

**FABAD**  
**JOURNAL of**  
**PHARMACEUTICAL**  
**SCIENCES**

ISSN 1300-4182  
e-ISSN: 2651-4648  
[www.fabad.org.tr](http://www.fabad.org.tr)

Volume: 50 • Issue: 1 • March 2025

An Official Journal of The Society of Pharmaceutical Sciences of Ankara (FABAD)



#### Publisher

Sevgi AKAYDIN (Gazi University, Department of Biochemistry, Ankara, Turkey)

#### Editor in Chief

Nesrin Gökhan KELEKÇİ (Hacettepe University, Department of Pharmaceutical Chemistry, Ankara, Turkey)

#### Co-Editors

Selen ALP (Ankara University, Department of Pharmaceutical Chemistry, Ankara, Turkey)  
Selin Seda TİMUR (Hacettepe University, Department of Pharmaceutical Technology, Ankara, Turkey)

#### Technical Editors

Gökçen TELLİ (Hacettepe University, Department of Pharmacology, Ankara, Turkey)  
Vahap Murat KUTLUAY (Hacettepe University, Department of Pharmacognosy, Ankara, Turkey)

#### Biostatistics Editor

Hatice Yağmur ZENGİN Hacettepe University, Faculty of Medicine, Department of Biostatistics, Ankara, Turkey

#### Editorial Board

- Almira RAMANAVIČIENĖ Vilnius University, Nanotechnology and Material Sciences Center, Vilnius, Latvia  
Alper GÖKBULUT Ankara University, Department of Pharmacognosy, Ankara, Turkey  
Ashok K. SHAKYA Al Ahliyya Amman University, Department of Pharmaceutical Chemistry, Amman, Jordan  
Aygin EKİNCİOĞLU Hacettepe University, Department of Clinical Pharmacy, Ankara, Turkey  
Ayşe KURUÜZÜM UZ Hacettepe University, Department of Pharmacognosy, Ankara, Turkey  
Bharat JHNAWAR Lovely Professional University, Pharmaceutical Sciences, Punjab, India  
Bülent KIRAN Ege University, Department of Pharmacy Management, Izmir, Turkey  
Ceyda Tuba ŞENGEL TÜRK Ankara University, Department of Pharmaceutical Technology, Ankara, Turkey  
Chia-Yi TSENG Chung Yuan Christian University, Biomedical Engineering, Taoyuan, Taiwan  
Didem DELİORMAN ORHAN Gazi University, Department of Pharmacognosy, Ankara, Turkey  
Emel Öykü ÇETİN UYANIKGİL Ege University, Department of Pharmaceutical Technology, Izmir, Turkey  
Filiz BAKAR ATEŞ Ankara University, Department of Biochemistry, Ankara, Turkey  
Francesco EPIFANÒ G. D'Annunzio University, Department of Pharmaceutical Chemistry, Chieti-Pescara, Italy  
Gerard LIZARD University of Burgundy, French Institute for Medical and Health Research, Dijon, France  
Gökçe CİHAN ÜSTÜNDAĞ Istanbul University, Department of Pharmaceutical Chemistry, Ankara, Turkey  
Gökçen EREN Gazi University, Department of Pharmaceutical Chemistry, Ankara, Turkey  
Hande GÜRER ORHAN Ege University, Department of Pharmaceutical Toxicology, Izmir, Turkey  
Hasan Abougazar YUSUFOĞLU King Saud University, Department of Pharmacognosy, Riyadh, Saudi Arabia  
Hasan KIRMIZIBEKMEZ Yeditepe University, Department of Pharmacognosy, Istanbul, Turkey  
Ikhlas KHAN University of Mississippi, National Center for Natural Product Research, USA.  
Işıl ÖZAKCA GÜNDÜZ Ankara University, Department of Pharmacology, Ankara, Turkey  
İnci Selin DOĞAN Karadeniz Technical University, Department of Pharmaceutical Chemistry, Trabzon, Turkey  
Leyla YURTTAŞ Anadolu University, Department of Pharmaceutical Chemistry, Eskişehir, Turkey  
Melike H. ÖZKAN Hacettepe University, Department of Pharmacology, Ankara, Turkey  
Meltem ÜNLÜSOY Ankara University, Department of Pharmaceutical Chemistry, Ankara, Turkey  
Merve BACANLI University of Health Sciences, Department of Pharmaceutical Toxicology, Ankara, Turkey  
Merve BECİT Afyonkarahisar University of Health Sciences, Department of Pharmaceutical Toxicology, Afyonkarahisar, Turkey  
Mesut SANCAR Marmara University, Department of Clinical Pharmacy, Istanbul, Turkey  
Ming-Wei CHAO Chung Yuan Christian University, Department of Bioscience Technology, Taoyuan, Taiwan  
Muharrem ÖLÇER Afyonkarahisar University of Health Sciences, Department of Pharmaceutical Technology, Afyonkarahisar, Turkey  
Natalizia MICELI University of Messina, Department of Chemistry and Biology, Messina, Italy  
Özlem Nazan ERDOĞAN Istanbul University, Department of Pharmacy Management, Ankara, Turkey  
Sevda ŞENEL Hacettepe University, Department of Pharmaceutical Technology, Ankara, Turkey  
Sevtap AYDIN DİLSİZ Hacettepe University, Department of Pharmaceutical Toxicology, Ankara, Turkey  
Suryakanta SWAIN The Assam Kaziranga University, Department of Pharmaceutical Sciences, Assam, India  
Şükrü BEYDEMİR Anadolu University, Department of Pharmaceutical Microbiology, Ankara, Turkey  
Tuba İNCEÇAYIR Gazi University, Department of Pharmaceutical Technology, Ankara, Turkey  
Tuğba TÜYLÜ KÜÇÜKKİLİÇ Hacettepe University, Department of Biochemistry, Ankara, Turkey  
Tuğçe YEŞİL Marmara University, Department of Pharmaceutical Toxicology, Istanbul, Turkey  
Uğur TAMER Gazi University, Department of Analytical Chemistry, Eskişehir, Turkey  
Vu Dang HOANG Hanoi University of Pharmacy, Department of Analytical Chemistry and Toxicology, Hanoi, Vietnam  
Wolfgang SCHUHLY University of Graz Institute of Pharmaceutical Sciences, Department of Pharmacognosy, Graz, Austria

The FABAD Journal of Pharmaceutical Sciences is published three times a year by the  
Society of Pharmaceutical Sciences of Ankara (FABAD)

All expressions of opinion and statements of supposed facts appearing in articles and / or advertisements carried in this journal are published on the responsibility of the author and / or advertiser, and are not to be regarded those of the Society of Pharmaceutical Sciences of Ankara. The manuscript submitted to the Journal has the requirement of not being published previously and has not been submitted elsewhere. Manuscript should be prepared in accordance with the requirements specified as in the back cover. The submission of the manuscript to the Journal is not a condition for acceptance; articles are accepted or rejected on merit alone. This Journal is published electronically and it is an open-access journal without publication fee. All rights reserved. Neither this work nor any part may be reproduced or transmitted in any form or by any means, electronic or mechanical, microfilming and recording, or by any information storage and retrieval systems without written permission from FABAD Journal of Pharmaceutical Sciences.

The FABAD Journal of Pharmaceutical Sciences is indexed in Chemical Abstracts,  
Analytical Abstracts, International Pharmaceutical Abstracts, Excerpta Medica (EMBASE), Scopus and TR Index

# CONTENTS

## Research Articles

- 1 Formulation and Evaluation of Orodispersible Tablet of Dolutegravir - Methionine Cocrystal  
**Rejoys TAMANG\***, **Ammon TAMANG\*\***, **Sayani BHATTACHARYYA\*\*\***
- 15 N-Alkylation of Some Imidazopyridines  
**Fatima DOGANC\***, **Hakan GOKER\*\***
- 21 Some 5-HT<sub>1A</sub>, 5-HT<sub>2A</sub> and 5-HT<sub>2C</sub> Receptor Ligands as Atypical Antipsychotic: In Silico Pharmacological Evaluation with ADME Predictions and Molecular Docking Techniques  
**Harun USLU\***
- 39 Is UR-144 Synthetic Cannabinoid Toxic to The Neuronal Cells: An *In Vitro* Evaluation  
**Mahmoud ABUDAYYAK\***, **Tuğçe BORAN\*\***
- 51 Formulation and Characterization of Lquisolid Tablets for Improving Dissolution of Telmisartan  
**Chinmaya Keshari SAHOO\***, **Nidhi SHREE\*\***, **Amiyakanta MISHRA\*\*\***
- 65 Antihypertensive Drug Box Sales Between January 2019 - June 2024 in Turkish Drug Market: Investigating the Drug Group and Fix-Dose Combination Sales  
**Elif Hilal VURAL\***, **Bülent GÜMÜŞEL\*\***
- 79 Phytochemical Analysis, Antibacterial, Anti-Fungi, and Antiradical Effects, Exploring Correlation Analysis of Lingonberry Leaf (*Vaccinium vitis-idaea* L.) Extracts  
**Olexander MASLOV\***, **Mykola KOMISARENKO\*\***, **Svitlana PONOMARENKO\*\*\***, **Tetiana OSOLOUDCHENKO\*\*\*\***, **Sergii KOLISNYK\*\*\*\*\***
- 95 An Experimental Investigation based on a Novel Gastro-Retentive Raft Liquid Dosage Form in Tandem with Controlled-Release Strategies for Oral Delivery of Metronidazole  
**Himangshu SARMA\***, **Taslima JAHAN\*\***, **Ashis Kumar GOSWAMI\*\*\***, **Hemanta Kumar SHARMA\*\*\*\***
- 111 A Blockchain-Based Approach to Securing the Pharmaceutical Supply Chain  
**Ahmed ALOUI\***, **Meftah ZOUAI\*\***, **Samir BOUREKKACHE\*\*\***, **Okba KAZAR\*\*\*\***
- 129 Characterization of Vasoactive Intestinal Polypeptide with LC-MS/MS Method  
**Sema KOYUTURK\***, **Erol SENER\*\***

- 145 Herbal Product Use and Drug-Herbal Product Interactions in Patients with Chronic Diseases-A Cross- Sectional Study  
**Eyup Can POLAT\*\* , Sefa GOZCU\*\***

#### **Review Articles**

- 157 Innovative Drug Delivery System: Aspasomes and Their Effectiveness in Treatment  
**Esmâ Nur USLU\* , Çiğdem YÜCEL\*\***
- 169 A Review on Calcium-alginate microspheres for Drug Delivery System: Characteristics, Drug Release, Activity, Stability and *In Vivo* Studies  
**Amiruddin AMIRUDDIN\* , Mahardian RAHMADI\*\* , Dewi Melani HARIYADI \*\*\*\*,\*\*\*\*\***
- 187 Forced Degradation and Stability Indicating Chromatographic Methods for the Analysis of Sofosbuvir Alone and in Combination with Velpatasvir, Daclatasvir, Voxilaprevir and Ledipasvir  
**Nastaran HEIDARZADEH KHORAMABADI\* , Nasrin NEMAYANDEH\*\* , Ali MOHAMMADI\*\*\* , Roderick B WALKER\*\*\*\***
- 211 Analytical Evaluation of the Chemical Content of HTPs Compared to Conventional Cigarettes  
**Bensu KARAHALİL\***

# Formulation and Evaluation of Orodispersible Tablet of Dolutegravir - Methionine Cocrystal

Rejoys TAMANG\*, Ammon TAMANG\*\*, Sayani BHATTACHARYYA\*\*\*

*Formulation and Evaluation of Orodispersible Tablet of Dolutegravir - Methionine Cocrystal*

## SUMMARY

Dolutegravir, a newly approved anti-HIV drug, is insoluble in the normal gastric pH range, resulting in a slow onset of action. The research proposes cocrystallization process to increase the solubility of the drug and hence dissolution. The cocrystals of dolutegravir were formulated using methionine as cofomers by solvent evaporation method. The cocrystals were evaluated for solubility, in vitro drug release, and solid-state characterization, study. The orodispersible tablets of dolutegravir cocrystal were successfully prepared by direct compression method. The solid-state characterization study showed the compatibility and amorphization of the drug in the cocrystal form. The cocrystal of drug: methionine (1:2) was found to enhance dissolution in pH 1.2 by 1.88 times compared to the pure drug. The orodispersible tablets disintegrated at  $10.05 \pm 0.5$  secs and  $90 \pm 0.64\%$  of the drug was released in 20 min. Hence, it can be concluded that the methionine-dolutegravir cocrystal can be a promising means to improve the solubility of the drug.

**Key Words:** Dolutegravir, methionine, solubility enhancement, orodispersible tablet, dissolution.

*Dolutegravir - Metionin Kokristalinin Ağızda Dağılabilen Tabletinin Formülasyonu ve Değerlendirilmesi*

## ÖZ

Yeni onaylanmış bir anti-HIV ilaç olan dolutegravir, normal gastrik pH aralığında çözünmez ve bu da etkisinin geç başlamasına neden olur. Araştırma, ilacın çözünürlüğünü ve dolayısıyla çözünmesini artırmak için birlikte kristalleştirme işlemi önermektedir. Dolutegravirin kokristalleri, çözücü buharlaştırma yöntemiyle koformer olarak metiyonin kullanılarak formüle edildi. Kokristaller çözünürlük, in vitro ilaç salınımı ve katı hal karakterizasyonu çalışmaları açısından değerlendirildi. Dolutegravir kokristalinin ağızda dağılabilen tabletleri doğrudan basım yöntemiyle başarılı bir şekilde hazırlandı. Katı hal karakterizasyon çalışması, ilacın kokristal formunda uyumluluğunu ve amorfizasyonunu gösterdi. İlacın kokristali : metiyoninin (1:2), pH 1.2'de çözünürlüğü saf ilaca göre 1.88 kat artırdığı bulundu. Ağızda dağılabilen tabletler  $10.05 \pm 0.5$  saniyede dağıldı ve ilacın  $90 \pm 0.64\%$ 'ü 20 dakikada salındı. Dolayısıyla, metiyonin-dolutegravir kokristalinin ilacın çözünürlüğünü iyileştirmede umut verici bir araç olabileceği sonucuna varılabilir.

**Anahtar Kelimeler:** Dolutegravir, metiyonin, çözünürlük artışı, ağızda dağılabilen tablet, çözünme.

Received: 15.07.2024

Revised: 03.10.2024

Accepted: 18.11.2024

\* ORCID: 0009-0009-0929-7158, Department of Pharmaceutics, Krupanidhi College of Pharmacy, Bengaluru, India.

\*\* ORCID: 0009-0002-7068-8616, Department of Pharmaceutics, Krupanidhi College of Pharmacy, Bengaluru, India.

\*\*\* ORCID: 0000-0002-4013-4316, Department of Pharmaceutics, Krupanidhi College of Pharmacy, Bengaluru, India.

## INTRODUCTION

Dolutegravir is an integrase strand transfer inhibitor (INSTI), recommended to be used in conjunction with other antiretroviral agents in the management of HIV-1 (Mattevi & Tagliari 2017). It is a newly approved BCS Class II drug and is insoluble over the gastric pH range (Yu et al., 2017). The poor solubility of the drug results in delayed onset of action and less oral bioavailability (Buchanan *et al.*, 2017). Therefore, the requirement for a new form of the drug with refined physicochemical properties is highly desirable.

Pharmaceutical co-crystals are composed of two or more ionic or molecular compounds mixed with a specific stoichiometric ratio with the active pharmaceutical ingredient (API) to yield a neutral single-phase system. They are a new and promising method for enhancing the performance of pharmaceuticals by modulating their mechanical, optical, release profile, and chemical stability, thereby improving bioavailability, and therapeutic efficacy (Guo *et al.*, 2021).

Tesson *et al.* researched cocrystals of lorcaserin, and patented the finding on the improvement of stability of the drug (Tesson *et al.* 2017). Nanubolu *et al.* summarized the findings on the solubility improvement of aripiprazole in their study (Nanubolu *et al.* 2016).

Co-crystal components combine via non-covalent interactions including hydrogen bonds, van der Waals interactions, ionic bonds, or  $\pi$ - $\pi$  interactions (Bhattacharyya & Manjunath, 2023). The co-crystallization process arises from the molecular interaction between similar molecules/homomers, and heteromers /different molecular structures (Qiao *et al.*, 2011).

Following USFDA regulations, an API and counter molecule must have a lower proton transfer potential to be categorized as cocrystals. Therefore, to restrict the salt formation, the difference in pKa between the two components must be less than 1 (Food and Drug Administration 2018).

The presence of polar groups in the structure of

amino acids capable of forming hydrogen bonds characterizes them as novel cofomer in the cocrystallization procedure. They support the “green method” co-crystallization of active molecules. The zwitterionic nature of the amino acids allows them to create hydrogen bonds with the API that strengthens the contacts and increases stability (Nugrahani & Jessica, 2021). They are also considered to be generally recognized as safe (GRAS), because of their low toxicity. Therefore, amino acids can be a good choice and potential co-former for co-crystallization of dolutegravir.

The research work plans to use methionine as a cofomer for improving the solubility of dolutegravir and formulate an orodispersible tablet of high effectiveness.

## MATERIALS AND METHODS

### Materials

Dolutegravir was procured as a gift sample from Strides Arcolab, Bangalore. The amino acid methionine was purchased from Sigma-Aldrich. Methanol, hydrochloric acid, and other analytical grade chemicals used for the analysis and preparation of tablets were purchased from SD Fine Chemicals, Bangalore, India.

### Method of preparation of Dolutegravir cocrystal

Cocrystals of dolutegravir were prepared by solvent evaporation method using methionine, as cofomers. The drug and the cofomer solutions were prepared separately using methanol and water. Both the solutions were mixed on a magnetic stirrer poured into the petri dish, and dried in the hot air oven at 50°C for 30 min. It was then allowed to cool at room temperature, weighed, and stored for further studies. Methionine was screened at two different ratios, drug: cofomer 1:1, 1:2 (Raheem Thayyil *et al.*, 2020).

### Determination of drug content

A known quantity (5 mg) of the sample was dissolved in a specific volume of diluting solution consisting of phosphate buffer solution pH 3.0, acetonitrile, and methanol at a ratio of 50:20:30. An aliquot

of 1 ml was withdrawn and diluted suitably and estimated spectrophotometrically at 322 nm. The same process was repeated for the pure drug of the same quantity (Bhattacharyya *et al.*, 2022). A standard graph was constructed previously in the range of 5-35 µg/ml using the diluting solution at 322 nm with an accuracy of 99.98%, a regression coefficient of 0.9998, and a linearity equation of  $Y=0.0174X$ . Experimentation was carried out in triplicates. Using the following formula the drug content was determined

$$\%Drug\ content = \frac{Absorbance}{Standard\ absorbance} \times 100$$

#### **Determination of solubility in different pHs**

The solubility of cocrystals of dolutegravir was determined in three different pH buffers (pH 1.2, pH 4.5, and pH 6.8). Cocrystal equivalent to the maximum dose of the drug was dissolved in 250 ml of three different buffers. The flasks were shaken in a mechanical shaker for 24 h at room temperature, after 24 h a known volume of solution was transferred to a centrifuge tube, and was centrifuged at 3000 rpm for 15 min, filtered, diluted, and assayed spectrophotometrically at 322 nm. All the tests were carried out in triplicates (Baka, Comer & Takács-Novák, 2008).

#### **Tukey's test to select the best drug cofomer ratio**

Dolutegravir cocrystals were compared with the pure drug and among themselves Tukey's multiple comparison tests (at a significance level of  $P < 0.05$ ) were used to identify the best combination of drug cofomer ratio of the selected amino acid.

#### **Selection of dissolution media based on solubility at different pHs**

The solubility of the best cocrystal of methionine and dolutegravir was determined in entire GI pH range buffers (pH 1.2, pH 3.0, pH 4.5, pH 5, pH 6.8, and pH 7.5). A maximum dose of the drug in its cocrystals was dissolved in 250 ml conical flasks containing different buffers. The solubility was determined by the same method as described earlier. The solubility data was used to calculate the Gibbs free energy and dose solubility ratio that helped to select

the dissolution media (Baka *et al.*, 2008). The Gibbs free energy of transfer ( $\Delta G$ ) was calculated using the following equation

$$\Delta G = - 2.303RT \log \frac{S_0}{S_s}$$

where  $S_0$  and  $S_s$  are the solubilities of the drug in water and dolutegravir cocrystal in the respective media respectively (Bhattacharyya *et al.*, 2022).

#### **Drug release study**

USP paddle-type II apparatus was used to conduct the dissolution study for the best cocrystal of dolutegravir. Dissolution media was selected after the solubility study using the concept of Gibbs free energy calculation and dose solubility ratio and was carried out in 900 ml of pH 1.2 HCl buffer. Cocrystal equivalent to 50 mg of dolutegravir was used for the drug release study stirring at a speed of 75 rpm, at  $37 \pm 0.5^\circ\text{C}$  for 60 min. The sampling was done at regular intervals (10 min) and was analyzed spectrophotometrically at 322 nm (Panzade P & Shendarkar G 2019). Three trials were carried out for each measurement

#### **Fourier Transform Infrared (FTIR) spectroscopy study**

The sample was analyzed using BRUKER FTIR Spectrometer Alpha II using the ATR technique from a range of  $3500\text{ cm}^{-1}$  to  $1000\text{ cm}^{-1}$ . The pure drug dolutegravir and the selected cocrystal were subjected to the analysis (Raheem Thayyil *et al.*, 2020).

#### **Powder X-ray Diffraction (PXRD)**

PXRD was used to identify the crystallinity of the drug in pure drug and best cocrystal. The data instrument used to analyze PXRD patterns was Rigaku Smartlab 3kW Japan. The powder X-ray diffraction study was carried out for pure drug and best cocrystal using Cu K $\alpha$  radiation at  $25^\circ\text{C}$  and scanned from 2 to 80,  $2\theta$  diffraction angle (Manjunath & Bhattacharyya, 2023).

#### **Differential Scanning Calorimetry (DSC) study**

The best cocrystal and reference standard drug are maintained at constant temperature and subjected to thermal analysis using the DSC Perkin-Elmer- 4000

series. Test samples were placed in aluminum pans and thematically sealed. Samples were heated from 20-400°C at an accelerating rate of 10°C per minute under nitrogen atmosphere. The thermograms were recorded.

#### Scanning electron microscopy (SEM)

The surface morphology of pure drug and the best cocrystal was imaged by a scanning electron microscope (Hitachi SU 3500) performed at an accelerating voltage of 10 kV. The powder in a few µg was fixed onto the stub, gold was sputtered, samples were adhered with a double-sided sticky carbon tape and images were taken (Raheem Thayyil *et al.*, 2020).

#### Nuclear Magnetic Resonance (NMR)

<sup>1</sup>H-NMR measurements were performed at ambient temperature Bruker NMR spectrometer, USA. The solid-state CP/MAS <sup>1</sup>H-NMR spectra of pure drug and DOLMET 1:2 were performed in DMSO solvent system using the cross-polarization magic angle spinning pulse sequence at measurement conditions of spinning 100 MHz, pulse delay 5s, contact time 10 minutes, and 24 h analysis time per sample. The signals were recorded (Kumar *et al.*, 2019).

#### Preparation of orodispersible tablets

##### Precompression characteristics of the powder blend of best cocrystal and method of preparation of tablet

Orodispersible tablets of Dolutegravir cocrystals were prepared by direct compression method. Each orodispersible tablet of 250 mg contains cocrystal of 30 mg equivalent dolutegravir, cross carmellose sodium (4%w/v), microcrystalline cellulose (46%w/v), mannitol (22%w/w), and lubricant (0.01%).

The angle of repose, bulk density, tapped density, Carr's index, and % porosity were carried out to get the precompression characteristics of the powder blend of best cocrystal before compression to tablets. All the tests were performed in triplicates (Martha *et al.*, 2017).

The drug and excipients were subjected to milling followed by sieving, mixing, and compression into a tablet using Rimek mini press-1 tablet punching machine with a compression force of 38±5 kN (Panzade *et al.*, 2017).

#### Post compression evaluation

##### Physical evaluation of tablets

The thickness of the tablets was determined using vernier calipers for randomly selected 30 tablets. Hardness was determined using a Monsanto hardness tester for 6 tablets selected randomly. Each of the 20 tablets was individually weighed using an electronic balance and the average weight of the tablets was checked. The % deviation of each tablet weight from the average weight was also estimated (Martha *et al.*, 2017).

##### Wetting time

The wetting test was performed using amaranth solution and cotton. The cotton was placed on the petri dish containing amaranth solution and the tablet was placed on top of the cotton. The time taken for the tablet to turn completely red was noted.

##### Disintegration test

The disintegration test was carried out for 6 tablets in 900 ml of distilled water using LAB-HOSP tablet disintegration test machine. The time taken for the tablet to disintegrate completely was noted. The test was performed in triplicates (Dey & Maiti, 2010).

##### Friability test

The friability test was carried out for 10 tablets using Electrolab friabilator (USP) EF-1W. The tablets were rotated at 25 rpm for 4 min. Initial and final weights were noted and % friability was calculated after the test (Pawar *et al.*, 2014). % Friability was calculated using the following equation

$$\text{Friability}(\%) = \frac{(W_1 - W_2)}{W_1} * 100$$

Where,  $W_1$  is the weight of tablets before tumbling, and  $W_2$  is the weight of tablets after tumbling.



### Drug release study of the orodispersible tablets

The same dissolution conditions as described prior were kept for the study of the dissolution of orodispersible tablets. The dissolution was carried out for 20 min. 1 ml of the sample was withdrawn at 5 min intervals and replaced with 1 ml of the fresh dissolution media. The diluted samples were analyzed spectrophotometrically at 322 nm. The analysis was carried out in triplicates (Panzade & Shendarkar, 2019).

### Stability studies of orodispersible tablets

The orodispersible tablets were stored at  $40^{\circ}\pm 2^{\circ}\text{C}$  at a relative humidity of  $75\% \pm 5\%$  for 3 months in sealed glass vials. The samples were observed for ap-

pearance, wetting, friability, disintegration, and *in vitro* drug release every month (Panzade & Shendarkar, 2017).

## RESULTS AND DISCUSSION

### Determination of solubility of cocrystals in different pH

Solubility studies of pure drug and Dolutegravir cocrystals (DOLMET 1:1 and DOLMET 1:2) in different pH (pH 1.2, pH 4.5, and pH 6.8) were carried out where the solubility of DOLMET 1:2 cocrystal was found to be the highest at pH 1.2 compared to the pure drug and DOLMET 1:1 cocrystal as shown in Figure 1.

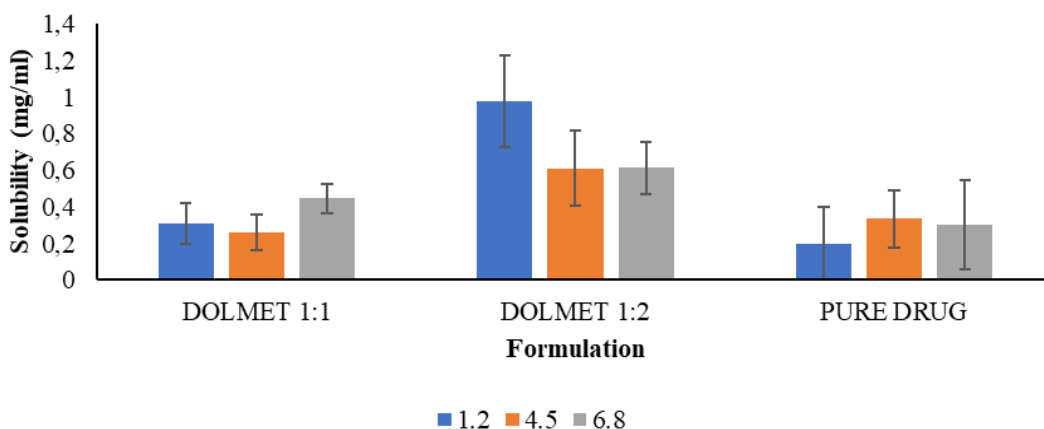


**Figure 1.** Comparative solubility of cocrystals of DOLMET 1:1, DOLMET 1:2, and pure drug in different pH (1.2, 4.5, and 6.8)

Dolutegravir is a weak acid and has a  $pK_a$  of 8.2. As per pH partition theory, the drug with  $pK_a > 8$ , will remain essentially unionized at all pHs, the entire gastrointestinal tract (GIT) thus serves as the absorption site for such molecules. Hence solubility improvement in the entire GIT is preferred for promoting absorption. The calculation of Gibbs's Free energy gives an understanding of the improvement of solubility. A negative Gibbs's free energy depicts the spontaneity of the solution process. The calculated Gibbs free energy of cocrystal DOLMET 1:2 predicted the dissolution can be spontaneous in all the media, but the highest might be in pH 1.2. The Gibbs free energy calculation was minimal for DOLMET 1:2 at pH 1.2 as shown in

Table 1. Dose solubility ratio was lowest at a value of 51.32. Hence considering the solubility parameters of DOLMET 1:2, pH 1.2 was selected as the dissolution media for the cocrystal.

**Table 1.** Thermodynamic solubility analysis of DOLMET 1:2

pH	Solubility (mg/ml)	Gibbs's Free energy	Dose solubility ratio
1.2	$0.97 \pm 0.25$	-10.54	51.32
3	$0.66 \pm 0.15$	-5.67	75
4.5	$0.609 \pm 0.20$	-7.19	82.07
5	$0.51 \pm 0.04$	-8.99	96.66
6.8	$0.61 \pm 0.14$	-6.87	81.69
7.4	$0.88 \pm 0.18$	-6.89	56.49

Tukey’s multiple comparison test ( $p < 0.05$ ) revealed that DOLMET 1:2 was significantly better than pure drug and DOLMET 1:1 as shown in Table 2.

Hence DOLMET 1:2 was selected as the best cocrystal for further evaluations.

**Table 2.** Tukey’s Multiple Comparison Test

Tukey’s Multiple Comparison Test	Mean Diff.	Significant? P < 0.05?	Summary	95% CI of diff
DOLMET 1:2 vs DOLMET 1:1	0.6657	Yes	***	0.6657 to 0.6657
DOLMET 1:2 vs PURE DRUG	0.7787	Yes	***	0.7787 to 0.7787
DOLMET 1:1 vs PURE DRUG	0.1130	Yes	***	0.1130 to 0.1130

**Determination of solubility of best cocrystal in the entire GI pH range**

Solubility of the pure drug and best cocrystal (DOLMET 1:2) in the entire GI pH range (pH 1.2, to pH 7.4) was carried out where DOLMET 1:2 cocrystal showed improved solubility than the pure drug in the entire GI pH range with maximum solubility at pH 1.2 as shown in Figure 2.

**In vitro drug release study**

*In vitro* drug release of pure drug and DOLMET 1:2, cocrystal was carried out for 60 min and graphically represented as % CDR v/s time profile. DOLMET 1:2 cocrystal showed remarkable improvement in dissolution compared to pure drugs. The *in vitro* dissolution rate of DOLMET 1:2 was more than 80 % in 60 min as shown in Figure 2.

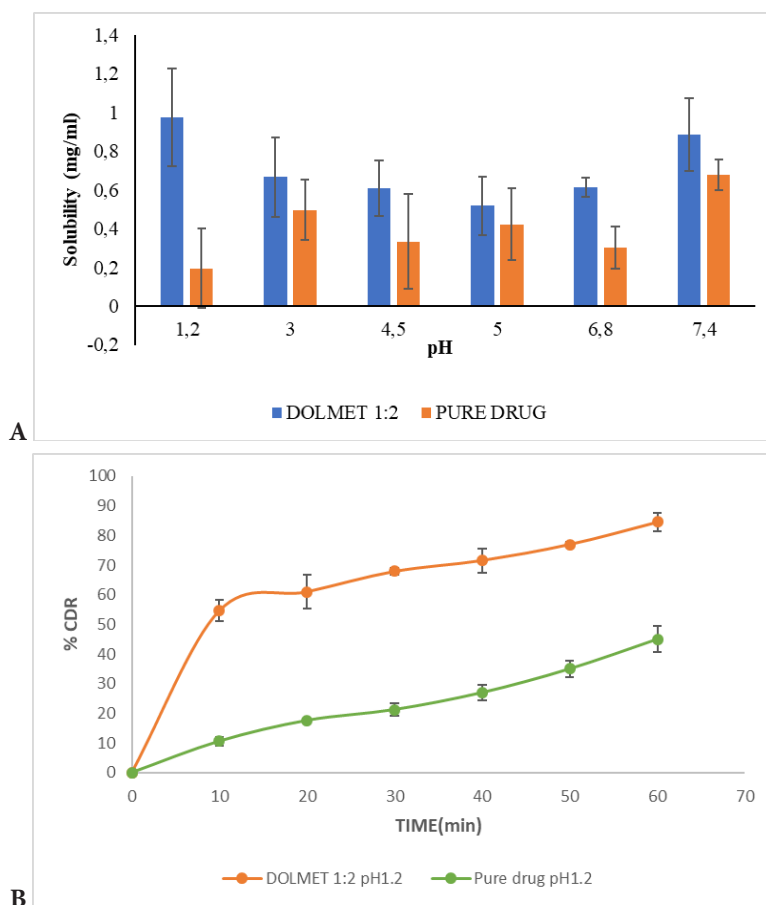


**Figure 2.** Solubility of DOLMET 1:2 and pure drug in the entire GI pH range (A)

*In vitro* drug release of DOLMET 1:2 and pure drug (B)

### **FTIR**

The compatibility of the drug and coformer was established through the FTIR study, Major peaks were found to be retained in the sample at a lower intensity indicating the formation of H bond with the coformer. The presence of peaks at  $1640.73\text{ cm}^{-1}$ (C=C),  $1363.95\text{ cm}^{-1}$ (C=F),  $1318.18\text{ cm}^{-1}$ (C=N),  $1271.48\text{ cm}^{-1}$ (C-O),  $854.50\text{ cm}^{-1}$ (C-H) and  $3064.96\text{ cm}^{-1}$ (O-H) of the pure drug was observed in the cocrystal of DOLMET 1:2 as shown in Figure 3 (Mupparaju *et al.*, 2021).

### **PXRD**

The PXRD diffraction pattern of the pure drug demonstrated high-intensity peaks, confirming the crystalline nature of the pure drug. The major peaks of the drug at  $2\theta$  6.4, 14.62, 19.25, 23.38, and 29.96 were significantly lowered in DOLMET 1:2 indicating amorphization of the drug in its cocrystal and supporting the dissolution enhancement. The presence of

new peaks at  $2\theta$  20.69, 23.10, 23.22,33.15, etc. confirms the formation of the cocrystal of dolutegravir. The PXRD patterns of pure drug and DOLMET 1:2 are shown in Figure 3 (Mupparaju *et al.*, 2021). The reduction in the intensity of the peaks in the cocrystals confirmed the amorphization of the drug which supported the high solubility of the cocrystals compared to the pure drug.

### **DSC**

A broad endothermic peak of the pure dolutegravir at its melting point of  $368.83\text{ }^{\circ}\text{C}$  indicated the crystalline nature of the drug. The thermogram of cocrystal DOLMET 1:2 showed a reduced peak at  $231\text{ }^{\circ}\text{C}$  that suggested the formation of the cocrystal. The reduced intensity of the peak depicts its amorphization. The DSC thermograms are presented in Figure 3 (Mupparaju *et al.*, 2021). These observations also supported the findings of PXRD studies and the improvement of solubility.

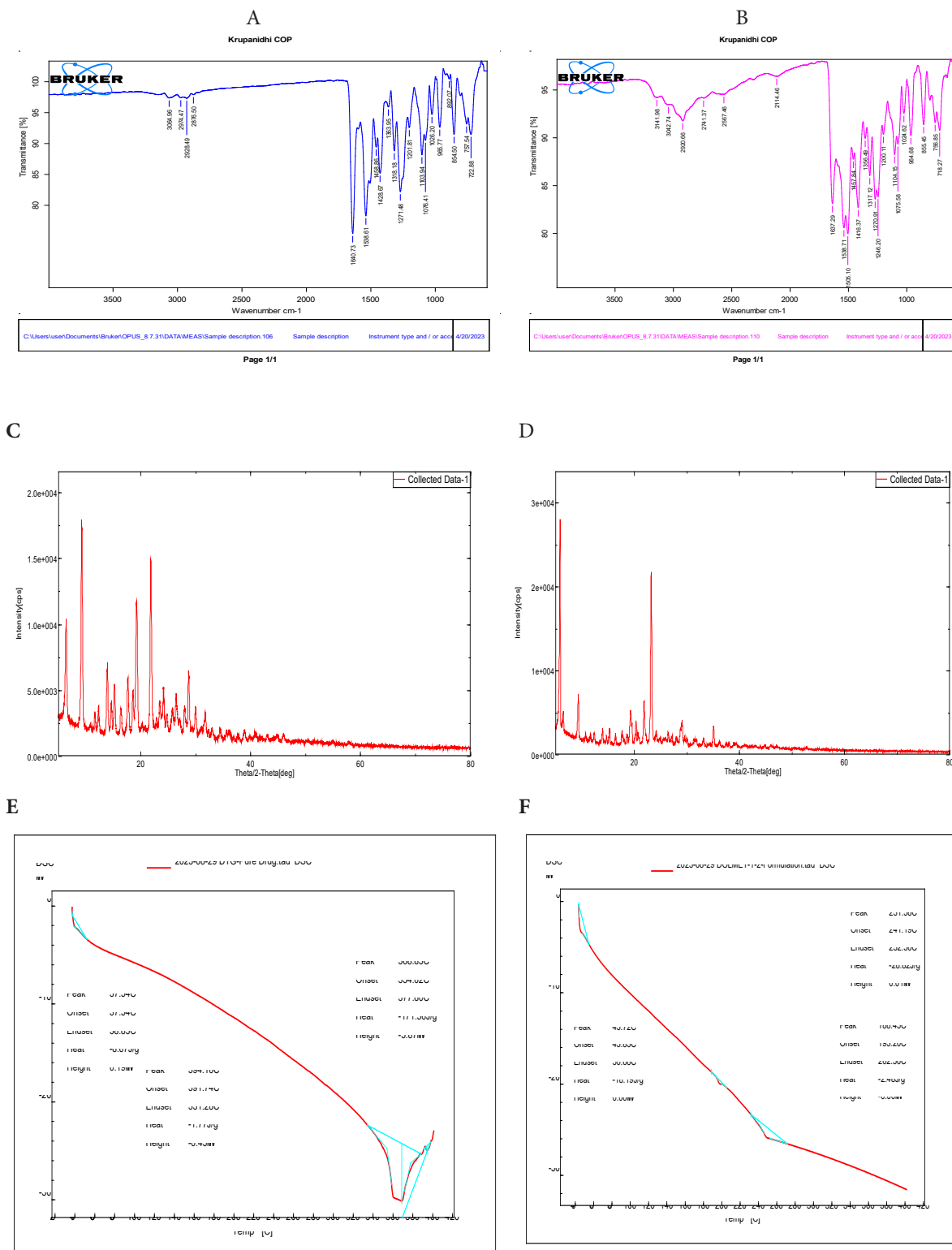


**Figure 3.** FTIR of Pure drug (A) and DOLMET 1:2 (B), PXRD of Pure drug (C) and DOLMET 1:2 (D), DSC of Pure drug (E) and DOLMET 1:2 (F).

### SEM

The surface morphology study of the pure drug and DOLMET 1:2 at the same magnifications is shown in Figure 4. The crystalline nature of the pure drug was observed in the images and the cocrystals were found to be discrete nano-sized particles. A significant change in shape and surface topography was observed in the cocrystal. The crystallinity of the drug was transformed into fine dispersed particles attached to the cofomers. These changes might have contributed to the flow properties of the cocrystals (Reham AK *et al.*, 2019).

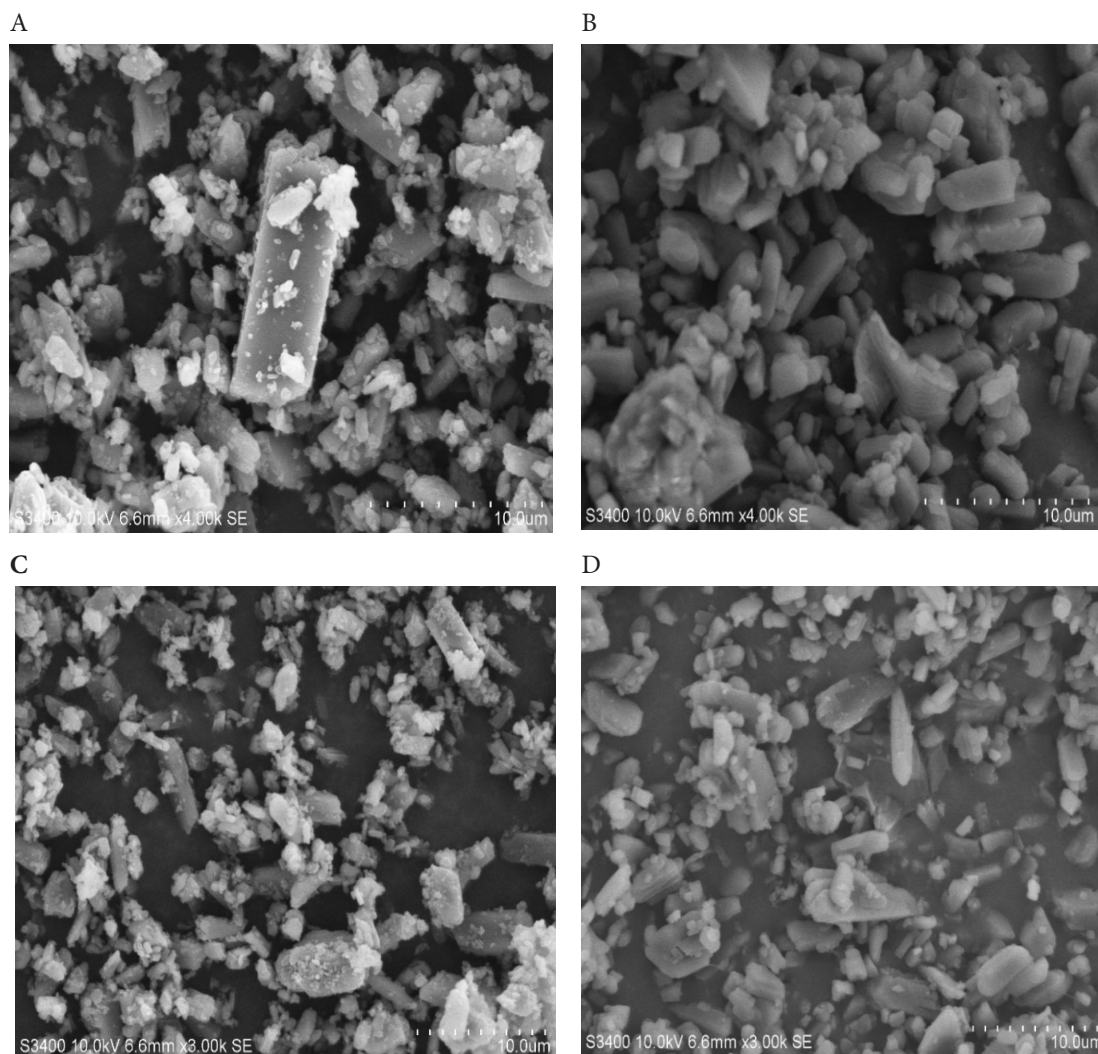
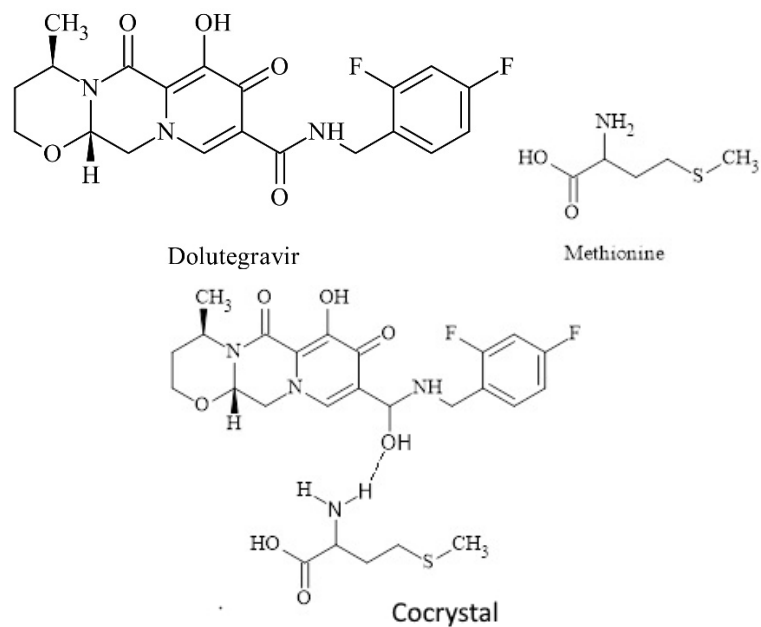


**Figure 4.** SEM images of Pure drug (A, B) and DOLMET1:2(C, D)

### NMR

The formation of hydrogen bonds in dolutegravir cocrystals was verified through NMR, which showed peak broadening at 3.321 for DOLMET 1:2. As de-

picted in Figure 5, this interaction involves the amino group and dioxo groups, confirming cocrystal formation and excluding salt formation.



**Scheme 1.** Structure of drug, coformer, and cocrystal

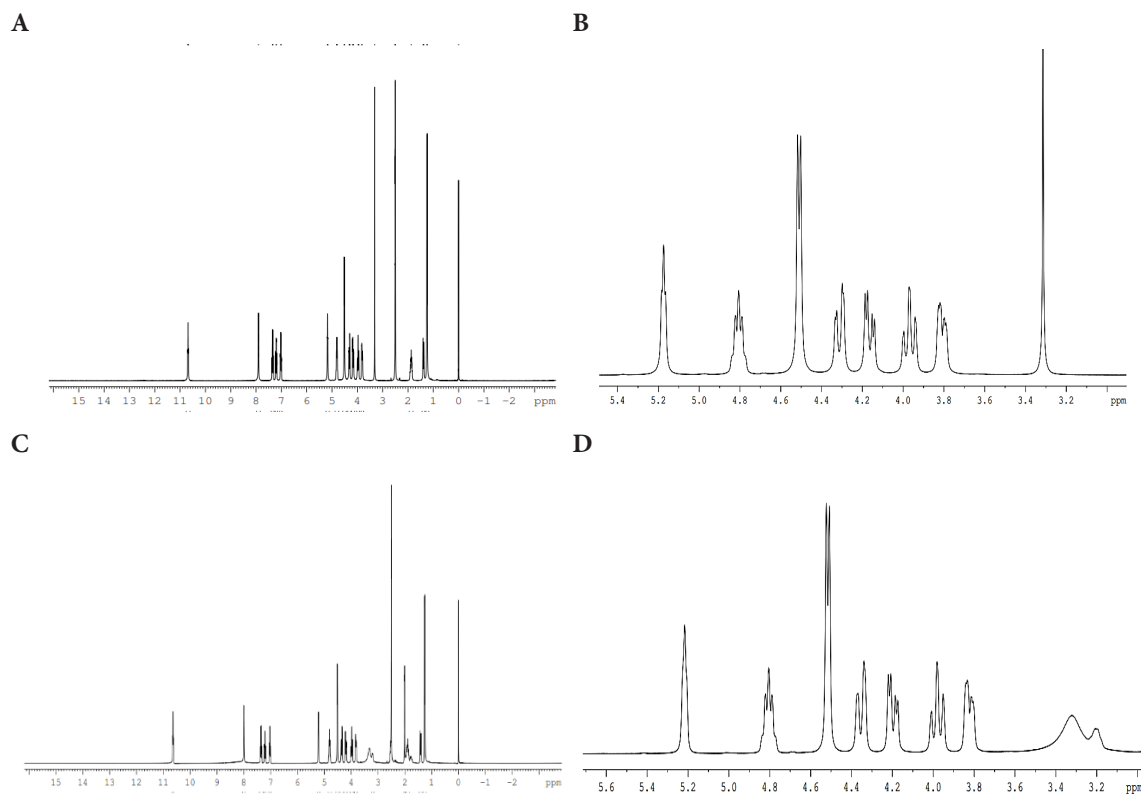


**Figure 5.** NMR of Pure drug (A, B) and DOLMET 1:2 (C, D)

### Precompression evaluation of the powder blend of cocrystal

The particle size, size distribution, shape, density, and surface area influence precompression properties and flow of powder. Precompression evaluation was carried out for the pure drug and powder blend of the cocrystal before compressing into tablets. It was observed that the powder blends of the cocrystal possessed good flow properties and acceptable compressibility index compared to the pure drug as shown

in Figure 6. An angle of repose of less than 25 was observed for the cocrystals, which is indicative of the excellent flow of the powder blend. Carr's index was found to be around 15, which indicated the compressibility of the cocrystal was good compared to the pure drug powder blend. % porosity was increased as it was calculated from the bulk density and particle density measurement. This might be the reason for the improvement in the dissolution (Sujitha *et al.*, 2014).

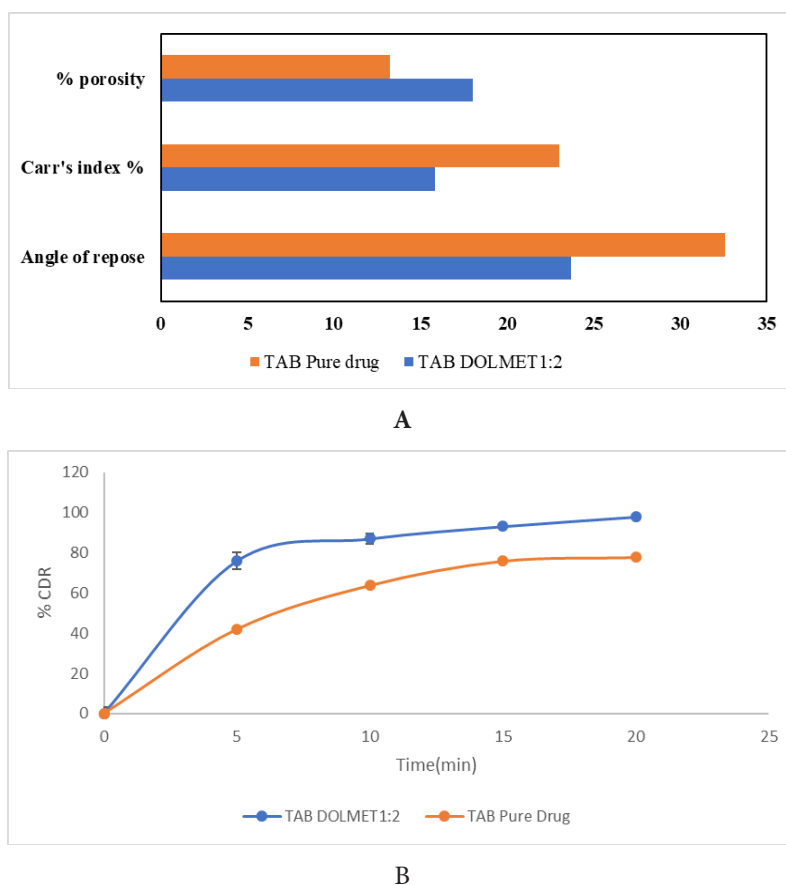


**Figure 6.** Precompression characteristics of the powder blend of DOLMET 1:2 and pure drug (A), *In vitro* drug release of orodispersible tablets of DOLMET 1:2 and pure drug

### Post-compression evaluation of orodispersible tablets

Post-compression studies such as weight variation, friability, disintegration, hardness, and wetting were carried out for orodispersible tablets. Weight variation was limited to the range of  $\pm 0.5\%$ , and friability was found to be  $0.00855\%$ . The tablets were disinte-

grated at  $10.05 \pm 0.5$  seconds. The hardness and wetting time were found to be  $3 \pm 0.87$  kg/cm<sup>2</sup> and  $13.62 \pm 0.05$  seconds respectively. All the findings supported the requirements of the orodispersible tablets. Hence the suitability of cocrystals of dolutegravir for developing fast-dissolving orodispersible tablets with excellent transportability was established.

### **In vitro drug release study of orodispersible tablets**

The *in vitro* drug release studies unequivocally demonstrated the superior dissolution performance of orodispersible tablets compared to pure drug tablets. Orodispersible tablets showed promising results in dissolution compared to pure drug tablets and the % CDR for orodispersible tablets was found to be more than 90% in 20 min as shown in Figure 6. This rapid and enhanced drug release profile suggested the potential of orodispersible tablets to improve bioavailability and accelerate therapeutic onset. The optimized formulation and cocrystal technology employed in these tablets successfully addressed the

limitations of pure drug tablets, paving the way for a more efficacious and patient-compliant treatment option.

### **Stability studies of orodispersible tablets**

Stability studies for the pure drug and orodispersible tablet were carried out for 3 months (temperature of  $40^{\circ} \pm 2^{\circ}\text{C}$  and relative humidity of  $75\% \pm 5\%$ ) and it was found that there was no significant change in the appearance, weight, hardness, and friability. The critical stability parameters are listed as shown in Table 3. There were no significant differences ( $p < 0.05$ ) observed in the tablets kept for stability study for 3 months.

**Table 3.** Stability studies of orodispersible tablets of DOLMET 1:2

Storage time(months)	Wetting time (Sec)	Disintegration time (Sec)	%CDR
0	13.62±0.05	10.05±0.5	97.95±0.02
1	13.7±0.09	10±0.3	97.8±0.05
2	13.7±0.06	10.1±0.4	97.76±0.04
3	13.71±0.05	10±0.5	97.7±0.06

### **CONCLUSION**

The cocrystallization process of dolutegravir in the presence of different amino acids was experimented out and revealed that a new improved physiochemical form of dolutegravir was obtained at a stoichiometric ratio of 1:2 of the drug; methionine. Methionine was found to be more effective in improving the solubility of the drug as evidenced from the dissolution studies. The solid-state characterization and surface morphology of the cocrystal showed amorphization of the pure drug. The orodispersible tablet formed with the crystal showed good precompression, post-compression, disintegration, and drug release. Hence the process of cocrystallization of dolutegravir with amino acids was found to be promising in overcoming the poor solubility of the drug.

### **ACKNOWLEDGEMENT**

No funding or other financial support was received for the study.

### **AUTHOR CONTRIBUTION STATEMENT**

All authors contributed to data collection, processing, writing, revision of the draft, reading and approval of the final manuscript.

### **CONFLICT OF INTEREST**

The authors declare that there is no conflict of interest.

### **REFERENCES**

- Baka, E., Comer, J.E., & Takács-Novák, K. (2008). Study of equilibrium solubility measurement by saturation shake flask method using hydrochlorothiazide as model compound. *Journal of Pharmaceutical Biomedical Analysis*, 46 (2), 335-41. <https://doi.org/10.1016/j.jpba.2007.10.030>.
- Bhattacharyya, S., Adhikari, H., Regmi, D., & HVR, R. (2022). A Study on solubility enhancement of etravirine by crystal engineering method. *Indian Journal of Pharmaceutical Science*, 84(3), 575-585. <https://doi.org/10.36468/pharmaceutical-sciences.952>.



- Bhattacharyya, S., & Manjunath, A. (2023). Pharmaceutical cocrystal-a deft technique for solubility enhancement, *Pharmaceutical Sciences Asia*, 50(4), 361-370. <https://doi.org/10.29090/psa.2023.04.23.618>.
- Buchanan, A.M., Holton, M., Conn, I., Davies, M., Choukour, M., & Wynne, B.R. (2017). Relative bioavailability of a dolutegravir dispersible tablet and the effects of low- and high-mineral-content water on the tablet in healthy adults. *Clinical Pharmacology in Drug Development*, 6(6), 577-583. <https://doi.org/10.1002/cpdd.332>.
- Dey, P., & Maiti, S. (2010). Orodispersible tablets: A new trend in drug delivery. *Journal of Natural Science Biology and Medicine*, 1(1), 2-5. <https://doi.org/10.4103/0976-9668.71663>.
- Food and Drug Administration, (2018). Regulatory classification of pharmaceutical cocrystals, guidance for industry, U.S. Department of Health and Human Services Food and Drug Administration Center for Drug Evaluation and Research (CDER). Access date: 30 March 2024.
- Guo, M., Sun, X., Chen, J., & Cai, T. Pharmaceutical cocrystals: A review of preparations, physico-chemical properties and applications. (2021). *Acta Pharmaceutica Sinica B*, 11(8), 2537-2564. <https://doi.org/10.1016/j.apsb.2021.03.030>.
- Kumar, T.N.V.G., Vidyadhara, S., & Narkhede, N.A. (2019). Study of dolutegravir degradation and spectroscopic identification of products by LCMS, 1H and 13C NMR techniques. *Pharmaceutical Chemistry Journal*, 53, 368-375. <https://doi.org/10.1007/s11094-019-02007-x>.
- Manjunath, A., & Bhattacharyya, S. (2023). Assessment of solid-state behaviour and in vitro release of artemether from liquisolid compact using mesoporous material as an excipient. *Indian Journal of Pharmaceutical Education and Research*, 57(1), 1321. <https://doi.org/10.5530/ijper.57.1s.3>.
- Martha, S., Nedanuri, A., Kalavathi, A., Vahini, B.S., Kumar, M.P., & Soumya, S. (2017). Design and in vitro characterization of dolutegravir sustained release matrix tablets. *International Journal of Pharmaceutical Sciences Review and Research*, 46(2), 136-141.
- Mattevi, V.S., & Tagliari, C.F. (2017). Pharmacogenetic considerations in the treatment of HIV. *Pharmacogenomics*, 18(1), 85-98. <https://doi.org/10.2217/pgs-2016-0097>.
- Mupparaju, S., Suryadevara, V., & Doppalapudi, S. (2021). Preparation and evaluation of dolutegravir solid dispersions. *International Journal of Applied Pharmaceutics*, 13(1), 193-198. <https://doi.org/10.22159/ijap.2021v13i1.40113>.
- Nanubolu, J.B., & Ravikumar, K. (2016). Correlating the melting point alteration with the supramolecular structure in aripiprazole drug cocrystals, *Cryst.Eng.Comm.*, 18(6), 1024-1038.
- Nugrahani, I., & Jessica, M.A. (2021). Amino acids as the potential co-former for co-crystal development: A review. *Molecules*, 26(11), 3279. <https://doi.org/10.3390/molecules26113279>.
- Panzade, P., & Shendarkar, G. (2019). Superior solubility and dissolution of zaltoprofen via pharmaceutical cocrystals. *Turkish Journal of Pharmaceutical Sciences*, 16(3), 310-316. <https://doi.org/10.4274/tjps.galenos>.
- Panzade, P., Shendarkar, G., Shaikh, S., & Balmukund Rathi, P. (2017). Pharmaceutical cocrystal of piroxicam: design, formulation, and evaluation. *Advance Pharmaceutical Bulletin*, 7(3), 399-408. <https://doi.org/10.15171/apb.2017.048>.
- Pawar, H., Varkhade, C., Jadhav, P., & Mehra, K. (2014). Development and evaluation of orodispersible tablets using a natural polysaccharide isolated from Cassia tora seeds. *Integrated Medicine Research*, 3(2), 91-98. <https://doi.org/10.1016/j.imr.2014.03.002>.

- Qiao, N., Li, M., Schlindwein, W., Malek, N., Davies, A., & Trappitt, G. (2011). Pharmaceutical cocrystals: an overview. *International Journal of Pharmaceutics*, 419(1-2), 1-11. <https://doi.org/10.1016/j.ijpharm.2011.07.037>.
- Raheem Thayyil, A., Juturu, T., Nayak, S., & Kamath, S. (2020). Pharmaceutical co-crystallization: regulatory aspects, design, characterization, and applications. *Advance Pharmaceutical Bulletin*, 10(2), 203-212. <https://https://doi.org/.org/: 10.34172/apb.2020.024>.
- Reham, A.K., Yacoub, A.B., & Aly, N. (2019). Dissolution enhancement of atorvastatin calcium by co-crystallization. *Advance Pharmaceutical Bulletin*, 9(4), 559-570. <https://doi.org/10.15171/apb.2019.064>.
- Sujitha, V., Sayani, B., & Geetha, T. (2014). Preparation and evaluation of orally disintegrating taste masking tablet of paracetamol with Kollicoat Smart Seal 30 D. *Der Pharmacia Lettre*, 6 (2), 82-89.
- Yu, J., Petrie, I.D., & Levy, R.H. (2019). Ragueneau-Majlessi I. mechanisms and clinical significance of pharmacokinetic-based drug-drug interactions with drugs approved by the U.S. Food and Drug Administration in 2017. *Drug Metabolism and Disposition*, 47(2), 135-144. <https://doi.org/10.1124/dmd.118.084905>.

# N-Alkylation of Some Imidazopyridines

Fatima DOGANÇ\*, Hakan GOKER\*\*

## N-Alkylation of Some Imidazopyridines

### SUMMARY

6-Bromo-2-(4-(4-fluorophenoxy)phenyl)-4H-imidazo[4,5-b]pyridine (I) and 2-[4-(4-fluorophenoxy)phenyl]-5H-imidazo[4,5-c]pyridine (III) were prepared by the reaction of 5-bromo-2,3-diaminopyridine and 3,4-diaminopyridine with sodyum metabisulfite adduct of 4-(4-fluorophenoxy)benzaldehyde (1), respectively. Alkylation of these compounds with 1-(chloromethyl)-4-methoxybenzene under basic conditions (K<sub>2</sub>CO<sub>3</sub> in DMF) was formed as mainly N<sub>4</sub> regioisomer (II) and N<sub>5</sub> regioisomer (IV). Their regioisomeric structures were assigned with 2D-NOESY (Nuclear Overhauser Effect Spectroscopy) spectra.

**Key Words:** Imidazopyridines, NOESY, regioisomers

## Bazı İmidazopiridinlerin N-Alkilyasyonu

### ÖZ

5-Bromo-2,3-diaminopiridin ve 3,4-diaminopiridin, 4-(4-florofenoksi)benzaldehitin (1) sodyum metabisülfid tuzuyla ile reaksiyona sokulmasıyla sırasıyla 6-bromo-2-(4-(4-florofenoksi)fenil)-4H-imidazo[4,5-b]piridin (I) ve 2-[4-(4-florofenoksi)fenil]-5H-imidazo[4,5-c]piridin (III) bileşikleri elde edildi. Bu bileşiklerin 1-(klorometil)-4-metoksibenzen ile bazik koşullar altında (DMF içinde K<sub>2</sub>CO<sub>3</sub>) alkilasyonu esas olarak N<sub>4</sub> regioizomeri (II) ve N<sub>5</sub> regioizomeri (IV) oluştu. Regioizomerik yapıları 2D-NOESY (Nükleer Overhauser Etki Spektroskopisi) spektrumları ile belirlendi.

**Anahtar Kelimeler:** İmidazopiridin, NOESY, regioizomer

Received: 01.11.2024

Revised: 12.11.2024

Accepted: 26.11.2024

\* ORCID: 0000-0002-1832-587X: Department of Pharmaceutical Chemistry, Faculty of Pharmacy, Ankara University, Ankara, Türkiye.

\*\* ORCID: 0000-0002-9366-6949: Department of Pharmaceutical Chemistry, Faculty of Pharmacy, Ankara University, Ankara, Türkiye.

## INTRODUCTION

Imidazopyridines, one of the most common heterocycles, are primarily used in medicinal chemistry, since they have potent several biological activities. The pharmacological profiles of imidazopyridines have been mentioned in many literatures, such as antibacterial, anti-inflammatory, antipyretic, analgesic, antiapoptotic, antitumor, antifungal, hypnotic, antiviral, and antiprotozoal agents (Dyminska, 2015;

Krause et al., 2017; Volpi, et al., 2024). Imidazopyridine scaffolds are formed by condensing imidazole and pyridine rings. In these condensed systems, the nitrogen bears a hydrogen atom ( $N^{1,3}$ ) as a pyrrole-like N-atom; the others ( $N^{4,5}$ ) resembles a pyridine-like N-atom. Hydrogen atom attached to nitrogen in the 1, 3, 4 and 5<sup>th</sup> position readily tautomerise in several positions depicted in Figure 1.

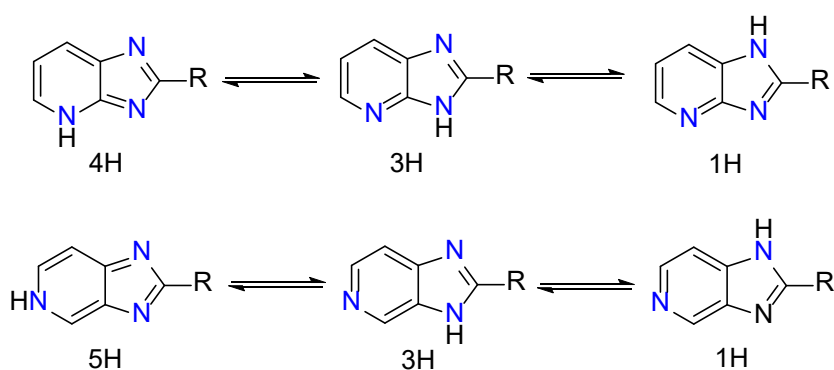


**Figure 1.** Tautomeric forms of imidazo[4,5-*b*]pyridine and imidazo[4,5-*c*]pyridine moieties

These relocations are entirely lost when the mobile hydrogen in imidazopyridines is replaced by any alkyl groups.

In our recently published papers, we have characterized the occurrence and structures of various regioisomers of imidazopyrimidines, imidazopyridines, imidazopyrazines, benzimidazoles and indazoles (Göker and Özden, 2019; Doganc et al., 2020; Karaaslan et al., 2020; Puskullu et al., 2021; Doganc and Göker, 2024). For this purpose, we used advanced 2D-NMR techniques for the structural elucidation. In continuation of these works, we now report, *N*-alkylation reaction of some imidazopyridines with 4-methoxybenzyl chloride, for investigation of the forming possible regioisomers. The 2D-NOESY (Nuclear Overhauser Effect Spectroscopy) technique was used for the structural elucidation.

## MATERIAL AND METHODS

Uncorrected melting points were measured on

a Büchi B-540 capillary melting point apparatus.  $^1\text{H}$  (500 MHz) and  $^{13}\text{C}$  (125 MHz) NMR spectra were recorded employing BRUKER AVANCE NEO 500 MHz FT spectrometer, chemical shifts ( $\delta$ ) are in ppm relative to TMS. The samples (5-10 mg) were prepared in 0.75 ml of  $\text{DMSO-}d_6$ . The liquid chromatography mass spectrometry (LC-MS) spectra were taken on a Waters Micromass ZQ connected with Waters Alliance HPLC (Waters Corporation), using the ESI (+) method with a C-18 column (XTerra<sup>®</sup>, 4.6 X 250 mm, 5  $\mu\text{m}$ ).

### Synthesis of sodium metabisulfite adduct of 4-(4-fluorophenoxy)benzaldehyde (1)

4-(4-Fluorophenoxy)benzaldehyde (30 mmol) was dissolved in EtOH (100 ml) and sodium metabisulfite (3.2 g) (in 5 ml of water) was added in portions. The reaction mixture was stirred vigorously. The mixture was kept in a refrigerator for a while. The precipitate was gained by filtration, dried and used for the further steps without purification and characterisation.

### General Synthesis of I and III

The mixture of related *o*-pyridine-diamine derivatives (1 mmol) and Na<sub>2</sub>S<sub>2</sub>O<sub>5</sub> adduct of 4-(4-fluorophenoxy)benzaldehyde (1 mmol) in DMF (0.5 ml) were heated at 130°C, for 4 h. The reaction mixture was cooled, poured into water. The resulting precipitate was collected by filtration washed with water and dried. The resulting precipitate was crystallized from EtOH.

#### 6 - B r o m o - 2 - ( 4 - ( 4 - f l u o r o p h e n o x y ) p h e n y l ) - 4 H - i m i d a z o [ 4 , 5 - b ] p y r i d i n e ( I )

Prepared from 5-bromopyridine-2,3-diamine (0.188 g) and Na<sub>2</sub>S<sub>2</sub>O<sub>5</sub> adduct of 4-(4-fluoro-phenoxy)benzaldehyde (0.320 g) as described in the general method. It was triturated with hot EtOH. Yield 0.286 g, 75%, m.p. = 310-312°C. <sup>1</sup>H-NMR δ ppm (DMSO-*d*<sub>6</sub>+one drop of TFA) : 7.18-7.19 (m, 4H), 7.23-7.26 (m, 2H), 8.24 (d, 2H, *J*=8.95 Hz), 8.49 (d, 1H, *J*=2 Hz), 8.64 (d, 1H, *J*=2Hz) ; <sup>13</sup>C-NMR δ ppm (DMSO-*d*<sub>6</sub> + one drop of TFA) : 162.35, 159.6 (d, *J*=240 Hz), 152.8, 150.9 (d, *J*=2.5 Hz), 146.29, 146.21, 130.8, 128.6, 125.9, 122.5 (d, *J*=8.7 Hz), 118.0, 117.2 (d, *J*=23 Hz), 115.5. MS (ESI+) *m/z* : 384 (M+H, 100%), 386 (M+H+2, 98%), C<sub>18</sub>H<sub>11</sub>BrFN<sub>3</sub>O.

#### 2 - [ 4 - ( 4 - f l u o r o p h e n o x y ) p h e n y l ] - 5 H - i m i d a z o [ 4 , 5 - c ] p y r i d i n e ( I I I )

Prepared from pyridine-3,4-diamine (0.109 g) and Na<sub>2</sub>S<sub>2</sub>O<sub>5</sub> adduct of 4-(4-fluoro-phenoxy)benzaldehyde (0.320 g) as described in the general method. It was triturated with hot EtOH. Yield 0.12 g, 39%, m.p. = 263-266°C. <sup>1</sup>H-NMR δ ppm (DMSO-*d*<sub>6</sub>+one drop of TFA) : 7.16-7.22 (m, 4H), 7.26-7.29 (m, 2H), 8.11 (d, 1H, *J*=6.45 Hz), 8.29 (d, 2H, *J*=8.9 Hz), 8.58 (d, 1H, *J*=6.55 Hz), 9.40 (s, 1H) ; <sup>13</sup>C-NMR δ ppm (DMSO-*d*<sub>6</sub> + one drop of TFA) : 161.3, 159.4 (d, *J*=239 Hz), 158.9, 151.4 (d, *J*=2 Hz), 147.5, 139.3, 133.7, 132.5, 130.4, 122.6, 122.4 (d, *J*=8.44 Hz), 118.8, 117.2 (d, *J*=23.2 Hz), 115.15. MS (ESI+) *m/z* : 306 (M+H, 100%), C<sub>18</sub>H<sub>12</sub>FN<sub>3</sub>O.

### General Synthesis of II and IV

K<sub>2</sub>CO<sub>3</sub> (1 mmol, 0.138 g) was added to a sus-

pension of the I or III (0.5 mmol) in DMF (0.7 ml) and stirred. One hour later, 1-(chloromethyl)-4-methoxybenzene (0.6 mmol, 0.094 g) was added. After overnight stirring at room temperature, water was added and precipitate was filtered.

#### 6 - B r o m o - 2 - ( 4 - ( 4 - f l u o r o p h e n o x y ) p h e n y l ) - 4 - ( 4 - m e t h o x y b e n z y l ) - 4 H - i m i d a z o [ 4 , 5 - b ] p y r i d i n e ( I I )

Prepared from I (0.192 g), 1-(chloromethyl)-4-methoxybenzene and K<sub>2</sub>CO<sub>3</sub> as described in the general method. The crude product was crystallised from EtOH. Yield 0.181 g, 72%, m.p. = 202-204°C. <sup>1</sup>H-NMR δ ppm (DMSO-*d*<sub>6</sub>): 3.70 (s, 3H, -OCH<sub>3</sub>), 5.78 (s, 2H, benzylic -CH<sub>2</sub>), 6.92 (d, 2H, *J*=8.65 Hz, H-3''',5'''), 7.09 (d, 2H, *J*=8.75 Hz, H-3',5'), 7.17-7.19 (m, 2H, H-2'',6''), 7.27-7.30 (m, 2H, H-3'',5''), 7.61 (d, 2H, *J*=8.65 Hz, H-2''',6'''), 8.36 (d, 1H, *J*=1.45 Hz, H-7), 8.40 (d, 2H, *J*=8.75 Hz, H-2',6'), 8.65 (d, 1H, *J*=1.4 Hz, H-5) ; COSY : [H-2',6' / H-3',5'], [H-2'',6'' / H-3'',5''], [H-2''',6''' / H-3''',5'''] ; NOESY : [N-CH<sub>2</sub> / H-5 & H-2''',6'''], [-OCH<sub>3</sub> / H-3''',5'''] ; <sup>13</sup>C-NMR & HSQC δ ppm (DMSO-*d*<sub>6</sub>) : 169.6, 159.9, 159.55, 159.0 (d, *J*=239 Hz, C-4''), 153.55, 152.3 (d, *J*=2 Hz, C-1''), 146.5, 130.93 (C-5H), 130.86 (C-2''',6'''), 130.3 (C-2',6'H), 129.7 (C-7H), 129.6, 127.9, 121.9 (d, *J*=7.5 Hz, C-2'',6''H), 118.1 (C-3',5'H), 117.2 (d, *J*=22.5 Hz, C-3'',5''H), 114.6 (C-3''',5''H), 105.8, 56.2 (benzylic -CH<sub>2</sub>), 55.6 (-OCH<sub>3</sub>). MS (ESI+) *m/z* : 504 (M+H, 100%), 506 (M+H+2, 98%), C<sub>26</sub>H<sub>19</sub>BrFN<sub>3</sub>O<sub>2</sub>.

#### 2 - ( 4 - ( 4 - F l u o r o p h e n o x y ) p h e n y l ) - 5 - ( 4 - m e t h o x y b e n z y l ) - 5 H - i m i d a z o [ 4 , 5 - c ] p y r i d i n e ( I V )

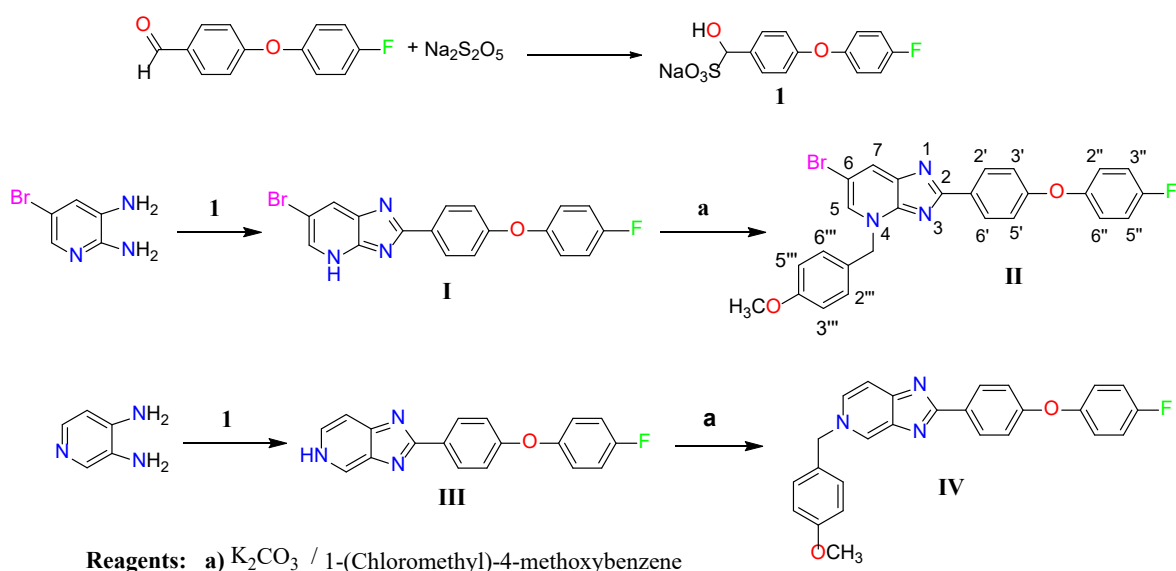
Prepared from III (0.153 g), 1-(chloromethyl)-4-methoxybenzene and K<sub>2</sub>CO<sub>3</sub> as described in the general method. The crude product was crystallized from EtOAc : *n*-Hexane. Yield 0.11 g, 52 %, m.p. = 196-198°C. <sup>1</sup>H-NMR δ ppm (DMSO-*d*<sub>6</sub>): 3.73 (s, 3H, -OCH<sub>3</sub>), 5.56 (s, 2H, benzylic -CH<sub>2</sub>), 6.95 (d, 2H, *J*=8.7 Hz, H-3''',5'''), 7.05 (d, 2H, *J*=8.85 Hz, H-3',5'), 7.15-7.17 (m, 2H, H-2'',6''), 7.25-7.28 (m, 2H, H-3'',5''), 7.46 (d, 2H, *J*=8.65 Hz, H-2''',6'''), 7.69 (d, 1H, *J*=6.75 Hz, H-7), 8.16 (dd, 1H, *J*=6.75 & 1.4 Hz, H-6), 8.36

(d, 2H,  $J=8.7$  Hz, H-2',6'), 9.06 (s, 1H, H-4); **COSY**: [H-6 / H-7], [H-2',6' / H-3',5'], [H-2'',6'' / H-3'',5''], [H-2''',6''' / H-3''',5''']; **NOESY**: [N-CH<sub>2</sub> / H-4 & H-6 & H-2'',6''], [-OCH<sub>3</sub> / H-3'',5'']; **<sup>13</sup>C-NMR & HSQC**  $\delta$  ppm (DMSO-*d*<sub>6</sub>): 171.2, 159.9, 158.94 (d,  $J=239$  Hz, C-4'), 158.87, 156.2, 152.5 (d,  $J=2$  Hz, C-1''), 145.9, 131.3 (C-4H), 131.1 (C-6H), 130.6, 130.2 (C-2'',6''H), 129.9 (C-2',6'H), 128.9, 121.7 (d,  $J=8.6$  Hz, C-2'',6''H), 118.0 (C-3',5'H), 117.1 (d,  $J=23.1$  Hz, C-3'',5''H), 114.8 (C-3'',5''H), 112.55 (C-7H), 61.2 (benzylic -CH<sub>2</sub>), 55.6 (-OCH<sub>3</sub>). **MS** (ESI+)  $m/z$ : 426 (M+H, 100%), C<sub>26</sub>H<sub>20</sub>FN<sub>3</sub>O<sub>2</sub>.

## RESULTS AND DISCUSSION

Targeted compounds were prepared using the methods outlined in Scheme 1. Cyclization of 5-bromo-2,3-diaminopyridine and 3,4-diaminopyridine with sodium metabisulfite adduct of 4-(4-fluorophenoxy)benzaldehyde (**1**) gave required imidazo[4,5-*b*]pyridines (**I**) and imidazo[4,5-*c*]pyridines (**III**), respectively. This group exhibits rapid prototropic tautomerism, resulting in equilibrium mixtures. Due to these tautomeric forms (Figure 1.) both <sup>1</sup>H and <sup>13</sup>C-NMR spectra of unsubstituted analogues (**I** and **III**) may not be sufficiently clear. It is typical for some proton and carbon signals to appear as broad peaks

and even certain hinge carbon signals may be undetectable. To address this, we utilized trifluoroacetic acid for running proton and carbon NMR spectra. The removal of the NH proton and subsequent substitution of this nitrogen atom would inhibit rapid tautomerism, leading to a separable mixture of regioisomers. When we have attempted alkylation of **I** and **III** with 1-(chloromethyl)-4-methoxybenzene under basic conditions (K<sub>2</sub>CO<sub>3</sub>, DMF), alkylation were formed as only *N*<sup>4</sup> (**II**) and *N*<sup>5</sup> (**IV**) position. Interestingly, we have never detected other possible regioisomers. The characterization of the individual isomeric products was achieved by observing the 2D-NOESY enhancements between the *N*-CH<sub>2</sub> and pyridine aromatic protons. As it is well known, NOESY is a valuable 2D NMR technique for identifying signals of protons in close spatial proximity (4-5 Å in distance) even if they are not directly bonded. In the NOESY spectrum of compound **II**, strong correlations have been observed between the benzylic and H-5 protons (Figure 2.). This finding showed us that, the synthesized final targeted compound **II** is the *N*<sup>4</sup> regioisomer form. Similarly, very strong NOE enhancements were seen between *N*-CH<sub>2</sub> and H-4,6 in the NOESY spectra of **IV** (Figure 3.).



**Scheme 1.** Synthesis of targeted compounds

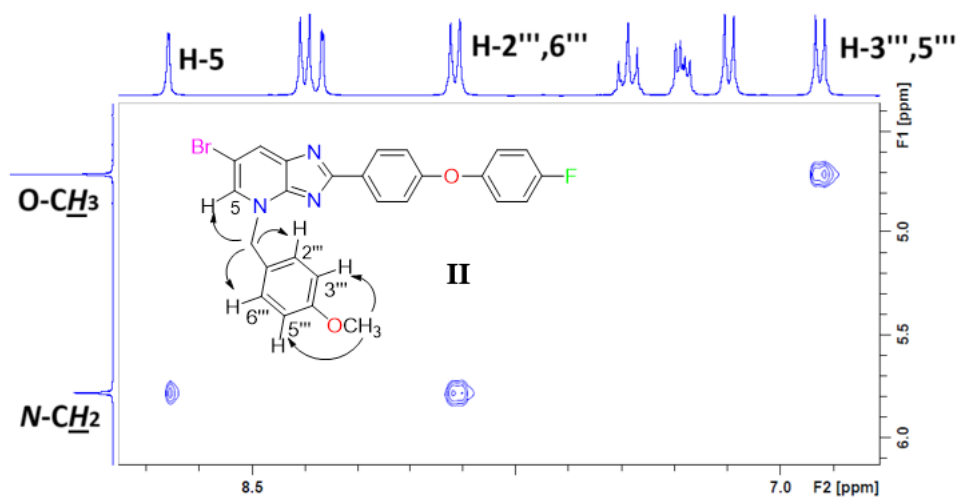


Figure 2. Partial NOESY spectrum of compound II

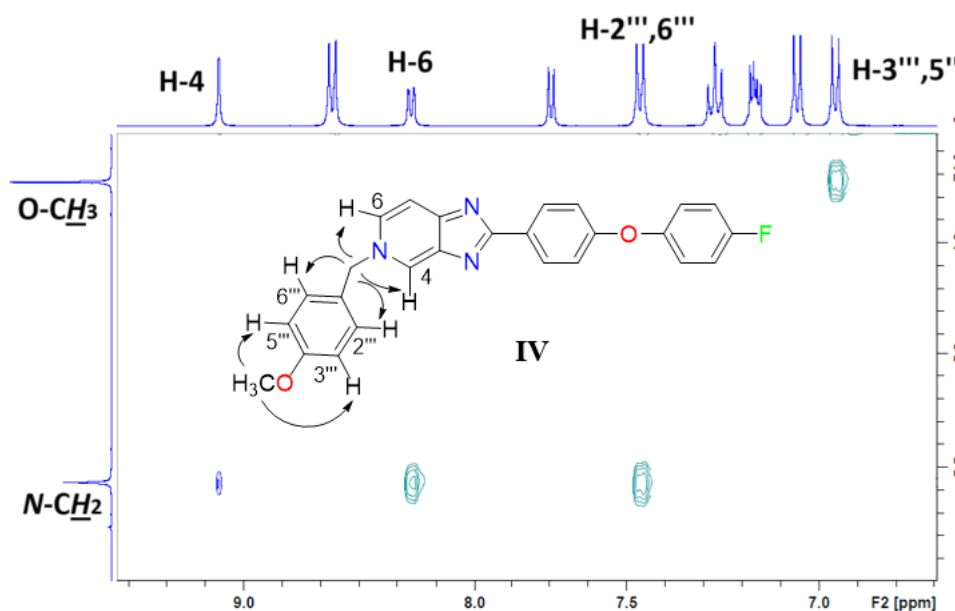


Figure 3. Partial NOESY spectrum of compound IV

## CONCLUSION

*N*-alkylation of 4*H*-imidazo[4,5-*b*]pyridines and 5*H*-imidazo[4,5-*c*]pyridines were mainly realized on the nitrogen atoms of pyridine ring, in the presence of anhydrous  $K_2CO_3$  in DMF with 4-methoxybenzyl chloride. 2D-NOESY experiment is the best method for structural elucidation of these types of regioisomers. The structure elucidation of synthesized compounds were performed using 1D and 2D NMR experiments including COSY, NOESY, gHSQC.

## ACKNOWLEDGEMENTS

Central Laboratory of Pharmacy, Faculty of Ankara University provided support for acquisition of NMR and mass spectrometer used in this work.

## AUTHOR CONTRIBUTION STATEMENT

Fatima Doganc and Hakan Goker were responsible for conducting developing the hypothesis, literature research, performing experiments, preparing and reviewing manuscript.

### CONFLICT OF INTEREST

The authors declare that there is no conflict of interest.

### REFERENCES

- Doganc, F., Aydin, A. S., Şahin, E., Göker, H. (2020). Regioselective *N*-alkylation of some 2 or 6-chlorinated purine analogues. *Journal of Molecular Structure*, 1272, 134200. doi : 10.1016/j.molstruc.2022.134200
- Doganc, F., Göker, H. (2024). Differentiation of regioisomeric *N*-alkylation of some indazoles and pyrazolopyridines by advanced NMR techniques. *Magnetic Resonance in Chemistry*, 62, 765-774. doi : 10.1002/mrc.5471
- Dyminska, L. (2015). Imidazopyridines as a source of biological activity and their pharmacological potentials infrared and raman spectroscopic evidence of their content in pharmaceuticals and plant materials. *Bioorganic & Medicinal Chemistry*, 23, 6087-6099. doi : 10.1016/j.bmc.2015.07.045
- Göker, H., Özden, S. (2019). Regioselective *N*-alkylation of 2-(3,4-dimethoxyphenyl)imidazo[4,5-*b*] and [4,5-*c*]pyridine oxide derivatives: Synthesis and structure elucidation by NMR. *Journal of Molecular Structure*, 1197, 183-195. doi : 10.1016/j.molstruc.2019.07.058
- Karaaslan, C., Doganc, F., Alp, M., Koc, A., Karabay, A. Z., Göker, H. (2020). Regioselective *N*-alkylation of some imidazole-containing heterocycles and their *in vitro* anticancer evaluation. *Journal of Molecular Structure*, 1205, 127673. doi : 10.1016/j.molstruc.2019.127673
- Krause, M., Foks, H., Gobis, K. (2017). Pharmacological potential and synthetic approaches of imidazo[4,5-*b*]pyridine and imidazo[4,5-*c*]pyridine derivatives. *Molecules* 22, 399. doi : 10.3390/molecules22030399
- Puskullu, M. O., Doganc, F., Ozden, S., Sahin, E., Celik, I., Göker, H. (2021). Synthesis, NMR, X-ray crystallography and DFT studies of some regioisomers possessing imidazole heterocycles. *Journal of Molecular Structure*, 1243, 130811. doi : 10.1016/j.molstruc.2021.130811
- Volpi, G., Laurenti, E., Rabezzana, R. (2024). Imidazopyridine family: Versatile and promising heterocyclic skeletons for different applications. *Molecules*, 29(11), 2668. doi : 10.3390/molecules29112668



# Some 5-HT<sub>1A</sub>, 5-HT<sub>2A</sub> and 5-HT<sub>2C</sub> Receptor Ligands as Atypical Antipsychotic: *In Silico* Pharmacological Evaluation with ADME Predictions and Molecular Docking Techniques

Harun USLU\*

*Some 5-HT<sub>1A</sub>, 5-HT<sub>2A</sub> and 5-HT<sub>2C</sub> Receptor Ligands as Atypical Antipsychotic: In Silico Pharmacological Evaluation with ADME Predictions and Molecular Docking Techniques*

*Atipik Antipsikotik Bazı 5-HT<sub>1A</sub>, 5-HT<sub>2A</sub> ve 5-HT<sub>2C</sub> Reseptör Ligandları: In Silico Farmakolojik Etkilerinin Moleküler Yerleştirme Teknikleriyle Değerlendirilmesi ve ADME Tahminleri*

## SUMMARY

Serotonin (5-HT) and its receptors are involved in various neuropsychiatric disorders, and altered serotonergic neurotransmission and interactions between the 5-HT and dopamine (DA) systems contribute to the pathophysiology of psychotic disorders. Interactions with 5-HT receptors may contribute to the elucidation of the properties of modern antipsychotic drugs, whose long-term effects on 5-HT receptors have not yet been adequately evaluated. Many people in society show at least one of the symptoms of psychotic disorder, and the mortality rate is twice as high as that of a healthy person. In this study, we revealed the molecular docking results of some drug molecules defined as atypical antipsychotics on 5-HT<sub>1A</sub>, 5-HT<sub>2A</sub>, and 5-HT<sub>2C</sub>. We aimed to contribute to the development of new compounds that may be useful in the treatment of psychotic disorders by trying to demonstrate the relationship between their computational inhibitory activities and their structural properties. Docking study showed that Lurasidone (e) was one drug molecule with the best docking scores on the receptors. Also, it showed that Risperidone (h), Paliperidone (f), and Brexpiprazole (b) were one drug molecules with the best pose on the receptors. Considering ADME predictions, all drug molecules (a-j) had good pharmacokinetic profiles, but Lurasidone was found to have some disadvantages. It seems that the use of Paliperidone and Risperidone may be more valuable, especially in the treatment of psychotic patients such as schizophrenia.

**Key Words:** Atypical antipsychotics, molecular docking, ADME predictions, 5-HT<sub>1A</sub>, 5-HT<sub>2A</sub>, 5-HT<sub>2C</sub>

## ÖZ

Serotonin (5-HT) ve reseptörleri çeşitli nöropsikiyatrik bozukluklarda rol oynamakta ve 5-HT ile dopamin (DA) sistemleri arasındaki değişen serotoninerjik nörotransmisyon ve etkileşimler, psikotik bozuklukların patofizyolojisine katkıda bulunmaktadır. 5-HT Reseptörleriyle etkileşimlerin araştırılması, 5-HT reseptörleri üzerindeki uzun vadeli etkileri henüz yeterince değerlendirilmemiş olan modern antipsikotik ilaçların özelliklerinin aydınlatılmasına katkıda bulunabilir. Toplumda psikotik bozukluk semptomlarından en az birini gösteren çok sayıda kişi vardır ve ölüm oranı sağlıklı bir kişiye göre iki kat daha yüksektir. Bu çalışmada, atipik antipsikotik olarak tanımlanan bazı ilaç moleküllerinin 5-HT<sub>1A</sub>, 5-HT<sub>2A</sub> ve 5-HT<sub>2C</sub> üzerindeki moleküler yerleştirme sonuçlarını ortaya koyduk. Hesaplamalı inhibe edici aktiviteleri ile yapısal özellikleri arasındaki ilişkiyi ortaya koymaya çalışarak psikotik bozuklukların tedavisinde yararlı olabilecek yeni bileşiklerin geliştirilmesine katkıda bulunmayı amaçladık. Yerleştirme çalışması, Lurasidon'un (e) reseptörler üzerinde en iyi yerleştirme skorlarına sahip ilaç moleküllerinden biri olduğunu gösterdi. Ayrıca, Risperidon (h), Paliperidon (f) ve Brexpiprazol'ün (b) reseptörler üzerinde en iyi poza sahip ilaç moleküllerinden biri olduğunu gösterdi. ADME tahminleri göz önüne alındığında, tüm ilaç moleküllerinin (a-j) iyi farmakokinetik profilleri vardı, ancak Lurasidon'un bazı dezavantajları olduğu bulundu. Paliperidon ve Risperidon kullanımının, özellikle şizofreni gibi psikotik hastaların tedavisinde daha değerli olabileceği anlaşılmaktadır.

**Anahtar Kelimeler:** Atipik antipsikotikler, moleküler yerleştirme, ADME tahminleri, 5-HT<sub>1A</sub>, 5-HT<sub>2A</sub>, 5-HT<sub>2C</sub>

Received: 26.09.2024

Revised: 12.11.2024

Accepted: 28.11.2024

\* ORCID: 0000-0001-8827-8557, Department of Pharmaceutical Chemistry, Faculty of Pharmacy, Firat University, Elazığ, Türkiye

## INTRODUCTION

Serotonin (5-hydroxytryptamine) has been found to play a substantial role in many basic physiological and pathophysiological processes, including mood and emotions, aggression and anxiety, circadian rhythms, sleep regulation, sexual behavior, memory and learning processes, thalamic blood pressure and nociception (Barnes & Sharp, 1999; Fiorino et al., 2017). 5-hydroxytryptamine (5-HT), one of the oldest known neurotransmitters, plays a role in the etiology of numerous disease states such as depression, anxiety, schizophrenia, social phobia, obsessive-compulsive disorder, and panic disorder; as well as hypertension, migraine, eating disorders, vomiting and irritable bowel syndrome (Hoyer, Hannon, & Martin, 2002). It is observed that the mortality rate of people with psychotic disorders is twice as high as that of healthy people, and the average life expectancy is 20 years less. Although these symptoms are observed at a rate of 3% in society, the rate of people showing at least one of the disorder's symptoms are relatively high in the general population (Moreno et al., 2013; Nuevo et al., 2012).

5-HT<sub>1A</sub>, the first 5-HT receptor to be fully elucidated, is found in the body, mainly around the brain, particularly in the hippocampus and cortical areas. At the cellular level, *in situ* hybridization and immunocytochemical studies also demonstrate the presence of 5-HT<sub>1A</sub> at receptors in pyramidal and granular neurons of the hippocampus. The pharmacological effects of 5-HT<sub>1A</sub> differ from those of other 5-HT<sub>1</sub> and 5-HT receptors. The 5-HT<sub>1A</sub> receptor agonists obtained in the first years were not selective, but over the years, selective agonists began to be obtained. The 5-HT<sub>1A</sub> receptor is known to have a neurotrophic role in the young brain and possibly in adults. Recent studies have highlighted that 5-HT<sub>1A</sub> receptor antagonists facilitate the effects of 5-HT reuptake inhibitors, monoamine oxidase inhibitors, and antidepressant (some tricyclics) drugs on 5-HT release. (Azmitia, Gannon, Kheck, & Whitaker-

Azmitia, 1996; Fletcher et al., 1993; Kobilka et al., 1987; Sharp & Hjorth, 1990).

5-HT<sub>2A</sub> was initially known as the 5-HT<sub>2</sub> receptor; it was later divided into a separate classification. The human 5-HT<sub>2A</sub> receptor is located on chromosome 13q14-q21 and is highly identical to the human 5-HT<sub>2C</sub> receptor. The 5-HT<sub>2A</sub> receptor is known to have potential sites for palmitoylation, phosphorylation, and glycosylation. Several recent studies have investigated the cellular location of the 5-HT<sub>2A</sub> receptor in the brain. Studies conducted so far have found 5-HT<sub>2A</sub> immunoreactivity in neurons. 5-HT<sub>2</sub> receptor antagonists such as Ritanserin have high affinity for various 5-HT<sub>2</sub> receptors. Ketanserin and Spiperon are approximately two orders of magnitude more selective for 5-HT<sub>2B</sub> receptors than 5-HT<sub>2A</sub>, while these drugs have an affinity for other monoamine receptors. Agonist action at 5-HT<sub>2</sub> receptors has been considered to be involved in hallucinogenic mechanisms because of their proximity to 5-HT<sub>2</sub> binding sites and the close relationship between the human hallucinogenic potential of 5-HT<sub>2</sub> receptor agonists (Baxter, Kennett, Blackburn, & Blaney, 1995; Boess & Martin, 1994; Glennon, 1990).

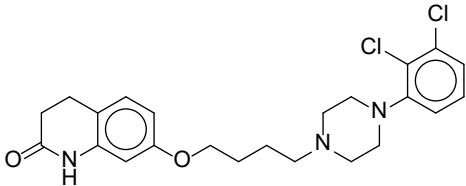
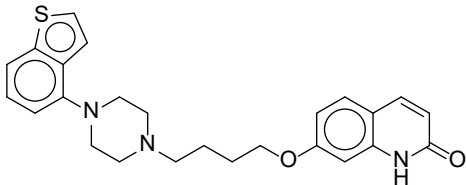
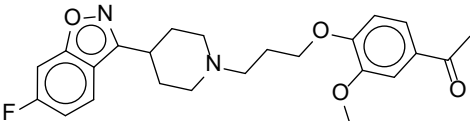
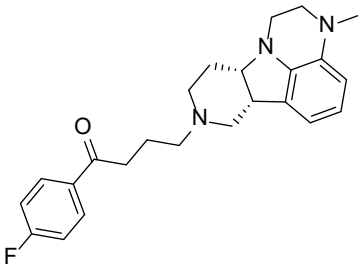
5-HT<sub>2C</sub> receptors are predominantly localized in the brain, and their dysregulation can lead to increased anxiety and depression. The fact that various psychotropic agents such as fluoxetine, clozapine, and tricyclic antidepressants have significant affinity for the 5-HT<sub>2C</sub> receptor has increased the interest in selective and high-affinity 5-HT<sub>2C</sub> receptor ligands. Recent studies have shown that 5-HT<sub>2C</sub> receptor agonists can reduce feeding when administered acutely to rats or mice and can also reduce body weight when administered to obese animals for a long time without causing tolerance. There are also reports that 5-HT<sub>2C</sub> antagonists increase the release of norepinephrine and dopamine (Bickerdike, 2003; Jenck et al., 1998; Millan, Dekeyne, & Gobert, 1998).

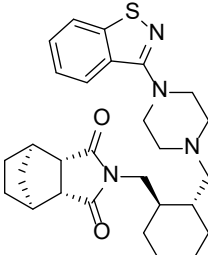
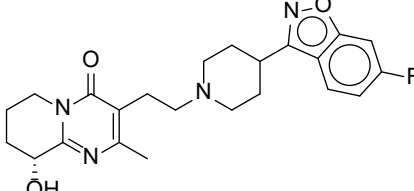
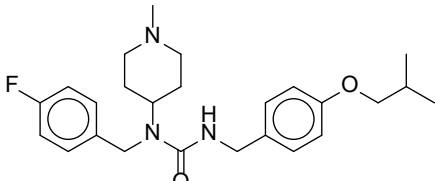
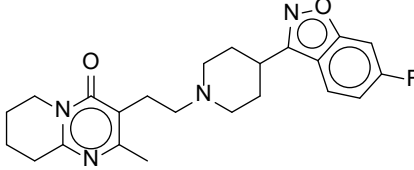
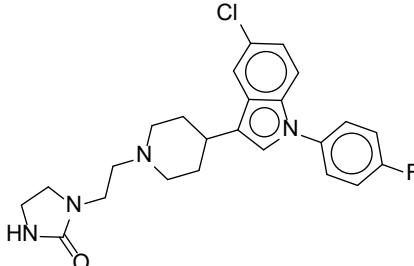
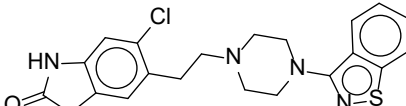
Known as a pharmacologically heterogeneous group of compounds, antipsychotics all act as D2

dopamine receptor antagonists. Atypical antipsychotic medications were developed in response to patients' failure to respond to typical psychotic problems with typical agents, including lack of effectiveness with the medications, lack of improvement in symptoms, and troublesome side effects, especially extrapyramidal symptoms. Atypical antipsychotic agents are often considered first-line agents in the treatment of schizophrenia. They are also seen as an area open to development as they are seen as agents that may be effective in other psychiatric and neurological conditions. Atypical antipsychotics are increasingly being used in the treatment of mania and depression as well as schizophrenia (Jibson & Tandon, 1998; Mackin & Thomas, 2011; Meltzer, 2013).

In this study, we revealed the molecular docking results of some drug molecules (Table 1.) characterized as atypical antipsychotic on 5-HT<sub>1A</sub>, 5-HT<sub>2A</sub>, and 5-HT<sub>2C</sub>. Since ideal pharmacokinetic properties, high pharmacological activity, and low toxicity are expected in drugs, so ADME predictions were also evaluated. In this context, the evaluation was made by comparing the molecular docking results and ADME predictions. We also aim to help reveal the relationship between their computational inhibitory activities and structural properties, contributing to the development of new compounds that may be useful in the treating of psychotic disorders.

**Table 1.** Chemical Structure of some atypical antipsychotic drug compounds

Compounds		Chemical Structure
Code	Name	
a	aripiprazole	
b	brexpiprazole	
c	iloperidone	
d	lumateperone	

e	lurasidone	
f	paliperidone	
g	pimavanserin	
h	risperidone	
i	sertindole	
j	ziprasidone	

## MATERIAL AND METHODS

### Molecular docking studies

The compounds analyzed in this study were selected with preference given to drugs that have received regulatory approval from the US Food and Drug Administration (FDA) or other regulators and have entered clinical practice globally. The chemical

structures of all selected compounds (a-j) used as ligands were carried out on a 64-bit operating system with Windows 11 Pro edition. The chemical structures of the compounds used as ligands, whose structures have been previously described in the literature (<https://pubchem.ncbi.nlm.nih.gov/>, access date: 23.09.2024), were created with the ChemDraw

2D program using their SMILES and their energy minimization was carried out with the ChemDraw 3D program. 5-HT<sub>1A</sub>, 5-HT<sub>2A</sub>, and 5-HT<sub>2C</sub> crystal structures were taken from protein data bank (Kimura et al., 2019; Peng et al., 2018; Xu et al., 2021). The grid boxes were positioned according to the previously determined regions for the active sites of the macromolecules, with dimensions of 40x40x40 Å<sup>3</sup> and a spacing of 0.375Å. The Pdb files of the macromolecules were optimized using Maestro Version 6.4.135, Release 2023-4 (Uslu et al., 2023). At least 50 runs were performed for each selected compounds while using standard settings for 5-HT<sub>1A</sub> receptor (PDB ID: 7E2Z), 5-HT<sub>2A</sub> receptor (PDB ID: 6A93), and 5-HT<sub>2C</sub> receptor (PDB ID: 6BQH). Lamarckian Genetic Algorithm was preferred in all studies; detailed results such as docking scores were obtained using both AutoDock 4.2 (Morris et al., 2009) and AutoDock Vina programs (Trott & Olson, 2010), and are presented. For docking validation, co-crystallized ligands were re-docked onto target sites of macromolecules, and RMSD values have been determined to be for existing ligand Aripiprazole (PDB ID: 9SC) as 1.88, existing ligand Risperidone (PDB ID: 8NU) as 0.79 and ligand Ritanserin (PDB ID: E2J) as 0.40, respectively for 5-HT<sub>1A</sub>, 5-HT<sub>2A</sub> and 5-HT<sub>2C</sub> (Table 2-4).

#### ADME predictions

The SwissADME online tool was used to calculate the pharmacokinetic and physicochemical properties of some selected atypical antipsychotic ligands (a-j) and compare the results (Table 5-6.) (<http://www.swissadme.ch/>, access date: 23.09.2024) (Daina, Michielin, & Zoete, 2014, 2017; Daina & Zoete, 2016).

## RESULT AND DISCUSSION

### Molecular docking studies

The interaction domain of 5-HT<sub>1A</sub> was determined previously. Weak hydrogen bonding with PHE362 and the chlorine attached to the 3rd position of the phenyl ring of Aripiprazole and van der Waals interaction with the phenyl ring were observed. A weak polar bond was observed between SER199 and the chlorine attached to the 3rd position of the phenyl ring, and weak polar and van der Waals interactions were observed with the phenyl ring. It has been observed that PHE361 forms hydrogen and weak polar bonds between chlorine attached to the second position of the phenyl ring. Hydrogen bonding and van der Waals interaction were observed between CYS120 and the piperazine ring. Weak hydrogen and weak polar bonding were observed between THR121 and the phenyl ring. Van der Waals interaction, weak polar and ionic bonding was observed between ASP116 and the piperazine ring. Weak hydrogen bonding was observed between ASP116 and the methylene group. Van der Waals interactions and weak polar bonding were observed between ASN386 and methylene groups. Van der Waals interactions and weak polar bonding were observed between TYR390 and the methylene group. A weak polar bond was observed between PHE112 and the oxygen atom. Weak hydrogen bonding and van der Waals interaction were observed between TYR96 and the dihydroquinolinone ring. It was observed that ALA93, GLN97, VAL117, ILE189, THR200, ALA203 and THR379 made hydrogen bonds with the compound (Figure 1.) (<https://www.ebi.ac.uk/pdbe/entry/pdb/7e2z/bound/9SC#501R>, access date: 23.09.2024) (Xu et al., 2021).

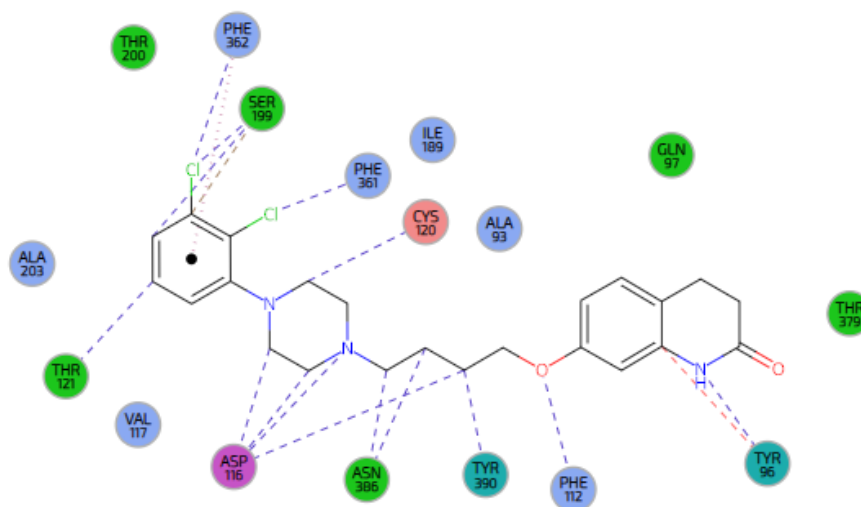


**Figure 1.** Interactions between aripiprazole (9SC) and 5-HT<sub>1A</sub> (quoted from the <https://www.ebi.ac.uk/pdbe/entry/pdb/7e2z/bound/9SC#501R>)

**Table 2.** Molecular docking scores, binding types, and estimated inhibition constants of some drug compounds on 7E2Z (5-HT<sub>1A</sub>)

Comp.	Based on Visual Results Interacting Residues			Autodock Results		Vina Results
	Hydrogen bond	Halogen Bond	Pi-Pi interaction	Estimated inhibition Constant, Ki	The best docking score	The best docking score
a	ASN386	THR379	-	117.04 nM	-9.46	-8.7
b	CYS187	-	PHE362	66.01 nM	-9.80	-9.4
c	SER199	-	PHE112 TRP387	133.98 nM	-9.38	-8.2
d	-	-	-	592.23 nM	-8.50	-7.7
e	-	-	TYR390	2.97 nM	-11.63	-10.2
f	-	-	PHE362 TRP358	42.05 nM	-10.06	-9.7
g	-	-	-	862.78 nM	-8.27	-8.8
h	-	-	PHE362	15.60 nM	-10.65	-9.4
i	ILE189	ASN386	PHE361	92.54 nM	-9.60	-9.4
j	-	-	-	125.87 nM	-9.41	-9.4

pM: picomolar, nM: nanomolar, Docking Score: Estimated Binding Free Energy (kcal/mol)

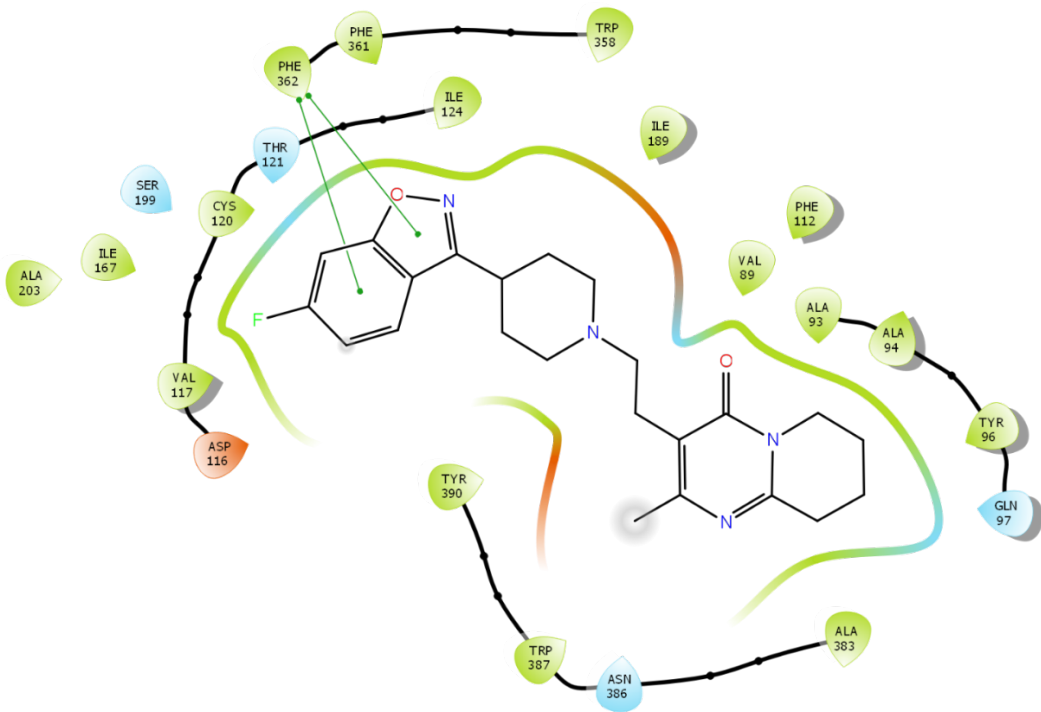


Figure 2. 2D interaction diagram with 5-HT<sub>1A</sub> (7E2Z) for Risperidone (h).

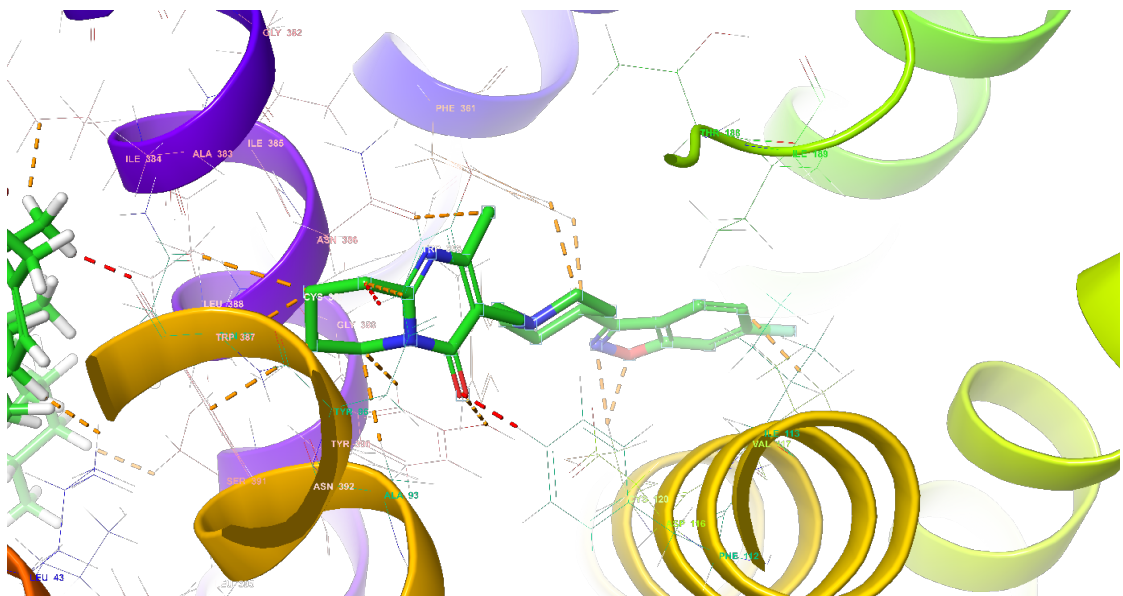
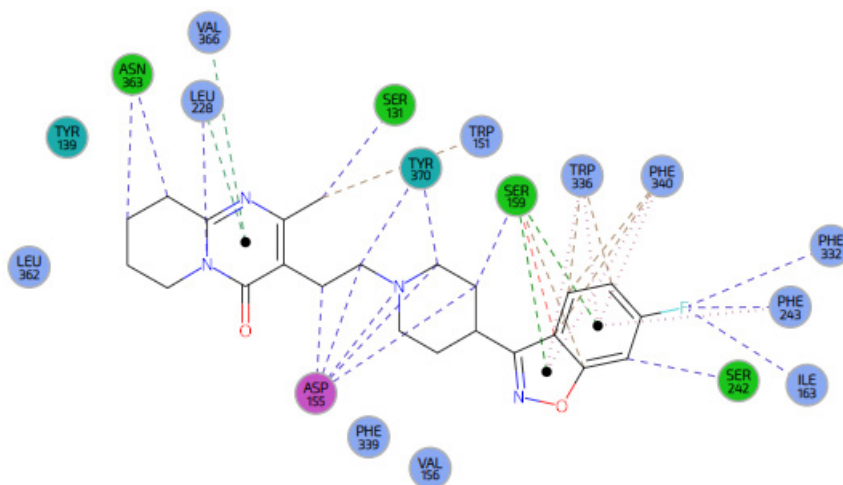


Figure 3. 3D interaction diagram with 5-HT<sub>1A</sub> (7E2Z) for Risperidone (h).

When the docking poses of Risperidone (**h**) were examined, it was seen that it had interaction such as pi-pi interaction. The pi-pi interactions were detected in the benzothiophene ring of Brexpiprazole (**b**) and PHE362 (Figure 2-3.). In this study, it was determined that Risperidone (**h**) with these residues of 5-HT<sub>1A</sub> in a similar way. All these interactions enabled Risperidone (**h**) to bind strongly to the active site, explaining why it exhibited a more robust inhibition profile (Table 2.).

The interaction domain of 5-HT<sub>2A</sub> was determined previously. One weak polar bond and one carbon- $\pi$  bond were observed between LEU228 and the pyrimidine ring. A carbon- $\pi$  bond was observed between VAL366 and the pyrimidine ring. Weak polar bond and van der Waals interaction were observed between SER131 and the methyl ring attached to pyrimidine. Van der Waals interaction was observed between TRP151 and the methyl ring attached to pyrimidine. Van der Waals interaction, weak hydrogen bond, and weak polar bond were observed between ASN363 and the tetrahydropyridine ring. A weak hydrogen bond was observed between TYR370 and the methylene group, and a weak polar bond was observed with the piperidine ring. One

weak polar bond and one van der Waals interaction were observed between ASP155 and methylene groups. Ionic bond, weak polar bond, and van der Waals interaction were observed between ASP155 and the pyrimidine ring. A weak polar bond was observed between SER159 and the pyrimidine ring. Two van der Waals interactions and two carbon- $\pi$  bonds were observed between SER159 and the benzoxazole ring. An aromatic hydrogen bond and a van der Waals interaction were observed between TRP336 and the benzoxazole ring. An aromatic hydrogen bond and a van der Waals interaction were observed between PHE340 and the benzoxazole ring. A weak polar bond was observed between PHE332 and the fluorine attached to the benzoxazole ring. A weak polar bond was observed between PHE243 and the fluorine attached to the benzoxazole ring. A weak polar bond was observed between ILE163 and the fluorine attached to the benzoxazole ring. Weak hydrogen bonding was observed between SER242 and the benzoxazole ring. It was observed that TYR139, LEU362, PHE339, and VAL156 made hydrogen bonds with the compound (<https://www.ebi.ac.uk/pdbe/entry/pdb/6a93/bound/8NU#3001A>, access date: 23.09.2024) (Figure 4.) (Kimura et al., 2019).



**Figure 4.** Interactions between risperidone (8NU) and 5-HT<sub>2A</sub> (quoted from the <https://www.ebi.ac.uk/pdbe/entry/pdb/6a93/bound/8NU#3001A>)



**Table 3.** Molecular docking scores, binding types, and estimated inhibition constants of some drug compounds on 6A93 (5-HT<sub>2A</sub>)

Comp.	Based on Visual Results Interacting Residues		Autodock Results		Vina Results
	Hydrogen bond	Pi-Pi interaction	Estimated inhibition Constant, Ki	The best docking score	The best docking score
<b>a</b>	A: LEU329	A: PHE340	14.31 nM	-10.70	-10.2
<b>b</b>	A: ASN343 A: LYS223	A: PHE243 A: TRP:336 A: PHE340	2.27 nM	-11.79	-10.3
<b>c</b>	A: ASN343	A: PHE340 A: TRP336	4.86 nM	-11.34	-10.5
<b>d</b>	-	A: PHE340 A: TRP336	38.28 nM	-10.12	-10.5
<b>e</b>	-	A: PHE340 A: TRP336	202.04 pM	-13.23	-11.8
<b>f</b>	A: ASN343 A: LEU229	A: PHE243 A: TRP:336 A: PHE340	692.56 pM	-12.50	-11.8
<b>g</b>	A: ASN343	A: PHE340 A: TRP336	15.45 nM	-10.66	-9.5
<b>h</b>	A: ASN343	A: PHE340 A: TRP336	1.04 nM	-12.26	-11.8
<b>i</b>	A: CYS227	A: PHE340 A: PHE339 A: TRP336	9.91 nM	-10.92	-11.1
<b>j</b>	A: LYS223	A: PHE340 A: TRP336	5.10 nM	-11.31	-10.2

When the docking poses of Paliperidone (**f**) were examined, it was seen that it had pi-pi interactions and hydrogen bonds. The pi-pi interactions were detected in the benzoxazole ring of Paliperidone (**f**) and PHE243, TRP336, and PHE340. Also, there were H-bond interactions between the pyrimidin-4-

one and LEU229 and ASN343 (Figure 5-6.). In this study, it was determined that Paliperidone (**f**) with these residues of 5-HT<sub>2A</sub> in a similar way. All these interactions enabled Paliperidone (**f**) to bind more vital to the active site, explaining why it exhibited a more robust inhibition profile (Table 3.).

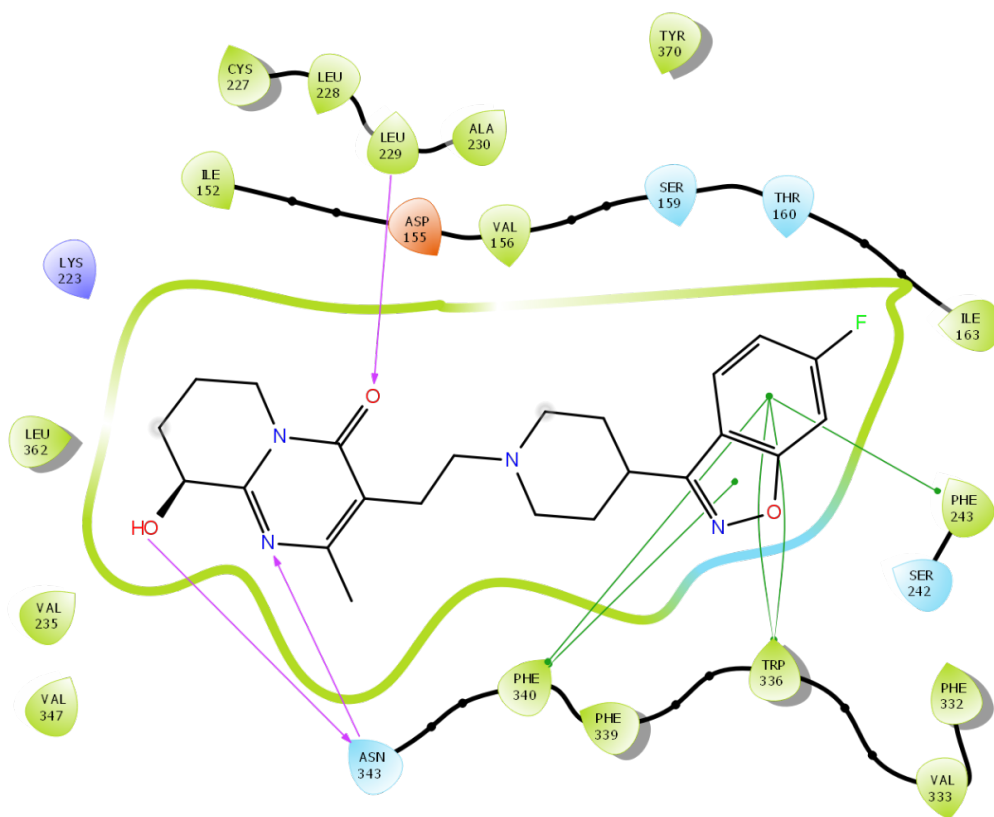


Figure 5. 2D interaction diagram with 5-HT<sub>2A</sub> (6A93) for Paliperidone (f).

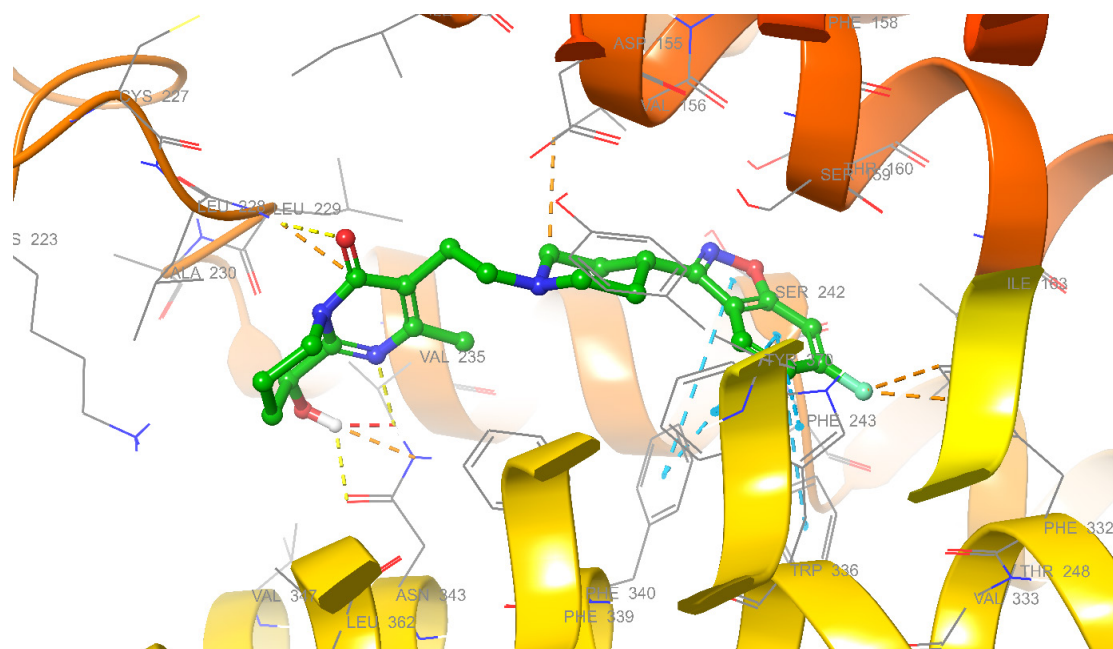
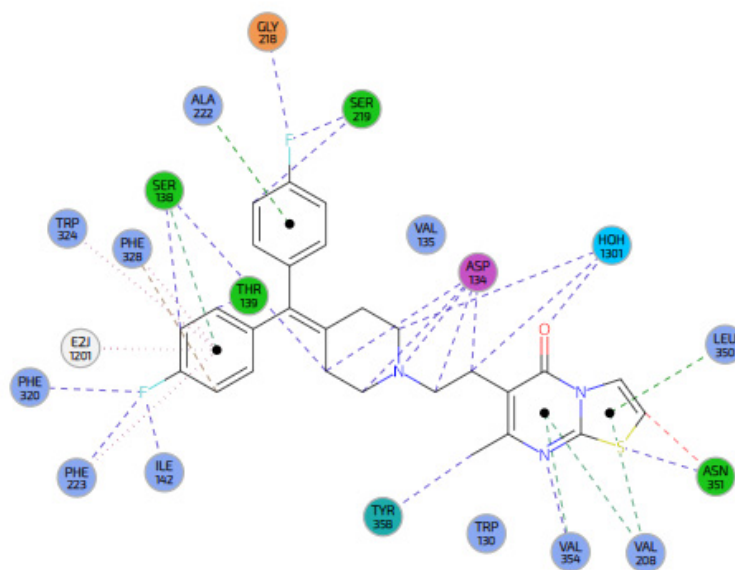


Figure 6. 3D interaction diagram with 5-HT<sub>2A</sub> (6A93) for Paliperidone (f).

The interaction domain of 5-HT<sub>2C</sub> was determined previously. A weak polar bond was observed between GLY218 and the fluorophenyl ring. A weak polar bond was observed between SER219 and the fluorophenyl ring. Weak hydrogen bonding was observed between SER219 and the fluorophenyl ring. A weak polar bond was observed between ILE142 and the fluorophenyl ring. A weak polar bond was observed between PHE223 and the fluorophenyl ring. A weak polar bond was observed between PHE320 and the fluorophenyl ring. Aromatic hydrogen bonding was observed between PHE328 and the phenyl ring. One weak polar bond and one carbon- $\pi$  bond were observed between SER138 and the phenyl ring. A weak polar bond was observed between SER138 and the piperidine ring. A weak polar bond was observed between TYR358 and the thiazolopyrimidine ring. A weak polar bond and carbon- $\pi$  bond were observed between VAL354 and the thiazolopyrimidine ring.

Two carbon- $\pi$  bonds were observed between VAL208 and the thiazolopyrimidine ring. Weak polar bonding and van der Waals interaction were observed between ASN351 and the thiazolopyrimidine ring. Weak polar bond, ionic bond, and van der Waals interaction were observed between ASP134 and the piperidine ring. Weak polar bonds and van der Waals bonds were observed between ASP134 and methylene groups. Hydrogen bonding was observed between HOH1301 and the piperidine ring, methylene group and the oxygen atom. Amiding bonds were observed between ALA222 and the fluorophenyl ring. Amiding bonds were observed between LEU350 and the thiazolopyrimidine ring. It was observed that VAL135 and TRP324 made hydrogen bonds with the compound (<https://www.ebi.ac.uk/pdbe/entry/pdb/6bqh/bound/E2J#1201A>, access date: 23.09.2024) (Figure 7.) (Peng et al., 2018).



**Figure 7.** Interactions between ritanserin (E2J) and 5-HT<sub>2C</sub> (quoted from the <https://www.ebi.ac.uk/pdbe/entry/pdb/6bqh/bound/E2J#1201A>)

**Table 4.** Molecular docking scores, binding types, and estimated inhibition constants of some drug compounds on 6BQH (5-HT<sub>2C</sub>)

Comp.	Based on Visual Results Interacting Residues			Autodock Results	Vina Results	
	Hydrogen bond	Halogen Bond	Pi-Pi interaction	Estimated inhibition Constant, Ki	The best docking score	The best docking score
<b>a</b>	LEU209	ALA222	TRP324 PHE328	51.17 nM	-9.95	-10.2
<b>b</b>	SER219	-	PHE223 TRP324 PHE328	3.88 nM	-11.48	-10.5
<b>c</b>	ASN331	-	PHE223 TRP324 PHE328	32.79 nM	-10.21	-10.8
<b>d</b>	-	-	PHE223 TRP324 PHE327 PHE328	134.18 nM	-9.38	-9.8
<b>e</b>	-	-	TRP130	204.48 pM	-13.22	-11.4
<b>f</b>	LEU209 ASN331	-	PHE223 TRP324 PHE328	7.06 nM	-11.12	-11.4
<b>g</b>	ASP134 LEU209	-	PHE223 TRP324 PHE328	51.99 nM	-9.94	-9.4
<b>h</b>	LEU209	-	PHE223 TRP324 PHE328	9.97 nM	-10.92	-11.3
<b>i</b>	LEU209	PHE214	PHE223 TRP324 PHE328	17.03 nM	-10.60	-11.4
<b>j</b>	VAL215	-	PHE223 TRP324 PHE328	11.13 nM	-10.85	-10.2

When the docking poses of Brexpiprazole (**b**) were examined, it was seen that it had pi-pi interactions and hydrogen bonds. The pi-pi interactions were detected in the benzothiophene ring of Brexpiprazole (**b**) and PHE223, TRP324, and PHE328. Also, there was a H-bond interaction between the quinolin-2-

one and SER219 (Figure 8-9.). In this study, it was determined that Brexpiprazole (**b**) with these residues of 5-HT<sub>2C</sub> in a similar way. All these interactions enabled Brexpiprazole (**b**) to bind more potent to the active site, explaining why it exhibited a more robust inhibition profile (Table 4.).

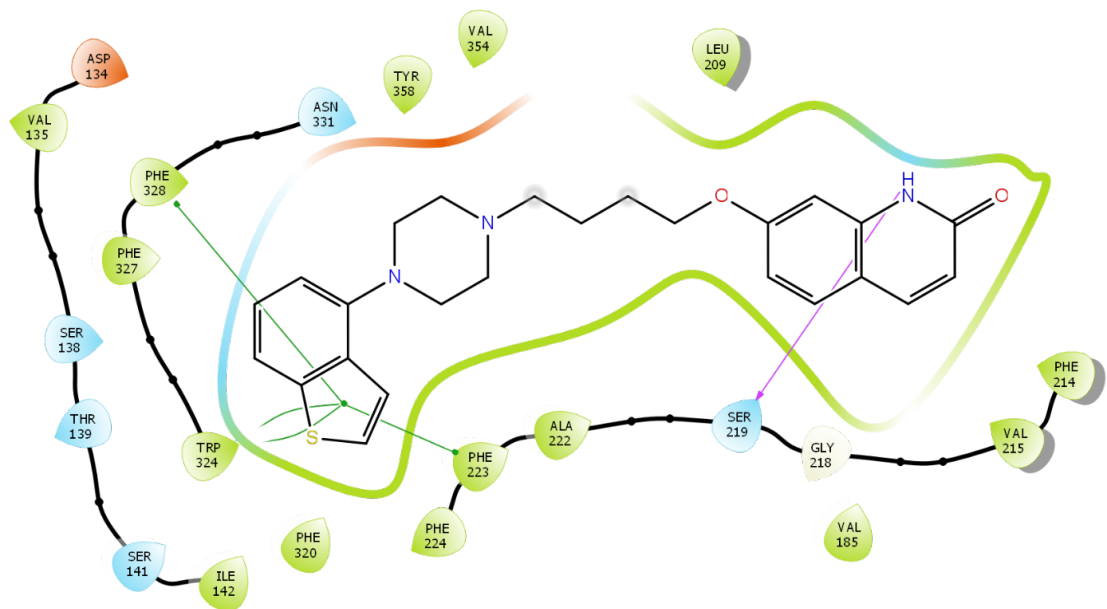


Figure 8. 2D interaction diagram with 5-HT<sub>2C</sub> (6BQH) for Brexpiprazole (b).

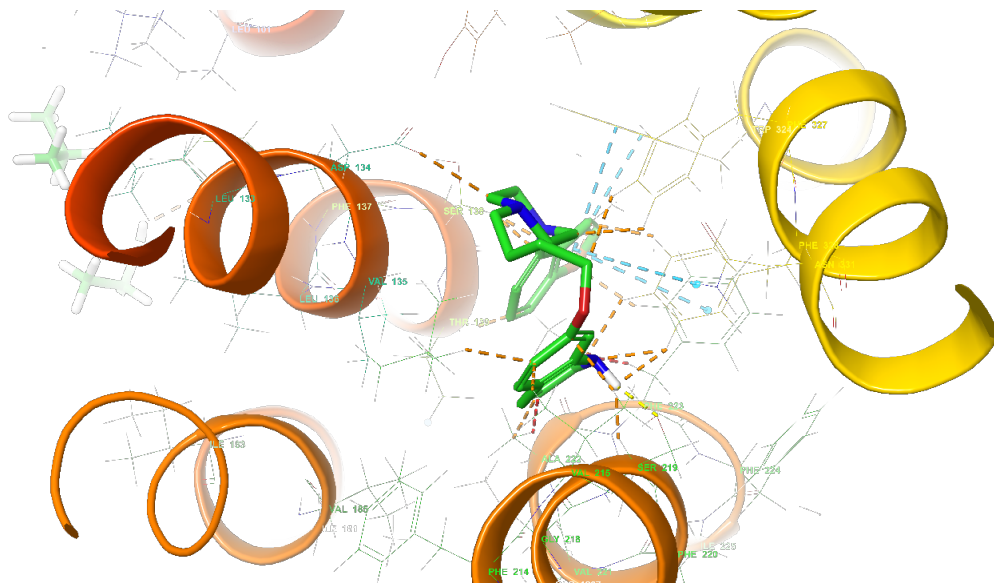


Figure 9. 3D interaction diagram with 5-HT<sub>2C</sub> (6BQH) for Brexpiprazole (b).

### ADME predictions

The software, known as SwissAdme, facilitates this process while providing some preliminary research results on turning molecules into drugs (Daina et al., 2014, 2017; Daina & Zoete, 2016). The physicochemical and pharmacokinetic properties of all synthesized compounds were evaluated appropriately to become drug candidates. Log S

values of the compounds are between -3.95 and -6.13, and their solubility is estimated to be between poorly and soluble. The F value, which indicates the oral bioavailability of the compounds, is 0.55 and is the most ideal (Table 5.). It was observed that all drug molecules were in full compliance with the Lipinski, Egan, and Veber rules. It was observed that all drug compounds except Lurasidone (e) complied

with Muegge's rules. The model that provides critically important information on passive human gastrointestinal absorption (HIA) and blood-brain barrier (BBB) permeability estimation is the Boiled Egg model from the SwissAdme software. All drug compounds are in the white region. This shows that they can pass through the gastrointestinal system. Except for compounds **e** and **f**, all other compounds

can easily cross the blood-brain barrier. This type of medicine is affect the central nervous system so this results are predictable. While the Total polar surface area (TPSA) values were found to be in the range of 26.79-84.99, the Consensus Log P (cLogP) values, which are the average of five predictions, were found to be in the range of 2.96-4.41 (Table 6., Figure 11.).

**Table 5.** Druglikeness, water solubility, and pharmacokinetic properties of some drug compounds.

Comp. Lipinski	Druglikeness				LogS	Water Solubility		Pharmacokinetics	
	Ghose	Veber	Egan	Muegge		Class	GI abs.	F	
<b>a</b>	+	-	+	+	+	-5.38	Moderately	High	0.55
<b>b</b>	+	-	+	+	+	-5.46	Moderately	High	0.55
<b>c</b>	+	+	+	+	+	-4.90	Moderately	High	0.55
<b>d</b>	+	+	+	+	+	-4.63	Moderately	High	0.55
<b>e</b>	+	-	+	+	-	-6.13	Poorly	High	0.55
<b>f</b>	+	+	+	+	+	-3.95	Soluble	High	0.55
<b>g</b>	+	+	+	+	+	-4.97	Moderately	High	0.55
<b>h</b>	+	+	+	+	+	-4.20	Moderately	High	0.55
<b>i</b>	+	-	+	+	+	-5.17	Moderately	High	0.55
<b>j</b>	+	-	+	+	+	-5.17	Moderately	High	0.55

LogS: ESOL, Class: -6 <Moderately <-4 GI abs: Gastrointestinal absorption, F: Bioavailability score.

**Table 6.** The physicochemical and lipophilicity properties of some drug compounds.

Comp.	Physicochemical Properties						Lipophilicity	
	MW	Fsp3	RB	HBA	HBD	MR	TPSA	cLogP
<b>a</b>	448.39	0.43	7	3	1	133.26	44.81	4.21
<b>b</b>	433.57	0.32	7	3	1	136.65	76.81	4.41
<b>c</b>	426.48	0.42	8	7	0	119.98	64.80	4.20
<b>d</b>	393.50	0.46	5	3	0	124.68	26.79	3.56
<b>e</b>	492.68	0.68	5	4	0	151.55	84.99	4.14
<b>f</b>	426.48	0.52	4	7	1	118.87	84.39	2.96
<b>g</b>	427.55	0.48	10	4	1	126.21	44.81	4.29
<b>h</b>	410.48	0.52	4	6	0	117.71	64.16	3.62
<b>i</b>	440.94	0.38	5	3	1	133.17	40.51	4.00
<b>j</b>	412.94	0.33	4	3	1	125.48	76.71	3.57

Comp: Compounds, MW: Molecular weight, Fsp3: Fraction Csp3, RB: Number of rotatable bonds, HBA: Number of hydrogen bond acceptors, HBD: Number of hydrogen bond donors, MR: Molar refractivity, TPSA: Total polar surface area, cLogP: Consensus Log P (average of five predictions)

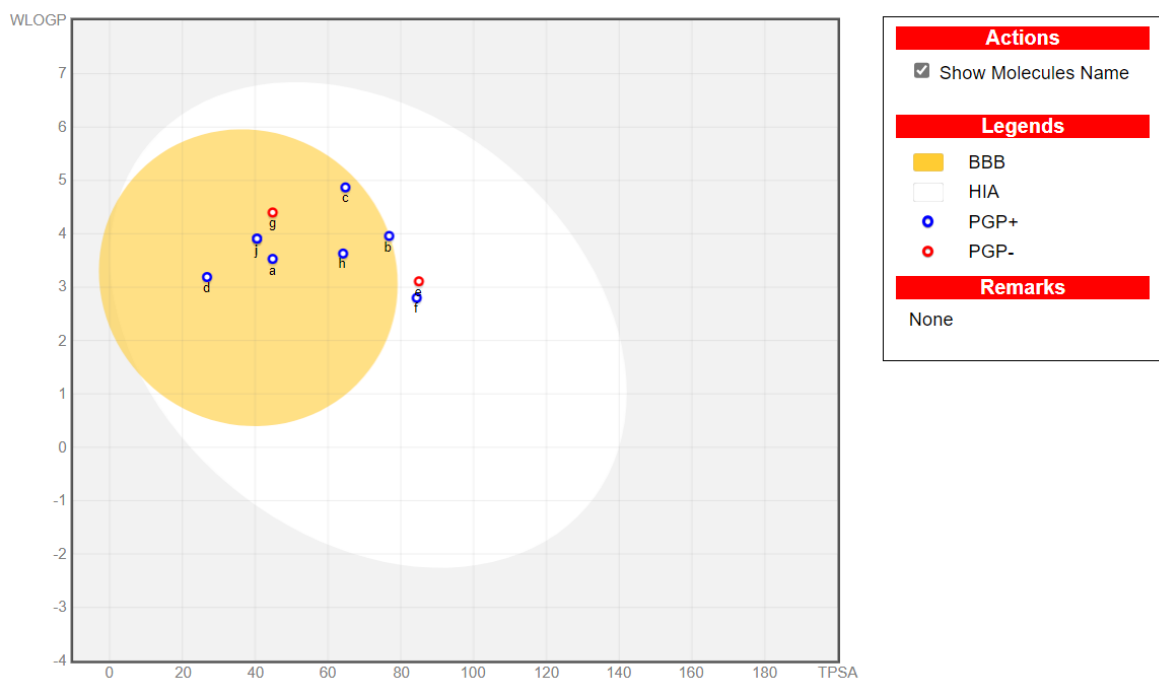


**Figure 11.** The BOILED-Egg model of some drug compounds

## CONCLUSION

As a result of the study, molecular docking and ADME studies of some atypical antipsychotic molecules were performed on 5-HT<sub>1A</sub>, 5-HT<sub>2A</sub>, and 5-HT<sub>2C</sub>, which are indicated as prominent receptors in psychotic disorders. Especially when the dock scores of Lurasidone (**e**) were examined, it was perceived to have the highest affinity for the mentioned receptors. However, when the poses and interaction types were examined, it was revealed that Risperidone (**h**) for 5-HT<sub>1A</sub>, Paliperidone (**f**) for 5-HT<sub>2A</sub>, and Brexpiprazole (**b**) for 5-HT<sub>2C</sub> may have higher affinity. Considering ADME predictions, all compounds (**a-j**) had good pharmacokinetic profiles, but Lurasidone (**e**) was found to have poorer druglikeness properties and have poorer BBB crossing. It was observed that all drug molecules fully complied with the Lipinski, Egan, and Veber rules, and especially all drug compounds

except Lurasidone (**e**) complied with the Muegge rules. Considering the calculated Ki values, it was predicted that the selected atypical antipsychotics would have nanomolar effects on 5-HT<sub>1A</sub> and picomolar effects on 5-HT<sub>2A</sub> and 5-HT<sub>2C</sub>. In light of the data in this study, it seems that the use of Paliperidone (**f**) and Risperidone (**h**) may be more valuable, especially in the treatment of psychotic patients such as schizophrenia.

## AUTHOR CONTRIBUTION STATEMENT

Writing-original draft, Methodology, Investigation, Formal analysis, Software, Conceptualization, Resources, Writing-review & editing, Supervision (H.U).

## CONFLICT OF INTEREST

The author declared that there is no conflict of interest.

## REFERENCES

- Azmitia, E. C., Gannon, P. J., Kheck, N. M., & Whitaker-Azmitia, P. M. (1996). Cellular localization of the 5-HT<sub>1A</sub> receptor in primate brain neurons and glial cells. *Neuropsychopharmacology*, *14*(1), 35-46. doi:10.1016/s0893-133x(96)80057-1
- Barnes, N. M., & Sharp, T. (1999). A review of central 5-HT receptors and their function. *Neuropharmacology*, *38*(8), 1083-1152. doi:https://doi.org/10.1016/S0028-3908(99)00010-6
- Baxter, G., Kennett, G., Blackburn, T., & Blaney, F. (1995). 5-HT<sub>2</sub> receptor subtypes: A family reunited? *Trends in Pharmacological Sciences*, *16*(3), 105-110. doi:https://doi.org/10.1016/S0165-6147(00)88991-9
- Bickerdike, J. M. (2003). 5-HT<sub>2C</sub> Receptor Agonists as Potential Drugs for the Treatment of Obesity. *Current Topics in Medicinal Chemistry*, *3*(8), 885-897. doi:http://dx.doi.org/10.2174/1568026033452249
- Boess, F. G., & Martin, I. L. (1994). Molecular biology of 5-HT receptors. *Neuropharmacology*, *33*(3-4), 275-317. doi:10.1016/0028-3908(94)90059-0
- Daina, A., Michielin, O., & Zoete, V. (2014). iLOGP: A Simple, Robust, and Efficient Description of n-Octanol/Water Partition Coefficient for Drug Design Using the GB/SA Approach. *Journal of Chemical Information and Modeling*, *54*(12), 3284-3301. doi:10.1021/ci500467k
- Daina, A., Michielin, O., & Zoete, V. (2017). SwissADME: a free web tool to evaluate pharmacokinetics, drug-likeness and medicinal chemistry friendliness of small molecules. *Scientific Reports*, *7*(1), 42717. doi:10.1038/srep42717
- Daina, A., & Zoete, V. (2016). A BOILED-Egg To Predict Gastrointestinal Absorption and Brain Penetration of Small Molecules. *ChemMedChem*, *11*(11), 1117-1121. doi:https://doi.org/10.1002/cmdc.201600182
- Fiorino, F., Magli, E., Kędzierska, E., Ciano, A., Corvino, A., Severino, B., . . . Caliendo, G. (2017). New 5-HT<sub>1A</sub>, 5HT<sub>2A</sub> and 5HT<sub>2C</sub> receptor ligands containing a picolinic nucleus: Synthesis, in vitro and in vivo pharmacological evaluation. *Bioorganic & Medicinal Chemistry*, *25*(20), 5820-5837. doi:https://doi.org/10.1016/j.bmc.2017.09.018
- Fletcher, A., Bill, D. J., Bill, S. J., Cliffe, I. A., Dover, G. M., Forster, E. A., . . . Reilly, Y. (1993). WAY100135: a novel, selective antagonist at presynaptic and postsynaptic 5-HT<sub>1A</sub> receptors. *Eur J Pharmacol*, *237*(2-3), 283-291. doi:10.1016/0014-2999(93)90280-u
- Glennon, R. A. (1990). Do classical hallucinogens act as 5-HT<sub>2</sub> agonists or antagonists? *Neuropsychopharmacology*, *3*(5-6), 509-517.
- Hoyer, D., Hannon, J. P., & Martin, G. R. (2002). Molecular, pharmacological and functional diversity of 5-HT receptors. *Pharmacol Biochem Behav*, *71*(4), 533-554. doi:10.1016/s0091-3057(01)00746-8
- Jenck, F., Bös, M., Wichmann, J., Stadler, H., Martin, J. R., & Moreau, J. L. (1998). The role of 5ht<sub>2c</sub> receptors in affective disorders. *Expert Opinion on Investigational Drugs*, *7*(10), 1587-1599. doi:10.1517/13543784.7.10.1587
- Jibson, M. D., & Tandon, R. (1998). New atypical antipsychotic medications. *Journal of Psychiatric Research*, *32*(3), 215-228. doi:https://doi.org/10.1016/S0022-3956(98)00023-5



- Kimura, K. T., Asada, H., Inoue, A., Kadji, F. M. N., Im, D., Mori, C., . . . Shimamura, T. (2019). Structures of the 5-HT<sub>2A</sub> receptor in complex with the antipsychotics risperidone and zotepine. *Nature Structural & Molecular Biology*, 26(2), 121-128. doi:10.1038/s41594-018-0180-z
- Kobilka, B. K., Frielle, T., Collins, S., Yang-Feng, T., Kobilka, T. S., Francke, U., . . . Caron, M. G. (1987). An intronless gene encoding a potential member of the family of receptors coupled to guanine nucleotide regulatory proteins. *Nature*, 329(6134), 75-79. doi:10.1038/329075a0
- Mackin, P., & Thomas, S. H. L. (2011). Atypical antipsychotic drugs. *BMJ*, 342, d1126. doi:10.1136/bmj.d1126
- Meltzer, H. Y. (2013). Update on Typical and Atypical Antipsychotic Drugs. *Annual Review of Medicine*, 64(Volume 64, 2013), 393-406. doi:https://doi.org/10.1146/annurev-med-050911-161504
- Millan, M. J., Dekeyne, A., & Gobert, A. (1998). Serotonin (5-HT)<sub>2C</sub> receptors tonically inhibit dopamine (DA) and noradrenaline (NA), but not 5-HT, release in the frontal cortex in vivo. *Neuropharmacology*, 37(7), 953-955. doi:10.1016/s0028-3908(98)00078-1
- Moreno, C., Nuevo, R., Chatterji, S., Verdes, E., Arango, C., & Ayuso-Mateos, J. L. (2013). Psychotic symptoms are associated with physical health problems independently of a mental disorder diagnosis: results from the WHO World Health Survey. *World Psychiatry*, 12(3), 251-257. doi:https://doi.org/10.1002/wps.20070
- Morris, G. M., Huey, R., Lindstrom, W., Sanner, M. F., Belew, R. K., Goodsell, D. S., & Olson, A. J. (2009). AutoDock4 and AutoDockTools4: Automated docking with selective receptor flexibility. *Journal of Computational Chemistry*, 30(16), 2785-2791. doi:https://doi.org/10.1002/jcc.21256
- Nuevo, R., Chatterji, S., Verdes, E., Naidoo, N., Arango, C., & Ayuso-Mateos, J. L. (2012). The Continuum of Psychotic Symptoms in the General Population: A Cross-national Study. *Schizophrenia Bulletin*, 38(3), 475-485. doi:10.1093/schbul/sbq099
- Peng, Y., McCorvy, J. D., Harpsøe, K., Lansu, K., Yuan, S., Popov, P., . . . Liu, Z.-J. (2018). 5-HT<sub>2C</sub> Receptor Structures Reveal the Structural Basis of GPCR Polypharmacology. *Cell*, 172(4), 719-730.e714. doi:https://doi.org/10.1016/j.cell.2018.01.001
- Sharp, T., & Hjorth, S. (1990). Application of brain microdialysis to study the pharmacology of the 5-HT<sub>1A</sub> autoreceptor. *Journal of Neuroscience Methods*, 34(1), 83-90. doi:https://doi.org/10.1016/0165-0270(90)90045-H
- Trott, O., & Olson, A. J. (2010). AutoDock Vina: Improving the speed and accuracy of docking with a new scoring function, efficient optimization, and multithreading. *Journal of Computational Chemistry*, 31(2), 455-461. doi:https://doi.org/10.1002/jcc.21334
- Uslu, H., Satilmiş, B., Uyumlu, A. B., Sağlık, B. N., Levent, S., Özkay, Y., . . . Benkli, K. (2023). Development of Some Antiplatelet Salts as Drug Active Ingredients and Investigation Biological Activities. *Pharmaceutical Chemistry Journal*, 57(8), 1260-1270. doi:10.1007/s11094-024-03032-1

Xu, P., Huang, S., Zhang, H., Mao, C., Zhou, X. E., Cheng, X., . . . Xu, H. E. (2021). Structural insights into the lipid and ligand regulation of serotonin receptors. *Nature*, 592(7854), 469-473. doi:10.1038/s41586-021-03376-8

# Is UR-144 Synthetic Cannabinoid Toxic to The Neuronal Cells: An *In Vitro* Evaluation

Mahmoud ABUDAYYAK<sup>\*</sup>, Tuğçe BORAN<sup>\*\*</sup>

*Is UR-144 Synthetic Cannabinoid Toxic to The Neuronal Cells: An In Vitro Evaluation*

## SUMMARY

The use of synthetic cannabinoids (SCs) increases dramatically among youth from different cultures. UR-144 is one of these SCs that was reported in 2012 for its first abuse. Case reports indicate symptoms of neuronal toxicity following UR-144 treatment, while several laboratory studies have demonstrated that UR-144 induces apoptosis and oxidative stress in various cell lines. However, none of those studies evaluate the effects of UR-144 in neuronal cells. This study aims to explore the molecular impacts of UR-144 on human neuroblastoma (SH-SY5Y) cells. MTT and neutral red uptake (NRU) assays were performed to evaluate the cytotoxicity. Oxidative stress was examined using the total antioxidant capacity test (TAC) and the changes in reactive oxygen species (ROS) and malondialdehyde (MDA) levels. The Comet assay was used to assess DNA damage. Results indicate that UR-144 did not cause cell death after 24 hours of treatment by MTT test. However, the cell death ratio at 50  $\mu$ M was 19.34%. UR-144 significantly decreased the levels of ROS and MDA in the cells, but no change in TAC levels was noticed. The comet assay results indicate no genotoxicity of UR-144 in SH-SY5Y cells. While these results indicate no significant toxicity of UR-144 SCs, further studies should be planned to illuminate the mechanism underlying the neuronal symptoms in UR-144 cases and approve or disapprove these results.

**Key Words:** Synthetic cannabinoids, UR-144, neurotoxicity, oxidative stress.

*Sentetik Kannabinoid UR-144 Nöronal Hücreler İçin Toksik Midir? Bir In Vitro Değerlendirme.*

## ÖZ

Sentetik kannabinoidlerin (SK) kullanımı, farklı kültürlerdeki gençler arasında önemli ölçüde artmaktadır. UR-144, bu SK'lerden biridir ve ilk kez 2012'de kötüye kullanımı rapor edilmiştir. Vaka raporları, UR-144 maruziyetinden sonra nöronal toksisite belirtilerine işaret ederken, çeşitli laboratuvar çalışmaları UR-144'ün farklı hücre hatlarında apoptoz ve oksidatif stresi indüklediğini göstermektedir. Ancak bu çalışmalardan hiçbiri UR-144'ün nöronal hücreler üzerindeki etkileri değerlendirmemektedir. Bu çalışmada, UR-144'ün insan nöroblastoma (SH-SY5Y) hücrelerinde moleküler etkilerinin araştırılması amaçlanmıştır. Sitotoksitesi değerlendirmek için MTT ve nötral kırmızı tutulum (NRU) testleri yapılmıştır. Oksidatif stres, toplam antioksidan kapasite testi (TAC) ile değerlendirilmiş ve reaktif oksijen türleri (ROS) ile malondialdehit (MDA) seviyelerindeki değişimler ölçülmüştür. DNA hasarını değerlendirmek için Comet testi kullanılmıştır. Sonuçlar, MTT testine göre UR-144'ün 24 saat maruz kalımından sonra hücre ölümüne neden olmadığını göstermektedir. Ancak 50  $\mu$ M'de hücre ölüm oranı %19.34'tür. UR-144 hücrelerdeki ROS ve MDA seviyelerini önemli ölçüde azaltırken, TAC seviyelerinde bir değişiklik fark edilmemiştir. Comet testi sonuçları, UR-144'ün SH-SY5Y hücrelerinde genotoksisiteye neden olmadığını göstermektedir. Bu sonuçlar UR-144'ün nöronal hücreler üzerinde önemli bir toksisitesi olmadığını gösterse de, UR-144 vakalarındaki nöronal semptomların altında yatan mekanizmayı aydınlatmak ve bu sonuçları doğrulamak veya reddetmek için daha fazla çalışma planlanmalıdır.

**Anahtar Kelimeler:** Sentetik kannabinoidler, UR-144, nörotoksisite, oksidatif stres.

Received: 08.08.2024

Revised: 15.11.2024

Accepted: 12.12.2024

<sup>\*</sup> ORCID: 0000-0003-2286-4777, Department of Pharmaceutical Toxicology, Faculty of Pharmacy, Istanbul University, Istanbul, Turkey

<sup>\*\*</sup> ORCID: 000-0003-4302-1947, Department of Pharmaceutical Toxicology, Faculty of Pharmacy, Istanbul University Cerrahpaşa, Istanbul, Turkey

## INTRODUCTION

According to the World Health Organization (WHO), “substance abuse refers to the harmful or hazardous use of psychoactive substances, including alcohol as well as illicit drugs”. “Psychotropic substance” is defined as a chemical substance that acts primarily upon the central nervous system, where it alters the person’s brain function, resulting in temporary changes in the person’s level of awareness, mood or attitude, consciousness, and demeanor. WHO further explains that psychoactive substance use can lead to dependence or an addictive syndrome, characterized by a cluster of behavioral, cognitive, and physiological phenomena that develop after repeated substance use (Atumeyi, Ligom & Tivkaa 2021; Bulska et al., 2020; Modrzyński, Pisarska, & Mańkowska 2022). New psychoactive substances or “legal highs” are synthetic compounds engineered to mimic the effects of illegal drugs like cocaine, ecstasy, amphetamines, and cannabis. Synthetic cannabinoids are a class of legal highs, designed to mimic the psychoactive effects of delta-9-tetrahydrocannabinol (THC), the primary active compound in *Cannabis sativa* (marijuana) (O’Hagan & Smith 2017). The use of *Cannabis sativa* (marijuana) as a hallucinogenic agent dates back to ancient human history. Although the identification of cannabinoid (CB) receptors was at the end of the 1980s, the research to develop chemicals that work similarly to THC was started in the 1960s, and the aim was to develop analogs with high analgesic and anti-inflammatory properties and low toxicity and side effects (Cacciola et al., 2010; Musselman & Hampton 2014).

Opposite to the expectations, synthetic cannabinoids show higher hallucination and psychological effects compared to the *Cannabis sativa*. In addition to their high addiction potential, synthetic cannabinoids such as JWHs and others were reported to cause toxic effects on the cardiovascular, kidney, lung, and neuronal systems (Riederer et al., 2016). While acute toxicity is the primary concern,

some studies have highlighted the chronic toxicity effects of synthetic cannabinoids, including psych-symptoms, change in the emotional state, damage in the nervous tissue, and changes in the release of the neurotransmitter, carcinogenic potential (Evren & Bozkurt 2013) and reproductive toxicity as depresses spermatogenesis are examples of this chronic effects (Cacciola et al., 2010)

UR-144 (indole-3-yl cycloalkyl ketone; Figure 1.) is one of the synthetic cannabinoids that developed in 2006. It was reported due to abusive use for the first time in 2012 (Al-Matrouk, Alqallaf, AlShemmeri, & BoJbarah 2019; Krotulski, Canaert, Stove, & Loganet 2021). UR-144 has been used alone or as a mixture with other herbs, tobacco, or other psychoactive drugs (Labay et al., 2016; Adamowicz et al., 2017). In general, UR-144 is primarily used in the form of cigarettes; however, some reports also suggest its use through vapor inhalation and oral consumption (Adamowicz & Lechowicz 2015; Adamowicz et al., 2017). Due to its distinct chemical structure compared to other synthetic cannabinoids, it became a “legal” alternative for marijuana in some countries at that time. The binding affinity of UR-144 to CB2 receptors is higher than that of CB1 receptors; however, According to WHO reports in 2014, the affinity of UR-144 to CBS receptors is lower than THC (WHO, 2014). WHO in 2017 reports mentioned a higher affinity of UR-144 to CBS compared to THC (WHO, 2017). The acute intoxication symptoms of UR-144, as reported in various clinical studies, include depression, convulsions, tachycardia, euphoria, hallucinations, and other symptoms (Adamowicz & Lechowicz 2015; Adamowicz et al., 2017). However, the toxicological and pharmacological effects of UR-144 and the mechanisms underlying those effects are still unclear and based generally on case reports and the abuser’s experiences (WHO, 2014). Studies indicate the carcinogenic effects of some synthetic cannabinoids and show the oxidative stress, genotoxicity, and cytotoxicity effects as mechanisms underlying their toxicity. In this study, it was hypothesized that UR-

144 could induce oxidative stress leading to cell death and DNA damage effects in the SH-SY5Y cells, which show neuroblast-like morphology, express some characteristics of catecholaminergic neurons' enzymes (Kovalevich & Langford, 2013), and important *in vitro* model for investigating neurotoxicology (Lopez-Suarez, Al Awabdh, Coumoul, & Chauvet 2022). For that, human neuroblastoma cells were exposed to UR-144 for 24 hours, and MDA level, ROS production, and TAC depletion were evaluated as endpoints for oxidative stress. Cytotoxicity was assessed using the MTT and NRU tests, while genotoxicity was evaluated using the comet assay.

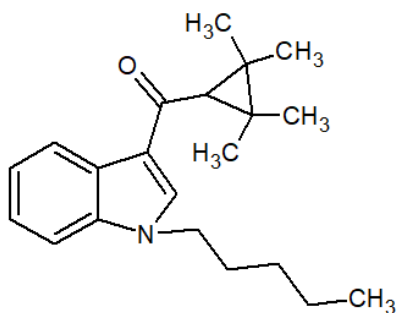


**Figure 1.** Chemical structure of UR-144

## MATERIAL AND METHODS

### Chemicals

UR-144 was purchased from Lipomed (Weil am Rhein, Germany). MTT (3-[4,5-dimethylthiazol-2-yl]-2,5-diphenyl-tetrazolium bromide), neutral red dye (NR), dimethylsulfoxide (DMSO), Triton-x, acetic acid, ethyl alcohol, Sodium chloride (NaCl), Ethylene diamine tetra acetic acid (EDTA), and ethidium bromide from Sigma Aldrich (Missouri, USA). Low melting agarose (LMA) and high melting agarose (HMA) from Himedia (Mumbai, India). Cell culture medium, fetal bovine serum (FBS), phosphate buffer saline (PBS), antibiotic solution, and trypsin solution were taken from Multicell Wisent Bioproducts (Quebec, Canada). Cell culture materials were taken from Nest Biotechnology (Wuxi, China).

### Cell culture and treatment

The SH-SY5Y cell line was purchased from ATCC (CRL-2266™). Cells were continued in EMEM cell culture medium with 10% FBS and 1% antibiotic-antimycotic mixture and incubated in 5% CO<sub>2</sub>, 37 °C, and 85% humidity. Cells were passaged by trypsinization when they reached about 70% confluence. About 10<sup>4</sup> cells /100 μL/ well were used for cytotoxicity assays, 10<sup>5</sup> cells /2 mL/ well for comet assay, and 5 x10<sup>6</sup> cells /12 mL/ flask for oxidative stress assays. Cells were treated with UR-144 for 24 hours. The treatment concentrations were chosen according to the preliminary study results and according to the previous articles. The unexposed cells were evaluated as the growth control group, and DMSO was used as the negative control.

### Cell viability determination

**MTT assay:** This test is based on the reduction of MTT dye to formazan crystals by a mitochondrial enzyme in viable cells (Fotakis & Timbrell 2006). After UR-144 treatment, 20 μL of 5 mg/ mL MTT dye solution was added to each well and incubated for 3 hours at 37 °C. The upper phase was thrown, and the formazan crystals were dissolved in 100 μL of DMSO. The absorbance (OD) was measured at 590 nm by a microplate reader (Biotek, Germany), and the cell viability was calculated as the relative percentage of the negative control.

**Neutral red uptake (NRU) assay:** To evaluate whether UR-144 causes cell death by affecting the lysosomal activity, the NRU assay was used (Borenfreund & Puerner 1985). While NR dye could be held in the viable cells, the disrupted cell membrane disallows it in the dead cells. At the end of the treatment period, the medium was replaced with a fresh medium containing 50 μg /mL of neutral red dye and incubated for three hours. After that, wells were washed with PBS, and the accumulated NR dye was dissolved with 100 μL/ well of glacial acetic acid: ethanol: water [1:49:50]. After 10 minutes of gentle shaking, the OD was determined at 540 nm by a microplate reader (Biotek Germany).

### **Oxidative stress determination**

**Reactive oxygen species (ROS) level:** ROS levels in the cells were investigated with molecular probe H<sub>2</sub>DCF-DA, which is converted to the fluorescent DCF in the presence of ROS. After the exposure to UR-144 treatment for 24 hours, the supernatant was removed, cells were trypsinized, washed with PBS (1X), and resuspended in PBS. 1 mL of 20 µM H<sub>2</sub>DCF-DA was added to the cells and incubated for 30 minutes. Then the cells were washed with PBS and suspended in 150 µL bovine serum albumin (BSA, 1%). The fluorescence intensity was measured in the FITC channel (488 nm/530 nm) on an ACEA NovoCyte flow cytometer (ACEA, San Diego, CA, USA). The results were represented as median fluorescence intensity ± standard deviation.

**Malondialdehyde (MDA) level:** Lipid peroxidation produces MDA as a final product, and an increase in MDA levels is commonly used as an indicator of oxidative stress in cells (Del Rio, Stewart, & Pellegrini 2005). For that, MDA levels in the cells were quantified manually by the thiobarbituric acid reactive substances assay (TBRAS) method, as previously described by Draper and Hadley (1990). The ODs were measured at 532 nm using a microplate reader (Epoch, Biotek). The protein amount of each sample was assessed with a Bicinchoninic acid (BCA) protein assay (ThermoScientific), whose principle is the reduction of Cu<sup>2+</sup> to Cu<sup>1+</sup> by amino acids in alkaline conditions using a commercial kit, and the results were calculated as the mean (µg/mg protein) ± standard deviation.

**Total antioxidant capacity (TAC) level:** TAC is a marker of antioxidant defense capacity in the cells. In this study, TAC levels were determined using a commercially available kit (Sigma, Missouri, USA) according to the manufacturer's instructions. 100 µL of Cu<sup>2+</sup> working solution was added to the standards and samples wells and incubated for 90 minutes in the dark at room temperature. The OD values were measured at 570 nm in a microplate reader (Epoch,

Biotek). Trolox was used as a standard for the calibration curve. The results are presented as the mean (nmol/ µL) ± standard deviation.

### **Genotoxicity evaluation**

DNA damage was evaluated with alkaline Comet assay as described in a previous study (Alpertunga et al. 2014) using a fluorescent microscope (Olympus BX53, Japan) with Comet assay IV image analysis system (Perceptive Instruments, Suffolk, UK). Briefly, the cells were collected at the end of the treatment period, washed, and counted. Then, the cells were mixed with low-melting agarose and spread on slides coated previously with high-melting agarose. Then, the cells were lysed using a high-salt solution for 24 hours. The next day, the lysed cells were treated with an alkaline (PH about 10.5) solution for 20 minutes before electrophoresis. The percentage of DNA in the tail was used to express the degree of damage in the individual cell. More than one hundred cells/slide were blindly assessed. The results were evaluated compared to the solvent control group and presented as the mean ± standard deviation. The cells treated with 100 µM H<sub>2</sub>O<sub>2</sub> for two hours were used as the positive control.

### **Statistical analysis**

All experiments were performed at least in three replicates and repeated three times (n= 9). Data were represented as the mean ± standard deviation (SD). The statistical differences were analyzed by one-way ANOVA and Post Hoc Tukey-test using SPSS version 20 for Windows (SPSS Inc., Chicago, IL) compared to the solvent control groups.

## **RESULTS and DISCUSSION**

The mortal effect of high-dose intake of synthetic cannabinoids has been approved by several clinical reports (Giorgetti, Busardò, Tittarelli, Auwärter, & Giorgetti 2020; Adamowicz 2021; Al-Matrouk et al., 2019); however, their chronic toxicity and the mechanisms underlying the toxicities are still insufficient and controversial (Coronado-´Alvarez et al., 2021); While a lot of studies show the toxicity of SCs

(Krotulski et al., 2020; Maida et al., 2021; Pellegrini, Marchei, Papaseit, Farré, & Zaami 2020), especially the neural toxicity (Gugelmann et al., 2014; Tomiyama and Funada, 2014; Cha et al., 2015), cardiotoxicity (Davis and Boddington, 2015), and nephrotoxicity (Silva, Carmo, & Carvalho 2018) and mentioned the cell death, oxidative stress, and inflammation induction (Oztas, Abudayyak, Celiksoz, & Özhan 2019; Akar, Ercin, Boran, Gezginici-Oktayoglu, & Özhan 2022) as the mechanisms underlying these toxicities, other studies show the benign- therapeutic effects of these chemicals (Coronado-´Alvarez et al., 2021; Muralidhar Reddy, Maurya, & Velmurugan 2019).

For UR-144, there is very little data related to their biological effects. According to a Scopus database search on 21 Dec. 2021 (TITLE-ABS-KEY(ur 144) AND TITLE-ABS-KEY(cannab\*) AND NOT TITLE-ABS-KEY(urethral)) AND ( LIMIT-TO ( DOCTYPE,"ar" )) there are 84 articles containing UR-144 in their title, abstract, and keywords. Of these, 55 articles were related to the analytical detection methods of UR-144 and other cannabinoids. While 11 articles focused on reports of the detection of UR-144 in the various products or the biological samples of the abusers.

UR-144 was developed by Abbott as an analgesic in 2006; however, it was not approved by the FDA. The first reports about the abuse were in 2012. Data mentioned the uses of different street names for UR-144 as Hardcore, Sonrisa, and Tio Tieso (Fabregat-Safont et al., 2020). Additionally, reports mentioned the uses of UR-144 alone or in combination with other synthetic cannabinoids like FUB-AMB, 5F-AKB48, and AB-FUBINACA (Al-Matrouk et al., 2019; Gugelmann et al., 2014; Kronstrand, Roman, Andersson, & Eklund 2013; Krotulski et al., 2020; Turcant et al., 2017). In addition to CB2 receptor activity, UR-144 has an agonist selectivity to CB1 (Coronado-´Alvarez et al., 2021). While the high

selectivity and affinity of SC to CB1 compared to THC make the side effects of SC higher than that of THC (Chung, Cha, Min, & Yun 2021), it could be concluded that UR-144 has a higher toxicity than THC.

Case reports mentioned different concentrations of UR-144 in the biological samples of the users; in Kronstrand et al. (2013) studies' the concentration was between 0.05 ng and 25.9 ng, and the mean was 1.26 ng per 1 mL blood sample (Kronstrand et al. 2013). In a study by Adamowicz (2021), it was reported, based on previous data analysis, that UR-144 blood concentrations in fatal cases vary between 1.4 and 12.3 ng/ mL (Adamowicz, 2021). In another study, 39 cases of UR-144 intoxication were reviewed, and 17 ng /mL was reported as the maximum concentration observed in those cases (Adamowicz et al., 2017).

Despite the possible toxicity of UR-144, there is a real lack of data related to the effect and toxicity of synthetic cannabinoids in general and UR-144 specifically (Kronstrand et al. 2013; Coronado-´Alvarez et al., 2021; Maida et al., 2021).

Behavior and cardiopathy symptoms were noticed in UR-144 intoxication cases (Adamowicz et al., 2017). Similarly, in a case reported by Al Fawaz et al. (2019), it was concluded that the UR-144 may cause prolonged epilepsy-like symptoms and stress cardiomyopathy (Al Fawaz et al., 2019). The neurotoxicity, like epileptic symptoms, was mentioned in a case that used the "Crazy Monkey" drug, where the blood and urine samples analysis revealed the presence of UR-144 metabolites in addition to PB-22 (QUIPIC) SCs; however, the researchers suggested PB-22 as a cause of those symptoms (Gugelmann et al., 2014).

In the present study, at the tested concentrations (12.5, 25, and 50  $\mu$ M; the higher dose was chosen based on solubility) UR-144 did not exhibit a significant cytotoxic effect. The median inhibition concentration ( $IC_{50}$ ) could not be calculated using either the MTT assay or the NRU (Figure 2.)

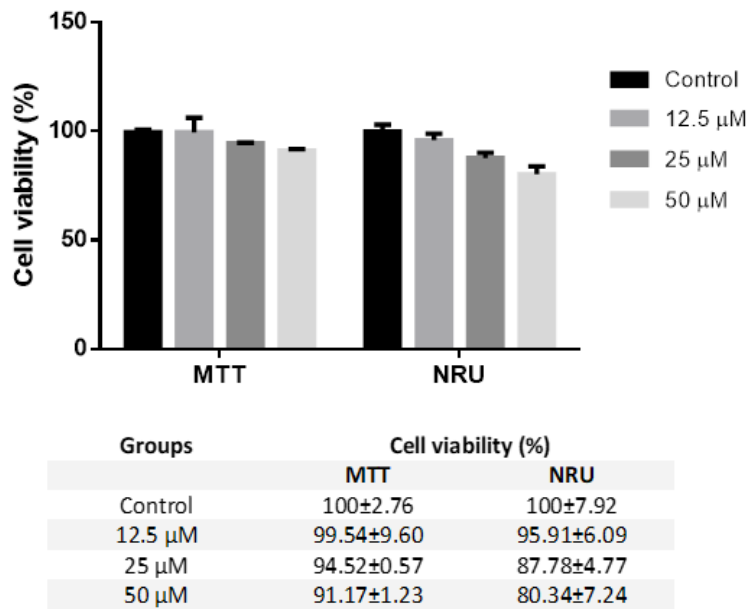


**Figure 2.** The effect of UR-144 on SH-SY5Y cell viability.

In a limited number of laboratory studies, Almada et al. (2020) evaluated UR-144 along with other SCs on BeWo human placental cytotrophoblast cells. A decrease in cell viability was observed; however, no significant changes were detected in LDH enzyme levels, a key parameter used to evaluate the damage in cells' metabolic activity. Their results also indicate the involvement of apoptotic pathways since Caspase 3, caspase 7, and caspase 9 were increased significantly. Additionally, a cell cycle arrest was noticed for all SCs including UR-144. While there was no change in the cellular ROS levels, UR-144 caused a loss of mitochondrial membrane potential. The comparison with  $\Delta 9$ -tetrahydrocannabinol (THC) indicates higher toxicity of SCs compared to TCH. Oppositely, Fonseca et al. (2019) hypothesized the effect of SCs on the endometrium remodeling process and tested this hypothesis using endometrial stromal (St-T1b) cells and decidual fibroblasts primary cells. A transitory increase in ROS and RNS levels and induction of the endoplasmic reticulum damage were detected following the treatment to UR-144 for 48 hours, but no cytotoxicity effects were noticed. Similarly, the

current study results reveal no cytotoxicity of UR-144 on SH-SY5Y cells. The decrease in ROS and MDA levels couldn't be assessed as a toxic effect since the induction of oxidative stress concurs with the increase in both ROS and MDA levels. Since the decrease was compared to the negative control and solvent control groups and the cells in the treatment groups did not treat previously with an oxidative stress inducer agent, the reduction in ROS and MDA couldn't also be assessed as an antioxidant effect. Herewith, it could be concluded that there is no significant oxidative stress effect on SH-SY5Y cells exposed to UR-144 for 24 hours.

In our study, the tested concentrations of UR-144 significantly reduced ROS levels in the cells compared to the control group. This reduction was further supported by a significant decrease in MDA levels observed in the 12.5 and 50  $\mu\text{M}$  exposure groups (Figure 3a., 3b.). However, the slight increase in TAC levels in the exposed groups was not statically significant compared to the control group (3c) ( $p > 0.05$ ).



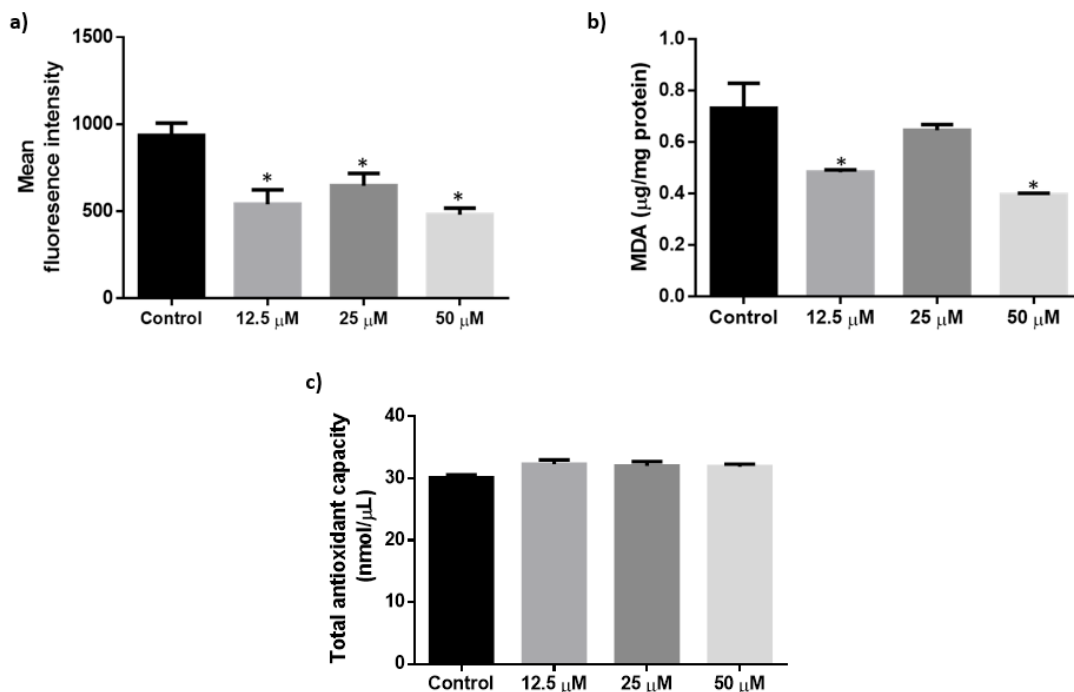


**Figure 3.** Effects of UR-144 on a) ROS level, b) MDA level, and c) TAC level in SH-SY5Y after 24 hours. \* $p < 0.05$  versus control group.

Koller et al. (2015) used SCGE assay and micronucleus assay on human lymphocyte cells and salmonella microsome assay to evaluate the genotoxicity potential of some SCs. Their results show inhibition of the cell division after treatment to 0.1 to 1 mM UR-144 for three hours. Additionally, an increase in the DNA migration and induction of micronucleus and chromosomal aberrations were noticed. Those results confirm the WHO's concerns

about its genotoxicity (WHO 2014). Conversely, the results of the present study show no significant DNA damage in the exposed cells compared to the negative group.

In the present study, the genotoxicity potential of UR-148 was evaluated by the Comet assay after the treatment with UR-144 for 24 hours. The results showed no significant differences between the groups UR-144- treated and the negative group (Figure 4.).

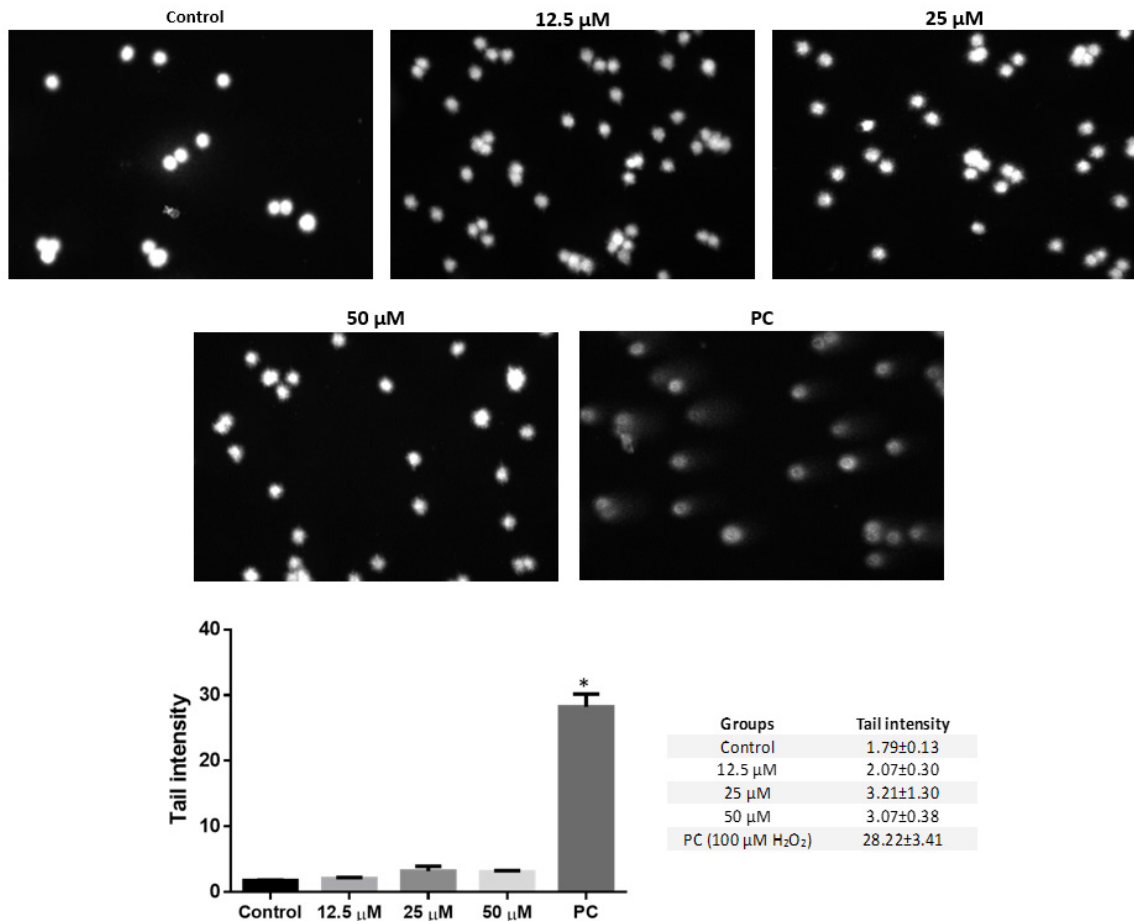


**Figure 4.** DNA damage induction by UR-144 in SH-SY5Y cell line. \* $p < 0.05$  versus the control group. PC: positive control (100  $\mu\text{M}$  H<sub>2</sub>O<sub>2</sub>)

Besides the possible toxicity of UR-144, Nielsen, Holm, Olsen, & Linnet (2015) mentioned the metabolism of UR-144 by CYP 450 enzymes as CYP3A4, CYP1A2, and CYP 2C enzymes; this indicated the possibility of drug/chemical-UR144 interaction, the uses of UR-144 in combination with other synthetic cannabinoids, herbs, and drugs increase the chance of UR-144 induced toxicity by the synergism effect or by decreasing the metabolism of that drugs. Similarly, Ashino, Hakukawa, Itoh, & Numazawa (2014) showed a weak inhibitory effect of UR-144 on CYP1A enzymes, which also could increase the risk of interaction. While the lab studies were done on highly pure chemicals, the street chemicals could contain high levels of organic and inorganic impurities that also increase the risk of

toxicity (Abdin, Yeboah, & Jacob 2020).

*In conclusion*, there is an increase in the use of SCs. UR-144 is an example of these SCs. The reported cases show the toxicity of UR-144 in the neuronal system that could be lethal. However, there are very few studies evaluating its toxicity. The negative results in this study and some previous works could draw a pink view for this chemical, especially since UR-144 was developed as a drug and passed some tests. However, the limited information, conflicting findings, and reports on the toxicity of other synthetic cannabinoids highlight the urgent need for further research to evaluate and better understand the toxicity of UR-144.

#### AUTHOR CONTRIBUTION STATEMENT

M.A. & T.B. designed and wrote the manuscript; M.A. & T.B. performed the experiments; M.A.

analyzed the data; M.A. performed the computational analyses; M.A. & T.B. assisted with the manuscript modification; M.A. supervised the study.

#### CONFLICT OF INTEREST

The authors declare that there is no conflict of interest.

#### REFERENCES

- Abdin, A. Y., Yeboah, P., & Jacob, C. (2020). Chemical Impurities: An Epistemological Riddle with Serious Side Effects. *International Journal of Environmental Research and Public Health*, 17(3), 1030. <https://doi.org/10.3390/ijerph17031030>
- Adamowicz, P. (2021). Blood concentrations of synthetic cannabinoids. *Clinical Toxicology*, 59(3), 246–251. <https://doi.org/10.1080/15563650.2020.1787429>
- Adamowicz, P., & Lechowicz, W. (2015). The Influence of Synthetic Cannabinoid UR-144 on Human Psychomotor Performance—A Case Report Demonstrating Road Traffic Risks. *Traffic Injury Prevention*, 16(8), 754–759. <https://doi.org/10.1080/15389588.2015.1018990>
- Adamowicz, P., Gieroń, J., Gil, D., Lechowicz, W., Skulska, A., & Tokarczyk, B. (2017). The effects of synthetic cannabinoid UR-144 on the human body—A review of 39 cases. *Forensic Science International*, 273, e18–e21. <https://doi.org/10.1016/j.forsciint.2017.02.031>
- Akar, M., Ercin, M., Boran, T., Gezginci-Oktayoglu, S., & Özhan, G. (2023). UR-144, synthetic cannabinoid receptor agonist, induced cardiomyoblast toxicity mechanism comprises cytoplasmic Ca<sup>2+</sup> and DAPK1-related autophagy and necrosis. *Toxicology Mechanisms and Methods*, 33(1), 56–64. <https://doi.org/10.1080/15376516.2022.2081829>
- Al Fawaz, S., Al Deeb, M., Huffman, J. L., al Kholaiif, N. A., Garlich, F., & Chuang, R. (2019). A case of status epilepticus and transient stress cardiomyopathy associated with smoking the synthetic psychoactive cannabinoid, ur-144. *American Journal of Case Reports*, 20, 1902–1906. <https://doi.org/10.12659/AJCR.918918>
- Almada, M., Alves, P., Fonseca, B. M., Carvalho, F., Queirós, C. R., Gaspar, H., Amaral, C., Teixeira, N. A., & Correia-da-Silva, G. (2020). Synthetic cannabinoids JWH-018, JWH-122, UR-144 and the phytocannabinoid THC activate apoptosis in placental cells. *Toxicology Letters*, 319, 129–137. <https://doi.org/10.1016/j.toxlet.2019.11.004>
- Al-Matrouk, A., Alqallaf, M., AlShemmeri, A., & Bojbarah, H. (2019). Identification of synthetic cannabinoids that were seized, consumed, or associated with deaths in Kuwait in 2018 using GC–MS and LC–MS–MS analysis. *Forensic Science International*, 303, 109960. <https://doi.org/10.1016/j.forsciint.2019.109960>
- Alpertunga, B., Kara, M., Abudayyak, M., Oztas, E., Ozden, S., & Özhan, G. (2014). Effects of prochloraz on DNA damage, lipid peroxidation and antioxidant system in vitro. *Toxicology Mechanisms and Methods*, 24(4), 268–275. <https://doi.org/10.3109/15376516.2014.881943>
- Ashino, T., Hakukawa, K., Itoh, Y., & Numazawa, S. (2014). Inhibitory effect of synthetic cannabinoids on CYP1A activity in mouse liver microsomes. *The Journal of Toxicological Sciences*, 39, 815–820. <https://doi.org/10.2131/jts.39.815>
- Atumeyi, A. U., Ligom, T. T., & Tivkaa, J. T. (2021). Intake and abuse of psychoactive substances and its relative consequences: a review. *Science Journal of Analytical Chemistry*, 9(2), 39–49. <https://doi.org/10.11648/j.sjac.20210902.12>
- Borenfreund, E., Puerner, J.A. (1985). Toxicity is determined in vitro by morphological alterations and neutral red absorption. *Toxicology Letters*, 24, 119–24. [https://doi.org/10.1016/0378-4274\(85\)90046-3](https://doi.org/10.1016/0378-4274(85)90046-3)
- Bulska, E., Bachliński, R., Cyrański, M. K., Michalska-Kacymirow, M., Kośnik, W., Małecki, P., Grela, K., & Dobrowolski, M. A. (2020). Comprehensive Protocol for the Identification and Characterization of New Psychoactive Substances in the Service of Law Enforcement Agencies. *Frontiers in Chemistry*, 8, 2020. <https://doi.org/10.3389/fchem.2020.00693>

- Cacciola, G., Chianese, R., Chioccarelli, T., Ciaramella, V., Fasano, S., Pierantoni, R., Meccariello, R., & Cobellis, G. (2010). Cannabinoids and reproduction: A lasting and intriguing history. *Pharmaceuticals*, 3(10), 3275-3323. <https://doi.org/10.3390/ph3103275>
- Cha, H. J., Seong, Y. H., Song, M. J., Jeong, H. S., Shin, J., Yun, J., ... & Kim, H. S. (2015). Neurotoxicity of synthetic cannabinoids JWH-081 and JWH-210. *Biomolecules & Therapeutics*, 23(6), 597. <https://doi.org/10.4062/biomolther.2015.057>
- Chung, E. Y., Cha, H. J., Min, H. K., & Yun, J. (2021). Pharmacology and adverse effects of new psychoactive substances: synthetic cannabinoid receptor agonists. *Archives of Pharmacal Research*, 44(4), 402-413. <https://doi.org/10.1007/s12272-021-01326-6>
- Coronado-Álvarez, A., Romero-Cordero, K., Macías-Triana, L., Tatum-Kuri, A., Vera-Barrón, A., Budde, H., Machado, S., Yamamoto, T., Imperatori, C., & Murillo-Rodríguez, E. (2021). The synthetic CB1 cannabinoid receptor selective agonists: Putative medical uses and their legalization. *Progress in Neuro-Psychopharmacology and Biological Psychiatry*, 110, 110301. <https://doi.org/10.1016/j.pnpbp.2021.110301>
- Evren, C., & Bozkurt, M. (2013). Synthetic Cannabinoids: Crisis of The Decade. *Dusunen Adam Journal of Psychiatry and Neurological Sciences*, 26, 1-11. <https://doi.org/10.5350/DA-JPN20132601001>
- Davis, C., & Boddington, D. (2015). Teenage cardiac arrest following abuse of synthetic cannabis. *Heart, Lung and Circulation*, 24(10), e162-e163. <https://doi.org/10.1016/j.hlc.2015.04.176>
- Del Rio, D., Stewart, A.J., Pellegrini N. A. (2005). Review of recent studies on malondialdehyde as toxic molecule and biological marker of oxidative stress. *Nutrition, Metabolism and Cardiovascular Diseases*, 15, 316-328. <https://doi.org/10.1016/j.numecd.2005.05.003>
- Draper, H. H., & Hadley, M. (1990). Malondialdehyde determination as index of lipid Peroxidation. *Methods in Enzymology*, 186, 421-431. [https://doi.org/10.1016/0076-6879\(90\)86135-I](https://doi.org/10.1016/0076-6879(90)86135-I)
- Fabregat-Safont, D., Ibáñez, M., Baquero, A., Sancho, J. V., Hernández, F., & Haro, G. (2020). Investigation on the consumption of synthetic cannabinoids among teenagers by the analysis of herbal blends and urine samples. *Journal of Pharmaceutical and Biomedical Analysis*, 186, 113298. <https://doi.org/10.1016/j.jpba.2020.113298>
- Fonseca, B. M., Fernandes, R., Almada, M., Santos, M., Carvalho, F., Teixeira, N. A., & Correia-da-Silva, G. (2019). Synthetic cannabinoids and endometrial stromal cell fate: Dissimilar effects of JWH-122, UR-144 and WIN55,212-2. *Toxicology*, 413, 40-47. <https://doi.org/10.1016/j.tox.2018.11.006>
- Fotakis, G., & Timbrell, J. A. (2006). In vitro cytotoxicity assays: comparison of LDH, neutral red, MTT and protein assay in hepatoma cell lines following exposure to cadmium chloride. *Toxicology letters*, 160(2), 171-177. <https://doi.org/10.1016/j.toxlet.2005.07.001>
- Giorgetti, A., Busardò, F. P., Tittarelli, R., Auwärter, V., & Giorgetti, R. (2020). Post-mortem toxicology: a systematic review of death cases involving synthetic cannabinoid receptor agonists. *Frontiers in Psychiatry*, 11, 464. <https://doi.org/10.3389/fpsy.2020.00464>
- Gugelmann, H., Gerona, R., Li, C., Tsutaoka, B., Olson, K. R., & Lung, D. (2014). "Crazy Monkey" poisons man and dog: Human and canine seizures due to PB-22, a novel synthetic cannabinoid. *Clinical Toxicology*, 52(6), 635-638. <https://doi.org/10.3109/15563650.2014.925562>

- Koller, V. J., Ferk, F., Al-Serori, H., Mišík, M., Nersesyan, A., Auwärter, V., Grummt, T., & Knasmüller, S. (2015). Genotoxic properties of representatives of alkylindazoles and aminoalkyl-indoles which are consumed as synthetic cannabinoids. *Food and Chemical Toxicology*, 80, 130–136. <https://doi.org/10.1016/j.fct.2015.03.004>
- Kovalevich, J., & Langford, D. (2013). Considerations for the use of SH-SY5Y neuroblastoma cells in neurobiology. *Neuronal cell culture: methods and protocols*, 9-21, Springer. [https://doi.org/10.1007/978-1-62703-640-5\\_2](https://doi.org/10.1007/978-1-62703-640-5_2)
- Kronstrand, R., Roman, M., Andersson, M., & Eklund, A. (2013). Toxicological findings of synthetic cannabinoids in recreational users. *Journal of Analytical Toxicology*, 37(8), 534–541. <https://doi.org/10.1093/jat/bkt068>
- Krotulski, A. J., Cannaert, A., Stove, C., & Logan, B. K. (2021). The next generation of synthetic cannabinoids: Detection, activity, and potential toxicity of pent-4en and but-3en analogues including MDMB-4en-PINACA. *Drug Testing and Analysis*, 13(2), 427–438. <https://doi.org/10.1002/dta.2935>
- La Maida, N., Papaseit, E., Martínez, L., Pérez-Mañá, C., Poyatos, L., Pellegrini, M., Pichini, S., Pacifici, R., Ventura, M., Galindo, L., Busardò, F. P., & Farré, M. (2021). Acute pharmacological effects and oral fluid biomarkers of the synthetic cannabinoid ur-144 and THC in recreational users. *Biology*, 10(4). <https://doi.org/10.3390/biology10040257>
- Labay, L. M., Caruso, J. L., Gilson, T. P., Phipps, R. J., Knight, L. D., Lemos, N. P., ... & Logan, B. K. (2016). Synthetic cannabinoid drug use as a cause or contributory cause of death. *Forensic Science International*, 260, 31-39. <https://doi.org/10.1016/j.forsciint.2015.12.046>
- Lopez-Suarez, L., Al Awabdh, S., Coumoul, X., & Chauvet, C. (2022). The SH-SY5Y human neuroblastoma cell line, a relevant in vitro cell model for investigating neurotoxicology in human: Focus on organic pollutants. *Neurotoxicology*, 92, 131-155. <https://doi.org/10.1016/j.neuro.2022.07.008>
- Maida, N., Pellegrini, M., Papaseit, E., Pérez-Mañá, C., Poyatos, L., Ventura, M., Galindo, L., Busardò, F. P., Pichini, S., Farré, M., & Marchei, E. (2020). Determination of the synthetic cannabinoids JWH-122, JWH-210, UR-144 in oral fluid of consumers by GC-MS and quantification of parent compounds and metabolites by UHPLC-MS/MS. *International Journal of Molecular Sciences*, 21(24), 1–14. <https://doi.org/10.3390/ijms21249414>
- Modrzyński, R., Pisarska, A., & Mańkowska, A. (2022). The Hazardous Use Scale of psychoactive substances. A pilot study. *Alcoholism and Drug Addiction/Alkoholizm i Narkomania*, 35(3), 187-204. <https://doi.org/10.5114/ain.2022.125279>
- Muralidhar Reddy, P., Maurya, N., & Velmurugan, B. K. (2019). Medicinal Use of Synthetic Cannabinoids—a Mini Review. *Current Pharmacology Reports*, 5, 1-13. <https://doi.org/10.1007/s40495-018-0165-y>
- Musselman, M. E., & Hampton, J. P. (2014). “Not for human consumption”: a review of emerging designer drugs. *Pharmacotherapy*, 34(7), 745-757. <https://doi.org/10.1002/phar.1424>
- Nielsen, L. M., Holm, N. B., Olsen, L., & Linnet, K. (2016). Cytochrome P450-mediated metabolism of the synthetic cannabinoids UR-144 and XLR-11. *Drug Testing and Analysis*, 8(8), 792–800. <https://doi.org/10.1002/dta.1860>
- O’Hagan, A., & Smith, C. (2017). A new beginning: an overview of new psychoactive substances. *Forensic Research & Criminology International Journal*, 5(3), 00159. <https://irep.ntu.ac.uk/id/eprint/31876>

- Oztaş, E., Abudayyak, M., Celiksoz, M., & Özhan, G. (2019). Inflammation and oxidative stress are key mediators in AKB48-induced neurotoxicity in vitro. *Toxicology in Vitro*, 55, 101-107. <https://doi.org/10.1016/j.tiv.2018.12.005>
- Pellegrini, M., Marchei, E., Papaseit, E., Farré, M., & Zaami, S. (2020). UHPLC-HRMS and GC-MS screening of a selection of synthetic cannabinoids and metabolites in urine of consumers. *Medicina (Lithuania)*, 56(8), 1-9. <https://doi.org/10.3390/medicina56080408>
- Riederer, A.M., Campleman, S.L., Carlson, R.G., ... Brent, A. (2016). Acute Poisonings from Synthetic Cannabinoids - 50 U.S. Toxicology Investigators Consortium Registry Sites, 2010-2015. *MMWR and Morbidity and Mortality Weekly Report*, 65(27), 692-695. Retrieved from <http://dx.doi.org/10.15585/mmwr.mm6527a2>
- Silva, J. P., Carmo, H., & Carvalho, F. (2018). The synthetic cannabinoid XLR-11 induces in vitro nephrotoxicity by impairment of endocannabinoid-mediated regulation of mitochondrial function homeostasis and triggering of apoptosis. *Toxicology Letters*, 287, 59-69. <https://doi.org/10.1016/j.toxlet.2018.01.023>
- Tomiyama, K. I., & Funada, M. (2014). Cytotoxicity of synthetic cannabinoids on primary neuronal cells of the forebrain: the involvement of cannabinoid CB1 receptors and apoptotic cell death. *Toxicology and Applied Pharmacology*, 274(1), 17-23. <https://doi.org/10.1016/j.taap.2013.10.028>
- Turcant, A., Deguigne, M., Ferec, S., Bruneau, C., Leborgne, I., Lelievre, B., Gegu, C., Jegou, F., Abbara, C., le Roux, G., & Boels, D. (2017). A 6-year review of new psychoactive substances at the Centre antipoison Grand-Ouest d'Angers: Clinical and biological data. *Toxicologie Analytique et Clinique*, 29(1), 18-33. <https://doi.org/10.1016/j.toxac.2016.12.001>
- World Health Organization Expert Committee on Drug Dependence (ECDD). (2014). UR-144 critical, review report. [https://ecddrepository.org/sites/default/files/2023-04/who\\_trs\\_991\\_eng.pdf](https://ecddrepository.org/sites/default/files/2023-04/who_trs_991_eng.pdf) <https://ecddrepository.org/en> Accessed: 07.12.2024
- World Health Organization WHO Expert Committee on Drug Dependence (ECDD). (2017). UR-144 critical, review report. [https://ecddrepository.org/sites/default/files/2023-04/criticalreview\\_ur144.pdf](https://ecddrepository.org/sites/default/files/2023-04/criticalreview_ur144.pdf) <https://ecddrepository.org/en> Accessed: 07.12.2024

# Formulation and Characterization of Liquisolid Tablets for Improving Dissolution of Telmisartan

Chinmaya Keshari SAHOO\*, Nidhi SHREE\*\*, Amiyakanta MISHRA\*\*\*

**Formulation and Characterization of Liquisolid Tablets for Improving Dissolution of Telmisartan**

## SUMMARY

The current study's objective was to create liquisolid tablets (LST) to improve the dissolution profile of telmisartan (TLS), a poorly soluble medication Biopharmaceutical Classification System (BCS) class II. To prepare LST, the following ingredients were used: microcrystalline cellulose (MCC) as the carrier, polyethylene glycol 600 (PEG 600) as the vehicle, croscarmellose sodium (CCS) as the superdisintegrant, and Aerosil 200 as the coating material. The tablet quality control tests, flow characteristics, and interactions between the medication and the excipient were assessed for each formulation. Higuchi, Korsmeyer-Peppas (KP), zero order, and first-order models were utilized to investigate the *in vitro* drug release (IVDR) kinetics for various batches. When the optimized formulation (TC3) was evaluated for stability at 75±5% RH and 40±2°C, it was shown to be steady for a maximum of three months. No interaction between the medication and excipients was confirmed by Fourier Transform Infrared Spectroscopy (FTIR) and Differential Scanning Calorimetry (DSC) investigations. The solubility studies were used to guide the selection of the dissolution medium. Comparing the TC3 to the conventional marketed tablet (MKT), TELVAS 20, a notable improvement in dissolution was observed. After three months of storage, there was no discernible change in the tablet's characteristics or the drug release profile.

**Key Words:** Dissolution, Poorly soluble, Stability, TLS.

**Telmisartanın Çözünmesini İyileştirmek İçin Sıvı Katı Tabletlerin Formülasyonu ve Karakterizasyonu**

## ÖZ

Mevcut çalışmanın amacı, Biyofarmasötik Sınıflandırma Sistemi (BCS) sınıf II'de zayıf çözünen bir ilaç olan telmisartanın (TLS) çözünme profilini iyileştirmek için sıvılaştırılmış katı tabletler (LST) oluşturmaktır. LST'yi hazırlamak için şu bileşenler kullanıldı: taşıyıcı olarak mikrokristal selüloz (MCC), taşıyıcı olarak polietilen glikol 600 (PEG 600), süper dağıtıcı olarak kroscarmeloz sodyum (CCS) ve kaplama malzemesi olarak Aerosil 200. Her formülasyon için tablet kalite kontrol testleri, akış özellikleri ve ilaç ile yardımcı madde arasındaki etkileşimler değerlendirildi. Çeşitli partiler için *in vitro* ilaç salım (IVDR) kinetiğini araştırmak için Higuchi, Korsmeyer-Peppas (KP), sıfırinci ve birinci dereceden modeller kullanıldı. Optimize edilmiş formülasyon (TC3), %75±5 RH ve 40±2°C'de kararlılık açısından değerlendirildiğinde, en fazla üç ay boyunca kararlı olduğu gösterildi. İlaç ve yardımcı maddeler arasında herhangi bir etkileşim, Fourier Dönüşümlü Infrared Spektroskopisi (FTIR) ve Diferansiyel Taramalı Kalorimetri (DSC) araştırmaları ile doğrulanmadı. Çözünme ortamının seçimi için çözünürlük analizi kullanıldı. TC3 piyasada bulunan geleneksel tablet (MKT), TELVAS 20 ile karşılaştırılarak, çözünmede kayda değer bir iyileşme gözlemlendi. Üç aylık depolamadan sonra, tabletin özelliklerinde veya ilaç salım profilinde fark edilebilir bir değişiklik olmadı.

**Anahtar Kelimeler:** Çözünme, Zayıf çözünürlük, Stabilite, TLS.

Received: 18.07.2024

Revised: 20.11.2024

Accepted: 18.12.2024

\* ORCID: 0000-0003-4290-4828, Associate Professor, Department of Pharmaceutics, College of Pharmaceutical Sciences, Puri (Affiliated to BPUT), Bidyaniketan, Puri-Konark Marine Drive Road, Puri, Odisha-752004

\*\* ORCID: 0009-0009-1490-4485, PG Scholar, Department of pharmaceutics, College of Pharmaceutical Sciences, Puri (Affiliated to BPUT), Bidyaniketan, Puri-Konark Marine Drive Road, Puri, Odisha-752004

\*\*\* ORCID: 0000-0002-5769-781X, Professor and Prinicipal, Department of pharmaceutics, College of Pharmaceutical Sciences, Puri (Affiliated to BPUT), Bidyaniketan, Puri-Konark Marine Drive Road, Puri, Odisha-752004

## INTRODUCTION

Many potentially novel medications fall into either BCS class IV (low solubility and low permeability) or BCS class II (low solubility and high permeability), and many of them show poor water solubility. The most crucial factors affecting bioavailability are the drug's solubility and dissolution behavior (Yadav et al., 2010). Poorly water-soluble drugs have numerous challenges while developing dosage forms for oral administration because of their low bioavailability (Javadzadeh et al., 2007). One crucial factor in achieving the appropriate drug concentration in the systemic circulation (Peddi et al., 2013) and demonstrating a pharmacological response is solubility.

Due to their limited solubility in the gastrointestinal tract (GIT), drugs that poorly soluble in water will naturally release their contents slowly. The task at hand for these medications is to optimize their rate of solubility or dissolution. This ultimately enhances bioavailability and absorption. For many pharmaceutical formulations, dissolution is the rate-limiting step. Solid dispersions (Merisko-Liversidge et al., 2003), inclusion complexes with  $\beta$ -cyclodextrins (Jarowski et al., 1992), micronization (Barzegar et al., 2005), liquid solid (LS) technology (Nokhodchi et al., 2011), spray drying technique (El-Houssieny et al., 2010), use of surfactants (Nighute et al., 2009), use of co-solvents (Millard et al., 2002), self-emulsification and self-micro emulsification (Balakrishnan et al., 2009), use of pro-drugs and drug derivatization (Tanino et al., 1998), formation of solid solutions or amorphous solids (Kapsi et al., 2001), and microencapsulation (Li et al., 2008) are some of the techniques for increasing drug solubility. The LS systems are the creative method to improve poorly soluble drug dissolution and *in vivo* bioavailability (Tiong et al., 2009).

The technology of solutions in powder form utilized to create "liquid medication," gave rise to the idea of LST. Solid medications dispensed in appropriate, vehicles for non-volatile liquids are called "liquid medication" (Nagabandi et al., 2011). The idea of LS allows for the physical blending process to be used with specific excipients such as carrier and coating material to transform a liquid into an easily com-

pressible, seemingly dry, and free-flowing powder. LS is described by (Spireas et al., 1999). To achieve a suitable flowable and compressible LS system, Spireas has developed a model to determine the right amounts of coating material and carrier. The excipients ratio (R) is the carrier/coating ratio.

$$R = Q/q \quad (1)$$

As a result, R is the ratio of the coating material (q) to the carrier material (Q) weights. The ideal value of R is 20. The weight ratio of the liquid drug (W) to Q in the LS system is known as the liquid loading factor (Lf) (Kasturi et al., 2021).

$$Lf = W/Q \quad (2)$$

The surface area of the medication accessible for disintegration and wetting qualities is greatly enhanced by the LS system. It is reasonable to anticipate that the LS system of water-insoluble compounds will exhibit improved medication dissolution, leading to increased bioavailability. The ideas behind the construction of LS are to use powdered liquid medications, such as drug solutions, suspensions, or liquid drugs. LS describes the process of combining liquid pharmaceuticals with appropriate additives, also known as transporters and coating materials, to create powder combinations that appear dry, loose-flowing, non-stick, and compressible (Kavitha et al., 2011) (Spireas, 2002).

A potent and specific angiotensin II type 1 (AT1) receptor antagonist used to treat essential hypertension is TLS (Kolatkar et al., 2007, 2005). BCS class II medication TLS has an aqueous solubility of 0.09  $\mu\text{g}/\text{mL}$  (Tran et al., 2008). Its solubility varies with pH, nearly becoming insoluble within the pH 3–9 range. Furthermore, its nature is strongly hydrophobic ( $\log P = 3.2$ ) (Sangwai et al., 2013). Poor drug water solubility is linked to irregular and sluggish drug absorption, slow drug breakdown, and ultimately, low and insufficient oral bioavailability (43%) (Wienen et al., 2000). Solid systems for liquid medications are created using LST technology. The current study is to formulate LST of TLS and its characterization.



## **MATERIALS AND METHODS**

### ***Materials***

TLS was gifted by Indchemie Health Specialties Pvt Ltd (Sikkim, India). PEG 600, Aerosil 200, croscarmellose sodium (CCS), and Hydrochloric acid (HCl) were acquired from Mumbai, India's S D Fine-Chem Ltd. We bought microcrystalline cellulose (MCC) from Signet Pharma in Mumbai. Analytical grade solutions, reagents, and other chemicals were all utilized. Marketed tablet (MKT) *TELVAS 20*, Aristo Pharmaceuticals Pvt. Ltd. Batch no: SPF231027 Sikkim was procured from a local pharmacy.

### ***Analytical techniques for TLS in vitro estimation and formulations***

Based on in vitro tests, the amount of TLS in the formulations was estimated using UV-visible spectrophotometric analytical methods. The pure medication and standard calibration curves were scanned for this procedure. Using an HCl buffer with a pH of 1.2, standard calibration curves were prepared.

### ***Lambda max determination***

100 mg of TLS was transferred to 100 ml volumetric flask and make up the volume upto the mark with 0.1N HCl to get concentration of 1000 µg/ml of standard stock solution. Further 5 milliliters was pipetted out from the above stock solution and transferred to a 50 ml volumetric flask make up the volume upto the mark with 0.1N HCl to obtain the concentration of 100 µg/ml (Padmavathi et al., 2013). Further 5 ml of solution was pipetted out from 100 µg/ml TLS solution and transfer to 10 ml volumetric flask, make up the volume upto the mark with 0.1N HCl to get concentration of 50 µg/ml. Then the 50 µg/ml solution was scanned in UV-visible spectrophotometer, and the  $\lambda_{max}$  was observed at 290 nm.

### ***Calibration curve for TLS***

A concentration of 1000 µg/ml standard stock solution (Tatane et al., 2011) was obtained by adding 100 mg of TLS medication to 100 ml of 0.1N HCl solution. Five milliliters of the solution was taken out from standard stock solution and diluted with fifty millili-

ters of 0.1 N HCl solution to create a concentration of 100 µg/ml. The 100 µg/ml solution was diluted using the same HCl buffer pH 1.2 to produce a sample solution at 10, 20, 30, 40, and 50 µg/ml concentrations. The absorbance corresponding to the concentrations was calculated at a 290 nm wavelength. A curve for calibration for pure TLS was made by plotting the measured absorbance against the respective concentrations.

### **Compatibility study**

#### ***FTIR***

The FTIR allows (Milam et al., 2013) the identification of functional groups in a variety of compounds and drug-excipient incompatibility. Using the KBr pellet method, the FTIR analysis (Bruker, αE, Germany) of antihypertensive medications was completed. To create a transparent pellet, a small portion of the mixture was squeezed at 10 kg per centimeter with a hydraulic press. The pellet remained inside the specimen container of the FTIR spectrophotometer and scanned between 4000 and 400  $\text{cm}^{-1}$ .

#### ***DSC***

The examination of potential incompatibilities between dosage forms' medication excipients is predicted using DSC (Shimadzu DSC-50, Japan). Drug and individual excipient physical mixes in a 1:1 ratio were prepared and subjected to DSC analysis (Milam et al., 2013). In a DSC pan, individual samples and a physical combination of the medication and excipients were weighed to a maximum of 5 mg. For efficient heat conduction, the sample pan was crimped and scanned between 50 and 300°C. A 20°C  $\text{min}^{-1}$  heating rate was employed, and the resulting thermogram was examined for signs of interaction. The thermograms were then compared (Jaydip et al., 2020).

#### ***Preparation of LST***

Spireas provided instructions for preparing TLS liquid-solid pills (Spireas et al., 1999; Swamy et al., 2013). To create a homogeneous dispersion, the weighed amount of TLS was combined with the non-volatile solvent (PEG 600), heated to (80–90)°C,

and then sonicated for 15 minutes. The carrier material (MCC) was then added to the melt in predetermined volumes, and following a standard mixing process, the resultant wet mass was mixed with the coating material (Aerosil 200). After spreading the powder mixture evenly, it was let to stand for five minutes. After scraping the powder mixture, it was

combined with CCS as superdisintegrant and mixed for an additional minute. A Rimek rotary tablet press machine was utilized to compress the LS powder admixtures, under pressure, into tablets with concave punches with the necessary weight. Table 1 displays the ingredients of LST.

**Table 1.** Composition of LST

Batches	TLS (mg)	PEG600 (W)	MCC (Q)	Aerosil 200 (q)	CCS	Total Weight (mg)	Lf = W/Q	R = Q/q
TC1	20	100	200	10	8	338	0.5	20
TC2	20	100	200	10	16	346	0.5	20
TC3	20	100	200	10	24	354	0.5	20

### Characterization LST of TLS

#### *Pre-compression parameters*

The angle of repose (AOR), tapped and bulk density, and Carr's index (C.I.) parameters were measured by specific procedures for prepared granules (Sahoo et al., 2015). The fixed funnel technique was used to measure the granular repose angle. AOR is determined by the classical method. Granules were to flow through the funnel freely and land on the spotless surface. The funnel was positioned so that its bottom tip would not make contact with the upper portion of the granule pile. Equation below is used to calculate AOR.

$$\tan = h/r \quad (3)$$

$$= \tan^{-1}(h/r) \quad (4)$$

Where the AOR measured in degrees,  $h$  is the heap's height in centimeters, and  $r$  is the circular support's (cone's) radius in centimeters.

The mass of an untapped powder sample divided by its bulk volume is known as the bulk density of a powder. A 100 ml graduated cylinder with a readable 1 ml is taken in order to determine the bulk density. Then it is fitted to bulk density apparatus (Sisco, India). When the bulk volume is leveled and the needed powder is carefully added to the cylinder without compacting, it is marked to the closest graded unit. Bulk density is then computed.

The bulk volume is determined using a measuring cylinder. A suitable 100 ml graduated cylinder readable 1 ml is taken and graduated measuring cylinder containing a powder sample fitted to bulk density apparatus is mechanically tapped. 10, 500, and 1250 taps on the powder sample were carried out, and the corresponding volumes  $V_{10}$ ,  $V_{500}$ , and  $V_{1250}$  to the nearest graduated unit were noted.  $V_{1250}$  is the tapped volume if the difference between  $V_{500}$  and  $V_{1250}$  is less than or equal to 1 ml. If the difference between  $V_{500}$  and  $V_{1250}$  exceeds 1 ml, continue in increments, such as 1250 taps, until the difference between subsequent measurements is less than or equal to 1 ml. Next, compute tapped density by dividing the powder mass by the tapped volume.

The following formula was utilized to calculate C.I. (Saeedi et al., 2021).

$$\% \text{ C.I} = 100 \quad (5)$$

H.R. was computed by dividing the tapped density by the bulk density.

#### **Post-compression parameters of LST**

##### *Appearance of the tablets*

Tablets were chosen randomly from each batch and formulation, and their surface texture, shape, overall elegance, consistency, color, and odor were all examined (Jadhav et al., 2011).

### **Thickness**

Utilizing a Vernier calliper, the thickness (Jadhav et al., 2011) of each LS tablet was determined.

### **Hardness**

Utilizing the Monsanto hardness tester, (Jadhav et al., 2011) the tablets' hardness was measured.

### **Friability**

The friability of LST was tested using a Roche friabilator (Gandhi et al., 2011). Twenty pills were added to the chamber after the group was weighed. Over the course of the friabilator's 100 revolutions, the tablets experienced the combined consequences of shock and abrasion because the plastic chamber holding them dropped them six inches away with each revolution. The pills are then weighed one more and finished (Naureen et al., 2022).

### **Weight variation test (WVT)**

Weight variation was assessed for each prepared LST in accordance (Suthar et al., 2016) with the USP monograph. Each of the twenty tablets is weighed individually, the average weight is established, and the weights of each tablet are compared to the average to conduct the WVT. After calculating the % weight deviation, the results were compared to the USP requirements (Patil et al., 2022).

### **Uniformity of drug content test**

Each batch of LS pills contained ten tablets, (The USP 26-National Formulary, 2003) which were triturated to create a powder. A 100 ml volumetric flask filled with 0.1N HCl was allowed to dissolve the powder weight equivalent to one tablet over the course of 24 h using a magnetic stirrer. After the solution was suitably diluted, then it was filtered using Whatman filter paper No. 1, and then subjected to spectrophotometric analysis.

### **Disintegration test**

The disintegration test was finished in accordance with IP 1996's strategy for uncoated tablets. The assembly was placed in the suitable vessel, preferably a 1000 ml beaker, and suspended in the liquid medium

(water). The fluid volume so that the wire mesh, at its highest position, is at least 25 mm below the liquid's surface and, at its lowest point, is at least 25 mm above the container's base. A thermostat was utilized to raise the liquid's temperature and keep it at  $37 \pm 2^\circ\text{C}$ . The apparatus was run for a predetermined amount while the assembly was suspended in a beaker filled with 1000 milliliters of pure water. The tablet's breakdown time was also noted. Ultimately, the liquid was removed from the assembly (Tiwari et al., 2021).

### **In vitro dissolution study (IVDS)**

IVDS was performed with USP type II (paddle) equipment (Electrolab, India). The pill is stored in 900 ml of HCl buffer pH 1.2 dissolution medium with a 75 rpm rotating stirrer, (Senthil et al., 2011) which keeps the dissolution media at  $37 \pm 0.5^\circ\text{C}$  for the necessary number of hours. At predetermined time intervals five milliliter aliquots were withdrawn by a sampling cannula then filtered using a  $0.45\text{-}\mu\text{m}$  cellulose acetate filter. They replaced with equivalent amount of HCl buffer pH 1.2 solutions to the dissolution medium. The samples were suitably diluted and analyzed for absorbance with a UV/Visible Spectrophotometer at  $\lambda_{\text{max}}$  of 290 nm. To ascertain the release profile of different batches, the percentage CDR was plotted against time.

### **Model-independent approach for dissolution comparison**

Results of the IVDR profile were expressed as mean  $\pm$  Standard Deviation (S.D). The model independent approach uses a difference factor ( $f_1$ ) and similarity factor ( $f_2$ ) to compare dissolution profiles (Sahoo et al., 2015). The  $f_1$  calculates the percent difference between the two curves at each time point and relative error between two curves. It is expressed as

$$f_1 = \frac{1}{n} \times 100 \quad (6)$$

Where  $n$  is the sampling number,  $R_j$  and  $T_j$  are the percent dissolved of the reference and test products at each time point  $j$ .

The  $f_2$  is a logarithmic transformation of the sum squared error of differences between the test  $T_j$  and reference products  $R_j$  over all time points.

$$f_2 = 50 \times \log [1 + 2^{\sum (T_j - R_j)^2}]^{-0.5} \times 100 \quad (7)$$

Where  $w_j$  is an optional weight factor, the two release profiles are considered to be similar if  $f_1$  value is lower than 15 (between 0 to 15), and  $f_2$  value is more than 50 (between 50 to 100).

#### IVDR kinetic study

To ascertain the method of release from tablets, the formulation's release data was investigated utilizing the Higuchi model, first-order kinetics, zero-order kinetics, Korsmeyer-Peppas (KP) equations, and the Hixson Crowell model (Senthil et al., 2011). The Higuchi model showed the percentage CDR versus square root of time. The KP model showed the log % CDR versus log time. The Hixson and Crowell model showed the drug proportion left in the matrix as a cube root vs. time, first-order log % drug remaining to release vs. time and the zero-order model, which showed the percentage CDR versus time, were the kinetic models that were used.

#### Accelerated Stability Study (ASS)

For three months, the tightly sealed tablets were kept in stability chambers at  $40 \pm 2^\circ\text{C}/75 \pm 5\% \text{RH}$  (Thermo Lab Scientific Equipment Pvt. Ltd., Mumbai, India) for ASS (ICH Harmonized Tripartite Guidelines, 2003). The tablets were removed from the container regularly to be checked for IVDS, drug content, and other characteristics.

#### Statistical Analysis of Data

The experiment results were presented as mean  $\pm$  S.D values (Rani et al., 2004). The degree of significance was ascertained using a paired and one-sided Student t-test. At  $p < 0.05$ , the difference was deemed statistically significant, whereas at  $p > 0.05$ , it was considered non-significant.

## RESULTS AND DISCUSSION

#### Analytical methods for the estimation of TLS

The drug content and IVDS of TLS were estimated by obtaining a calibration curve in a pH 1.2 HCl buffer. The estimated  $\lambda_{\text{max}}$  at a standard concentration of TLS in the HCl buffer, pH 1.2 was observed to be 290 nm. Regression values ( $R^2$ ), which were found to be 0.9995, demonstrated the linearity of the calibration curve for HCl buffer pH 1.2.  $Y = 0.0205X - 0.0015$  calibration curves were used to derive the straight-line equations for drug content and IVDS. The scanning graph for  $\lambda_{\text{max}}$  of TLS in HCl buffer pH 1.2 was presented in Figure 1. The values of absorbance to corresponding concentration in different buffer for TLS were presented in Table 2 and calibration curve was presented in Figure 2. The analytical parameters for UV-visible spectroscopic method (Systronics double beam India) were presented in Table 3.

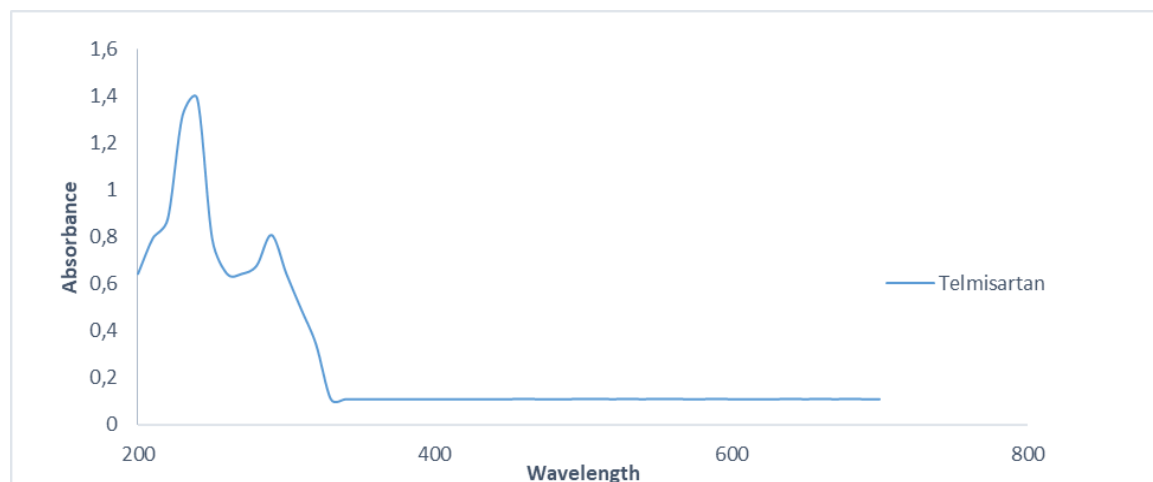
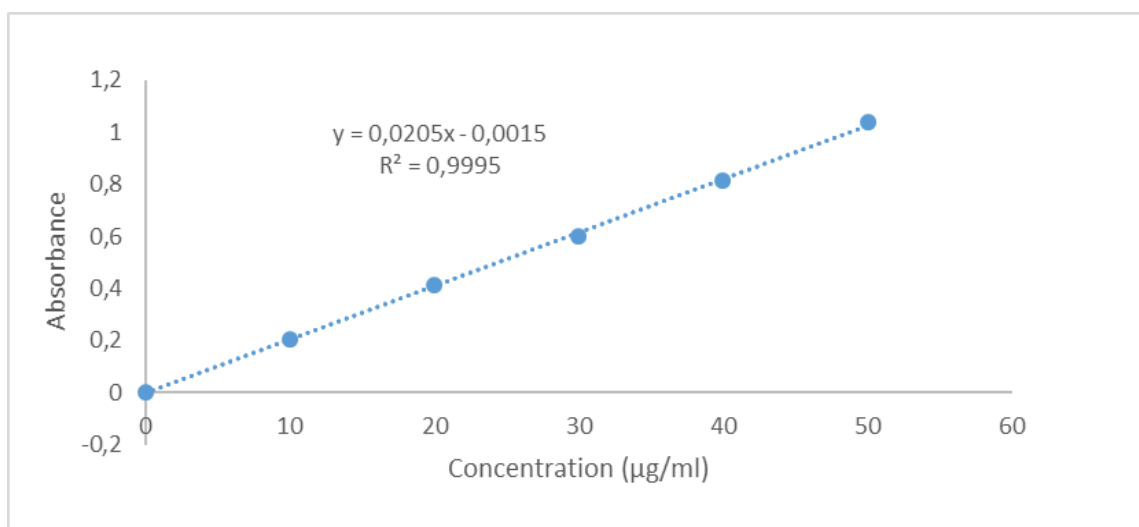


Figure 1. Scanning spectrum curve of TLS in HCl buffer pH 1.2

**Table 2.** Absorbance values to the corresponding concentration of TLS in HCl buffer pH 1.2 at 290 nm

Concentration (µg/ml)	Absorbance (Mean ± S.D.)
0	0
10	0.207 ± 0.013
20	0.414 ± 0.011
30	0.601 ± 0.017
40	0.815 ± 0.015
50	1.036 ± 0.018

Where S.D. is Standard Deviation, n 3



**Figure 2.** Calibration curve of TLS in HCl buffer pH 1.2 at 290 nm

**Table 3.** Analytical parameters of TLS for the development of the UV method

Parameters	Values for HCl buffer pH 1.2
λmax (nm)	290
Beer's law limit (µg/ml)	0-50
Regression equation	Y = 0.0205X-0.0015
Slope	0.0205
Intercept	0.0015
Correlation coefficient (R <sup>2</sup> )	0.9995

### Compatibility study

#### FTIR study

Pure TLS's FTIR spectra revealed the drug's distinctive peak at 2955.38 cm<sup>-1</sup> caused by the aromatic group's C-H stretching vibration, the carbonyl group at 1693.19 cm<sup>-1</sup> (Figure 3), and the C=C. The physical mixture's FTIR spectrum showed that the med-

ication's unique peaks (at 1693.19 cm<sup>-1</sup> and 1459.85 cm<sup>-1</sup>) remained unchanged and did not exhibit any interaction, as demonstrated by the aromatic bend and stretch at that location (Figure 4). Consequently, there was no appreciable distinction between the FTIR spectra and those obtained for their physical mixing, indicating compatibility.

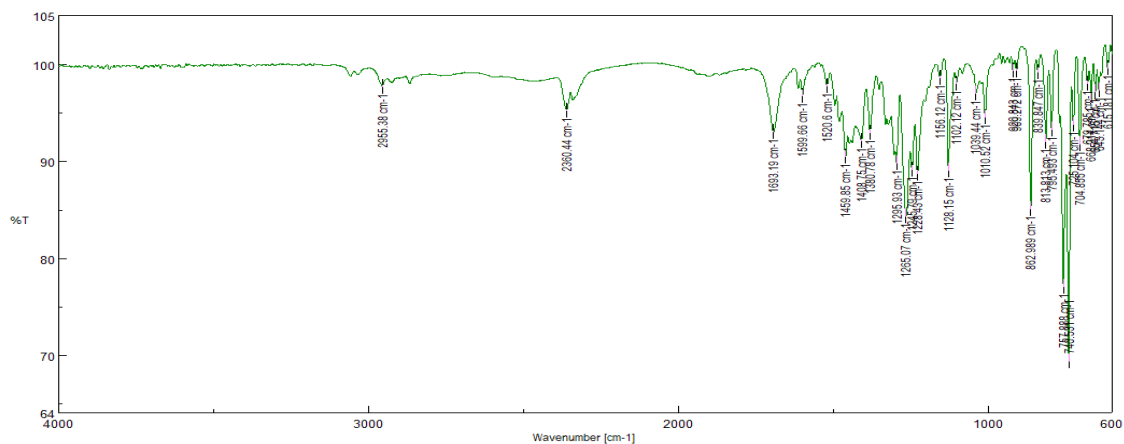


Figure 3. FTIR study of TLS

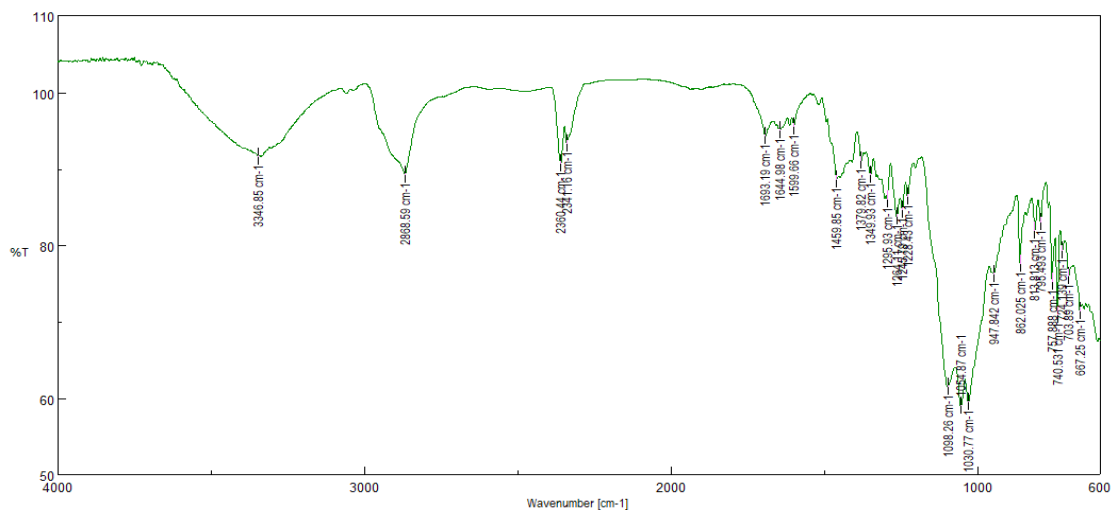


Figure 4. FTIR spectroscopy study of TC3

The formulation spectra also show the distinctive absorption peaks of TLS without much of a shift, suggesting no interaction between TLS and the additions (Swamy et al., 2013).

**DSC Study**

DSC thermogram of pure drug, and physical mixture of excipients used for LS formulations were

obtained and shown in figure 5 and 6. Out of 3 formulations one formulation was found to be good i.e. TC3. DSC thermogram showed an endothermic peak at 275.42 °C which is corresponding melting point of drug. DSC thermogram showed a peak at 268.75 °C in TC3 formulation. Hence, physical mixture showed that there was compatibility with the drug.

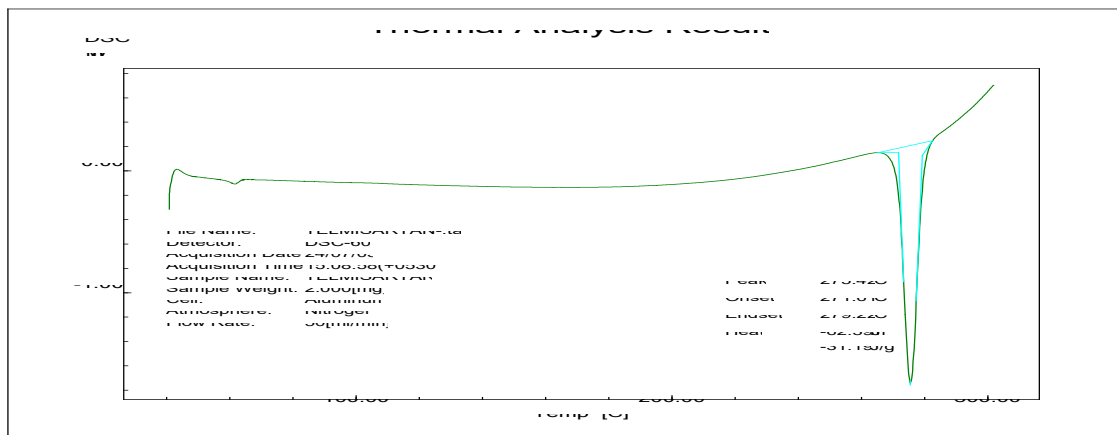


Figure 5. DSC thermogram of TLS

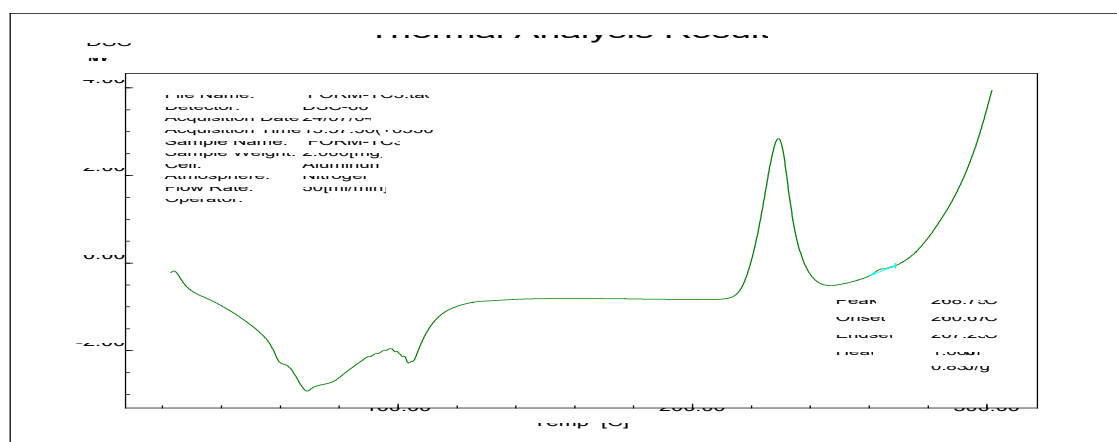


Figure 6. DSC thermogram of TC3

Since the steep peak at 266.45 on the TLS DSC thermogram is identical to the drug’s melting point, it indicates no drug-excipient interaction (Mishra et al., 2023).

**Characterization LST of TLS**

**Pre-compression parameters**

All formulations had an angle of repose between  $32.01 \pm 1.60$  and  $47.2 \pm 2.36$ . All formulations’ bulk densities of TLS fell between  $0.16 \pm 0.008$  and  $0.26 \pm 0.013$  g/ml. It was discovered that the tapped densities ranged from  $0.20 \pm 0.01$  to  $0.35 \pm 0.017$  g/ml. These findings indicated that the formulation powders were TC1-poor, TC2-fair, and TC3-good, in that order. The range of results for Carr’s index across all TLS formu-

lations was  $11.54 \pm 0.57$  to  $30 \pm 1.5$ . The optimized formulation TC3’s C.I. value ranges from 5 to 15%, indicating excellent granule flow properties. In contrast, the TC2 formulation’s C.I. value ranges from 16 to 20%, indicating fair granule flow properties. The granules of TLS had H.R. values ranging from  $1.13 \pm 0.05$  to  $1.42 \pm 0.07$  in all formulations. When the granule H.R. is less than 1.25, it typically shows that the TLS formulations TC2 and TC3 under investigation have outstanding flow properties. However, TC1 had a weak flow. According to the pre-compression parameter data, all TLS formulations’ dry granules had good flow characteristics, making it easier to manufacture LST. Table 4 displays it.

**Table 4.** Pre-compression parameters of powder blend

Batches	AOR (degree) ± S.D (n = 3)	Bulk density (g/ ml) ± S.D (n = 3)	Tapped density (g/ml) ± S.D (n = 3)	C.I (%) ± S.D (n = 3)	H.R ± S.D (n = 3)
TC1	47.2 ± 2.36	0.26 ± 0.013	0.3 ± 0.015	30 ± 1.5	1.42 ± 0.07
TC2	36.50 ± 1.83	0.16 ± 0.008	0.20 ± 0.01	20.43 ± 1.021	1.25 ± 0.06
TC3	32.01 ± 1.60	0.30 ± 0.015	0.35 ± 0.017	11.54 ± 0.57	1.13 ± 0.05

**N.B.**-Each value is given as mean ± S.D.

CI values ranged from 11.5 to 15.5, while AOR values varied from 28.89° to 34.07° among the pre-compression investigations. H.R. results ranged from 1.12 to 1.19 indicating good powder mix flow, which is very much needed for final processing into tablets (Swamy et al., 2013)

#### **Post compression parameters**

All of the TLS LSTs were found to have identical morphological features. It was discovered that every tablet had a smooth, concave, round, and white surface. The TLS LST ranged in average thickness from 5.67 ± 0.28 to 6.5 ± 0.47 mm. It was within permissible bounds, with average value variations not exceeding

± 5%. Every TLS LST had a hardness ranging from 2 ± 0.19 to 3 ± 0.11 kg/cm<sup>2</sup>. All formulations had a percentage friability ranging from 0.08 ± 0.0008% to 0.11 ± 0.001%. The % friability for each formulation was good in the current trials. The range of weight variation for the average pill weight was 2.9 ± 0.016 to 3.53 ± 0.017 percent. All of the formulations fell within the permitted range. The drug content percentages for TLS LST were discovered to be within allowable bounds, ranging from 97.98 ± 1.04 % to 99.12 ± 1.25 %. Within the defined range, the disintegration time of TLS LST was determined to be 2.20 ± 0.16 to 5.94 ± 0.21 minutes. Table 5 refers to it.

**Table 5.** Post-compression parameters of LST.

Batches	Thickness (mm) ± S.D (n = 10)	Hardness (kg/cm <sup>2</sup> ) ± S.D (n = 10)	%Friability (%) ± S.D (n = 20)	%Weight variation (%) <sup>b</sup> ± S.D (n = 20)	%Drug content (%) ± S.D (n = 10)	Disintegration time (min) ± S.D (n = 10)
TC1	5.67 ± 0.28	2 ± 0.19	0.11 ± 0.001	2.9 ± 0.016	97.98 ± 1.04	5.94 ± 0.21
TC2	6.34 ± 0.56	2.5 ± 0.11	0.08 ± 0.0008	3.44 ± 0.017	98.26 ± 1.06	5.16 ± 0.19
TC3	6.5 ± 0.47	3 ± 0.11	0.10 ± 0.001	3.53 ± 0.017	99.12 ± 1.25	2.20 ± 0.16

**N.B.**-Each value is given where mean ± S.D.

LS compacts ranged in hardness from 3.8 to 4.6 kg/cm<sup>2</sup>. For LS compacts, the friability value varied from 0.5 to 0.72%. The drug content ranges from 91.29 ± 0.03 to 94.62 ± 0.01 %, whereas the thicknesses vary from 5.80 ± 0.01 to 5.87 ± 0.02 mm. The disintegration time ranges from 185 to 276 seconds (Swamy et al., 2013).

#### **IVDS**

After 30 minutes, the % cumulative drug release

(% CDR) of TLS for TC1, TC2, TC3, and MKT was 85.63%, 92.97%, 98.30%, and 88.95%, respectively. Figure 7 displays the graph, which was created by plotting the % CDR (Y-axis) against time (X-axis). The % CDR of optimized formulation is highest as compared to others because of its high concentration of CCS. Significantly (p 0.05) higher values of % CDR of TC3 compared to MKT further indicate superiority of developed formulation over MKT.



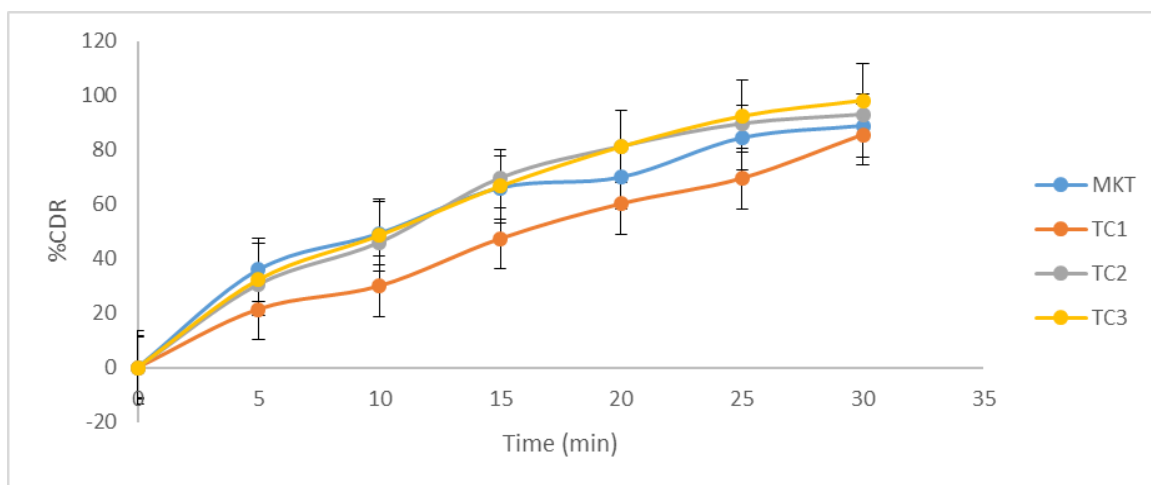


**Figure 7.** IVDS is showing TLS release from various fabricated formulations TC1-TC3 and MKT (n=3).

From the dissolution profile data for TLS LS compacts, a % CDR of 85.97 to 94.05 was recorded for the formulations at the end of 60 min. The drug surface available for dissolution is significantly increased with LS compacts because the drug is present in a non-volatile component solution, meaning that the drug is available in a molecularly distributed state in the dissolving media (Swamy et al., 2013). According to the data, the medication started to release from the compacts at minute five, and after sixty minutes, 70.00% to 93.28% of the drug was visible in the dissolving media. The commercial formulation of TLS, recognized for its favorable in-vitro drug release profile, was contrasted with the F5 formulation, which demonstrated the maximum release (Mishra et al., 2023)

The reason for the high dissolving rate of LST is that their formulations have a drug solution in a non-volatile vehicle that is used to generate the LS compact, which significantly increases the amount of drug surface area available for dissolution. As a result, compared to MKT, the surface area of the medication that is available for dissolving in an LS compact is significantly larger (Kalbhor et al., 2020).

**Model-independent approach for dissolution comparison**

IVDR profiles of developed formulations TC1-TC3 were compared with commercial tablet TELVAS 20. The values of f1 and f2 were depicted in Table 6. From the data TC3 formulation was found to best among all showing f2 value 80.5 and f1 value 2.4.

**Table 6.** Estimation of f1 and Similarity f2 of TC1-TC3

Formulations	f1	f2	Observation
TC1	34	49.25	Dissimilar
TC2	3	68	Similar
TC3	2.4	80.5	Similar

**IVDR kinetic study**

The TC3 exhibits a non-Fickian transport mechanism and KP release kinetics, as shown from the kinetic. TC3 was determined to be the optimal formulation among the three developed formulations. The R<sup>2</sup> values were 0.953, 0.912, 0.986, 0.999, and 0.987 for the zero-order, first-order, Higuchi, KP, and

Hixson-Crowell models, respectively. In comparison to other models, it was discovered that the KP model had the highest R<sup>2</sup> value due to its excellent linearity. It therefore adheres to KP kinetics. The KP model's release exponent for the TC3 formulation was found to be 0.650, which appears to support Non-Fickian diffusion. It is shown in Table 7.

**Table 7.** Fitting of IVDR data in various mathematical models

Models	Zero-order		First-order		Higuchi		KP			Hixson-Crowell	
	Batches	R <sup>2</sup>	K <sub>0</sub>	R <sub>1</sub> <sup>2</sup>	K <sub>1</sub>	R <sub>H</sub> <sup>2</sup>	K <sub>H</sub>	R <sub>K</sub> <sup>2</sup>	Kp	N	R <sup>2</sup>
TC1	0.991	2.738	0.933	0.059	0.941	15.35	0.975	5.61	0.785	0.972	0.069
TC2	0.932	3.088	0.989	0.092	0.979	18.19	0.977	10.77	0.654	0.992	0.094
TC3	0.953	3.199	0.912	0.126	0.986	18.71	0.999	11.15	0.650	0.987	0.111

**ASS**

ASS was determined for TC3. It was noted that no discernible alterations had occurred to optimized batch's weight variation, physical appearance, friabili-

ty, drug content etc. There was no significant ( $p < 0.05$ ) difference between TC3 accelerated values vs. initial values of TC3 parameters. Hence it was confirmed that TC3 was found to be stable. Table 8 displays it.

**Table 8.** Comparative physicochemical analysis of TC3

Parameters	Initial	Following thirty days	Following sixty days	Following ninety days
Physical appearance	White, circular, and concave smooth surface	Nothing alters	Nothing alters	Nothing alters
Thickness (mm) $\pm$ S.D (n = 10)	6.5 $\pm$ 0.47	6.5 $\pm$ 0.47	6.5 $\pm$ 0.47	6.4 $\pm$ 0.47
Hardness (kg/cm <sup>2</sup> ) $\pm$ S.D (n = 10)	3 $\pm$ 0.11	3 $\pm$ 0.11	3 $\pm$ 0.11	3 $\pm$ 0.11
Friability (%) $\pm$ S.D (n = 20)	0.10 $\pm$ 0.001	0.10 $\pm$ 0.001	0.10 $\pm$ 0.001	0.9 $\pm$ 0.001
Weight variation (%) $\pm$ S.D (n = 20)	3.53 $\pm$ 0.017	3.53 $\pm$ 0.017	3.52 $\pm$ 0.017	3.51 $\pm$ 0.017
Drug content (%) $\pm$ S.D (n = 10)	99.12 $\pm$ 1.25	99.12 $\pm$ 1.25	99.12 $\pm$ 1.25	98.12 $\pm$ 1.25
Disintegration time (min) $\pm$ S.D (n = 10)	2.20 $\pm$ 0.16	2.20 $\pm$ 0.16	2.19 $\pm$ 0.22	2.19 $\pm$ 0.23

**N.B.** Every value is presented as mean  $\pm$  S.D.

**CONCLUSION**

According to the current study's findings, LST shows great promise in enhancing the dissolving of medications that are difficult to dissolve, such as TLS. It was discovered that the LST made with Aerosil 200 and MCC was a superior product, exhibiting an enhanced dissolution profile and satisfactory tableting qualities. When compared to commercial tablets, IVDS showed an improvement in dissolution from LST tablets. The medication and excipients did not interact, according to the FTIR spectra. According to stability experiments, aging did not affect the LS formulation's capacity to dissolve. Ultimately, it may be said that TC3's LST can more effectively lessen the adverse effects of traditional tablets.

**ACKNOWLEDGEMENTS**

The authors thank the College of Pharmaceutical Sciences, Puri, Odisha, India, Pharmaceutics Department, for providing the facilities needed to conduct the research.

**AUTHOR CONTRIBUTION STATEMENT**

Chinmaya Keshari Sahoo (CKS) gave the concept and idea for research, Nidhi Shree (NS) performed the literature survey and research work. CKS, and Amiyakanta Mishra (AKM) reviewed the research data, manuscript, and approved the final version.

**CONFLICT OF INTEREST**

The authors declare that there is no conflict of interest.

**REFERENCES**

- Balakrishnan, P., Le, B., Oh, DH., Kim, JO., Hong, MJ., Jee, J., Kim, JA., Yoo, BK., Woo, JS., Yong, CS., Choi, H. (2009). Enhanced oral bioavailability of dexibuprofen by a novel solid self-emulsifying drug delivery system (SEDDS). *European Journal of Pharmaceutics and Biopharmaceutics*, 72, 539–545.

- Barzegar, JM., Javadzadeh, Y., Nokhodchi, A., Siahi-Shadbad, MR. (2005). Enhancement of dissolution rate of piroxicam using liquisolid compacts. *Il Farmaco*, 60(4), 361-365.
- El-Houssieny, BM., Wahman, LF., Arafa, NMS. (2010). Bioavailability and biological activity of liquisolid compact formula of repaglinide and its effect on glucose tolerance in rabbits. *BioScience Trends*, 4(1), 17-24.
- Gandhi, GS., Dharmendra, R., Mundhada, BS. (2011). Levocetirizine orodispersible tablet by direct compression method. *Journal of Applied Pharmaceutical Science*, 1(5), 145-150.
- ICH Harmonized Tripartite Guidelines, (2003). Stability testing of New Drug Substances and Products. *Q1A (R2)*.
- Jadhav, SB., Kaudewar, DR., Kaminwar, GS., Jadhav, AB., Kshirsagar, RV., Skarkar, DM. (2011). Formulation and evaluation of dispersible tablets of Diltiazem hydrochloride. *International Journal of PharmTech Research*, 3(3), 1314-21.
- Jarowski, CI., Rohera, BD., Spireas, S. (1992). Powdered solution technology: principles and mechanism. *Pharmaceutical Research*, 9, 1351-1358.
- Javadzadeh, Y., Siahi, MR., Asnaashari, S., and Nokhodchi, A. (2007). Liquisolid technique as a tool for enhancement of poorly water-soluble drugs and evaluation of their physicochemical properties. *Acta Pharmaceutica*, 57, 99-109.
- Jaydip, B., Dhaval, M., Soniwala, MM., Chavda, J. (2020). Formulation and optimization of liquisolid compact for improving the dissolution profile of efavirenz by using DoE approach. *Saudi Pharmaceutical Journal*, 28, 737-745.
- Kalbhor, MG., Deshmukh, MA., Tilak, P. (2020). Dissolution enhancement of telmisartan by liquisolid compact. *World Journal of Pharmacy and Pharmaceutical Sciences*, 9(9), 1721-1736.
- Kapsi, SG., Ayres, JW., (2001). Processing factors in development of solid solution formulation of itraconazole for enhancement of drug dissolution and bioavailability. *International Journal of Pharmaceutics*, 229, 193-203.
- Kasturi, M. Malviya, N. (2021). Formulation and evaluation of liquisolid compacts of BCS class II drug ketoprofen. *Journal of Pharmaceutical Research International*, 33(45B), 322-334.
- Kavitha, K., LovaRaju, KNS., Ganesh, NS., Ramesh, B. (2011). Effect of dissolution rate by liquisolid compacts approach: An overview. *Der Pharmacia Lettre*, 3, 71-83.
- Kolatkar, G., Zisman, E. (2007, 2005). Pharmaceutical compositions of telmisartan. *USA Patent US20070116759A1*.
- Li, DX., Oh, Y., Lim, S., Kim, JO., Yang, HJ., Sung, JH., Yong, CS., Choi, H. (2008). Novel gelatin microcapsule with bioavailability enhancement of ibuprofen using spray-drying technique. *International Journal of Pharmaceutics*, 355, 277-284.
- Merisko-Liversidge, E., Liversidge, GG., Cooper, ER. (2003). Nanosizing: a formulation approach for poorly-water-soluble compounds. *European Journal of Pharmaceutical Sciences*, 2, 113-120.
- Milam, P., Jayavadan, KP. (2013). Analytical method for determination of telmisartan: An overview. *International journal of Pharmacy and Pharmaceutical Sciences*, 5(1), 17-22.
- Millard, JW., Alvarez-Núñez, FA., Yalkowsky, SH. (2002). Solubilization by cosolvents establishing useful constants for the log-linear model. *International Journal of Pharmaceutics*, 245, 153-166.
- Mishra, S., Singh, S., Verma, N. (2023). Telmisartan liquisolid compact formulation development for enhanced aqueous solubility. *European Chemical Bulletin*, 12(6), 7175-7184.
- Nagabandi, VK., Ramarao, T., Jayaveera, KN. (2011). Liquisolid compacts: A novel approach to enhance bioavailability of poorly soluble drugs. *International Journal of Pharmacy and Biological Sciences*, 1, 89-102.
- Nighute, AB., Bhise SB. (2009). Enhancement of dissolution rate of Rifabutin by preparation of microcrystals using solvent change method. *International Journal of PharmTech Research*, 1, 142-148.
- Naureen, F., Shah, Y., Shah, SI., Abbas, M., Rehman, IU., Muhammad, S., Hamdullah, Goh, KW., Khuda, F., Khan, A., Chan, SY., Mushtaq, M., Ming, LC. (2022). Formulation development of mirzapine liquisolid compacts: optimization using central composite design. *Molecules*, 27, 4005.
- Nokhodchi, A., Hentzschel, CM., Leopold, CS. (2011). Drug release from liquisolid system: speed it up, slow it down. *Expert Opinion on Drug Delivery*, 8, 191-205.

- Peddi, MG., (2013). Novel Drug Delivery System: Liquid Solid Compacts. *Journal of Molecular Pharmaceutics & Organic Process Research*, 1, 3.
- Padmavathi, M., Reshma, MSR., Sindhuja, YV., Venkateshwararao, KCh., Nagaraju, K. (2013). Spectrometric Methods for Estimation of TLS Bulk Drug and its Dosage Form. *International Journal of Research in Pharmacy and Chemistry*, 3(2), 320-325.
- Patil, A., Kauthankar, B., Kavatagimath, S., Masaredy, R., Dandagi, P. (2022). Central composite design for the development and evaluation of liquisolid compacts of glyburide. *Indian Journal of Pharmaceutical Education and Research*, 56, 56.
- Rani, M., Mishra B. (2004). Comparative in vitro and in vivo evaluation of matrix, osmotic matrix, and osmotic pump tablets for controlled delivery of diclofenac sodium. *AAPS PharmSciTech*, 5(4), 1-7.
- Saeedi, M., Akbari, J, Enayatifard, R., Semnani, KM., Hashemi, SMH., Babaei, A., Mashhadi, SA., Eghbali, M. (2021). Liquisolid tablet: an effective approach towards improvement of dissolution rate of famotidine as poorly soluble drugs. *International Journal of Pharmaceutical Sciences and Research*, 12(2), 803-812.
- Sahoo, CK., Rao, SRM.,Sudhakar, M., and Kokkula, S. (2015). The kinetic modeling of drug dissolution for drug delivery systems: an overview. *Der Pharmacia Lettre*. 7(9), 186-194.
- Sangwai, M., and P. Vavia, P. (2013). Amorphous ternary cyclodextrin nanocomposites of telmisartan for oral drug delivery: improved solubility and reduced pharmacokinetic variability. *International Journal of Pharmaceutics*, 453(2), 423-432.
- Senthil, A., Sivakumar, T., Narayanaswamy, VB., Ashish, SP., Viral, GP. (2011). Formulation and evaluation of Metoprololtartarate by direct compression using super disintegrants. *International Journal of Research in Ayurveda and Pharmacy*, 2(1), 224-29.
- Spireas, S., (2002). Liquisolid system and method of preparing same. *US Patent*, 6423339B1.
- Spireas, S., Bolton, SM. (1999). Liquisolid systems and methods of preparing same. *US5968550*.
- Suthar, M., Raval, A., Patel, R., Dr. Patel, L. (2016). Formulation and Evaluation of Immediate Release Tablet of Rosuvastatin Calcium by Liquisolid Compact Technique. *Journal of Biological Sciences*, 2(5), 18-35.
- Swamy, NGN., Shiny, EK. (2013). Formulation and Evaluation of Telmisartan Liquisolid Tablets. *RGUHS Journal of Pharmaceutical Sciences*, 3, 49-57.
- Tanino, T., Ogiso, T., Iwaki, M., Tanabe, G., and Muraoka, O. (1998). Enhancement of oral bioavailability of phenytoin by esterification, and in vitro hydrolytic characteristics of prodrugs. *International Journal of Pharmaceutics*, 163, 91-102.
- Tatane, S. (2011). Development of UV spectrophotometric method of telmisartan in tablet formulation. *Journal of Advances in Pharmacy and Healthcare Research*, 1, 23-6.
- The USP 26-National Formulary 21 Rockville MD *US Pharmacopoeial Convention 2003*.
- Tiong, N., Elkordy, AA. (2009). Effects of liquisolid formulations on dissolution of naproxen. *European Journal of Pharmaceutics and Biopharmaceutics*, 73,373-384.
- Tiwari, D., Sharma, V., Soni, SL. (2021). Formulation and in-vitro evaluation of oxcarbazepine liquisolid compacts. *Asian Journal of Pharmaceutical Research and Development*, 9(1), 71-77.
- Tran, PHL., Tran, HTT., and Lee, BJ. (2008). Modulation of microenvironmental pH and crystallinity of ionizable Telmisartan using alkalizers in solid dispersions for controlled release. *Journal of Controlled Release*, 129(1), 59-65.
- Wienen, W., Entzeroth, M., Van Meel, JCA. (2000). A review on telmisartan: a novel, long-acting angiotensin II-receptor antagonist. *Cardiovascular Drug Reviews*, 18(2), 127- 156.
- Yadav, AV., Shete, AS., Dabke, AP. (2010). Formulation and evaluation of orodispersible liquid solid compacts of aceclofenac. *Indian Journal of Pharmaceutical Education and Research*, 44, 227-235.

# Antihypertensive Drug Box Sales Between January 2019 - June 2024 in Turkish Drug Market: Investigating the Drug Group and Fix-Dose Combination Sales

Elif Hilal VURAL<sup>\*</sup>, Bülent GÜMÜŞEL<sup>\*\*</sup>

*Antihypertensive Drug Box Sales Between January 2019 - June 2024 in Turkish Drug Market: Investigating the Drug Group and Fix-Dose Combination Sales*

## SUMMARY

The financial and emotional burden of chronic diseases, including hypertension, has been rising. The objective of this study was to assess the trends in box sales of antihypertensive medications in Türkiye and to compare these trends across the antihypertensive medicine subgroups. This study analyzed retail and hospital box sales of antihypertensive drug groups recommended by guidelines between January 2019 and June 2024. The data used in this study were obtained from IQVIA. While antihypertensive drugs sold a total of 176,453,254 boxes in 2019, they were sold 203,690,099 boxes in 2023, a 15.44% increase. The best-selling drug group is the Renin-Angiotensin System (RAS) antagonists. Angiotensin Receptor Blocker-Diuretic fixed-dose combination (FDC) is the best-selling subgroup in the RAS antagonists. FDCs of RAS antagonists are more often used than their mono forms, and in 2022 and 2023, FDCs of calcium channel blockers have begun to outsell their combined formulations. Triple FDCs of the RAS antagonists with calcium channel blockers and diuretics have been increasing regularly. In Türkiye, drug groups that have had the highest share in the antihypertensive drug market in recent years are the groups recommended in the guidelines. Increasing the triple FDC consumption is valuable for the rational treatment of hypertension.

**Key Words:** Antihypertensive drugs; Rational drug use; box sales; Fixed-dose combination.

*Türkiye İlaç Pazarında Ocak 2019 - Haziran 2024 Arası Antihipertansif İlaç Kutusu Satışları: İlaç Grubu ve Sabit Doz Kombinasyon Satışlarının Araştırılması*

## ÖZ

Hipertansiyonun da içinde bulunduğu kronik hastalıkların finansal ve duygusal yükü artmaktadır. Bu çalışmanın amacı Türkiye'de antihipertansif ilaçların kutu satış eğilimlerini değerlendirmek ve bu eğilimleri antihipertansif ilaç alt grupları arasında karşılaştırmaktır. Bu çalışmada Ocak 2019 ile Haziran 2024 arasındaki kılavuzlarda önerilen antihipertansif ilaç gruplarının perakende ve hastane kutu satışları analiz edildi. Bu çalışmada kullanılan veriler IQVIA'dan elde edildi. Antihipertansif ilaçlar 2019 yılında toplam 176.453.254 kutu satarken, 2023 yılında %15,44 artarak 203.690.099 kutu satıldı. En çok satan ilaç grubu Renin-Anjiyotensin Sistem (RAS) antagonistleridir. RAS antagonistleri içinde en çok satan alt grup Anjiyotensin Reseptör Blokörü-Diüretik sabit doz kombinasyonudur (SDK). RAS antagonistlerinin SDK'ları mono formlarından daha sık kullanılmaktadır ve 2022 ve 2023'te kalsiyum kanal blokörlerinin SDK'ları da kombine formülasyonlarından daha fazla satmaya başlamıştır. RAS antagonistlerinin kalsiyum kanal blokörleri ve diüretiklerle üçlü SDK'ları düzenli olarak artmaktadır. Türkiye'de son yıllarda antihipertansif ilaç pazarında en yüksek paya sahip olan ilaç grupları kılavuzlarda önerilen gruplardır. Üçlü SDK tüketiminin artması hipertansiyonun rasyonel tedavi uygulamaları açısından değerlidir.

**Anahtar Kelimeler:** Antihipertansif ilaçlar; Akılcı ilaç kullanımı; kutu satışları; Sabit doz ilaç kombinasyonu.

Received: 12.11.2024

Revised: 01.12.2024

Accepted: 13.01.2025

<sup>\*</sup> ORCID: 0000-0003-1309-6606, Lokman Hekim University, Faculty of Medicine, Department of Medical Pharmacology, Ankara, Türkiye

<sup>\*\*</sup> ORCID: 0000-0002-7533-7949, Istanbul Okan University, Faculty of Pharmacy, Department of Pharmacology, Istanbul, Türkiye

## INTRODUCTION

In the last decades, the increase in the geriatric population has raised the concern of many chronic diseases in terms of the burden of disease and financial aspects. Currently, chronic diseases such as hypertension, diabetes, and coronary heart disease have been causing significant financial and emotional burdens (Sağlık Teknolojileri Değerlendirme Raporu 3). The World Health Organization (WHO) states that cardiovascular diseases cause nearly 18 million deaths worldwide each year. A significant portion of these deaths are due to heart attacks and strokes (WHO, 2021). In 2021, 28% of the total deaths in OECD countries were due to circulatory system diseases (ischemic heart disease 11%, stroke 6%), while this rate was 35% in Türkiye (ischemic heart disease 15%, stroke 7%) (Health Statistics Yearbook 2022). WHO estimates that approximately 1.28 billion adults aged 30-79 worldwide, most of whom (two-thirds) live in low- and middle-income countries, have hypertension (WHO, 2023). It is seen that the primary health problem experienced by individuals aged fifteen and over in 2022 is hypertension, with a rate of 16.1%, after waist and neck problems (Health Statistics Yearbook 2022). According to a prevalence study published in 2021, more than one-third of the adult population in Türkiye suffers from hypertension. (Bayram et al., 2021).

According to the data of the Ministry of Health, a total of 2,268.5 million boxes of medicine were sold in Türkiye in 2017, while this number reached 2,643.2 million in 2022. The sales volume of cardiovascular system drugs was 225.9 million boxes in 2017, while it was 291 million boxes in 2022. In other words, while the total box increase was 17%, it was 29% for cardiovascular system drugs in that period. When the amount of medicine consumed per 1000 people was investigated, it was seen that the consumption of cardiovascular system drugs increased from 176.4 to 232.6 between those years (Health Statistics Yearbook 2022).

Various drug groups with different pharmacological mechanisms of action are used in the treatment of hypertension. These drug groups include diuretics (thiazide diuretics, potassium-sparing diuretics, loop diuretics), those that block angiotensin production or affect Angiotensin Receptor Blockers (ARB), Angiotensin Converting Enzyme (ACE) inhibitors, renin inhibitors, sympatholytics (alpha-blockers, beta-blockers, adrenergic neuron blockers, ganglion blockers) and vasodilators (calcium channel blockers, other direct-acting vasodilators) (Benowitz, 2018). Some of these drugs are recommended in the guidelines for the first-stage pharmacotherapy of hypertension. Although there are some differences between these guidelines, ACE inhibitors, ARBs, calcium channel blockers (some guidelines recommend dihydropyridines which are vasoselective calcium channel blockers), and diuretics (thiazide group diuretics, some guidelines also recommend potassium-sparing diuretics) are recommended as first-line hypertension pharmacotherapy. Beta-blockers are also recommended as first-line treatment in patients with ischemic heart disease or in patients who want to manage heart rate (Arıcı et al., 2015; Whelton et al., 2018; Guideline for the pharmacological treatment of hypertension in adults, 2021; Hipertansiyon Tanı Ve Tedavi Kılavuzu, 2022; McEvoy et al., 2024). In addition, the effectiveness and safety of fixed-dose combinations of these antihypertensive drugs have been demonstrated, and WHO included these drugs in the essential medicines list in 2019 (Salam et al., 2020).

In this study, we aimed to evaluate the box sales trends of essential drugs recommended in national and international guidelines for treating hypertension in Türkiye according to drug groups and subgroups and to compare these trends among themselves and with total cardiovascular system drug sales trends.

## MATERIAL AND METHOD

This study analyzed retail and hospital box sales of antihypertensive drug groups recommended by national and international guidelines. The data used

in this study were obtained from IQVIA. IQVIA is a global pharmaceutical consultancy company that collects sales and price data of medicines from many different countries. The company collects data from the pharmaceutical market supply and distribution chain. The IQVIA data used herein includes the number of boxes sold from wholesalers for the selected sample of medical preparations for 66 months between January 2019 and June 2024. The data includes 3-month periods starting from the first quarter of 2019 and ending in the second quarter of 2024. Thus, 22 time points were used in the study. In addition, box sales data for 5 years between 2019 and 2023 were used as annual box sales. The data were provided by IQVIA as monthly drug box sales, indicating the active ingredients and Anatomical Therapeutic Chemical (ATC) groups. ATC is a system for the categorization of pharmaceutical active ingredients based on their effects on the organs or systems (ATC/DDD Toolkit). In the study, the pharmaceuticals were grouped according to ATC groups and active ingredients. The data does not contain any patient or personal information or prescription information.

First, cardiovascular system drugs (Class C according to ATC classification) were grouped at the ATC3 level and annual box sales volume between 2019-2023 was calculated. Data for double and triple fixed-dose combination pharmaceuticals containing active ingredients from different groups have been included only under the drug groups they are classified within the ATC system. Data for cerebral and peripheral vasotherapeutic drugs, topical antihemorrhoid drugs, and medications used in the treatment of pulmonary arterial hypertension were excluded from the study.

Then, the annual box sales data of antihypertensive drugs between 2019 and 2023 were examined. The data of drug groups included in national and international guidelines as antihypertensive drugs were examined within the framework of ATC4 level classification (Arıcı et al., 2015; Whelton et al., 2018; Guideline for the pharmacological treatment of hyper-

tension in adults, 2021; Hipertansiyon Tani Ve Tedavi Kılavuzu, 2022; McEvoy et al., 2024). The antihypertensive drug groups whose sales data were examined were ACE inhibitors, ARBs, calcium channel blockers, beta-blockers, centrally acting sympatholytics, other peripherally acting sympatholytics, thiazide group diuretics, and potassium-sparing diuretics. In addition to the mono forms of these drugs, their fixed-dose combination forms were also examined as separate subgroups. The fixed-dose combination subgroups are ACE inhibitors + diuretics, ACE inhibitors + calcium channel blockers, ARB + diuretics, ARB + calcium channel blockers, ARB + neprilysin inhibitors, calcium channel blockers + statins, thiazide + potassium-sparing diuretics and beta blockers + diuretics in two drug fixed-dose combinations, and ACE inhibitors + calcium channel blockers + diuretics and ARB inhibitors + calcium channel blockers + diuretics in triple-drug fixed-dose combinations.

The box sales data of diuretics, drugs that block angiotensin production or effect (ARB and ACE inhibitors), beta-blockers, and calcium channel blockers were examined independently. These four groups were classified separately according to their mono and fixed-dose combination, and the 3-month box sales data between the first quarter of 2019 and the second quarter of 2024, change rates, and the amounts of medical preparations in these groups were shared separately.

The changes in the total sales volume data of the drugs examined in the study were compared with the sales volume changes of cardiovascular system drugs in the same period. In this study, grouping, addition, and percentage calculations were performed using Microsoft Excel. Additionally, graphs and tables were created with Microsoft Excel.

## RESULTS AND DISCUSSION

While cardiovascular system drugs sold a total of 225,038,590 boxes in 2019, it increased by 18.10% and sold 265,766,918 boxes in 2023. Below are box sales for cardiovascular system medication classes at the ATC3 level from 2019 to 2023 (Table 1).

**Table 1.** Box sales for cardiovascular system medication classes at the ATC 3 level between 2019-2023.

Drug Groups (ATC3 Level)	2019	2020	2021	2022	2023
Cardiac Glycosides	685,330	694,589	709,389	658,176	576,250
Antiarrhythmics	2,478,259	2,387,156	2,602,548	3,036,789	2,949,973
Other Vasodilators Used in Cardiac Diseases (excluding nitrates, calcium canal blockers, renin-angiotensin system inhibitors)	8,401,191	9,383,448	9,630,685	9,110,695	8,893,443
Nitrites and Nitrates	4,330,763	4,498,612	4,166,555	4,053,054	3,786,499
Cardiac Stimulants (excluding cardiac glycosides)	84,090	80,810	110,709	94,500	99,471
Other Antihypertensives (Central and Peripheral Effects)	4,154,420	4,415,927	4,354,237	5,002,136	5,290,594
Diuretics (mono and fixed-dose combination)*	15,229,910	16,001,615	16,286,815	15,311,724	15,949,625
Beta Blockers (mono and fixed-dose combination)*	60,543,231	65,598,097	67,151,393	67,979,337	70,110,291
Calcium Canal Blockers (mono and fixed-dose combination)*	19,525,661	21,304,975	21,148,323	20,891,310	21,146,152
Angiotensin Converting Enzyme Inhibitors (mono and fixed-dose combination)*	37,194,441	40,861,750	42,420,237	43,293,906	43,764,708
Angiotensin Receptor Blockers (mono and fixed-dose combination)*	49,635,836	55,163,416	53,396,957	57,628,803	58,367,238
Cholesterol and Triglyceride Regulators (mono)	22,710,158	28,143,144	30,264,136	34,448,434	34,603,590
Cholesterol and Triglyceride Regulators (fixed-dose combination)	0	0	4,268	88,761	173,076
Cholesterol and Triglyceride Regulators (fixed-dose combinations with other groups)*	65,300	69,567	71,711	65,579	56,008
<b>TOTAL</b>	<b>225,038,590</b>	<b>248,603,106</b>	<b>252,317,963</b>	<b>261,663,204</b>	<b>265,766,918</b>

\* Data for double and triple fixed-dose combination pharmaceuticals containing active ingredients from different groups have been included only in the drug groups they are included in the ATC classification

Among the antihypertensive drug groups whose sales data were investigated, box sales of ACE inhibitors increased by 17.67% in 2023 compared to 2019, while ARBs increased by 17.59%. The increase rate for this period was 8.30% for calcium channel blockers, 15.80% for beta blockers, and 4.73% for diuretics. The following table presents the sales of antihypertensive medications from 2019 to 2023, which were examined by categorizing them at the ATC4 level by national and international norms (Table 2).



**Table 2.** Box sales for antihypertensive medications at the ATC4 level between 2019 – 2023.

Drug Groups (ATC4 Level)	2019	2020	2021	2022	2023
Potassium-Sparing Diuretics (mono)	458,448	513,015	516,805	567,169	619,750
Thiazide Group Diuretics (mono)	3,129,853	3,302,538	3,251,199	2,957,196	2,834,971
Potassium-Sparing Diuretics+Thiazide Group Diuretics (Fixed-Dose Combination)	1,713,848	1,550,639	1,527,162	1,499,500	1,473,525
Vasopressin Antagonist Diuretics (mono)	32,216	72,456	99,237	8,791	26,862
Centrally Acting Sympatholytics (mono)	521,857	524,883	458,251	482,232	479,470
Peripherally Acting Sympatholytics (excluding beta blockers) (mono)	3,632,563	3,891,044	3,895,986	4,519,904	4,811,124
Beta Blockers (mono)	58,826,819	63,632,381	64,943,282	65,614,292	67,418,808
Beta Blockers+Diuretics (Fixed-Dose Combination)	1,716,412	1,965,716	2,208,111	2,365,045	2,691,483
Calcium Channel Blockers (mono)	19,525,661	21,304,975	21,148,323	20,891,310	21,146,152
Calcium Channel Blockers+Statines (Fixed-Dose Combination)	65,300	69,567	71,711	65,579	56,008
Angiotensin Converting Enzyme Inhibitors (mono)	13,335,618	14,412,486	14,782,213	15,134,327	15,163,892
Angiotensin Converting Enzyme Inhibitors+ Diuretics (Fixed-Dose Combination)	15,339,761	16,281,795	16,425,520	16,177,343	15,931,795
Angiotensin Converting Enzyme Inhibitors+ Calcium Channel Blockers (Fixed-Dose Combination)	7,092,512	8,127,127	8,525,833	8,498,466	8,849,164
Angiotensin Converting Enzyme Inhibitors+ Calcium Channel Blockers+ Diuretics (Fixed-Dose Combination)	1,426,550	2,040,342	2,686,671	3,483,770	3,819,857
Angiotensin Receptor Blockers (mono)	9,005,003	10,246,494	9,860,478	11,158,966	10,803,069
Angiotensin Receptor Blockers+Diuretics (Fixed-Dose Combination)	34,036,946	37,138,626	35,273,668	35,867,229	35,394,639
Angiotensin Receptor Blockers+ Calcium Channel Blockers (Fixed-Dose Combination)	5,826,507	6,576,560	6,610,773	7,661,228	8,128,012
Angiotensin Receptor Blockers+ Calcium Channel Blockers+ Diuretics (Fixed-Dose Combination)	688,554	1,093,796	1,501,926	2,737,964	3,795,568
Angiotensin Receptor Blockers+ Nephilysin Inhibitors (Fixed-Dose Combination)	78,826	107,940	150,112	203,416	245,950
<b>TOTAL</b>	<b>176,453,254</b>	<b>192,852,380</b>	<b>193,937,261</b>	<b>199,893,727</b>	<b>203,690,099</b>

While antihypertensive drugs sold a total of 176,453,254 boxes in 2019, they increased by 15.44% and sold 203,690,099 boxes in 2023. The 3-month box sales data of antihypertensive drug groups between the first quarter of 2019 and the second quarter of 2024 are shared in Figure 1. The best-selling drug group in all quarters examined in the study of drugs that inhibit the Renin-Angiotensin System is the ARB-Diuretic fixed-dose combinations (Figure 1). The sales rate of ARB-Diuretic fixed-dose combination in all drug groups that inhibit the Renin-Angiotensin System was 38.85% in the first quarter, while it was 32.30% in the last quarter. In this

group, mono and fixed-dose combination pharmaceuticals of ACE inhibitor drugs were sold at a total rate of 43.54% in the first quarter and 43.80% in the last quarter.

In contrast, ARB mono and fixed-dose combination pharmaceuticals were sold at a rate of 56.46% in the first quarter and 56.20% in the last quarter. Investigations on the use of mono and fixed-dose combination medicines revealed that the sales of mono medications in this category (ARB+ACE inhibitors) were 25.98% in the first quarter and 25.35% in the last. In the first quarter, the fixed-dose combination pharmaceutical sales rates of ACE inhibitors and ARBs were 74.02%; in the last quarter, they were 74.65%. When

the sales rates of fixed-dose combination pharmaceuticals were investigated among themselves, it was seen that the triple-drug fixed-dose combination pharmaceuticals of ACE inhibitors (ACE inhibitor + Calcium channel blocker + Diuretic combination) sold at a rate of 5.27% in the first quarter. In comparison, the sales rate increased to 15.74% in the last quarter. Similarly, it is seen that the triple-drug fixed-dose combination pharmaceuticals of ARBs (ARB + Calcium channel blocker + Diuretic combination) sold at a rate of 1.51% in the first quarter, while the sales rate increased to 11.21% in the last quarter. The usage rates of two and triple-drug fixed-dose combination pharmaceuticals of ACE inhibitors and ARBs between 2019-2023 are shared in Figure 2.

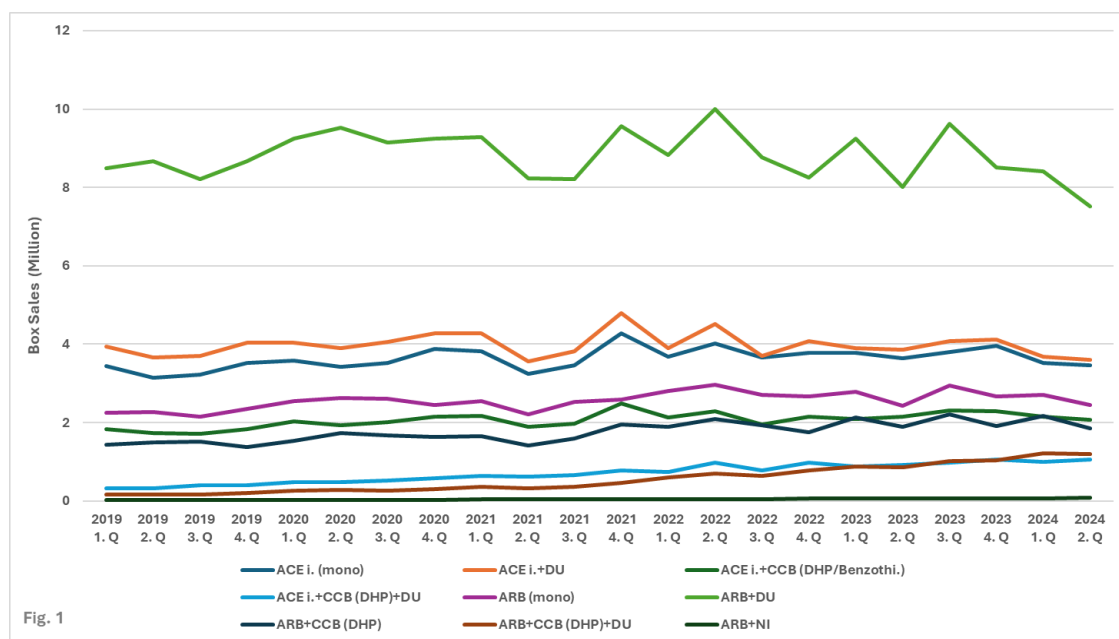


**Figure 1.** Box Sales of Drugs Acting on the Renin-Angiotensin System (Both Mono and Fixed-dose Combinations)

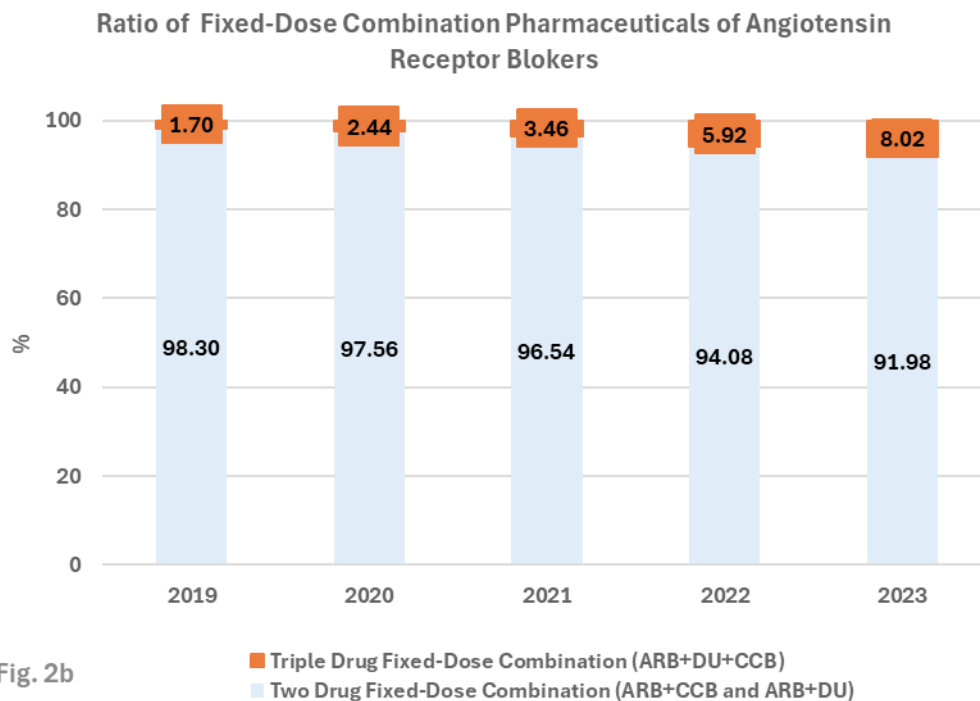
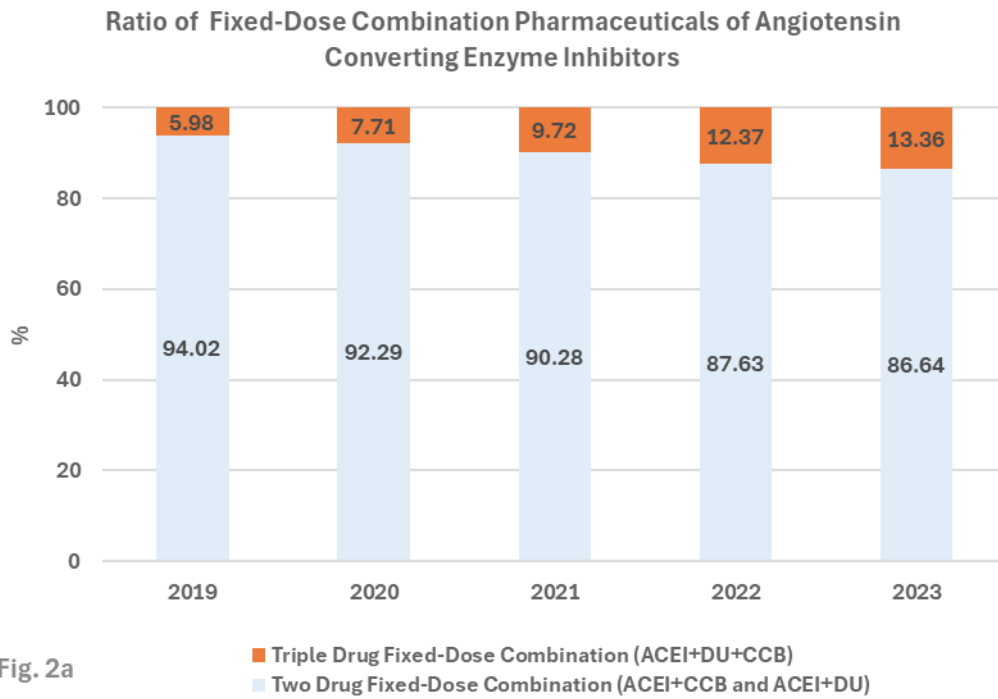


**Figure 2a.** Ratio of Fixed-Dose Combination Pharmaceuticals of Angiotensin Converting Enzyme Inhibitors

**Figure 2b.** Ratio of Fixed-Dose Combination Pharmaceuticals of Angiotensin Receptor Blockers

Dihydropyridine derivative medications were the best-selling mono calcium channel blocker pharmaceuticals across all research quarters (Figure 3). While the sales rate of mono dihydropyridine derivative calcium channel blockers in all calcium channel blocker groups was 45.18% in the first quarter, it was 36.89% in the last quarter. This group's overall sales rate for mono and fixed-dose combination medications containing dihydropyridine derivatives was 82.73% in the first quarter and 89.00% in the last. In contrast, sales of benzothiazepine mono and fixed-dose combination medications were 15.61% in the first quarter and 10.15% in the last. Phenylalkylamine derivatives, on the other hand, sold at a rate of 0.85% in the most recent quarter and 1.66% in the first. According to calculations, the overall sales rates of calcium channel blocker fixed-dose combination medications were 43.15% in the first quarter and 56.11% in the last. When the sales rates of fixed-dose combination pharmaceuticals were examined among themselves, it was seen that the triple-drug fixed-dose combination pharmaceuticals of dihydropyridine derivative calcium channel blockers (ACE inhibitor + Calcium Channel Blocker + Diuretic Combination and ARB + Calcium Channel Blocker) sold at a rate of 12.58% in the first quarter. In comparison, the sales rate increased to 36.35% in the last quarter.

Among diuretic pharmaceuticals, thiazides were the best-selling drug group in all quarters investigated (Figure 4). When all the fixed-dose combinations and mono forms were analyzed, ARB-Diuretic fixed-dose combinations were the best-selling drug subgroup. In the first quarter, the sales rate of ARB-Diuretic fixed-dose combinations across all diuretic medication groups was 57.71%; however, in the final quarter, it dropped to 49.84%. It was determined that the overall sales rate of diuretic fixed-dose combination medications was 93.64% in the first quarter and 94.98% in the last. When the sales rates of fixed-dose combination drugs are examined among themselves, it was seen that the triple-drug fixed-dose combinations of diuretics (ACE inhibitor + Calcium Channel Blocker + Diuretic Combination and ARB + Calcium Channel Blocker + Diuretic Combination) sold at a rate of 3.54% in the first quarter. In comparison, the sales rate increased to 16.43% in the last quarter.

Cardioselective beta-blockers are the best-selling class of beta-blocker medications throughout all study quarters (Figure 5). Cardioselective beta-blockers were sold at a rate of 78.85% in the first quarter and 81.71% in the last quarter across all beta-blocker medication categories. According to calculations, the overall sales rate of beta-blocker fixed-dose combinations was 2.96% in the first quarter and 3.64% in the last quarter.

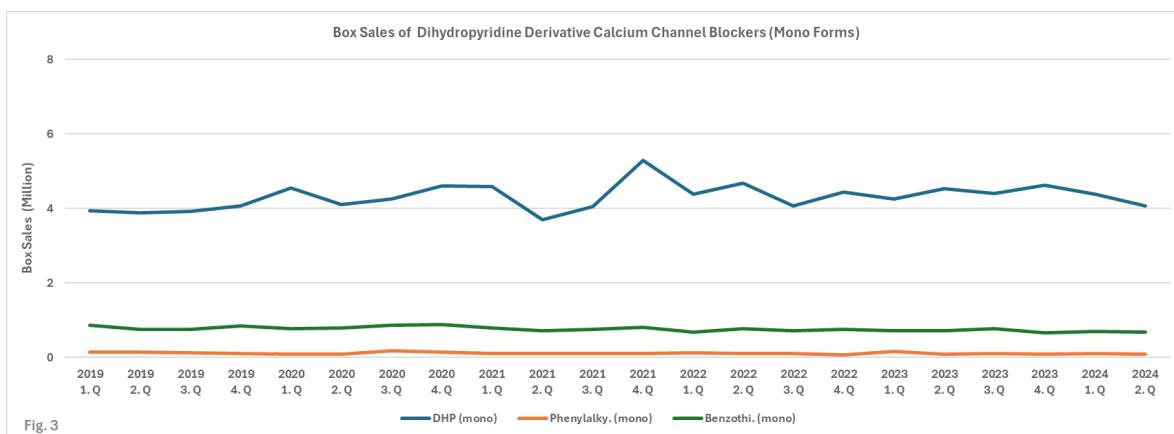


**Figure 3.** Box Sales of Dihydropyridine Derivative Calcium Channel Blockers (Both Mono and Fixed-dose Combinations)

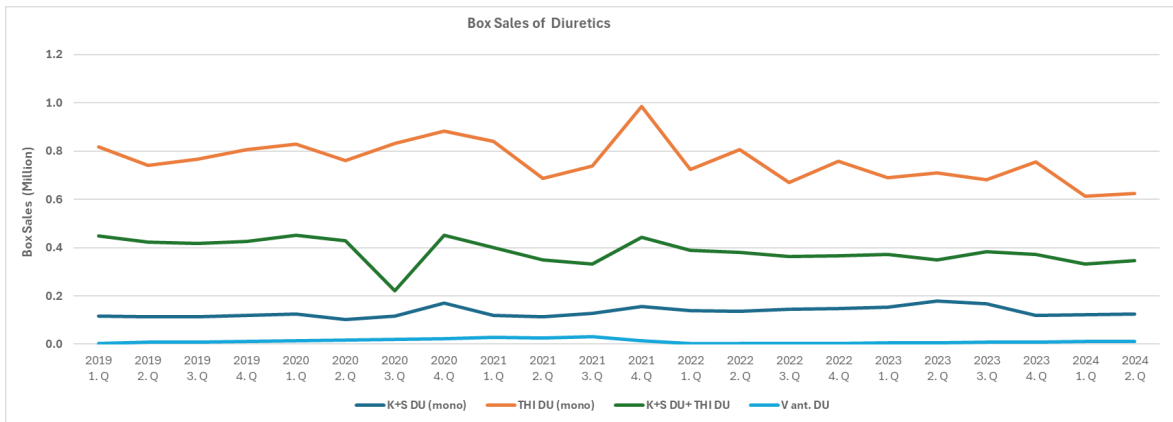


Figure 4. Box Sales of Diuretics

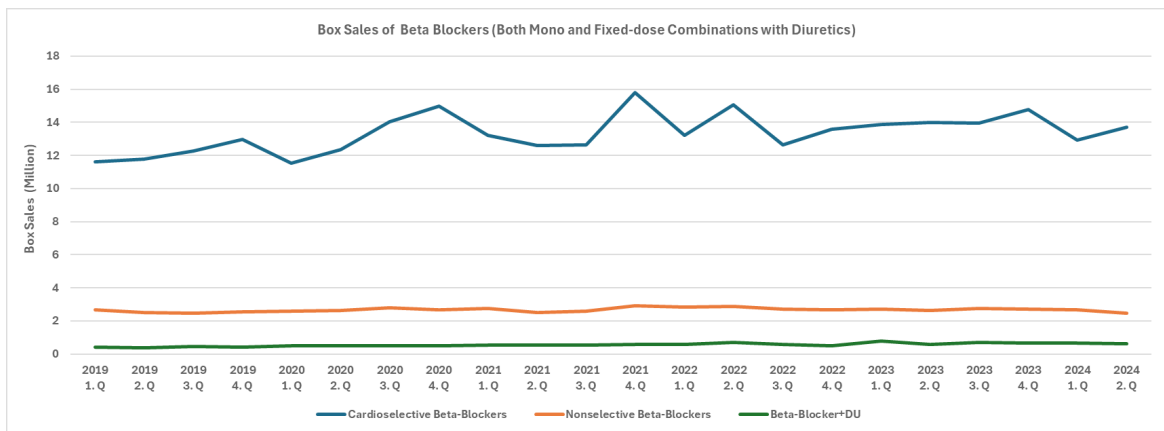


Figure 5. Box Sales of Beta Blockers (Both Mono and Fixed-dose Combinations with Diuretics)

WHO estimates that approximately 1.28 billion adults aged 30-79 suffer from hypertension worldwide. It is also stated that the number of adults with hypertension increased from 594 million to 1.13 billion between 1975 and 2015 and that this increase was seen mainly in low- and middle-income countries (WHO, 2023). In Türkiye, various studies have demonstrated the prevalence of hypertension. In the Turkish Hypertension Prevalence Study PatenT1 the prevalence of hypertension adjusted for age and gender was determined 31.8% in 2003 (Altun et al., 2005). In a recent study, Bayram et al. showed that 36.5% of adults in Türkiye had hypertension in 2021 (Bayram et al., 2021). Common chronic diseases, including hypertension, are shifting the disease burden of coun-

tries from acute diseases to chronic diseases. Chronic diseases, especially hypertension, and diabetes, cause significant economic and moral burdens also in our country (Sağlık Teknolojileri Değerlendirme Raporu 3). The Ministry of Health's Health Statistics report indicated that the sales volume of cardiovascular medicines increased by approximately 28% from 225.9 million boxes in 2017 to 291 million boxes in 2022 (Health Statistics Yearbook 2022). In this study, we determined that the total sales volume of anti-hypertensive drugs recommended in the guidelines increased by 15.44% between 2019 and 2023 in the Turkish market.

Hypertension treatment includes lifestyle changes such as achieving an ideal body weight, healthy diet,

salt restriction, quitting smoking, alcohol restriction, being active, and managing stress, as well as pharmacotherapy. The Turkish Hypertension Consensus report prepared in 2015 recommended drugs from the diuretic, beta-blocker, calcium channel blocker, angiotensin-converting enzyme (ACE) inhibitor, and angiotensin receptor blocker (ARB) groups for use in hypertension pharmacotherapy (Arıcı et al., 2015). Again, in the guide prepared by the Turkish Endocrinology and Metabolism Association, thiazide group diuretics, calcium channel blockers, ACE inhibitors, and ARBs are the four major antihypertensive drug groups (Hipertansiyon Tani Ve Tedavi Kılavuzu, 2022). In the guideline published by the World Health Organization in 2021, thiazide diuretics, ACE inhibitors, ARBs, and long-acting dihydropyridine derivative calcium channel blockers were recommended in pharmacotherapy as first-line hypertension treatment. At the same time, it was stated that beta-blockers should be evaluated in patients with ischemic heart disease (Guideline for the pharmacological treatment of hypertension in adults, 2021). In the guideline prepared by the American College of Cardiology and the American Heart Association published in the United States (US) in 2017, ACE inhibitors, ARBs, dihydropyridine-derivative and non-dihydropyridine-derivative calcium channel blockers, and thiazide group diuretics were recommended in the first-line hypertension treatment (Whelton et al., 2018). In the latest guideline published by the European Society of Cardiology, ACE inhibitors, ARBs, dihydropyridine-derivative calcium channel blockers, thiazide group diuretics, and potassium-sparing diuretics are recommended in first-line hypertension treatment. Additionally, beta-blockers are advised as first-line therapy for individuals with heart failure or angina, following myocardial infarction, or for those seeking to regulate their heart rate (McEvoy et al., 2024). However, different publications criticize the use of beta-blockers in first-line therapy because of their slightly reducing effect on the risk of stroke (Messerli et al., 2023).

## CONCLUSION

In this study, the last 66-month sales data of antihypertensive medication groups recommended by guidelines were analyzed separately. In 2019, ARB mono and combination preparations sold approximately 49.6 million boxes in Türkiye, while ACE inhibitors sold approximately 37.1 million boxes. It is observed that the market share between the two drug groups that inhibit the renin-angiotensin system, ACE inhibitors, and ARBs, did not change during the period examined in the study. These box sales reached approximately 58.3 million for ARBs and approximately 43.7 million for ACE inhibitors in 2023. In a different study examining the market distribution of hypertension drugs in Türkiye in 2020 and 2021, the highest box sales were in drugs that block angiotensin production or effect, followed by beta blockers. Among drugs that block angiotensin production or its effect, the highest box sales were in ARB and thiazide fixed-dose combinations (Tengiz et al., 2023). A prior study indicated that the consumption of ARB group antihypertensives increased by 175% from 2005 to 2010, and ACE inhibitors by 17% in Türkiye (Koçkaya et al., 2012). In a recent study ACE inhibitor and ARB sales in various European countries were examined using different parameters. Mono and fixed-dose combination pharmaceuticals of ACE inhibitors and ARBs were evaluated together, and the total sales of both pharmaceuticals were examined. When the amount of drug consumption per capita in 2016 was examined, the consumption of ARB and ACE inhibitors was close to each other in France and Spain, while ACE inhibitor consumption was determined to be dominant over ACE inhibitor consumption, especially in Poland, Hungary, Romania, and the UK. It was determined that the ARB consumption rate in the total consumption of these two drug groups was 1% in Poland, Hungary, and Romania in 2001, over 15% in 2009, and over 25% in 2016. The increase in ARB consumption in Eastern European countries was explained by the entry of generic medications in these markets. However, this increase was not detected in

other European countries, the Netherlands, England, and Italy. ARB sales data reached a certain plateau and remained at that level for a long time. It was stated that this situation shows that drug policies and regulations are essential factors affecting drug consumption at the country level (Kovács et al., 2021). Another study conducted in the Baltic countries (Estonia, Lithuania, and Latvia) found that the most commonly used medicine class was medications that block the action or synthesis of angiotensin and that the usage of antihypertensive agents has grown between 2008 and 2018. The mono forms of ACE inhibitors were determined as the most commonly used subgroup. Another critical data in that study is a remarkable increase in ARB use between 2008 and 2018 (Treciokiene et al., 2022). In a study in Bosnia and Herzegovina and Serbia, it was demonstrated that the use of antihypertensive drugs increased more than threefold between 2009 and 2019. ACE inhibitors were the most often used medication class during the years under review, followed by calcium channel blockers. The difference in use between the two groups is about 2-fold. It was found that the combination of ACE inhibitors with thiazide diuretics was close to calcium channel blockers in those years (Kalinić et al., 2022).

On the other hand, a study examining the antihypertensive drug market in India showed that the market grew by 6.9% between 2016 and 2018. In that study, it was demonstrated that the group with the highest market share among mono drugs was calcium channel blockers, while beta blockers and ARBs followed this group (Sahoo et al., 2021). We showed that mono forms of beta-blocker agents have sold over 60 million boxes annually since 2020, and cardioselective beta-blockers accounted for more than 80% of these sales. The point to remember here is that beta-blockers are also used in the treatment of other cardiovascular diseases. Therefore, it cannot be concluded from the data in our study that the group of drugs used as mono to treat hypertension in Turkey is cardioselective beta blockers. On the other hand, while mono forms of calcium channel blockers were

sold around 20 million boxes annually during the five years, box sales of their fixed-dose combined forms increased by over 60% since 2019, approaching 25 million. When the data of calcium channel blockers are examined, it is seen that the group predominantly used in Türkiye is dihydropyridine derivatives under the guidelines.

Fixed-dose drug combinations have also been shown to increase patient compliance with antihypertensive drug treatment (Tsioufis et al., 2020). Fixed-dose drug combinations are recommended in terms of effectiveness and cost in the treatment of hypertension, and in recent years, WHO has added some of these drugs to the essential drug list (Salam et al., 2020). In our study, we showed that combinations of drugs used in the treatment of hypertension are widely used, and their use has increased over the years. In contrast to their mono formulations, we discovered that fixed-dose combinations of ACE inhibitors and ARBs are more often used. In recent years, fixed-dose calcium channel blockers have begun to outsell their combined formulations. In a study that investigated data from 75 countries between 2010 and 2021, it was stated that the use of fixed-dose combined antihypertensive drugs increased in low-income countries compared to middle- and high-income countries. However, it was found that antihypertensive drug consumption rates were significantly lower in these countries compared to middle- and high-income countries (Jayawardana et al., 2024). In a study in Germany, it was stated that, despite the recommendation of fixed-dose combination drugs in the joint guideline of the European Society of Cardiology and the European Society of Hypertension in 2018, fixed-dose combination drugs had a share of 15.4% in antihypertensive drug box sales in 2016. Still, this share decreased to 10.9% in 2020 (Mahfoud et al., 2023). In the study in India between 2016-2018, mentioned in the paragraph above, it was seen that fixed-dose combinations of two drugs had a share of 36% in the entire antihypertensive drug market (Sahoo et al., 2021). In the study in Bosnia and Herzegovina and Serbia be-

tween 2009 and 2019, as mentioned above, it was seen that the combination of ACE inhibitors and thiazide diuretics were the two most preferred antihypertensive drug groups after mono ACE inhibitors, together with calcium channel blockers (Kalinić et al., 2022). One of the essential results of this study is the demonstration that sales dates of triple fixed-dose drug combinations have been increasing over the years in Türkiye. It has been determined that triple fixed-dose combinations of ARBs and ACE inhibitors that suppress the renin-angiotensin system with calcium channel blockers and diuretics have been increasing regularly in the period examined in the study. We believe that these rising rates should be evaluated concerning the diagnosis, management, and treatment of hypertension in Türkiye.

In each country, the choice of antihypertensive drug group in the treatment is different. Generic formulations, pharmaceutical strategies, legal frameworks, and other variables in various nations contribute to this circumstance. As a result, according to the data in our study, we demonstrated that the drug groups that have the highest share in the antihypertensive drug market in Türkiye in recent years are the groups recommended in the guidelines. We found that the total box sales of these drugs increased by 15.44% between 2019 and 2024. However, it is not possible to conclude that this data only covers medicine sales for the treatment of hypertension, particularly beta blockers, because our analysis only includes wholesaler sales data without prescription and diagnosis information. It would be more beneficial for future studies to include clinical data such as diagnosis and the treatment step in which the drugs are used. As mentioned above, an essential finding of this study is that triple fixed-dose combination sales are increasing regularly. This data is essential for assessing the rational treatment of hypertension in our nation. Such studies are helpful because they contribute to the assessment of whether drugs used in the treatment of chronic diseases are used rationally following the

guidelines, as well as to the status of access to drugs in countries. More detailed studies are needed on medications used in the treatment of all chronic diseases, especially hypertension, to evaluate health systems and public health.

#### AUTHOR CONTRIBUTION STATEMENT

Concept: E.H.V., B.G; Design: E.H.V., B.G; Control: E.H.V., B.G; Sources: E.H.V., B.G; Materials: -; Data Collection and/or Processing: E.H.V.,B.G.; Analysis and/or Interpretation: E.H.V.,; Literature Review: E.H.V., B.G.; Manuscript Writing: E.H.V., B.G.; Critical Review: E.H.V., B.G; Other:-

#### CONFLICT OF INTEREST

The authors declare that there is no conflict of interest.

#### REFERENCES

- Altun, B., Arıcı, M., Nergizoğlu, G., Derici, U., Karatan, O., Turgan, C., Sindel, S., Erbay, B., Hasanoglu, E., Cağlar, S., & Turkish Society of Hypertension and Renal Diseases (2005). Prevalence, awareness, treatment and control of hypertension in Turkey (the PatenT study) in 2003. *Journal of Hypertension*, 23(10), 1817–1823. <https://doi.org/10.1097/01.hjh.0000176789.89505.59>
- Arıcı, M., Birdane, A., Güler, K., Yıldız, B. O., Altun, B., Ertürk, Ş., Aydoğdu, S., Özbakkaloğlu, M., Ersöz, H. Ö., Süleymanlar, G., Tükek, T., Tokgözoğlu, L., Erdem, Y., Türk Kardiyoloji Derneği (TKD), Türk İç Hastalıkları Uzmanlık Derneği (TİHUD), Türkiye Endokrinoloji ve Metabolizma Derneği (TEMED), Türk Nefroloji Derneği (TND), & Türk Hipertansiyon ve Böbrek Hastalıkları Derneği (2015). Türk Hipertansiyon Uzlaşı Raporu [Turkish Hypertension Consensus Report]. *Türk Kardiyoloji Derneği arsivi: Türk Kardiyoloji Derneğinin yayın organidir*, 43(4), 402–409. <https://doi.org/10.5543/tkda.2015.16243>
- ATC/DDD Toolkit. Anatomical Therapeutic Chemical (ATC) Classification. Retrieved from <https://www.who.int/tools/atc-ddd-toolkit>



- Bayram, F., Demir, Ö., Sabuncu, T., Eren M.A., Gedik A.V., Çorapçıoğlu D, Kaya A. (2021). Prevalence and Awareness of Hypertension in Seven Distinct Geographic Regions of Turkey: The SEMT HT Study. *The Turkish Journal of Endocrinology and Metabolism*, 25(1), 1–10. <https://doi.org/10.25179/tjem.2020-78532>
- Benowitz NL (2018). Antihypertensive Agents. B. Katzung (Ed.) *Basic and clinical Pharmacology* (pp.173-193) 14<sup>th</sup> Edition. USA: McGraw Hill Education.
- Guideline for the pharmacological treatment of hypertension in adults.* (2021) Geneva: World Health Organization; 2021. Licence: CC BY-NC-SA 3.0 IGO. Retrieved from <https://iris.who.int/bitstream/handle/10665/344424/9789240033986-eng.pdf?sequence=1>
- Health Statistics Yearbook* (2022) T.C. Sağlık Bakanlığı, Ankara. Ministry of Health Publication no: 1280. ISBN: 978-975-590-901-1 Retrieved from <https://dosyasb.saglik.gov.tr/Eklenti/48055/0/siy2022eng-050420241pdf.pdf>
- Hipertansiyon Tani Ve Tedavi Kılavuzu* (2022). Türkiye Endokrinoloji ve Metabolizma Derneği. 6. Baskı ISBN: 978-605-66410-4-6. Retrieved from <https://file.temd.org.tr/Uploads/publications/guides/documents/Hipertansiyon-Kilavuzu-2022.pdf>
- Jayawardana, S., Campbell, A., Aitken, M., Andersson, C. E., Mehra, M. R., & Mossialos, E. (2024). Global consumption patterns of combination hypertension medication: An analysis of pharmaceutical sales data from 2010-2021. *PLOS Global Public Health*, 4(9), e0003698. <https://doi.org/10.1371/journal.pgph.0003698>
- Kalinić, D., Škrbić, R., Vulić, D., Stojaković, N., Stoisavljević-Šatara, S., Stojiljković, M. P., Marković-Peković, V., Golić Jelić, A., Pilipović-Broćeta, N., Wong, N. D., & Godman, B. (2022). Trends in Antihypertensive Medicine Utilization in the Republic of Srpska, Bosnia and Herzegovina: An Eleven-Year Follow-Up. *Frontiers in Pharmacology*, 13, 889047. <https://doi.org/10.3389/fphar.2022.889047>
- Koçkaya, G., Tanyeri, P., Kılıç, P., Vural, İ. M., Akbulat, A., Artıran, G., Kerman, S. (2012). Türkiye’de anjiyotensin reseptör blokerleri ve anjiyotensin dönüştürücü enzim inhibitörlerinin yıllar içerisinde tüketim, bütçe ve fiyat değişim analizi. *MN Kardiyoloji*, 19(3), 112 - 119.
- Kovács, B., Darida, M., & Simon, J. (2021). Drugs Becoming Generics-The Impact of Genericization on the Market Performance of Antihypertensive Active Pharmaceutical Ingredients. *International Journal of Environmental Research and Public Health*, 18(18), 9429. <https://doi.org/10.3390/ijerph18189429>
- Mahfoud, F., Kieble, M., Enners, S., Kintscher, U., Laufs, U., Böhm, M., & Schulz, M. (2023). Use of fixed-dose combination antihypertensives in Germany between 2016 and 2020: an example of guideline inertia. *Clinical Research in Cardiology: Official Journal of the German Cardiac Society*, 112(2), 197–202. <https://doi.org/10.1007/s00392-022-01993-5>
- McEvoy, J. W., McCarthy, C. P., Bruno, R. M., Brouwers, S., Canavan, M. D., Ceconi, C., Christodorescu, R. M., Daskalopoulou, S. S., Ferro, C. J., Gerdtts, E., Hanssen, H., Harris, J., Lauder, L., McManus, R. J., Molloy, G. J., Rahimi, K., Regitz-Zagrosek, V., Rossi, G. P., Sandset, E. C., Scheenaerts, B., ... ESC Scientific Document Group (2024). 2024 ESC Guidelines for the management of elevated blood pressure and hypertension. *European Heart Journal*, 45(38), 3912–4018. <https://doi.org/10.1093/eurheartj/ehae178>
- Messerli, F. H., Bangalore, S., & Mandrola, J. M. (2023).  $\beta$  blockers switched to first-line therapy in hypertension. *Lancet (London, England)*, 402(10414), 1802–1804. [https://doi.org/10.1016/S0140-6736\(23\)01733-6](https://doi.org/10.1016/S0140-6736(23)01733-6)
- Sahoo, S. K., Pathni, A. K., Krishna, A., Moran, A. E., Cohn, J., Bhatia, S., Maheshwari, N., & Sharma, B. (2021). Research Letter: Antihypertensive Drugs Market in India: An Insight on Size, Trends, and Prescribing Preferences in the Private Health Sector, 2016-2018. *Global heart*, 16(1), 51. <https://doi.org/10.5334/gh.999>

- Sağlık Teknolojileri Değerlendirme Raporu 3 (2016). Türkiye İlaç ve Tıbbi Cihaz Kurumu, Ankara/Türkiye. Retrieved from <https://titck.gov.tr/Dosyalar/Ilac/SaglikTeknolojileriDegerlendirme/STDRaporu3.pdf>
- Salam, A., Huffman, M. D., Kanukula, R., Hari Prasad, E., Sharma, A., Heller, D. J., Vedanthan, R., Agarwal, A., Rodgers, A., Jaffe, M. G., R Frieden, T., & Kishore, S. P. (2020). Two-drug fixed-dose combinations of blood pressure-lowering drugs as WHO essential medicines: An overview of efficacy, safety, and cost. *Journal of Clinical Hypertension (Greenwich, Conn.)*, 22(10), 1769–1779. <https://doi.org/10.1111/jch.14009>
- Tengiz, I., Atila, D., & Ercan, E. (2023). Market Distributions and Pricing/Reimbursement Policies of Antihypertensive Drugs in Turkey. Türkiye'de Antihipertansif İlaçların Pazar Dağılımları ve Fiyatlandırma/Geri Ödeme Politikaları. *Türk Kardiyoloji Dernegi arsivi: Turk Kardiyoloji Derneginin yayin organidir*, 51(5), 299–303. <https://doi.org/10.5543/tkda.2023.84039>
- Treciokiene, I., Bratickoviene, N., Gulbinovic, J., Wettermark, B., & Taxis, K. (2022). Trend of Antihypertensive Medicine Use in the Baltic States between 2008 and 2018: A Retrospective Cross-National Comparison. *Pharmacoepidemiology*, 1(1), 1-11. <https://doi.org/10.3390/pharma1010001>
- Tsioufis, K., Kreutz, R., Sykara, G., van Vugt, J., & Hassan, T. (2020). Impact of single-pill combination therapy on adherence, blood pressure control, and clinical outcomes: a rapid evidence assessment of recent literature. *Journal of Hypertension*, 38(6), 1016–1028. <https://doi.org/10.1097/HJH.0000000000002381>
- Whelton, P. K., Carey, R. M., Aronow, W. S., Casey, D. E., Jr, Collins, K. J., Dennison Himmelfarb, C., DePalma, S. M., Gidding, S., Jamerson, K. A., Jones, D. W., MacLaughlin, E. J., Muntner, P., Ovbigele, B., Smith, S. C., Jr, Spencer, C. C., Stafford, R. S., Taler, S. J., Thomas, R. J., Williams, K. A., Sr, Williamson, J. D., ... Wright, J. T., Jr (2018). 2017 ACC/AHA/AAPA/ABC/ACPM/AGS/APhA/ASH/ASPC/NMA/PCNA Guideline for the Prevention, Detection, Evaluation, and Management of High Blood Pressure in Adults: Executive Summary: A Report of the American College of Cardiology/American Heart Association Task Force on Clinical Practice Guidelines. *Hypertension (Dallas, Tex.: 1979)*, 71(6), 1269–1324. <https://doi.org/10.1161/HYP.0000000000000066>
- World Health Organization (WHO) (2021). *Cardiovascular diseases (CVDs)*. Retrieved from [https://www.who.int/news-room/fact-sheets/detail/cardiovascular-diseases-\(cvds\)](https://www.who.int/news-room/fact-sheets/detail/cardiovascular-diseases-(cvds))
- World Health Organization (WHO) (2023). *Hypertension*. Retrieved from <https://www.who.int/news-room/fact-sheets/detail/hypertension>

# Phytochemical Analysis, Antibacterial, Anti-Fungi, and Antiradical Effects, Exploring Correlation Analysis of Lingonberry Leaf (*Vaccinium vitis-idaea* L.) Extracts

Olexander MASLOV\*, Mykola KOMISARENKO\*\*, Svitlana PONOMARENKO\*\*\*, Tetiana OSOŁODCHENKO\*\*\*\*, Sergii KOLISNYK\*\*\*\*\*

*Phytochemical Analysis, Antibacterial, Anti-Fungi, and Antiradical Effects, Exploring Correlation Analysis of Lingonberry Leaf (*Vaccinium vitis-idaea* L.) Extracts*

*Fitokimyasal Analiz, Antibakteriyel, Anti-Fungal ve Antiradikal Etkiler ve Lingonberry Yaprağı (*Vaccinium vitis-idaea* L.) Ekstrelerinin Korelasyon Analizinin Araştırılması*

## SUMMARY

Nowadays, infectious diseases are a significant catastrophe for modern public health and society, especially due to the spread of Gram-negative and Gram-positive bacterial strains, as well as fungi, that are resistant to antibiotics. The purpose of this work was to study the total content of some biologically active substances, determine the antibacterial, antifungal, and antioxidant activities of lingonberry leaf extracts, and perform a correlation analysis between the content of natural compounds and their antibacterial, antifungal, and antioxidant activities. The results demonstrated the highest amounts of polyphenols, flavonoids, catechins, and organic acids in the extracts, with respective values of  $2.20 \pm 0.06\%$ ,  $1.39 \pm 0.01\%$ ,  $0.65 \pm 0.01\%$ , and  $0.21 \pm 0.01\%$  in the 60% ethanolic extract. Organic acids were most abundant in the aqueous extract ( $0.89 \pm 0.01\%$ ), while hydroxycinnamic acids were most prevalent in the 40% ethanolic extract ( $0.80 \pm 0.04\%$ ). The 60% ethanolic extract of lingonberry leaf exhibited the most potent antioxidant properties. There was a strong correlation between the content of polyphenols, flavonoids, and the inhibition of *S. aureus*, *P. aeruginosa*, *B. subtilis*, *P. vulgaris*, *C. albicans*, and *E. coli*, which depended significantly on the content of hydroxycinnamic acids. These findings highlight the great potential for developing and creating new medicines with antimicrobial, antioxidant, and antifungal effects that are not only comparable to but may even surpass those of synthetic analogues.

**Key Words:** Lingonberry leaf, correlation analysis, antiradical effect, antimicrobial effect, phenolic compounds

## ÖZ

Günümüzde bulaşıcı hastalıklar, özellikle antibiyotiklere dirençli Gram-negatif ve Gram-pozitif bakteri suşlarının yanı sıra mantarların yayılması nedeniyle, modern halk sağlığı ve toplum için önemli bir felakettir. Bu çalışmanın amacı, bazı biyolojik olarak aktif maddelerin toplam içeriğini incelemek, kızılçık yaprağı ekstrelerinin antibakteriyel, antifungal ve antioksidan aktivitelerini belirlemek ve doğal bileşiklerin içeriği ile antibakteriyel, antifungal ve antioksidan aktiviteleri arasında bir korelasyon analizi yapmaktır. Sonuçlar, %60 etanolik ekstredeki sırasıyla  $2,20 \pm 0,06\%$ ,  $1,39 \pm 0,01\%$ ,  $0,65 \pm 0,01$  ve  $0,21 \pm 0,01$  değerleriyle, ekstrelerde en yüksek polifenol, flavonoid, kateşin ve organik asit miktarlarını göstermiştir. Organik asitler sulu ekstrede en bol miktarda bulunurken ( $0,89 \pm 0,01$ ), hidroksisinnamik asitler %40 etanolü ekstrede en yaygındı ( $0,80 \pm 0,04$ ). Yaban mersini yaprağının %60 etanolü özütü en güçlü antioksidan özelliklerini sergiledi. Polifenoller, flavonoidler ve *S. aureus*, *P. aeruginosa*, *B. subtilis*, *P. vulgaris*, *C. albicans* ve *E. coli* inhibisyonu arasında güçlü bir korelasyon vardı ve bu korelasyon önemli ölçüde hidroksisinnamik asitlerin içeriğine bağlıydı. Bu bulgular, yalnızca sentetik analoglarla karşılaştırılabilir değil, hatta onları aşabilecek antimikrobiyal, antioksidan ve antifungal etkilere sahip yeni ilaçlar geliştirme ve yaratma konusunda büyük bir potansiyel olduğunu vurgulamaktadır.

**Anahtar Kelimeler:** Lingonberry yaprağı, korelasyon analizi, antiradikal etki, antimikrobiyal etki, fenolik bileşikler.

Received: 02.09.2024

Revised: 28.11.2024

Accepted: 21.01.2025

\* ORCID: 0000-0001-9256-0934, Department of General Chemistry, National University of Pharmacy, Kharkiv, Ukraine.

\*\* ORCID: 0000-0002-1161-8151, Department of Pharmacognosy and Nutriology, National University of Pharmacy, Kharkiv, Ukraine.

\*\*\* ORCID: 0000-0003-3994-3500, Laboratory of Biochemistry and Biotechnology, Mechnikov Institute of Microbiology and Immunology of the NAMS of Ukraine, Kharkiv, Ukraine.

\*\*\*\* ORCID: 0000-0001-7258-3880, Laboratory of Biochemistry and Biotechnology, Mechnikov Institute of Microbiology and Immunology of the NAMS of Ukraine, Kharkiv, Ukraine.

\*\*\*\*\* ORCID: 0000-0002-4920-6064, Department of General Chemistry, National University of Pharmacy, Kharkiv, Ukraine

\* Corresponding Author; Olexander Maslov

Pushkinskaya Str. 53, 61001, Kharkiv, E-mail: alexmaslov392@gmail.com

## INTRODUCTION

Bacterial and fungal infections remain among the leading causes of human mortality worldwide. Statistical analyses indicate that 13.7 million people die annually due to infectious diseases, with a mortality rate of 99 deaths per 100,000 individuals. Among these, 3.6 million deaths are attributed to bacterial infections caused by Gram-positive strains, such as *Staphylococcus aureus*, and Gram-negative strains, including *Streptococcus pneumoniae*, *Klebsiella pneumoniae*, *Pseudomonas aeruginosa*, and *Escherichia coli*. In 2019 alone, approximately 1 million deaths were linked to *S. aureus* infections (Ikuta et al., 2022). This issue is further exacerbated by the increasing resistance of bacteria to commonly used antibiotics, making treatment more challenging, time-consuming, and costly (Bongomin et al., 2017). Given this scenario, the search for new antibacterial natural compounds has become a highly relevant and promising area of research today.

The scientific community has devoted significant attention to studying the pharmacological activities of natural compounds, particularly derivatives of flavon-3-ols and flavonols (Maslov et al., 2024; Di Pede et al., 2022; Panche et al., 2016). According to the literature, natural compounds offer several advantages over synthetic alternatives (Chaachouay et al., 2024). Firstly, they are generally safer and associated with fewer side effects. Secondly, natural compounds often demonstrate higher efficacy. Lastly, their production is more cost-effective, making them an attractive option for therapeutic development (Abdallah et al., 2023).

Lingonberry (*Vaccinium vitis-idaea* L.), an evergreen shrub from the *Ericaceae* family, is one of the richest plant sources of phenolic compounds. Its distribution spans Russia, the Baltic countries, the northern regions of Ukraine and Belarus, and Canada (Ryyti et al., 2020; Hirabayashi et al., 2023). The chemical composition of lingonberry leaves includes a wide variety of biologically active substances: hydroquinone derivatives (arbutin, methylarbutin),

catechins (epicatechin, (+)-catechin), flavonoids (rutin, quercetin), hydroxycinnamic acids (ferulic and caffeic acids), and organic acids (citric and malic acids) (Kowalska et al., 2021; Cvetkova et al., 2024).

Numerous scientific studies have focused on determining the antioxidant activity of *Vaccinium vitis-idaea* leaf extracts (Vyas et al., 2013; Feriemi and Lamari, 2016). However, no data are available on assessing the antioxidant, antibacterial, and antifungal activities and their correlation with the content of biologically active substances using the potentiometric method.

The purpose of this research was to quantify the total polyphenols, flavonoids, hydroxycinnamic acids, organic acids, and catechins in *V. vitis-idaea* leaf extracts. Additionally, the study aimed to evaluate their antibacterial and antifungal activities against Gram-positive strains (*S. aureus*, *B. subtilis*), Gram-negative strains (*E. coli*, *P. vulgaris*, *P. aeruginosa*), and fungi (*C. albicans*). Finally, a correlation analysis was conducted to explore the relationship between the content of biologically active substances in the extracts and their antibacterial, antifungal, and antioxidant activities.

## MATERIALS AND METHODS

Leaves of *Vaccinium vitis-idaea* were harvested in the Zhytomyr region, Ukraine (50°32'94" N, 29°53'68" E), during autumn 2021. A green tea (*Camellia sinensis* L.) leaves were collected in Anhui Province, China (30°63'41" N, 116°33'25" E).

Six samples of *V. vitis-idaea* leaf (10.0 g each, exact mass) with particle sizes of 1–2 mm were prepared. The extraction was conducted using distilled water, 20%, 40%, 60%, and 96% ethanol at 80°C for 1 hour with a condenser, maintaining a raw material-to-solvent ratio of 1:20. The extraction process was performed twice to ensure the complete extraction of biologically active substances. The filtrates were then combined and evaporated under vacuum using a rotary evaporator to achieve a final extract-to-raw material ratio of 1:2. As a result, six extracts were obtained: aqueous and ethanol extracts at 20%, 40%,

60%, and 96% concentrations. Additionally, a green tea (*Camellia sinensis*) extract was prepared using the same method with 60% ethanol.

The sum of polyphenols was quantified using the Folin-Ciocalteu method, with absorbance readings taken at 760 nm (Blainski et al., 2013). The phosphomolybdotungstic reagent was used for performing an assay. The calibration curve ( $Y = 0.1055X + 0.1745$  ( $R^2=0.9951$ )) was plotted with interval concentrations 1.0 – 5.0  $\mu\text{g/mL}$ , the calibration equation. The total phenolic compounds content in extracts (X), expressed as gallic acid was calculated according to equation 2:

$$X(\%) = \frac{C_x \times K_{dil} \times 100}{V}$$

where,  $C_x$  – concentration of gallic acid according to the calibration curve,  $C \times 10^{-6}$ , g/mL;  $V$  – extract volume, mL;  $K_{dil}$  – coefficient of dilution, mL.

The total catechin content was determined using the vanillin reagent assay, with optical density measured at 505 nm. (Maslov et al., 2023, a). A calibration curve ( $Y = 0.0025X - 0.0851$  ( $R^2 = 0.9951$ )) was plotted with 100 – 400  $\mu\text{g/mL}$  interval concentrations of epigallocatechin-3-*O*-gallate. The total catechins content in extracts (X), expressed as epigallocatechin-3-*O*-gallate was calculated according to the equation:

$$X(\%) = \frac{C_x \times K_{dil} \times 100}{V}$$

where,  $C_x$  – concentration of epigallocatechin-3-*O*-gallate according to the calibration curve,  $C \times 10^{-6}$ , g/mL;  $V$  – extract volume, mL;  $K_{dil}$  – coefficient of dilution, mL.

The total flavonoid was evaluated by  $\text{AlCl}_3$  complex assay, with absorbance measurement at 415 nm (Upyr et al., 2019). The concentration of standard solution of rutin was 0.02 mg/mL. The total flavonoid content in extracts (X), expressed as rutin, was calculated according to the equation:

$$X(\%) = \frac{A \times K_{dil} \times m_s \times 100}{A_s \times V}$$

where,  $A$  – absorbance of analyzed solution;  $A_{st}$  – absorbance of standard solution of rutin;  $V$  – volume of extract, mL;  $K_{dil}$  – coefficient of dilution, mL,  $m_s$  – mass of rutin, g.

The total hydroxycinnamic acids were quantified using a reaction with  $\text{NaNO}_2$  and  $\text{Na}_2\text{MoO}_4$ , with optical density measured at 525 nm. (Upyr et al., 2022). The total content of hydroxycinnamic acids derivatives in extracts (X), expressed as chlorogenic acid was calculated according to the equation:

$$X(\%) = \frac{A \times K_{dil} \times 1000}{188 \times V}$$

where,  $A$  – absorbance of analyzed solution; 188 – specific adsorption coefficient of chlorogenic acid;  $V$  – volume of extract, mL;  $K_{dil}$  – coefficient of dilution, mL.

The content of total organic acids was established through acid-base titration, using a potentiometric method to determine the end-point (Maslov et al., 2023, b). The total content of organic acids in extracts, expressed as citric acid was calculated according to equation:

$$X(\%) = \frac{(V_{equiv} - V_x) \times 0.0032 \times K_{dil} \times K \times 100}{V}$$

where, 0.0032 – the amount of citric acid, equivalent to 1 mL of sodium hydroxide solution (0.05 mol/L), g;  $V_{equiv}$  is the volume (mL) of sodium hydroxide solution (0.05 mol/L), which was used for titration;  $V_x$  – the volume (mL) of sodium hydroxide solution (0.05 mol/L), which was spent for titration in a blank experiment;  $V$  – volume of extract, mL;  $K_{dil}$  – coefficient of dilution, mL.;  $K$  is the correction coefficient for 0.05 mol/L sodium hydroxide solution.

The antioxidant effect was determined by the potentiometric assay (Maslov et al., 2023, c). A 5.00 mL aliquot of 2 mmol/L solution of  $\text{K}_3[\text{Fe}(\text{CN})_6]$

and 0.02 mmol/L of  $K_4[Fe(CN)_6]$  was taken and transferred into a 250.0 mL volumetric flask and made up to the mark by 0.067 mol/L phosphate buffer solution. A 50.00 mL of prepared mediator solution was transferred in an electrochemical cell. The initial potential of mediator solution was measured after initial one was established, a 1.00 mL of aliquot of the prepared solutions was added and a final potential was measured. The difference ( $\Delta E$ ) between the initial ( $E_0$ ) and final ( $E_1$ ) potentials was found.

Antioxidant activity was calculated according to equation and expressed as mmol-eqv./m<sub>dry res.</sub>:

$$AOA = \frac{C_{ox} - \alpha \times C_{red}}{1 + \alpha} \times K_{dil} \times 10^3 \times \frac{m_1}{m_2}$$

where,  $\alpha = C_{ox}/C_{red} \times 10^{(\Delta E - E_{ethanol})nF/2.3RT}$ ;  $C_{ox}$  – concentration of  $K_3[Fe(CN)_6]$ , mol/L;  $C_{red}$  – concentration of  $K_4[Fe(CN)_6]$ , mol/L;  $E_{ethanol}$  – 0.0546· $C_{\%}$  – 0.0091;  $C_{\%}$  – concentration of ethanol;  $\Delta E$  – change of potential;  $F = 96485.33$  C/mol – Faraday constant;  $n = 1$  – number of electrons in electrode reaction;  $R = 8.314$  J/molK – universal gas constant;  $T = 298$  K;  $K_{dil}$  – coefficient of dilution, mL.;  $m_1$  – mass of dry residue;  $m_2$  – mass of dry residue in 1.0 mL of extract.

Test strains of fungi – *C. albicans* ATCC 885/653, Gram-positive strains – *S. aureus* ATCC 25923, *B. subtilis* ATCC 6538, Gram-negative strains – *E. coli* ATCC 25922, *P. vulgaris* NTCS 4636, *P. aeruginosa* ATCC 27853 were applied with the recommendations for the assessment of antimicrobial effect of drugs.

The diffusion method using agar “wells” was employed to evaluate the drug’s activity (Tsemenko et al., 2018). Microorganism suspensions with standardized concentrations (optical density) were prepared according to the McFarland turbidity standard (0.5 units) using a Densi-La-Meter (Czech Republic) at a wavelength of 540 nm. Suspensions were prepared following the equipment’s manual and information guidelines. The colony-forming unit (CFU) concentration was  $10^7$  microorganisms per milliliter of growth medium, as determined by the

McFarland standard.

On solidified agar in sterile Petri dishes, 1 mL of the microorganism suspension was pipetted under sterile conditions. After uniformly distributing the microorganisms across the agar surface, the plates were incubated at room temperature for 15–20 minutes. Wells with a diameter of 6 mm were then created in the agar, and solutions of the test substances were introduced.

The samples were incubated at 37°C for 16–24 hours. Following incubation, the plates were inverted and placed on a dark matte surface under light angled at 45° for measurement. The diameters of the growth inhibition zones were measured using a caliper. Gentamicin and fluconazole were used as reference drugs for assessing antibacterial and antifungal activity.

Pearson’s (r) correlation coefficient was applied to analyze the correlation relation. The correlation coefficient to takes a value in the range of -1 to +1. Correlation is negligible from 0.00 to 0.30; low – from 0.30 to 0.50; moderate – from 0.50 to 0.70; high – from 0.70 to 0.90 and very high from 0.90 to 1.00. (Akoglu et al., 2018)

## RESULTS AND DISCUSSION

According to the results presented in Table 1, the 60% EtOH extract (2.20±0.06%) contained the highest amount of polyphenols, followed by the 40% EtOH extract (2.10±0.07%), while the aqueous extract had the lowest amount (1.90±0.06%).

The content of catechins increased in the following order: 96% EtOH extract (1.13±0.03%) < aqueous extract (1.34±0.04%) < 20% EtOH extract (1.36±0.04%) < 40% EtOH extract (1.37±0.04%) < 60% EtOH extract (1.39±0.04%). The proportion of catechins in relation to the total polyphenol content was 55%, 63%, 65%, 68%, and 71% for the 96%, 60%, 40%, 20%, and aqueous extracts, respectively. The highest percentage of catechins was found in the aqueous extract, while the lowest was in the ethanolic extracts (Table 1).

Table 1 shows that the 60% EtOH extract (0.65±0.02%) contained the highest amount of flavonoids, while the aqueous extract (0.41±0.01%) had the lowest. The percentage of flavonoids relative to the total polyphenol content was 21%, 30%, 28%, 22%, and 22% for the 96%, 60%, 40%, 20%, and aqueous extracts, respectively. The highest percentage of flavonoids was found in the 60% EtOH extract, while the lowest was in the aqueous extract.

The amount of hydroxycinnamic acids increased in the following order: 96% EtOH extract (0.20±0.01%) < 60% EtOH extract (0.21±0.01%) < aqueous extract (0.28±0.01%) < 20% EtOH extract (0.57±0.03%). The proportion of hydroxycinnamic acids relative to the

total polyphenol content was 10%, 10%, 38%, 29%, and 15% for the 96%, 60%, 40%, 20%, and aqueous extracts, respectively. The highest proportion of hydroxycinnamic acids was found in the 40% EtOH extract, while the lowest was in the 96% EtOH extract (Table 1).

The highest amount of organic acids was found in the aqueous extract (0.89±0.01%), followed by the 20% EtOH extract (0.51±0.02%), while the lowest amount was in the 96% EtOH extract (0.38±0.01%). The total organic acid content was 82%, 78%, 80%, 75%, and 53% lower than the polyphenol content in the 96%, 60%, 40%, 20% EtOH, and aqueous extracts, respectively.

**Table 1.** The sum of different group of biologically active substances in *V. vitis-idaea* leaf liquid extracts

Sample	Amount of polyphenols expressed as gallic acid, %±SD	Amount of catechins expressed as epigallocatechin-3-O-gallate, %±SD	Amount of flavonoid expressed as rutin, %±SD	Amount of hydroxycinnamic acids expressed as chlorogenic acid, %±SD	Amount of organic acids expressed as citric acid, %±SD
96% EtOH extract	2.06±0.06	1.13±0.03	0.44±0.01	0.20±0.01	0.38±0.01
60% EtOH extract	2.20±0.06	1.39±0.04	0.65±0.02	0.21±0.01	0.48±0.01
40% EtOH extract	2.10±0.07	1.37±0.04	0.59±0.02	0.80±0.04	0.41±0.01
20% EtOH extract	2.00±0.06	1.36±0.04	0.44±0.01	0.57±0.03	0.51±0.02
H <sub>2</sub> O extract	1.90±0.06	1.34±0.04	0.41±0.01	0.28±0.01	0.89±0.01

A potentiometric method for determining antioxidant activity was used to evaluate the effect of the obtained extracts of *V. vitis-idaea* leaf. Table 2 shows that the level of antiradical effect grows in the order: 96% EtOH extract (105.00±1.05 mmol-eqv./m<sub>dry res.</sub>) > 20% EtOH extract (114.56±1.15 mmol-eqv./m<sub>dry res.</sub>) > aqueous extract (119.88±0.89 mmol-eqv./m<sub>dry res.</sub>) > 40% EtOH extract (142.44±1.42 mmol-eqv./m<sub>dry res.</sub>) > 60% EtOH extract (148.39±1.48 mmol-eqv./m<sub>dry res.</sub>). In light of the data obtained, it can be established that the 60% EtOH extract has the top level of antiradical effect. According to the modern classification of antioxidant activity, which was previously developed in our previous research (Mikulic-Petkovsek et al., 2012), it was found that all extracts obtained have a great level of antiradical effect. Moreover, a comparative analysis of the

“strength” of antioxidant activity was carried out with the gold standard 60% EtOH extract of *C. sinensis* leaf. The *C. sinensis* leaf extract was obtained by the same technological method as *V. vitis-idaea* leaf extracts. The obtained extracts were significantly inferior in antioxidant effect to *C. sinensis* leaf extract. Further, a 0.03 mol/L solutions (in terms of the amount of polyphenols expressed as gallic acid) of extracts of *V* and *C. sinensis* leaf were prepared. As a result of the study, it was found that when compared at the same concentrations, the aqueous extract had the highest antioxidant effect, and the least - 96% extract. (Table 3)

The potentiometric assay was chosen to evaluate antioxidant activity for several reasons: firstly, it is highly expressive; secondly, it is cost-effective; and thirdly, it is both accurate and precise. To compare the

antioxidant effects, we used the green tea leaf extract. The results showed that green tea extract significantly inactivates free radicals more effectively than *V. vitis-idaea* leaf extracts. Among the *V. vitis-idaea* extracts, the 60% EtOH extract exhibited the highest level of antiradical activity.

Next, we compared the antioxidant effects of the extracts at the same concentration of phenolic compounds. The results showed that the green tea extract was less effective than both the 60% EtOH and aqueous extracts of *V. vitis-idaea*. Moreover, the order of antioxidant activity changed significantly with varying concentrations of phenolic compounds. At higher concentrations, the 60% EtOH extract exhibited the greatest antiradical effect, while at equal

concentrations, the aqueous extract was the most effective.

Kryvtsova *et al.* reported on the antioxidant effects of ethyl acetate, methanolic, 60%, and 96% EtOH extracts of *V. vitis-idaea* leaves and fruits. Their research showed that the ethyl acetate extract had the highest antioxidant activity, followed by methanolic, ethanolic, and 60% EtOH extracts. In comparison, our study found that the 60% EtOH extract exhibited higher antioxidant activity than the 60% EtOH extract in their research. This difference may be due to the application of different analytical methods. In our study, we employed the electrochemical method, while Kryvtsova *et al.* used the spectrophotometric method, which is less accurate and sensitive.

**Table 2.** The level of antiradical effect of *V. vitis-idaea* leaf liquid extracts

Analyzed Sample	Antiradical effect, mmol-eqv./m <sub>dry res.</sub> ±SD	Conditional term of antioxidant level
96% EtOH extract	105.00±1.05	High level
60% EtOH extract	148.39±1.48	High level
40% EtOH extract	142.44±1.42	High level
20% EtOH extract	114.56±1.15	High level
H <sub>2</sub> O extract	119.88±0.89	High level
Green tea leaf 60% EtOH extract	548.79±10.98	Very high level

**Table 3.** Comparing the value of antiradical activity of *V. vitis-idaea* leaf liquid extracts with *C. sinensis* leaf 60% EtOH extract at the concentration 0.03 mol/L expressed as sum polyphenols as gallic acid

Sample	Concentration of polyphenols, mol/L	Antiradical effect, mmol-eqv./m <sub>dry res.</sub>
96% EtOH extract	0.03	26.25±0.26
60% EtOH extract		34.27±0.34
40% EtOH extract		30.50±0.31
20% EtOH extract		29.15±0.29
H <sub>2</sub> O extract		36.00±0.36
Green tea leaf 60% EtOH extract		30.78±0.31

In this research work, the antibacterial and antifungal activity of the obtained *V. vitis-idaea* leaf extracts was investigated against the following strains of G(+) – *B. subtilis*, *S. aureus*, G(–) – *P. vulgaris*, *E. coli*, *P. aeruginosa*, as well as a strain of the fungus *C. albicans*. According to the obtained results, all extracts obtained from the *V. vitis-idaea* leaf had an effective antibacterial and antifungal effect. (Table 4)

*S. aureus* was the most penetrating to the 60% EtOH extract (22.5±0.4 mm) and more resistant to the 20% EtOH extract (16.5±0.5 mm). When comparing the results of the gentamicin standard and the 60% EtOH extract, it was found that the 60% EtOH extract was 3% better at inhibiting the growth of the *S. aureus* strain of bacteria. According to the results presented in Table 3, it was found that *B. subtilis*, as



well as *S. aureus*, was less resistant to the 60% EtOH extract ( $21.0 \pm 0.4$  mm), followed by 40% EtOH extract ( $19.5 \pm 0.5$  mm), and the 20% EtOH extract ( $17.0 \pm 0.4$  mm) inhibited the growth of the bacterial strain the least. *P. aeruginosa*, *E. coli* were most sensitive to the action of 60% EtOH extract, whereas *P. vulgaris* were most sensitive to the action of aqueous extract. Antifungal effect research showed that 60% EtOH extract of *V. vitis-idaea* leaf was the most actively inhibited the growth of the fungus, whereas the 20% EtOH extract were least active inhibited the growth of fungi. (Table 4)

The *V. vitis-idaea* leaf extract studied in our research showed antibacterial and antifungal activity against the following strains: *S. aureus*, *P. aeruginosa*, *P. vulgaris*, *B. subtilis*, and *C. albicans*. Kryvtsova *et al.* (2019) reported the antimicrobial activity of ethyl acetate and methanolic extracts of leaves and fruits against both test and resistant G(+) and G(-) strains. The highest antibacterial activity of both extracts was observed against *S. aureus*. In comparison with our results, the highest inhibition zone in our extracts was also found against *S. aureus*. This suggests that *V. vitis-idaea* leaf extract could be useful in developing new antibacterial drugs against resistant *S. aureus* strains.

Tsamenko *et al.* (2018) reported that the native 96% EtOH *V. vitis-idaea* leaf extract was most active against *P. vulgaris*, followed by *C. albicans*. In contrast, our research showed that the 96% EtOH extract highly inhibited *S. aureus*, followed by *P. vulgaris* and *P. aeruginosa*, while the *C. albicans* strain was less sensitive to the 96% EtOH *V. vitis-idaea* extract.

Furthermore, when comparing the antibacterial effects of our extracts with the results of Tsamenko *et al.* and Kryvtsova *et al.*, we found that our results were more pronounced. This difference may be attributed to variations in the content of phenolic compounds and hydroquinone derivatives.

Based on the obtained data, it may initially appear that the antimicrobial and antifungal activity of *V. vitis-idaea* leaf extracts is significantly lower than that of gentamicin and fluconazole, as their solution concentrations were much lower than the polyphenol content in the extract. However, it is important to note that gentamicin has serious toxicity to the auditory nerve, kidneys, and liver, potentially leading to severe complications (Ispiryan *et al.*, 2024).

When comparing the antifungal effects of fluconazole and *V. vitis-idaea* leaf extract, it was observed that both inhibited fungal growth to the same extent, despite fluconazole being used at a lower concentration, similar to gentamicin. While fluconazole is a leading antifungal medication, it has limited effectiveness against both gram-negative and gram-positive bacteria. In contrast, *V. vitis-idaea* leaf extracts show sensitivity against both bacterial strains and fungi.

Thus, *V. vitis-idaea* leaf extracts represent a combined pharmaceutical with the ability to affect various vital mechanisms of bacteria and fungi, offering a broad spectrum of activity against different strains. Additionally, these extracts do not exhibit serious toxicity, making them a promising alternative.

**Table 4.** The value of antibacterial and anti-fungi activity of *V. vitis-idaea* leaf liquid extracts

Sample	Concentration mmol/L, (expressed in total polyphenols as gallic acid)	Diameter of the growth retardation zone, mm					
		Gramm-positive		Gramm-negative			Fungi
		<i>Staphylococcus aureus</i>	<i>Bacillus subtilis</i>	<i>Escherichia coli</i>	<i>Proteus vulgaris</i>	<i>Pseudomonas aeruginosa</i>	<i>Candida albicans</i>
96% EtOH extract	0.036	21.0±0.4	18.5±0.5	18.5±0.5	19.0±0.4	19.0±0.4	16.0±0.4
60% EtOH extract	0.039	22.5±0.5	21.0±0.4	20.0±0.4	21.0±0.4	21.0±0.4	17.0±0.4
40% EtOH extract	0.042	19.5±0.5	19.5±0.5	17.5±0.5	19.5±0.5	19.5±0.5	16.0±0.4
20% EtOH extract	0.035	16.5±0.5	17.0±0.4	17.0±0.4	16.5±0.5	17.0±0.4	14.5±0.5
H <sub>2</sub> O extract	0.035	17.0±0.4	18.0±0.4	18.0±0.4	16.0±0.4	17.0±0.4	15.0±0.4
<b>Gentamycin</b>	0.003	22.0±0.4	24.0±0.3	25.3±0.3	25.0±0.3	25.6±0.3	12.0±0.6
<b>Fluconazole</b>	0.003	18.0±0.4	12.0±0.6	14.3±0.6	12.3±0.6	10.0±0.8	20.0±0.4

The dependence of antioxidant, antibacterial and antifungal activity on the content of different groups of biologically active substances was studied using the method of linear regression. In Fig. 1 shows that the correlation between the antioxidant effect and the sum polyphenols was moderate (R=0.6566), in the case of catechins was moderate (R=0.7318), flavonoids was very high (R=0.9230), in the case of hydroxycinnamic acids was moderate (R=0.6512), and the lowest correlation value was observed for organic acids.

According to the research results presented in Fig. 2 it was found that there is a high correlation between phenolic compounds (R=0.8643), flavonoids (R=0.7031), moderate correlation – organic acids (R=0.5902), and inhibition of the growth of *S. aureus*, in the case of catechins (R=0.2258), hydroxycinnamic acids (R=0.3936), and antioxidant activity (R=0.4479) – low correlation.

In Fig. 3 shows that the antimicrobial effect against *B. subtilis* is very highly dependent on the content of flavonoids (R=0.9064), high dependent on polyphenols (R=0.8643), and antioxidant activity (R=0.8167), in turn, the sum hydroxycinnamic acids is observed moderate correlation and in the case of catechins there is no dependence.

The study showed that there is no correlation between organic acids (R=0.1229), catechins (R=0.036), and inhibition of *E. coli* growth, while polyphenols, flavonoids, have moderate correlation on the growth inhibition of *E. coli*, whereas a high correlation is observed in case of hydroxycinnamic acid. (Fig. 4)

When studying the relationship between inhibition of growth of *P. vulgaris* and the content of different groups of biologically active substances, there is a very high dependence of antibacterial activity on the polyphenols (R=0.9623), high correlation – flavonoids (R=0.8704), in turn, the antioxidant effect, organic acids had a moderate correlation, while catechins, hydroxycinnamic acids had not correlation at all. (Fig. 5)

Fig. 6 shows that the correlation between the growth inhibition of *P. aeruginosa* and the sum of polyphenols (R=0.9470) is very high, with the sum of flavonoids was high, in the case of organic acids and antioxidant effect it was found moderate correlation. Whereas, the sum hydroxycinnamic acids was not effect on the inhibition of growth *P. aeruginosa*.

In Fig. 7 shows a high correlation between inhibition of the growth of *C. albicans* and the sum

polyphenols (R=0.8665), flavonoids (R=0.8133), in turn, with the sum of polyphenols (R=0.6316) was found a moderate dependence, a low correlation was

determined of content organic acids, and the total content of catechins was not effect on the inhibition of growth of *C. albicans*.

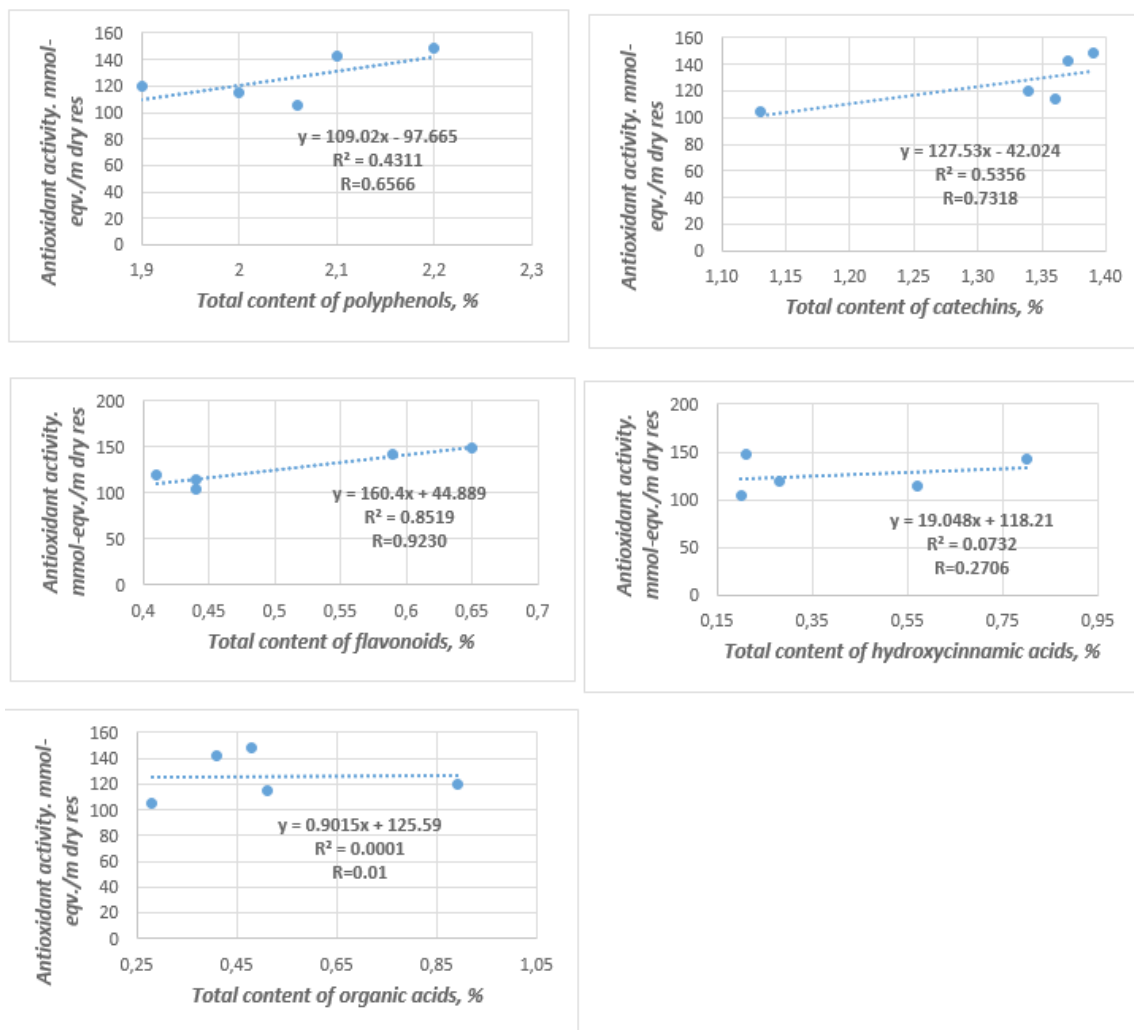


Figure 1. Correlation relationship between value of antioxidant activity and biologically active substances

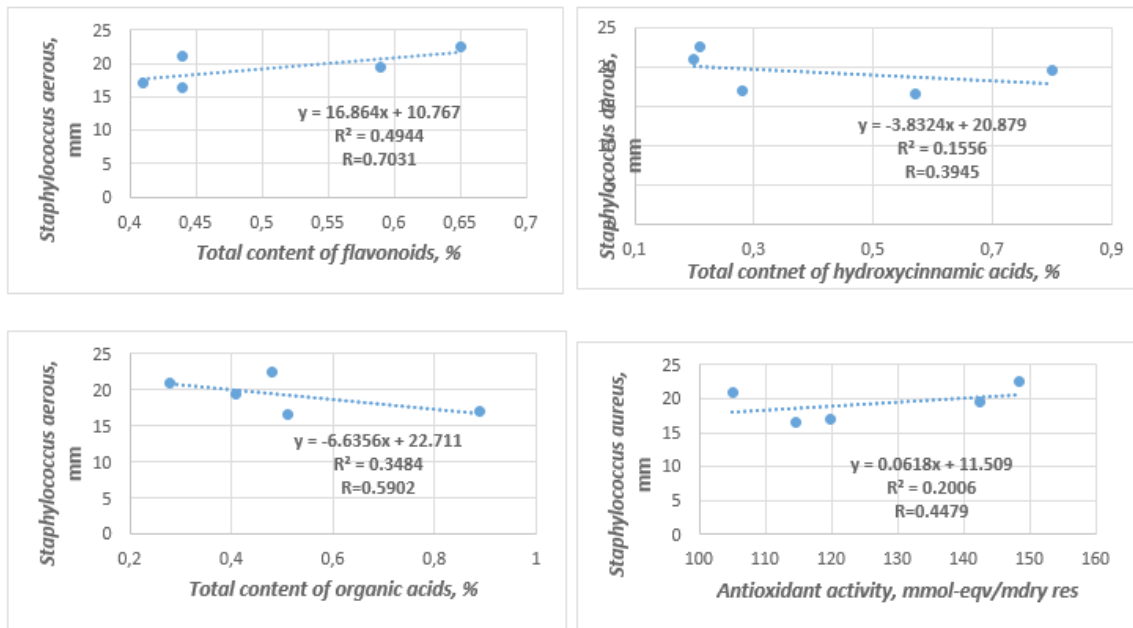


Figure 2. Correlation relationship between value of antimicrobial activity against *S. aureus* and sum of biologically active substances, antioxidant activity

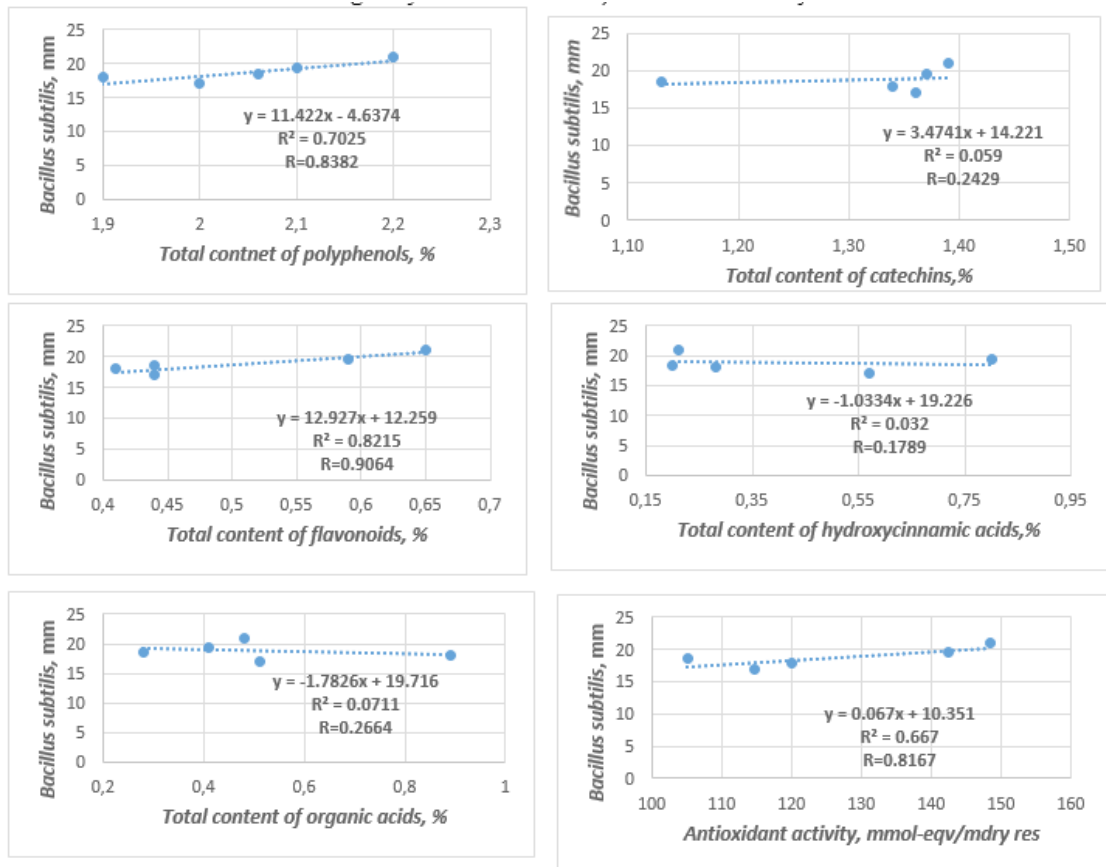


Figure 3. Correlation relationship between value of antimicrobial activity against *B. subtilis* and sum of biologically active substances, antioxidant effect

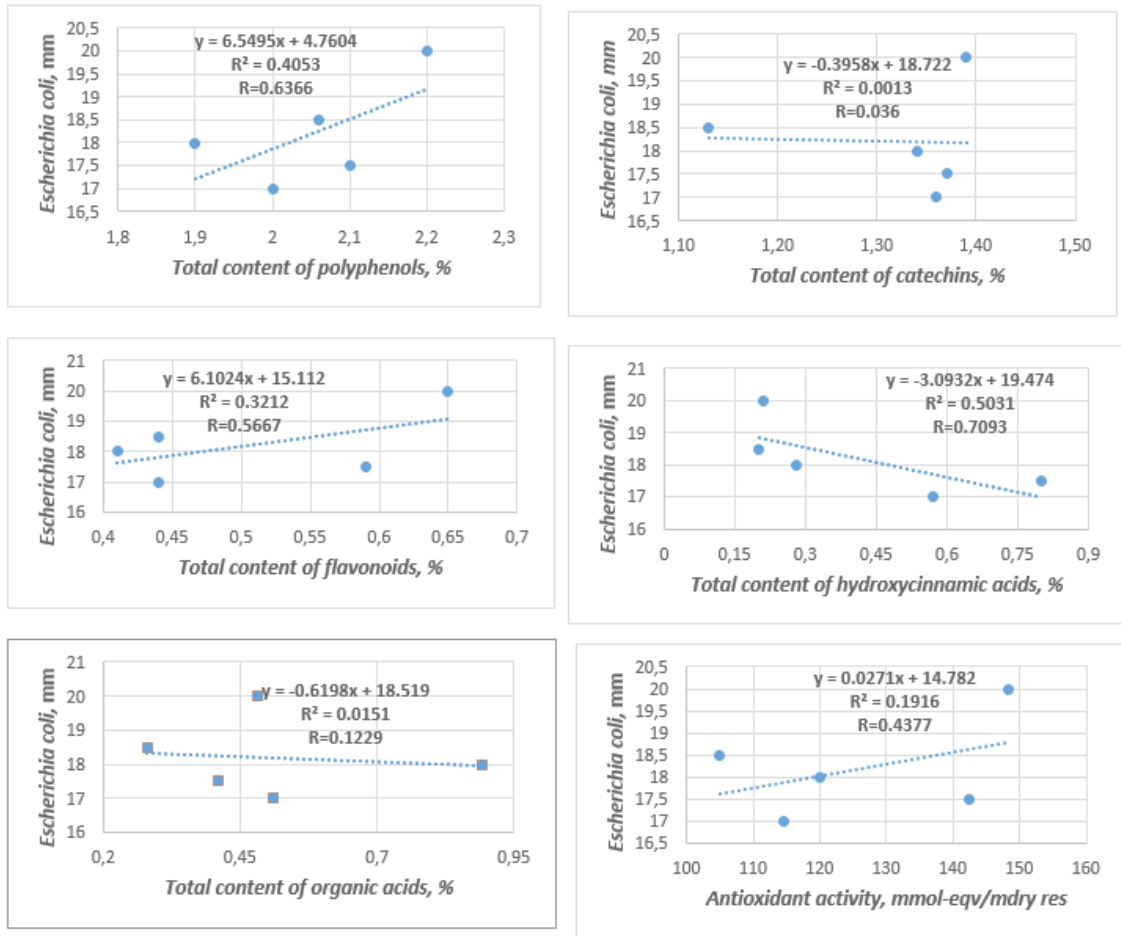
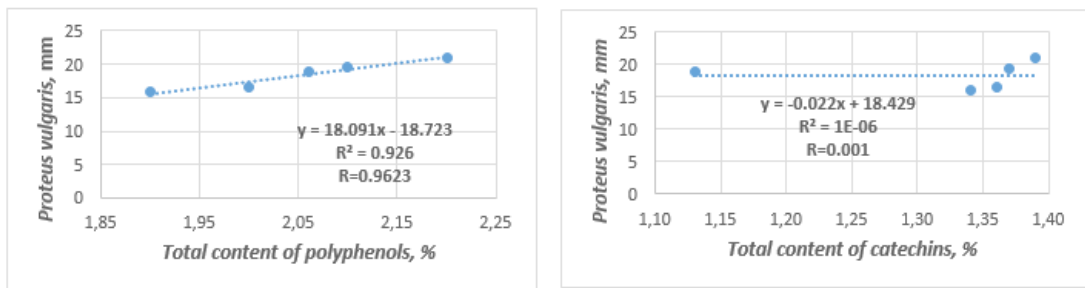


Figure 4. Correlation relationship between value of antimicrobial activity against *E. coli* and sum of biologically active substances, antioxidant activity



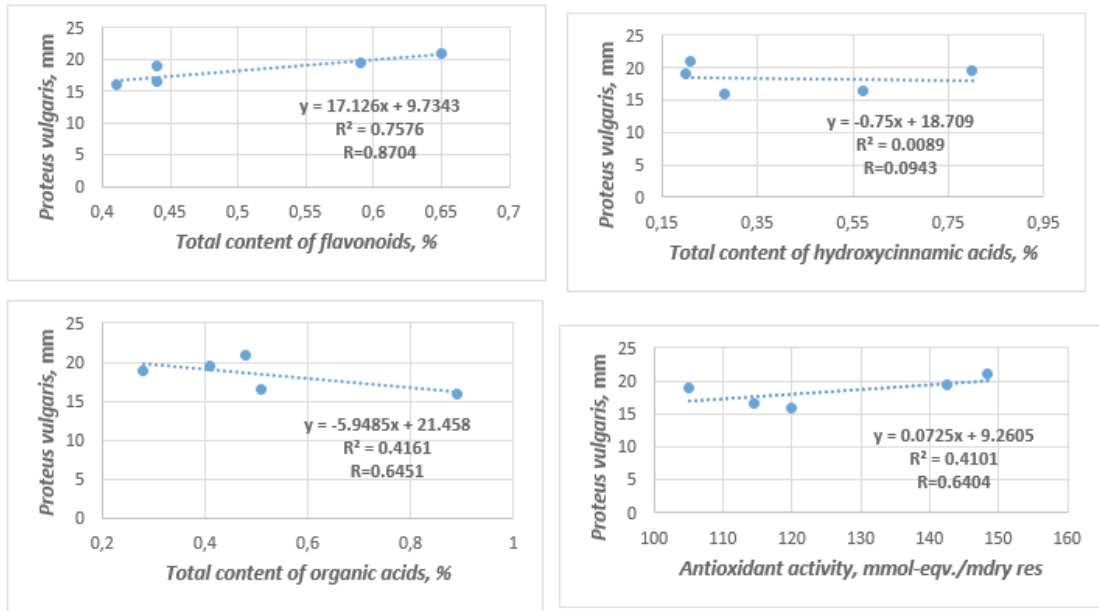


Figure 5. Correlation relationship between value of antimicrobial activity against *P. vulgaris* and sum of biologically active substances, antioxidant activity

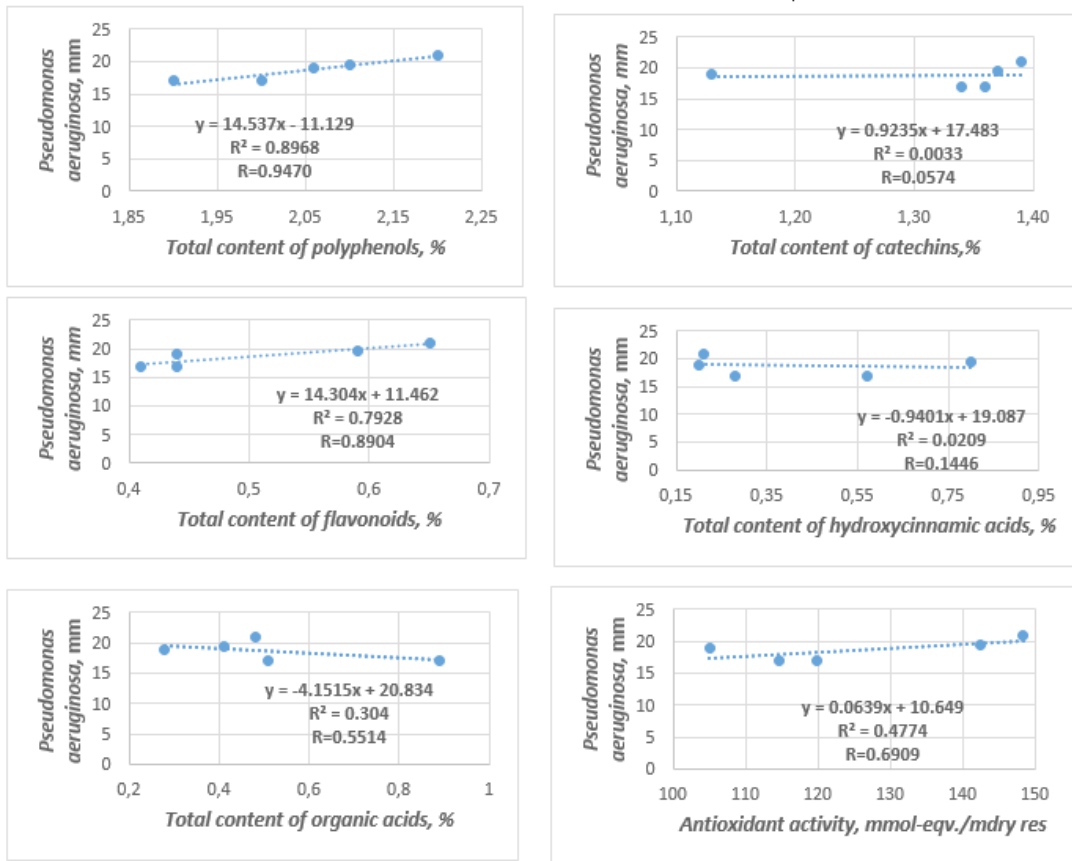
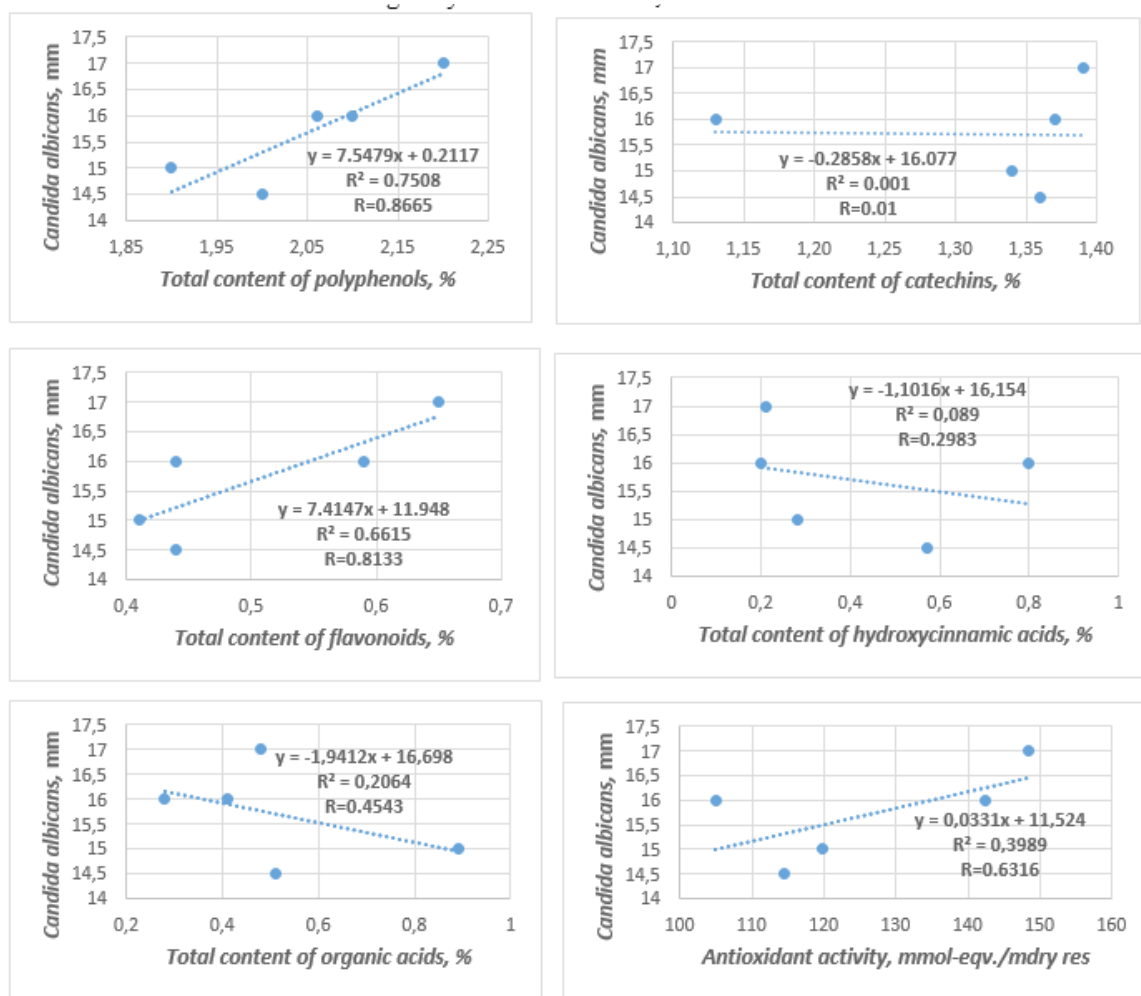


Figure 6. Correlation relationship between value of antimicrobial activity against *P. aeruginosa* and sum of biologically active substances, antioxidant effect



**Figure 7.** Correlation relationship between value of antimicrobial activity against *C. albicans* and sum of biologically active substances, antioxidant activity

Ispiryán *et al.* (2024) reported on the study of the relationship between antiradical and antibacterial activity and the total polyphenol and flavonoid content in extracts of raspberry shoots, leaves, seeds, and fruits. A significant correlation was found between the content of biologically active compounds and the antiradical effect. However, no correlation was observed for antibacterial activity ( $R = 0.3$ ). When studying the dependence of antioxidant activity on the content of different groups of biologically active substances, it was found that phenolic compounds and catechins had the strongest influence on antioxidant activity.

In the investigation of the correlation between the inhibition of bacterial growth (*S. aureus*, *B. subtilis*, *P. aeruginosa*) and fungi (*C. albicans*) and the content of biologically active substances, it was shown that microbial growth was most strongly influenced by phenolic compounds, flavonoids, and antioxidant effects. The growth of *E. coli* was most strongly influenced by the content of hydroxycinnamic acids.

### CONCLUSION

In the research, it has been determined the content of biologically active compounds, antiradical, antibacterial and antifungal activity of the obtained

extracts of *V. vitis-idaea* leaf. The dominant content of the sum of polyphenols, flavonoids, catechins was observed in 60% extract, whereas the organic acids in aqueous extract. The 60% EtOH extract has a high level of antioxidant activity, all obtained extracts actively inhibits the growth of all studied G(+), G(-) strains and *C. albicans* in the range from 14.5 to 22.5 mm (diameter of growth inhibition). We have shown that there is a high correlation between the content of polyphenols, flavonoids and inhibition of G(+) strain – *S. aureus*, *B. subtilis*, G(-) strain – *P. aeruginosa*, *P. vulgaris*, and *C. albicans* as well as *E. coli* is depends on content of hydroxycinnamic acids. These findings show the great potential in the development and creation of new medicines with antibacterial, antioxidant and antifungal effects that are not inferior to, and even superior to, the effects of synthetic analogues.

#### CONFLICT OF INTEREST

The authors declare that there is no conflict of interest.

#### ACKNOWLEDGMENTS

We are grateful for the provided scientific and material help pharmaceutical company “Zdravopharm”, Kharkiv, Ukraine

#### REFERENCES

- Abdallah, E. M., Alhatlani, B. Y., de Paula Menezes, R., & Martins, C. H. G. (2023). Back to Nature: Medicinal Plants as Promising Sources for Antibacterial Drugs in the Post-Antibiotic Era. *Plants*, 12(17), 3077. <https://doi.org/10.3390/plants12173077>
- Blainski, A., Lopes, G., & de Mello, J. (2013). Application and Analysis of the Folin Ciocalteu Method for the Determination of the Total Phenolic Content from *Limonium Brasiliense* L. *Molecules*, 18(6), 6852–6865. <https://doi.org/10.3390/molecules18066852>
- Bongomin, F., Gago, S., Oladele, R., & Denning, D. (2017). Global and Multi-National Prevalence of Fungal Diseases—Estimate Precision. *Journal of Fungi*, 3(4), 57. <https://doi.org/10.3390/jof3040057>
- Chaachouay, N., & Zidane, L. (2024). Plant-Derived Natural Products: A Source for Drug Discovery and Development. *Drugs and Drug Candidates*, 3(1), 184–207. <https://doi.org/10.3390/ddc3010011>
- Cvetkova, M., Bandere, D., Lauberte, L., Niedra, S., & Teterovska, R. (2024). Polyphenol Content, Antiradical Properties, and  $\alpha$ -Amylase Inhibition Activity of *Vaccinium myrtillus* L. (Bilberry) and *Vaccinium vitis-idaea* L. (Lingonberry) Leaf and Aerial Parts Extracts. *Applied Sciences*, 14(12), 5237. <https://doi.org/10.3390/app14125237>
- Di Pede, G., Mena, P., Bresciani, L., Achour, M., Lamuela-Raventós, R. M., Estruch, R., Landberg, R., Kulling, S. E., Wishart, D., Rodriguez-Mateos, A., Crozier, A., Manach, C., & Del Rio, D. (2022). Revisiting the bioavailability of flavan-3-ols in humans: A systematic review and comprehensive data analysis. *Molecular Aspects of Medicine*, 101146. <https://doi.org/10.1016/j.mam.2022.101146>
- Ferlemi, A.-V., & Lamari, F. (2016). Berry Leaves: An Alternative Source of Bioactive Natural Products of Nutritional and Medicinal Value. *Antioxidants*, 5(2), 17. <https://doi.org/10.3390/antiox5020017>
- Hirabayashi, K., Debnath, S. C., & Owens, G. L. (2023). Unveiling the evolutionary history of lingonberry (*Vaccinium vitis-idaea* L.) through genome sequencing and assembly of European and North American subspecies. *G3: Genes, Genomes, Genetics*. <https://doi.org/10.1093/g3journal/jkad294>



- Ikuta, K. S., Swetschinski, L. R., Robles Aguilar, G., Sharara, F., Mestrovic, T., Gray, A. P., Naghavi, M. (2022). Global mortality associated with 33 bacterial pathogens in 2019: a systematic analysis for the Global Burden of Disease Study 2019. *The Lancet*. [https://doi.org/110.1016/s0140-6736\(22\)02185-7](https://doi.org/110.1016/s0140-6736(22)02185-7)
- Ispiryan, A., Atkociuniene, V., Makstutiene, N., Sarkinas, A., Salaseviciene, A., Urbonaviciene, D., Raudone, L. (2024). Correlation between Antimicrobial Activity Values and Total Phenolic Content/Antioxidant Activity in *Rubus idaeus* L. *Plants*, 13(4), 504. <https://doi.org/10.3390/plants13040504>
- Kowalska, K. (2021). Lingonberry (*Vaccinium vitis-idaea* L.) Fruit as a Source of Bioactive Compounds with Health-Promoting Effects—A Review. *International Journal of Molecular Sciences*, 22(10), 5126. <https://doi.org/110.3390/ijms22105126>
- Kryvtsova, M. V., Trush, K., Eftimova, J., Koscova, J., & Spivak, M. J. (2019). Antimicrobial, Antioxidant and some Biochemical Properties of *Vaccinium vitis-idaea* L. *Mikrobiolohichni Zhurnal*, 81(3), 40–52. <https://doi.org/10.15407/microbiolj81.03.040>
- Maslov, O. Y., Komisarenko, M. A., Golik, M. Y., Kolisnyk, S. V., Altukhov, A. A., Baiurka, S. V., . . . Iuliia, K. (2023a). Study of total antioxidant capacity of red raspberry (*Rubus idaeus* L.) shoots. *Vitae*, 30(1), 1 – 9. <https://doi.org/110.17533/udea.vitae.v30n1a351486>
- Maslov, O., Komisarenko, M., Kolisnyk, S., & Derymedvid, L. (2024). Evaluation of Anti-Inflammatory, Antioxidant Activities and Molecular Docking Analysis of *Rubus idaeus* Leaf Extract. *Jordan Journal of Pharmaceutical Sciences*, 17(1), 105–122. <https://doi.org/110.35516/jjps.v17i1.1808>
- Maslov, O., Komisarenko, M., Kolisnyk, S., Kostina, T., Golik, M., Moroz, V., Akhmedov, E. (2023b). Investigation of the extraction dynamic of the biologically active substances of the raspberry (*Rubus idaeus* L.) shoots. *Current Issues in Pharmacy and Medical Sciences*. 36(4), 194-198. <https://doi.org/10.2478/cipms-2023-0034>
- Maslov, O., Komisarenko, M., Kolisnyk, S., Tkachenko, O., Akhmedov, E., Poluain, S., Kostina, T., & Kolisnyk, O. (2023c). Study of qualitative composition and quantitative content of free organic acids in lingonberry leaves. *Fitoterapia*, (1), 77–82. <https://doi.org/10.32782/2522-9680-2023-1-77>
- Mikulic-Petkovsek, M., Schmitzer, V., Slatnar, A., Stampar, F., & Veberic, R. (2012). Composition of Sugars, Organic Acids, and Total Phenolics in 25 Wild or Cultivated Berry Species. *Journal of Food Science*, 77(10), C1064–C1070. <https://doi.org/10.1111/j.1750-3841.2012.02896.x>
- Panche, A. N., Diwan, A. D., & Chandra, S. R. (2016). Flavonoids: an overview. *Journal of Nutritional Science*, 5. <https://doi.org/10.1017/jns.2016.41>
- Ryyti, R., Hämäläinen, M., Peltola, R., & Moilanen, E. (2020). Beneficial effects of lingonberry (*Vaccinium vitis-idaea* L.) supplementation on metabolic and inflammatory adverse effects induced by high-fat diet in a mouse model of obesity. *PLOS ONE*, 15(5), Стаття e0232605. <https://doi.org/10.1371/journal.pone.0232605>
- Tsamenko, K. (2018). Antibacterial activity of phytosubstances from *Vaccinium vitis-idaea* leaves. *Annals of Mechnikov Institute*, (3), 23–26.

Vyas, P., Kalidindi, S., Chibrikova, L., Igamberdiev, A. U., & Weber, J. T. (2013). Chemical Analysis and Effect of Blueberry and Lingonberry Fruits and Leaves against Glutamate-Mediated Excitotoxicity. *Journal of Agricultural and Food Chemistry*, 61(32), 7769–7776. <https://doi.org/110.1021/jf401158a>

# An Experimental Investigation based on a Novel Gastro-Retentive Raft Liquid Dosage Form in Tandem with Controlled-Release Strategies for Oral Delivery of Metronidazole

Himangshu SARMA\*, Taslima JAHAN\*\*, Ashis Kumar GOSWAMI\*\*\*,  
Hemanta Kumar SHARMA\*\*\*\*°

*An Experimental Investigation based on a Novel Gastro-Retentive Raft Liquid Dosage Form in Tandem with Controlled-Release Strategies for Oral Delivery of Metronidazole*

*Metronidazolün Oral Uygulamasını için Kontrollü Salm Stratejileriyle Birlikte Yeni Bir Gastro-Retentif Raft Sıvı Dozaj Formuna Dayalı Deneysel Bir Araştırma*

## SUMMARY

Peptic ulcers are lesions that form on the mucosal lining of the stomach and duodenum. The most common inducer of peptic ulcers is *Helicobacter pylori* (*H. pylori*) as the primary pathogen. The present study aimed to design and develop a novel gastro retentive raft liquid dosage formulation to prolong the gastric retention time of the medicament for the treatment of *H. pylori* infection. Metronidazole-loaded raft formulations were prepared using ion-sensitive in situ gel-forming polymers. The formulation was floated within 1 minute on the liquid surface of the in vitro model and maintained floatation for more than 24 hours. Among those formulations, formulation F-5 exhibited results within acceptable limits compared with the other batches of formulations. The in vitro drug release was  $81.83 \pm 0.54$  % after 8 hours in 0.1 M HCl. The drug, metronidazole, was released from the dosage form slowly in the stomach. The formulation followed first-order release kinetics, and metronidazole was released from the formulation as a combination of diffusion and erosion mechanisms. Thus, the proposed metronidazole-loaded raft formulation would be a promising novel site-specific drug delivery system and has a potential utility in the therapy of peptic ulcers induced by *H. pylori*.

**Key Words:** Floating drug delivery system, Metronidazole, Peptic ulcer, Stomach-specific delivery, *H. pylori*.

## ÖZ

Peptik ülserler, mide ve duodenumun mukoza yüzeyinde oluşan lezyonlardır. Peptik ülserlerin en yaygın nedenlerinden biri, birincil patojen olarak *Helicobacter pylori*'dir (*H. pylori*). Bu çalışma, ilacın mide içinde kalış süresini uzatarak *H. pylori* enfeksiyonunu tedavi etmek amacıyla yeni bir gastro-retentif raft sıvı dozaj formülasyonu tasarlamayı ve geliştirmeyi amaçlamıştır. Metronidazol yüklü raft formülasyonları, iyon duyarlı in situ jel oluşturan polimerler kullanılarak hazırlanmıştır. Formülasyon, in vitro modelde sıvı yüzeyinde 1 dakika içinde yüzmeye başlamış ve 24 saatten fazla süreyle yüzmeye durumunu korumuştur. Bu formülasyonlar arasında, F-5 formülasyonu diğer formülasyon gruplarıyla karşılaştırıldığında kabul edilebilir sınırlar içinde sonuçlar göstermiştir. In vitro ilaç salım, 0.1 M HCl'de 8 saat sonra  $81.83 \pm 0.54$  % olarak gerçekleşmiştir. Metronidazol, dozaj formundan midede yavaşça salınmıştır. Formülasyon birinci dereceden salım kinetiğini izlemiş ve metronidazol, formülasyondan difüzyon ve erozyon mekanizmalarının bir kombinasyonu olarak salınmıştır. Bu nedenle, önerilen metronidazol yüklü raft formülasyonu, bölgeye özgü yeni bir ilaç taşıma sistemi olarak umut vadetmektedir ve *H. pylori*'nin neden olduğu peptik ülserlerin tedavisinde potansiyel bir kullanıma sahiptir.

**Anahtar Kelimeler:** Yüzen ilaç taşıma sistemi, Metronidazol, Peptik ülser, Mideye özgü taşıma, *H. pylori*.

Received: 25.10.2024

Revised: 28.12.2024

Accepted: 03.02.2025

\* ORCID: 0000-0002-8585-8182, Department of Pharmaceutical Sciences, Faculty of Science and Engineering, Dibrugarh University, Dibrugarh-786004, Assam, India

\*\* ORCID: Department of Pharmaceutical Sciences, Faculty of Science and Engineering, Dibrugarh University, Dibrugarh-786004, Assam, India

\*\*\* ORCID: 0000-0002-9994-0849, Department of Pharmaceutical Sciences, Faculty of Science and Engineering, Dibrugarh University, Dibrugarh-786004, Assam, India

\*\*\*\* ORCID: 0000-0003-2632-4903, Department of Pharmaceutical Sciences, Faculty of Science and Engineering, Dibrugarh University, Dibrugarh-786004, Assam, India

° Corresponding Author: Dr. Hemanta Kumar Sharma  
Email: hemantasharma123@yahoo.co.in

## INTRODUCTION

Peptic ulcers are lesions that form on the mucosal lining of the stomach and duodenum. The most common inducer of peptic ulcers is *Helicobacter pylori* (*H. pylori*) as the primary pathogen. Other non-pathogenic causes of peptic ulcers include the prolonged use of medicaments such as steroids, non-steroidal anti-inflammatory drugs (NSAIDs), anticoagulants, alcohol, spicy food, etc. Low antibiotic levels and limited medication accessibility at the site of infection are two of the many challenges in eliminating *H. pylori* infections (Adebisi et al., 2015). According to researchers, antibiotics absorbed via the mucus layer are more successful than those that are absorbed through the basolateral membrane in eliminating *H. pylori* (Nori et al., 2011). Hence, the nitroimidazole group of drugs like metronidazole is preferred for the treatment of anaerobic or facultative anaerobic microbes like *H. pylori*. *H. pylori* exhibits redox potential in the electron transport segments, which reduces the metronidazole nitro group to nitro radicals and leads to the production of toxic metabolites, which can disrupt *H. pylori* DNA replication (Hernández Ceruelos et al., 2019).

The application of nitro-imidazole derivatives, such as metronidazole, tinidazole, etc., is an active adjuvant antibiotic in the management of peptic ulcers caused by *H. pylori* (Emara et al., 2014). However, metronidazole has a plasma  $t_{1/2}$  of 8 hours. Generally, 400 mg three times daily is prescribed in the treatment of *H. pylori*. The frequent administration of metronidazole aggravates the adverse effects such as anorexia, nausea, vomiting, peripheral neuropathy, and can develop bacterial resistance. The effects on the central nervous system are mainly dose-dependency related, which can negatively impact patient compliance (Tripathi, 2013). Therefore, it was thought to be worthy of formulating in site-specific dosage forms, which act locally at the site of disease occurrence. It would reduce the frequency of the therapeutic dose of the medicament, minimize the

potential adverse effects as well as raise the efficacy of the treatment and patient compliance. Accordingly, preparing gastro retentive dosage forms is crucial for the complete eradication of *H. pylori*. Additionally, metronidazole offers the advantage of having pH-independent activity, unlike the other anti-*H. pylori* antibiotics such as clarithromycin. The researchers have made several attempts to eradicate microorganisms from the stomach completely (Koga, 2022; Nori et al., 2011; Rajinikanth & Mishra, 2008).

Pharmaceutical scientists have designed various novel drug delivery systems to enhance the gastric residence time of anti-*H. pylori* medicaments. Thus, raft liquid, floating, swellable, mucoadhesive, high-density formulations, etc., are being developed to achieve gastro retention (Nori et al., 2011). Among the various novel gastro retentive drug delivery systems (GRDDS), raft liquid delivery dosage form is a progressed revolution in liquid oral controlled drug delivery. Raft dosage forms are liquid at room temperature but go through gelation once the pH changes, wherein each part of the liquid swells organizing a continuous layer called a raft (Vinod et al., 2010). Each layer of gel floats on the gastric fluid owing to its bulk density which is less than gastric fluids. It remains buoyant inside the stomach without being affected by the gastric emptying rate for a long duration of time, which has been assessed for sustaining as well as targeting the dosage form for drug delivery (Abou Youssef et al., 2015; Prajapati et al., 2013). The raft remains intact inside the stomach contents for more than 48 hours, raising gastric residence time and sustaining drug delivery in the gastrointestinal tract (GIT) (Ibrahim, 2009).

The goal of designing this raft formulation is to slowly release the medicament from the dosage form at a desired rate in the stomach. This raft formulation significantly prolongs the gastric residence time of a medicament, improves oral bioavailability, and simultaneously minimizes dosing intervals. Additionally, raft liquid formulation is simple to formulate as well

as cost-effective. Moreover, it is absorbed from the proximal part of GIT, so this raft formulation allows for prolonged drug release in the vicinity of the bacterium (Rajinikanth et al., 2007).

Keeping this concept in mind, the present study aimed to improve the gastric residence time of metronidazole via formulating a raft liquid formulation to eradicate *H. pylori* and control the release of the medicament into the local site of action. This dosage formulation could offer a revolutionary solution for the treatment of *H. pylori*.

## MATERIAL AND METHODS

### Chemicals

Metronidazole was obtained as a gift sample from Ozone Pharmaceutical Pvt. Ltd. Guwahati, India. Eudragit® NE 30D was procured from Yarrow Chem Product, Mumbai, India. Calcium carbonate ( $\text{CaCO}_3$ ), sodium alginate, sodium citrate, and sodium bicarbonate ( $\text{NaHCO}_3$ ) were procured from Himedia Ltd. Mumbai, India. Barium sulphate ( $\text{BaSO}_4$ ) and Hydrochloric acid (HCl) were procured from Merck Specialities Pvt. Limited, Mumbai, India

### Preparation of Metronidazole loaded gastro retentive raft forming formulation

#### *Coating of Metronidazole*

Metronidazole was initially dispersed in Eudragit® NE 30D and then dried in the hot air oven at 70°C till completely dry. The achieved dried mixture was then kept in tightly closed containers until further use.

#### *Preparation of the raft-forming formulation*

According to Table 1 composition, the eight raft formulations were prepared (Abouelatta et al., 2018). Rafts were prepared by dissolving sodium alginate at the concentration of 1-3 % w/v in deionized water containing 0.17 % w/v of sodium citrate and 1 % w/v of  $\text{NaHCO}_3$ . Then  $\text{CaCO}_3$  solution of (0.5-3 % w/v) different concentrations was with continuous stirring on a magnetic stirrer (Model AI-021, Alfa instru-

ments, New Delhi, India). Then, previously coated metronidazole was suspended in the resulting solution with continuous stirring until it was thoroughly dispersed, and the final volume was made to 100 mL with deionized water. The obtained raft-forming formulations were stored in amber-colored containers and protected from light for further experimental study.

### Drug excipients compatibility study of the model drug with excipients

It was carried on by Fourier transform Infrared spectroscopy (FT-IR) and Differential Scanning Calorimetry (DSC).

#### *Differential Scanning Calorimetry*

DSC was performed to measure the heat exchange during thermal transitions, which gave information on the structural properties of the ingredients. Metronidazole, metronidazole with Eudragit® NE 30D, and physical mixtures of metronidazole with all excipients were performed separately by using a Perkin Elmer JADE DSC (USA) instrument. The samples were kept in an aluminum pan and scanned at a speed of 10 °C minute<sup>-1</sup> at the temperature range of 20 °C to 300 °C under the inert nitrogen gas atmosphere. The thermograms were observed for any phase changes during the analysis process if there were any changes in thermograms compared to individual components used in formulation, indicating their interaction with each other.

#### *Fourier transform infrared spectroscopy (FT-IR)*

FT-IR was performed to study the compatibility of ingredients. In this technique, the nature of the interacting force can be evaluated during the gelation process. The FT-IR spectra of metronidazole, metronidazole with Eudragit® NE 30D, and physical mixtures of metronidazole with all excipients were analyzed in Bruker Alpha FT-IR spectrophotometer, Germany, to distinguish if there is any interaction between drug and polymers.

**Evaluation of post-formulation parameters and gastro retentive study of developed formulation**

*Rheological property of the raft formulations*

The rheological property is the characteristic function of raft formulations. It was carried out on a rotating viscometer (Anton Paar Rheometer MCR 102SN81260812) at 25 ± 2 °C. Viscosity was measured at speeds ranging from 0.3 to 60 rpm.

*Measurement of raft weight, volume, density, and buoyancy*

The raft’s weight, volume, and density were measured according to a modified method of Abbas et al. (2017), Bunlung et al. (2021), and Hampson et al. (2005). The maximum dose of the prepared raft formulation was transferred to 150 mL of 0.1 M HCl (pH1.2) in a glass beaker, which was previously maintained at the temperature of 37± 1 °C and waited for 30 minutes till the raft was formed. Before preparing the raft, each beaker was pre-weighed (W<sub>1</sub>). The top of each raft was observed from the outer surface of the beaker, and the position of each raft reached on top was marked on the outside of the beaker. The total weight of the beaker containing the raft was noted after raft formation (W<sub>2</sub>). The weight of each raft formation was calculated from the formula (Eq 1).

$$Raft\ weight\ (g) = W_2 - W_1 \dots\dots\dots Eq\ 1$$

Where, W<sub>1</sub> is the weight of the empty beaker, and W<sub>2</sub> is the weight of the beaker containing the raft.

The raft was transferred from the beaker to a measuring cylinder and the final volume of each raft was determined. We assumed that in the formula, the density of the subnatant liquid is the same as that of water. Finally, the density of each raft was calculated as per the following equation (Eq 2).

$$Raft\ density = \frac{Raft\ weight\ (g)}{Raft\ volume\ (ml)} \dots\dots\dots Eq\ 2$$

Each formulation was tested in triplicate. The density of each raft was expressed as g mL<sup>-1</sup>

A buoyancy index was calculated as,

$$Raft\ bouncy\ (ml) = \frac{Raft\ Volume - Raft\ weight}{Raft\ weight} \quad Eq\ 3$$

*Measurement of raft strength of the formulation*

Raft strength is used to determine the firmness, consistency, cohesiveness, and gelling properties of the prepared formulation. The strength was with a modified balanced method. Here, rafts were developed in a 250 mL glass beaker under the same conditions as described above, but with an additional suspended L-shaped stainless-steel probe (diameter: 1.2 mm) placed in the center of the beaker, with the lower third immersed in acid. The beaker was positioned on the balance after 30 minutes of raft development. Then water was added dropwise until the raft surface was back drowned, and the force was recorded in grams. (Note: A double pan dispensing balance was modified to facilitate the measurement of raft strength, where one of the pans was replaced with the same volume of a beaker containing water) (Abbas et al., 2017; Hampson et al., 2005).

*In vitro floating and gelling capacity of the raft formulation*

The maximum dose of the prepared raft formulation was carefully and slowly transferred to 250 mL of a glass beaker, as above condition, but without suspending an L-shaped stainless steel probe, and waited for 30 minutes till the raft was formed. The gelation was noticed by visual observation. The time that the formulation takes to emerge on the medium, i.e., floating log time, and the duration of time during which the formulation continued to levitate on the surface of the medium, i.e., floating duration, were recorded. The floating behavior of each formulation was recorded in three categories based on the time and period for which the formed gel remained floating in a medium, such as the formation of the raft after a few minutes, dispersed rapidly, formation of immediate raft remains for 12 hours and formation of immediate raft remains for over 12 hours.

### *In vitro* determination of drug release

Raft forming formulation is administered through the oral route; thus, the release rate of metronidazole from raft formulation was carried out using a USP type II rotating paddle dissolution apparatus (Abou Youssef et al., 2015) (Electro lab, Mumbai) in 900 mL 0.1M HCl at  $37 \pm 1$  °C and rotating speed of 50 rpm. 10 mL of the raft formulation was carefully injected using a disposable syringe into the dissolution vessel without much disturbance and in the paddle device, the raft was capable of floating freely on the surface of the liquid, due to the minimum surface stress of the surface. 5 mL aliquots were withdrawn and replaced by fresh samples at predetermined fixed time intervals. The quantity of metronidazole in the withdrawn samples was analyzed by a UV Spectrophotometer (UV- 1800, Shimadzu Spectrophotometer, Japan) at approximately 276 nm. Tests were carried out repeatedly for each formulation three times, and data were reported as mean value  $\pm$  S.D. The cumulative percentage release of the drug against time was plotted to depict the metronidazole release profile (Kerdsakundee et al., 2015).

### *In vitro* drug release kinetics

To facilitate the easier comparison of each formulation and analyze the impact of various factors on drug release profiles, we calculated the cumulative percentage of drugs released at predetermined time intervals. Drug release data were analyzed according to various *in vitro* drug release kinetics models such as zero-order, first-order, Korsmeyer- Peppas, and Higuchi models (Abbas et al., 2017; Das et al., 2010).

### *In situ* gel-forming activity in rabbit stomach using Roentgenography

The Roentgenography method is widely used to locate dosage forms in the GIT; therefore, it can be assumed and correlated with the duration of gastric evacuation along with the passage of dosage forms in the GIT. It involves radio-opaque markers such as BaSO<sub>4</sub> (Hooda, 2011; Prajapati et al., 2013).

### *Preparation of radio-opaque raft formulation*

As mentioned previously, the optimized raft formulation was prepared and made radio-opaque by adding 500 mg of BaSO<sub>4</sub> in the same formulation instead of metronidazole. Then, the formulation was homogeneously mixed to form a homogeneous dispersion and finally stored in containers (El-Mahrouk et al., 2016).

### *Radiographic examination of optimized raft formulation in the rabbit model*

The experiment was reviewed, approved (Approval No.-IAEC/DU/164), and conformed with the guidelines of the IAEC (Institutional Animal Ethics Committee) for Animal experiments.

*In vivo* gel-forming activity was carried on through the X-ray method in young and healthy male albino rabbits (6–8 weeks, 2.0 - 2.2 kg). They were kept for one week in an animal house in spacious, labeled cages maintained in standard laboratory conditions at a temperature of  $26 \text{ }^\circ\text{C} \pm 2 \text{ }^\circ\text{C}$  and relative humidity of 44–56 % with 12 hours of light and dark cycle prior to the experiment acclimatizing them and were given food as well as water *ad libitum*. None of the animals had symptoms or a history of GI disease. The rabbits were kept in fast condition for 24 hours with free access to water prior to the commencement of the experiment, which maintained the constant GI motility. In this study, the first X-ray image of the rabbit was taken to ensure the absence of radio-opaque compounds in the GIT. The formulation prepared for radiography was orally administered to rabbits with the help of a gastric lavage tube. The rabbits were not allowed to eat during the experiment, but water *ad libitum* was provided.

In this model, 5 mL of the optimized formulation, instead of the drug, was orally administered to each rabbit. Radiographs were taken from the ventral portion of the rabbit at predetermined time intervals af-

ter dosing. The X-ray generating unit (Allengers Mars 3.5/4.2 Mobile X-ray machine) was set at 50 kv, 100 mA, and 1 second. Radiographs were taken to assess gel formation and demonstrate gastric retention for an extended period (El-Mahrouk et al., 2016).

### Statistical analysis

All the tests were expressed in triplicates, and the results are shown in mean  $\pm$  standard deviation. All statistical analyses were performed in GraphPad Prism 7.04. Statistical significance within the variables was determined by employing a one-way ANOVA. The correlation between the cumulative percent *in vitro* drug release profile, raft strength, and viscosity was analyzed using Pearson's correlation (two-tailed test). The significance level was studied at  $p < 0.05$ .

## RESULTS AND DISCUSSION

### Drug-excipients compatibility study

#### *Differential scanning calorimetric study*

The DSC thermogram of metronidazole (Supplementary Figure 1) showed a sharp endothermic peak at 170.58 °C. When metronidazole was coated with Eudragit® NE 30D (Supplementary Figure 1), a sharp endothermic peak was observed at 168.76 °C, where a slight change was observed compared to the uncoated metronidazole peak in its melting point range. In sodium alginate, a broad endothermic peak appeared at 109.20 °C (Supplementary Figure 1), assigned to the loosely bound water release from the molecule. In  $\text{Ca}_2\text{CO}_3$  (Supplementary Figure 1), the thermogram did not exhibit any endothermic or exothermic peak within 50-300 °C. The  $\text{NaHCO}_3$  (Supplementary Figure 1) showed an endothermic peak at 165.23 °C (starting from 142.98 °C and ending at 216.76 °C), which may be characterized by the evaporation of adsorbed water from  $\text{NaHCO}_3$ .

The sharp endothermic peak of metronidazole and the broad endothermic peak of sodium alginate were slightly shifted (Supplementary Figure 1) at 167.43 °C and 112.17 °C in the physical mixtures of different excipients in the ratio of 1:1. The slight shift in the melting endotherm of metronidazole could be due to drug mixing with the contaminant existing in the excipients. The endothermic peak of each excipient, as well as the physical mixture of excipients with metronidazole, clearly depicts the integrity. It remained intact in crystalline form, confirming the absence of interaction between the metronidazole and excipients used in the raft formulation.

#### *Fourier Transform Infrared (FT-IR) spectroscopy*

The FT-IR spectra of metronidazole showed the typical characteristics peak [Supplementary Figure 2(A)] of aromatic -C-H stretching, aromatic -C-N-, aromatic -N-O- of  $\text{NO}_2$  stretching, and -O-H stretching band at 3093  $\text{cm}^{-1}$ , 1261  $\text{cm}^{-1}$ , 1531  $\text{cm}^{-1}$ , 1361  $\text{cm}^{-1}$  (i.e., 3° -N-O- group is attached to an aromatic ring) and 3679  $\text{cm}^{-1}$  in their respective position. All the characteristic bands of metronidazole were also present in the FT-IR spectrum of Eudragit® NE 30D coated as well as physical mixture [Supplementary Figure 2 (B&C)].

### Physical characteristics of raft forming formulation

The formulations were liquid, which could be easily swallowable, rapidly transforming into a gel raft in the stomach. The following were the physical attributes of the developed raft-forming systems-

#### *Measurement of raft strength, weight, volume, and raft density*

After the liquid formulation was poured in 0.1M HCl (pH 1.2), it sank to the bottom of the medium and formed a gel, as illustrated in Figure 1.



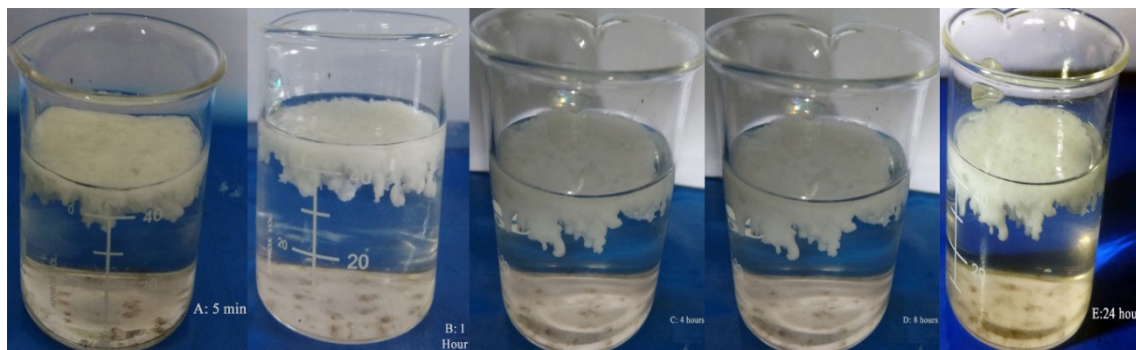


**Figure 1.** Floating behavior of the metronidazole-loaded raft liquid formulation.

The floating lag time and duration of floating are shown in Table 1. All the formulations were floated on the surface within 60 seconds. The formed *in situ* gel of all the raft formulations maintained floatation for more than 24 hours, encouraging further *in vivo* study. Figure 1 shows the floating behavior of the optimized metronidazole raft formulation at different time intervals in a rabbit stomach.

The raft strength and density of the formulation are presented in Table 2. The raft strength was found within the range of  $2.48 \pm 0.41$  to  $8.76 \pm 0.13$  g. The density was found within the range from  $0.33 \pm 0.03$  to  $0.93 \pm 0.07$  g.cm<sup>-3</sup>.

#### Measurement of rheological properties of raft formulation

The flow behavior was studied according to Farrow's equation:  $\text{Log } D = N \text{ Log } S - \text{Log } \eta$ , where, D implies shear rate (sec<sup>-1</sup>), S implies shear stress (Pa),

N is Farrow's constant, and  $\eta$  is the viscosity (Pa. s). The flow index (N) is characteristic for each formulation, as N = 1 indicates Newtonian behavior, while N is less than one (N < 1), indicating a thickening shear rate. If N is greater than one (N > 1) indicates a thinning shear rate (Table 3) (Abouelatta et al., 2018) (The viscosity shear rate profiles of the metronidazole raft forming optimized formulation are illustrated in Supplementary Figure 3).

#### *In vitro* drug release study

The metronidazole release profiles of raft formulation are shown in Figure 2 (A, B). The *in vitro* drug releases were  $87.53 \pm 2.87\%$ ,  $84.37 \pm 1.04\%$ ,  $95.96 \pm 0.01\%$ ,  $90.27 \pm 1.93 \%$ ,  $81.83 \pm 0.54\%$ ,  $84.78 \pm 0.98\%$ ,  $88.57 \pm 1.81\%$  and  $92.24 \pm 0.94\%$  from F-1, F-2, F-3, F-4, F-5, F-6, F-7 and F-8 formulation respectively after 8 hours in 0.1M HCl medium. The 8-hour release values are mentioned considering the half-life of Metronidazole.

**Table 1.** Physical characteristics of the batches of raft forming formulation

Formulation Code	Floating lag time (in Seconds)	Duration of floating (in Hours)	Raft strength (g)	Raft weight (g)	Raft volume (mL)	Density (g.mL <sup>-1</sup> )	Buoyancy index
F-1	7	>24	4.05 ± 0.43	5.16 ± 0.11	6.96±0.14	0.74±0.026	0.34±0.10
F-2	7	>24	6.56 ± 0.16	2.32±0.17	5.81±0.31	0.394±0.055	1.50±0.22
F-3	5	>24	3.97 ± 0.56	1.89±0.17	5.69±0.13	0.33±0.032	1.86±0.12
F-4	6	>24	6.65 ± 0.31	3.18±0.24	5.20±0.43	0.61±0.035	0.67±0.06
F-5	16	>24	3.74 ± 0.23	6.04±0.27	6.44±0.22	0.93±0.070	0.16±0.07
F-6	56	>24	8.76 ± 0.13	6.63±0.15	12.24±0.08	0.544±0.028	0.84±0.13
F-7	45	>24	5.98 ± 0.22	5.53±0.12	9.73±0.12	0.56±0.030	0.61±0.26
F-8	6	>24	2.84 ± 0.41	2.02±0.19	5.29±0.24	0.38±0.041	1.47 ±0.35

Table represent mean ± SD, n=3

**Table 2.** Composition of raft formulations

Composition of Raft	Formulation Code and quantity in percentage (W/V)							
	F-1	F-2	F-3	F-4	F-5	F-6	F-7	F-8
Sodium alginate	3	1	1	1	3	3	3	1
Sodium bicarbonate	0.5	0.5	1	1	1	1	0.5	0.5
Calcium carbonate	0.5	3	0.5	3	0.5	3	3	0.5
Sodium citrate	0.17	0.17	0.17	0.17	0.17	0.17	0.17	0.17
Coated API	0.1	0.1	0.1	0.1	0.1	0.1	0.1	0.1

**Table 3.** Rheological properties of the batches of raft formulation

Formulation Code	Viscosity of sols (Pa. s)	N (Furrow's Constant of sols)	Flow behavior	Zeta Potential (milli volts)
F-1	0.0175±0.001	1.001	Thixotropic	45.7
F-2	0.0148±0.015	1.021	Thixotropic	43.2
F-3	0.003±0.001	1.01	Thixotropic	38.2
F-4	0.003±0.001	1.01	Thixotropic	43.1
F-5	0.231±0.37	1.06	Thixotropic	41.0
F-6	0.021±0.001	1.025	Thixotropic	45.7
F-7	0.024±0.001	1.010	Thixotropic	46.4
F-8	0.003±0.006	1.0101	Thixotropic	43.0

**Table 4 -** Correlation coefficient ( $r^2$ ) and diffusional exponent ( $n$ ) of raft forming formulation

Formulation Code	Drug release kinetic correlation coefficients ( $r^2$ )				Release exponent ( $n$ )
	Zero order	First order	Higuchi	Korsmeyer-Peppas	
	$r^2$	$r^2$	$r^2$	$r^2$	
F-1	0.6665	0.9462	0.8903	0.141	0.663
F-2	0.7082	0.9727	0.8939	0.083	0.45
F-3	0.5616	0.7496	0.9603	0.707	0.674
F-4	0.6037	0.9157	0.9497	0.727	0.811
F-5	0.7354	0.9715	0.8752	0.763	0.781
F-6	0.7339	0.9755	0.8436	0.172	0.581
F-7	0.6532	0.9141	0.9188	0.808	0.45
F-8	0.5824	0.8989	0.9378	0.099	0.543

## DISCUSSION

The principal prerequisites of raft formulations are optimum viscosity of the prepared liquid sol, gelling, and floating capacities. The formulation should have an optimal viscosity that will allow easy swallowing as a liquid dosage form. Thus, it undergoes a rapid sol-gel transition and floats owing to the ionic reaction. Furthermore, the *in situ* formed gel should preserve its integrity without dissolving or eroding. The viscous raft formulation is being floated in the stomach for a prolonged period to locally encourage a sustained release of medicament. Eudragit NE 30 D, a copolymer of methyl acrylate, enables the pH-dependent release of metronidazole through salt formation. Metronidazole coated with Eudragit NE 30 D forms a thin film

in the raft formulation, is insoluble in the GI tract, has extremely low permeability, and exhibits pH-independent swelling (Ahmed et al., 2020; Thakral et al., 2012). The sodium alginate can form a floating gel mass or raft in the stomach, an essential ingredient of anti-reflux products such as Gaviscon Advance, Gastrocote, Gaviscon Liquid, Paptac, and Rennie Duo, etc. intended to work by a barrier action. It has also imparted mucoadhesive properties in the formulation (Hampson et al., 2005). Also,  $\text{NaHCO}_3$  and  $\text{CaCO}_3$  have an antacid function, so the formulation has an acid-neutralizing capacity (Shakya et al., 2013).

Sol-to-gel transformation of sodium alginate occurs due to either monovalent or divalent cations in the acidic pH (Siew et al., 2005). Sodium alginate

is freely dissociated into alginate and  $\text{Na}^+$  ion at an aqueous media and forms double helices at room temperature when the solution has a viscosity near that of water. The helices are weakly connected by the Van der Waals attraction force. When gel-promoting cations are present, some helices associate with cation-mediated aggregates, which cross-link the polymer. For instance, the divalent ions, calcium, are superior to monovalent cations in encouraging the gelation of the polysaccharide (Tang et al., 1997). This is the result of the internal ionotropic gelation effect of  $\text{Ca}^{2+}$  on the polymer used (Choi et al., 2002). In the present work,  $\text{CaCO}_3$  was used as a source of  $\text{Ca}^{2+}$  and a gas-generating ingredient. While insoluble in water,  $\text{CaCO}_3$  dissolves in acidic media (pH 1.2- 3.5). When the formulation is in contact with the acidic medium of the stomach, it produces  $\text{CO}_2$ , which may get entrapped and protected within the gel layer formed by cross-linking with the polymeric alginate chain in an acidic medium. The  $\text{Ca}^{2+}$  interaction with alginate can create a firm and strong gel network that can entrap the  $\text{CO}_2$  more efficiently (Jiang et al., 2015). Simultaneously,  $\text{Na}^+$  from sodium alginate is exchanged with divalent  $\text{Ca}^{2+}$ , which can lead to a low-viscosity solution to a gel by forming an egg-box structure. This interaction would be essential to create a strong, coherent raft in the post-prandial stomach weakly acidic medium.  $\text{NaHCO}_3$  was used to avoid any internal ionotropic gelation effect of calcium on alginates during storage (Poncelet et al., 1999). Various literature has reported that the amount of  $\text{NaHCO}_3$  and  $\text{CaCO}_3$  are directly related to the floating lag time. If the amount of  $\text{NaHCO}_3$  and  $\text{CaCO}_3$  is increased, floating lag time decreases due to the production of a significant amount of  $\text{CO}_2$ . Moreover, increasing the amount of alginate resulted in increased weight, which then requires a prolonged period to achieve a density below that of the gastric fluids and float. In contrast,  $\text{NaHCO}_3$  and  $\text{CaCO}_3$  reduced the floating lag time owing to the increase in  $\text{CO}_2$  produced by an increased amount of  $\text{NaHCO}_3$ , which resulted in a shorter time to reach a suitable density. At the same time, the drug loading did not affect the floating ability.

Thus, sodium citrate (0.17% w/v) was added to the formulation as a chelating agent; it complexes with the free  $\text{Ca}^{2+}$  ions. It prevents premature gelation, which may occur during storage, and only releases it in the stomach's acidic environment (Abou Youssef et al., 2015; Abouelatta et al., 2018). The formulation thus remains in the liquid phase until it reaches the stomach, where gelation is instantaneous. Optimum quantities of  $\text{CaCO}_3$  that guaranteed fluidity during storage, then immediate gelation and floatation, were determined by preliminary tests.

The density of a raft formulation was less than the density of gastric content ( $\sim 1.0597 \text{ g.mL}^{-1}$ ) (Table 2). This result confirmed that the raft was buoyant in the GI fluid and remained withheld in the stomach, facilitating the local release of medicament. The buoyancy of the raft can be anticipated to enhance the effectiveness of the product in resisting reflux since a more buoyant raft would be more likely to displace corrosive gastric content in the upper part of the stomach, and it would also be less likely to be emptied along with the meal. The buoyancy of the raft was generated by the entanglement of  $\text{CO}_2$  in the gel network. Additionally, the gel elevated and retained buoyant on the surface of the medium. The floating raft was favorable as it behaved as a hindrance to avert gastric fluid reflux into the esophagus.

Different alginate concentrations disturbed the raft density. The raft density rises with the enhancement of the alginate content. However, all raft formulations could form a gel and float in an acidic medium. The amount of  $\text{CO}_2$  did not affect the gelled raft density, although the weight of  $\text{CaCO}_3$  raised the raft volume.

The raft formulations showed thixotropic due to the sodium alginate solution exhibiting a shear-thinning behavior or pseudoplastic flow of the viscosity resulting in an inverse proportion to the shear rate. The viscosity of the formulation was enhanced with the increment in the alginate concentration. On the other hand, the amount of metronidazole did not affect the viscosity of the formulation.

The raft formulations exhibited raft strengths within the same range as commercial antacid products (between 1.1 to 16.5 g) (Hampson et al., 2005). Moreover, it was noticed that raft was present in the rabbit's stomach more than 7 hours after taking the X-ray through oral feeding (Figure 3). It indicates that the developed formulation could resist GI peristalsis. Thus, a formulation with the highest strength (F6, F7) resists breakup for the longest time, whereas a formulation with low raft strength (<5 g) has little or no resistance to raft breakup in the resilience test.

The capability to retain the raft within the gastric cavity constituted the exclusive attribute, in addition to the necessity for it to withstand peristaltic contractions. The force (g) exerted for extracting the probe transpires through the strength of the gel raft. Consequently, the robustness of the raft is contingent upon the concentrations of sodium alginate and CaCO<sub>3</sub>. This investigation has elucidated that an escalation

in the concentration of sodium alginate and CaCO<sub>3</sub> results in enhanced raft integrity, attributable to an increase in its density as well as augmented cross-linking interactions among adjacent alginate chains.

### In vitro drug release study

The impacts of all components in the raft-forming formulations on metronidazole release are represented in Figure 2 (A, B). Coating metronidazole with Eudragit® NE 30D played a key role in the release from the raft formulation. The *in vitro* drug release pattern could be partitioned into two steps. The initial step involved a burst release, likely due to incomplete gelation and rapid drug release upon contact with 0.1M HCl (pH 1.2). Radiological observation revealed that the burst release effect was not due to raft damage (Figure 3). After the raft was formed entirely, the residual metronidazole was limited and gradually released from the gel network, representing the second phase; the drug was released moderately in this phase.

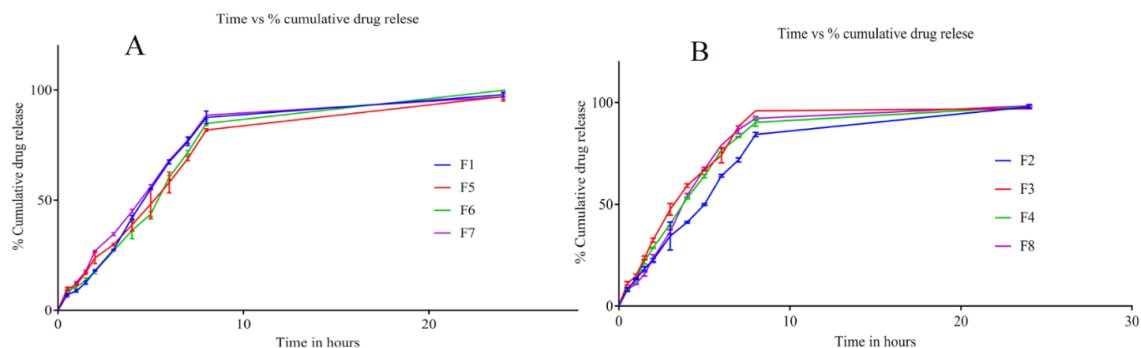


**Figure 2.** (A) Effect of Sodium alginate concentration on the *in vitro* metronidazole release of the raft forming systems incorporating Eudragit NE30D coated metronidazole; (B) Effect of CaCO<sub>3</sub> concentration on the *in vitro* metronidazole release of the raft forming systems incorporating Eudragit NE 30D coated metronidazole.

Bars represent mean ± SD (n = 3)

The amount of metronidazole released at 30 and 60 minutes did not differ significantly at varying concentrations of alginate. This suggests that the drug was not effectively trapped within the gel network and was released into the media independently of the polymer matrix control.

Nevertheless, the rate of metronidazole release after a duration of 60 minutes exhibited a pronounced reduction with an elevation in alginate concentration. The increased concentration of alginate augmented the density of the polymer matrix and contributed to the formation of a more viscous gel raft. Conse-

quently, the drug was subjected to an extended path length and time for diffusion as a result of the gel network's properties. The quantity of  $\text{CaCO}_3$  exerted a minor influence on the drug release characteristics of the raft formulations. Nonetheless, the presence of  $\text{Ca}^{2+}$  facilitated the formation of a more robust raft in conjunction with sodium alginate, while the  $\text{CO}_2$  gas generated within the gel network resulted in a gel of enhanced permeability, which in turn improved the release rate. As a result, the elevated concentration of  $\text{CaCO}_3$  yielded a greater quantity of  $\text{Ca}^{2+}$  and produced increased amounts of  $\text{CO}_2$ , which collectively exerted a negligible overall impact on the drug release profile.

#### ***In vitro* drug release kinetics**

The drug loading in the formulation did not significantly affect the *in vitro* release profile of the raft formulation. The release profile was analyzed to identify the most appropriate mechanisms for elucidating the release characteristics by utilizing linear regression analysis alongside various kinetic models. The model exhibiting the highest coefficient of determination (i.e.,  $r^2$  approaching 1) was deemed the most suitable kinetic model. The Korsmeyer-Peppas model parameter 'n' represents the release exponent linked to the drug release mechanism. The raft formulation adhered to first-order release kinetics (Table 4). The release exponents (n) for the formulations ranged from 0.45 to 0.81, indicating that the metronidazole release from the formulation occurs via a combi-

nation of diffusion and erosion mechanisms (i.e., a non-Fickian diffusion mechanism where  $0.45 < n < 0.89$ ) (Das et al., 2010; Dhar et al., 2020).

#### **Assortment of optimized formulation**

The chosen optimized formulation was based on the significant characteristics ( $p < 0.05$ , general appearance, raft strength, viscosity, and *in vitro* drug release profile) of the raft formulation. Among the parameters mentioned above, the F-5 formulation was found to be a suitable formulation in all aspects ( $p < 0.05$ ). The strength of the raft was found to be  $3.74 \pm 0.23\text{g}$ , which assured that the raft has adequate mechanical strength as well as constant drug release from the gel network. The viscosity of the formulation was  $0.93 \pm 0.070$  Pa.s, which was less than GI fluid. The floating lag time was less than 60 seconds, ensuring that the formulation floated immediately after oral administration (Figure 1). The *in vitro* drug release was  $81.83 \pm 0.54$  % after 8 hours in 0.1M HCl.

#### ***In vivo* gel-forming activity in rabbit stomach using Roentgenography**

Figure 3 demonstrates the appearance of gel formation in rabbit stomach after oral administration of  $\text{BaSO}_4$  disperses optimized formulation. The presence of  $\text{BaSO}_4$  in the stomach confirms the GI retentive property of the drug-free optimized formulation. The amount of gel was reduced over time, as shown in Figure 3. The findings indicated a gradual degradation of the synthesized gel, thereby underscoring the enhanced gel integrity of the optimized formulation.

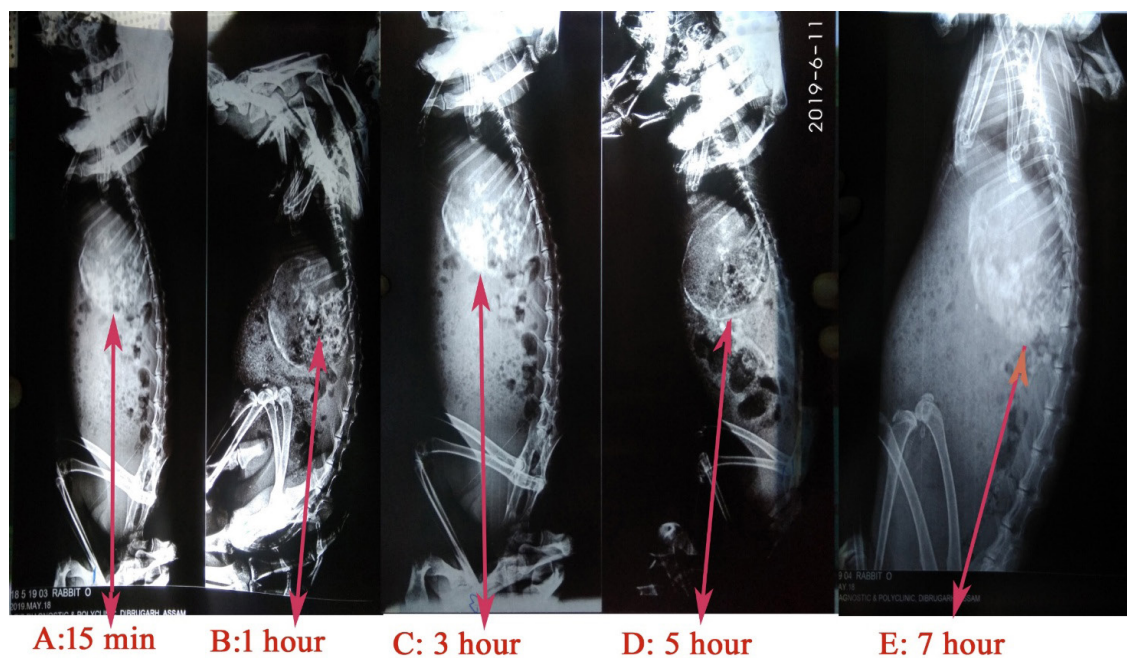


**Figure 3.** X-ray images of rabbit stomach at different time intervals after oral administration raft liquid

## CONCLUSION

This study successfully formulated a gastro retentive raft-forming formulation incorporating metronidazole. The optimized F-5 formulation contains 3% w/v of sodium alginate, 0.5% w/v of  $\text{CaCO}_3$ , and 1% w/v of  $\text{NaHCO}_3$ . The formulation was characterized by having an optimum viscosity that will permit smooth ingestion as a liquid dosage form, which undergoes a rapid sol-gel transition and floating due to ionic interaction. Excellent floating behavior and controlled release profile for more than 8 hours were observed.

The drug, metronidazole, was released from the dosage form slowly in the stomach, significantly extending its residence time, which may facilitate its direct antibacterial action and consequently enhance the healing of chronic gastric ulcers and stimulate mucosal regeneration in the affected area. Furthermore, the administration interval for metronidazole would be minimized, resulting in enhanced efficacy compared to conventional oral dosage formulations. Therefore, the proposed raft formulation would be a promising site-specifying dosage form for treating peptic ulcers caused by *H. pylori*. Also, it could be suitable for geriatrics who find difficulty swallowing other

solid dosage forms of metronidazole, thus improving efficacy due to enhancing patient compliance. Moreover, the thick barrier of raft formulation on top of the GI fluid may prevent or minimize gastroesophageal reflux disease symptoms. This study has illustrated the potential utility of a novel raft liquid formulation for stomach-specific delivery.

## ACKNOWLEDGEMENTS

We would like to acknowledge the All India Council for Technical Education (AICTE), Govt. of India, New Delhi, and Aziz Diagnostic & Poly Clinic, Dibrugarh.

## AUTHOR CONTRIBUTION STATEMENT

We declare that this study was done by the authors named in this article. HS & HKS were involved in the conceptualization; TJ & HS were contributed to the methodology, involved in the formal analysis, and investigation; HS & AKG contributed to writing original draft preparation and writing, review and editing; HKS was involved in the supervision, contributed to the project administration and funding acquisition. All the authors read and approved the final manuscript.

### CONFLICT OF INTEREST

Authors declare that there is no conflict of interest.

### REFERENCES

- Abbas, G., Hanif, M., & Khan, M. A. (2017). pH responsive alginate polymeric rafts for controlled drug release by using box behnken response surface design. *Designed Monomers and Polymers*, 20(1), 1–9. <https://doi.org/10.1080/15685551.2016.1231046>
- Abou Youssef, N. A. H., Kassem, A. A., El-Massik, M. A. E., & Boraie, N. A. (2015). Development of gastroretentive metronidazole floating raft system for targeting *Helicobacter pylori*. *International Journal of Pharmaceutics*, 486(1–2), 297–305. <https://doi.org/10.1016/j.ijpharm.2015.04.004>
- Abouelatta, S. M., Aboelwafa, A. A., & El-Gazayerly, O. N. (2018). Gastroretentive raft liquid delivery system as a new approach to release extension for carrier-mediated drug. *Drug Delivery*, 25(1), 1161–1174. <https://doi.org/10.1080/10717544.2018.1474969>
- Adebisi, A. O., Laity, P. R., & Conway, B. R. (2015). Formulation and evaluation of floating mucoadhesive alginate beads for targeting *Helicobacter pylori*. *Journal of Pharmacy and Pharmacology*, 67(4), 511–524. <https://doi.org/10.1111/jphp.12345>
- Ahmed, A. R., Mota, J. P., Shahba, A. A. W., & Irfan, M. (2020). Aqueous polymeric coatings: New opportunities in drug delivery systems. In R. Shergokar (Ed.), *Drug Delivery Aspects: Expectations and Realities of Multifunctional Drug Delivery Systems* (1st ed., Vol. 4, pp. 33–56). Elsevier. <https://doi.org/10.1016/B978-0-12-821222-6.00003-8>
- Bunlung, S., Nualnoi, T., Issarachot, O., & Wiwattanapatapee, R. (2021). Development of raft-forming liquid and chewable tablet formulations incorporating quercetin solid dispersions for treatment of gastric ulcers. *Saudi Pharmaceutical Journal*, 29(10), 1143–1154. <https://doi.org/10.1016/J.JSPS.2021.08.005>
- Choi, B. Y., Park, H. J., Hwang, S. J., & Park, J. B. (2002). Preparation of alginate beads for floating drug delivery system: Effects of CO<sub>2</sub> gas-forming agents. *International Journal of Pharmaceutics*, 239(1–2), 81–91. [https://doi.org/10.1016/S0378-5173\(02\)00054-6](https://doi.org/10.1016/S0378-5173(02)00054-6)
- Das, S., Murthy, P. N., Nath, L. K., & Chowdhury, P. (2010). Kinetic Modeling on Drug Release from Controlled Drug Delivery Systems. *Acta Poloniae Pharmaceutica- Drug Research*, 67(3), 217–223.
- Dhar, P., Sarma, H., & Sharma, H. K. (2020). Fixed Dose Oral Dispersible Tablet of Bitter Drug Using Okra Mucilage: Formulation and Evaluation. *Journal of Drug Delivery and Therapeutics*, 10(5), 149–158. <https://doi.org/10.22270/jddt.v10i5.4393>
- El-Mahrouk, G. M., Aboul-Einien, M. H., & Makhoul, A. I. (2016). Design, Optimization, and Evaluation of a Novel Metronidazole-Loaded Gastro-Retentive pH-Sensitive Hydrogel. *AAPS PharmSciTech*, 17(6), 1285–1297. <https://doi.org/10.1208/s12249-015-0467-x>
- Emara, L. H., Abdul, A. R., Ahmed, E.-A., & Mursi, N. mohamed. (2014). Preparation and evaluation of metronidazole sustained release floating tablets. *International Journal of Pharmacy and Pharmaceutical Sciences*, 6(9), 198–204.
- Hampson, F. C., Farndale, A., Strugala, V., Sykes, J., Jolliffe, I. G., & Dettmar, P. W. (2005). Alginate rafts and their characterisation. *International Journal of Pharmaceutics*, 294(1–2), 137–147. <https://doi.org/10.1016/j.ijpharm.2005.01.036>
- Hernández Ceruelos, A., Romero-Quezada, L. C., Ruvalcaba Ledezma, J. C., & López Contreras, L. (2019). Therapeutic uses of metronidazole and its side effects: an update. *European Review for Medical and Pharmacological Sciences*, 23(1), 397–401. [https://doi.org/10.26355/EUR-REV\\_201901\\_16788](https://doi.org/10.26355/EUR-REV_201901_16788)



- Hooda, A. (2011). Gastrointestinal mucoadhesive drug delivery system: A review. *Journal of Pharmacy Research*, 4(5), 1448–1453.
- Ibrahim, H. K. (2009). A Novel Liquid Effervescent Floating Delivery System for Sustained Drug Delivery - PubMed. *Drug Discoveries Therapeutics*, 3(4), 168–175.
- Jiang, H., Tian, R., Hu, W., Jia, Y., Yuan, P., Wang, J., & Zhang, L. (2015). Formulation and evaluation of gastroretentive floating drug delivery system of dipyrindamole. *Drug Development and Industrial Pharmacy*, 41(4), 674–680. <https://doi.org/10.3109/03639045.2014.893355>
- Kerdsakundee, N., Mahattanadul, S., & Wiwattanapatapee, R. (2015). Development and evaluation of gastroretentive raft forming systems incorporating curcumin-Eudragit® EPO solid dispersions for gastric ulcer treatment. *European Journal of Pharmaceutics and Biopharmaceutics*, 94, 513–520. <https://doi.org/10.1016/j.ejpb.2015.06.024>
- Koga, Y. (2022). Microbiota in the stomach and application of probiotics to gastroduodenal diseases. *World Journal of Gastroenterology*, 28(47), 6715. <https://doi.org/10.3748/WJG.V28.I47.6702>
- Nori, L. P., Prasanthi, C. H., Prasanthi, N. L., Manikiran, S. S., & Rao, N. R. (2011). Focus on current trends in the treatment of Helicobacter pylori infection: An update. *International Journal of Pharmaceutical Sciences Review and Research*, 9(1), 42–51.
- Poncelet, D., Babak, V., Dulieu, C., & Picot, A. (1999). A physico-chemical approach to production of alginate beads by emulsification-internal ionotropic gelation. *Colloids and Surfaces A*, 155, 171–176.
- Prajapati, V. D., Jani, G. K., Khutliwala, T. A., & Zala, B. S. (2013). Raft forming system - An upcoming approach of gastroretentive drug delivery system. *Journal of Controlled Release*, 168(2), 151–165. <https://doi.org/10.1016/j.jconrel.2013.02.028>
- Rajinikanth, P. S., Balasubramaniam, J., & Mishra, B. (2007). Development and evaluation of a novel floating in situ gelling system of amoxicillin for eradication of Helicobacter pylori. *International Journal of Pharmaceutics*, 335(1–2), 114–122. <https://doi.org/10.1016/j.ijpharm.2006.11.008>
- Rajinikanth, P. S., & Mishra, B. (2008). Floating in situ gelling system for stomach site-specific delivery of clarithromycin to eradicate H. pylori. *Journal of Controlled Release*, 125(1), 33–41. <https://doi.org/10.1016/j.jconrel.2007.07.011>
- Shakya, R., Thapa, P., & Saha, R. N. (2013). In vitro and in vivo evaluation of gastroretentive floating drug delivery system of ofloxacin. *Asian Journal of Pharmaceutical Sciences*, 8(3), 191–198. <https://doi.org/10.1016/j.ajps.2013.07.025>
- Siew, C. K., Williams, P. A., & Young, N. W. G. (2005). New insights into the mechanism of gelation of alginate and pectin: Charge annihilation and reversal mechanism. *Biomacromolecules*, 6(2), 963–969. <https://doi.org/10.1021/bm049341l>
- Tang, J., Tung, M. A., & Zeng, Y. (1997). Gelling Properties of Gellan Solutions Containing Monovalent and Divalent Cations. *Journal of Food Science*, 62(4), 688–712. <https://doi.org/10.1111/j.1365-2621.1997.tb15436.x>
- Thakral, S., Thakral, N. K., & Majumdar, D. K. (2012). Eudragit®: a technology evaluation. *Expert Opinion on Drug Delivery*, 10(1), 131–149. <https://doi.org/10.1517/17425247.2013.736962>
- Tripathi, K. D. (2013). Drugs for Peptic Ulcer and Gastroesophageal Reflux Disease. In *Essentials of Medical Pharmacology* (7th ed., pp. 648–660). Jaypee Bothers Medical Publishers (P) Ltd.

Vinod, K. R., Vasa, S., Banji, D., Padmasri, A., & Sandhya, S. (2010). Approaches for gastrotentive drug delivery systems. *International Journal of Applied Biology and Pharmaceutical Technology*, 1(1), 589–601.

# A Blockchain-Based Approach to Securing the Pharmaceutical Supply Chain

Ahmed ALOUI<sup>\*</sup>, Meftah ZOUAI<sup>\*\*</sup>, Samir BOUREKKACHE<sup>\*\*\*</sup>, Okba KAZAR<sup>\*\*\*\*</sup>

*A Blockchain-Based Approach to Securing the Pharmaceutical Supply Chain*

## SUMMARY

Securing the pharmaceutical supply chain is a significant global challenge, as the integrity of drug distribution is critical for patient safety. Traditional supply chain systems are often opaque, making it difficult to track and verify the authenticity of pharmaceutical products. This lack of transparency leads to vulnerabilities where counterfeit drugs can infiltrate the market, posing severe health risks to millions of patients worldwide. Data manipulation and lack of accountability in centralized systems further exacerbate these issues, undermining trust in the pharmaceutical supply chain. Algerian industrial companies are confronted with numerous changes and challenges impacting their various activities, particularly in the drug distribution sector. In this paper, we propose a new Blockchain-based system to ensure the security and transparency of the drug distribution process. Blockchain technology provides a decentralized, tamper-resistant record that enhances security in drug distribution. This system offers transparency and security across all transaction stages, addressing core issues in the pharmaceutical supply chain.

**Key Words:** Pharmaceutical Supply Chain, Drug Distribution, Transparency, Security, Counterfeit Drugs, Blockchain, Data Integrity, Decentralized Systems, Patient Safety, Data Manipulation, Transaction Records.

*İlaç Tedarik Zincirinin Güvenliğini Sağlamak İçin Blokzincir Tabanlı Bir Yaklaşım*

## ÖZ

İlaç tedarik zincirinin güvenliğini sağlamak, ilaç dağıtımının bütünlüğünün hasta güvenliği açısından kritik olması nedeniyle küresel çapta önemli bir zorluktur. Geleneksel tedarik zinciri sistemleri genellikle şeffaf olmayıp, farmasötik ürünlerin orijinalliğinin takibini ve doğrulanmasını zorlaştırmaktadır. Bu şeffaflık eksikliği, sahte ilaçların pazara sızmasına ve dünya çapında milyonlarca hasta için ciddi sağlık riskleri oluşturmasına yol açabilen güvenlik açıklarına yol açar. Merkezi sistemlerdeki veri manipülasyonu ve hesap verebilirlik eksikliği bu sorunları daha da kötüleştirerek ilaç tedarik zincirine olan güveni zedeler. Cezayir'deki sanayi şirketleri, özellikle ilaç dağıtım sektöründe, çeşitli faaliyetlerini etkileyen çok sayıda değişim ve zorlukla karşı karşıyadır. Bu çalışmada, ilaç dağıtım sürecinin güvenliğini ve şeffaflığını sağlamak için yeni bir Blockchain tabanlı sistem öneriyoruz. Blockchain teknolojisi, ilaç dağıtımında güvenliği artıran, merkezi olmayan, müdabaleye karşı dayanıklı bir kayıt sağlamaktadır. Bu sistem, ilaç tedarik zincirindeki temel sorunları ele alarak tüm işlem aşamalarında şeffaflık ve güvenlik sunmaktadır.

**Anahtar Kelimeler:** İlaç Tedarik Zinciri, İlaç İletimi, Şeffaflık, Güvenlik, Sahte İlaçlar, Blokzincir, Veri Bütünlüğü, Merkezi olmayan sistemler, Hasta Güvenliği, Veri Manipülasyonu, İşlem Kayıtları.

Received: 12.08.2024

Revised: 21.12.2024

Accepted: 05.02.2025

<sup>\*</sup> ORCID ID: 0000-0003-2623-5118, Computer Science, Intelligent Computer Science Laboratory, Biskra University, Biskra, Algeria.

<sup>\*\*</sup> ORCID ID: 0000-0003-0950-2667, Computer Science, Intelligent Computer Science Laboratory, Biskra University, Biskra, Algeria.

<sup>\*\*\*</sup> ORCID ID: 0000-0003-2038-6257, Computer Science, Intelligent Computer Science Laboratory, Biskra University, Biskra, Algeria.

<sup>\*\*\*\*</sup> ORCID ID: 0000-0003-0522-4954, College of Arts, Sciences & Information Technology, University of Kalba, Sharjah, UAE.

## INTRODUCTION

In recent years, the pharmaceutical industry has encountered significant challenges in maintaining the authenticity, security, and efficiency of its supply chain operations. One of the most pressing concerns is the rise of counterfeit drugs, which not only jeopardizes patient safety but also results in significant financial losses for manufacturers. It is estimated that counterfeit medicines account for over 15% of the global pharmaceutical market, posing severe risks to public health and creating distrust in pharmaceutical systems (Tiwari et al., 2024). These counterfeit products can enter the supply chain at various stages, exploiting vulnerabilities in tracking and verification processes.

Beyond the issue of counterfeiting, inefficiencies within the supply chain—such as delivery delays, inaccurate inventory management, and the absence of real-time monitoring—have also become significant challenges. Traditional supply chain systems often lack the transparency required for stakeholders to monitor the movement of drugs across different stages, from manufacturers to pharmacies, creating opportunities for errors or malicious tampering (Tiwari et al., 2024; Musamih et al., 2021).

Blockchain technology presents an effective solution to these challenges due to its decentralized and tamper-proof nature. By creating an immutable record of transactions, Blockchain can provide complete transparency and traceability in the supply chain. Every stakeholder, including manufacturers, distributors, and pharmacists, has access to a shared ledger, ensuring that any changes or discrepancies are immediately visible and verifiable. Furthermore, Blockchain's use of cryptographic hashing mechanisms prevents unauthorized modifications, making it nearly impossible for counterfeit drugs to enter the system undetected (Abdallah et al., 2023; Farooq et al., 2020). Blockchain's features make it ideal for ensuring security, transparency, and efficiency in pharmaceutical supply chain management.

The proliferation of counterfeit drugs and inefficiencies in real-time tracking and verification pose significant challenges to the pharmaceutical supply chain. Counterfeit drugs are a significant threat to public health and safety, infiltrating global markets and undermining consumer trust. Traditional supply chain systems lack the transparency and traceability required to effectively track pharmaceuticals from production to delivery, allowing counterfeit drugs to enter the market undetected (Gligor et al., 2022; Jadhav et al., 2022).

The pharmaceutical supply chain, which involves distributors, pharmacists, and patients, is typically managed by a centralized system. However, this traditional approach has several drawbacks. Maintaining accurate records can be difficult, leading to data inconsistencies, delays, and challenges in monitoring shipping or theft issues. Relying on a single central server reduces efficiency, increases maintenance costs, and makes the system more vulnerable to cyber-attacks and breakdowns. Furthermore, these centralized networks lack transparency and traceability, as users have no control over the data, which is often unreliable and lacks proper authentication. Therefore, transitioning away from this model is essential for a more secure and efficient supply chain (Akram et al., 2024).

Blockchain technology facilitates the exchange and transfer of distributed data among organizations without the need for a central authority (Akram et al., 2024; Raparathi et al., 2021). This fosters direct engagements between participants in the supply chain, eliminating the reliance on trust in a central entity. These secure direct communications enhance transparency, clarity, and efficiency while reducing the costs and risks of tracking shipments.

Our Blockchain-based system provides a secure, decentralized ledger that improves traceability for pharmaceutical products. With this approach, each transaction is recorded and verified in real-time, pre-

venting counterfeit drugs from entering the supply chain. Furthermore, our system eliminates the inefficiencies associated with traditional systems, where real-time monitoring is often fragmented or non-existent.

In this paper, we have refined the problem definition to address two significant issues in the pharmaceutical supply chain: counterfeit drugs and inefficiencies in real-time tracking. Focusing on these key challenges, we underline the need for a secure, transparent system to manage and track pharmaceutical products. The scope of our project is clearly defined, emphasizing the application of Blockchain technology to enhance traceability, visibility, and security within the supply chain. Our system is designed to mitigate the risk of counterfeit drugs and improve real-time tracking for safer pharmaceutical delivery. Additionally, we recognize that aspects such as regulatory compliance and broader supply chain management practices fall outside the scope of this project.

Several research studies have been conducted to address these concerns and enhance the transparency and visibility of supply chains. A notable approach involves the elimination of a central authority by utilizing innovative technologies such as Blockchain (Gomasta et al., 2023; Mishra et al., 2024; Faulkner et al., 2020). Through its distributed ledger technology (a distributed database that records transactions across multiple nodes), Blockchain can revolutionize supply chain operations, resulting in improved efficiency, transparency, and security by ensuring trust and security.

Traditional supply chain management solutions have typically relied on barcodes and RFID tags for identification. Wireless Sensor Networks (WSN) have been employed for data collection, along with Electronic Product Codes (EPC), which serve the functions of identifying, capturing, and sharing product information to facilitate the tracking of goods across different stages (Gruchmann et al., 2024; Akram et al., 2024). Smart-Track (Al Huraimel et al., 2020; Go-

masta et al., 2023) functions within this framework by leveraging GS1 standard barcodes, which include unique serialized product identifiers along with lot production and expiration dates. In (Abdallah et al., 2023), the authors explored the application of Blockchain technology to address various issues in the healthcare sector, but the discussion lacked technical details or specific applications.

In (Tiwari et al., 2024; Alla et al., 2024), the authors have put forward traceability solutions; however, these rely on centralized databases, making it relatively easy to tamper with goods information and challenging to detect such tampering. Moreover, utilizing various types of centralized databases can lead to issues with interoperability and scalability in the proposed solutions. (Mishra et al., 2024; Faulkner et al., 2020) propose an NFC-driven mechanism designed to enhance transparency across various stages of the pharmaceutical distribution network. Every pharmaceutical product undergoes registration and validation through a unique key value, with an NFC label affixed for identification purposes. Like previous solutions, individuals or patients can verify the authenticity and origin of medication by scanning the assigned NFC label using a mobile application.

This section examines recent research aimed at improving supply chain transparency and security, emphasizing the vulnerabilities of traditional centralized methods, including their susceptibility to tampering and lack of interoperability.

### **Differences Between Traditional Databases and Blockchain Technology**

Blockchain, a distributed ledger technology (DLT), integrates digital systems to record asset transactions across multiple locations simultaneously. It is a widely recognized DLT that facilitates direct data exchange between different parties within a network, eliminating the need for intermediaries. Blockchain technology has applications across various domains, such as voting, banking, and healthcare. A Blockchain comprises a series of blocks that store diverse types of information. It is often defined as a transparent, secure

technology that operates without a central control body (Ayati et al., 2020). Each block in the Blockchain contains two parts: the body, which includes recorded transactions or facts (like medical data or monetary transactions), and the header, which includes details such as the transaction hash, timestamp, and the hash of the previous block. These linked blocks form a sequential chain, making the Blockchain tamper-proof due to the difficulty of altering the chain (Faulkner et al., 2020). For a malicious user to modify a transaction, they would need to adjust all subsequent blocks due to their interconnected hashes and change the version of the Blockchain stored by each participating node, making tampering highly impractical.

Unlike traditional databases that operate on centralized servers and allow for modifications such as Create, Read, Update, and Delete (CRUD) operations, Blockchain technology only permits data to be added, enhancing its security and immutability. Traditional databases rely on a central administrator who can modify or delete records, making them more vulnerable to cyberattacks and internal threats due to the potential for a single point of failure. In contrast, Blockchain's decentralized structure replicates data across multiple nodes, requiring consensus among participants for any changes, thereby reducing the risk of unauthorized alterations. Furthermore, while traditional databases rely on integrity rules that administrators can bypass, Blockchain ensures data security through cryptographic hashing, making any alterations easily detectable and providing a more robust and transparent solution for applications requiring high data integrity. This section explains the foundational aspects of Blockchain technology, including its decentralized structure, tamper-resistant nature, and advantages over traditional databases.

### Pharmaceutical Supply Chain Infrastructure

The pharmaceutical supply chain must facilitate the delivery of pharmaceutical products to patients, ensuring safety and traceability in compliance with the extensive regulations governing pharmaceutical products and their distribution (Tiwari et al., 2024).

The pharmaceutical distribution cycle (as shown in Figure 1) encompasses nine primary activities:

- **Pharmaceutical Procurement:** The process entails the acquisition of goods and services at the optimal total cost of ownership, ensuring the appropriate quality and quantity, timely delivery, and sourcing from the correct provider for direct advantages. The effectiveness of procurement plays a pivotal role in ensuring the availability of drugs and managing the overall expenses of pharmaceuticals.
- **Port Clearing:** Efficient port clearance is crucial for the smooth operation of pharmaceutical procurement in public organizations, ensuring the rapid and hassle-free movement of goods through customs.
- **Receipt and Inspection:** Inbound management involves receiving and inspecting goods upon arrival to ensure they are stored correctly in the warehouse. This procedure involves a comprehensive assessment of each shipment from either the port or local suppliers to verify compliance with contractual obligations. Prompt and precise inspections are essential for upholding quality standards.
- **Inventory Control:** This process focuses on optimizing stock management to maximize returns while minimizing inventory costs, ensuring efficient resource utilization and maintaining high customer satisfaction.
- **Storage:** The warehousing of pharmaceutical products allows for necessary testing before their introduction to the market, ensuring adherence to quality standards and regulatory requirements.
- **Supplier Requisition:** The requisition system, whether manual, computerized, or a combination of both, is structured to streamline the distribution process, aiding in inventory management and offering an audit trail to monitor the drug flow, thereby enhancing transparency and accountability.

- **Delivery:** Pharmaceuticals can be transported directly from the warehouse or collected by health-care facility personnel using various transportation modes such as air or river. Transportation managers must meticulously plan routes and deliveries to guarantee punctual and cost-efficient services.
- **Distribution to Patients:** Efficient dispensing practices are essential for the rational use of drugs. The distribution mechanism must facilitate the delivery of medications to hospital departments, outpatient facilities, health clinics, and community health

workers, ensuring appropriate administration to patients in doctors' care. Adopting of point-of-care drug dispensation has emerged as a secure, effective, and economically viable approach to bolster patient treatment initiatives.

- **Consumption Reports:** The reporting of data on drug consumption and inventory status back to the procurement unit represents the final stage in the distribution chain. This information is instrumental in forecasting future procurement requirements and maintaining an uninterrupted supply chain.

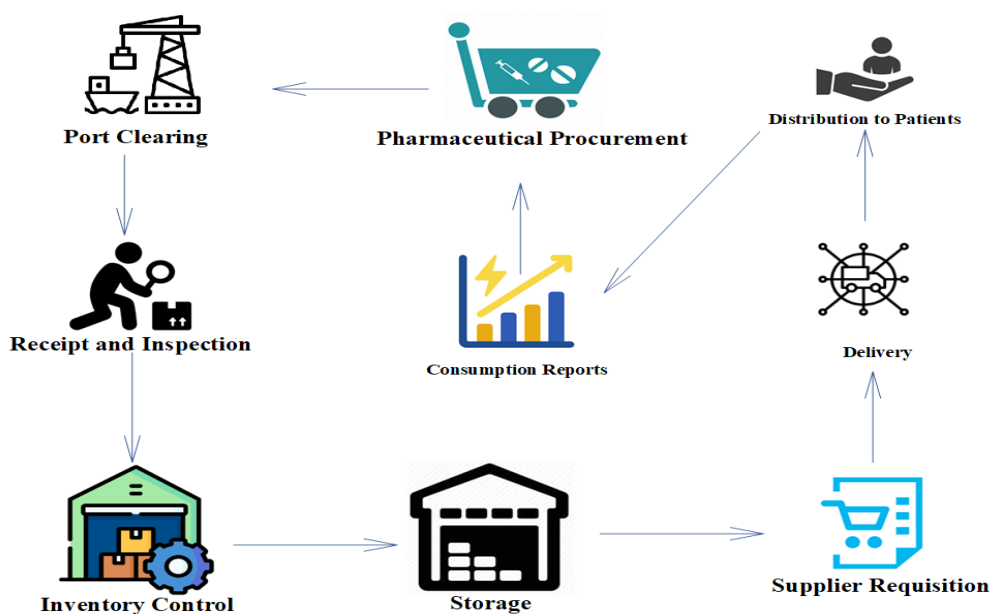


Figure 1. Pharmaceutical supply chain.

### Problem Definition and Project Aims

Counterfeit pharmaceuticals pose significant public health risks, including ineffective treatment and heightened drug resistance, at the same time the complexities of tracking the origin and movement of goods across the supply chain contribute to inefficiencies.

To address these challenges, we propose a Blockchain-based system to improve transparency, traceability, and security. Our solution utilizes an immutable, decentralized ledger to enhance product

authenticity verification and enable real-time tracking of pharmaceuticals across the supply chain. This system directly combats the issue of counterfeit drugs and inefficiencies by offering secure, verifiable records of transactions. The scope of our project is clearly defined to focus on the application of Blockchain technology to enhance the traceability and security of pharmaceutical products. Broader aspects, such as regulatory compliance and overall supply chain management practices, are outside the current scope of this work but remain areas for future research.

This section describes the key stages of the pharmaceutical supply chain and its challenges, particularly with counterfeit drugs and inefficiencies in tracking. The proposed Blockchain-based solution aims to improve transparency, traceability, and security by providing an immutable, decentralized ledger for real-time tracking and product verification.

## MATERIALS AND METHODS

### Blockchain Integration in Pharmaceutical Supply Chains

Drug fraud presents a notable challenge within the pharmaceutical sector. As indicated by the World Health Organization (WHO), approximately 15% of medications distributed worldwide are counterfeit. The prevalence of fake drugs poses serious risks to patients' well-being, potentially resulting in treatment inefficacies, adverse effects, and even mortality (Xu et al., 2023). The integration of Blockchain technology provides a significant benefit in improving drug traceability. By allowing for precise monitoring of pharmaceutical items across the complete supply chain, Blockchain establishes a secure and transparent framework. This innovation guarantees a closed loop impenetrable to fraudulent products, thus upholding the credibility of the distribution network and ensuring patient safety. Through the provision of an unalterable and verifiable account of each transaction, Blockchain not only enhances transparency but also nurtures trust among all involved parties in the pharmaceutical sector (Raparathi et al., 2021).

Moreover, Blockchain technology enables patients to authenticate the source of their prescribed medications. Pharmaceutical corporations can create their individual Blockchain networks, documenting each package of pharmaceuticals within the distribution channel. Details about each medication are modified within the Blockchain to portray alterations in whereabouts, facilitating pharmacists in validating the authenticity of drugs originating from accredited laboratories. This framework additionally empowers patients to oversee the credibility of the voyage undertaken by their prescribed medications. Furthermore, in the event of a pharmaceutical product recall,

pharmacists can quickly identify affected patients and notify them, ensuring their safety and well-being (Xu et al., 2023).

Several pharmaceutical companies have successfully implemented Blockchain technology to improve supply chain transparency and security. Pfizer's partnership with ChroniLed and the MediLedger Project have focused on tracking drug authenticity and preventing counterfeits (Akram et al., 2024).

VeChain and Bayer China have utilized Blockchain to manage clinical trial data, ensuring its integrity and traceability (Hossain et al., 2021). Modum has employed Blockchain and IoT to monitor temperature-sensitive products, ensuring compliance with cold chain regulations. These case studies demonstrate the potential of Blockchain to revolutionize the pharmaceutical supply chain by enhancing efficiency, security, and trust.

### Challenges and Limitations: Case Study Insights

The pharmaceutical supply chain represents one of the most intricate and stringently regulated systems globally, encountering a multitude of challenges that jeopardize its integrity and operational efficacy. Some of the primary concerns include:

- 1. Counterfeit Drugs:** A critical issue is the encroachment of counterfeit pharmaceuticals, which can pose significant health risks to patients and result in substantial financial detriments for legitimate pharmaceutical enterprises. The presence of counterfeit medications not only undermines patient safety but also erodes public confidence in the healthcare infrastructure.
- 2. Supply Chain Complexity:** The pharmaceutical supply chain encompasses a variety of intermediaries, including manufacturers, distributors, and retailers, each fulfilling specific functions. This inherent complexity may precipitate inefficiencies, inaccuracies, and increased susceptibility to fraud or tampering at various junctures within the chain.



- 3. Data Security and Privacy:** The management of sensitive information, encompassing patient data and proprietary drug formulations, necessitates the implementation of rigorous data security measures. Conventional data-sharing frameworks generally depend on centralized entities, which may be vulnerable to data breaches or unauthorized access, particularly in international transactions.
- 4. Regulatory Compliance:** Every phase of the supply chain is governed by regulatory stipulations to ensure product safety and effectiveness. Nonetheless, maintaining compliance across all stakeholders can prove to be arduous, particularly when regulatory frameworks differ across various jurisdictions.

#### **Blockchain's Role in Addressing These Challenges**

Blockchain technology provides innovative solutions to numerous challenges inherent within the pharmaceutical supply chain by capitalizing on its distinctive attributes, including decentralization, immutability, and transparency. Some of the principal applications encompass:

- 1. Augmented Traceability:** Blockchain facilitates real-time monitoring of pharmaceuticals throughout the supply chain, encompassing production, distribution, and retail phases. With an immutable ledger, stakeholders are empowered to trace each batch of pharmaceuticals back to its source, thereby simplifying the identification of counterfeit products and executing product recalls when warranted.
- 2. Data Security and Privacy:** Blockchain's decentralized ledger enhances data security by distributing data across the network, making it more resilient to attacks. Sensitive data can be disseminated exclusively among authorized participants, mitigating the risk of data breaches and ensuring adherence to privacy regulations. Furthermore, sophisticated encryption methods guarantee that data remains protected even during cross-border transactions.

- 3. Transparency and Accountability:** Blockchain furnishes a collective, unalterable record of every transaction within the supply chain. This transparency fosters accountability among all participants, diminishing opportunities for fraudulent activities and assuring that each stakeholder can rely on the integrity of the data they engage with.
- 4. Smart Contracts for Regulatory Compliance:** Smart contracts, defined as self-executing agreements on the Blockchain, automate the verification of regulatory compliance at various stages within the supply chain. For example, a smart contract can be designed to verify that specific conditions (such as temperature and handling specifications) are satisfied before progression to the subsequent phase, thus minimizing human error and aiding in preserving regulatory compliance.

Pfizer and Chronicle's blockchain initiatives, as well as other projects like MediLedger and VeChain, encountered significant challenges that have slowed their widespread adoption in the pharmaceutical supply chain (Akram et al., 2024). These challenges include scalability limitations, integration difficulties, high costs, regulatory hurdles, privacy concerns, and the need for full stakeholder participation. Overcoming these obstacles is crucial for realizing the full potential of Blockchain technology in the pharmaceutical industry.

This sub-section has highlighted the significant role of Blockchain technology in enhancing transparency, traceability, and security within the pharmaceutical supply chain. By addressing issues such as counterfeit drugs, supply chain complexity, data security, and regulatory compliance, Blockchain offers solutions that ensure patient safety, improve operational efficiency, and foster trust.

#### **Proposed System**

This section presents our proposed system, which integrates key stakeholders involved in patient care, including physicians, pharmacists, producers, distributors, and patients. The primary rationales behind the

incorporation of Blockchain technology in our system are as follows:

- **Security:** Blockchain technology provides heightened security in contrast to conventional database systems, rendering it notably less vulnerable to cyber attacks. This ensures the security of medications and grants patients transparency and confidence in relation to their pharmaceuticals.
- **Interoperability:** Blockchain facilitates improved interoperability among diverse stakeholders in the pharmaceutical distribution network, such as pharmacists, producers, distributors, physicians, and patients. Blockchain fosters seamless cooperation within a unified system.
- **Transparency:** Blockchain offers increased transparency, empowering patients with a clear view of their medication’s journey. Moreover, the inherent characteristics of Blockchain offer safeguards against deliberate tampering and human error, thereby bolstering the reliability of the system.

A robust database is essential for storing critical medication data, including manufacturing and expiration dates, batch numbers, and distribution records. This database serves as the backbone of our system, ensuring that all essential information is securely stored and easily accessible to authorized parties.

Our system eliminates the traditional need for trust between manufacturers, distributors, pharmacists, and patients. This is where Blockchain technology becomes a highly suitable solution, as it inherently provides a trustless environment. Blockchain’s decentralized nature ensures that all transactions and data entries are verified and immutable, meaning that no single party can alter the records without consensus. This greatly reduces the risk of data manipulation or fraud, which is particularly crucial in the pharmaceutical industry, where the integrity of information can directly impact patient safety.

The decision to deploy a private Blockchain was made with careful consideration of our need for centralized control while still reaping the benefits of Blockchain’s decentralized features. A private Blockchain allows us to maintain oversight and enforce strict access controls, ensuring only authorized entities can participate in the network. This centralized control is crucial for regulatory compliance, data security, and maintaining the integrity of the pharmaceutical supply chain. At the same time, the use of Blockchain technology enhances transparency, traceability, and security, providing a comprehensive solution that addresses the unique challenges of managing pharmaceutical data.

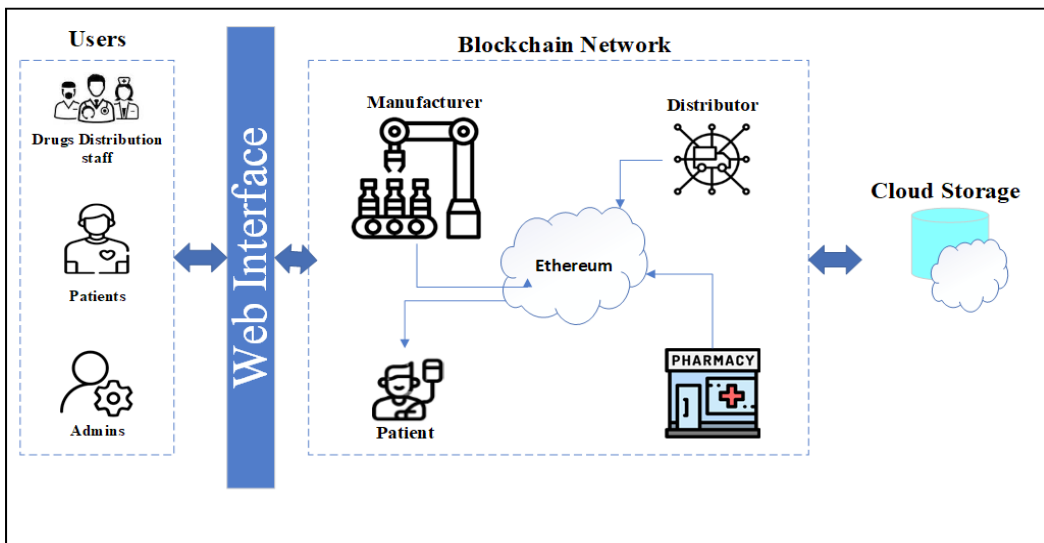


Figure 2. System architecture.

### System Architecture

The system architecture is established on the Ethereum Blockchain, utilizing intelligent contracts to obviate the necessity for intermediary oversight. Our application revolves around an Ethereum intelligent contract responsible for managing essential supply chain functions. This arrangement also affords the capacity to archive and retrieve data from the Blockchain ledger, facilitating product tracking and ensuring data integrity and tamper resistance.

The suggested architecture, as illustrated in Figure 2, integrates various stakeholders in the pharmaceutical distribution sector, each assigned specific duties and responsibilities by public health regulations:

- **Administrators:** Responsible for overseeing the system's overall operations and adherence to public health standards.
- **Patients:** End-users benefiting from the secure and transparent delivery of pharmaceuticals.
- **Manufacturers:** Interested in a supply chain that efficiently delivers their products to target markets at a reasonable cost.
- **Distributors:** Crucial in ensuring sustainable access to high-quality medications, justifying distribution expenses with the benefits conferred to the public and health organizations.
- **Retailers:** Encompassing public and private pharmacies, drugstores, online merchants, supermarkets, and prescribing physicians, all tasked with dispensing medications to patients.
- **Storage:** Encompasses decentralized and distributed data management, guaranteeing secure information storage throughout the Blockchain network.
- **Blockchain Network:** The foundational infrastructure supporting these operations, ensur-

ing transparency, security, and dependability throughout the supply chain.

This comprehensive framework ensures that each participant in the pharmaceutical distribution network complies with their designated responsibilities, thereby enhancing the overall efficiency, transparency, and security of the pharmaceutical supply chain.

### Practical Applications: Real-World Cases of Blockchain and Smart Contracts

Blockchain acts as a decentralized, immutable ledger where all transactions between participants (e.g., manufacturers, distributors, wholesalers, pharmacies) are recorded transparently. Each entity communicates through the Blockchain network, ensuring that every step in the supply chain is securely documented, as shown in Figure 3:

- **Manufacturers:** Add new drug batches to the Blockchain and initiate smart contract verification.
- **Distributors:** Transport drugs and participate in smart contract verification at each handoff.
- **Wholesalers:** Receive drugs and verify their authenticity using smart contracts.
- **Pharmacies:** Receive drugs and validate transactions using smart contracts.
- **Patients:** Can verify the authenticity of their medication using Blockchain technology.
- **Authority:** Regulatory bodies that monitor and approve transactions on the Blockchain.
- **Consensus Mechanism:** Ensures the validity of all transactions and maintains Blockchain integrity.
- **Smart contracts:** Automate various aspects of the pharmaceutical supply chain, including drug verification, payment processing, and shipment tracking, by using self-executing code to enforce predefined terms and conditions.

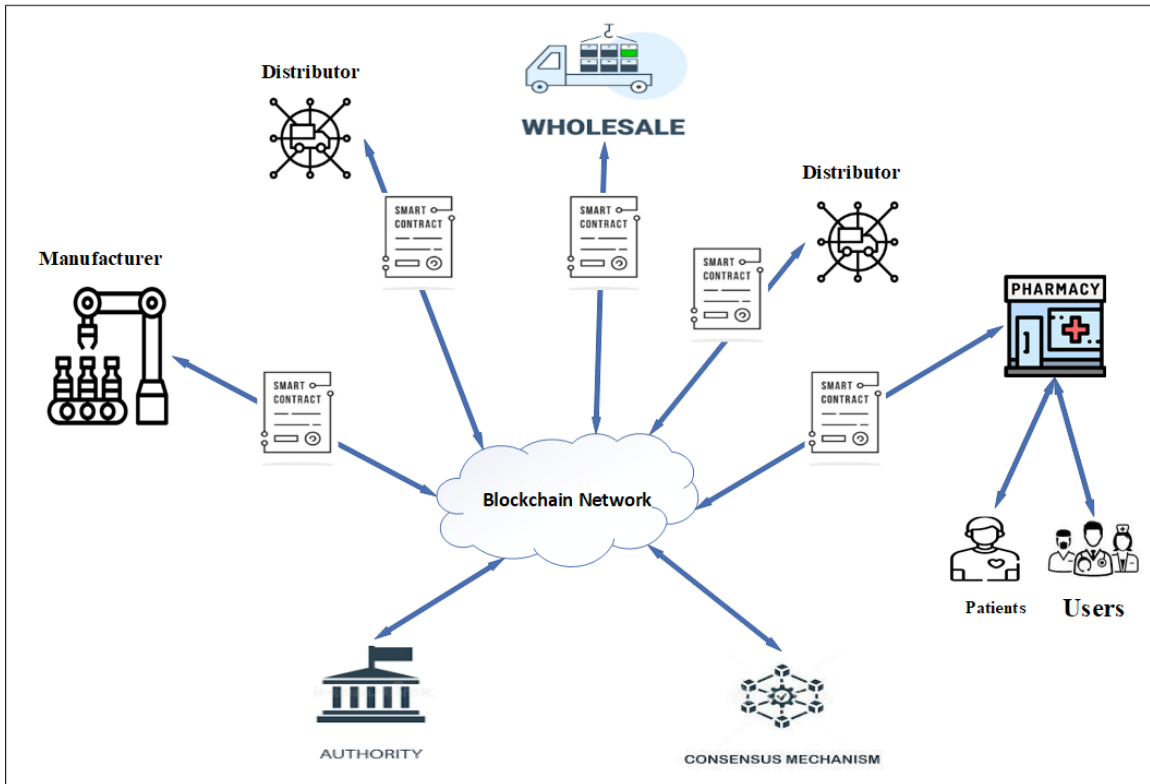


Figure 3. Blockchain Network in Pharmaceutical Supply Chain.

### System Components

The primary component is Blockchain technology, which enhances transparency and accuracy in tracking the supply chain, playing a crucial role in reducing drug counterfeiting. The monitoring of the complete production process, from manufacturing to final delivery or end-user usage, is enabled through a combination of physical digitization and a decentralized, unchangeable ledger that securely logs all transactions. Through granting all supply chain participants equal access to shared data, the Blockchain network effectively diminishes the chances of communication mistakes or inconsistencies in data transmission.

Secondly, smart contracts are automated software programs used by all participants in the supply chain to initiate, manage, and execute transactions seamlessly. These contracts are programmed to autonomously enforce the terms of an agreement autonomously, guaranteeing the precise execution of each transaction without the necessity of intermediaries. Once the smart contracts are created, they are deployed on an Ethereum test network called Ropsten. Ropsten replicates the primary Ethereum network (mainnet) and functions according to the same protocol, providing an optimal setting for testing and validating smart contracts before their deployment on the mainnet. Figure 4 shows the smart contract sequence diagram and the relationship among the participants.

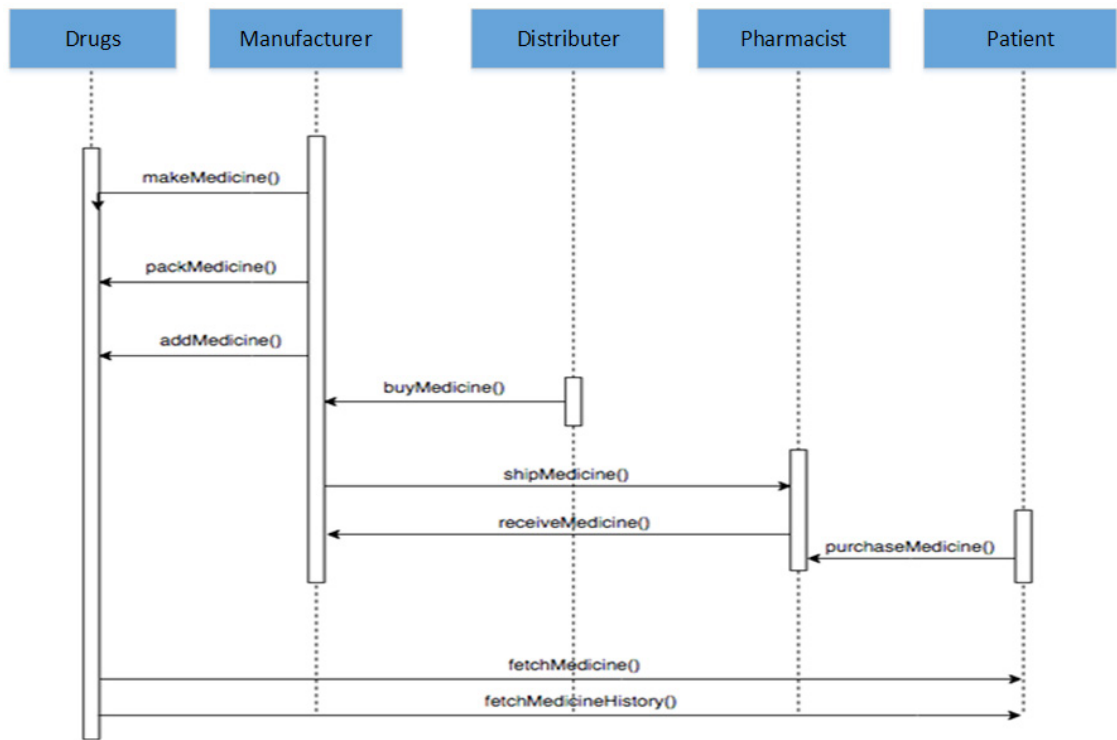


Figure 4. Sequence Diagram of Smart Contract Function.

To deploy the smart contract, a connection is established with a specific node on the Ropsten network. This connection enables the contract to be directly published to that node, allowing for monitoring and validation of its performance within a controlled testing environment. Through these assessments on

Ropsten, any potential issues can be identified and resolved, ensuring the dependable and secure operation of the smart contracts before their integration into the live Ethereum network. Figure 5 shows the smart contract functions activity diagram.

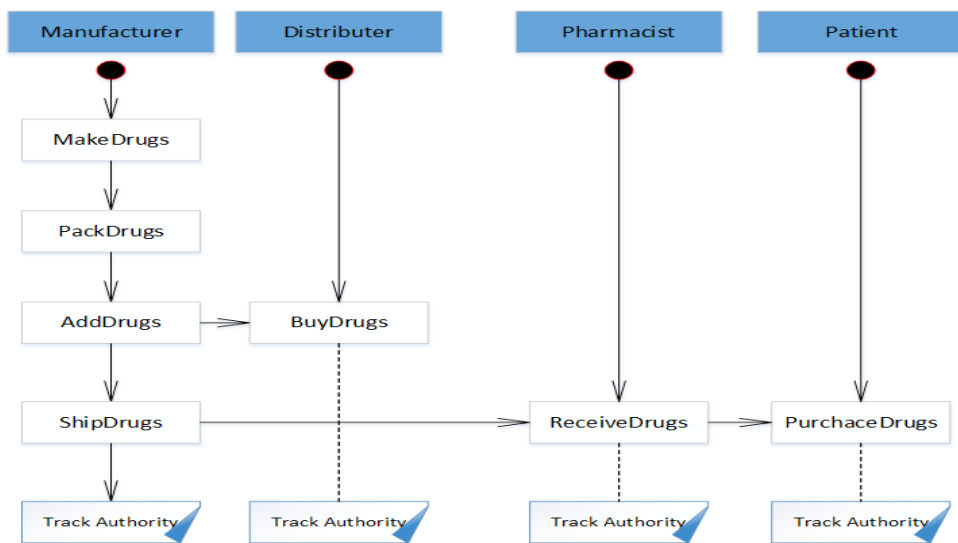


Figure 5. Activity Diagram of Smart Contract Function.

The contract outlines the various functions and actions within the supply chain, and we will detail the role of each participant step by step:

- *Manufacturer's Role:* Initially, the manufacturer is responsible for providing the drugs and essential information such as the drug name, code, and quantity. This data is securely stored on the Blockchain, enabling other participants to transparently trace the drug supply chain. After production, the manufacturer packages the drugs and sells them to distributors. From the outset, distributors place the payment into a smart contract. Once the shipping company confirms receipt of the order, the smart contract automatically releases the payment to the manufacturer.
- *Distributor's Role:* After receiving the drugs from the manufacturers, distributors verify the origin of the drugs using a product code (UPC) that is stored on the Blockchain. This allows them to trace back information provided by the manufacturers, such as drug quantities and manufacturing locations. Distributors then validate the received drugs and digitally sign the transaction, which is subsequently recorded on the Blockchain. The signed transactions trigger smart contracts that initiate the shipment of drugs to pharmacists. Once the shipment is confirmed, the smart contract releases payment to the shipping company.
- *Pharmacist's Role:* Pharmacists receive the drugs and can verify their origin using the UPC recorded on the Blockchain. For instance, if a dishonest distributor attempts to tamper with the drugs or delay delivery, any fraudulent activity will invalidate their transaction due to the integrity of the Blockchain records. This allows pharmacists to detect any discrepancies in the transactions immediately. Upon approval of the received drugs, the transaction between the pharmacist and the distributor is recorded on the Blockchain, ensuring a legally binding agreement. Additionally, when pharmacists sell drugs to customers (pa-

tients), these transactions are also added to the Blockchain, maintaining transparency and traceability throughout the supply chain.

This system ensures that every step of the drug supply chain is securely recorded and verifiable, preventing fraud and ensuring that all parties are held accountable for their actions.

Thirdly, API Infura provides a direct approach for accessing multiple Blockchain networks without the need to establish a complete node for each one, making it an efficient solution for Blockchain integration. Infura effectively manages its personal infrastructure, offering a smooth and effective means of reaching various Blockchain networks, including Ethereum. Through the utilization of Infura, developers can readily engage with Blockchain platforms via its application programming interfaces (APIs), which are tailored to streamline connections to the Ethereum network and other decentralized systems. Infura accounts empower users to execute code and interact with numerous networks like Mainnet, Ropsten, RinkeBy, and Kovan, all while avoiding the complexities of maintaining a full node. We use the Ropsten Testnet, which mirrors the Ethereum main network, for testing and development before deploying to production.

Fourthly, Web3.js represents a prominent framework utilized for developing decentralized applications (DApps). It streamlines the process of engagement with smart contracts on the Ethereum Blockchain by furnishing a user-friendly interface. Through this JavaScript API, developers can establish communication with an Ethereum node via JSON RPC endpoints, which are reachable through HTTP, IPC, or WebSocket. This functionality allows for smooth data transmission and contract interaction directly from a web page, thus establishing Web3.js as a crucial instrument for advancing Ethereum-based DApps.

Fifthly, the fundamental role of a smart contract is to oversee essential operations and manage funds securely. Nonetheless, to render these contracts acces-

sible to users, an intuitive means for interaction with the Blockchain nodes must be in place. This is where user interfaces assume significance. In our case, we use the Ropsten Testnet, which closely replicates the Ethereum main network, providing an ideal environment for testing and development before deploying to production. React was explicitly selected for its extensive adoption and robust backing, rendering it an optimal choice for crafting responsive and dynamic user interfaces. For the backend infrastructure, we have deployed Node.js in conjunction with Express, alongside MongoDB as the document-oriented database. The API stratum, empowered by Node.js/Express, manages server-side logic and facilitates communication between the front end and the Blockchain. Mon-

goDB stores essential data in a flexible and scalable format. This amalgamation of technologies guarantees that the system is both efficient and scalable, delivering a seamless user experience for individuals engaging with the Blockchain through the web interface.

### System implementation and realization

To develop and implement our system, we utilized various essential tools, including Remix IDE, Visual Studio Code, Truffle, Ganache, Node.js, React, and MetaMask. Each of these tools plays a crucial role in different stages of the development process.

Initially, we compiled the smart contract to ensure its functionality and detect potential errors. This step is crucial as it validates the correctness of the contract before deployment, as depicted in Figure 6.

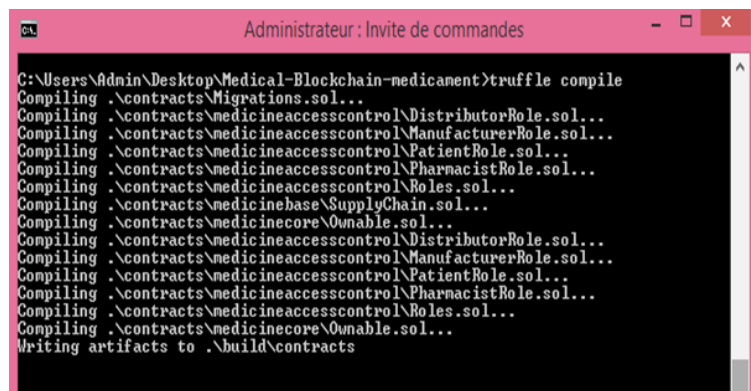


Figure 6. Smart Contract Development and Integration.

Once the contract is successfully compiled, the next step is to deploy it onto the Blockchain network.

Deployment requires establishing a connection to the Blockchain, which is illustrated in Figure 7.

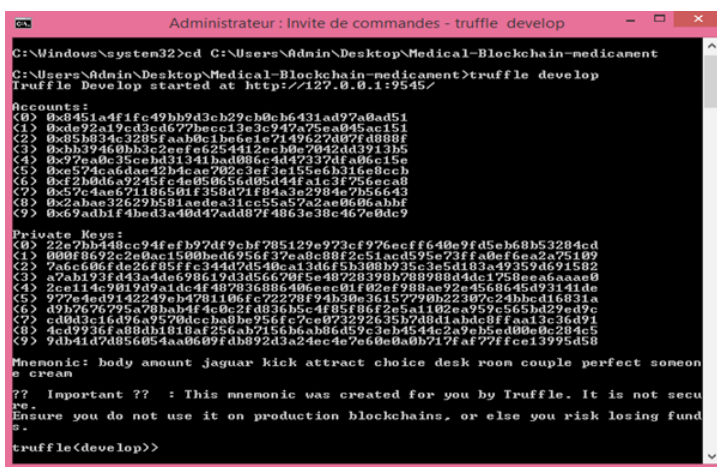


Figure 7. Creating a Blockchain network with Truffle

Testing smart contracts is a vital part of the Blockchain development process, ensuring that the contracts behave as expected under various conditions.

The Truffle framework simplifies this testing phase, providing tools that make it easy to write, run, and debug tests, as shown in Figure 8.

```
C:\Users\Admin\Desktop\Medical-Blockchain-medicament>truffle test
Using network 'development'.

Compiling .\contracts\medicineaccesscontrol\DistributorRole.sol...
Compiling .\contracts\medicineaccesscontrol\ManufacturerRole.sol...
Compiling .\contracts\medicineaccesscontrol\PatientRole.sol...
Compiling .\contracts\medicineaccesscontrol\PharmacistRole.sol...
Compiling .\contracts\medicineaccesscontrol\Roles.sol...
Compiling .\contracts\medicore\Ownable.sol...
ganache-cli accounts used here...
Contract Owner: accounts[0] 0xaE5B002b1Be1413Cd143794d51D33986118325C1
Manufacturer: accounts[1] 0x9e7e6E0662E2D52C419c23e179aCf1511A074B04
Distributor: accounts[2] 0x7faF8Cf40C899abb6013702087BE566cB77982b8
Pharmacist: accounts[3] 0x6F19d17Be1a8183705FBCDAFCB3bF5FD0217f8F4
Patient: accounts[4] 0xe6f19468A3a7e035363cAEB6563e63c883C3e2C

Contract: SupplyChain
  > Testing smart contract function makeMedicine() that allows a manufacturer
  to make medicine (634ms)
  > Testing smart contract function packMedicine() that allows a manufacturer
  to pack medicine (253ms)
  > Testing smart contract function sellMedicine() that allows a manufacturer
  to sell medicine (245ms)
  > Testing smart contract function buyMedicine() that allows a distributor to
  buy medicine (256ms)
  > Testing smart contract function shipMedicine() that allows a distributor to
  ship medicine (429ms)
  > Testing smart contract function receiveMedicine() that allows a pharmacist
  to mark medicine received (196ms)
  > Testing smart contract function purchaseMedicine() that allows a patient to
  purchase medicine (250ms)
  > Testing smart contract function fetchMedicineBufferOne() that allows anyone
  to fetch medicine details from blockchain
  > Testing smart contract function fetchMedicineBufferTwo() that allows anyone
  to fetch medicine details from blockchain
```

Figure 8. Smart contract test.

Following successful testing, we proceeded with deploying the smart contract on the Ganache local Blockchain, which simulates the Ethereum network

for testing and development purposes. Figure 9 demonstrates this deployment process.

```
Administrator - Invite de commandes
Starting migrations...
> Network name: 'development'
> Network id: 5297
> Block gas limit: 4712195

1. Initial migration.js
  > Deploying 'Migrations'
    > Transaction hash: 0x4ca29e1eef66c70464a0bc932124204ccb8ac02dd1a67de196
    > Blocks: 0
    > contract address: 0xc7208124a5316744c435e2ccaab8f4c41a2f09
    > account: 0xaE5B002b1Be1413Cd143794d51D33986118325C1
    > balance: 99.99992802
    > gas used: 38359
    > gas price: 20 gwei
    > gas sent: 0 ETH
    > value sent: 0.00407118 ETH
    > total cost: 0.00407118 ETH
  > Saving migration to chain.
  > Saving artifacts
  > Total cost: 0.00407118 ETH

2. deploy_contracts.js
  > Deploying 'ManufacturerRole'
    > Transaction hash: 0x021126584aa3d216ee42aba4a59f518eed206ef99a1bbae9294
    > Blocks: 0
    > contract address: 0x8c4798046E8123499762cb95c88c23fc28c80db
    > account: 0xaE5B002b1Be1413Cd143794d51D33986118325C1
    > balance: 99.99892324
    > gas used: 36724
    > gas price: 20 gwei
    > gas sent: 0 ETH
    > value sent: 0.006459 ETH
    > total cost: 0.006459 ETH
  > Deploying 'DistributorRole'
    > Transaction hash: 0x44b4924392d1392184a72506e5d46e1b9f76915105ef9910f6
    > Blocks: 0
    > contract address: 0x7272fcd9c61ca54725c132623f54ee984fae1
    > account: 0xaE5B002b1Be1413Cd143794d51D33986118325C1
    > balance: 99.99276472
    > gas used: 36726
    > gas price: 20 gwei
    > gas sent: 0 ETH
    > value sent: 0.00645852 ETH
    > total cost: 0.00645852 ETH
  > Deploying 'PharmacistRole'
    > Transaction hash: 0x0419196e0c50f98288ac914fa53f39a134f7d5e295336261e
    > Blocks: 0
    > contract address: 0x751c1c34a938E48a159d2f31f34125E22B80
    > account: 0xaE5B002b1Be1413Cd143794d51D33986118325C1
    > balance: 99.994052
    > gas used: 36726
    > gas price: 20 gwei
    > gas sent: 0 ETH
    > value sent: 0.00645852 ETH
    > total cost: 0.00645852 ETH
  > Deploying 'PatientRole'
    > Transaction hash: 0x4cb4e085e66773cabd44f72502ebc130feef6e2bf00170c6
    > Blocks: 0
    > contract address: 0x9a88814a06527b8Ca024b94324042BEE0
    > account: 0xaE5B002b1Be1413Cd143794d51D33986118325C1
    > balance: 99.9949764
    > gas used: 36724
    > gas price: 20 gwei
    > gas sent: 0 ETH
    > value sent: 0.00645852 ETH
    > total cost: 0.00645852 ETH
  > Deploying 'SupplyChain'
    > Transaction hash: 0xa63e3fb414087b02eccf5404b6b68f9444bd8fad41ed6e8987
    > Blocks: 0
    > contract address: 0x03f30311207a2639D8A2336954f47988846407
    > account: 0xaE5B002b1Be1413Cd143794d51D33986118325C1
    > balance: 99.99262316
    > gas used: 38359
    > gas price: 20 gwei
```

Figure 9. Smart Contract on Ganache.

The Figure 10. displays a snapshot illustrating the execution of a smart contract on the Ethereum Blockchain through the Remix IDE. The contract pertains to a system for managing the supply chain, as evidenced by its designation as “SupplyChain.sol.” A manufacturer is being incorporated into the supply chain by

the user by inputting an Ethereum address into the addManufacturer function, followed by the execution of the transaction. The transaction is currently pending, as indicated by the console output displayed at the bottom of the interface. The user is currently linked to the Ethereum network using the MetaMask



wallet, which is observable on the right-hand side of the interface. Within the MetaMask wallet, it is apparent that the user is connected to the “manufacture”

account, possessing a balance of 0.9975 ETH, and the transaction is undergoing processing on the Ropsten test network.

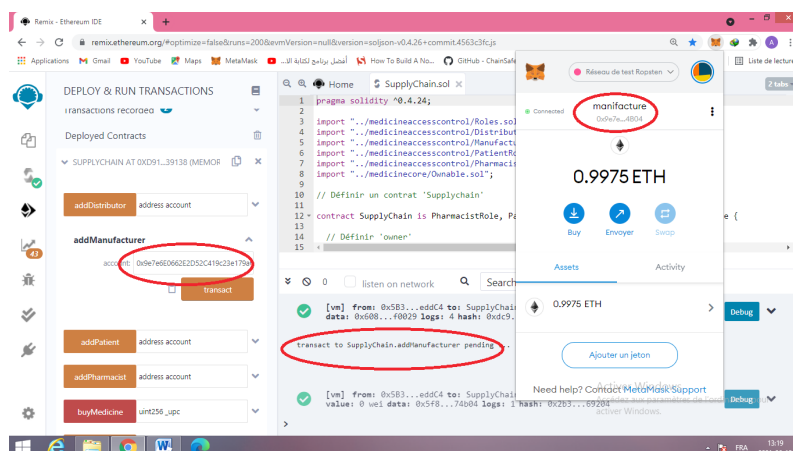


Figure 10. Sample functionalities of the addManufacturer smart contract

On the Manufacturer page, manufacturers can register new drugs into the system by providing detailed information such as the manufacturer’s name, product code, drug name, and quantity. Clicking the

“Make” button initiates a transaction that securely stores all relevant information on the Blockchain and systematically records it in the MongoDB database, as shown in Figure 11.

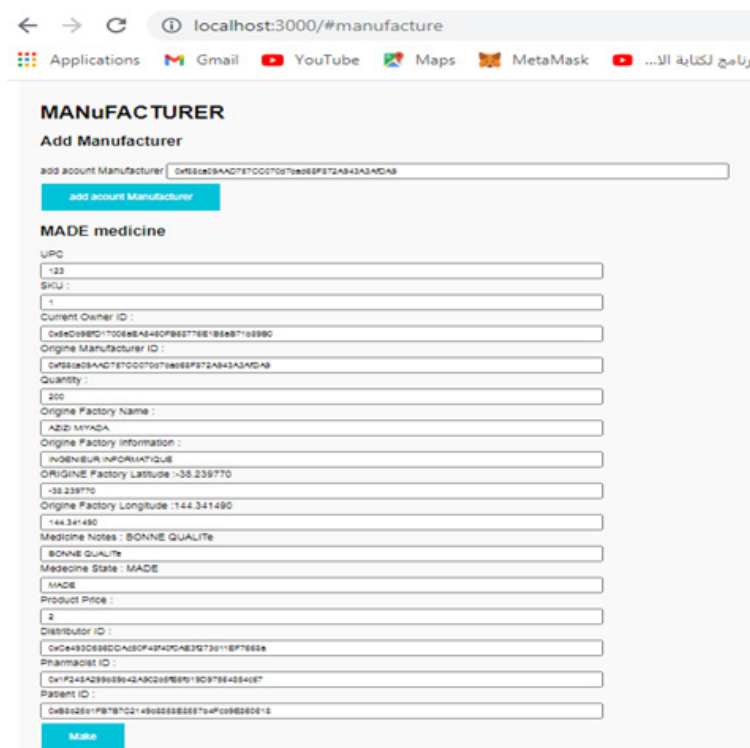


Figure 11. Manufacturer page.

After a drug is registered, the manufacturer can change its status to “packed” after verifying that it has entered the supply chain. Subsequently, the manufacturer can update the drug’s status to “sell” by adding the unit price once the drug is confirmed to follow

the supply chain. The drug is then marked as “For Sale,” allowing a distributor to purchase it. Upon verification, the smart contract facilitates the transfer of payment to the manufacturer, and the drug’s status is updated to “Buy,” as illustrated in Figure 12.

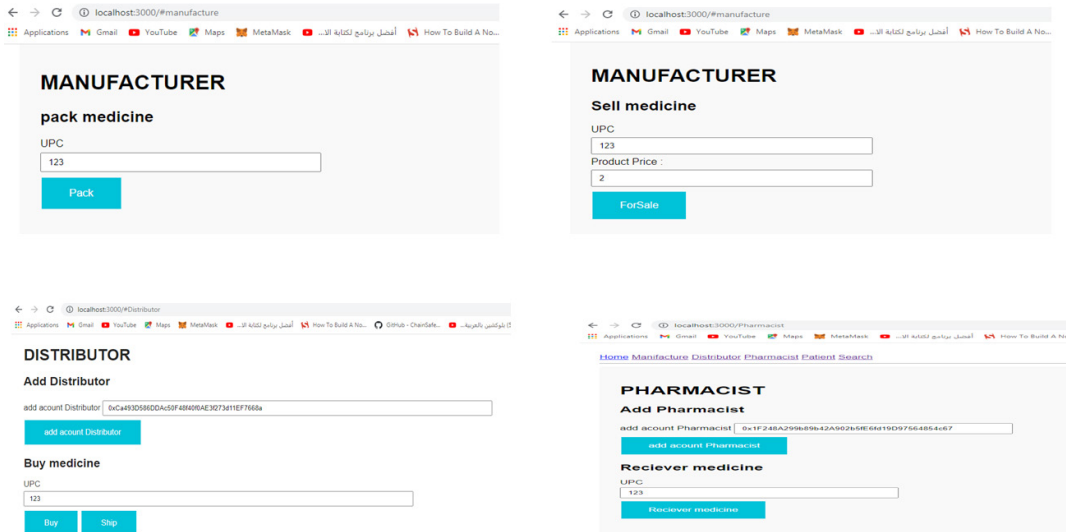


Figure 12. Drug states.

Finally, after the patient verifies the drug’s journey through the supply chain, they can change the drug’s status to “Purchase,” indicating that the transaction is

complete and the drug has been successfully acquired by the end-user, as shown in Figure 13.

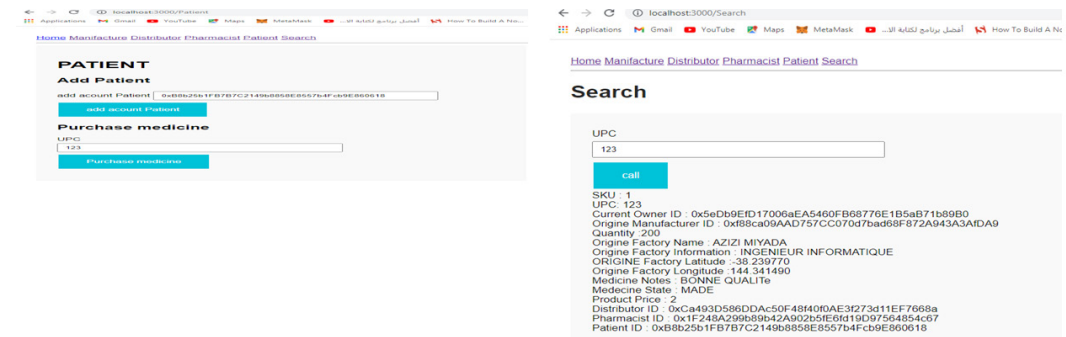


Figure 13. Purchase drugs.

This comprehensive process, supported by the integration of various tools and technologies, ensures a secure, transparent, and efficient drug supply chain, leveraging Blockchain’s immutable ledger and smart contracts to manage transactions and maintain trust across all participants.

### Difference Between our Proposed System and a Traditional Database

The table highlights several key differences between the proposed Blockchain-based system and traditional databases. In terms of operations, Blockchain only allows data insertion, preventing modifi-

cations or deletions, which enhances data security. At the same time, traditional databases support CRUD operations, making them more flexible but potentially vulnerable to tampering. Regarding replication, Blockchain ensures full replication across all peers, promoting decentralization and redundancy, unlike traditional databases that use master-slave or multi-master replication, which introduces central points of failure. Consensus in Blockchain requires agreement among participants before committing data, ensuring trust without central control, whereas traditional databases rely on internal consistency

mechanisms. Lastly, Blockchain allows transaction validation by any participant, fostering transparency, while traditional databases depend on integrity constraints managed by administrators, which could be bypassed. Overall, Blockchain offers enhanced security and transparency, making it ideal for sensitive applications like pharmaceutical supply chains. However, traditional databases provide greater flexibility for tasks that require frequent data modifications.

The Table 1 illustrates the fundamental differences between our proposed Blockchain-based system and a traditional database.

**Table 1.** Differences between our proposed system and a traditional database.

Properties	Our proposed Blockchain-based system	Traditional Database
<b>Operations</b>	It only allows insert operations.	Supports CRUD operations (Create, Read, Update, Delete).
<b>Replication</b>	Full replication for each peer	Uses master-slave or multi-master replication.
<b>Consensus</b>	Achieves consensus on transactions.	Relies on distributed transactions.
<b>Validation</b>	Transactions can be validated by anyone.	Enforces integrity constraints.

## CONCLUSION

This paper presents a Blockchain-based system designed to enhance transparency and traceability in the pharmaceutical supply chain by providing verifiable information on the origin and distribution of medications. By enabling producers to authenticate sourcing and distribution without data manipulation risks, the system gives participants access to a drug's complete history, building trust and accountability. Additionally, the Blockchain framework authenticates each product at every stage, preventing counterfeit drugs from entering the market and enhancing patient safety.

A Blockchain-secured supply chain further supports regulatory compliance, reduces supply chain fraud, and strengthens confidence among healthcare providers, patients, and stakeholders. Future research should prioritize regulatory and ethical challenges, integration with current systems, and scalability and cost-efficiency. Expanding these capabilities could also involve Big Data for in-depth analysis, cloud computing for scalable storage, and IoT for real-time monitoring, which would collectively improve the safety and reliability of the pharmaceutical supply chain. Addressing these challenges is crucial to maximizing Blockchain's impact in this sector.

## AUTHOR CONTRIBUTION STATEMENT

Ahmed Aloui: Conceptualization, Methodology, Writing – Original Draft. Meftah Zouai: Data Collection, Experiments, Formal Analysis. Samir Bourekache: Writing – Review & Editing, Visualization, Validation. Okba Kazar: Supervision, Project Administration, Final Approval.

## CONFLICT OF INTEREST

The authors declare that there is no conflict of interest.

## REFERENCES

- Abdallah, S., & Nizamuddin, N. (2023). Blockchain-based solution for Pharma Supply Chain Industry. *Computers & Industrial Engineering*, 177, 108997. <https://doi.org/10.1016/j.cie.2023.108997>
- Akram, W., Joshi, R., Haider, T., Sharma, P., Jain, V., Garud, N., & Singh, N. (2024). Blockchain technology: A potential tool for the management of pharma supply chain. *Research in Social and Administrative Pharmacy*, 20(6), 156-164. <https://doi.org/10.1016/j.sapharm.2024.02.014>

- Al Huraimel, K., & Jenkins, R. (2020). Smart Track. Accessed: May 26, 2020. Available: <https://smart-track.ae/>
- Alla, S., Sriraman, H., & Chattu, V. K. (2024). Securing Drug Supply Chain Management Using Blockchain. In P. Kumar & A. Kumari (Eds.), *Blockchain for Biomedical Research and Healthcare* (p. 9). Springer. [https://doi.org/10.1007/978-981-97-4268-4\\_9](https://doi.org/10.1007/978-981-97-4268-4_9)
- Ayati, N., Saiyarsarai, P., & Nikfar, S. (2020). Short and long-term impacts of COVID-19 on the pharmaceutical sector. *DARU Journal of Pharmaceutical Sciences*, 28(2), 799-805.
- Faulkner, C. (2020). What is NFC? Everything you need to know. *TechRadar*. Accessed: Jun. 3, 2020. Available: <https://techradar.com>
- Farooq, M. S., Khan, M., & Abid, A. (2020). A framework to make charity collection transparent and auditable using blockchain technology. *Computers & Electrical Engineering*, 83, 106588.
- Gligor, D. M., Holcomb, M. C., McCarthy, T. M., & Pfohl, H. C. (2022). Utilizing blockchain technology for supply chain transparency: A resource orchestration perspective. *Journal of Business Logistics*, 43(1), 140-159.
- Gomasta, S. S., Dhali, A., Tahlil, T., Anwar, M. M., & Ali, A. B. M. S. (2023). PharmaChain: Blockchain-based drug supply chain provenance verification system. *Heliyon*, 9(7), e17957. <https://doi.org/10.1016/j.heliyon.2023.e17957>
- Gruchmann, T., Elgazzar, S., & Ali, A. H. (2024). Blockchain technology in pharmaceutical supply chains: A transaction cost perspective. *Modern Supply Chain Research and Applications*. ISSN: 2631-3871
- Hossain, M. Z. (2021). The applicability of blockchain technology in healthcare contexts to contain COVID-19 challenges. *Library Hi Tech*, ahead-of-print(ahead-of-print). <https://doi.org/10.1108/LHT-02-2021-0071>
- Jadhav, J. S., & Deshmukh, J. (2022). A review study of the blockchain-based healthcare supply chain. *Social Sciences & Humanities Open*, 6(1), 100328.
- Kumar, A., Liu, R., & Shan, Z. (2020). Is blockchain a silver bullet for supply chain management? Technical challenges and research opportunities. *Decision Sciences*, 51(1), 8-37.
- Mishra, R., Ramesh, D., Mohammad, N., et al. (2024). Blockchain enabled secure pharmaceutical supply chain framework with traceability: An efficient searchable Pharmachain approach. *Cluster Computing*, 27, 13621–13641. <https://doi.org/10.1007/s10586-024-04626-w>
- Musamih, A., Alsabah, M., Omar, M., Ahmed, A., Alsmadi, S., & Salah, K. (2021). A blockchain-based approach for drug traceability in healthcare supply chain. *IEEE Access*, 9, 9728-9743.
- Raparathi, M. (2021). Blockchain-Based Supply Chain Management Using Machine Learning: Analyzing Decentralized Traceability and Transparency Solutions for Optimized Supply Chain Operations. *Blockchain Technology and Distributed Systems*, 1(2), 1-9.
- Tiwari, A., & Rueboon, W. (2024). Transforming Supply Chain Management: Leveraging Blockchain Technology for Enhanced Security, Transparency, and Efficiency. *Journal of Electrical Systems*, 20(9s), 1073-1079.
- Xu, X., et al. (2023). A survey on application of blockchain technology in drug supply chain management. In *2023 IEEE Eighth International Conference on Big Data Analytics (ICBDA)*. IEEE.

# Characterization of Vasoactive Intestinal Polypeptide with LC-MS/MS Method

Sema KOYUTURK\*, Erol SENER\*\*o

## Characterization of Vasoactive Intestinal Polypeptide with LC-MS/MS Method

### SUMMARY

Neuropeptides are peptides used by neurons for communication. Vasoactive intestinal polypeptide (VIP) is a polypeptide belonging to the glucagon/secretin family obtained from the hypothalamus region of the brain. In this study, VIP was analytically characterized and examined using a sensitive Liquid Chromatography-Mass Spectrometry (LC-MS/MS) method. For the analysis of VIP, chromatographic (such as separation column, organic solvent and acid content of the mobile phase, flow rate) and mass spectrometric (observation of precursor ions and fragments of peptides, fragmentation voltage, collision energy) parameters were examined. In the analysis, 799.5 and 770.7 m/z fragment ions were observed, consisting of the 665.9 ( $M^+$ ) m/z precursor ion for VIP. Moreover, the VIP adsorption problem that emerged during the analyses was investigated, and factors preventing adsorption were tested using LC-MS/MS analyses. Additionally, the effect of albumin solution on the analyses as a barrier to the adsorption of the peptide to the surface was investigated. As a result of these studies, the suitability of the application has been demonstrated in that the masses and fragments of the polycharged species of VIP in the presence of adsorption can be observed with the developed LC-MS/MS method.

**Key Words:** Vasoactive intestinal polypeptide (VIP), LC-MS/MS, peptide adsorption.

## Vazoaktif Intestinal Polipeptitlerinin LC-MS/MS Yöntemi ile Karakterizasyonu

### ÖZ

Nöropeptitler, nöronlar tarafından iletişim için kullanılan peptitlerdir. Vazoaktif intestinal polipeptid (VIP), beynin hipotalamus bölgesinden elde edilen glukagon/sekretin ailesine ait bir polipeptittir. Bu çalışmada VIP; analitik olarak karakterize edilmiş ve hassas Sıvı Kromatografisi-Kütle Spektrometrisi (LC-MS/MS) yöntemi ile incelenmiştir. VIP analizi için kromatografik (ayırma kolonu, organik çözücü ve hareketli fazın asit içeriği, akış hızı gibi) ve kütle spektrometrik (peptit öncül iyonlarının ve parçalarının gözlenmesi, parçalanma voltajı, çarpışma enerjisi gibi) parametreler incelenmiştir. Analizde VIP için 665.9 ( $M^+$ ) m/z öncül iyon ve 799.5 ve 770.7 m/z parça iyonları gözlenmiştir. Ayrıca analizler sırasında ortaya çıkan peptidin adsorpsiyon probleminin kaynakları araştırılmış ve LC-MS/MS analizlerinde adsorpsiyonu engelleyen faktörler test edilmiştir. Ek olarak, albümin çözeltisinin peptidin yüzeye adsorpsiyonuna bir bariyer olarak analizler üzerindeki etkisi araştırılmıştır. Bu çalışmalar sonucunda, geliştirilen LC-MS/MS yöntemi ile adsorpsiyon varlığında VIP'nin çoklu yüklenmiş türlerinin kütlelerinin ve parçalarının gözlenebilmesi bakımından uygulamanın uygunluğu gösterilmiştir.

**Anahtar Kelimeler:** Vazoaktif intestinal polipeptid (VIP), LC-MS/MS, peptid adsorpsiyonu.

Received: 28.09.2024

Revised: 12.12.2024

Accepted: 05.02.2025

\* ORCID: 0000-0002-3323-9902, School of Pharmacy Department of Analytical Chemistry, Istanbul Medipol University, Kavacik South Campus, Beykoz, Istanbul, Turkey  
\*\* ORCID: 0000-0003-1902-4785, School of Pharmacy Department of Analytical Chemistry, Anadolu University, Yunusemre Campus, Eskisehir, Turkey

## INTRODUCTION

Neuropeptides have long been known as chemical signals in the brain. They are small protein-structured substances that function on neural surfaces and are spread by neurons through regular secretion. These are the most diverse class of signaling molecules that have many physiological functions in the brain (Burbach, 2011). Studies have proven that peptides are bioactive compounds throughout the body (Sewald & Jakubke, 2002).

According to the gastroenteropancreatic peptide classification made by Rehfeld (Rehfeld, 1998), vasoactive intestinal polypeptide (VIP) is among the peptides in the secretin group. It is a neuropeptide containing 28 amino acids that is very common in the central and peripheral nervous system (Watanabe, 2016).

VIP is produced in many tissues in the brain, such as the suprachiasmatic nucleus of the hypothalamus, pancreas, and intestine. In addition to its many general functions, it increases glycogenolysis, lowers arterial blood pressure, strengthens the immune system without causing an autoimmune reaction, prevents apoptosis in brain cells, has neuroprotective effects, and has antioxidant properties. Due to these

properties, its protective and therapeutic effects point out in a wide variety of pathologies such as septic shock, hemorrhagic shock, ischemia-reperfusion injury, Parkinson's disease, and Alzheimer's disease (Tunçel & Korkmaz, 2010).

When the literature on VIP is reviewed, numerous medical, physiological and pharmacological studies have been existed since it is a neuropeptide. These are studies primarily aimed at the diagnosis and treatment of diseases; however, there are limited analytical studies. It is believed that this might be due to the very low concentrations of neuropeptides in the brain, the challenges faced in peptide analysis (like surface adsorption), and the absence of a method that can effectively analyze them.

Recently, chromatography, isoelectric point-electrophoresis, and their combination methods have been used for peptide analysis. Immunocytochemistry, radioimmunoanalysis (RIA), enzyme-linked immunosorbent analysis (ELISA), and mass spectrometry (MS) are other methods that provide information about the determination and distribution of neuropeptides (Soloviev & Finch, 2005). A summary of the studies in the literature using these and combined methods is given in (Table 1).

**Table 1.** Research for VIP Analysis in Literature

Analysis Method	Analyte	Sample	Linear Range	LOD	LOQ	References
HPCE	VIP	Rat brain	$1 \times 10^{-6}$ - $5 \times 10^{-4}$ M	$\sim 10^{-6}$ M	NA	Soucheleau & Denoroy, 1992
CE-LIF	VIP	Tissue	10-800 pg	5 pg/mL	NA	Phillips, 1998
RIA	VIP and PACAP	-	NA	NA	NA	Wasilewska-Dzubinska et al., 2002
HPLC	Neuropeptide Y and VIP	Gingival Tissue	19-1000 pg/mL	NA	NA	El-Karim et al., 2003
ESI-QTOF-MS	CGRP and VIP	-	1-1000 ng/mL	NA	NA	Abaye et al., 2011
RIA	VIP and PACAP	-	NA	NA	NA	Hansen et al., 2013
HPLC	VIP	-	9-150 $\mu$ g/mL	360 ng/mL	900 ng/mL	Cui et al., 2013
CE-MS	VIP and PACAP	-	1-200 ng/mL	1 ng/mL	NA	Lock et al., 2015
HPLC	VIP, Glutamate and GABA	-	NA	NA	NA	Korkmaz et al., 2021

\*NA: No application

Since neuropeptides exist in extremely low amounts, they are usually analyzed by methods that require high sensitivity, excellent selectivity, and a wide dynamic detection range (Yin et al., 2011). The MS method is indispensable for the identification of the peptide (Baggerman et al., 2004). It is possible to determine the main mass by MS analysis and to observe the masses of fragment ions belonging to this mass by MS/MS. The LC-ESI-MS/MS or LC-MALDI-MS/MS methods are generally used for these studies.

The feature that makes MS analysis of proteins/peptides possible is that their structures are not disrupted by methods such as MALDI/ESI during evaporation/ionization. The ESI method enables multiple charging of the same peptide in an MS spectrum, allowing the use of mass analyzers with a limited  $m/z$  range for peptide analysis, and provides more accurate molecular weight calculations through various calculations (Trauger et al., 2002).

There are also several challenges encountered during peptide/protein analysis, as well as factors that limit the analysis. Because of the polar, nonpolar, and charged parts in the structures of these substances, they are adsorbed to silica by hydrogen bonding or ionic interaction (Baker, 1995). Therefore, the choice of materials used during sample preparation is critical. Given that they are generally glass and polypropylene/polyethylene, adsorption may occur depending on these surfaces and vary depending on the material. Additionally, adding organic, or nonionic surfactant to the medium and keeping the medium acidic, basic or neutral helps prevent adsorption.

This study aimed to develop an analytical method that is as sensitive, simple, and fast as possible, to characterize VIP using a highly sensitive technique such as LC-MS/MS, and to refine the analysis method.

## **MATERIALS AND METHOD**

### **Chemicals**

Albumin (>98%), acetonitrile (HPLC purity), formic acid (~98% for LC-MS), methanol (HPLC purity), ultra-pure water, reference standard ( $\geq 95\%$ ) of VIP were purchased from Sigma-Aldrich (Germany), acetic acid (100%) was purchased from Merck (Germany).

### **Instruments**

The analysis column used in LC-MS/MS studies, Ascentis Express Peptides, ES-C18, 100×2.1 mm, 2.7  $\mu\text{m}$ , was obtained from Supelco, Sigma-Aldrich (Germany). Sartorius Stedim Biotech distilled water instrument, Arium Pro VF (Germany); Excellence Plus XP-205 model, Mettler Toledo (Switzerland) analytical balance; Mettler Toledo Seven Compact pH/ion meter S220 (Switzerland) pH meter; 1290 LC system and 6460 Triple Quad MS system Agilent Technologies (USA), Bandelin Electronic RK510 H (Germany) ultrasonic bath and Jeio Tech VM 96 B (Korea) vortex mixer are other instruments used in the studies.

### **Solvent Selection and Preparation of Stock Solutions**

To facilitate the ionization of VIP during the analysis, 1% acetic acid (AcAc) was chosen as the solvent. The reference standard of VIP was dissolved in 1% AcAc to a stock concentration of 0.25 mg/mL and stored at  $-80^\circ\text{C}$ . Working solutions with concentrations of 1.25, 2.50, and 5.00  $\mu\text{g}/\text{mL}$  were prepared from this stock solution. Additionally, 1% AcAc was used as a dilution solution and stored at  $-18^\circ\text{C}$ .

### **Chromatographic Parameters**

The analytical column used for the separation process is a C18 column with a length of 100 mm, an inner diameter of 2.1 mm, and a particle size of 2.7  $\mu\text{m}$ . It has a pore size of 160  $\text{Å}$  to increase the capacity factor of the analyte peak and improve the peak morphology in the analysis of large molecules such as peptides.

When examining the mobile phases used in the literature, they generally include acidic mobile phases, as VIP is basic and will ionize before entering the MS. A 0.2% formic acid-water solution (A) and a 0.2% formic acid-acetonitrile solution (B) were prepared in separate lines, and the experiments were started with this mobile phase. Furthermore, experiments were started with a low flow rate of 0.2 mL/min to ensure that the analyte coming from the column was completely ionized when it entered the ionization chamber and to prevent peptide loss.

Since VIP has a polar structure due to its amino acid content (Watanabe, 2016), it was anticipated that VIP would not be retained for a long time because of the mobile phase and column used, and the analyses were started with the gradient shown in (Table 2). These gradient and flow rate values were used during MS optimization and were later re-evaluated and optimized.

**Table 2.** Initial Gradient

R <sub>t</sub> (min) <sup>a</sup>	A%	B%	Flow Rate (mL/min)
0	90	10	0.2
8	30	70	0.2

<sup>a</sup> Retention Time

In addition, other parameters, such as the injection volume, were set to 2 µL, and the column temperature was set to 30°C.

**RESULTS**

**Optimization of Method**

Analyses launched by examining the parameters of

MS. VIP is a large peptide with a molecular weight of 3325.8 g/mol. since scanning can be done up to 3000 m/z with the Triple Quad. mass analyzer, it is not possible to analyze VIP by charging with 1+/1-. However, it can be analyzed with multiple ionization by charging it as 2+, 3+, and 4+.

Moreover, since the pI value of VIP is greater than 11, it will act as a cation in acidic environments, that is, at pH lower than the pI value, so only positive polarity analyses were carried out.

Considering the mass analyzer and the properties of VIP, scanning was first carried out in the 100-3000 m/z range in MS<sup>2</sup> Scan mode. In the source parameters, the gas temperature is set to 300°C, and the gas flow is 5 L/min, the nebulizer pressure is 45 psi, the sheath gas temperature is 350°C, the sheath gas flow is 7 L/min, the capillary voltage is 3500 V, and the nozzle voltage is 500 V. The chromatogram of 5.00 µg/mL VIP obtained after scanning is shown in Figure 1(a) and MS spectrum for 1108.9(M<sup>3+</sup>), 832.3(M<sup>4+</sup>), 665.9(M<sup>5+</sup>), and 554.6(M<sup>6+</sup>) m/z values is provided in Figure 1(b).

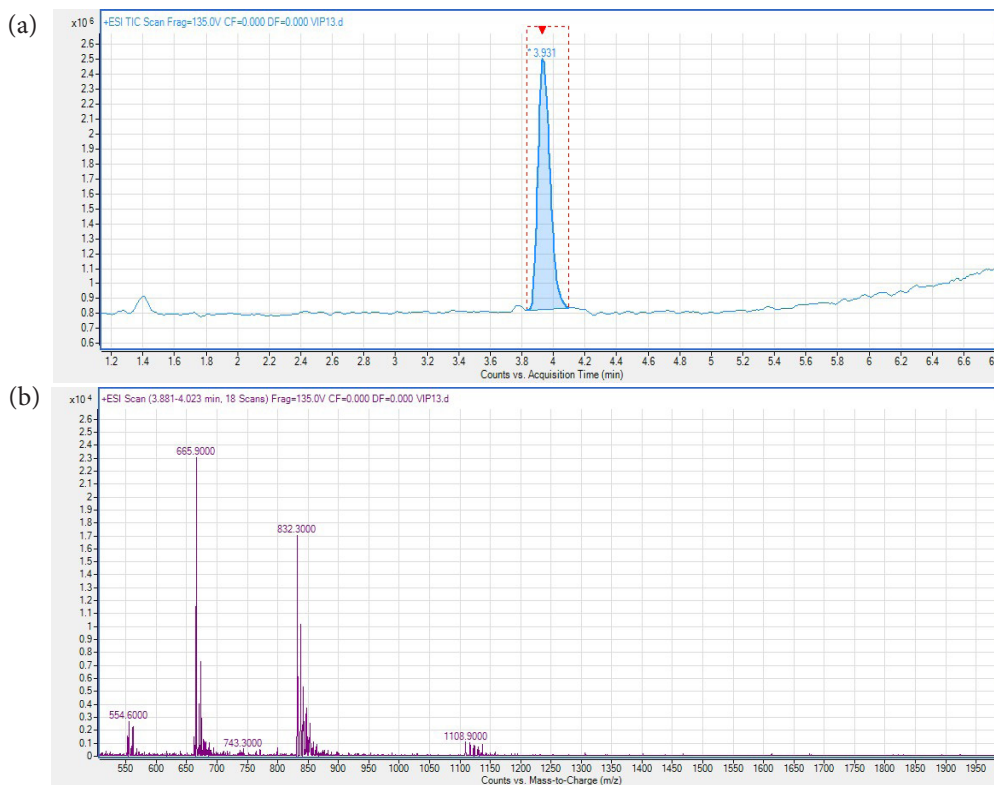


**Figure 1.** (a) 5.00 µg/mL VIP chromatogram with SCAN mode (b) MS spectrum for 554.6 (M<sup>6+</sup>), 665.9 (M<sup>5+</sup>), 832.3 (M<sup>4+</sup>), 1108.9 (M<sup>3+</sup>) m/z masses



To increase the selectivity of these masses and to confirm that they belong to VIP, these masses ( $M^{6+}$ ,  $M^{5+}$ ,  $M^{4+}$ , and  $M^{3+}$ ) were examined with the selected

ion monitoring (SIM) mode known as  $MS^2$  SIM and confirmed by performing analysis with increasing concentrations of 1.25, 2.50 and 5.00  $\mu\text{g/mL}$  VIP.

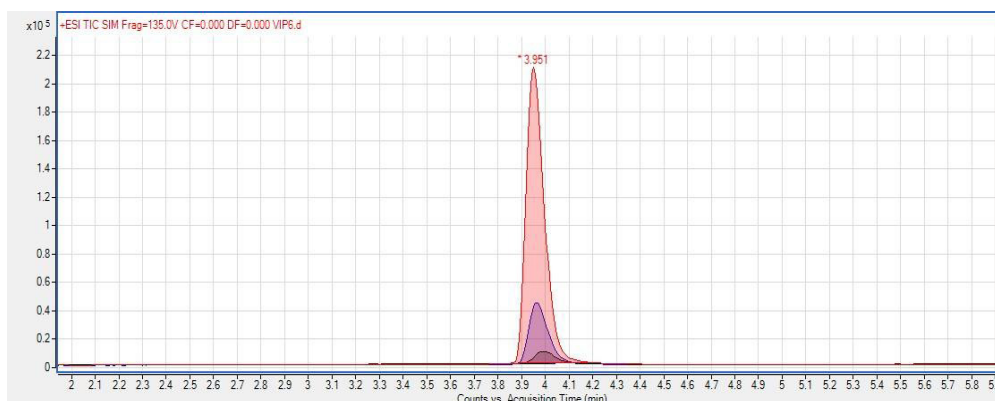


**Figure 2.** 1.25, 2.50, and 5.00  $\mu\text{g/mL}$  VIP analysis with SIM mode

As seen in (Figure 2), reproducible retention times, the stability of these three masses belonging to VIP in each analysis, and the correlation between concentration and peak areas confirmed that the peak at 3.9 min was VIP.

Since the selected  $m/z$  values will be analyzed with fragments in MRM mode in subsequent stages, a fragmentation voltage scan was performed. The

fragmentation voltage scan of each  $m/z$  value (1109.1, 832.1, and 665.9) was examined between 10-200 V on SIM mode using 2.50  $\mu\text{g/mL}$  VIP solution during the analyses. Differences in peak areas and their corresponding signal-to-noise ratios (SNR) were observed in the result of the fragmentation voltage scan. The peak areas obtained for each mass versus the fragmentation voltage are given graphically (Figure 3).

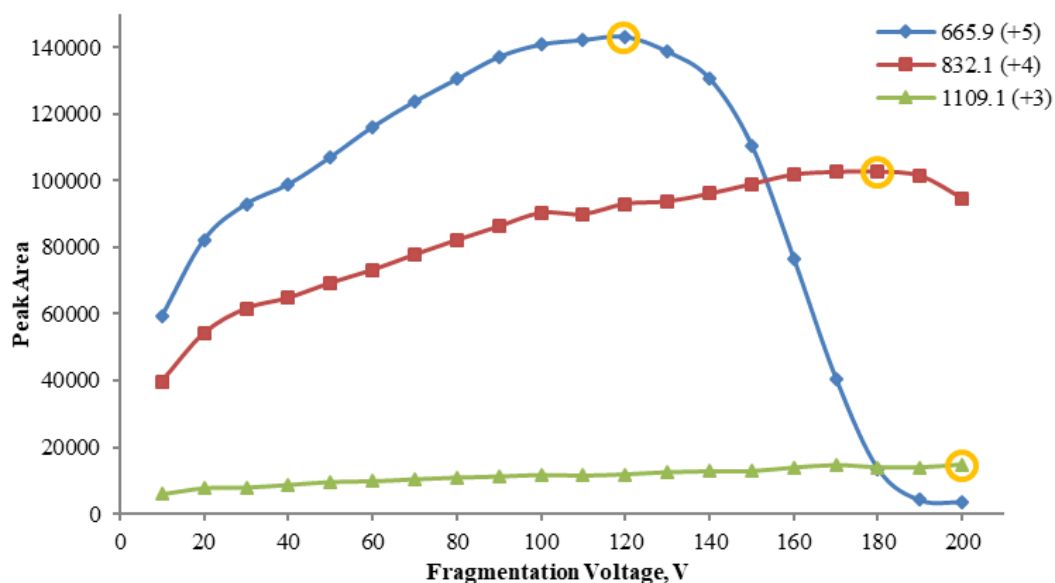


**Figure 3.** Fragmentation Voltage-Peak Area Graph

As it stands in the graph in Figure 3, the largest peak areas were obtained with fragmentation voltages of 120 V for 665.9 ( $M^{5+}$ ), 180 V for 832.1 ( $M^{4+}$ ), and 200 V for 1109.1 ( $M^{3+}$ ). However, the peak areas obtained from the  $M^{+3}$  mass were much lower than those of the  $M^{4+}$  and  $M^{5+}$  m/z masses, indicating that this mass cannot be used at lower concentrations. Therefore, we focused on 832.1 and 665.9 m/z masses. Repetitive

analyses were performed at a fragmentation voltage of 135 V, which is the device's default value, as well as at 180 V for 832.1 and 120 V for 665.9, corresponding to  $M^{4+}$  and  $M^{5+}$ , respectively, where the largest peak areas were observed. According to the analysis results, evaluations were made on the RSD, and the results are given in (Table 3).

**Table 3.** Analysis results obtained as the consequence of repetitive analyses at different fragmentation voltages (n=6)

	120 V		135 V		180 V	
	832.1	665.9	832.1	665.9	832.1	665.9
	A <sup>a</sup>	A <sup>a</sup>	A <sup>a</sup>	A <sup>a</sup>	A <sup>a</sup>	A <sup>a</sup>
mean	224085.46	322957.12	231300.72	308692.70	235300.88	35760.87
SD <sup>b</sup>	3426.99	4559.14	5932.42	7302.12	5209.73	1436.86
RSD% <sup>c</sup>	1.53	1.41	2.56	2.37	2.21	4.02

<sup>a</sup> Area, <sup>b</sup> Standard Deviation, <sup>c</sup> Relative Standard Deviation

According to (Table 3), the one with the highest peak area and lowest RSD was 665.9 ( $M^{5+}$ ) at 120 V fragmentation voltage. Since a higher signal was obtained compared to other m/z masses, it was decided to continue with 665.9 ( $M^{5+}$ ) and 120 V fragmentation voltage in subsequent analyses.

In the later stages of the study, the multiple reaction monitoring (MRM) mode, which significantly enhances the method's selectivity, was employed. The fragments of the 665.9 ( $M^{5+}$ ) m/z value of VIP were identified using the Product Ion mode. Fragment scanning was performed in the range of 50-3000 m/z. The reason for scanning in such a wide m/z range is that since the 665.9 m/z mass has a 5+ charge, it is considered the main mass (3328.5 g/mol), and when it

is broken down, it is predicted that it may have larger fragments. Fragments of 665.9 m/z were examined with different energies (10, 20, 30, and 40 V) applied to the collision cell.

Although no fragments were formed at low fragmentation energies, such as 10 V, it was observed that small fragments were generated as the applied energy increased. When 20 V was applied, m/z values of 799.4, 770.8, and 132.1 were observed, and these values were also included in the repetitive analyses. The amino acid sequence of VIP and its predicted fragmentation in MS are given as the VIP chromatogram in Figure 4(a) and together with the MS spectrum in Figure 4(b).

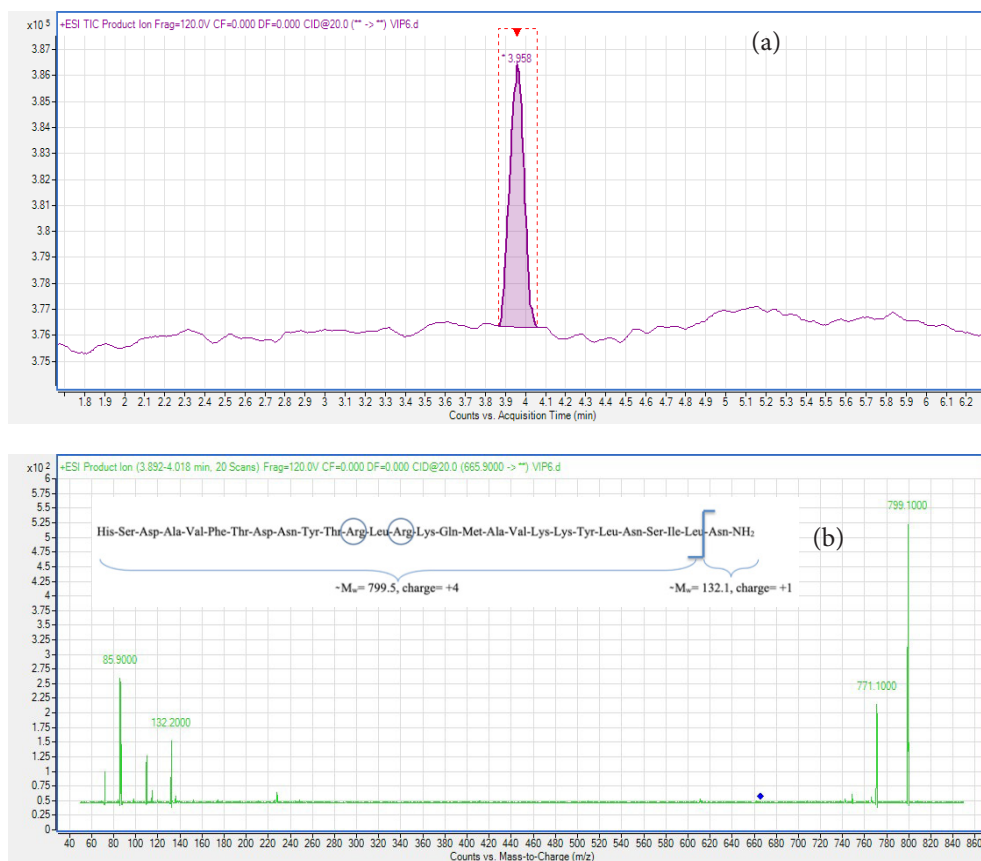


**Figure 4.** (a) 2.50 µg/mL VIP chromatogram (b) Fragments obtained from the analysis of the 665.9 ( $M^{5+}$ )  $m/z$  using the Product Ion mode and the estimated fragmentation of VIP

Since the amino acid arginine (Arg) in its structure is basic (pKa 13.2), it is estimated that 4+ ionization occurs via Arg, and 1+ ionization occurs via asparagine (Asn) in MS. In this case, VIP fragments were obtained by breaking the Leu-Asn bond, as shown in Figure 4(b). When calculations were made based on the observed masses and predicted charges, it was thought that the 5+ charged mass of 665.9 might have disintegrated into 4+ charged masses of 799.4 and 1+ charged mass of 132.1. As a result of the calculations  $((799.4 \times 4) + (132.1 \times 1) = (665.9 \times 5))$ , the main mass of the VIP was reached. Because of the limited scanning range of the mass analyzer, the 1+ charged mass of VIP (directly 3326.8  $m/z$  mass without a multiply charged species since its molecular weight is 3325.8 Da) could not be observed, and deconvolution could not be performed through the software. However, by

verifying the calculations based on this algorithm, the fragments of the 665.9 ( $M^{5+}$ )  $m/z$  mass were identified as 799.4 and 132.1  $m/z$ .

The scanning range was narrowed to focus on the fragmentation energy, specifically around 20 V. The fragmentation voltage scanning was carried out between 15-20 V with the Product Ion mode; when 16 V fragmentation energy was applied, the maximum areas of the peaks belonging to 799.4 and 132.1  $m/z$  masses were obtained. The 770.7  $m/z$  mass, which has a higher mass amount after the 799.4  $m/z$  mass, is encountered in the spectra. In this case, while the 799.4  $m/z$  mass was chosen for quantitative analysis (as quantifier), the 770.7  $m/z$  mass was selected to qualitatively confirm the VIP (as qualifier). In the following stages, analyses with MRM were carried out on these two masses.

The parameter that affects the dwelling time of the mass coming from the first mass analyzer in the collision cell and accelerates or slows down the mass is the cell accelerator voltage (CAV). Since it varies for each analyte, it is recommended to optimize it. If  $CAV \geq 7$ , the analyte will move very quickly inside the cell, causing ion loss; in contrast, if  $CAV \leq 3$ , as it moves very slowly, it may cause problems in MRM

transitions in such a way that it will be subjected to simultaneous fragmentation with the subsequent ion, known as cross-contamination. To examine the effects of this parameter on the fragments of 665.9 m/z, CAV scanning was first performed in Product Ion mode. As a result of these analyses, the change in mass abundance of the fragments was examined and given in (Figure 5).

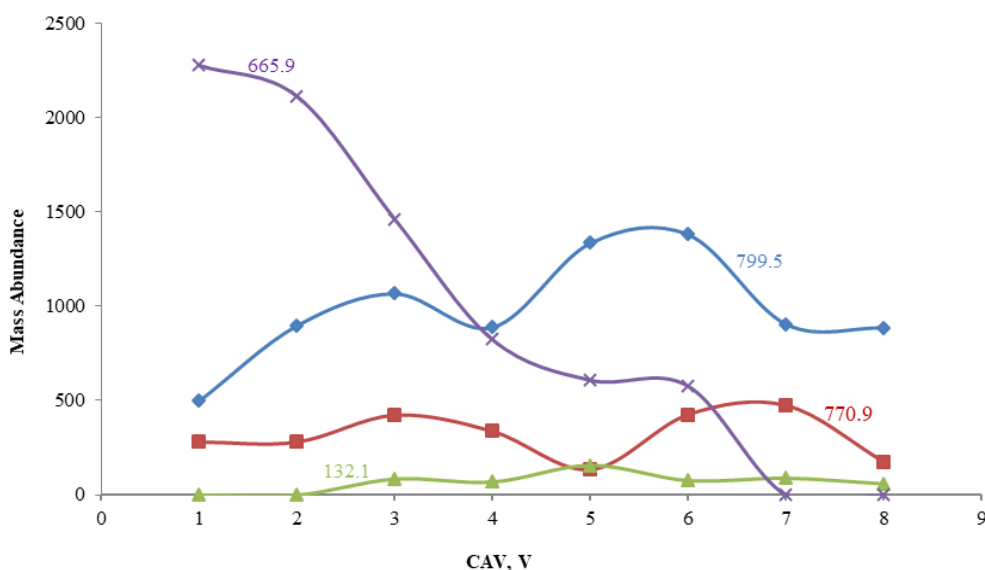


**Figure 5.** CAV- Fluctuation of mass abundance for precursor and fragment ions

As seen in the graph in Figure 5, fragmentation increased with the rise of CAV, and after a certain point, the 665.9 ( $M^{5+}$ ) precursor ion was no longer observed when the fragments became abundant in the environment. However, after approximately 6 V, a decrease in the desired masses was observed. The reason for this may be that the 665.9 ( $M^{5+}$ ) m/z ion moves too quickly in the collision cell, preventing sufficient exposure to fragmentation and resulting in mass loss. Afterward, CAV scanning was performed between 1-8 V with the MRM mode. The relevant

graphs, plotted against applied voltage, peak area, and RSD values from repetitive analyses using 2.50  $\mu\text{g/mL}$  VIP, are shown in Figures 6, 7, and 8.

As seen from the graphs of the peak areas of 799.5 m/z, 770.7 m/z, and the ratio of these two masses to each other, although the peak areas are not very high, the point with the lowest RSD% was observed when CAV was set to 5 V. This indicated that by applying 5 V energy, VIP underwent fragmentation at the optimal rate, resulting in stable fragments.

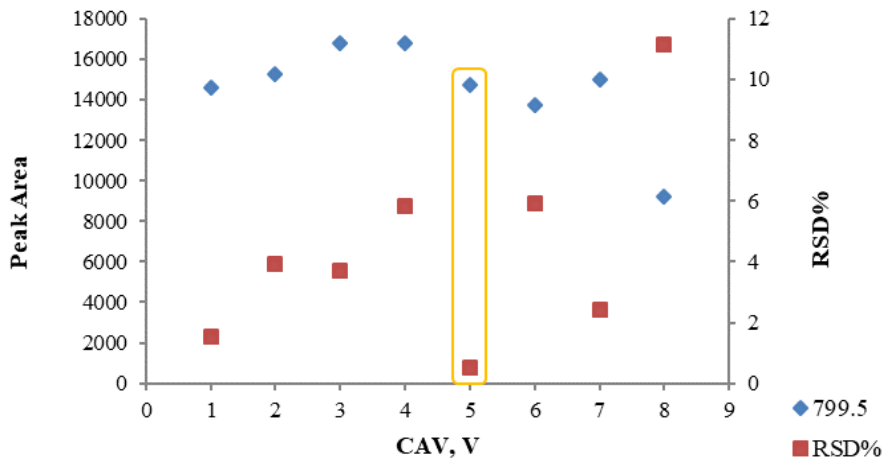


Figure 6. CAV-peak area-RSD graph for 799.5 m/z

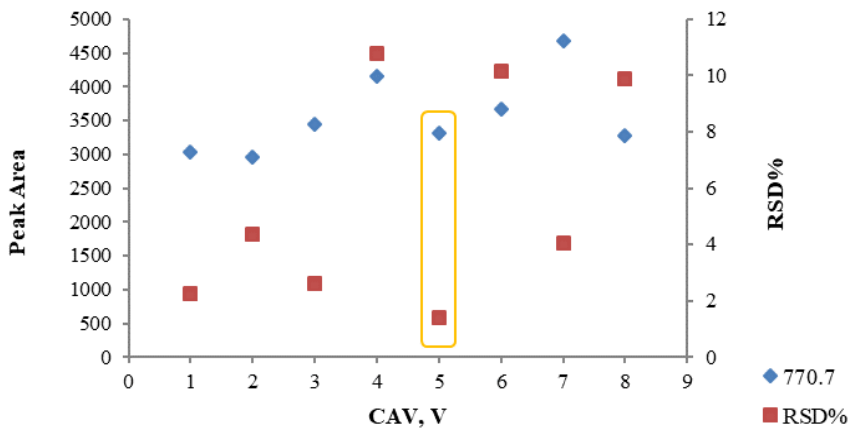


Figure 7. CAV-peak area-RSD graph for 770.7 m/z

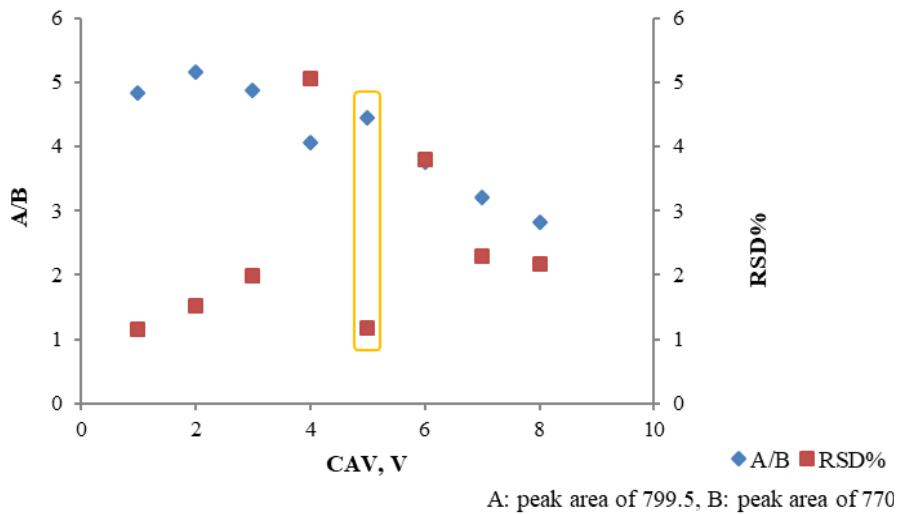


Figure 8. CAV-799.5/770.7 m/z peak area ratio-RSD graph

Before the CAV scanning was performed (when CAV was 7 V), the fragmentation energy had been scanned and found to be 16 V. However, optimizing the CAV to 5 V required slowing down the VIP in the cell and re-scanned the fragmentation energy accordingly. The fragmentation energy was re-scanned between 10-20 V with the Product Ion mode as before. As a result of the analyses carried out in increasingly narrow ranges, the fragments were intensely observed at 18 V. In the analyses performed by applying 18 V fragmentation energy with the MRM mode, larger and more repetitive peak areas were obtained compared to 16 V. Consequently, the analysis continued with the fragmentation energy as 18 V and CAV as 5 V.

After optimizing the MS parameters, the effect of VIP solvent on peak morphology, area and retention time was examined. To observe this difference, 1.25, 2.50, and 5.00 µg/mL VIP solutions were separately

prepared in water:ACN (1:1) and 1% AcAc and analysed using the MRM mode. As a result of repetitive analyses, higher and more reproducible peak areas were obtained in the analyses of VIP dissolved in 1% AcAc.

To increase and facilitate the ionization efficiency of VIP in the MS ionization chamber, aqueous (A line), and ACN (B line) solutions containing 0.1, 0.2, 0.3, and 0.4% formic acid (FA) were prepared and a 2.50 µg/mL VIP was analysed in duplicate for each mobile phase separately. As a consequence of the analyses, the peak area and RSD% of VIP analyzed with mobile phase containing different amounts of FA were examined and are given in (Figures 9 and 10). Analyzes were performed on MRM mode with 799.5 and 770.7 m/z masses. When these data were evaluated, it was shown that 0.2% FA was most suitable for the VIP peak in terms of high peak area and low RSD.

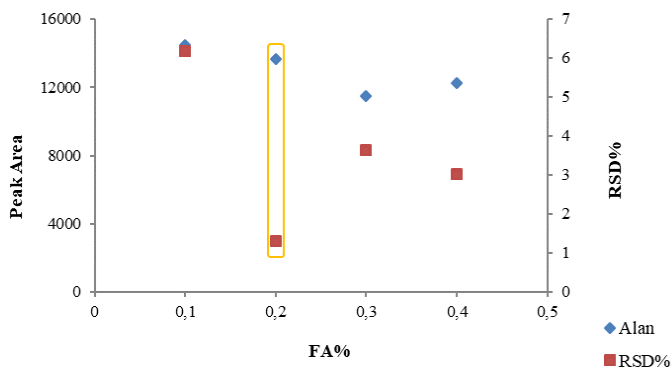


Figure 9. FA%-peak area(n=5)-RSD% graph for 799.5 m/z

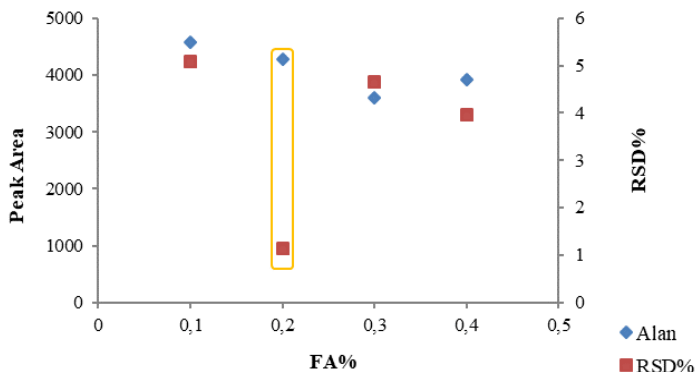


Figure 10. FA%-peak area(n=5)-RSD% graph for 770.7 m/z

To investigate the effect of the pH of the mobile phase containing 0.2% FA (pH 2.45) on the VIP peak, VIP analyses were carried out with two different mobile phases, with the pH of the medium adjusted to 2.94 and 3.15, based on the  $pK_a$  value of FA ( $pK_a$  3.8). The analysis results are given in (Table 4), and

it was seen that the pH change did not have any positive effect on the symmetry of the VIP peak. For this reason, it was decided not to change the pH of the mobile phase, that is, to continue the studies at approximately pH 2.45.

**Table 4.** pH Effect on VIP peak

		mean	SD <sup>a</sup>	RSD% <sup>b</sup>		
pH= 2.45	799.5	$R_t$ (min) <sup>c</sup>	3.95	0.00	0.10	
		A <sup>d</sup>	13766.77	396.27	2.88	
		SNR <sup>e</sup>	10297.42	4248.03	41.25	
		S <sup>f</sup>	1.96	0.07	3.68	
	770.7	$R_t$ (min) <sup>c</sup>	3.94	0.00	0.10	
		A <sup>d</sup>	4174.89	82.95	1.99	
		SNR <sup>e</sup>	9852.20	5368.70	54.49	
		S <sup>f</sup>	2.05	0.14	6.58	
	pH= 2.94	799.5	$R_t$ (min) <sup>c</sup>	4.27	0.06	1.31
			A <sup>d</sup>	1029.03	120.81	11.74
			SNR <sup>e</sup>	4488.72	2511.34	55.95
			S <sup>f</sup>	2.17	0.24	11.03
770.7		$R_t$ (min) <sup>c</sup>	4.24	0.01	0.15	
		A <sup>d</sup>	327.94	42.88	13.08	
		SNR <sup>e</sup>	1412.90	1058.35	74.91	
		S <sup>f</sup>	2.30	0.26	11.15	
pH= 3.15		799.5	$R_t$ (min) <sup>c</sup>	4.25	0.01	0.14
			A <sup>d</sup>	483.01	17.36	3.59
			SNR <sup>e</sup>	3217.00	1344.08	41.78
			S <sup>f</sup>	1.78	0.14	7.92
	770.7	$R_t$ (min) <sup>c</sup>	4.25	0.01	0.18	
		A <sup>d</sup>	148.17	8.84	5.96	
		SNR <sup>e</sup>	1210.18	318.36	26.31	
		S <sup>f</sup>	1.60	0.13	8.22	

<sup>a</sup> Standard deviation, <sup>b</sup> Relative standard deviation, <sup>c</sup> Retention time, <sup>d</sup> Area, <sup>e</sup> Signal noise ratio, <sup>f</sup> Peak symmetry

To investigate the effect of organic solvent polarity in the mobile phase on the VIP peak, ACN and MeOH phases were separately used near the aqueous phase containing 0.2% FA. The effects of ACN and MeOH in

terms of ionizing VIP in MS were monitored by MRM mode with 799.5 and 770.7 m/z masses. 2.50 µg/mL VIP solution was used in the analyses, and the results are given in tables (Table 5 and Table 6).

**Table 5.** Results for 2.50 µg/mL VIP analyzed with mobile phase containing 0.2% FA-ACN (n=5)

0.2% FA with ACN								
799.5					770.7			
	R <sub>t</sub> (min) <sup>c</sup>	A <sup>d</sup>	SNR <sup>e</sup>	T <sup>f</sup>	R <sub>t</sub> (min) <sup>c</sup>	A <sup>d</sup>	SNR <sup>e</sup>	T <sup>f</sup>
Mean	3.99	13667.37	11818.22	2.78	3.98	4277.70	4610.32	2.79
SD <sup>a</sup>	0.00	179.99	5800.85	0.17	0.00	49.09	2633.69	0.11
RSD% <sup>b</sup>	0.00	1.32	49.08	6.23	0.11	1.15	57.13	4.06

<sup>a</sup> Standard deviation, <sup>b</sup> Relative standard deviation, <sup>c</sup> Retention time, <sup>d</sup> Area, <sup>e</sup> Signal Noise Ratio, <sup>f</sup> Tailing factor

**Table 6.** Results for 2.50 µg/mL VIP analyzed with mobile phase containing 0.2% FA-MeOH (n=5)

0.2% FA with MeOH								
799.5					770.7			
	R <sub>t</sub> (min) <sup>c</sup>	A <sup>d</sup>	SNR <sup>e</sup>	T <sup>f</sup>	R <sub>t</sub> (min) <sup>c</sup>	A <sup>d</sup>	SNR <sup>e</sup>	T <sup>f</sup>
mean	7.45	7414.41	3099.88	3.83	7.44	2270.60	1401.50	3.91
SD <sup>a</sup>	0.02	174.30	1668.05	0.22	0.02	81.73	725.10	0.33
RSD% <sup>b</sup>	0.29	2.35	53.81	5.70	0.33	3.60	51.74	8.48

<sup>a</sup> Standard deviation, <sup>b</sup> Relative standard deviation, <sup>c</sup> Retention time, <sup>d</sup> Area, <sup>e</sup> Signal Noise Ratio, <sup>f</sup> Tailing factor

It can be seen from Tables 5, and 6 that the VIP peak was retained more by the MeOH mobile phase, the peak symmetry was disrupted, the tailing factor increased, and its area decreased. For this reason, it was decided to continue with the mobile phase with ACN.

At the end of the mobile phase optimization, the best VIP peak was obtained under conditions where 0.2% FA-water and 0.2% FA-ACN were used.

Therefore, studies were continued with 0.2% FA-water and 0.2% FA-ACN mobile phase.

After optimizing the mobile phase, the flow rate, which is another chromatographic parameter, was checked. VIP was analyzed at different flow rates with 799.5 and 770.7 m/z masses by MRM using 0.2% FA-water and 0.2% FA-ACN mobile phase and 2.50 µg/mL VIP solution. Data obtained at flow rates of 0.15-0.35 mL/min are given in (Tables 7 and 8).

**Table 7.** Effect of flow rate on 799.5 m/z fragment ion peak (n=3)

		799.5							
Flow rate (mL/min)		R <sub>t</sub> (min) <sup>c</sup>	A <sup>d</sup>	SNR <sup>e</sup>	S <sup>f</sup>	T <sup>g</sup>	W <sup>h</sup>	k' <sup>i</sup>	N <sup>j</sup>
0.35	mean	3.16	3798.17	3336.30	0.38	2.20	0.48	1.30	7026.67
	SD <sup>a</sup>	0.01	22.49	1022.84	0.02	0.10	0.01	0.00	281.79
	RSD% <sup>b</sup>	0.21	0.59	30.66	4.06	4.55	2.39	0.00	4.01
0.30	mean	3.34	4424.45	2930.60	0.40	2.10	0.48	1.40	7514.67
	SD <sup>a</sup>	0.00	38.86	418.22	0.02	0.10	0.00	0.00	206.73
	RSD% <sup>b</sup>	0.10	0.88	14.27	4.33	4.76	0.85	0.00	2.75
0.25	mean	3.60	5083.50	3687.20	0.38	2.07	0.53	1.60	7286.67
	SD <sup>a</sup>	0.01	164.05	515.40	0.03	0.06	0.01	0.00	360.22
	RSD% <sup>b</sup>	0.18	3.23	13.98	7.53	2.79	1.95	0.00	4.94
0.20	mean	3.98	6218.69	5945.00	0.42	2.03	0.56	1.80	7247.67
	SD <sup>a</sup>	0.00	90.64	3024.66	0.01	0.06	0.01	0.00	130.94
	RSD% <sup>b</sup>	0.10	1.46	50.88	1.39	2.84	1.15	0.00	1.81
0.15	mean	4.61	7934.30	20447.83	0.43	1.93	0.65	2.30	6928.67
	SD <sup>a</sup>	0.00	112.72	18867.81	0.02	0.06	0.03	0.00	151.14
	RSD% <sup>b</sup>	0.09	1.42	92.27	3.53	2.99	4.37	0.00	2.18

<sup>a</sup> Standard Deviation, <sup>b</sup> Relative standard deviation, <sup>c</sup> Retention time, <sup>d</sup> Area, <sup>e</sup> Signal noise ratio, <sup>f</sup> Symmetry, <sup>g</sup> Tailing factor, <sup>h</sup> Peak width, <sup>i</sup> Capacity factor, <sup>j</sup> Theoretical plate number



**Table 8.** Effect of flow rate on 770.7 m/z fragment ion peak (n=3)

		770.7							
Flow rate (mL/min)		R <sub>t</sub> (min) <sup>c</sup>	A <sup>d</sup>	SNR <sup>e</sup>	S <sup>f</sup>	T <sup>g</sup>	W <sup>h</sup>	k <sup>i</sup>	N <sup>j</sup>
0.35	mean	3.15	1171.67	5580.83	0.37	2.27	0.46	1.27	6827.33
	SD <sup>a</sup>	0.01	31.15	2597.53	0.01	0.15	0.01	0.06	168.74
	RSD% <sup>b</sup>	0.32	2.66	46.54	3.09	6.74	1.77	4.56	2.47
0.3	mean	3.34	1214.21	7277.03	0.40	2.03	0.46	1.40	7355.00
	SD <sup>a</sup>	0.00	26.72	2594.51	0.03	0.06	0.03	0.00	824.29
	RSD% <sup>b</sup>	0.00	2.20	35.65	6.61	2.84	6.99	0.00	11.21
0.25	mean	3.60	1377.41	3031.30	0.41	2.03	0.49	1.60	7616.67
	SD <sup>a</sup>	0.01	7.96	1677.14	0.02	0.06	0.02	0.00	213.88
	RSD% <sup>b</sup>	0.18	0.58	55.33	5.68	2.84	3.53	0.00	2.81
0.2	mean	3.98	1753.57	2795.93	0.43	1.97	0.53	1.80	8170.00
	SD <sup>a</sup>	0.00	49.06	1516.71	0.01	0.06	0.02	0.00	534.87
	RSD% <sup>b</sup>	0.10	2.80	54.25	2.66	2.94	3.21	0.00	6.55
0.15	mean	4.61	2268.58	5898.47	0.43	2.03	0.67	2.30	6090.00
	SD <sup>a</sup>	0.01	26.96	158.50	0.05	0.15	0.03	0.00	937.33
	RSD% <sup>b</sup>	0.14	1.19	2.69	10.83	7.51	4.20	0.00	15.39

<sup>a</sup> Standard Deviation, <sup>b</sup> Relative standard deviation, <sup>c</sup> Retention time, <sup>d</sup> Area, <sup>e</sup> Signal noise ratio, <sup>f</sup> Symmetry, <sup>g</sup> Tailing factor, <sup>h</sup> Peak width, <sup>i</sup> Capacity factor, <sup>j</sup> Theoretical plate number,

According to the data in (Tables 7 and 8), 799.5 m/z (quantifier) and 770.7 m/z (qualifier) peaks were evaluated according to system suitability parameters. Considering parameters such as peak area, SNR, symmetry, and plate numbers, the optimum flow rate was determined as 0.2 mL/min.

**Adsorption Inhibiting Studies for VIP**

Peptides can adhere to glass or polypropylene surfaces due to their chemical properties under the environmental conditions in which they are brought into solution. While standard solutions are being prepared, they can be adsorbed on experimental materials such as tubes, pipette tips, and vials. Taking this situation into consideration, the studies were continued by examining the parameters that prevent adsorption.

Albumin (bovine serum albumin, BSA) helps to prevent adsorption by covering the surfaces in contact with the peptide and preventing the interaction. BSA solution (1%) was prepared for the coating process. Materials such as pipette tips, tubes, and vials used in

experimental studies were shaken with this albumin solution and dried. Then, standard peptide solutions and working solutions were all prepared using these coated materials. Additionally, BSA was added to the stock peptide solution. VIP stock (0.25 mg/mL) was mixed with 1% BSA solution in a 1:1 ratio and kept in an ultrasonic bath for 1 hour. Working solutions were prepared using this mixture.

At the same time, the effect of the solvent on adsorption was examined. To determine whether it has an inhibitory/reducing effect on adsorption, three different dilutions were prepared: 1% AcAc, 1% AcAc-50% ACN mixture, and 5% AcAc-50% ACN mixture. Three different sets of VIP working solutions (250 and 500 ng/mL) were prepared with these solutions and analyzed respectively by SCAN-SIM-MRM modes. To 500 ng/mL VIP, the peaks belonging to 665.9 m/z mass were evaluated, and the analysis results are presented in table (Table 9). There was no significant difference in the peaks between dilution solutions, and tailing occurred in the VIP peak with all three dilution

solutions. While there was no difference between the retention times and areas of the peaks, the evaluation was made according to SNR. While increasing acidity did not show a significant difference for adsorption, the presence of organic solvent in the environment increased the non-polarity, thus reducing the solubility of polar VIP, preventing its ionization, and stopping it from adhering to the surface, which may be ionic even though it is covered with albumin.

**Table 9.** Comparison of peaks for 500 ng/mL VIP (665.9 m/z) with different dilution solutions (SIM mode)

VIP	R <sub>t</sub> (min) <sup>a</sup>	A <sup>b</sup>	SNR <sup>c</sup>
VIP with %1 AcAc	4.038	160799.98	8863.4
VIP with %1AcAc-%50 ACN	4.015	156932.27	11948.9
VIP with %5AcAc-%50 ACN	4.008	154503.54	11701.6

<sup>a</sup> Retention time, <sup>b</sup> Area, <sup>c</sup> Signal Noise Ratio

The LOD and LOQ values of the developed LC-MS/MS method were calculated using the SNR as 0.14 and 0.42 ng/mL, respectively.

The stability of the VIP standard solution under different storage conditions was also examined during these studies. 500 ng/mL VIP solutions were prepared with the three different dilution solutions above, using VIP solutions in albumin-free and uncoated vials kept at -80°C for 16 months and -20°C for 2 months. These solutions were analysed on SIM mode and comparisons were made based on peaks with 665.9 and 832 m/z masses. While no significant difference was observed between the peaks obtained from different dilution solutions using VIP stored at -80°C for 16 months, it was observed that the peak areas increased as the amount of acid and organic solvent raised in VIP solutions stored at -20°C for 2 months. This indicated that the adsorption at -20°C was greater than at -80°C, and the stability of the peptide was greater at lower temperatures.

## DISCUSSION

This study aimed to develop an analytical method for the characterization of VIP using the sensitive and selective LC-MS/MS technique, which will pave the way for the analysis of VIP in biological tissues and fluids.

In LC-MS analyses for VIP, chromatographic and MS parameters were examined. Chromatographically, the mobile phase content was comparatively examined in terms of the amount and type of organic solvent and the amount of acid that influences the ionization of the peptide. In addition, the flow rate was also optimized as it would affect the ionization and ion intensity of the peptide in MS. Chromatographically, the best VIP peak was obtained with a mobile phase containing 0.2% FA-water and 0.2% FA-ACN at a flow rate of 0.2 mL/min. Since it is known that VIP ionizes positively in an acidic environment due to its pI value being greater than 11, MS analyses were carried out in positive mode. Together with the main ion of VIP, the fragmentation voltage and cell accelerator voltage were also optimized, and the multiply charged species obtained due to the fragmentation of the peptide could be observed. When mass 665.9, the 5+ charged ion of VIP, was fragmented by the MRM mode, fragment masses of 799.5 m/z (quantifier) and 770.7 m/z (qualifier) were successfully characterized. The method has become highly selective in the analyses performed using SCAN, SIM, and MRM modes.

Throughout the analysis of VIP, issues such as a decrease in peak areas and the inability to observe VIP masses emerged, which were attributed to peptide adsorption onto surfaces and the instability of VIP. To prevent VIP adsorption to the materials used in experimental studies, they were coated with a 1% BSA solution, which was also added to the stock and working solutions. Furthermore, dilution solutions containing different ratios of acid and organic solvents were prepared for VIP, and their adsorption inhibition powers were compared.

The intense positive charge of VIP, due to its basic Lys and Arg amino acids, causes it to strongly adhere to negatively charged surfaces with which it interacts. However, thanks to a highly sensitive and selective method such as LC-MS/MS and a mass analyzer known as Triple quadrupole, multiply charged masses and fragments for VIP could be observed successfully. However, because of adsorption, the ion intensity of the masses remained very low.

Given the low peptide concentrations in biological samples (such as brain tissue and fluid), different studies can be conducted considering adsorption for VIP analysis. The foundation for methods to be developed was laid in this study. Among the studies reviewed, excluding the CE-LIF method, the LOD and LOQ values of the studies conducted using the LC-MS method, as shown in (Table 1), are approximately 1 ng/mL. The LOD and LOQ values (0.14 and 0.42 ng/mL) of the developed LC-MS/MS method are lower than those reported in these studies. This highlights another contribution of our study to the scientific literature.

It has been demonstrated that the chosen LC-MS/MS method is a unique option for VIP analysis, as it can reach very low levels and perform quantification in biological samples with high accuracy, with an adsorption inhibitor method that does not suppress peptide ions.

#### ACKNOWLEDGMENT

The Anadolu University Scientific Research Projects Commission (Eskisehir, project grant 1601S036) is acknowledged for financial support.

#### AUTHOR CONTRIBUTION STATEMENT

Concept (SK, ES), Design (SK, ES), Supervision (ES), Resources (SK, ES), Materials (SK, ES), Data Collection and/or Processing (SK), Analysis and/or Interpretation (SK, ES), Literature Search (SK), Writing (SK), Critical Reviews (SK, ES)

#### CONFLICT OF INTEREST

The authors declare that there is no conflict of interest.

#### REFERENCES

- Abaye, D. A., Pullen, F. S., & Nielsen, B. V. (2011). Practical considerations in analyzing neuropeptides, calcitonin gene-related peptide and vasoactive intestinal peptide, by nano-electrospray ionization and quadrupole time-of-flight mass spectrometry: monitoring multiple protonation. *Rapid Communications Mass Spectrometry*, 25(8), 1107-1116. <https://doi.org/10.1002/rcm.4961>.
- Baggerman, G., Verleyen, P., Clynen, E., Huybrechts, J., De Loof, A., & Schoofs, L. (2004). Peptidomics. *Journal of Chromatography B*, 803(1), 3-16. <https://10.1016/j.jchromb.2003.07.019>.
- Baker, D. L. (1995). *Capillary Electrophoresis*. New York: John Wiley & Sons, Inc.
- Burbach, J. P. (2011). What are neuropeptides? *Methods in Molecular Biology*, 789, 1-36. [https://10.1007/978-1-61779-310-3\\_1](https://10.1007/978-1-61779-310-3_1).
- Cui, X., Cao, D., Qu, C., Zhang, X., & Zheng, A. (2013). A study of the chemical and biological stability of vasoactive intestinal peptide. *Drug Development and Industrial Pharmacy*, 39(12), 1907-1910. <https://10.3109/03639045.2012.693503>.
- El-Karim, I., Lundy, F. T., Linden, G. J., & Lamey, P. J. (2003). Extraction and radioimmunoassay quantitation of neuropeptide Y (NPY) and vasoactive intestinal polypeptide (VIP) from human dental pulp tissue. *Archives of Oral Biology*, 48(3), 249-254. [https://10.1016/s0003-9969\(02\)00213-3](https://10.1016/s0003-9969(02)00213-3).
- Hansen, J. M., Fahrenkrug, J., Petersen, J., Wienecke, T., Olsen, K. S., & Ashina, M. (2013). Vasoactive intestinal peptide (VIP) and pituitary adenylate cyclase-activating polypeptide (PACAP) in the circulation after sumatriptan. *Scandinavian Journal of Pain*, 4(4), 211-216. <https://doi.org/10.1016/j.sjpain.2013.04.002>

- Korkmaz, O. T., Arkan, S., Oncü-Kaya, E. M., Ates, N., & Tuncel, N. (2021). Vasoactive intestinal peptide (VIP) conducts the neuronal activity during absence seizures: GABA seems to be the main mediator of VIP. *Neuroscience Letters*, 765, 136268. <https://doi.org/10.1016/j.neulet.2021.136268>
- Lock, S., Thorn, J., & Fox, S. (2015). *CESI-MS A new way to Analyze for PACAP and VIP*. Retrieved from [https://www.researchgate.net/profile/James-Thorn/publication/284020013\\_CESI-MS\\_A\\_new\\_way\\_to\\_Analyze\\_Vasoactive\\_intestinal\\_peptide\\_VIP\\_and\\_Pituitary\\_adenylate\\_cyclase-activating\\_polypeptide\\_PACAP/links/564af63f08ae295f64507ff6/CESI-MS-A-new-way-to-Analyze-Vasoactive-intestinal-peptide-VIP-and-Pituitary-adenylate-cyclase-activating-polypeptide-PACAP.pdf](https://www.researchgate.net/profile/James-Thorn/publication/284020013_CESI-MS_A_new_way_to_Analyze_Vasoactive_intestinal_peptide_VIP_and_Pituitary_adenylate_cyclase-activating_polypeptide_PACAP/links/564af63f08ae295f64507ff6/CESI-MS-A-new-way-to-Analyze-Vasoactive-intestinal-peptide-VIP-and-Pituitary-adenylate-cyclase-activating-polypeptide-PACAP.pdf)
- Phillips, T. M. (1998). Determination of in situ tissue neuropeptides by capillary immunoelectrophoresis. *Analytica Chimica Acta*, 372(1-2), 209-218. [https://doi.org/10.1016/S0003-2670\(98\)00342-0](https://doi.org/10.1016/S0003-2670(98)00342-0).
- Rehfeld, J. F. (1998). The new biology of gastrointestinal hormones. *Physiological Reviews*, 78(4), 1087-1088. <https://doi.org/10.1152/physrev.1998.78.4.1087>.
- Sewald, N., & Jakubke, H. D. (2002). Biologically Active Peptides. *Peptides: Chemistry and Biology*. (pp. 90, 99, 107, 109). Weinheim: Wiley-VCH Verlag GmbH & Co. KGaA.
- Soloviev, M., & Finch, P. (2005). Peptidomics, current status. *Journal of Chromatography B*, 815(1-2), 11-24. <https://doi.org/10.1016/j.jchromb.2004.11.011>.
- Soucheleau, J., & Denoroy, L. (1992). Determination of vasoactive intestinal peptide in rat brain by high-performance capillary electrophoresis. *Journal of Chromatography A*, 608(1-2), 181-188. [https://doi.org/10.1016/0021-9673\(92\)87122-O](https://doi.org/10.1016/0021-9673(92)87122-O).
- Trauger, S. A., Webb, W., & Siuzdak, G. (2002). Peptide and Protein Analysis in Mass Spectrometry. *Journal of Spectroscopy*, 16, 15-28. <https://doi.org/10.1155/2002/320152>.
- Tunçel, N., & Korkmaz, O. T. (2010). *Vazoaktif İntestinal Polipeptid'in (VIP) Dünü, Bugünü, Yarını*. Retrieved from [http://www.tfbd.org.tr/yuklemeler/kongre\\_36.pdf](http://www.tfbd.org.tr/yuklemeler/kongre_36.pdf)
- Wasilewska-Dzubinska, E., Borowiec, M., Chmielowska, M., Wolinska-Witort, E., & Baranowska, B. (2002). Alfa 1 Adrenergic Potantiation of Progesterone Accumulation Stimulated by Vasoactive Intestinal Peptide (VIP) and Pituitary Adenylate Cyclase-Activating Polypeptide (PACAP) in Cultured Rat Granulosa Cell. *Neuroendocrinology*, 23, 141-148.
- Watanabe, J. (2016). Subchapter 18E-Vasoactive Intestinal Peptide. Peptides and Proteins in Vertebrates. In Y. Takei, H. Ando and K. Tsutsui (Eds.), *Handbook of Hormones, Comparative Endocrinology for Basic and Clinical Research* (pp. 150-152). Elsevier Inc.
- Yin, P., Hou, X., Romanova, E. V., & Sweedler, J. V. (2011). Neuropeptidomics: Mass Spectrometry-Based Qualitative and Quantitative Analysis. *Methods in Molecular Biology*, 89, 223-236. [https://doi.org/10.1007/978-1-61779-310-3\\_14](https://doi.org/10.1007/978-1-61779-310-3_14).

# Herbal Product Use and Drug-Herbal Product Interactions in Patients with Chronic Diseases-A Cross-Sectional Study

Eyup Can POLAT<sup>°</sup>, Sefa GOZCU<sup>\*\*</sup>

*Herbal Product Use and Drug-Herbal Product Interactions in Patients with Chronic Diseases-A Cross-Sectional Study*

## SUMMARY

Herbal products are frequently used to prevent and treat diseases in the community. Although they are considered safe because they are natural, the simultaneous use of herbal products with drugs may cause drug-related problems and negatively affect therapeutic outcomes. Our study aimed to determine the herbal product use rates of patients with chronic diseases and the interactions of the herbal products used with drugs. This study is a cross-sectional survey conducted in a community pharmacy. The study included adult patients with chronic diseases who used regular drugs and had a history of using herbal products within the previous three months. The surveys included questions about patients' demographics, diseases, drugs, and herbal products. Drug-herbal product interactions were examined through databases, monographs, and books. 93 of 148 patients were using herbal products. Most of the patients were diagnosed with hypertension and diabetes. The use of herbal products was found to be positively correlated with undergraduate educational status, asthma, COPD, diabetes, and anxiety ( $p < 0.05$ ). The herbal product that was most used and had the most drug interactions was garlic. The majority of drug-herbal product interactions were determined by the "drugs.com" interaction checking tool and the WHO monographs. Pharmacists should provide consultancy services to their patients on the use of herbal products. It is advisable for community pharmacists to keep their knowledge on drug-herbal product interactions updated. They can benefit from training programs on drug-herbal product interactions organized by clinical pharmacists. Thus, drug-herbal product interactions that may occur in patients can be reduced.

**Key Words:** Drug-herbal product interactions, clinical pharmacy, chronic disease, community pharmacy

*Kronik Hastalığı Olan Hastalarda Bitkisel Ürün Kullanımı ve İlaç-Bitkisel Ürün Etkileşimleri-Kesitsel Bir Anket Çalışması*

## ÖZ

Bitkisel ürünler toplumda hastalıkları önlemek ve tedavi etmek için sıklıkla kullanılmaktadır. Doğal oldukları için güvenli olarak kabul edilen bitkisel ürünlerin ilaçlarla eş zamanlı kullanımı ilaç kaynaklı sorunlara neden olabilmekte ve tedavi sonuçlarını olumsuz etkileyebilmektedir. Çalışmamızda, kronik hastalığı olan hastalarda bitkisel ürün kullanım oranları ve kullanılan bitkisel ürünlerin ilaçlarla etkileşimlerinin belirlenmesi amaçlanmıştır. Bu çalışma bir toplum eczanesinde kesitsel anket çalışması olarak yürütülmüştür. Çalışmaya kronik hastalığı olan ve son 3 ay içerisinde bitkisel ürün kullanmış olan hastalar dahil edilmiştir. Uygulanan anketlerde hastaların demografik özellikleri, mevcut hastalıkları, kullandıkları ilaçlar ve bitkisel ürünlerle ilgili sorular yer almaktaydı. İlaç-bitkisel ürün etkileşimleri ilaç veri tabanları, monograflar ve basılı kitaplar aracılığıyla incelenmiştir. Çalışmaya dahil edilen 148 hastadan 93'ünün bitkisel ürün kullandığı belirlenmiştir. Çalışmadaki hastaların çoğunun hipertansiyon ve diyabet tanılarının olduğu tespit edilmiştir. Bitkisel ürün kullanımının lisans eğitim durumu, astım, KOAH, diyabet ve anksiyete ile pozitif korelasyon gösterdiği bulunmuştur ( $p < 0,05$ ). En çok kullanılan ve en çok ilaç etkileşimi gösteren bitkisel ürünün sarımsak olduğu belirlenmiştir. İlaç-bitkisel ürün etkileşimlerinin çoğu "drugs.com" etkileşim kontrol aracı ve WHO monografi aracılığıyla tespit edilmiştir. Eczacılar, hastalarına bitkisel ürünlerin kullanımı konusunda danışmanlık hizmeti vermelidir. Toplum eczacılarının ilaç-bitkisel ürün etkileşimleri konusundaki bilgilerini güncel tutmaları tavsiye edilir. Toplum eczacıları, klinik eczacılar tarafından düzenlenen ilaç-bitkisel ürün etkileşimlerine yönelik eğitim programlarından faydalanabilirler. Böylece hastalarda oluşabilecek ilaç-bitkisel ürün etkileşimleri azaltılabilir.

**Anahtar Kelimeler:** İlaç-bitkisel ürün etkileşimi, klinik eczacılık, kronik hastalık, toplum eczanesi

Received: 10.10.2024

Revised: 05.02.2025

Accepted: 11.02.2025

<sup>°</sup> ORCID: 0000-0002-9455-5423, Department of Clinical Pharmacy, Faculty of Pharmacy, Erzincan Binali Yıldırım University, 24002, Erzincan, Turkey

<sup>\*\*</sup> ORCID: 0000-0002-0735-4229, Department of Pharmacognosy, Faculty of Pharmacy, Erzincan Binali Yıldırım University, 24002, Erzincan, Turkey

## INTRODUCTION

Herbal products are one of the primary complementary and alternative treatment methods used in the treatment of diseases in the population. Herbal products are frequently preferred for the treatment of acute and chronic conditions in the population, as well as to prevent diseases and support existing drug treatments (Tulunay, Aypak, Yikilkan, & Gorpelioglu, 2015). The rate of herbal product use in the community reaches up to 80% (Ekor, 2014). Considered safe due to their natural origin, herbal products may alter the effectiveness of drugs in patients undergoing drug therapy and, when misused, may impact the prognosis of pre-existing disorders (Robinson & Zhang, 2011).

Community pharmacies serve as primary healthcare institutions offering counseling services for patients regarding their diseases and drug treatments (Abudalo et al., 2022). Due to the constraints of healthcare settings and physician workloads, patients are often unable to provide sufficient information to their physicians about their nutritional habits, use of herbal products, and drugs they use (Goldstein et al., 2007; Williams, Rondeau, Xiao, & Francescutti, 2007). This situation causes the interactions of non-pharmaceutical products used by patients with prescribed drugs to be ignored.

Clinical pharmacy is defined as; "... a health science discipline in which pharmacists provide patient care that optimizes medication therapy and promotes health, wellness, and disease prevention" (ACCP, 2008). The consultancy services provided by clinical pharmacists to healthcare personnel on issues such as drug selection, dosage adjustment, drug interactions, side effects, toxicity, and therapeutic drug monitoring contribute to improving treatment outcomes (ACCP, 2023). The services provided by clinical pharmacists contribute to the prevention and solution of medication-related problems (Abunahlah, Elawaisi, Velibeyoglu, & Sancar, 2018; Polat, Koc, & Demirkan, 2022). Additionally, In addition to consultancy services, clin-

ical pharmacists contribute to increasing the knowledge level of pharmacists through professional training (Hersberger & Messerli, 2016). In-service training provided by clinical pharmacists to community pharmacists will help reduce the incidence of drug-related problems. Drug-related problems are a common issue in treatment that can negatively affect patients' response to therapy, increase morbidity and mortality rates, and escalate treatment costs (Abunahlah et al., 2018). Drug-herbal product interactions have a special place among the factors that cause drug-related problems in patients. These interactions may either reduce drug efficacy or enhance drug toxicity and adverse effects. Drug-herbal product interactions are neglected in routine treatment and have a negative impact on therapeutic outcomes. Several factors contribute to these interactions, such as patients' failure to inform physicians, pharmacists, and other healthcare providers about the herbal products they take and healthcare providers' lack of sufficient knowledge about herbal product-drug interactions (Ahmed et al., 2021; Parvez & Rishi, 2019). Investigating the effect of herbal products that patients use in conjunction with drug treatments will help to improve patient safety and treatment outcomes. Therefore, our study aimed to determine the prevalence of herbal product use in patients with chronic diseases and the potential interactions between the patients' drugs and the herbal products they use.

## MATERIAL AND METHOD

The study was designed as a cross-sectional descriptive survey conducted in a community pharmacy in Erzincan, Turkey, between April and September 2023. The pharmacy is located near the family health center. The study included adult patients with chronic diseases who consented to participate, used regular drugs to treat these conditions and had a history of using herbal products within the previous three months. Patients who did not give consent to participate in the study and who did not have chronic diseases were excluded from the study. The research team comprised one faculty member from the Department of Clinical

Pharmacy and one faculty member from the Department of Pharmacognosy. The structured survey questions were developed by the researchers and reviewed by three field experts to ensure content and face validity. After incorporating the necessary revisions, the final version of the survey was created. The survey included 5 open-ended and 10 closed-ended questions. The research team administered it to patients face-to-face. In addition to the demographic data of the patients, the surveys included questions about patients' existing diseases, the use of medicines and herbal products. Medscape®, drugs.com, and UpToDate® databases were used to determine the interactions between drugs and herbal products. In addition, Physicians' Desk Reference (PDR), World Health Organization (WHO) and Turkish Pharmacognosy and Phytotherapy Association (FFD) monographs, Novel Drug Target With Traditional Herbal Medicines and Kanıta Dayalı Fitoterapi-I books were used to detect drug-herbal product interactions. Drug-herbal product interactions were investigated by the clinical pharmacist in the research team. This study was approved by the Erzincan Binali Yildirim University Health and Sports Sciences Ethics Committee with the decision dated 31.03.2023 and numbered 03/06.

### **Statistical analysis**

The sample size targeted in the study, based on the studies in the literature, a total of 103 patients were determined with a power level of 90% and an error level of 5%, with the prediction that the herbal product use prevalence of the patients planned to be included in the study would be 40% (Tulunay et al., 2015; Turkmenoglu, Kutsal, Dolgun, Diker, & Baydar, 2016). The sample size was calculated with G-power v3.1.9.7 software. Student's t-Test was used in the analysis of continuous parametric variables where normal distribution conditions were met, and Mann Whitney U Test, which is the non-parametric counterpart of this test, was used in cases where normal distribution conditions were not met. Analysis of categorical data was done with the Chi-Square Test. The relationship between patients' herbal product use

and gender, educational status, and comorbid diseases was examined with binary logistic regression analysis. Statistical analyses were performed with IBM SPSS v22.0 software. Statistical significance was accepted as  $p < 0.05$ .

### **RESULTS AND DISCUSSION**

Drug-related problems are defined as an event or situation that prevents or has the potential to prevent drug therapy from achieving the desired therapeutic results. Drug-related problems result in increased morbidity and mortality rates for patients, as well as increased treatment costs. Clinical pharmacists play a key role in the prevention, identification, and management of drug-related problems. One of the factors that cause drug-related problems to be observed in patients is drug-herbal product interactions (Abunahlah et al., 2018; Polat et al., 2022). The perception that herbal products are safe because they are natural contributes to their widespread use in society. However, the unconscious use of herbal products poses potential risks to patient health. In particular, the simultaneous use of herbal products and prescription drugs can alter the effects of the medication and lead to adverse drug reactions. Studies indicate that the usage rate of herbal products worldwide reaches up to 80% (Ekor, 2014). The high rate of herbal product use among the public also increases the likelihood of drug-related problems being observed.

The pharmacy, where our study was carried out, is mostly visited by patients with chronic diseases (such as hypertension, diabetes, and coronary artery disease). The pharmacy staff consists of one pharmacist and one pharmacy technician. On average, the pharmacy fills 150 prescriptions per day.

A total of 148 patients were included in the study. Demographic data of patients are presented in Table 1. The percentage of patients using herbal products was 62.84% (n=93). Previous studies have reported herbal product usage rates of 29% and 56.6% in patients with chronic conditions (Tulunay et al., 2015; Welz, Emberger-Klein, & Menrad, 2019). In another study, the

herbal product use rate of patients was reported to be 62.9%, similar to our results (Souza-Peres et al., 2023).

In our study, the mean age (mean±SD) of the patients was 56.61±11.470 years, while the mean age of patients using herbal products was 55.59±10.204 years ( $p>0.05$ ). The median (minimum-maximum) number of drugs used by the patients included in our study was 2 (1-7), and for those using herbal products, it was 2 (1-6). The number of male patients was more than the number of female patients ( $n=78$ , 52.70% and  $n=70$ , 47.30%, respectively) ( $p>0.05$ ). Among the patients using herbal products, 48 (51.61%) were male and 45 (48.39%) were female ( $p>0.05$ ) (Table 1).

The average age of the patients in our study with a history of herbal product use was similar to the previous study (56.4±9.9) (Tulunay et al., 2015). However, some studies have reported higher usage rates of herbal products in female patients, contrary to our results (Al-Windi, 2004; Grymonpre, McKechnie, & Briggs, 2010; Peltzer & Pengpid, 2019; Tezcan & Butur, 2022;

Ünlüyol et al., 2023). Differences in the patient populations and the geographic locations where the studies were conducted likely account for these variations.

The majority of patients using herbal products were elementary school graduates ( $n=30$ , 32.26%). In addition, the educational level of patients using herbal products was statistically different from those not using them ( $p<0.05$ ) (Table 1). Statistical analysis was carried out to determine the impact of education level on the use of herbal products by patients. The use of herbal products and undergraduate patients' educational status were found to be positively correlated and statistically significant (OR: 6.50; 95% CI: 1.39-30.49;  $p=0.018$ ) (Table 2). Previous studies have reported similar findings (Abunahlah et al., 2018; Al-Windi, 2004; Peltzer & Pengpid, 2019; Pradipta et al., 2023; Ünlüyol et al., 2023). In a study on patients with chronic conditions found that herbal product use increased with education level ( $p<0.05$ ) (Pearson et al., 2018). These data show that herbal product use rates increase with higher levels of education.



**Table 1.** Demographic data of patients

	Patients who do not use herbal products (n=55)	Patients who use herbal products (n=93)	Total (n=148)	p
Age (year), (mean±SD) <sup>a</sup>	58.35±13.26	55.59±10.20	56.61±11.47	0.118
Sex, n (%) <sup>b</sup> ;				
Female	25 (45.45)	45 (48.39)	70 (47.30)	0.730
Male	30 (54.55)	48 (51.61)	78 (52.70)	
Rate of cigarette use, n (%) <sup>b</sup>	10 (18.18)	30 (32.26)	40 (27.03)	0.062
Rate of alcohol use, n (%) <sup>b</sup>	4 (7.27)	7 (7.53)	11 (7.43)	1.00
Educational status, n (%) <sup>b</sup> ;				<b>p=0.004</b>
Illiterate	7 (12.73)	5 (5.38)	12 (8.11)	
Literate	12 (21.82)	6 (6.45)	17 (11.49)	
Elementary school	16 (29.09)	30 (32.26)	46 (31.08)	
High school	4 (7.27)	26 (27.96)	30 (20.27)	
Undergraduate	10 (18.18)	20 (21.51)	30 (20.27)	
Postgraduate and Doctorate	6 (10.91)	6 (6.45)	12 (8.11)	
Drug groups, n (%) <sup>c</sup> ;				
Cardiovascular System Drugs	41 (35.04)	99 (52.38)	140 (45.75)	<b>0.048</b>
Antidiabetic Drugs	37 (31.62)	40 (21.16)	77 (25.16)	<b>0.019</b>
Respiratory System Drugs	13 (11.11)	8 (4.23)	21 (6.86)	<b>0.031</b>
Central Nervous System Drugs	12 (10.26)	6 (3.17)	18 (5.88)	<b>0.006</b>
Haematologic Drugs	2 (1.71)	14 (7.41)	14 (7.41)	<b>0.044</b>
Other	12 (10.26)	22 (11.64)	34 (11.11)	>0.05
Diseases, n (%) <sup>b</sup> ;				
Hypertension	21 (21.86)	48 (33.33)	69 (28.75)	0.113
Diabetes	31 (32.29)	35 (24.31)	66 (28.5)	<b>0.027</b>
Benign Prostatic Hyperplasia	4 (4.17)	14 (9.72)	18 (7.5)	0.162
Dyslipidemia	5 (5.21)	12 (8.33)	17 (7.08)	0.482
Psychiatric Disease	8 (8.33)	5 (3.47)	13 (5.42)	0.204
Heart Failure	3 (3.13)	11 (7.64)	14 (5.83)	0.20
Asthma and Chronic Obstructive Lung Disease	7 (7.29)	4 (2.78)	11 (4.58)	0.118
Other	17 (17.71)	15 (10.42)	32 (13.33)	>0.05

<sup>a</sup> Student's T Test, <sup>b</sup> Chi-Squared Test, <sup>c</sup> Mann Whitney U Test

**Table 2.** The relationship between the educational status of patients and the use of herbal products

Education Status	OR	OR (%95 CI)		p
		Min	Max	
Illiterate	-	-	-	<b>0.09</b>
Literate	0.714	0.143	3.579	0.682
Elementary school	0.500	0.112	2.234	0.364
High school	1.875	0.519	6.771	0.337
Undergraduate	6.500	1.386	30.487	<b>0.018</b>
Postgraduate and Doctorate	2.000	0.512	7.813	0.319

The majority of the patients in the study were diagnosed with hypertension and diabetes (n=69 (28.75%) and n=66 (28.50%), respectively). The prevalence of diabetes was statistically significantly higher in patients using herbal products than in patients without a history of using herbal products (p<0.05)

(Table 1). Similar to our results, it has been reported that hypertension and diabetes diagnoses come to the fore among patients with a history of herbal product use (Peltzer & Pengpid, 2019; Tulunay et al., 2015). When the impact of patients' chronic diseases on their herbal product usage preferences was

analyzed, a significant and positive relationship was found between the diagnoses of diabetes (OR: 5.74; 95% CI 2.01-16.37; p=0.001), anxiety (OR: 10.42; 95% CI 1.27-85.61; p=0.029), asthma and Chronic obstructive lung disease (COPD) (OR: 8.27; 95% CI 1.36-50.17; p=0.022) and the rates of herbal product use (Table 3). The number of studies investigating the relationship between patients' use of herbal products and their existing diseases is limited in the literature. In a study, it was determined that there was a positive

and significant relationship between asthma, arthritis, cancer, cardiac diseases, dyslipidemia, hypertension, migraine, and gastrointestinal system diseases and patients' use of herbal products (p<0.05) (Peltzer & Pengpid, 2019). However, in contrast to our results, there was no significant relationship between diabetes, anxiety, and herbal product use in this study (p>0.05). The fact that the studies were conducted in different patient populations explains the variation in the reported results.

**Table 3.** The relationship between the diseases of patients and the use of herbal products

Disease	OR	OR (%95 CI)		P
		Min	Max	
Asthma and Chronic Obstructive Lung Disease	8.265	1.361	50.173	<b>0.022</b>
Depression	0.950	0.112	8.030	0.962
Hypertension	0.973	0.355	2.667	0.958
Diabetes	5.738	2.011	16.371	<b>0.001</b>
Hypothyroidism	1.475	0.099	21.978	0.778
Parkinson's Disease	9347983460.403	0	-	1.000
Heart Failure	0.232	0.042	1.281	0.094
Benign Prostatatic Hyperplasia	0.671	0.168	2.676	0.571
Dyslipidemia	0.688	0.188	2.515	0.572
Epilepsy	9098014877.572	0	-	0.999
Ankylosing spondylitis	0.000	0	-	1.000
Chronic Venous Insufficiency	3172540955.156	0	-	0.999
Pulmonary Embolism	0	0	-	0.999
Anxiety	10.421	1.269	85.606	<b>0.029</b>
Neuropathy	191864126.318	0	-	1.000
Rheumatoid Arthritis	1.069	0.079	14.394	0.960
Familial Mediterranean Fever	0	0	-	1.000
Lupus Erythematosus	9347979125.376	0	-	1.000
Psoriasis	873020163.740	0	-	1.000
Cancer	1585688405.889	0	-	1.000
Kidney Stone	0	0	-	1.000
Peptic Ulcer	2.893	0.218	38.396	0.421
Gastroesophageal Reflux Disease	1.768	0.057	54.688	0.745
Bipolar Disease	6339476654.783	0	-	1.000
Osteoporosis	2.867	0.222	36.957	0.419
Neurogenic Bladder	1100838317.606	0	-	1.000

Cardiovascular drugs were the most commonly used drugs among the patients in our study (n=140, 45.75%). The rates of the use of cardiovascular system, antidiabetic, respiratory system, central nervous system, and hematological system drugs were statistically significantly different between patients with and without a history of herbal product use (p<0.05) (Table 1). It was determined that cardiovascular (n=99, 52.38%) and antidiabetic drugs (n=40, 21.16%) were mostly used in patients with a history of herbal product use. Consistent with our findings, it has been shown previously that cardiovascular system and antidiabetic drugs were mostly used in patients with chronic diseases who used herbal products (Albassam

et al., 2021).

Patients with a history of herbal product use in the past three months most frequently used Garlic, Olive Leaf, Turmeric, and Saw Palmetto (Table 4). It was determined that 76.34% (n = 71) of the patients with a history of using herbal products used these products every day. While different studies have reported varying herbal product usage rates among chronic disease patients, the increased use of Garlic is particularly notable (Grymonpre et al., 2010; Mazrouei et al., 2022; Olisa & Oyelola, 2010; Tulunay et al., 2015; Ünlüyol et al., 2023). These differences likely stem from a combination of traditional influences and variations in study populations.

**Table 4.** Herbal products most used by patients in the last 3 months

Herbal products	n (%)
Garlic	17 (14.05)
Olive Leaf	10 (8.26)
Turmeric	10 (8.26)
Saw palmetto	10 (8.26)
Hawtorn	8 (6.61)
Ginger	6 (4.96)
Green tea	6 (4.96)
Parsley juice	6 (4.96)
Lemon juice	5 (4.13)
Licorice root	4 (3.31)
Nettle seed	4 (3.31)
Sambucus nigra	4 (3.31)
Black cumin oil	4 (3.31)
Cinnamon juice	4 (3.31)
Other	23 (19.01)

When the patients' answers to the survey questions were analyzed, 81 (87.10%) patients stated that they knew the content of the herbal product they used. The majority of patients stated that they thought herbal products would not have harmful effects on health (n=60, 64.52%). Additionally, 74 (79.57%) patients stated that herbal products and drugs had similar success rates in treating diseases (Table 5). In a study, the

majority of patients stated that herbal products were effective in treating diseases. In the same study, more than half of the patients thought that herbal products were harmless (Ünlüyol et al., 2023). In another study, patients stated that herbal products were more effective and safer than drugs (Mazrouei et al., 2022). The belief that herbal products are harmless contributes to their high prevalence of use in populations.

**Table 5.** Patients' answers to survey questions

Questions	n (%)
Do you know the ingredients of the herbal product you use? No Yes	12 (12.90) 81 (87.10)
Have you used herbal products with your drugs? No Yes I don't remember	0 (0) 91 (97.85) 2 (2.15)
Can herbal products be harmful to your health? Yes, it can be harmful. No, I don't think herbal products can be harmful. I have no idea.	22 (23.66) 60 (64.52) 11 (11.83)
How did you make your decision to use herbal products? My physician recommended. My pharmacist recommended. I decided to use it after watching it on TV. I decided to use it after seeing the posts on social media. I decided to use it on the advice of my family/friends/relatives. Other	13 (13.98) 2 (2.15) 11 (11.83) 45 (48.39) 9 (9.68) 13 (13.98)
Do herbal products have the same success as drugs in treating diseases? No Yes I have no idea	5 (5.38) 74 (79.57) 14 (15.05)

It is noteworthy that most of the patients selected the option "I decided to use herbal products after seeing them in social media posts" when asked to find out how the patients decided to use herbal products (n=45, 48.39%) (Table 5). Studies have reported that different factors such as physician/pharmacist recommendations, family members' recommendations, television programs, and social media posts play a role in patients' decisions to use herbal products (Albassam et al., 2021; Mazrouei et al., 2022; Tulunay et al., 2015; Ünlüyol et al., 2023). In our study, social media channels -which are becoming increasingly influential in our daily lives- play an active role in patients' decision to use herbal products.

In the literature, studies investigating the interactions between herbal products and drugs are limited compared to those examining drug-drug interactions. This lack of research increases the likelihood of unexpected treatment outcomes, particularly in patients using herbal products alongside drugs. In our study, potential interactions between herbal products and

patients' drugs were examined using databases and monographs. In our study, the majority of drug-herbal product interactions were identified using the "drugs.com" interaction checker (n=57). Most potential drug-herbal product interactions (n=29) were at the "moderate" level. The monograph in which drug-herbal product interactions were most frequently detected was the WHO monograph (n=34) (Table 6). The herbal product with the most potential drug interactions detected in both drugs.com and WHO monographs was Garlic (n=21 and n=18, respectively). In a study examining drug-herbal product interactions, it was reported that most of the interactions detected were at a moderate level, similar to the results in our study (Albassam et al., 2021). Studies assessing drug-herbal product interactions that used monographs were absent from the literature. In addition, the identified potential drug interactions do not always make sense of clinically. Generally, moderate, major, or contraindicated drug interactions are clinically significant (Rodrigues et al., 2015).

**Table 6.** Drug-herbal products interactions

Interaction Control Source	Number of Interaction (n)
UpToDate (Lexicomp)	32 (total) 29 (monitor therapy) 3 (no action needed)
Medscape	16 1 (serious) 13 (monitor closely) 2 (minor)
drugs.com	57 1 (major) 29 (moderate) 27 (minor)
WHO monographs	34
PDR	30
<i>Kanıtı Dayalı Fitoterapi-I</i>	31
Novel Drug Target With Traditional Herbal Medicines	4
FFD monographs	4

Garlic was the herbal product that most frequently interacted with drugs in our study, particularly with antihypertensive, antiplatelet, and antidiabetic drugs. In a study, it was stated that Garlic potentiates the antiplatelet effect of aspirin (Souza-Peres et al., 2023). Garlic was found to enhance the effects of captopril in an animal study investigating the antihypertensive properties of Garlic (Asdaq & Inamdar, 2010). Additionally, studies on both humans and animals have demonstrated that Garlic improves the effects of hypoglycemic drugs (Hu et al., 2005). Due to its various pharmacological effects, patients taking cardiovascular or endocrine system drugs should be warned about using garlic.

This study has several limitations. As the study was limited to one community pharmacy, it was mandatory to work together with patients who shared a similar demographic. Expanding the study to include community pharmacies in various locations would increase the number of participants and allow for the examination of patients with more different profiles. Another limitation was the limited number of studies on drug-herbal product interactions. Finally, since the interactions identified by drug interaction tools are potential drug-herbal product interactions, they may not always have clinical significance.

**CONCLUSION**

Our findings show that herbal products used in patients with chronic diseases are not always safe and may even interact with the drugs used and cause life-threatening adverse drug reactions in patients. It is particularly important to investigate about herbal product use in patients taking cardiovascular or antidiabetic medications who visit pharmacies, to evaluate potential interactions between herbal products and their medications, and to provide appropriate guidance to these patients. Pharmacists should provide consultancy services to their patients on the use of herbal products. It is advisable for community pharmacists to keep their knowledge on drug-herbal product interactions updated. They can benefit from training programs on drug-herbal product interactions organized by clinical pharmacists.

**ACKNOWLEDGEMENTS**

None.

**AUTHOR CONTRIBUTION STATEMENT**

Developing hypothesis: EP. Methodology: EP. Survey question: EP and SG. Implementation of surveys: SG. Data management: EP and SG. Statistics, analysis and interpretation of the data: EP. Writing — original draft: EP. Writing — reviewing and editing: EP and SG.

### CONFLICTS OF INTEREST

The authors declare that there is no conflict of interest.

### REFERENCES

- Abudalo, R., Abudalo, R., Alqudah, A., Abuqamar, A., Abdelaziz, A., Alshawabkeh, M., & Taha, L. (2022). Pharmacy practitioners' practice, awareness and knowledge about herbal products and their potential interactions with cardiovascular drugs. *F1000Res*, 11, 912. doi:10.12688/f1000research.121709.2
- Abunahlah, N., Elawaisi, A., Velibeyoglu, F. M., & Sancar, M. (2018). Drug related problems identified by clinical pharmacist at the Internal Medicine Ward in Turkey. *Int J Clin Pharm*, 40(2), 360-367. doi:10.1007/s11096-017-0585-5
- ACCP. (2008). The definition of clinical pharmacy. *Pharmacotherapy*, 28(6), 816-817.
- ACCP. (2023). Standards of practice for clinical pharmacists. *JACCP: Journal of the American Collage of Clinical Pharmacy*, 6(10), 1156-1159. doi:https://doi.org/10.1002/jac5.1873
- Ahmed, S., Khan, H., Mirzaei, H., Hasan, M. M., Eddouks, M., & Daglia, M. (2021). Herbal Drug Interaction: Mechanistic Details through Pharmacokinetic Portfolio. *CNS & Neurological Disorders - Drug Targets*, 20(8), 677-686. doi:10.2174/1871527319666201008151710
- Al-Windi, A. (2004). Predictors of herbal medicine use in a Swedish health practice. *Pharmacoepidemiol Drug Saf*, 13(7), 489-496. doi:10.1002/pds.901
- Albassam, A. A., Alanazi, A., Alhaqbani, N., Alhoti, F., Almalki, Z. S., Alshehri, A. M., & Alzahrani, J. (2021). The potential of drug-herbal interaction among patients with chronic diseases in Saudi Arabia. *Complementary Therapies in Clinical Practice*, 43, 101324. doi:10.1016/j.ctcp.2021.101324
- Asdaq, S. M., & Inamdar, M. N. (2010). Potential of garlic and its active constituent, S-allyl cysteine, as antihypertensive and cardioprotective in presence of captopril. *Phytomedicine*, 17(13), 1016-1026. doi:https://doi.org/10.1016/j.phymed.2010.07.012
- Ekor, M. (2014). The growing use of herbal medicines: issues relating to adverse reactions and challenges in monitoring safety. *Front Pharmacol*, 4, 177. doi:10.3389/fphar.2013.00177
- Goldstein, L. H., Elias, M., Ron-Avraham, G., Biniaurishvili, B. Z., Madjar, M., Kamargash, I., . . . Golik, A. (2007). Consumption of herbal remedies and dietary supplements amongst patients hospitalized in medical wards. *Br J Clin Pharmacol*, 64(3), 373-380. doi:10.1111/j.1365-2125.2007.02878.x
- Grymonpre, R. E., McKechnie, M., & Briggs, C. (2010). Community pharmacists' identification of natural health product/drug interactions in older persons. *International Journal of Pharmacy Practice*, 11(4), 217-223. doi:10.1211/0022357022674
- Hersberger, K. E., & Messerli, M. (2016). Development of Clinical Pharmacy in Switzerland: Involvement of Community Pharmacists in Care for Older Patients. *Drugs Aging*, 33(3), 205-211. doi:10.1007/s40266-016-0353-6
- Hu, Z., Yang, X., Ho, P. C. L., Chan, S. Y., Heng, P. W. S., Chan, E., . . . Zhou, S. (2005). Herb-Drug Interactions. *Drugs*, 65(9), 1239-1282. doi:10.2165/00003495-200565090-00005
- Mazrouei, N. A., Meslamani, A. Z. A., Alajeel, R., Alghadban, G., Ansari, N., Kaabi, M. A., . . . Ibrahim, O. M. (2022). The patterns of herbal medicine use in the United Arab Emirates; A national study. *Pharmacy Practice (Granada)*, 20(3), 2698. doi:10.18549/PharmPract.2022.3.2698

- Olisa, N. S., & Oyelola, F. T. (2010). Evaluation of use of herbal medicines among ambulatory hypertensive patients attending a secondary health care facility in Nigeria. *International Journal of Pharmacy Practice*, 17(2), 101-105. doi:10.1211/ijpp.17.02.0005
- Parvez, M. K., & Rishi, V. (2019). Herb-Drug Interactions and Hepatotoxicity. *Curr Drug Metab*, 20(4), 275-282. doi:10.2174/1389200220666190325141422
- Pearson, H., Fleming, T., Chhoun, P., Tuot, S., Brody, C., & Yi, S. (2018). Prevalence of and factors associated with utilization of herbal medicines among outpatients in primary health centers in Cambodia. *BMC Complementary Medicine and Therapies*, 18(1), 114. doi:10.1186/s12906-018-2181-1
- Peltzer, K., & Pengpid, S. (2019). The use of herbal medicines among chronic disease patients in Thailand: a cross-sectional survey. *J Multidiscip Healthc*, 12, 573-582. doi:10.2147/jmdh.S212953
- Polat, E. C., Koc, A., & Demirkan, K. (2022). The role of the clinical pharmacist in the prevention of drug-induced acute kidney injury in the intensive care unit. *J Clin Pharm Ther*, 47(12), 2287-2294. doi:10.1111/jcpt.13811
- Pradipta, I. S., Aprilio, K., Febriyanti, R. M., Ningsih, Y. F., Pratama, M. A. A., Indradi, R. B., . . . Abdullah, R. (2023). Traditional medicine users in a treated chronic disease population: a cross-sectional study in Indonesia. *BMC Complementary Medicine and Therapies*, 23(1), 120. doi:10.1186/s12906-023-03947-4
- Robinson, M. M., & Zhang, X. (2011). The world medicines situation 2011, traditional medicines: Global situation, issues and challenges. World Health Organization, Geneva, 31, 1-2.
- Rodrigues, A. T., Stahlschmidt, R., Granja, S., Falcão, A. L., Moriel, P., & Mazzola, P. G. (2015). Clinical relevancy and risks of potential drug-drug interactions in intensive therapy. *Saudi Pharm J*, 23(4), 366-370. doi:10.1016/j.jsps.2014.11.014
- Souza-Peres, J. V., Flores, K., Umloff, B., Heinan, M., Herscu, P., & Babos, M. B. (2023). Everyday Evaluation of Herb/Dietary Supplement-Drug Interaction: A Pilot Study. *Medicines (Basel)*, 10(3). doi:10.3390/medicines10030020
- Tezcan, S., & Butur, M. (2022). Evaluation of the attitudes and practices of patients regarding the use of herbal products. *Journal of Faculty of Pharmacy of Ankara University*, 46(3), 817-826.
- Tulunay, M., Aypak, C., Yikilkan, H., & Gorpelioglu, S. (2015). Herbal medicine use among patients with chronic diseases. *Journal of Intercultural Ethnopharmacology*, 4(3), 217.
- Turkmenoglu, F. P., Kutsal, Y. G., Dolgun, A. B., Diker, Y., & Baydar, T. (2016). Evaluation of herbal product use and possible herb-drug interactions in Turkish elderly. *Complementary Therapies in Clinical Practice*, 23, 46-51. doi:https://doi.org/10.1016/j.ctcp.2016.03.004
- Ünlüyol, D., Gökçekuş, H., Kassem, Y., Tezer, M., Meriçli, F., & Yavuz, D. (2023). Complementary and Alternative Medicines in Northern Cyprus: Public Awareness, Patterns of Use, and Attitudes. *Healthcare (Basel)*, 11(7). doi:10.3390/healthcare11070977
- Welz, A. N., Emberger-Klein, A., & Menrad, K. (2019). The importance of herbal medicine use in the German health-care system: prevalence, usage pattern, and influencing factors. *BMC Health Serv Res*, 19(1), 952. doi:10.1186/s12913-019-4739-0

Williams, E. S., Rondeau, K. V., Xiao, Q., & Francescutti, L. H. (2007). Heavy physician workloads: impact on physician attitudes and outcomes. *Health Serv Manage Res*, 20(4), 261-269. doi:10.1258/095148407782219067



# Innovative Drug Delivery System: Aspasomes and Their Effectiveness in Treatment

Esmâ Nur USLU\*, Çiğdem YÜCEL\*\*

## Innovative Drug Delivery System: Aspasomes and Their Effectiveness in Treatment

### SUMMARY

Aspasomes recently discovered by Gopinath et al. are defined as a double-layered vesicular system formed by ascorbyl palmitate. Ascorbyl palmitate is the ester form that is more lipophilic, stable and bioavailable than ascorbic acid. Ascorbyl palmitate, which can be stored in the lipid cell membrane until used in the body, has important advantages that make aspasomes stand out in dermal application, with its properties that increase drug solubility and permeability in the skin. Considering the studies carried out, it is seen that even aspasomes that do not contain active compounds have high antioxidant activity, and they have also been developed for different purposes such as anti-aging effect, photoprotection, skin lightening effect by using different active compounds.

This review focuses on the structure, advantages, disadvantages, preparation methods, characterization, therapeutic potential and future of aspasomes, are new drug carrier systems that serves to increase the effectiveness of treatment.

**Key Words:** Aspasome, drug delivery system, therapeutic efficiency

## Yenilikçi İlaç Dağıtım Sistemi: Aspazomlar ve Tedavideki Etkinliği

### ÖZ

Yakın geçmişte Gopinath ve arkadaşları tarafından keşfedilen aspazomlar, askorbil palmitatın oluşturduğu çift tabakalı veziküller sistem olarak tanımlanmaktadır. Askorbil palmitat, askorbik asite göre daha lipofilik, kararlı ve biyoyararlanımı daha yüksek olan ester formudur. Vücutta kullanıma kadar lipid hücre zarında depolanabilen askorbil palmitat, ilaç çözünürlüğünü ve deride permeabiliteyi artırıcı özellikleriyle aspazomları dermal uygulamada ön plana çıkaran önemli avantajlara sahiptir. Yapılan çalışmalara bakıldığında, etkin madde içermeyen aspazomların bile antioksidan etkinliğinin yüksek olduğu, bunun yanı sıra farklı aktif bileşikler kullanılarak yaşlanma karşıtı etki, foto koruma, deri rengini açıcı etki gibi farklı amaçlar için geliştirildiği görülmektedir.

Bu derleme, tedavide etkinliği artırmak amacıyla hizmet eden yeni ilaç taşıyıcı sistem olan aspazomların yapısı, avantajları, dezavantajları, hazırlama yöntemleri, karakterizasyonu, terapötik potansiyelleri ve geleceği üzerinde durmaktadır.

**Anahtar Kelimeler:** Aspazom, ilaç taşıyıcı sistem, terapötik etkinlik

Received: 18.04.2024

Revised: 04.11.2024

Accepted: 18.11.2024

\* ORCID: 0009-0004-9469-9402, Department of Pharmaceutical Technology, Faculty of Pharmacy, Erciyes University, 38280, Kayseri, Türkiye

\*\* ORCID: 0000-0002-0622-5150, Department of Pharmaceutical Technology, Faculty of Pharmacy, Erciyes University, 38280, Kayseri, Türkiye

## INTRODUCTION

Micro and nanoparticulate drug forms are a group that has been intensively studied to increase the treatment effectiveness provided by traditional drug forms and reduce side effects and the therapeutic dose used in treatment. Studies on these systems, which aim to increase the patient's quality of life and eliminate side and harmful effects by extending the dosing interval at lower doses, are increasing day by day in parallel with the advantages provided by the solubility, permeability and applicability properties of nano-sized particles. (Zırh-Gürsoy, 2002; Wilczewska et al., 2012).

Aspasomes were first discovered by Gopinath and others in 2004, and they pioneered the study of aspasomes with the article they published. Aspasomes are defined as double-layered ascorbyl palmitate (AP) vesicles. Additionally, negatively charged phospholipids such as cholesterol and dicethyl phosphate are used as formulation components (Figure 1) (Gopinath et al., 2004).

Ascorbic acid also known as vitamin C, provides wide-ranging support for the human body. AP is a fat-soluble ester derivative with much higher

bioavailability than ascorbic acid, synthesized with a traditional esterification process of between the main alcohol group of ascorbic acid and the carboxylic group of palmitic acid (Figure 2). Studies have shown that amphiphilic AP, especially when incorporated into a phospholipid monolayer, effectively reduces the surface tension of the air/water interface. This ester structure has a molecular weight of 414.55 g/mol and a melting point range of 115–118°C (Yadav and Lariya, 2018; Imran et al., 2024).

When Web of Science (2024) is scanned, there are 18 manuscripts about aspasomes, one of which belongs to the author's team. Since aspasomes have been described recently, studies in this field are quite limited. Considering the studies carried out; it is observed that even empty aspasomes have high antioxidant activity, and they have also been developed for different purposes such as anti-aging effect, photoprotection, skin lightening, melasma, androgenic alopecia and rheumatoid arthritis by using different active compounds (Ghosh et al., 2018; Hatem et al., 2018; Yadav and Lariya, 2018; Kar et al., 2020; Shinde et al., 2022; Yücel et al., 2023).

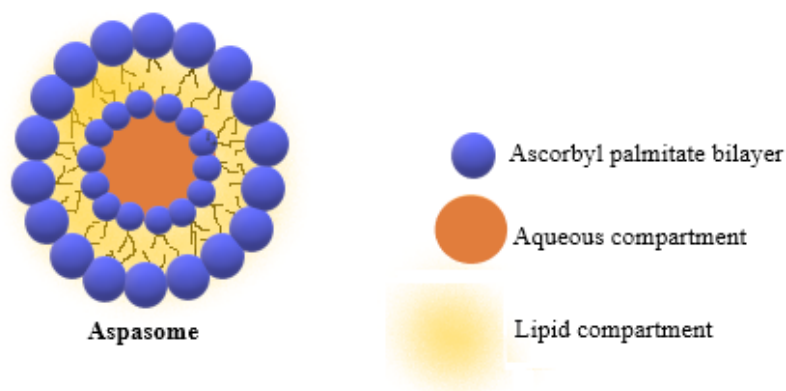


**Figure 1.** Aspasome structure

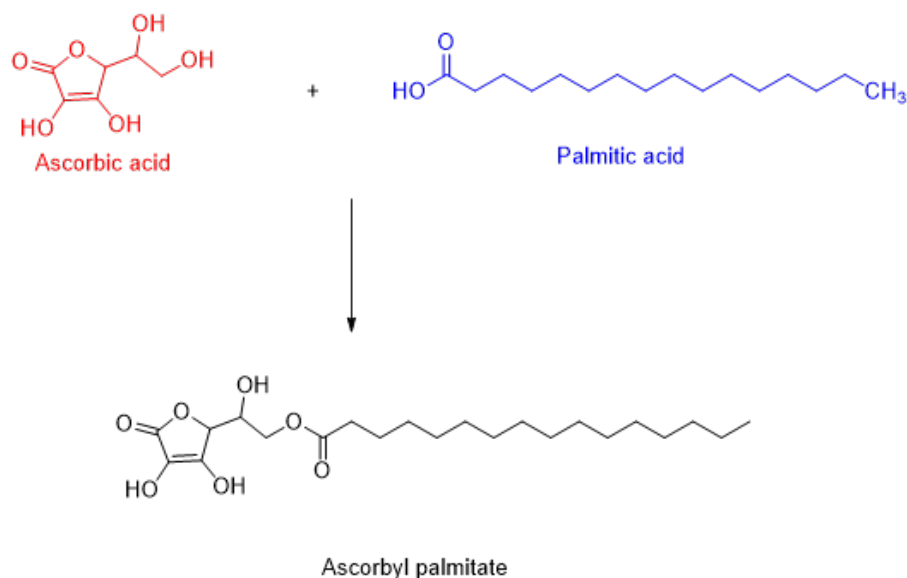


**Figure 2.** Chemical production reaction of AP

#### Advantages of aspasomes

Although aspasomes have been named as AP liposomes in some sources, they have gained a new identity over time. It is seen that they have been developed with different active compounds and their effectiveness has been determined, especially thanks to the advantages they provide for topical use. The advantages of aspasomes and AP, the main component in their formation are listed below.

- AP plays an important role in the formation of the structure of aspasomes and is in ester form and more lipophilic and stable than ascorbic acid.
- AP has been granted Generally Recognized as Safe (GRAS) status by the Food and Drug Administration (FDA).
- Unlike ascorbic acid, AP is water-soluble and can be stored in the lipid cell membrane until it is ready to be used by the body.
- AP shows better antioxidant activity than ascorbic acid.
- When taken orally or applied topically, AP hydrolyzes to its metabolites ascorbic acid and palmitic acid, and is considered safer compared to other synthetic antioxidants.
- Aspasomes are biocompatible thanks to their composition. Since they contain hydrophilic and

lipophilic regions, they allow the encapsulation of both hydrophilic and lipophilic compounds.

- Aspasomes, thanks to the AP they contain, have important roles such as increasing skin elasticity by triggering collagen production, increasing drug solubility and the permeability of encapsulated active ingredients through the skin and helping moisturize the skin (Yadav and Lariya, 2018; Kar et al., 2020; Aboul-Einien et al., 2020; Ledinski et al., 2022; Imran et al., 2024).

#### Disadvantages of aspasomes

- Although AP is a well-known antioxidant, it may have a prooxidant effect depending on the high concentration (Let et al., 2007).
- Despite its increased stability compared to ascorbic acid, AP can become relatively unstable when exposed to temperature, oxygen, light, and excess moisture, which can lead to gradual oxidation and discoloration. One of the most important factors that can disrupt the stability of AP, which is the main component of aspasomes, is temperature. Higher temperatures have the potential to accelerate most reactions and initiate oxidation. In addition, operating conditions and storage conditions may also have an impact on physical stability, causing aggregation. (Imran et al., 2024).

• In addition, it is well known that light can initiate a process that leads to the production of free radicals. Stability in the presence of UV radiation needs to be assessed. Numerous studies have shown that AP exhibits both biological activity and instability when exposed to UV light. The presence of certain transition metals can potentially catalyze oxidation and lead to oxidation-reduction processes that destabilize the compound (Gorain et al., 2018).

#### **Preparation methods and *in vitro* characterization of aspasomes**

In recently discovered and limited studies, the film hydration method, which is widely used in the preparation of vesicular systems, and sonication have also been used for aspasomes. For the quality control of the developed aspasomal formulations, *in vitro* characterization is required immediately after preparation and during storage. Among the parameters examined in this context, thermotropic properties and phase transition behavior, surface morphology, vesicle size and size distribution, polydispersity index, zeta potential, percent drug encapsulation, and *in vitro* release (Gopinath et al., 2004; Aboul-Einien et al., 2020)

#### **Uses of aspasomes in treatment**

As mentioned above, aspasomal formulation studies are quite limited today and these studies are summarized below.

Gopinath et al. (2004), who first mentioned the structure and characterization of aspasomes, prepared aspasomal formulations containing AP, cholesterol, dicetyl phosphate, a negatively charged lipid, and azidothymidine (zidovudine) by the film hydration method. In this study, which formed the basis for the development of aspasomes, *in vitro* characterization, antioxidant effect, and skin penetration activity were investigated in comparison with ascorbic acid. Their high antioxidant effect and greater skin permeability have led to further studies, especially topical application (Gopinath et al., 2004).

In another study, Lamie et al. (2022) investigated the effects of aspasomes loaded with the antifungal active ingredient itraconazole (ITZ) in the treatment

of skin cancer. In this study, optimized aspasomes were applied for the first time as a new delivery platform by dispersing in a cream base and their effectiveness was evaluated. The cream was chosen as the dosage form because it can stay on the skin longer with its viscous texture. Clinical studies demonstrated that ITZ-loaded aspasomes resulted in a significant increase in necrotic tissue and a 62.68% reduction in subcutaneous tumor mass compared to the 14% tumor weight reduction achieved with traditional ITZ cream. Additionally, research highlighted the ability of aspasomes as nanocarriers with superior physicochemical properties to improve skin permeability and lipophilic drug dermal targeting via cream form (Lamie et al., 2022).

Rheumatoid arthritis (RA) is a common form of arthritis and is a chronic inflammatory disease that causes inflammation of the membranes inside the joints (synovium) and/or other internal organs. Current management of RA is provided by disease-modifying antirheumatic drugs such as symptom-relieving nonsteroidal anti-inflammatory drugs, corticosteroids, methotrexate (MTX), and biologics (Demirel and Kirnap, 2010; Ghosh et al., 2018). MTX is one of the most widely used basic effective drugs in the treatment of inflammatory rheumatic diseases (reducing inflammation and pain and stopping the progression). Additionally, intra-articular injection of the free drug has been reported to show poor efficacy due to rapid drug clearance (Prabhu et al., 2012; Gottschalk et al., 2015; Garg et al., 2016; Ghosh et al., 2018). Based on this point, Ghosh et al. prepared and evaluated methotrexate-loaded aspasomes in terms of drug-excipient interaction, particle size, zeta potential, encapsulation efficiency, and surface properties. It was found that the optimized aspasome formulation had a particle size of 386.8 nm, a smooth surface with high drug loading, negative zeta potential, and a constant permeation rate with *in vitro* controlled drug release over 24 hours. The best formulation selected as a result of the characterization study was loaded into the hydrogel to evaluate *in vitro* drug release and tested

*in vivo* against the adjuvant-induced arthritis model in Wistar rats. On the other hand, the effectiveness of AP, which was combined with MTX and has an antioxidant effect, in the treatment of RA was also evaluated. It was determined that rat paw diameter, TNF $\alpha$  and IL  $\beta$  levels, cartilage damage, inflammation and bone resorption decreased after the application of MTX-loaded aspasome hydrogel for 12 days (Ghosh et al., 2018).

Psoriasis is a chronic inflammatory skin disease that can flare up in any cutaneous area and is seen on the scalp, outer surfaces of the sacral areas, elbows and knees. In psoriasis, there are options such as systemic, topical (corticosteroid creams) treatment, as well as phototherapy. Mometasone Furoate (MMF) is an important topical corticosteroid used in the treatment of various skin diseases such as dermatitis and psoriasis. Topical application of MMF once daily has proven to be beneficial in the treatment of Psoriasis vulgaris (Tiplica and Salavastru, 2009). In psoriasis, traditional medications cannot penetrate the thickened skin, while MMF-loaded ASP gel increases permeability through the stratum corneum. Dry and rough skin is a big problem for psoriasis patients, so, gel forms are thought to help moisturize the skin and increase skin elasticity of aspasomes with the presence of AP. In the investigation conducted by Shinde et al., aspasomes were produced by the film hydration method, optimized and characterized in terms of drug entrapment efficiency, vesicle size and size distribution, charge, and morphology. After the optimized aspasomes were dispersed into the carbopol gel structure, they were evaluated in terms of pH, viscosity, and spreadability, and the drug release study was carried out using a dialysis membrane and goat skin. The antioxidant activity was determined. *In vivo* performance on skin irritation and inflammation was performed using Wistar rats. The optimized aspasomes had a particle size of  $282.9 \pm 1.7$  nm, a polydispersity index of 0.2, a zeta potential of  $-20.2$  mV, and an encapsulation efficiency of  $74.72 \pm 1.8\%$ . Results recorded showed sustained release (24

hours) against commercial cream (5 hours). Using a fluorescent marker, the accumulation of MMF-loaded aspasomal gel in the epidermis was approved by a skin penetration study (Shinde et al., 2020).

Tizanidine hydrochloride (TZN) is a potent, centrally-acting muscle relaxant, but its bioavailability is low because the marketed tablet dosage form is subject to a first-pass effect in the liver when administered orally. TZN is a rapidly absorbed, narrow therapeutic index active substance with a half-life of approximately 2.5 hours and a T<sub>max</sub> of approximately 1 hour. It was revealed that TZN showed good stability in the skin environment and did not form a reservoir in the stratum corneum while partitioning into intercellular spaces. According to a study by Khalil et al., it was reported that transdermal delivery of TZN active ingredient may benefit bioavailability, and the possibility that aspasomes could be potential carriers was evaluated. In the study, an optimal formulation was developed using a full factorial design that evaluated the effects of selected variables on the properties of vesicles, encapsulation efficiency, vesicle size, cumulative percentage released, and the stability of aspasomes under different conditions was evaluated. A 4.4-fold increase in steady-state flux was observed in an *ex vivo* permeation study using rat skin compared to free drug. In an *in vivo* study in albino rats administered aspasomal formulation and free drug, the bioavailability of TZN was significantly increased compared to Sirdalud®, a commercial product. Additionally, skin irritation tests confirmed that the vesicles are non-invasive and safe for the skin (Khalil et al., 2021).

Androgenetic alopecia (AGA) is also known as male pattern hair loss (baldness), which generally begins in the 20s and 30s and typically begins with bitemporal regression of the frontal hairline, resulting in thinning of the hair, especially at the crown, and complete hair loss in the center of the crown. In the treatment of AGA, local use of liquid and foam forms of minoxidil at 2% and 5% (w/v) concentration has been approved by the FDA for the treatment of hair

loss in men and women. In addition, finasteride, which is an antiandrogen and an inhibitor of the type 2 5- $\alpha$ -reductase enzyme that converts testosterone to dihydrotestosterone, is approved for use only in men in the treatment of AGA. However, due to the need for a long time to evaluate the effectiveness of these compounds and the observation of some side effects (erectile problems, decreased libido, ejaculatory dysfunction, decrease in sperm count), the necessity of new approaches in treatment has emerged by formulating alternative compounds and using them more effectively with drug delivery systems (Martinez-Jacobo et al., 2018; Ho et al., 2021; Wu and Du, 2023). Additionally, Fischer et al. suggested that it is necessary to investigate alternative agents to oral finasteride and topical minoxidil in the treatment of AGA, and melatonin hormone, a strong antioxidant and growth modulator, was determined as a potentially effective candidate and was investigated in *in vitro* and *in vivo* studies (Fischer et al., 2012). Hatem et al. aimed to develop melatonin-loaded vitamin C-based aspasomes for use in the clinical treatment of AGA. Aspasomes were evaluated for vesicular size, entrapment efficiency, morphology, antioxidant potential, physical stability, *in vitro* release, and ex-vivo skin accumulation. Clinically, melatonin aspasomes were tested in AGA patients and the degree of improvement was evaluated by performing a hair-pulling test and histometric analysis. The results showed that the developed aspasomal melatonin exhibited clinically favorable pharmaceutical properties compared to its solution form, providing increased hair thickness, density and reduced hair loss along with photographic improvement in most patients (Hatem et al., 2018).

The demand for skin-lightening cosmetics is increasing in the treatment of skin darkening and blemishes, which are more common with age. Skin whitening may be possible if inhibitors of tyrosinase, the main enzyme involved in melanin synthesis, are used. Quercetin, a flavonoid with a strong antioxidant effect (Özgen et al., 2016), is a tyrosinase

enzyme inhibitor and inhibits melanin biosynthesis. However, its practical applications are limited due to its low chemical stability. Increased skin absorption was observed when AP was used in combination with quercetin, especially for topical application. Aspasomes can act as a local repository for different drug classes, increasing drug effectiveness in skin whitening, providing anti-aging effects, photo protection, moisturizing, etc (Ghosh et al., 2018; Yadav and Lariya, 2018; Kar et al., 2020; Shinde et al., 2022; Yücel et al., 2023). In one study, quercetin-loaded aspasomes were developed for skin lightening and prepared by the film hydration method using AP, cholesterol, and negatively charged lipids. Afterward, aspasomal gel was prepared by dispersing it into Carbopol. The encapsulation efficiency of aspasomes was high (52.41%) and released up to 78% of the drug. Quercetin-loaded aspasomes were more successful in passing through rat dorsal skin than unformulated quercetins and were reported to be effective for skin pigmentation disorders (Kar et al., 2020).

In another study on quercetin-loaded aspasomes, their beneficial effects in acne treatment were investigated. Aspasomes were characterized *in vitro* in terms of their particle size, zeta potential, entrapment efficiency, stability, cytotoxic effect on the 3T3 CCL92 cell line, skin accumulation/permeability, antioxidant potential and morphology. Antibacterial activity on *Propionibacterium acnes* was tested and the percentage reduction in acne lesions was determined. It was observed that quercetin-loaded aspasomes were developed at nano sizes (125-184 nm) in accordance with the target, exhibiting negative charge and high skin accumulation reaching 40%. The antioxidant activity of quercetin was preserved with the formulation, resulting in a significantly higher antibacterial effect against *Propionibacterium acnes* compared to free quercetin (Amer et al., 2020).

Magnesium ascorbyl phosphate (MAP) is a stable and water-soluble form of ascorbic acid. It is easily absorbed by the skin, has a moisturizing effect on the skin, reduces transepidermal water loss, and it is

a free radical scavenger with a photoprotective effect that increases collagen production. (Lakra et al., 2020; Telang, 2013). In a study assessed by Aboul-Einien et al., nine different aspasomal formulations were produced to evaluate the effectiveness of aspasomes in the treatment of melasma, in which MAP was formulated in different topical formulations such as aspasomal cream. They assessed in terms of particle size and distribution, zeta potential and encapsulation efficiency. Then, after examining the three formulations in terms of drug release, skin penetration, and retention, a formulation suitable for topical application in two different forms, cream and gel, was selected. Aspasomal cream has been shown to provide better drug permeability and skin retention than gel and suspended aspasom formulations. MAP aspasomal cream was clinically evaluated for its potential as an effective treatment for melasma versus 15% trichloroacetic acid, and aspasomal cream showed the greatest improvement in hemi-MASI scores, and 35% of patients were very positive about the treatment (Aboul-Einien et al., 2020).

In the study where aspasomes were prepared for the simultaneous application of idebenone and naproxen, it was decided to use L-ascorbic acid 6-palmitate, cholesterol, and dimyristoyl phosphatidic acid or dimyristoyl phosphatidyl glycerol at a lipid molar ratio of 35:55:10 as a result of the use of different lipid compositions. The average diameter of the formed aspasomes was below 160 nm, the size distribution was narrow and there was a clear negative zeta potential (~50 mV), and capture efficiency of ~50-75% was obtained for idebenone and naproxen,

respectively. It was observed that the co-loading of idebenone and naproxen did not change the physicochemical properties and long-term stability of aspasomes. Continuous and controlled drug release was observed from *in vitro* drug release studies for up to 24 hours. In the viability test performed on the human keratinocyte cell line, its viability was found to be 93%. *In vivo* study showed increased therapeutic efficacy and rapid reduction of chemical-induced erythema compared to commercially available naproxen gel Naprosyn® 1 hour after topical application (d'Avanzo et al., 2022).

In the use of anti-aging active ingredients in cosmetic formulas, vesicular lipid structured systems such as aspasomes, which seem to be advantageous in penetrating the skin, are preferred. Ferulic acid is a phenolic compound that is found in skincare and anti-aging products thanks to its antioxidant properties and is increasingly used in pharmaceuticals and cosmetics. Its poor water solubility and the instability of its physicochemical structure create problems in formulation development. It needs a formulation that increases its stability, protects its chemical structure, and demonstrates its effectiveness. In one study by our team, ferulic acid-loaded aspasomal formulations were developed, characterized, and *in vitro* release and penetration studies through *ex vivo* mouse abdominal skin were performed. The anti-aging activity of aspasomes has been proven with its antioxidant activity and inhibitory effect on collagenase and elastase enzymes in the skin penetration study (Yücel et al., 2023).

**Table 1.** Aspasomal formulations with different active compounds

Active compound	Reason for use	Results	Reference
Zidovudine	Lipo-peroxidation	Increased antioxidant effect Due to its nano size, it can better adhere to the membranes of blood cells and be well localized within the cell. Showing amphipathic properties Contains a free polar head	Gopinath et al., 2004
Itraconazole	Skin cancer	Increased antioxidant and anticancer effects Increased skin permeability Do not cause irritation Good spreadability Usability of nanovesicles on skin Good moisturizing effectiveness	Lamie et al., 2022
Methotrexate	Rheumatoid arthritis	Reduction in side effects More active than MTX alone Providing controlled release Adequate drug permeation rate in topical application High drug retention efficiency	Ghosh et al., 2018
Mometasone furoate	Psoriasis	Increasing skin elasticity by promoting collagen formation Helps MF penetrate the skin Reduces pigmentations that cause psoriasis Helping moisturize the skin Does not cause irritation and inflammation	Shinde et al., 2020
Tizanidine	Muscle relaxation	Increased bioavailability Increased stability Does not cause irritation	Khalil et al., 2021
Quercetin	Skin whitening	Whitening effect on skin Increased penetration through the skin	Kar et al., 2020
	Acne treatment	Higher antibacterial effect against <i>Propionibacterium acnes</i>	Amer et al., 2020
Melatonin	Androgenetic alopecia	Significant improvement in hair growth Accumulation of melatonin in all layers of the skin High drug release High antioxidant activity	Hatem et al., 2018
Magnesium ascorbyl phosphate	Melasma	High efficiency in topical application Good stability Reduction in hyperpigmentation Anti-inflammatory effect	Aboul-Einien et al., 2020
Idebenone and naproxen	Inflammation	Continuous and controlled drug release Long-term stability Increased therapeutic effect Decreased the induced skin chemical erythema	D'Avanzo et al., 2022
Ferulic acid	Skin aging	An effective permeation rate Increased antioxidant effect Increased anti-aging effect Improving skin permeability Slowing down skin aging	Yücel et al., 2023



## CONCLUSION

To sum up, the innovative drug delivery system aspasomes, which have come to the fore in recent years, are systems that can be safely applied to carry many molecules, especially in topical use, to the lower layers of the skin and increase their effectiveness. It seems possible to increase the formulation quality, effectiveness, stability, and bioavailability of biopharmaceuticals with prepared aspasomes. The antioxidant and anti-inflammatory effects of AP, as well as its lipophilic properties, make aspasomes valuable in the cosmetic industry for being effective in skin moisturizing, collagen synthesis, and anti-aging treatment. It offers opportunities for the increased use of aspasomes. However, when used, AP is metabolized to ascorbic acid and palmitic acid, and there is not enough research to understand how it affects biological activities. More detailed studies and clinical applications are needed.

## ACKNOWLEDGEMENT

We would like to thank the Proofreading & Editing Office of the Dean for Research at Erciyes University for the copyediting and proofreading service for this manuscript.

This study was produced from the master's thesis titled "Development and investigation of the efficacy of aspasomal formulations containing some effective natural compounds in the treatment of androgenetic alopecia" and coded 10663777, carried out within the scope of Erciyes University Health Sciences Institute.

## AUTHOR CONTRIBUTION STATEMENT

Determination of the subject, literature research, preparation of the manuscript (EU) Determination of the subject, literature research, reviewing the manuscript and supervision (ÇY)

## CONFLICT OF INTEREST

The authors declare that there is no conflict of interest.

## REFERENCES

- Aboul-Einien, M. H., Kandil, S. M., Abdou, E. M., Diab, H. M., & Zaki, M. S. (2019). Ascorbic acid derivative-loaded modified aspasomes: formulation, in vitro, ex vivo and clinical evaluation for melasma treatment. *Journal of Liposome Research*, 30(1), 54–67. <https://doi.org/10.1080/08982104.2019.1585448>
- Amer, S. S., Nasr, M., Abdel-Aziz, R. T., Moftah, N. H., El Shaer, A., Polycarpou, E., Mamdouh, V., & Sammour, O. (2020). Cosm-nutraceutical nanovesicles for acne treatment: Physicochemical characterization and exploratory clinical experimentation. *International Journal of Pharmaceutics*, 577, 119092. <https://doi.org/10.1016/j.ijpharm.2020.119092>
- Chan, S. A., Hussain, F., Lawson, L. G., & Ormerod, A. D. (2011). Factors affecting adherence to treatment of psoriasis: comparing biologic therapy to other modalities. *Journal of Dermatological Treatment*, 24(1), 64–69. <https://doi.org/10.3109/09546634.2011.607425>
- d'Avanzo, N., Cristiano, M. C., Di Marzio, L., Bruno, M. C., Paolino, D., Celia, C., & Fresta, M. (2022). Multidrug Idebenone/Naproxen co-loaded aspasomes for significant in vivo anti-inflammatory activity. *ChemMedChem*, 17(9). <https://doi.org/10.1002/cmdc.202200067>
- Demirel, A., & Kırnar, M. (2010). Romatoid artrit tedavisinde geleneksel ve güncel yaklaşımlar. *Sağlık Bilimleri Dergisi*, 19(1), 74-84.
- Fischer, T., Hänggi, G., Innocenti, M., Elsner, P., & Trüeb, R. (2012). Topical melatonin for treatment of androgenetic alopecia. *International Journal of Trichology*, 4(4), 236. <https://doi.org/10.4103/0974-7753.111199>

- Garg, N. K., Singh, B., Tyagi, R. K., Sharma, G., & Katare, O. P. (2016). Effective transdermal delivery of methotrexate through nanostructured lipid carriers in an experimentally induced arthritis model. *Colloids and Surfaces B: Biointerfaces*, 147, 17–24. <https://doi.org/10.1016/j.colsurfb.2016.07.046>
- Ghosh, S., Mukherjee, B., Chaudhuri, S., Roy, T., Mukherjee, A., & Sengupta, S. (2018). Methotrexate aspasomes against rheumatoid arthritis: optimized hydrogel loaded liposomal formulation with in vivo evaluation in wistar rats. *AAPS PharmSciTech*, 19(3), 1320-1336. <https://doi.org/10.1208/s12249-017-0939-2>
- Gopinath, D., Ravi, D., Rao, B., Apte, S., Renuka, D., & Rambhau, D. (2004). Ascorbyl palmitate vesicles (Aspasomes): formation, characterization and applications. *International Journal of Pharmaceutics*, 271(1–2), 95-113. <https://doi.org/10.1016/j.ijpharm.2003.10.032>
- Gorain, B., Choudhury, H., Pandey, M., Madheswaran, T., Kesharwani, P., Rakesh K. & Tekade R. K. (2018). Drug–excipient interaction and incompatibilities, *Dosage Form Design Parameters*, 2, 363-402. <https://doi.org/10.1016/B978-0-12-814421-3.00011-7>
- Gottschalk, O., Metz, P., Trong, M. D., Altenberger, S., Jansson, V., Mutschler, W., & Schmitt-Sody, M. (2015). Therapeutic effect of methotrexate encapsulated in cationic liposomes (EndoMTX) in comparison to free methotrexate in an antigen-induced arthritis study in vivo. *Scandinavian Journal of Rheumatology*, 44(6), 456-463. <https://doi.org/10.3109/03009742.2015.1030448>
- Hatem, S., Nasr, M., Mofthah, N. H., Ragai, M. H., Geneidi, A. S., & Elkheshen, S. A. (2018). Melatonin vitamin C-based nanovesicles for treatment of androgenic alopecia: Design, characterization and clinical appraisal. *European Journal of Pharmaceutical Sciences*, 122, 246-253. <https://doi.org/10.1016/j.ejps.2018.06.034>
- Ho, C. H., Sood, T., & Zito, P. M. (2024). Androgenetic alopecia. In StatPearls. StatPearls Publishing.
- Imran, M., Titilayo, B., Adil, M., Zhang, L., Mehmood, Q., Shahzada Hammad Mustafa, S. H., & Shen, Q. (2024). Ascorbyl palmitate: A comprehensive review on its characteristics, synthesis, encapsulation and applications. *Process Biochemistry*, 142, 68-80. <https://doi.org/10.1016/j.procbio.2024.04.015>
- Kar, M., Saquib, M., & Jain, D. K. (2020). Formulation development and evaluation of aspasomes containing skin whitening agent. *Manipal Journal of Pharmaceutical*, 6(1), 47-53.
- Khalil, R. M., Abdelbary, A., El-Arini, S. K., Basha, M., El-Hashemy, H. A., & Farouk, F. (2019). Development of tizanidine loaded aspasomes as transdermal delivery system: ex-vivo and in-vivo evaluation. *Journal of Liposome Research*, 31(1), 19-29. <https://doi.org/10.1080/08982104.2019.1684940>
- Lakra, R., Kiran, M. S., & Korrapati, P. S. (2021). Effect of magnesium ascorbyl phosphate on collagen stabilization for wound healing application. *International Journal of Biological Macromolecules*, 166, 333–341. <https://doi.org/10.1016/j.ijbiomac.2020.10.193>
- Lamie, C., Elmowafy, E., Attia, D., Elmazar, M. M., & Mortada, N. D. (2022). Diversifying the skin cancer-fighting worthwhile frontiers: How relevant are the itraconazole/ascorbyl palmitate nanovectors? *Nanomedicine*, 43, 102561. <https://doi.org/10.1016/j.nano.2022.102561>

- Ledinski, M., Marić, I., Peharec Štefanić, P., Ladan, I., Caput Mihalić, K., Jurkin, T., Gotić, M., Urlić, I. (2022). Synthesis and In vitro characterization of ascorbyl palmitate-loaded solid lipid nanoparticles. *Polymers*, 14, 1751. <https://doi.org/10.3390/polym14091751>
- Let, M. B., Jacobsen, C., & Meyer, A. S. (2007). Ascorbyl palmitate, gamma-tocopherol, and EDTA affect lipid oxidation in fish oil enriched salad dressing differently. *Journal of Agricultural and Food Chemistry*, 55(6), 2369-2375. <https://doi.org/10.1021/jf062675c>
- Martínez-Jacobo, L., Villarreal-Villarreal, C. D., Ortiz-López, R., Ocampo-Candiani, J., & Rojas-Martínez, A. (2018). Genetic and molecular aspects of androgenetic alopecia. *Indian Journal of Dermatology, Venereology, and Leprology*, 84(3), 263. [https://doi.org/10.4103/ijdv.ijdv1\\_262\\_17](https://doi.org/10.4103/ijdv.ijdv1_262_17)
- Ogbechie-Godec, O. A., & Elbuluk, N. (2017). Melasma: an Up-to-Date Comprehensive Review. *Dermatology and Therapy*, 7(3), 305-318. <https://doi.org/10.1007/s13555-017-0194-1>
- Ozgen, S., Kilinc, O. K., & Selamoğlu, Z. (2016). Antioxidant activity of quercetin: A mechanistic review. *Turkish Journal of Agriculture - Food Science and Technology*, 4(12), 1134. <https://doi.org/10.24925/turjaf.v4i12.1134-1138.1069>
- Prabhu, P., Shetty, Koland, M., Bhat, V., Vijayalakshmi, K., Nairy, H., & Shetty, N. (2012). Investigation of nano lipid vesicles of methotrexate for anti-rheumatoid activity. *International Journal of Nanomedicine*, 177. <https://doi.org/10.2147/ijn.s25310>
- Prabhu, P., Shetty, Koland, M., Bhat, V., Vijayalakshmi, K., Nairy, H., & Shetty, N. (2012). Investigation of nano lipid vesicles of methotrexate for anti-rheumatoid activity. *International Journal of Nanomedicine*, 177. <https://doi.org/10.2147/ijn.s25310>
- Shinde, G., Desai, P., Shelke, S., Patel, R., Bangale, G., & Kulkarni, D. (2020). Mometasone furoate-loaded aspasomal gel for topical treatment of psoriasis: formulation, optimization, in vitro and in vivo performance. *Journal of Dermatological Treatment*, 33(2), 885-896. <https://doi.org/10.1080/09546634.2020.1789043>
- Şenyiğit, T., Padula, C., Özer, Z., & Santi, P. (2009). Different approaches for improving skin accumulation of topical corticosteroids. *International Journal of Pharmaceutics*, 380(1-2), 155-160. <https://doi.org/10.1016/j.ijpharm.2009.07.018>
- Tiplica, G., & Salavastru, C. (2009). Mometasone furoate 0.1% and salicylic acid 5% vs. mometasone furoate 0.1% as sequential local therapy in psoriasis vulgaris. *Journal of the European Academy of Dermatology and Venereology*, 23(8), 905-912. <https://doi.org/10.1111/j.1468-3083.2009.03214.x>
- Wilczewska, A. Z., Niemirowicz, K., Markiewicz, K. H., & Car, H. (2012). Nanoparticles as drug delivery systems. *Pharmacological Reports*, 64(5), 1020-1037. [https://doi.org/10.1016/s1734-1140\(12\)70901-5](https://doi.org/10.1016/s1734-1140(12)70901-5)
- Wu, J., Du, J., Wu, J., & Du, X. (2023). Modification of high temperature radiation absorption properties of solid particles with surface coating. *Solar Energy Materials and Solar Cells*, 263, 112567. <https://doi.org/10.1016/j.solmat.2023.112567>
- Yadav, P., & Lariya, N. (2018). Formulation And Evaluation of Nanocarrier Drug Delivery System For Hyperpigmentation. *Journal of Pharma Research*, 7(1), 13-18. <https://doi.org/10.5281/zenodo.1159012>

Yücel, Ç., Şeker Karatoprak, G., Ilbasımış-Tamer, S., Değim, İ. T. (2023). Ferulic acid-loaded aspasomes: A new approach to enhance the skin permeation, anti-aging and antioxidant effects. *Journal of Drug Delivery Science and Technology*, 86, 104748. <https://doi.org/10.1016/j.jddst.2023.104748>

Zırh Gürsoy, A. (2002). *Kontrollü salım sistemleri*. İstanbul, Türkiye: Kontrollü Salım Sistemleri Derneği, 3-5.

# A Review on Calcium-alginate microspheres for Drug Delivery System: Characteristics, Drug Release, Activity, Stability and *In Vivo* Studies

Amiruddin AMIRUDDIN<sup>\*,\*\*</sup>, Mahardian RAHMADI<sup>\*\*\*</sup>,  
Dewi Melani HARIYADI<sup>\*\*\*\*,\*\*\*\*\*</sup>

*A Review on Calcium-alginate microspheres for Drug Delivery System: Characteristics, Drug Release, Activity, Stability and In Vivo Studies*

## SUMMARY

Microspheres are one of the drug delivery systems that allow therapeutic agents to penetrate the body to increase their efficacy and safety by regulating their rate of release, timing, and site of action in the body. Alginate is a natural polymer of polysaccharides that has the advantages of being biocompatible, low toxicity, inexpensive, easy to obtain, and capable of chemical modifications. Calcium chloride is the most suitable crosslinker for sodium alginate. Research on calcium-alginate microspheres has been widely developed to deliver various drugs. Therefore, this review provides a comprehensive summary of research focusing on the characteristics, drug release, activity, stability, and in vivo studies of calcium-alginate microspheres for drug delivery.

**Key Words:** Microspheres, alginate, calcium chloride, characteristics, in vitro studies, stability, in vivo studies

*İlaç Taşıma Sistemi için Kalsiyum-aljinat mikroküreleri Üzerine Bir Derleme: Özellikler, İlaç Salımı, Aktivite, Stabilitate ve In Vivo Çalışmaları*

## ÖZ

Mikroküreler, terapötik ajanların vücutta salım hızını, zamanlamasını ve etki alanını düzenleyerek etkinliğini ve güvenliğini artırmak için vücuda nüfuz etmesini sağlayan ilaç taşıma sistemlerinden biridir. Aljinat, biyoyumlu, düşük toksisiteli, ucuz, kolay elde edilebilir, kimyasal modifikasyonlara uygun olma gibi avantajlara sahip, doğal bir polisakkarit polimeridir. Kalsiyum klorür, sodyum aljinat için en uygun çapraz bağlayıcıdır. Çeşitli ilaçların taşınmasında kalsiyum-aljinat mikroküreleri üzerine araştırmalar yaygınlaşmıştır. Bu nedenle, bu derleme kalsiyum-aljinat mikrokürelerinin ilaç salımı için karakteristikleri, ilaç salımı, aktivitesi, stabilitesi ve in vivo çalışmaları üzerine odaklanan araştırmaların kapsamlı bir özetini sunmaktadır.

**Anahtar Kelimeler:** Mikroküreler, aljinat, kalsiyum klorür, özellikler, in vitro çalışmalar, stabilite, in vivo çalışmalar.

Received: 06.07.2024

Revised: 22.10.2024

Accepted: 27.11.2024

\* ORCID: 0009-0001-2376-4527, Doctoral Programme of Pharmaceutical Sciences, Faculty of Pharmacy, Universitas Airlangga, Surabaya 60115, Indonesia.

\*\* ORCID: 0009-0001-2376-4527, Department of Pharmaceutical Sciences, Faculty of Pharmacy, Universitas Airlangga, Campus C Mulyorejo, Surabaya 60115, Indonesia.

\*\*\* ORCID: 0000-0002-7256-2446, Department of Pharmacy Practice, Faculty of Pharmacy, Universitas Airlangga, Campus C Mulyorejo, Surabaya 60115, Indonesia.

\*\*\*\* ORCID: 0000-0001-9357-3913, Department of Pharmaceutical Sciences, Faculty of Pharmacy, Universitas Airlangga, Campus C Mulyorejo, Surabaya 60115, Indonesia.

\*\*\*\*\* ORCID: 0000-0001-9357-3913, Pharmaceutics and Delivery Systems for Drugs, Cosmetics and Nanomedicine (Pharm-DCN) Research Group, Faculty of Pharmacy, Universitas Airlangga, Campus C Mulyorejo, Surabaya 60115, Indonesia.

## INTRODUCTION

Drug delivery systems are defined as formulations or devices that allow the entry of therapeutic agents into the body to increase their efficacy and safety by regulating their release rate, timing, and site of action in the body (Jain, 2020). One of the carriers for drug delivery is the microspheres. Microspheres may be used for controlled release of drugs, antibiotics, vaccines, and hormones (Prasad et al., 2014). Microspheres consist of a drug or core of active agents and polymers (Kadam et al., 2015). The type of polymer used can be derived from natural or synthetic. Still, natural polymers have the advantages of being cheap, readily to use, biocompatible, biodegradable, and able to do a multitude of chemical modifications (Rajeswari et al., 2017). Alginate is a naturally occurring polysaccharide polymer that is generally found in the cell walls of brown algae (Phaeophyceae) species (Lee & Mooney, 2012). The structure consists of  $\beta$ -D-Mannuronic acid (M) and  $\alpha$ -L-Guluronic acid (G) residues linked through 1,4 bound in various proportions and arrangements. Alginic acid containing a sodium salt is sodium alginate (Patil et al., 2010).

Over several decades, alginates have been extensively utilized in the design and improvement of various biopolymeric systems for a multitude of scientific and biomedical purposes, one of which is drug delivery due to its capability of carrying out many chemical modifications with the simple addition of crosslinkers such as divalent calcium ions from  $\text{CaCl}_2$  (Dhamecha et al., 2019; Hasnain et al., 2020). Calcium chloride with sodium alginate can be cross-linked because sodium alginate has a carboxyl group that bonds with  $\text{Ca}^{2+}$  ions (Fadhilah et al., 2019). Research on microspheres using sodium alginate polymers and  $\text{CaCl}_2$  crosslinkers has been widely developed to deliver various drugs. This review aims to comprehensively analyze characteristics, drug release, activity, stability, and *in vivo* studies of calcium-alginate microspheres for drug delivery.

## Alginate

Alginate is a naturally occurring polysaccharide polymer that is generally found in the cell walls of brown algae (Phaeophyceae) species (Lee & Mooney, 2012). The structure consists of  $\beta$ -D-Mannuronic acid (M) and  $\alpha$ -L-Guluronic acid (G) residues linked through 1,4 bound in various proportions and arrangements. Alginate when compared to gelatin, agar, and other polysaccharides, has a more remarkable ability to form gels that are not affected by temperature (Ching et al., 2017). Among the many alginates, that have received the most attention in the pharmaceutical and biomedical industries is sodium alginate (Szekalska et al., 2016). Sodium alginate is an alginic acid containing sodium salt with a chemical structure  $(\text{C}_6\text{H}_7\text{NaO}_6)_n$  and a mean molecular weight of 216.121g/mol (Frent et al., 2022). Sodium alginate has the advantages of being cheaper, biocompatible, biodegradable, low toxicity, readily to be had, having excellent thickening and gelling properties, and provides the highest mucoadhesive ability compared to other polymers, so it is widely used in drug delivery systems (Batista et al., 2019; Adrian et al., 2019; Fernando et al., 2020). Sodium alginate was exploited within the design and improvement of various biopolymeric systems for a multitude of scientific and biomedical purposes, one of which is drug delivery because sodium alginate is capable of carrying out many chemical modifications with the simple addition of crosslinkers such as divalent calcium ions from  $\text{CaCl}_2$  (Dhamecha et al., 2019; Uyen et al., 2019; Hasnain et al., 2020).

## Calcium Chloride

Calcium chloride is an inorganic salt substance with the chemical formula  $\text{CaCl}_2$ . Organoleptic calcium chloride is a white crystalline powder, granules, or crystalline mass and is hygroscopic (Rowe et al., 2009).  $\text{Ca}^{2+}$  ions are most preferred for developing microparticles compared to  $\text{Rb}^+$ ,  $\text{Cs}^+$ ,  $\text{K}^+$ ,  $\text{Na}^+$ ,  $\text{Li}^+$ ,  $\text{Ba}^{2+}$ ,  $\text{Sr}^{2+}$ , and  $\text{Mg}^{2+}$  because  $\text{Ca}^{2+}$  is the safest for the body (Tecante et al., 2012; Thi et al., 2019). Calcium

chloride is often used as a crosslinker to make alginate beads (Skrzypczak et al., 2019). Calcium chloride with sodium alginate can crosslink because sodium alginate has a carboxyl group at the guluronic acid (G) position, which binds to  $\text{Ca}^{2+}$  ions (Fadhilah et al., 2019). Based on competitive inhibition studies, the mechanism involved in the complexation of divalent cations and the G-block region of the polymer is the dimerization of G residues, is two G chains are

bonded to opposite sides of the alginate polymer by the addition of Ca ions. This alignment creates hydrophilic cavities with diamond-shaped holes that bind calcium ions through the multi-coordination of the oxygen atoms of the carboxyl groups. This tightly bonded polymer configuration causes the formation of a junction zone with an “egg box” shape (Ching et al., 2017). Figure 1. shows the egg-box structure of calcium-alginate.

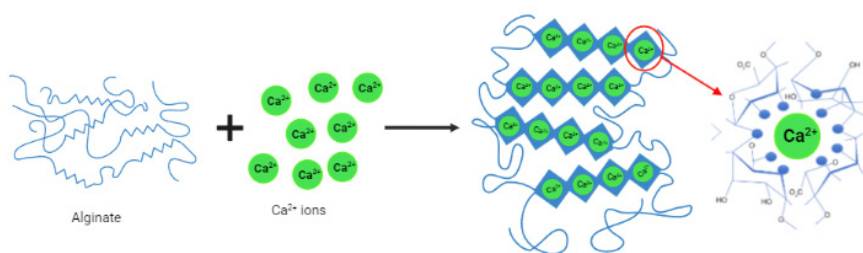


**Figure 1.** Schematic structure of “egg box” calcium-alginate (Ching et al., 2017).

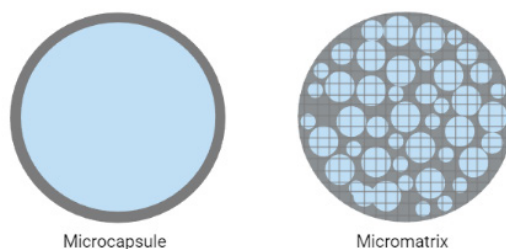


**Figure 2.** Schematic structure of microcapsule and micromatrix (Uyen et al., 2019).

### Microspheres

Microspheres serve as carriers for drug delivery, enabling the controlled release of various substances, including drugs, antibiotics, vaccines, and hormones (Prasad et al., 2014). Microspheres have a diameter of 1  $\mu\text{m}$  to 1000  $\mu\text{m}$  with spherical particles, consisting of drugs and polymers (Kadam et al., 2015). Microspheres are divided into microcapsules and micromatrices depending on how they are encapsulated, as shown in Figure 2. Microcapsules contain substances entrapped and ringed by distinct capsule walls whereas in micromatrices, entrapped materials are scattered all over the matrix (Solanki, 2018; Uyen et al., 2019). Microspheres have several benefits when compared to conventional drug delivery systems, including:

- The therapeutic effect of microspheres is prolonged and sustained.
- Microspheres increase bioavailability and reduce the frequency or severity of side effects.
- It improves patient adherence by reducing the frequency of dosing.
- Microspheres are small, spherical particles that are easy to inject into the body.
- The first-pass metabolism and toxicity of drugs are decreased by microspheres.
- Protection of drugs against the environment (Ramteke et al., 2012; Prasad et al., 2014; Verma, 2019; Tandale et al., 2020).

On the other hand, the microspheres have limitations:

- a. Release rates can vary due to diet and transit rates through the gut.
- b. Variations in the rate of release between doses.
- c. Materials and processing for the preparation of controlled release are significantly more expensive than for the conventional formulations (Prasad et al., 2014; Verma, 2019).

Calcium-alginate microspheres for drug delivery systems can be prepared using several methods. Three standard methods for preparing calcium-alginate microspheres are spray drying, extrusion, and emulsification/gelation techniques. The spray drying method for producing dry powder microspheres is fast, sustainable, economical, repeatable, and scalable. This method involves atomizing the alginate solution with hot air after mixing it with organic reagents (Sosnik & Seremeta, 2015). The extrusion method is the most straightforward and popular method for preparing drug-filled microspheres by alginate ionic gelation involving simple diffusion and crosslinking reactions by  $\text{Ca}^{2+}$  ions. The alginate solution is added dropwise to the crosslinking solution in the extrusion method (Uyen et al., 2019). The emulsification/gelation method can produce microspheres with a simple and inexpensive experimental setup. The emulsification/gelation process generally involves two key steps: first, the formation of stable polymer droplets, and second, the hardening of these droplets within the emulsion system. In this procedure, the gelation happens when the cross-linker ions and the alginate solution collide (Mishra, 2015). Calcium-alginate microspheres for drug delivery systems have been widely developed to date. Several evaluations of calcium-alginate microspheres have been conducted in vitro or in vivo. This evaluation aims to verify the effectiveness of the calcium alginate microspheres used in the drug delivery system, ensuring maximum and stable drug delivery.

### **Characteristics of Calcium-Alginate Microspheres for Drug Delivery System**

Generally, the characteristics of microspheres are influenced by several factors such as sodium alginate concentration, crosslinker concentration, crosslinking time, and preparation method (Kadam et al., 2015). Factors that affected the physical characteristics of calcium-alginate microspheres are as follows:

#### **Alginate concentration**

The concentration of alginate is a significant variable affecting the characteristics of calcium-alginate microspheres (yield, particle size, drug loading, and entrapment efficiency). The size of the droplet would increase due to the increase in the solution's viscosity brought on by the rise in alginate concentration, and the larger particle size of the large microsphere would result in an improvement in drug loading and entrapment efficiency (Hariyadi et al., 2019).

#### **Crosslinker concentration**

The concentration of  $\text{CaCl}_2$  used as a crosslinker, significantly influences the characteristics of the calcium-alginate microspheres. When the  $\text{CaCl}_2$  crosslinker solution comes into contact with the alginate polymer solution, it forms an egg-box structure (Ching et al., 2017). This occurs because of the bond between  $\text{Ca}^{2+}$  ions and the G-alginate structure containing carboxyl groups (Fadhilah et al., 2019). The increase in crosslinker concentration would provide more availability of  $\text{Ca}^{2+}$  ions to bind with the alginate polymer solution, causing the drug loading and entrapment efficiency to increase (Amiruddin et al., 2023). On the other hand, it was discovered that as the calcium chloride concentration increased, the mean particle size of the microspheres decreased. According to some reports, gelation happens right away when drops of alginate solution interact with calcium ions. When  $\text{Ca}^{2+}$  ions enter the droplet's interior, the water is squeezed out of the droplet, which causes the microspheres to contract and cause a smaller particle size (Manjanna et al., 2010).



### Crosslinking time

The crosslinking time significantly impacts the characteristics of calcium-alginate microspheres, especially in particle size and encapsulation efficiency. It was discovered that as the crosslinking time increased, the mean particle size of the microspheres shrank (Loquercio et al., 2015; Choukaife et al., 2020). According to some reports, gelation happens right away when drops of alginate solution interact with calcium ions. Longer crosslinking time causes Ca<sup>2+</sup> ions to enter the interior of the droplets, and water to be squeezed out of the droplets, which causes the microspheres to contract and smaller particle sizes to form (Manjanna et al., 2010). On the other hand, crosslinking time may decrease the entrapment efficiency of microspheres because longer stirring duration may cause polymer molecules to aggregate on the surface of microspheres and reduce the amount of free space in the alginate matrix, but shorter stirring time may not be enough to generate strong electrolyte interactions that condense polymer chains on the

microspheres (Mali et al., 2010; Łętocha et al., 2022).

### Preparation method

The method of preparation of calcium alginate microspheres affects the particle size because each method has advantages and disadvantages. In spray drying, the percent yield of the laboratory scale is not optimal due to product loss on the drying chamber walls and a low cyclone capacity to separate fines, less than <2 μm (Sosnik & Seremeta, 2015). The extrusion method has large particle sizes when compared to other methods, which can range from hundreds of micrometers to millimeters (Uyen et al., 2019). In the drop method, the crosslinker solution is added to the alginate-protein dispersion drop by drop using a burette, resulting in larger microsphere particle sizes comparing the aerosolization technique used in spray drying, so the resulting particle size is smaller (Mishra, 2015; Uyen et al., 2019). A summary of research on the characteristics of calcium-alginate microspheres for drug delivery systems is shown in Table 1.

**Table 1.** Characteristics of Calcium-Alginate Microspheres for Drug Delivery System

No.	Drug	Use	Alginate Conc.	CaCl <sub>2</sub> Conc.	Method	Characteristics	Ref.
1.	Ciprofloxacin HCl	Antibiotic	1%; 1.5%; 2%  2% - 3.5%	3%; 5%  0.5M; 1.5M	Ionotropic gelation method involving aerosolization	Microspheres were smooth and spherical, with a particle size of less than 5 μm, a moisture content <10%, a yield of 70.63%-82.94%, and drug loading and entrapment efficiencies between 2.58%-4.32% and 27.39%-80.74%. Particle size less than 5 μm with 89% yield, 80% drug loading, and entrapment efficiencies up to 95%.	(Hariyadi et al., 2019)  (Hariyadi et al., 2020)
2.	Gatifloxacin	Antibiotic	1% - 2.2%	7%; 10%	Ionotropic gelation method	The various formulations of Gatifloxacin microspheres exhibited distinct spherical shapes, and it was observed that those with a higher drug concentration had a rougher surface texture. The optimal formulation contained 1.8% sodium alginate, 0.432 mg of pectin, and 10% calcium chloride. This formulation achieved a yield of 96.30% and an entrapment efficiency of 95.66%.	(Nagasree et al., 2016)

3.	Ovalbumin	Protein Antigen	1%; 1.5%	0.25M; 0.5M; 1.5M	Ionotropic gelation using aerosolization and drop technique	Ovalbumin-loaded alginate microspheres have maximum loadings and encapsulation effectiveness of about 89%. Ovalbumin-loaded alginate microspheres produced by aerosolization have a smooth and spherical surface with an average particle size of 12 to 30 $\mu\text{m}$ smaller than the drop technique with microsphere sizes made of 1-3 mm.	(Hariyadi et al., 2014)
4.	Resveratrol	Antioxidant	0.5%; 1%	0.5%; 1%	Ionic gelation	Microspheres have an average particle size of 175.52 $\mu\text{m}$ and 244.03 $\mu\text{m}$ , with an entrapment efficiency of over 95%. Increasing $\text{CaCl}_2$ concentration resulted in higher entrapment efficiency and smaller particle size of microspheres.	(Ra et al., 2014)
5.	Risedronate Sodium	Osteoporosis drug	3%	2%; 4 %	Emulsification crosslinking method	The yield of Risedronate sodium microspheres is 61.29-89.33%, with entrapment efficiency of around 42.25-62.58% and mucoadhesion strength 68.15-82.24.	(Gedam et al., 2018)
6.	Gliclazide	Antidiabetic	1%	2-10%	Ionic gelation	Gliclazide microspheres had spherical shapes and rough surfaces with particle sizes between 752.12 $\mu\text{m}$ -948.49 $\mu\text{m}$ . These microspheres had a drug entrapment efficiency of around 58.12-82.78%. The entrapment efficiency of gliclazide microspheres decreased with increasing particle size, but on the other hand, the entrapment efficiency increased with decreasing TSP to alginate ratio and increasing crosslinker concentration.	(Pal & Nayak, 2012)
7.	Olmесartan	Antihypertensive	1% - 2.5%	6%; 10%	Ionotropic gelation method	The formula of microspheres containing sodium alginate 1.75%, ethyl cellulose 250 mg, and calcium chloride 10% showed a spherical shape with a good percentage yield of 98.34% and entrapment efficiency of 97.36%.	(Kumar & Suresh, 2018)
8.	Quercetin	Anti-inflammatory	1% - 2.5%	5.5%	Ionic gelation with aerosolization	Quercetin-loaded alginate microspheres have a percentage of yield 41.33%-76.14%, drug loading <6%, and entrapment efficiency 74.153%-93.805%. They also had particle sizes of less than 2 $\mu\text{m}$ with excellent flow.	(Kalalo et al., 2022)
9.	Cefixime	Antibiotic	3% - 6%	5%	Ionic gelation technique	Microspheres had more spherical shapes, smooth surfaces, good flowing characteristics with particle size 642-720 $\mu\text{m}$ , and efficiency of entrapment 88.30%-89.01%. The entrapment efficiency of microspheres increased with the increase of polymer.	(Vasam et al., 2016)

10.	Aceclofenac	NSAID	1% - 6%	5%	Ionic gelation technique	Microspheres have a particle size that ranges from 650 to 802 $\mu\text{m}$ , with a yield between 88.71% and 96.64%. The drug loading varies from 13.19% to 28.65%, while the entrapment efficiency lies between 51.29% and 89.34%. The entrapment efficiency and particle size of aceclofenac microspheres increased with higher polymer concentration.	(Chakraborty et al., 2012)
11.	Erythropoietin	Glycoprotein hormone	2%	0.5M; 0.75M; 1M	Ionotropic gelation method involving aerosolization	Microspheres have smooth and spherical surfaces with particle size of about 2.86-3.23 $\mu\text{m}$ and mass swelling index at 24h between 1.11-1.25; at 30 h, it was 1.72-2.00 and yield around 77.76-82.97%.	(Hariyadi et al., 2018)
12.	Risperidone	Antipsychotic	1.5%; 3%	5%	Employing cross-linking method	The formed microspheres exhibited good drug loading 78.6-59.9% and encapsulation efficiencies 71.97-72.63%. Increasing the drug-to-alginate ratio increased the percentage of loading.	(Al-Tahami, 2014)
13.	Glutathione	Antioxidant	2%	1M	Ionotropic gelation method involving aerosolization	Alginate microspheres loaded with glutathione and surfactants have been successfully created. Alginate 2% was used to produce the small and spherical microspheres.	(Hariyadi et al., 2018)
14.	Bordetella pertussis	Vaccine	3.8%	8%	Emulsification method	The microspheres, both empty and loaded with <i>Bordetella pertussis</i> , have smooth and spherical surfaces. The microspheres containing <i>Bordetella pertussis</i> produced under ideal circumstances had an average particle size of 151.1 $\mu\text{m}$ , a polydispersity index of 0.43, an 89.6% loading efficiency, and a 36.3% loading capacity.	(Dounighi et al., 2017)

### In Vitro Drug Release of Calcium-Alginate Microspheres for Drug Delivery System

The process by which drug molecules in the drug delivery system are transferred to the external surface and then, as solutes, into the release medium is referred to as drug release (Talevi & Ruiz, 2021). It is a complicated phenomenon that may include one or more processes depending on the delivery system (Bruschi et al., 2015). Diffusion, swelling, erosion, and degradation are common mechanisms by which drugs are released from the microspheres (Asmatulu et al., 2009; Balagani et al., 2011), shown in Figure 3.

#### Diffusion

Diffusion is the process of moving a substance mass in individual molecules from one area of a system to another where there is a gradient concentration. The spontaneous flow of matter reduces the concentration difference during this process. Mass transfer in diffusion is a kinetic process in non-equilibrium

systems (Bruschi et al., 2015). When drug molecules in the system dissolve in body fluids surrounding or contained by the particles and move away from the particles, this is known as diffusion of microspheres (Balagani et al., 2011).

#### Swelling

The mechanism of release by swelling of the microspheres is initially dry microspheres. Still, when the microspheres are placed in the body in contact with aqueous, the microspheres expand, increasing the pressure and porosity inside of them, allowing drug molecules to escape from the swollen tissue (Balagani et al., 2011; Talevi & Ruiz, 2021). The swelling mechanism has three sequential steps: water diffusion, polymer chain relaxation, and drug dissolution, and diffusion (Wang et al., 2020).

#### Erosion

Some coating using polymers can be designed to gradually erode over time and release the drug that is

contained within the particles. The polymer erosion begins with a change in the carrier microstructure due to water penetrating it which leads to matrix plasticization so that the coating becomes thin and causes the entrapped drug to escape from the microsphere system (Balagani et al., 2011).

**Degradation**

Polymer degradation in the microsphere system occurs when the polymer chains are hydrolyzed so

that the microspheres that have a significant molecular weight become in the polymer chains (Asmatulu et al., 2009). In general, there are three degradation molecules with a lower molecular weight, and then successfully dissolve the drug molecules entrapped processes associated with the release of drug microspheres: physical methods, chemical processes, and biological processes (Wang et al., 2020).

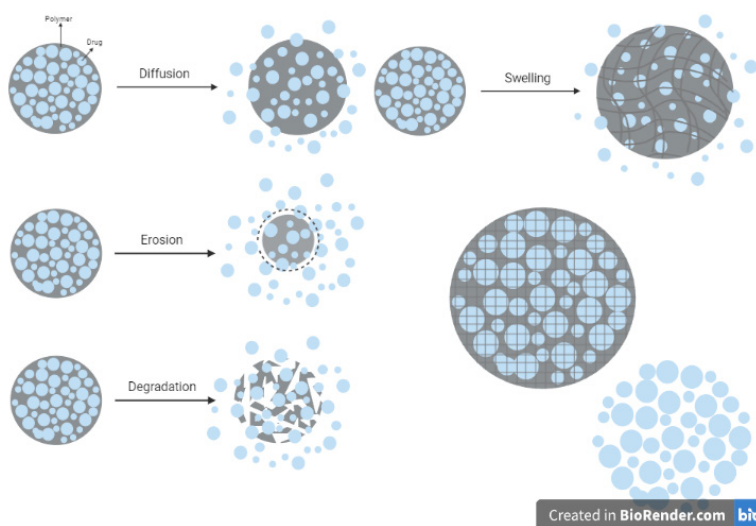


**Figure 3.** Schematic illustration of the drug release mechanism from the microspheres through diffusion, swelling, erosion, and degradation (Asmatulu et al., 2009).

Drug release of calcium-alginate microspheres follows several kinetics models including zero-order kinetics, first-order kinetics, Korsmeyer-Peppas, and Higuchi (Salome et al., 2013). Drug release is in zero-order kinetics, and time is only considered a function of drug release because the process moves forward at a constant rate regardless of drug concentration. First-order release kinetics describes the drug release from a system where the release rate is dependent on concentration. Both Fickian and non-Fickian drug release from swelling as well as non-swelling polymeric delivery systems were examined using the Korsmeyer-Peppas model. The Higuchi model describes the release of water-soluble

and low-solubility drugs, including in semisolid and solid matrices. The Higuchi model is based on several hypotheses, including that the initial concentration of the drug in the formulation is greater than the drugs solubility, that the drug is only dispersed in one dimension, that the substance’s particles are smaller than the size of the carrier, that swelling of the system and the drug’s dissolution are not significant, that the drug’s diffusivity is unaltered, and that sink conditions are reached (Salome et al., 2013; Wang et al., 2020). A summary of *in vitro* drug release studies of calcium-alginate microspheres for drug delivery systems is shown in Table 2.

**Table 2.** *In Vitro* Drug Release of Calcium-Alginate Microspheres

No.	Drug	Release Medium	<i>In Vitro</i> Release	Release Kinetics Profile	Ref.
1.	Ciprofloxacin HCl	Phosphate buffer saline (pH 7.4)	The amount of ciprofloxacin released for 24 hours ranged from 80 to 100%. The release rate was shown to decrease with increasing alginate and CaCl <sub>2</sub> .	Zero order with a mechanism based on non-Fickian diffusion	(Hariyadi et al., 2019)
2.	Gatifloxacin	N HCl (pH 1.2)	The optimum formulation, containing sodium alginate 1.8%, pectin 0.432 mg, and calcium chloride 10%, showed the highest release, 95.21%, after 12 h. This formulation provides a controlled release compared to the innovator product.	Higuchi model with non-Fickian diffusion release mechanism	(Nagaree et al., 2016)
3.	Resveratrol	Phosphate buffer saline (pH 7.4)	In comparison to wet microspheres, freeze-dried resveratrol microspheres showed a slower initial burst release. Dry microspheres only release 30% of their load while more than 60% of their loadings are released by wet microspheres during 30 minutes. Increasing alginate and crosslinker concentrations resulted in a slower release rate for microspheres.	Korsmeyer-Peppas model with anomalous transport mechanism	(Ra et al., 2014)
4.	Olmesartan	N HCl (pH 1.2)	The formulation containing sodium alginate 1.75%, ethyl cellulose 250 mg, and CaCl <sub>2</sub> 10% was the optimum formula and showed the highest drug release 96.98% ± 5.28 within 12 hours. Olmesartan microspheres may represent a viable option for sustained drug delivery, providing a secure and efficient method that increases bioavailability.	Zero order with anomalous non-Fickian diffusion	(Kumar & Suresh, 2018)
5.	Aceclofenac	0.1 N HCl (pH 1.2) for 2 hours followed by phosphate buffer (pH 6.8)	Aceclofenac was released slowly in an acidic medium (3.16% to 11.31%) and more rapidly in a phosphate buffer due to the swelling and rapid erosion of sodium alginate in the higher pH environment. Additionally, the release of aceclofenac slowed as the polymer concentration increased, with a sustained release observed for up to 12 hours.	Korsmeyer-Peppas model with Fickian diffusion mechanism	(Chakraborty et al., 2012)
6.	Metronidazole	0.1 M HCl (pH 1.2) and simulated vaginal fluid (SVF pH 4.2)	After 0.5 hours, significant burst releases of metronidazole were seen in SVF, and for the next 4 hours, the drug continued to be released continuously. In contrast, there was no burst effect in 0.1M HCl, and after 3 hours, 80% metronidazole was released and lasted for up to 6 hours. Metronidazole is sustained and released in 0.1M HCl when sodium alginate is converted to insoluble (at acidic pH) alginic acid.	First order with a mechanism based on fiction diffusion in SVF and anomalous transport in HCl	(Szekalska et al., 2015)
7.	Diclofenac Sodium	HCL/NaCl (pH=1.2) and Phosphate buffer saline (pH 6.8)	Diclofenac microspheres did not swell and did not dissolve in acidic media so the cumulative release obtained was only less than 1%. In contrast, in phosphate-buffered saline solution, the release of diclofenac approached 100% within 3 hours. Sustained release of diclofenac is obtained by a first-order kinetics model.	First order with a mechanism based on Fickian diffusion	(Song et al., 2018)
8.	Curcumin	Phosphate buffer saline (pH 7.4).	The formulation containing alginate 4% (w/v) was the optimum formula. The alginate matrix system effectively encapsulated curcumin, resulting in a prolonged drug release pattern over an extended period, with 98.32% of the drug released cumulatively after 672 h. Furthermore, the high Ca <sup>2+</sup> crosslinker concentration may have contributed to the extended drug release behavior.	Zero order with anomalous non-Fickian diffusion	(Uyen et al., 2020)

9.	Zidovudine	0.1 M HCl and Phosphate buffer saline (pH 7.4)	It was discovered that the total percentage of medication released from the various formulations ranged between 84.63% and 97.17%. Zidovudine release from the microspheres was prolonged for 8 to 12 hours. Microspheres produced with sodium alginate and 1% chitosan as the coated polymer showed a satisfactory sustained release profile.	Zero order with a mechanism based on bizarre and super case (II) transport	(Rao & Kanakamn, 2019)
10.	Histone Deacetylase Inhibitor (HDACi)	Phosphate buffer saline (pH 7.4)	The drug release time gradually increased as the concentration of Ca <sup>2+</sup> increased. At a concentration of 2% crosslinked calcium ions, the duration of drug release was approximately 7 minutes. This duration was extended to about 25 minutes when the calcium ion concentration increased to 10%.	-	(Man et al., 2022)
11.	Gallic Acid and Crocin	Distilled water (pH 6.8)	Gallic acid and crocin, as bioactive substances, were released from microcapsules with rapid kinetics (85% within the first 20 minutes for gallic acid and 75% within the first 50 minutes for crocin) at a pH of 6.8 in distilled water (as a hydrophilic system) with no observed effect of alginate polymer concentration on the release kinetics. The release mechanism is affected by the structure and physicochemical properties of the encapsulated molecules.	The release kinetics of gallic acid and crocin follow the Korsmeyer–Peppas model with the Fickian diffusion mechanism.	(Essifi et al., 2021)

*In vitro* drug release studies of calcium-alginate microspheres have shown that increasing concentration of polymers and crosslinker causes a decrease in drug release (Hariyadi et al., 2014; Ra et al., 2014; Al-Tahami, 2014; Hariyadi et al., 2019; Kalalo et al., 2022) this occurs due to an increase in the viscosity and bond strength of the crosslinker so that the surface of the formed microspheres is thicker and denser, resulting in a more extended drug release from the microspheres due to a slower rate of diffusion of the loose media into the microspheres, thereby preventing burst release (Ra et al., 2014) and obtaining extended drug release such as risperidone microspheres showed extended drug release for 8 hours in phosphate buffer

(Al-Tahami, 2014), controlled drug release (Nagasree et al., 2016), sustained drug release (Szekalska et al., 2015; Kumar & Suresh, 2018; Song et al., 2018; Uyen et al., 2020) and prolonged release (Rao & Kanakamn, 2019).

***In Vitro* Activity of Calcium-Alginate Microspheres for Drug Delivery System**

*In vitro* activity studies of calcium alginate microspheres were carried out to assess the activity capabilities of drugs encapsulated in the microsphere system compared with conventional preparations. Several studies regarding the use of microspheres as a drug delivery system to increase drug activity are shown in Table 3.

**Table 3.** *In Vitro* Activity of Calcium-Alginate Microspheres

No.	Drug	Application	<i>In Vitro</i> Activity	Ref.
1.	Ciprofloxacin HCl	Antibacterial activity	The <i>in vitro</i> diffusion technique was used to test the antibacterial activity. An inhibitory diameter ranging from 15.05 ± 0.07 mm and 15.30 ± 0.36 mm was observed in the ciprofloxacin-alginate formula antibacterial activity test against <i>Staphylococcus aureus</i> (ATCC 6538). Similarly, an inhibitory diameter ranging from 15.37 ± 0.38 mm and 15.92 ± 0.28 mm was observed in the antibacterial activity test against <i>Escherichia coli</i> (ATCC 8739).	(Hariyadi et al., 2019 <sup>a</sup> )
2.	Curcumin	Antibacterial activity	The agar well diffusion technique was used to test for antibacterial activity. The microsphere sample displayed an inhibition zone measuring 1.21 cm in diameter on the <i>Staphylococcus aureus</i> (ATCC 12600), but no inhibition zone was visible on the <i>Escherichia coli</i> (ATCC 25922). Therefore, the <i>in vitro</i> analysis indicates that Cur-AMs were resistant to <i>E. coli</i> and susceptible to <i>S. aureus</i> .	(Uyen et al., 2020)
3.	Ciprofloxacin HCl	Antibacterial activity	The <i>in vitro</i> diffusion technique was used to test the antibacterial activity. It was shown that the activity of every formula microsphere against <i>Staphylococcus aureus</i> (ATCC 25923) was greater than that of ciprofloxacin HCl. However, ciprofloxacin HCl was only effective at alginate polymer concentration greater than 0.75%, according to results for the formula against <i>Pseudomonas aeruginosa</i> (ATCC 27853).	(Hariyadi et al., 2019 <sup>b</sup> )
4.	Nystatin	Antifungal activity	The antifungal activity of the microspheres was tested using the <i>Candida albicans</i> (ATCC 10231). In all nystatin-loaded microspheres, fungicidal activity was shown for up to 48 hours. When the commercial product and microspheres were separated for four hours, no statistically significant differences were seen. Nystatin microspheres showed marked fungicidal activity, as evidenced by a drastic reduction in the initial load of <i>Candida albicans</i> .	(Martin et al., 2015)
5.	Metformin	Hypoglycemic activity	The hypoglycemic effect was studied <i>in vitro</i> using a glucose uptake assay by <i>Saccharomyces cerevisiae</i> cells. Alginate microspheres improve the hypoglycemic activity of metformin, according to the evaluation of its <i>in vitro</i> hypoglycemic activity.	(Szekalska et al., 2016)
6.	Astaxanthin	cell proliferation inhibition of hepatoma cells	The growth of THLE-2 cells was not inhibited by astaxanthin. However, after 96 hours of incubation at 40 μM, the development of HepG2 cells was significantly suppressed, with an inhibition rate that could reach 40%. The current investigation showed that astaxanthin encapsulated in calcium alginate could inhibit the division of HepG2 cells, but had little to no influence on the proliferation of THLE-2 cells.	(Zhang et al., 2020)
7.	Doxorubicin and NaHCO <sub>3</sub>	Anticancer activity	The cytotoxicity of alginate microspheres with or without NaHCO <sub>3</sub> and, or with or without Dox was assessed using two cell lines generated from hepatocellular carcinomas: Huh-7 [Tumor Protein 53 (TP53)-positive] and Hep-3B (TP53-deficient). The results showed that cell viability decreased in microspheres containing Dox with a relatively high NaHCO <sub>3</sub> ratio in both time- and dose-dependent manners.	(Pan et al., 2021)

**Stability of Calcium-Alginate Microspheres for Drug Delivery Systems**

Pharmaceutical product stability is a complex set of processes for developing the effectiveness, quality, and safety of pharmaceutical product formulations. According to ICH, based on temperature and humidity, the stability test is divided into four climate zones: Zone I (temperature climate), Zone II (subtropical and Mediterranean climates), Zone III (hot and dry

climate), and Zone IV (hot and humid environment). Generally, stability carried out on calcium alginate microspheres includes long-term/real-time stability and accelerated (WHO, 2018). Factors that affect drug stability include temperature, humidity, pH, excipients, oxygen, and light (Zothanpuui et al., 2020). The stability of calcium-alginate microspheres for drug delivery is shown in Table 4.

**Table 4.** Stability Study of Calcium-Alginate Microspheres

No.	Drug	Method	Stability Result	Ref.
1.	Ciprofloxacin HCl	The accelerated stability test was conducted for 28 days at 0, 7, 14, 21, and 30 days in a room at 25±2°C and an oven at 40±2°C with RH 75±5%.	After 30 days of storage, it was confirmed that all the microspheres were stable because there had been no appreciable changes to their morphology, organoleptic, and drug content.	(Hariyadi et al., 2020)
2.	Gatifloxacin	According to ICH guidelines, the stability study was conducted under various conditions and stored in a stability chamber. Accelerated stability tests were run for 6 months at 40°C and 75% RH.	Stability studies were conducted over 6 months to measure the yield percentage, entrapment efficiency, and in-vitro drug release profile. The results indicate that the optimized formulation is stable and maintains its original properties.	(Nagasree et al., 2016)
3.	Risedronate Sodium	The effect of temperature and humidity on the microspheres was tested during a 30-day stability test that was conducted at 4°C and 45% RH.	Microspheres kept at room temperature lose their stability over time, but those kept at 4°C retain their strength. This is indicated by the decreased entrapment efficiency and different drug release patterns after storage at room temperature for 30 days.	(Gedam et al., 2018)
4.	Olmесartan	Following ICH recommendations, the stability test of the optimum formulas was performed under various circumstances. The accelerated stability test was conducted for 6 months in a stability chamber at 40±2°C with RH 75±5%.	Stability test results show minor variations in yield percentage, entrapment efficiency, and cumulative percent of drug released so that the optimized formulation is stable and retains its original properties.	(Kumar & Suresh, 2018)
5.	Quercetin	The stability of quercetin-loaded calcium alginate microspheres was tested for 28 days at two different temperatures 25°C±2°C and 40°C±2°C, RH 75±5%.	The findings revealed that particle size increased at both 25°C and 40°C. However, the four formulas still meet the inhalation delivery requirement of a particle size of >6 µm.  Because quercetin was degraded during storage under the influence of temperature and storage time, thereby decreasing the drug loading and entrapment efficiency of the microsphere.	(Kalalo et al., 2022)
6.	Aceclofenac	Following ICH guidelines, the formulation of microspheres aceclofenac was tested for stability. Six sets of microsphere samples were prepared, sealed in tubes, and stored for 30 days in a room at 25±2°C with RH 60±5% and under accelerated conditions at 40±2°C with RH 75±5%.	The optimized alginate microsphere formulation had a shelf life of 3.57 years at room temperature and 1.96 years under accelerated conditions. The texture of the microspheres had barely changed after 150 days. Within 180 days, the drug loading in the accelerated condition dropped to 97.55%, whereas good stability was seen in the case of room temperature (98,61±3.26%).	(Chakraborty et al., 2012)
7.	Glutathione	Storage in an oven for five days at 50, 60, 80°C and 75%RH was required for the glutathione microspheres stress test.	According to the results of the stress test, glutathione belonged to the first-order. Furthermore, the glutathione is more stable with surfactants than glutathione alone.	(Hariyadi et al., 2018)
8.	Zidovudine	According to ICH guidelines, the microspheres produced in this study were kept in HDPE containers for 3 months at 40°C/75% RH. Next, the drug loading was characterized.	The accelerated stability test findings indicated that the microsphere formulation was stable. This is demonstrated by the fact that the percentage of drug loading in the microsphere formulation has not changed significantly.	(Rao & Kanakamn, 2019)

Based on the results of research on the stability of calcium-alginate microspheres that have been developed for drug delivery, it can be concluded that drug stability can be increased and maintained when the drug is encapsulated in a matrix such as calcium-alginate microspheres with a preparation that uses sodium alginate as a polymer and CaCl<sub>2</sub> as a crosslinker.

#### ***In Vivo* Studies of Calcium-Alginate Microspheres for Drug Delivery Systems**

An *in vivo* study tests drugs or chemicals in living organisms, such as animals or humans. This method aims to determine the effect of drugs or chemicals on the organism, including possible side effects. *In vivo* testing is often used to develop new drugs, including the development of calcium-alginate microspheres for drug delivery systems. A summary of the *in vivo* studies of calcium-alginate microspheres is shown in Table 5.



**Table 5.** *In Vivo* Studies of Calcium-Alginate Microspheres

No.	Drug	Pharmaceutical Applications	<i>In Vivo</i> Study	Ref.
1.	Gliclazide	Antidiabetic	<p>Gliclazide microspheres were used in <i>in vivo</i> investigations comparing pure gliclazide solution to diabetic albino rats caused by alloxan. When pure gliclazide solution is administered, blood glucose levels can drop sharply for up to 2 hours before swiftly returning to normal. In contrast, when gliclazide microspheres are administered, the most significant drop in blood glucose levels is observed 4 hours after oral administration and the decrease in blood glucose levels lasts 12 hours.</p> <p>These <i>in vivo</i> studies demonstrate that gliclazide microspheres effectively lower blood glucose levels when administered orally. These <i>in vivo</i> investigations show the gliclazide microspheres have significant hypoglycemic effects when taken orally. They may be beneficial for the extended systemic absorption of gliclazide to sustain appropriate blood glucose levels and improve patient adherence.</p>	(Pal & Nayak, 2012)
2.	Aceclofenac	Anti-inflammatory	<p>Aceclofenac microspheres, pure drug, and marketed formulations were tested for their anti-inflammatory, based on their ability to prevent rat hind paw edema caused by carrageenan.</p> <p>The anti-inflammatory action of the pure medication is remarkably rapid (<math>88.71 \pm 7.78\%</math> inhibition in 4 hours) when compared to the marketed product (<math>74.47 \pm 3.64\%</math> inhibition in 8 hours) and optimized alginate microsphere formulation (<math>84.41 \pm 4.82\%</math> inhibition in 8 hours).</p> <p>Studies conducted <i>in vivo</i> have demonstrated that aceclofenac microspheres had a much stronger and longer-lasting anti-inflammatory effect than pure aceclofenac.</p>	(Chakraborty et al., 2012)
3.	Nystatin	Antifungal	<p>According to <i>in vivo</i> research, nystatin was not detected in the bloodstream, indicating the treatment's safety.</p> <p>The levels of nystatin that were kept in the mucosa were more than sufficient to have a fungicidal impact that was successful and without causing tissue damage.</p> <p>The resulting levels of nystatin kept in the microsphere-retained porcine mucosa were <math>4.73 \pm 0.18 \mu\text{g/g tissue/cm}^2</math>. The concentration of nystatin that was retained in the mucosa was six times higher than the <math>0.78 \mu\text{g/mL}</math>, or <math>0.79 \mu\text{g/g}</math>, minimum inhibitory concentration (MIC).</p>	(Martin et al., 2015)
4.	Carvedilol	Pharmacokinetics  Deposition and Clearance	<p>A pharmacokinetics investigation showed that the area under the curve (AUC) of carvedilol microspheres increased. Following intranasal delivery of carvedilol microspheres and carvedilol solution intravenously, the AUC was approximately <math>215.83 \pm 18.56</math> and <math>54.06 \pm 6.45 \mu\text{g h/mL}</math>, and <math>C_{\text{max}}</math> values of microspheres were <math>64.85 \pm 4.15 \mu\text{g h/mL}</math>.</p> <p>Carvedilol microspheres had a relative bioavailability of 67.87%, suggesting that nasal administration enhances carvedilol absorption from alginate microspheres in rabbits.</p> <p>As demonstrated by pharmacokinetic studies, the gamma scintigraphy showed that the microspheres cleared more slowly and stayed in the nasal cavity longer than the lactose powder (61.55% of the alginate microspheres and 87.36% of the lactose powder were cleared from the nasal cavity after 4 hours). This implies that the nasal mucosa's sustained and improved medication absorption is provided by the microspheres.</p>	(Patil et al., 2012)
5.	Mesalamine	Anti-inflammatory	<p><i>In vivo</i> research was carried out on rats with inflammatory colonic lesions, and a decrease in the ulcer index was observed. The colon damage score for healthy controls was <math>0.0 \pm 0.0</math>, colitis controls was <math>5.0 \pm 0.0</math>, and the scores for those treated with conventional mesalamine and mesalamine microspheres were <math>2.2 \pm 0.8</math> and <math>1.6 \pm 0.6</math>, respectively.</p> <p>Compared to other groups, the mesalamine microsphere formulation intended for the colon demonstrated a notable decrease in ulcer index.</p> <p>Moreover, tissue sample histological analysis verified the outcomes. The amount and severity of histological indications of cell damage were significantly reduced in the mesalamine microsphere formulation. There were no indications of bleeding or ulceration, and the colon looked normal.</p>	(Patole & Pandit, 2018)

6.	Vascular Endothelial Growth Factor (VEGF)	Angiogenesis protein for Revascularization	Adipose tissue transplantation receptors were created using BALB/c nude mice. Mice were given subcutaneous implants of adipocytes combined with VEGF-CA microspheres in their dorsum. In comparison to the other groups, the mass and microvascular density of the grafts in the VEGF-CA microspheres were observed to be statistically higher in a time-dependent way. Adipose graft neovascularization was markedly enhanced by VEGF-CA microspheres, which also increased adipocyte survival.	(Ding et al., 2015)
7.	Dendritic Cell	Tumor Vaccine	Tumor lysates, live tumor cells, a recombinant MIP-3a adenovirus, and BCG were all encapsulated in an alginate microsphere (PaLlTcAdMIP3a). PaLlTcAdMIP3a was employed as a model vaccination to evaluate its antitumor activity. PaLlTcAdMIP3a was injected into tumor-bearing mice, and the results demonstrated antitumor immunity in CT26, Meth A, B16-F10, and H22 models, both therapeutically and prophylactically, without increasing side effects.  The antitumor activity was partially eliminated with the depletion of CD8 <sup>+</sup> and CD4 <sup>+</sup> T cells. Additionally, the number of CD4 <sup>+</sup> CD25 <sup>+</sup> FOXP3 <sup>+</sup> regulatory T cells (Treg) in the tumor tissues decreased. In contrast, the number of IFN-g-producing CD8 <sup>+</sup> T cells increased significantly in both the spleen and the tumor tissues. These findings strongly imply that microspheres might be a helpful vaccination for tumor models.	(Huang et al., 2015)
8.	Isoniazid	Pharmacokinetics	Microspheres were prepared by encapsulating isoniazid into a calcium alginate-piperine matrix (INH-CaSP Ms) to improve the encapsulation efficiency and oral bioavailability of isoniazid. The oral bioavailability results showed that, compared to pure INH, INH-CaSP Ms significantly increased the oral bioavailability of INH by raising the C <sub>max</sub> , T <sub>max</sub> , t <sub>1/2</sub> , and AUC values.	(Telange et al., 2022)

## CONCLUSION

This review study explores a range of studies on the development of calcium alginate microspheres for drug delivery, primarily focusing on characteristics, drug release, activity, stability, and *in vivo* studies. Calcium-alginate microspheres have advantages over other formulations because alginate when compared to other polysaccharides, has a more remarkable ability to form gels that are not affected by temperature so that it has excellent thickening and gelling properties and provides the highest mucoadhesiveness and is capable of multiple chemical modifications with CaCl<sub>2</sub>. It has been determined in those studies that various formulations of calcium alginate-based microspheres possess diverse characteristics. Additionally, it has been shown that specific formulations exhibit a steady-slow release profile, thereby preventing burst release, and the microsphere formulation increased the drug activity through *in vitro* studies with good stability when the drug is encapsulated in a matrix such as calcium-alginate microspheres.

Furthermore, *in vivo* studies demonstrated increased drug effectiveness on calcium-alginate

microspheres compared with conventional formulations.

## ACKNOWLEDGMENTS

The authors thank the Faculty of Pharmacy Universitas Airlangga for the facilities and research support.

## AUTHOR CONTRIBUTION STATEMENT

Determination of the Subject (A, DMH), Literature Research (A, DMH, MR), Preparing the Study Text (A), Reviewing the Text (MR, DMH).

## CONFLICT OF INTEREST

The authors declare that there is no conflict of interest.

## REFERENCES

- Adrian, G., Mihai, M., & Vodnar, D. C. (2019). The Use of Chitosan, Alginate, and Pectin in the Biomedical and Food Sector- Biocompatibility, Bioadhesiveness, and Biodegradability. *Polymers*, 11(1837), 7–11.
- Al-Tahami Alkhaled Pharma, K. (2014). Preparation of Alginate Microspheres for the Delivery of Risperidone. *Yemeni Journal for Medical Sciences*, 8, 19–23.

- Amiruddin, Muh. Agus Syamsur Rijal, & Dewi Melani Hariyadi. (2023). Effect of CaCl<sub>2</sub> Crosslinker Concentration On The Characteristics, Release, and Stability of Ciprofloxacin HCl-Alginate-Carrageenan Microspheres. *Jurnal Farmasi Dan Ilmu Kefarmasian Indonesia*, 10(3), 312–323.
- Asmatulu, R., Fakhari, A., Wamocha, H. L., Chu, H. Y., Chen, Y. Y., Eltabey, M. M., Hamdeh, H. H., & Ho, J. C. (2009). Drug-Carrying Magnetic Nanocomposite Particles for Potential Drug Delivery Systems. *Journal of Nanotechnology*, 2009(January), 1–6.
- Balagani, P. K., Chandiran, I., B.Bhavya, & Manubolu, S. (2011). Microparticulate drug delivery system: a review. *Indian Journal of Pharmaceutical Science & Research*, 1, 19–37.
- Batista, P. S. P., de Morais, A. M. M. B., Pintado, M. M. E., & de Morais, R. M. S. C. (2019). *Alginate: Pharmaceutical and Medical Applications BT - Extracellular Sugar-Based Biopolymers Matrices* (E. Cohen & H. Merzendorfer (eds.); pp. 649–691). Springer International Publishing.
- Bruschi ML. (2015). Main mechanisms to control the drug release. *Strategies to Modify the Drug Release from Pharmaceutical Systems*, 37–62.
- Chakraborty, S., Khandai, M., Sharma, A., Khanam, N., Patra, C., Dinda, S., & Sen, K. (2012). Preparation and in vitro in vivo evaluation of aceclofenac loaded alginate microspheres: An investigation of effects of polymer using multiple comparison analysis. *Current Drug Delivery*, 9(5), 495–505.
- Ching, S. H., Bansal, N., & Bhandari, B. (2017). Alginate gel particles – A review of production techniques and physical properties. *Critical Reviews in Food Science and Nutrition*, 57(6), 1133–1152.
- Choukaife, H., Doolaanea, A. A., & Alfatama, M. (2020). Alginate nanoformulation: Influence of process and selected variables. *Pharmaceuticals*, 13(11), 1–35.
- Dhamecha, D., Movsas, R., Sano, U., & Menon, J. U. (2019). Applications of alginate microspheres in therapeutics delivery and cell culture: Past, present and future. *International Journal of Pharmaceutics*, 569(May), 118627.
- Ding, S. L., Zhang, M. Y., Tang, S. J., Yang, H., & Tan, W. Q. (2015). Effect of calcium alginate microsphere loaded with vascular endothelial growth factor on adipose tissue transplantation. *Annals of Plastic Surgery*, 75(6), 644–651.
- Dounighi N, Shahcheraghi F, Razzaghi-Abyaneh M, Nofeli M, Z. H. (2017). A New Vaccine Delivery Vehicle and Adjuvant Candidate: Bordetella pertussis Inactivated Whole Cells Entrapped in Alginate Microspheres. *Current Pharmaceutical Design*, 23(12), 2665–2672.
- Essifi, K., Brahmi, M., Berraouan, D., Ed-Daoui, A., El Bachiri, A., Fauconnier, M. L., & Tahani, A. (2021). Influence of Sodium Alginate Concentration on Microcapsules Properties Foreseeing the Protection and Controlled Release of Bioactive Substances. *Journal of Chemistry*, 2021.
- Fadhilah, S., Aisyah, N., Mohd, N., & Mat, K. A. (2019). Sodium alginate film: the effect of crosslinker on physical and mechanical properties. *IOP Conference Series: Materials Science and Engineering*, 209, 1–6.
- Fernando, I. P. S., Lee, W., Han, E. J., & Ahn, G. (2020). Alginate-based nanomaterials: Fabrication techniques, properties, and applications. *Chemical Engineering Journal*, 391.
- Frent, O. D., Vicas, L. G., Duteanu, N., Morgovan, C. M., Jurca, T., Pallag, A., Muresan, M. E., Filip, S. M., Lucaciu, R., & Marian, E. (2022). Sodium Alginate — Natural Microencapsulation Material of Polymeric Microparticles. *International Journal of Molecular Sciences Review*, 23(12108), 1–24.
- Gedam, S., Jadhav, P., Talele, S., & Jadhav, A. (2018). Effect Of Crosslinking Agent On Development Of Gastroretentive Mucoadhesive Microspheres Of Risedronate Sodium. *International Journal of Applied Pharmaceutics*, 10(4), 133–140.

- Hariyadi, D., & Hendradi, E. (2020). *Optimization Performance and Physical Stability of Ciprofloxacin HCL- Ca Alginate Microspheres : Effect of Different Concentration of Alginate*. 89–94.
- Hariyadi, D. M., & Hendradi, E. (2019a). Effect of Polymer Concentration on Micromeritics, Kinetics, and Activity of Ciprofloxacin HCL- Alginate Microspheres. *Asian Journal of Pharmaceutics*, 13(4), 349–355.
- Hariyadi, D. M., Hendradi, E., & Kurniawan, T. D. (2019b). Alginate Microspheres Encapsulating Ciprofloxacin HCL: Characteristics, Release and Antibacterial Activity. *International Journal of Pharma Research and Health Sciences*, 7(4), 3020–3027.
- Hariyadi, D. M., Hendradi, E., Purwanti, T., Fadil, F. D. G. P., & Ramadani, C. N. (2014). Effect of cross-linking agent and polymer on the characteristics of ovalbumin loaded alginate microspheres. *International Journal of Pharmacy and Pharmaceutical Sciences*, 6(4), 469–474.
- Hariyadi, D. M., Purwanti, T., & Adilla, S. (2018). Influence of crosslinker concentration on the characteristics of erythropoietin-alginate microspheres. *Journal of Pharmacy & Pharmacognosy Research*, 6(4), 250–259.
- Hariyadi, D. M., Rosita, N., & Nugrahaeni, F. (2018). Formulation, characteristic evaluation, stress test, and effectiveness study of matrix metalloproteinase-1 (MMP-1) expression of glutathione-loaded alginate microspheres and gel. *Pharmaceutical Sciences*, 24(4), 304–312.
- Hasnain, S., Jameel, E., Mohanta, B., Dhara, A. K., Alkahtani, S., & Nayak, A. K. (2020). Chapter 1. Alginates: sources, structure, and properties. In *Alginates in Drug Delivery*. INC.
- Huang, F. Y., Huang, F. R., Chen, B., Liu, Q., Wang, H., Zhou, S. L., Zhao, H. G., Huang, Y. H., Lin, Y. Y., & Tan, G. H. (2015). Microencapsulation of tumor lysates and live cell engineering with MIP-3 $\alpha$  as an effective vaccine. *Biomaterials*, 53, 554–565.
- Jain, K. K. (2020). *An Overview of Drug Delivery Systems* (Vol. 2059).
- Kadam N. R. and Suvarna. (2015). Microsphere: A Brief Review. *Asian Journal of Biomedical and Pharmaceutical Sciences*, 05(47), 13–19.
- Kalalo, T., Miatmoko, A., Tanojo, H., Erawati, T., Hariyadi, D. M., & Rosita, N. (2022). Effect of Sodium Alginate Concentration on Characteristics, Stability and Drug Release of Inhalation Quercetin Microspheres. *Jurnal Farmasi Dan Ilmu Kefarmasian Indonesia*, 9(2), 107–114.
- Kumar, K. R., & Suresh, G. (2018). Development and Characterization of Alginate Microspheres Containing Olmesartan by Ionotropic Gelation Method. *International Journal of Pharmaceutical Sciences and Drug Research*, 10(4), 335–341.
- Lee, K. Y., & Mooney, D. J. (2012). Alginate: Properties and biomedical applications. *Progress in Polymer Science (Oxford)*, 37(1), 106–126.
- Łętocha, A., Miastkowska, M., & Sikora, E. (2022). Preparation and Characteristics of Alginate Microparticles for Food, Pharmaceutical and Cosmetic Applications. *Polymers*, 14(18).
- Loquercio, A., Castell-Perez, E., Gomes, C., & Moreira, R. G. (2015). Preparation of Chitosan-Alginate Nanoparticles for Trans-cinnamaldehyde Entrapment. *Journal of Food Science*, 80(10), N2305–N2315.
- Mali, K. K., Dias, R. J., Ghorpade, V. S., & Havaldar, V. D. (2010). Sodium alginate microspheres containing multicomponent inclusion complex of domperidone. *Latin American Journal of Pharmacy*, 29(7), 1199–1207.
- Man, J., Wang, X., Li, J., Cui, X., Hua, Z., Li, J., Mao, Z., & Zhang, S. (2022). Intravenous Calcium Alginate Microspheres as Drug Delivery Vehicles in Acute Kidney Injury Treatment. *Micromachines*, 13(4), 1–9.
- Manjanna, K. M., Kumar, T. M. P., & Shivakumar, B. (2010). Calcium alginate cross-linked polymeric microbeads for oral sustained drug delivery in arthritis. *Drug Discoveries & Therapeutics*, 4(2), 109–122.

- Martín, M. J., Calpena, A. C., Fernández, F., Mallandrich, M., Gálvez, P., & Clares, B. (2015). Development of alginate microspheres as nystatin carriers for oral mucosa drug delivery. *Carbohydrate Polymers*, 117, 140–149.
- Mishra, M. (2015). Handbook of Encapsulation and Controlled Release. In *CRC Press* (Issue 11).
- Nagasree, K., Chowdary, G. V, Kumar, C. B. M., Reddy, T. R. M., Bhikshapathi, D. V. R. N., & Nagasree, K. (2016). *Design and evaluation of sodium alginate microspheres loaded with gatifloxacin*. 8(4), 361–370.
- Pal, D., & Nayak, A. K. (2012). Novel tamarind seed polysaccharide-alginate mucoadhesive microspheres for oral gliclazide delivery : in vitro – in vivo evaluation. *Drug Delivery*, 19(January), 123–131.
- Pan, C. T., Yu, R. S., Yang, C. J., Chen, L. R., Wen, Z. H., Chen, N. Y., Ou, H. Y., Yu, C. Y., & Shiue, Y. L. (2021). Sustained-release and pH-adjusted alginate microspheres-encapsulated doxorubicin inhibit the viabilities in hepatocellular carcinoma-derived cells. *Pharmaceutics*, 13(9).
- Patil, J. S., Kamalapur, M. V., Marapur, S. C., & Kadam, D. V. (2010). Iontropic gelation and polyelectrolyte complexation: The novel techniques to design hydrogel particulate sustained, modulated drug delivery system: A review. *Digest Journal of Nanomaterials and Biostructures*, 5(1), 241–248.
- Patil, S. B., Kaul, A., Babbar, A., Mathur, R., Mishra, A., & Sawant, K. K. (2012). In vivo evaluation of alginate microspheres of carvedilol for nasal delivery. *Journal of Biomedical Materials Research - Part B Applied Biomaterials*, 1, 249–255.
- Patole, V. C., & Pandit, A. P. (2018). Mesalamine-loaded alginate microspheres filled in enteric-coated HPMC capsules for local treatment of ulcerative colitis: in vitro and in vivo characterization. *Journal of Pharmaceutical Investigation*, 48(3), 257–267.
- Prasad, B. S. G., Gupta, V. R. M., Devanna, N., & Jayasurya, K. (2014). Microspheres as Drug Delivery System – A Review. *Journal of Global Trends in Pharmaceutical Sciences*, 5(3), 1961–1972.
- Ra, A., Yong, C., Chun, G., Keun, B., & Park, D. J. (2014). Preparation of alginate – CaCl<sub>2</sub> microspheres as resveratrol carriers. *J Mater Sci.*, 49, 4612–4619.
- Ramteke K.H, V.B, J., & S.N., D. (2012). Microspheres: as carriers used for novel drug delivery systems. *IOSR Journal of Pharmacy (IOSRPHR)*, 2(4), 44–48.
- Rao, P. S., & Kanakamn, V. (2019). Formulation and evaluation of Zidovudine alginate microspheres. *Journal of Drug Delivery and Therapeutics*, 9(5-s), 57–64.
- Rowe et al. (2009). Handbook of Pharmaceutical Excipients. Sixth Edition. In *Pharmaceutical Press* (Issue 1).
- Salome, A. C., Godswill, C. O., & Ikechukwu, I. O. (2013). Kinetics and mechanisms of drug release from swellable and nonswellable matrices: A review. *Research Journal of Pharmaceutical, Biological and Chemical Sciences*, 4(2), 97–103.
- Saripilli Rajeswari<sup>1\*</sup>, Teella Prasanthi<sup>1</sup>, Navya Sudha<sup>1</sup>, Ranjit Prasad Swain<sup>1</sup>, S. P. and V. G. (2017). Natural Polymers: A Recent Review. *World Journal of Pharmacy and Pharmaceutical Sciences*, 6(8), 472–494.
- Skrzypczak, K. M. D., & Witek, B. L. A. (2019). Preparation of hydrogel composites using Ca<sup>2+</sup> and Cu<sup>2+</sup> ions as crosslinking agents. *SN Applied Sciences*, 1(6), 1–15.
- Solanki, N. (2018). *Microspheres are an innovative approach to drug delivery systems*. 56–58.
- Song, P., Wu, Y., Zhang, X., Yan, Z., Wang, M., & Xu, F. (2018). Preparation of Covalently Crosslinked Sodium Alginate/Hydroxypropyl Methylcellulose Ph-Sensitive Microspheres for Controlled Drug Release. *BioResources*, 13(4), 8614–8628.
- Sosnik, A., & Seremeta, K. P. (2015). Advantages and challenges of the spray-drying technology for producing pure drug particles and drug-loaded polymeric carriers. *Advances in Colloid and Interface Science*.

- Szekalska, M., Puciłowska, A., Szymańska, E., Ciosek, P., & Winnicka, K. (2016). Alginate: Current Use and Future Perspectives in Pharmaceutical and Biomedical Applications. *International Journal of Polymer Science*, 2016.
- Szekalska, M., Winnicka, K., Sosnowska, K., & Amelian, A. (2015). Evaluation of Alginate Microspheres with Metronidazole Obtained by The Spray Drying Technique. *Acta Poloniae Pharmaceutica- Drug Research*, 72(3), 569–578.
- Szekalska, M., Wroblewska, M., Sosnowska, K. (2016). Influence of Sodium Alginate on Hypoglycemic Activity of Metformin Hydrochloride in the Microspheres Obtained by the Spray Drying. *International Journal of Polymer Science*, 1–12.
- Talevi, A., & Ruiz, M. E. (2021). Drug Release. In *The ADME Encyclopedia* (pp. 1–7). Springer International Publishing.
- Tandale, S. R., Mole, M. M., & Gawade, V. R. (2020). *Review on Novel Drug Delivery System of Microsphere: Type, Material, Method of Preparation and Evaluation of Microsphere: Method Evaluation*”.
- Tecante, A., & Núñez, C. (2012). Solution Properties of  $\kappa$ -Carrageenan and Its Interaction with Other Polysaccharides in Aqueous Media. In *Rheology In Tech* (pp. 241–264).
- Telange, D. R., Pandharinath, R. R., Pethe, A. M., Jain, S. P., & Pingale, P. L. (2022). Calcium Ion-Sodium Alginate-Piperine-Based Microspheres: Evidence of Enhanced Encapsulation Efficiency, Bio-Adhesion, Controlled Delivery, and Oral Bioavailability of Isoniazid. *AAPS PharmSciTech*, 23(4).
- Thanh Uyen, N. T., Abdul Hamid, Z. A., Thi, L. A., & Ahmad, N. B. (2020). Synthesis and characterization of curcumin-loaded alginate microspheres for drug delivery *Journal of Drug Delivery Science and Technology*.
- Uyen, T. N. T., Ain, Z., Hamid, A., Xuan, N., Tram, T., & Ahmad, N. B. (2019). Fabrication of alginate microspheres for drug delivery : a review. *International Journal of Biological Macromolecules*.
- Vasam, M., Sriharsha, S. N., & Bhukya, S. (2016). Composition, formulation, and in-vitro evaluation studies of cefixime microspheres. *International Conference on Electrical, Electronics, and Optimization Techniques, ICEEOT 2016*, 3391–3396.
- Verma, S. (2019). Microsphere A Novel Drug Delivery System. *Research Chronicle in Health Sciences*, 5(July).
- Wang, S., Liu, R., Fu, Y., & Kao, W. J. (2020). Release Mechanisms and Applications of Drug Delivery Systems for Extended-Release. *Expert Opinion on Drug Delivery*.
- World Health Organization. (2018). Q1F Stability testing of active pharmaceutical ingredients and finished pharmaceutical products.
- Zhang, X., Li, W., Dou, X., Nan, D., & He, G. (2020). Astaxanthin Encapsulated in Biodegradable Calcium Alginate Microspheres for the Treatment of Hepatocellular Carcinoma In Vitro. *Applied Biochemistry and Biotechnology*, 191(2).
- Zothanpuii, F, R, R., & K, S. (2020). A Review on Stability Testing Guidelines of Pharmaceutical Products. *Asian Journal of Pharmaceutical and Clinical Research*, 13(October), 3–9.

# Forced Degradation and Stability Indicating Chromatographic Methods for the Analysis of Sofosbuvir Alone and in Combination with Velpatasvir, Daclatasvir, Voxilaprevir and Ledipasvir

Nastaran HEIDARZADEH KHORAMABADI\*, Nasrin NEMAYANDEH\*\*, Ali MOHAMMADI\*\*\* °, Roderick B WALKER\*\*\*\*

*Forced Degradation and Stability Indicating Chromatographic Methods for the Analysis of Sofosbuvir Alone and in Combination with Velpatasvir, Daclatasvir, Voxilaprevir and Ledipasvir*

## SUMMARY

Sofosbuvir (SOF) is an antiviral compound used alone to treat hepatitis C or in combination with drugs such as ribavirin and ledipasvir (LED). FDA approval as monotherapy was granted in 2013, and for combination treatment of hepatitis C in 2014. Different studies have reported on the analysis of SOF in bulk and tablet forms. However, a monograph for SOF has not yet been included in official pharmacopeias. Therefore, no consensus with respect to the identification of impurities and concerns relating to the safety of the drug exists. A review of the development of stability indicating chromatographic methods for the analysis of SOF was undertaken using PubMed and the Google Scholar databases from initial reports to January 2023. Our focus pertained to studies in which a stability-indicating chromatographic method had been designed and validated for analysis of SOF in bulk and tablet form alone and in combination with LED, daclatasvir (DAC), velpatasvir (VEL) and voxilaprevir (VOX) and also reported the use of stress testing. This review aims to summarize the information reported in different studies concerning the development of stability-indicating methods conducted using stress studies to analyze SOF and the results of such stress studies.

**Key Words:** Sofosbuvir, anti-virus drug, stability indicating, method development, stress studies.

*Sofosbuvir'in Tek Başına ve Velpatasvir, Daklatasvir, Voksilaprevir ve Ledipasvir ile Kombinasyonunun Analizi İçin Hızlandırılmış Degradasyon ve Stabilitite Göstergesi Kromatografik Yöntemler*

## ÖZ

Sofosbuvir (SOF), hepatit C tedavisinde tek başına ya da ribavirin ve ledipasvir (LED) gibi ilaçlarla birlikte kullanılan antiviral bir bileşiktir. Monoterapi olarak FDA onayı 2013 yılında, hepatit C'nin kombinasyon tedavisi için ise 2014 yılında verilmiştir. Bulk ve tablet formlarında SOF analizine ilişkin farklı çalışmalar rapor edilmiştir. Ancak SOF için bir monografi henüz resmi farmakopelerde yer almamıştır. Bu nedenle, safsızlıkların tanımlanması konusunda bir fikir birliği oluşmamış olup, ilacın güvenliğine ilişkin endişeler de bulunmaktadır. SOF analizi için stabiliteyi gösteren kromatografik yöntemlerin geliştirilmesine ilişkin bir inceleme, ilk raporlardan Ocak 2023'e kadar PubMed ve Google Akademik veri tabanları kullanılarak gerçekleştirildi. Odak noktamız, SOF'un bulk ve tablet formunda tek başına ve LED, daklatasvir (DAC), velpatasvir (VEL) ve voksilaprevir (VOX) ile kombinasyonu halinde analizi için stabiliteyi gösteren bir kromatografik yöntemin tasarlandığı ve doğrulandığı ve ayrıca stres testinin kullanımını bildiren çalışmalarına yöneliktir. Bu derlemenin amacı, SOF'u analiz etmek için stres çalışmaları kullanılarak yürütülen stabilite gösterge yöntemlerinin geliştirilmesine ilişkin farklı çalışmalarda bildirilen bilgileri ve bu stres çalışmalarının sonuçlarını özetlemektir.

**Anahtar Kelimeler:** Sofosbuvir, antiviral ilaç, stabilite göstergesi, yöntem geliştirme, stres çalışmaları.

Received: 08.01.2024

Revised: 18.11.2024

Accepted: 08.12.2024

\* ORCID: 0000-0001-5565-3664; Department of Drug and Food Control, Faculty of Pharmacy, Tehran University of Medical Sciences, Tehran, Iran.

\*\* ORCID: 0000-0001-5602-5088; Department of Drug and Food Control, Faculty of Pharmacy, Tehran University of Medical Sciences, Tehran, Iran.

\*\*\* ORCID: 0000-0003-3686-7602; Pharmaceutical Quality Assurance Research center, The Institute of Pharmaceutical Sciences (TIPS), Tehran University of Medical Sciences, Tehran, Iran.

\*\*\*\* ORCID: 0000-0003-2781-4154; Division of Pharmaceutics, Faculty of Pharmacy, Rhodes University, Makhanda 6140, Eastern Cape, South Africa.

° Corresponding Author; Ali Mohammadi

E-mail: alimohammadi@tums.ac.ir, Tel: +98-21-88358801, +98-9123212724

## INTRODUCTION

Sofosbuvir (SOF) is a nucleotide analog NS5B polymerase inhibitor used to treat chronic hepatitis C infection caused by genotypes 1, 2, 3, or 4 in adult patients. (Singh, Bhatt, & Prasad, 2017). It is a direct-acting antiviral compound used alone or in combination with other drugs such as ribavirin and ledipasvir (LED) (Wang et al., 2017; Nebsen et al., 2016) and was approved in 2013 for monotherapy and in 2014 for combination treatment of hepatitis C (WHO, 2016). This compound is better than previously approved therapies as it exhibits better recovery rates and fewer side effects achieved with shorter duration treatment times (Wang & You, 2017). Currently, SOF is produced in many countries globally and different studies relating to analysis in bulk and tablet forms have been undertaken (Agarwal et al., 2022; Ganji et al., 2021; Hamdache et al., 2021; Abdel-Razeq et al., 2019; Bhujbal et al., 2019; Annapurna et al., 2018; Hassouna et al., 2018; Lalitha et al., 2018; Vanitha et al., 2018; Shaikh et al., 2017; Swathi et al., 2017; Nebsen et al., 2016; Pottabathini et al., 2016; Swain et al., 2016; Vejjendla et al., 2016). In addition, a study using a Quality by Design (QbD) approach has been used for the development and validation of analytical methods for this drug (Bhujbal & Darkunde, 2019) has been reported and others have estimated SOF content in pharmaceutical formulations (Shaikh & Manjusri, 2017; Vejjendla, Subramanyam, & Veerabhadram, 2016). Several stability indicating methods have been designed to simultaneously estimate SOF with LED, daclatasvir (DAC), velpatasvir (VEL) and voxilaprevir (VOX) (Balaswami, Ramana, Rao, & Sanjeeva, 2018; Bandla & Ganapaty, 2017; Bandla & Ganapaty, 2018; Bhavani & Maduri, 2020; Damle & Kalaskar, 2020; Deepthi & Sankar, 2020; El-Waey, Abdel-Salam, Hadad, & El-Gindy, 2023; El-Yazbi, Elashkar, Abdel-Hay, Talaat, & Ahmed, 2020; R Godela & Sowjanya, 2020; Ramreddy Godela & Sowjanya, 2021; Harshalatha, Chandrasekhar, & Mv, 2018; Hassouna, Abdelrahman, & Mohamed, 2017; Hemchand, Babu, & Annapurna, 2018; Jahnavi & Ganapaty, 2018; Kokkiralala & Suryakala, 2020; Kumar & Rao, 2018;

Kumari & Sankar, 2019; Lakshmana Rao & Pallavi, 2019; Lakshmi, Chaitanya, & Chandrasekar, 2018; Lakshmi Maneka S, Saravanakumar RT, & Anjana, 2020; Mankar, Bhawar, & Dalavi, 2019; Mastanamma, Chandini, Reehana, & Saidulu, 2018; Namratha & Vijayalakshmi, 2021; Narla & Pappula, 2020; Padmini M, Venkata D, & Sankar, 2019; Priyanka, Vinutha, Sridevi, Ramya, & Bhagavan Raju, 2018; Rao, Reddy, & Rao, 2017; Rao, Rao, & Prasad, 2018; Reddy, Alam, Khanam, & Adhkrishnanand, 2018; Rote, Alhat, & Kulkarni, 2017; Saroja, Lakshmi, Rammohan, Divya, & Kumar, 2018; Suganthi, Satheshkumar, & Ravi, 2019; Susmita & Rajitha, 2018; Veereswara Rao, Deshmukh, & Kumar, 2018; Yeram, Hamrapurkar, & Mukhedkar, 2019; Zaman & Hassan, 2021).

The presence of impurities and degradation products (DPs) may affect the efficacy and safety of drugs. Consequently, it is essential to conduct stability studies to identify such impurities (Fakhari, Nojavan, Haghgoo, & Mohammadi, 2008). Drug stability is an important quality attribute for the pharmaceutical industry, and analytical methods designed for quality control should preferably be stability-indicating (Montazeri, Mohammadi, Adib, & Naemy, 2018). According to the International Council for Harmonization (ICH) of Technical Requirements for Pharmaceuticals for Human Use and USP guidelines, the assay method for a drug-active substance must be stability-indicating to permit determination of the active substance in the presence of any potential DPs of that compound (Souri et al., 2011). The best approach for developing stability-indicating analytical methods is to undertake forced degradation studies during method development and validation (Pourmoslemi, Mirfakhraee, Yaripour, & Mohammadi, 2016). There are several analytical techniques used for the analysis of drugs, of which HPLC methods are commonly used for quality control and consistency of medicines as the approach is reliable, simple, cost-effective, and robust, and the familiarity of the analysts with this technique is a reason for the plethora of separations reported using this approach (Mohammadi et al., 2007). Therefore, our focus in this review is on the



chromatographic methods that have reported the analysis of SOF only or in combination with other antivirus drugs and the purpose of the review is to summarize information relating to the conduct of stress studies, results of such stress studies in reports in which the design and validation of stability indicating chromatographic methods of analysis for SOF had been published. For this purpose, we report information from articles that have reported the design of stability indicating chromatographic methods for SOF alone or with other antiviral drugs. For this purpose, the inclusion and exclusion criteria for this review resulted in 45 studies being considered suitable for inclusion from the scientific databases searched.

## METHODS

### Literature search

A review of the design, development, and validation of stability-indicating methods for the analysis of SOF was performed up to the beginning

of 2023 using the updated PubMed and Google Scholar databases. In addition, the references from the list of identified and subsequently selected articles were reviewed to identify additional sources. Our focus was on chromatographic studies that involved the development and validation of stability-indicating methods of analysis for SOF alone or with other antivirus drugs simultaneously, during which stress testing was performed. Studies in which SOF was analyzed simultaneously with other drugs were considered in the inclusion criteria, and only chromatographic studies that analyzed the drug were included in our review. Only studies published in English were included. All selected reports were saved in an Endnote library, after which duplications were removed, and the titles and abstracts were screened to establish whether they met the inclusion criteria.

### Search strategy

Our search strategy for Google Scholar and PubMed databases is depicted in (Figure 1.).

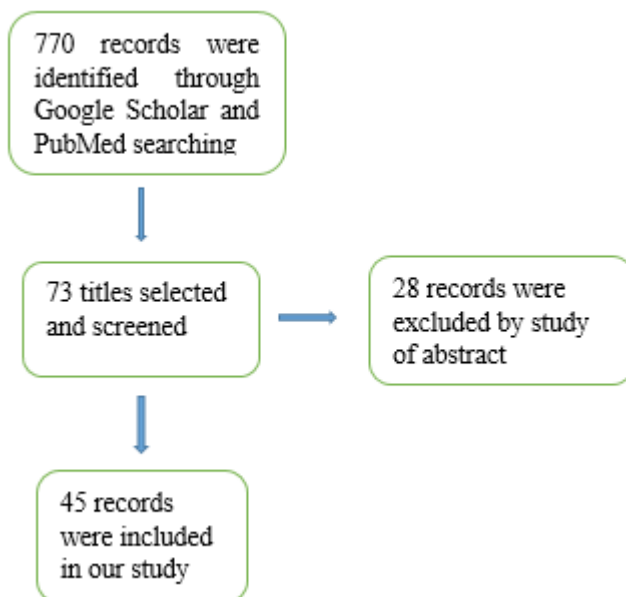


Figure 1. Flow Diagram of Study Selection Process

## **FINDINGS AND DISCUSSION**

### **Summary of studies conducted with SOF alone**

Ten studies were finally identified, selected and used following review of the actual analytical approach for SOF alone (Abdel-Razeq, Nasr, & S Said, 2019; Agarwal, Jagdale, & Gandhi, 2022; Annapurna, Teja, & Chaitanya, 2018; Hamdache et al., 2021; Hassouna & Mohamed, 2018; Lalitha, Reddy, & Devanna, 2018; Nebsen & Elzanfaly, 2016; Pottabathini, Gugulothu, Kaliyaperumal, & Battu, 2016; Swain et al., 2016; Vanitha, Bhaskar Reddy, & Satyanarayana, 2018).

The study conducted by Nebzen et al. aimed to investigate the degradation behavior of SOF under different stress conditions through a green validated stability-indicating method. The optimized LC-MS-MS method was used to identify fragmentation patterns of DP of SOF (Nebsen & Elzanfaly, 2016). The primary purposes of a study conducted by Pottabathini were to develop a stability-indicating method for the analysis of SOF, investigate the degradation behavior of the drug, separate and characterize the DP (Pottabathini, Gugulothu, Kaliyaperumal, & Battu, 2016). In another study, structural information generated using MS measurements was used for *in silico* toxicity studies of the DP, which were performed using two toxicity prediction software packages. The primary peak was well separated from the peaks of the DP, which were also resolved from each other, confirming the method was selective and stability-indicating. The LC-MS method used a LC-ESI-QTOF-MS/MS to identify the DP (Swain et al., 2016). In a study by Vanitha et al., a QbD approach was used to develop a simple, robust and selective RP-HPLC method for the estimation of SOF active pharmaceutical ingredient (API) in which degradation studies were performed under different stress conditions for the

purposes of method optimization (Vanitha, Bhaskar Reddy, & Satyanarayana, 2018). Annapurna et al. designed a stability-indicating RP-UFLC method for the analysis of SOF in bulk form. For this purpose, forced degradation studies were performed under acidic, alkaline, oxidation, thermal and photolysis conditions. The specific and selective method was validated using ICH guidelines (ICH, 1997) and was applied to the analysis of SOF in commercial formulations (Annapurna, Teja, & Chaitanya, 2018). In a study conducted in 2022, a stability-indicating RP-HPLC method for drug analysis was reported and included forced degradation studies performed according to ICH guidelines (Guideline, 2003). Samples were analyzed by MS (Mass Spectrometry), and drug degradation pathways were identified and profiled (Agarwal, Jagdale, & Gandhi, 2022). Two stability-indicating methods using UPLC and HPTLC were developed and validated according to ICH guidelines for the determination of SOF (bulk form) in the presence of its DPs and included performing stress tests under acidic and alkaline hydrolytic and oxidative conditions (Abdel-Razeq, Nasr, & S Said, 2019). In three other studies, a stability-indicating RP-HPLC method was developed and validated to determine SOF and included degradation studies carried out under acidic, alkaline, oxidation, thermal, and photolysis conditions (Hamdache et al., 2021; Hassouna & Mohamed, 2018; Lalitha, Reddy, & Devanna, 2018).

A summary of the stress conditions and the extent of SOF degradation under different stress conditions used in each study is listed in (Table 1). In Study No. 3, stress tests were performed on the tablet form, and in Study No. 10, stress tests were performed on both bulk and tablet dosage forms.

**Table 1.** Summary of stress studies and % degradation of SOF

Study (Form) and %Degradation	Hydrolysis			Oxidation	Thermal	Photolytic	Reference
	Acidic	Basic	Neutral				
<b>Study 1 (Bulk)</b>	0.1 N HCl 60°C 30 min	0.1 N NaOH 25°C 2 min	NR <sup>1</sup>	30% v/v H <sub>2</sub> O <sub>2</sub> 60°C 1 h	60°C 1 h (In solution state)	UV 48 h (In solid state)	(Annapurna et al., 2018)
<b>%Degradation</b>	11.65%	27.03%	NR	32.85%	ND <sup>2</sup>	ND	
<b>Study 2 (Bulk)</b>	0.1 M HCl 25°C 6 h	0.1 M NaOH 25°C 6 h	Water 72 h	3%, 6% v/v H <sub>2</sub> O <sub>2</sub> 25°C 10 days	80°C 72 h In oven (In solid state)	UV 6 h 254 nm (In solid state)	(Nebsen & Elzanfaly, 2016)
<b>%Degradation</b>	2.5%	90%	ND	11%	ND	ND	
<b>Study 3 (Tablet)</b>	1 N HCl 80°C 10 h	0.5 N NaOH 60°C 24 h	NR	30% v/v H <sub>2</sub> O <sub>2</sub> 80°C 2 days	Thermal study was performed but NR	254 nm 24 h (In solid state)	(Pottabathini et al., 2016)
<b>%Degradation</b>	8.66%	45.97%	NR	0.79%	ND	ND	
<b>Study 4 (Bulk)</b>	0.1 M HCl 60°C 3 h	0.1 M NaOH 25°C 15 min	(Water: Acetonitrile 50:50% v/v) 60°C 6 h	30% v/v H <sub>2</sub> O <sub>2</sub> 25°C 72 h	80°C In oven 48 h (In solid state)	UV (200 Whrm <sup>-2</sup> ) Fluorescent light (1.2 million lux hours) (In solid state)	(Swain et al., 2016)
<b>%Degradation</b>	Two DPs	Three DPs	One DP	One DP	ND	ND	
<b>Study 5 (Bulk)</b>	0.1 M HCl 25°C 25 h	0.1 M NaOH 25°C 100 min	Water 25°C 72 h	0.3% v/v H <sub>2</sub> O <sub>2</sub> 25°C 50 h	60°C In oven 72 h (In solid state)	Sunlight 10 h (In solid state)	(Vanitha et al., 2018)
<b>%Degradation</b>	One DP	Two DPs	NR	ND	ND	NR	
<b>Study 6 (Bulk)</b>	0.1N HCl 70°C 6 h	0.1N NaOH 70°C 10 h	NR	3% v/v H <sub>2</sub> O <sub>2</sub> 25°C 7 days	50°C 21 Days (In solution state)	Sunlight 21 Days (In solution state)	(Agarwal et al., 2022)
<b>%Degradation</b>	One DP	One DP	NR	One DP	ND	ND	
<b>Study 7 (Bulk)</b>	1N HCl 50-60°C 14 h	1N NaOH 50-60°C 14 h	Water 50-60°C 48 h	3% v/v H <sub>2</sub> O <sub>2</sub> 25°C 48 h	75% Humidity 40°C 1 Month (In solid state)	Sunlight 48 h (In solid state)	(Abdel-Razeq et al., 2019)
<b>%Degradation</b>	18.36%	70.81%	NR	4.56%	4.31%	7.03%	
<b>Study 8 (Bulk)</b>	5N HCl 100°C 7 h	5N NaOH 100°C 3 h	NR	3% v/v H <sub>2</sub> O <sub>2</sub> 25°C One week	NR	NR	(Hassouna & Mohamed, 2018)
<b>%Degradation</b>	25%	19%	NR	32%	NR	NR	
<b>Study 9 (Bulk)</b>	0.1N HCl 60°C 6 h	0.1N NaOH 60°C 6 h	NR	3% v/v H <sub>2</sub> O <sub>2</sub> 25°C 15 min	110°C 24 h (In solid state)	Sunlight 24 h (In solution state)	(Lalitha et al., 2018)
<b>%Degradation</b>	6.7%	8.9%	NR	8.1%	5.1%	8.5%	
<b>Study 10 (Bulk And Tablet)</b>	1N HCl 8°C 3 h	1N NaOH 8°C 3 h	NR	30% v/v H <sub>2</sub> O <sub>2</sub> 8°C 1 h	105°C 48 h (In solid state)	UV light 72 h (In solid state)	(Hamdache et al., 2021)
<b>%Degradation</b>	10.68% 10.72%	14.57% 16.12%	NR NR	0.31% 0.27%	0.55% 0.67%	0.94% 0.84%	

<sup>1</sup>NR: Not Reported

<sup>2</sup>ND: No Degradation

### **Summary of studies conducted with SOF in combination with VEL**

Thirteen studies have designed as stability indicating analysis method for SOF and VEL, simultaneously (Bandla & Ganapaty, 2017; Damle & Kalaskar, 2020; Godela & Sowjanya, 2020; Harshalatha et al., 2018; Hemchand et al., 2018; Lakshmana Rao & Pallavi, 2019; Lakshmi et al., 2018; Namratha & Vijayalakshmi, 2021; Priyanka et al., 2018; Rao et al., 2018; Saroja et al., 2018; Susmita & Rajitha, 2018; Zaman & Hassan, 2021).

In a study by Damle et al., a stability-indicating HPTLC method for SOF and VEL was designed and validated according to the ICH guidelines with a shorter run-time than previously reported methods (Damle & Kalaskar, 2020). Lakshmana Rao et al., developed and validated an accurate, simple stability-indicating RP-HPLC method for estimating SOF and VEL in tablet form with short retention times suitable for quality control testing (Lakshmana Rao & Pallavi, 2019). A stability-indicating RP-HPLC method was developed to estimate SOF and VEL in tablets to separate the compounds and their DP (Saroja et al., 2018). In another study, RP-HPLC, UPLC, and a new stability-indicating RP-UPLC method were designed to determine SOF and VEL in tablets, and stress studies were also conducted (Hemchand et al., 2018). Bandla et al., developed a stability-indicating RP-HPLC method for rapid simultaneous quantification of SOF and VEL in the final product (Bandla & Ganapaty, 2017). A simple and specific stability-indicating RP-HPLC method was designed to simultaneously determine SOF and VEL, which exhibited a much shorter retention time than previously reported

methods (Rao et al., 2018). Lakshmi et al., reported the development of a stability-indicating RP-UPLC method for the simultaneous estimation of SOF and VEL, which was accurate, rapid, simple, and economical (Lakshmi et al., 2018). A stability-indicating RP-HPLC designed for the simultaneous determination of SOF and VEL in bulk form, which can also be used for the routine analysis of two drugs in pharmaceutical products, was reported by Priyanka et al. (Priyanka et al., 2018). Zaman et al. developed an accurate and simple stability-indicating HPLC-UV method for analyzing process impurities and DP of SOF and VEL in pharmaceutical formulations and characterized the DP (Zaman & Hassan, 2021). A rapid and simple stability-indicating RP-HPLC method for the simultaneous determination of SOF and VEL in tablet form was developed by Harshalata et al. (Harshalatha et al., 2018) as well as an accurate and simple stability-indicating UPLC method for the simultaneous estimation of SOF and VEL in tablets has been reported by Susmita et al. (Susmita & Rajitha, 2018). Namratha et al. have also designed a stability-indicating UPLC method for the simultaneous estimation of SOF and VEL in tablets (Namratha & Vijayalakshmi, 2021). Godela et al., reported sensitive, simple and specific stability- indicating RP-HPLC method for the simultaneous estimation of SOF and VEL in bulk form, which was useful for monitoring the quality of these two drugs (R Godela & Sowjanya, 2020).

The conditions and results of the stress tests used are listed in (Tables 2 and 3), respectively. In Studies No. 1, 8 and 13, stress tests were performed on the bulk form. The rest of the tests were performed on tablet dosage forms.

**Table 2.** Summary of stress studies of SOF and VEL simultaneously

Study (Form)	Hydrolysis			Oxidation	Thermal	Photolytic	Reference
	Acidic	Basic	Neutral				
<b>Study 1 (Bulk)</b>	0.1N HCl Immediately	0.1N NaOH 20 min	Water Immediately	30% H <sub>2</sub> O <sub>2</sub> 1h	80°C 4 h (In solid state)	Fluorescence (1.2 million lux hrs/m <sup>2</sup> ) or UV light (200-watt-hrs/m <sup>2</sup> ) (In solid state)	(Damle & Kalaskar, 2020)
<b>Study 2 (Tablet)</b>	2N HCl 60°C 30 min	2N NaOH 60°C 30 min	Water 60°C 1 h	20% H <sub>2</sub> O <sub>2</sub> 60°C 30 min	105°C 1 h (In solution state)	UV light in UV chamber 1 day or 200-watt hrs/m <sup>2</sup> (In solution state)	(Lakshmana Rao & Pallavi, 2019)
<b>Study 3 (Tablet)</b>	0.1N HCl 25°C 30 min	0.1N NaOH 25°C 30 min	NR	30% H <sub>2</sub> O <sub>2</sub> 25°C 30 min	105°C 30 min (In solution state)	Sunlight 1 day (In solution state)	(Saroja et al., 2018)
<b>Study 4 (Tablet)</b>	0.1N HCl 60°C 30 min	0.1N NaOH 60°C 2 min	NR	30% H <sub>2</sub> O <sub>2</sub> 40°C 1 h	60°C 1 h (In solution state)	UV light in a photostability chamber 48 h (In solid state)	(Hemchand et al., 2018)
<b>Study 5 (Tablet)</b>	2N HCl 60°C 30 min	2N NaOH 60°C 30 min	Water 60°C 6 h	H <sub>2</sub> O <sub>2</sub> 60°C 30 min	105°C 6 h (In solution state)	UV light 7 days or 200-watt hrs/m <sup>2</sup> (In solution state)	(Bandla & Ganapaty, 2017)
<b>Study 6 (Tablet)</b>	2N HCl 60°C 30 min In dark	2N NaOH 60°C 30 min In dark	Water 60°C 30 min In dark	20% H <sub>2</sub> O <sub>2</sub> 25°C 1 day In dark	105°C 1 h (In solid state)	UV light in UV chamber 1 day or 200-watt hrs/m <sup>2</sup> (In solution state)	(Rao et al., 2018)
<b>Study 7 (Tablet)</b>	0.1N HCl 60°C 24 h	0.1N NaOH 60°C 24 h	NR	12.5% H <sub>2</sub> O <sub>2</sub> 25°C 15 min	110°C 3 h (In solid state)	UV light in UV chamber 24 h (In solution state)	(Lakshmi et al., 2018)
<b>Study 8 (Bulk)</b>	NR	NR	NR	NR	NR	NR	(Priyanka et al., 2018)
<b>Study 9 (Tablet)</b>	0.1N HCl 25°C 8 h	0.1N NaOH 25°C 8 h	NR	3% H <sub>2</sub> O <sub>2</sub> 25°C 7 days	105°C 8 h (In solid state)	UV light 25°C 7 days or Fluorescent light 1.2 million lux hrs/m <sup>2</sup> 7 days (In solid state)	(Zaman & Hassan, 2021)
<b>Study 10 (Tablet)</b>	0.1N HCl 85°C 5 h	0.1N NaOH 85°C 6 h	NR	3% H <sub>2</sub> O <sub>2</sub> 55°C 8 h	85°C 30 h (In solid state)	UV degradation in 256 nm 30 h (In solution state)	(Harshalatha et al., 2018)
<b>Study 11 (Tablet)</b>	NR	NR	NR	NR	NR	NR	(Susmita & Rajitha, 2018)
<b>Study 12 (Tablet)</b>	2N HCl 60°C 30 min	2N NaOH 60°C 30 min	Water 6 h	20% H <sub>2</sub> O <sub>2</sub> 60°C 30 min	105°C 6 h (In solution state)	NR	(Namratha & Vijayalakshmi, 2021)
<b>Study 13 (Bulk)</b>	0.1N HCl 70°C 24 h	0.1N NaOH 70°C 24 h	NR	3% H <sub>2</sub> O <sub>2</sub> 70°C 24 h	80°C 24 h (In solution state)	UV light 24 h (In solution state)	(Godela & Sowjanya, 2020)

**Table 3.** Summary % degradation results for SOF and VEL tested simultaneously

Study		Hydrolysis			Oxidation	Thermolysis	Photolysis	Reference
		Acidic	Basic	Neutral				
Study 1	SOF	16.3	16.46	17.34	21.97	18.67	UV:25.98 Fluorescence:12.99	(Damle & Kalaskar, 2020)
	VEL	23.96	7.84	7.78	14.05	11.87	UV:20.75 Fluorescence:6.76	
Study 2	SOF	4.66	4.04	2.83	3.77	2.86	2.83	(Lakshmana Rao & Pallavi, 2019)
	VEL	4.92	4.24	0.94	3.18	2.97	2.68	
Study 3	SOF	7.45	7.16	NR	7.39	6.45	6.73	(Saroja et al., 2018)
	VEL	6.80	6.19	NR	5.88	7.21	6.27	
Study4	SOF	3.87	71.06	NR	5.07	5.02	4.04	(Hemchand et al., 2018)
	VEL	0.16	0.09	NR	2.99	0.61	0.22	
Study5	SOF	4.79	2.79	0.81	1.96	0.84	0.59	(Bandla & Ganapaty, 2017)
	VEL	4.97	2.66	0.96	1.67	0.51	0.76	
Study6	SOF	3.49	3.49	0.84	3.61	4.57	1.79	(Rao et al., 2018)
	VEL	3.64	3.64	0.90	2.90	4.11	2.44	
Study7	SOF	5.60	5.20	NR	5.30	3.00	5.5	(Lakshmi et al., 2018)
	VEL	6.50	5.20	NR	5.80	2.00	7.00	
Study8	SOF	3.78	3.77	NR	5.69	4.37	4.38	(Priyanka et al., 2018)
	VEL	5.17	5.00	NR	5.80	2.51	3.19	
Study9	SOF	5.88	85.64	NR	3.48	1.82	UV:0.33 Fluorescence:0.14	(Zaman & Hassan, 2021)
	VEL	1.84	1.03	NR	18.40	2.09	UV:1.25 Fluorescence:0.90	
Study10	SOF	12.76	10.82	NR	11.26	7.30	8.74	(Harshalatha et al., 2018)
	VEL	12.41	10.74	NR	6.24	8.21	8.30	
Study11	SOF	3.56	2.10	NR	0.95	0.05	-0.19	(Susmita & Rajitha, 2018)
	VEL	5.42	3.23	NR	2.34	1.14	1.29	
Study12	SOF	5.09	4.33	0.23	2.59	2.21	NR	(Namratha & Vijayalakshmi, 2021)
	VEL	7.18	5.60	0.67	2.79	1.93	NR	
Study 13	SOF	22.00	18.40	NR	19.50	0.85	0.45	(Godela & Sowjanya, 2020)
	VEL	13.60	12.70	NR	12.70	4.20	0.21	

### Summary of studies conducted on SOF and DAC

Two studies of SOF and DAC were identified (Bandla & Ganapaty, 2018; Ramreddy Godela & Sowjanya, 2021) and the results are summarized in (Tables 4. and 5.).

In a study conducted by Bandla et al., a stability-indicating RP-HPLC method was developed for the simultaneous estimation of SOF and DAC in the bulk

form in which stress studies were also conducted has been reported (Bandla & Ganapaty, 2018). A stability-indicating RP-HPLC for the simultaneous determination of SOF and DAC in the bulk form in which the well-resolved separation of SOF and DAC from their DP has been reported and can be used to analyze these two drugs by the pharmaceutical industry (Ramreddy, Godela & Sowjanya, 2021).

**Table 4.** Summary of stress studies conducted with SOF and DAC simultaneously.

Study (Form)	Hydrolysis			Oxidation	Thermal	Photolytic	Reference
	Acidic	Basic	Neutral				
Study 1 (Bulk)	2N HCl 60°C 30 min	2N NaOH 60°C 30 min	Water 60°C 6 h	20% H <sub>2</sub> O <sub>2</sub> 60°C 30 min	105°C 6 h (In solution state)	UV light in UV chamber 7 days Or 200-watt hours/m <sup>2</sup> (In solution state)	(Bandla & Ganapaty, 2018)
Study 2 (Bulk)	0.1N HCl 70°C 2 h	0.1N NaOH 70°C 2 h	NR	3% H <sub>2</sub> O <sub>2</sub> 70°C 2 h	In a hot air oven at 80°C/75% RH 24 h <sup>1</sup> (In solution state)	NR	(Ramreddy Godela & Sowjanya, 2021)

<sup>1</sup> The problem in this part of the study is that there is no need to control the humidity in the solution state.

The summary of stress studies results of SOF and DAC is given in (Table 5.).

**Table 5.** Summary of % degradation results of SOF and DAC stress testing

Study		Hydrolysis			Oxidation	Thermolysis	Photolysis	Reference
		Acidic	Basic	Neutral				
Study 1	SOF	4.42	5.25	0.77	7.92	2.23	1.71	(Bandla & Ganapaty, 2018)
	DAC	4.26	4.41	0.15	5.09	2.02	1.07	
Study 2	SOF	15.6	51.20	NR	2.00	1.20	NR	(Ramreddy Godela & Sowjanya, 2021)
	DAC	9.80	16.40	NR	7.00	0.60	NR	

**Summary of studies conducted on SOF, VEL and VOX**

Five combination studies, which included SOF, VEL and VOX, were identified (Balaswami et al., 2018; Deepthi & Sankar, 2020; Kokkiralala & Suryakala, 2020; Lakshmi Maneka S et al., 2020; Padmini M et al., 2019) and the conditions and results of stress testing are summarized in (Tables 6. and 7.).

A stability-indicating RP-HPLC developed for the determination of SOF, VEL, and VOX in the tablets was reported to be rapid and suitable for the routine analysis and quality control of these drugs (Deepthi & Sankar, 2020). A simple, rapid and linear stability indicating RP-HPLC method for estimating SOF, VEL, VOX and DP simultaneously in bulk has also been reported (Kokkiralala & Suryakala, 2020).

Balaswami et al., reported a simple and economic stability-indicating RP-HPLC method for the simultaneous estimation of SOF, VEL and VOX which was applied to routine analysis of these three drugs in the bulk form (Balaswami et al., 2018). Padmini et al., reported stability- indicating RP-HPLC method for the simultaneous estimation of SOF, VEL, and VOX in the bulk form (Padmini M et al., 2019). A stability-indicating RP-UPLC for the simultaneous estimation of SOF, VEL, and VOX in the bulk form with much shorter retention and run times when compared to conventional HPLC methods was reported (Lakshmi Maneka S et al., 2020).

It is worth noting that Studies No. 2 -5 were undertaken using bulk API, whereas Study No. 1 used the tablet form.

**Table 6.** Summary of stress study conditions for SOF, VEL and VOX

Study (Form)	Hydrolysis			Oxidation	Thermolysis	Photolysis	Reference
	Acidic	Basic	Neutral				
<b>Study 1 (Tablet)</b>	2 N HCl 60°C 30 min	2 N NaOH 60°C 30 min	Water 60°C 6 h	20% H <sub>2</sub> O <sub>2</sub>	105°C 6 h (In solution state)	UV light 7 days Or 200-watt hours/m <sup>2</sup> (In solution state)	(Deepthi & Sankar, 2020)
<b>Study 2 (Bulk)</b>	2N HCl 60°C 30 min	2N NaOH 60°C 30 min	Water 60°C 6 h	20% H <sub>2</sub> O <sub>2</sub> 60°C 30 min	105°C 1 h (In solution state)	UV light 1 day Or 200-watt hours/m <sup>2</sup> (In solution state)	(Kokkerala & Suryakala, 2020)
<b>Study 3 (Bulk)</b>	2N HCl 60°C 30 min	2N NaOH 60°C 30 min	Water 60°C 6 h	20% H <sub>2</sub> O <sub>2</sub> 60°C 30 min	105°C 6 h (In solution state)	UV light 7 days Or 200-watt hours/m <sup>2</sup> 3 days (In solution state)	(Balaswami et al., 2018)
<b>Study 4 (Bulk)</b>	1N HCl 60°C 30 min	1N NaOH 60°C 30 min	NR	20% H <sub>2</sub> O <sub>2</sub> 60°C 30 min	105°C 6 h (In solution state)	UV light 3 days Or 200-watt hours/m <sup>2</sup> (In solution state)	(Padmini M et al., 2019)
<b>Study 5 (Bulk)</b>	2N HCl 60°C 30 min	2N NaOH 60°C 30 min	Water 60°C 30 min	20% H <sub>2</sub> O <sub>2</sub> 60°C 30 min	105°C 6 h (In solution state)	UV light 3 days Or 200-watt hours/m <sup>2</sup> (In solution state)	(Lakshmi Meneka S et al., 2020)

**Table 7.** % Degradation data following stress testing of SOF, DAC and VOX in combination

Study		Hydrolysis			Oxidation	Thermolysis	Photolysis	Reference
		Acidic	Basic	Neutral				
<b>Study 1</b>	SOF	5.77	4.65	0.63	4.05	1.75	2.27	(Deepthi & Sankar, 2020)
	VEL	5.96	4.90	0.49	4.42	3.57	2.42	
	VOX	5.86	5.51	0.33	3.39	1.29	0.92	
<b>Study 2</b>	SOF	Two DPs	One DP	ND	Two DPs	ND	ND	(Kokkerala & Suryakala, 2020)
	VEL	Two DPs	One DP	ND	Two DPs	ND	ND	
	VOX	Two DPs	One DP	ND	Two DPs	ND	ND	
<b>Study 3</b>	SOF	95.50	94.60	0.90	3.84	4.40	3.00	(Balaswami et al., 2018)
	VEL	96.23	95.92	0.48	2.84	1.88	1.24	
	VOX	95.50	94.60	0.90	3.43	4.40	3.00	
<b>Study 4</b>	SOF	8.90	7.97	0.67	6.11	3.84	1.56	(Padmini M et al., 2019)
	VEL	4.39	3.55	0.55	3.06	2.37	1.51	
	VOX	7.72	6.39	0.75	4.54	2.31	1.28	
<b>Study 5</b>	SOF	5.90	4.44	0.58	3.19	2.88	1.18	(Lakshmi Meneka S et al., 2020)
	VEL	5.83	4.31	0.90	3.10	2.26	1.58	
	VOX	4.72	3.64	0.32	3.58	2.96	1.51	

**Summary of studies conducted on SOF and LED**

Fifteen studies in which a combination of SOF and LED were analyzed were identified and included (Bhavani & Maduri, 2020; El-Waey et al., 2023; El-

Yazbi et al., 2020; Hassouna et al., 2017; Jahnavi & Ganapaty, 2018; Kumar & Rao, 2018; Kumari & Sankar, 2019; Mankar et al., 2019; Mastanamma et al., 2018; Narla & Pappula, 2020; Rao et al., 2017; Reddy et al., 2018; Rote et al., 2017; Suganthi et al., 2019;



Veereswara Rao et al., 2018; Yeram et al., 2019).

In a study conducted by Hassouna et al. assay and dissolution methods were developed to determine LED and SOF in bulk. Furthermore, stress studies were undertaken to develop and validate a RP-HPLC method to determine LED selectively and SOF with precision (Hassouna et al., 2017). Rao et al. reported a precise and accurate RP-HPLC method that had been developed for the determination of LED in tablets and forced degradation studies were performed using the conditions recommended in the ICH guideline and photodiode array detection (PDA) used to monitor the API and impurities (Rao et al., 2017). A RP-HPLC stability-indicating method to determine LED and SOF in the bulk form with forced degradation studies was performed according to ICH guidelines (Rote et al., 2017). The study conducted by Mastanamma et al. aimed to develop an analytical method for the simultaneous estimation of LED and SOF in the presence of DP produced under stress conditions using RP-HPLC with UV detection (Mastanamma et al., 2018). Kumar et al. aimed to develop a stability-indicating RP-HPLC method to determine LED and SOF in tablets using ICH guidelines (Kumar & Rao, 2018), whereas Veereswara reported a new stability-indicating RP-HPLC method for the determination of LED and SOF in tablets (Veereswara Rao et al., 2018). Bandla et al. reported a RP-HPLC stability-indicating method for determining LED and SOF in tablets in the presence of DP, produced under stress conditions (Jahnvi & Ganapaty, 2018). A precise, simple, and stability-indicating RP-HPLC method was developed to estimate LED and SOF in tablets, and the method was validated as recommended in the ICH guidelines (Reddy et al., 2018).

By 2019 a simple, robust and selective RP-HPLC method for the estimation of LED and SOF in bulk had been developed using a QbD approach and forced degradation studies were applied for the purposes of method optimization (Yeram et al., 2019). An accurate, precise, simple RP-HPLC method was developed to estimate LED and SOF in tablets and forced degradation studies, applied according to

ICH guidelines, and revealed the final method was stability-indicating (Mankar et al., 2019). In a study conducted by Kumari et al., a stability-indicating UPLC method was developed and validated using the ICH guidelines, and the method was faster, more accurate, and more precise when compared to other methods. All samples subjected to stress conditions were analyzed using the optimized method, and based on the ICH guidelines, the method was found to be stability-indicating (Kumari & Sankar, 2019). Bhavani et al. reported that no stability-indicating method existed for the analysis of LED and SOF in multi-component tablets, and the primary purpose of their study was to develop a stability-indicating method for the analysis of LED and SOF in bulk. The RP-HPLC method using photodiode array detection was developed and optimized with the aid of forced degradation studies, which resulted in a highly specific approach to analysis (Bhavani & Maduri, 2020). In a study conducted by Suganthi et al., it was reported that no stability-indicating method had been published to determine LED and SOF in tablets. Therefore, their study aimed to develop a rapid, simple, and robust HPLC method for the assay of LED and SOF in tablets, and forced degradation studies were performed according to ICH guidelines (Suganthi et al., 2019). El Yazbi et al. reported a precise, rapid, simple, and eco-friendly HPTLC method for the simultaneous analysis of LED and SOF in tablets. Forced degradation studies performed according to ICH guidelines under acidic and alkaline hydrolysis, oxidative, and photolytic conditions revealed the method was stability-indicating (El-Yazbi et al., 2020). Narla et al. developed a stability-indicating UHPLC method for the simultaneous estimation of SOF and LED in tablets. The proposed method is simple and accurate and was used to analyze tablets in the presence of DP (Narla & Pappula, 2020).

A summary of the stress test conditions and % degradation is reported in (Tables 8. and 9.), respectively. In studies No. 1, 3, 4, 9, and 12, forced degradation studies were performed on bulk API, whereas in all other studies, forced degradation studies were undertaken using tablets.

**Table 8.** Summary of stress study conditions for SOF and LED

Study (Form)	Hydrolysis			Oxidation	Thermolysis	Photolysis	Reference
	Acidic	Basic	Neutral				
<b>Study 1 (Bulk)</b>	1N HCl 25°C 48 h	1N NaOH 25°C 48 h	NR	3% H <sub>2</sub> O <sub>2</sub> 25°C 48 h	80°C 8 h in dry heat or Stability chamber 40°C±2,75%±5%RH 7 days in wet heat (In solid state)	Sunlight 48 h (In solid state)	(Hassouna et al., 2017)
<b>Study 2 (Tablet)</b>	1.1N HCl 25°C 30 min	1.1N NaOH 25°C 30 min	NR	3% H <sub>2</sub> O <sub>2</sub> 25°C 30 min	105°C 30 min (In solid state)	Sunlight 24 h (In solid state)	(Rao et al., 2017)
<b>Study 3 (Bulk)</b>	1.1N HCl 25°C 24 h	1.1N NaOH 25°C 24 h	Water 25°C 24 h	3% H <sub>2</sub> O <sub>2</sub> 25°C 24 h	NR	NR	(Rote et al., 2017)
<b>Study 4 (Bulk)</b>	5N HCl 60°C 30 min	5N NaOH 70°C 60 min	Water 70°C 3 h	30% H <sub>2</sub> O <sub>2</sub> 70°C 1 h	105°C 72 h (In solid state)	UV light 1.2 million lux hours 24 h (In solid state)	(Mastanamma et al., 2018)
<b>Study 5 (Tablet)</b>	2N HCl 60°C 30 min	2N NaOH 60°C 30 min	Water 60°C 6 h	20% H <sub>2</sub> O <sub>2</sub> 60°C 30 min	105°C 6 h (In solution state)	UV chamber 7 days or 200-watt hours/ m <sup>2</sup> (In solution state)	(Kumar & Rao, 2018)
<b>Study 6 (Tablet)</b>	2N HCl 60°C 30 min	2N NaOH 60°C 30 min	Water 60°C 1 h	20% H <sub>2</sub> O <sub>2</sub> 60°C 30 min	105°C 6 h in dry heat Stability chamber 40±2°C,75%±5%RH 1 day in wet heat. (In solution state)	UV light (In solution state)	(Veereswara Rao et al., 2018)
<b>Study 7 (Tablet)</b>	2N HCl 60°C 30 min	2N NaOH 60°C 30 min	NR	20% H <sub>2</sub> O <sub>2</sub> 60°C 30 min	105°C 6 h (In solution state)	UV light 7 days or 200-watt hours/ m <sup>2</sup> (In solution state)	(Jahnavi & Ganapaty 2018)
<b>Study 8 (Tablet)</b>	2N HCl 60°C 30 min	2N NaOH 60°C 30 min	NR	20% H <sub>2</sub> O <sub>2</sub> 60°C 30 min	105°C 6 h (In solution state)	UV light 254nm 7 days or 200-watt hours/m <sup>2</sup> (In solution state)	(Reddy et al., 2018)
<b>Study 9 (Bulk)</b>	1N HCl 80°C 1 h	1N NaOH 80°C 1h	NR	3% H <sub>2</sub> O <sub>2</sub> 25°C 25 min	80°C 2 h (In solution state)	UV light 290nm 7 days (In solid state)	(Yeram et al., 2019)
<b>Study 10 (Tablet)</b>	5N HCl 60°C 30 min	5N NaOH 70°C 60 min	NR	30% H <sub>2</sub> O <sub>2</sub> 70°C 48 h	105°C 48 h (In solution state)	UV light 1.2 million lux hours 48 h (In solution state)	(Mankar et al., 2019)
<b>Study 11 (Tablet)</b>	2N HCl 60°C 30 min	2N NaOH 60°C 30 min	Water 60°C 6 h	20% H <sub>2</sub> O <sub>2</sub> 60°C 30 min	105°C 6 h (In solution state)	UV light 7 days (In solution state)	(Kumari & Sankar, 2019)
<b>Study 12 (Bulk)</b>	1N HCl 70°C 48 h	1N NaOH 70°C 48 h	NR	3% H <sub>2</sub> O <sub>2</sub> 70°C 48 h	70°C 14 days (In solid state)	UV light 14 days (In solid state)	(Bhavani & Maduri, 2020)
<b>Study 13 (Tablet)</b>	0.1 N HCl 80°C 5 h	0.1 N NaOH 80°C 5 h	Water 80°C 5 h	6% H <sub>2</sub> O <sub>2</sub> 25°C 5 h	80°C 5 h (In solid state)	UV light 5 h (In solid state)	(Suganthi et al., 2019)
<b>Study 14 (Tablet)</b>	1N HCl 90°C 1 h	1N NaOH 90°C 1 h	NR	30% H <sub>2</sub> O <sub>2</sub> 80°C 1h	NR	UV light 254 nm for 12 h UV light 365 nm for 12 h (In solution state)	(El-Yazbi et al., 2020)
<b>Study 15 (Tablet)</b>	1N HCl 25°C 2 h	1N NaOH 25°C 2 h	NR	30% H <sub>2</sub> O <sub>2</sub> 25°C 2 h	110°C 2 h (In solution state)	Sunlight 8 h (In solution state)	(Narla & Pappula, 2020)

**Table 9.** % Degradation following analysis simultaneous analysis of SOF and LED

Study		Hydrolysis			Oxidation	Thermolysis	Photolysis	Reference
		Acidic	Basic	Neutral				
Study 1	SOF	12.44	12.60	NR	5.40	Dry: 7.89 Wet: 12.54	6.36	(Hassouna et al., 2017)
	LED	10.32	10.05	NR	1.60	Dry: 6.12 Wet: 10.6	4.63	
Study 2	SOF	2.27	2.14	NR	1.67	1.74	1.39	(Rao et al., 2017)
	LED	1.97	1.71	NR	1.92	1.06	1.32	
Study 3	SOF	4.03	1.35	2.15	0.35	NR	NR	(Rote et al., 2017)
	LED	0.08	0.99	0.22	0.22	NR	NR	
Study 4	SOF	29.7	28.1	24.00	26.4	20.00	24.10	(Mastanamma et al., 2018)
	LED	26.40	29.50	28.30	26.00	24.80	25.10	
Study 5	SOF	2.97	2.17	0.16	1.65	0.85	0.38	(Kumar & Rao, 2018)
	LED	4.72	2.29	0.19	1.24	0.85	0.61	
Study 6	SOF	5.41	3.67	2.69	2.88	Dry: 1.15 Wet: 3.75	0.87	(Veerewara 2018)
	LED	4.75	4.20	2.57	5.95	Dry: 2.00 Wet: 3.5	1.00	
Study 7	SOF	4.90	3.03	NR	1.30	0.70	0.48	(Jahnavi & Ganapaty, 2018)
	LED	3.65	3.26	NR	2.25	1.09	0.94	
Study 8	SOF	5.67	3.93	NR	3.35	2.67	1.70	(Reddy et al., 2018)
	LED	5.05	4.43	NR	3.66	2.99	1.83	
Study 9	SOF	3.10	7.80	NR	1.40	3.20	0	(Yeram et al., 2019)
	LED	17.13	12.45	NR	11.91	9.20	18.72	
Study 10	SOF	0.44	0.02	NR	0.41	0.04	0.01	(Mankar et al., 2019)
	LED	1.18	0.05	NR	1.73	0.05	0.07	
Study 11	SOF	6.09	5.49	0.72	3.83	2.69	1.99	(Kumari & Sankar, 2019)
	LED	6.21	4.84	0.83	3.14	2.35	1.52	
Study 12	SOF	NR	NR	NR	NR	NR	NR	(Bhavani & Maduri, 2020)
	LED	NR	NR	NR	NR	NR	NR	
Study 13	SOF	NR	NR	NR	NR	NR	NR	(Suganthi et al., 2019)
	LED	NR	NR	NR	NR	NR	NR	
Study 14	SOF	52.29	58.96	NR	16.90	NR	0	(El-Yazbi et al., 2020)
	LED	10.96	8.57	NR	37.99	NR	0	
Study 15	SOF	7.72	9.55	NR	8.72	8.03	8.03	(Narla & Pappula, 2020)
	LED	5.41	5.35	NR	5.64	4.45	4.70	

The summary of chromatographic conditions used in all studies is listed in (Table 10.).

**Table 10.** Summary of chromatographic conditions used in all studies

Study	Method	Mobile Phase and Elution Mode	Stationary Phase	Detector Wavelength (nm)	LOQ (µg/ml)	Reference	
SOF ONLY	1	RP-UFLC	0.1% FA <sup>1</sup> : ACN <sup>2</sup> (40: 60% v/v)	C8	PDA <sup>3</sup> , 259	0.76	(Annapurna et al., 2018)
	2	RP-HPLC	Methanol: Water (70: 30% v/v)	C18	UV <sup>4</sup> , 254	1.00	(Nebsen & Elzanfaly, 2016)
	3	UPLC	ACN: 0.1% FA	C18	PDA, 260	0.83	(Pottabathini et al., 2016)
	4	HPLC	AA <sup>5</sup> :ACN	C18	PDA, 260	NR	(Swain et al., 2016)
	5	RP-HPLC	Methanol: Water (65: 35% v/v)	C18	PDA, 261	NR	(Vanitha et al., 2018)
	6	RP-HPLC	Methanol: Water with 0.1% FA (50:50 %v/v)	C18	PDA, 261	NR	(Agarwal et al., 2022)
	7	RP-HPLC	PDP <sup>6</sup> : ACN (60:40 %v/v)	C18	PDA, 260	30.62	(Hassouna & Mohamed., 2018)
	8	UPLC	0.1% OPA <sup>7</sup> : Methanol (40:60% v/v)	C18	UV, 260	0.55	(Abdel-Razeg et al., 2019)
	9	RP-HPLC	0.1% OPA: ACN (30:70% v/v)	C18	UV, 260	1.07	(Lalitha et al., 2018)
	10	RP-HPLC	0.05% PA <sup>8</sup> : ACN	C18	PDA, 260	1.45	(Hamdache et al., 2021)
SOF&VEL	1	HPTLC	EA <sup>9</sup> : IPA <sup>10</sup> (9:1 %v/v)	Silica gel 60 F 254	UV, SOF: 260 VEL:302	SOF: 76.25 ng/band VEL: 30.19 ng/band	(Damle & Kalaskar, 2020)
	2	RP-HPLC	ODP <sup>11</sup> (0.01%): ACN (50:50% v/v)	C18	UV, 240	SOF: 1.32 VEL: 1.01	(Lakshmana Rao & Pallavi, 2019)
	3	RP-HPLC	PDP: Methanol (60:40% v/v)	C18	PDA, 240	SOF: 1.60 VEL: 0.62	(Saroja et al., 2018)
	4	RP-HPLC	0.1% FA:ACN	C8	PDA, 259	SOF: 3.83 VEL: 0.91	(Hemchand et al., 2018)
	5	RP-HPLC	PDP: ACN (50:50% v/v)	C18	PDA, 240	SOF: 0.78 VEL: 0.50	(Bandla & Ganapaty, 2017)
	6	RP-HPLC	PDP: ACN (50:50% v/v)	C8	PDA, 240	SOF: 0.61 VEL: 0.65	(Rao et al., 2018)
	7	RP-UPLC	Phosphate buffer: ACN (50:50% v/v)	C18	PDA, 240	SOF: 4.49 VEL: 5.13	(Lakshmi et al., 2018)
	8	RP-HPLC	PDP: ACN (50:50% v/v)	YMC Column	UV, 255	SOF: 1.20 VEL: 0.30	(Priyanka et al., 2018)
	9	HPLC	AA <sup>12</sup> : ACN (45:55% v/v)	C18	UV, 268	SOF: 0.38 VEL: 0.24	(Zaman & Hassan, 2021)
	10	RP-HPLC	SDOP <sup>13</sup> : ACN (85:15% v/v)	C18	PDA, 292	SOF: 0.04 VEL: 0.06	(Harshalatha et al., 2018)
	11	UPLC	PDP: ACN (45:55% v/v)	C18	UV, 250	SOF: 0.35 VEL: 0.03	(Susmita & Rajitha, 2018)
	12	UPLC	PPM <sup>14</sup> : ACN (50:50% v/v)	C8	PDA, 260	SOF: 0.29 VEL: 1.25	(Namratha & Vijayalakshmi, 2021)
	13	HPLC	FA in Water: ACN: Methanol (30:30:40% v/v)	Phenyl XDB	PDA, 273	SOF: 1.20 VEL: 0.30	(R Godela & Sowjanya, 2020)
SOF & DAC	1	RP-HPLC	PDP: ACN (50:50% v/v)	C18	PDA, 254	SOF: 0.07 DAC: 0.03	(Bandla & Ganapaty, 2018)
	2	RP-HPLC	ACN: TFA <sup>15</sup> in water (50:50% v/v)	XDB Phenyl	PDA, 275	SOF: 15.80 DAC: 7.80	(Ramreddy Godela & Sowjanya, 2021)

SOF&VEL&VOX	1	RP-HPLC	OPA: ACN (55:45% v/v)	C18	PDA, 220	SOF: 0.34 VEL: 0.29 VOX: 0.17	(Deepthi & Sankar, 2020)
	2	RP-HPLC	SDOP: ACN (60:40% v/v)	C18	PDA, 220	SOF: 1.14 VEL: 0.99 VOX: 0.24	(Kokkerala & Suryakala, 2020)
	3	RP-HPLC	OPA: ACN (50:50% v/v)	C18	PDA, 220	SOF: 0.25 VEL: 0.87 VOX: 0.31	(Balaswami et al., 2018)
	4	RP-HPLC	ACN: Water (65:35% v/v)	C18	PDA, 220	SOF: 2.32 VEL: 0.53 VOX: 0.70	(Padmini M et al., 2019)
	5	RP-UPLC	PDP: Methanol (50:50% v/v)	C18	PDA, 260	SOF: 0.02 VEL: 0.40 VOX: 0.02	(Lakshmi Meneka S et al., 2020)
SOF&LED	1	RP-HPLC	Phosphate buffer: ACN (50:50% v/v)	C18	UV, 254	SOF: 12.54 LED: 11.03	(Hassouna et al., 2017)
	2	RP-HPLC	DHP <sup>16</sup> : ACN (60:40% v/v)	C18	PDA, 282	SOF: 0.75 LED: 0.25	(Rao et al., 2017)
	3	RP-HPLC	Methanol: Water with 0.05% acetic acid (83:17% v/v)	Purospher RP-18	UV, 245	SOF: 10.19 LED: 3.30	(Rote et al., 2017)
	4	RP-HPLC	ACN: TEA <sup>17</sup> (50:50% v/v)	C18	UV, 227	SOF: 0.50 LED: 0.51	(Mastanamma et al., 2018)
	5	RP-HPLC	ACN: 0.1% OPA buffer (35:65% v/v)	C18	UV, 272	SOF: 3.70 LED: 0.56	(Kumar & Rao, 2018)
	6	RP-HPLC	ACN: 0.1% OPA (50:50% v/v)	C8	UV, 230	SOF: NR LED: NR	(Veereswara Rao et al., 2018)
	7	RP-HPLC	ACN: 0.1% OPA (55:45% v/v)	C18	PDA, 270	SOF: 0.65 LED: 0.19	(Jahnvi & Ganapaty, 2018)
	8	RP-HPLC	ACN: OPA (55:45% v/v)	C8	PDA, 260	SOF: 0.76 LED: 1.13	(Reddy et al., 2018)
	9	RP-HPLC	Methanol: AA with GAA <sup>18</sup> (70:30% v/v)	C18	PDA, 254	SOF: 1.50 LED: 11	(Yeram et al., 2019)
	10	RP-HPLC	TFA: ACN (70:30% v/v)	C18	UV, 245	SOF: 1.20 LED: 0.40	(Mankar et al., 2019)
	11	UPLC	PDP: ACN (50:50% v/v)	C18	UV, 220	SOF: 3.91 LED: 1.29	(Kumari & Sankar, 2019)
	12	RP-HPLC	OPA: Methanol (45:55% v/v)	C8	PDA, 238	SOF: 2.21 LED: 0.70	(Bhavani & Maduri, 2020)
	13	HPTLC	Hexane: EA: Methanol (5:3:2 %v/v)	Silica gel 60 F <sub>254</sub>	UV, 288	SOF: 1.32 ng/spot LED: 0.40 ng/spot	(Suganthi et al., 2019)
	14	HPTLC	EA: Methanol: Water: GAA (30:1.5:1:0.2 %v/v)	Silica gel F <sub>254</sub>	PDA, SOF 260 LED 320	SOF: 1.90 µg/band LED: 0.33 µg/band	(El-Yazbi et al., 2020)
	15	RP-HPLC	ACN: Phosphate (55:45% v/v)	C18	PDA, 247	SOF: 0.28 LED: 0.32	(Narla & Pappula, 2020)

<sup>1</sup>FA: Formic Acid

<sup>2</sup>ACN: Acetonitrile

<sup>3</sup>PDA: Photo Diode Array

<sup>4</sup>UV: Ultra Violet

<sup>5</sup>AA: Acetic Acid

<sup>6</sup>PDP: Potassium Dihydrogen Phosphate

<sup>7</sup>OPA: Ortho Phosphoric Acid

<sup>8</sup>PA: Phosphoric Acid

<sup>9</sup>EA: Ethyl Acetate

<sup>10</sup>IPA: Iso Propyl Alcohol

<sup>11</sup>ODP: Ortho Dihydrogen Phosphate

<sup>12</sup>AA: Ammonium Acetate

<sup>13</sup>SDOP: Sodium Dihydrogen Orthophosphate

<sup>14</sup>PPM: Potassium Phosphate Monobasic

<sup>15</sup>TFA: Trifluoro Acetic Acid

<sup>16</sup>DHP: Disodium Hydrogen Phosphate

<sup>17</sup>TEA: Triethylamine

<sup>18</sup>GAA: Glacial Acetic Acid

### **Analysis of SOF alone**

Ten studies in which the analysis of SOF alone with stress testing and designated stability-indicating method for the drug was identified and included (Abdel-Razeq et al., 2019; Agarwal et al., 2022; Annapurna et al., 2018; Hamdache et al., 2021; Hassouna & Mohamed, 2018; Lalitha et al., 2018; Nebsen & Elzanfaly, 2016; Pottabathini et al., 2016; Swain et al., 2016; Vanitha et al., 2018).

In Study No. 1 (Annapurna et al., 2018), the conditions used for stress testing were not based on those recommended in the ICH guidelines (Guideline, 2003). The API was tested under extremely severe stress conditions for a short period. By way of example, the concentrations of H<sub>2</sub>O<sub>2</sub> were 30% v/v, and the temperature was 60°C for the oxidative stress test. However, oxidative stress testing with H<sub>2</sub>O<sub>2</sub> should be performed at or lower than room temperature as at high temperatures, H<sub>2</sub>O<sub>2</sub> decomposes to form hydroxyl radicals, which are highly reactive in their own right and may result in the formation of DPs that would never form under normal storage conditions in bulk and pharmaceutical dosage forms (Yaripour, Rashid, Alibakhshi, & Mohammadi, 2015). Therefore, when severe stress conditions are applied over a period of time, the API may be destroyed instead of undergoing degradation. This study stated that the API was sensitive to alkaline hydrolytic and oxidative stress conditions but did not degrade under thermal and photolytic conditions. Different results may have been observed if the conditions and duration of stress were selected based on the relevant guidelines. In Study No. 2 (Nebsen & Elzanfaly, 2016), the duration of alkaline hydrolysis was not selected according to the published guidelines and 90% and 100% of API degraded in 6 and 24 hours, respectively. The ICH guideline states that the duration of stress testing should be selected such that a maximum of 5-20% of API degrades during the test period (Baertschi, Alsante, & Reed, 2016). In addition, for the thermal studies, the API was tested at 80°C while the recommendation is that the temperature range used fall between 50 and 70°C

(Baertschi et al., 2016). It was reported that the API did not degrade under this condition. However, the thermal study test period should be extended to ensure the API is or is not sensitive to the test conditions. According to the ICH guideline, the recommended concentration of H<sub>2</sub>O<sub>2</sub> should be between 0.3-3% v/v (Baertschi et al., 2016), whereas in this study, 3% and 6% v/v concentrations were used. Consequently, the DP produced at the 6% v/v concentration may not be reliable. Furthermore, the ICH guideline states that photolytic studies should be performed in the presence of UV and visible light (Baertschi et al., 2016), but in this study, the API was only exposed to UV light for 6 hours in an aqueous solution of the API which turned yellow in these conditions with an apparent 70% degradation, suggesting the study is incomplete and possibly unreliable. In Study No. 3 (Pottabathini et al., 2016), a temperature of 80°C was used to perform acid hydrolysis testing of SOF, which is higher than that recommended in guidelines which require testing at room temperature or temperatures up to a maximum of 70°C (Baertschi et al., 2016). In addition, 30% v/v H<sub>2</sub>O<sub>2</sub> at 80°C was used for the oxidative stress study, which, as previously mentioned, is outside the recommended concentration of H<sub>2</sub>O<sub>2</sub> of 0.3-3% v/v at ambient temperature. In Study No. 4 (Swain et al., 2016), the decomposition behavior of API under different stress conditions was monitored using a 30% v/v concentration of H<sub>2</sub>O<sub>2</sub> for the oxidative stress study, and a temperature of 80°C was used for the thermal stress test. In Study No. 5 (Vanitha et al., 2018), no decomposition was reported to have occurred when oxidative and thermal stress conditions were used however, the API was found to be sensitive to acidic and alkaline hydrolytic stress conditions. The drawback of these studies is that their duration was too short, and it is unclear whether more decomposition products would have been produced if a longer exposure time had been used. In Study No. 6 (Agarwal et al., 2022), what can be considered acceptable stress conditions were used. For acidic and alkaline hydrolysis, 0.1N HCl

and 0.1N NaOH were used, respectively. The rate of degradation in acidic hydrolysis was remarkable, and a major DP was produced, whereas, during alkaline hydrolysis, 50% of the drug degraded, and another major DP was produced. The conditions used for oxidative stress testing were also acceptable according to guidelines and > 10% API degraded with a major DP produced. The API was stable under thermal and photolytic stress test conditions. It is considered better to select conditions according to approved guidelines to evaluate the effects of light on an API while monitoring the effects of UV light and fluorescence on API degradation. In Study No. 7 (Hassouna & Mohamed., 2018), high concentrations of acid and alkali were used for acid and alkaline hydrolysis experiments. During the oxidation study, a 3% v/v concentration of H<sub>2</sub>O<sub>2</sub> was used at room temperature for 48 hours, which resulted in 4.56% degradation. If the duration of this study had been extended, the extent of degradation would have been greater, and the study would have been more accurate. The photolysis study was also conducted for 48 hours, after which 7% degradation had occurred. It would have been better if this study had been continued for a longer time so that the percent degradation would be greater. For thermal studies, the API was exposed to 40°C and 75% humidity in a climatic chamber for one month, which resulted in 4% degradation that suggests the conditions and duration of the study were acceptable. In Study No. 8 (Abdel-Razeg et al., 2019), the API was subjected to acidic, alkaline and oxidative stress conditions. The 5 N concentration of acid and base used was very high. In addition, a very high temperature of 100°C was used for acid and alkaline hydrolysis studies. These conditions are severe and are well beyond those recommended in the guidelines. Furthermore at temperature >70°C, the decomposition kinetics of the API do not follow the Arrhenius model because, at temperatures <70°C, the mechanism of drug degradation may change, and products may be formed that are never formed under normal conditions of drug storage (Yaripour

et al., 2015). In Study No. 9 (Lalitha et al., 2018) listed in (Table 1.) the use of mild stress conditions was reported. However, the results suggest the conditions for degradation used were appropriate and degradation between 5-10 % was observed (Baertschi et al., 2016). In Study No. 10 (Hamdache et al., 2021), stress tests were performed on API and tablets. The 1N concentration of acid and alkali used was high. However, the temperature used was 8°C, which is different from the normal storage conditions for the drug. The 30% v/v H<sub>2</sub>O<sub>2</sub> used is also high, but the stress was applied at 8°C. The duration of all tests was one hour, which is also different from the conditions for drug storage and is not aligned with the guidelines (Baertschi et al., 2016). The low percent degradation of < 1% under oxidative and photolytic conditions is more than likely due to the short duration of exposure during stress testing.

#### **Analysis of SOF and VEL**

The simultaneous stability indicating analysis of SOF and VEL, which included stress testing, was reported in 13 studies (Bandla & Ganapaty, 2017; Damle & Kalaskar, 2020; R Godela & Sowjanya, 2020; Harshalatha et al., 2018; Hemchand et al., 2018; Lakshmana Rao & Pallavi, 2019; Lakshmi et al., 2018; Namratha & Vijayalakshmi, 2021; Priyanka et al., 2018; Rao et al., 2018; Saroja et al., 2018; Susmita & Rajitha, 2018; Zaman & Hassan, 2021).

Different stress test conditions applied to the two compounds resulted in different outcomes (Bandla & Ganapaty, 2017). In addition, the concentration of stress agent used was as recommended in guidelines, and the time of exposure to the stress conditions was more reasonable. However, these studies are not comparable. By way of example, in Study No. 4 (Hemchand et al., 2018), 0.1 N acid and alkali were used however, in Study No. 5 (Bandla & Ganapaty, 2017), a 2 N acid and alkali concentration was used. In both cases, the duration of exposure was 30 min at a temperature of 60°C. However, Study No. 4 (Hemchand et al., 2018), in which an appropriate

concentration of the stress factor was used, revealed lower degradation. A comparison of the results of hydrolytic studies shows that the duration of the stress test is influential on the extent of hydrolysis. Temperature also has an impact on the rate of hydrolysis. In Studies No. 9 and 10 (Harshalatha et al., 2018; Zaman & Hassan, 2021), the same concentration of acid and alkali and duration used were the same. However, Study No. 9 (Zaman & Hassan, 2021) was conducted at room temperature and Study No. 10 (Harshalatha et al., 2018) at 85°C.

In a comparison of the results of these two studies, the effect of temperature is evident, and greater degradation was observed for both drugs under acidic and alkaline conditions. Greater degradation was observed for VEL under higher temperatures. As previously mentioned, using temperatures higher than ambient conditions for oxidative stress tests may result in the formation of hydroxyl radicals, which are known to be very corrosive. Also, according to the guidelines, H<sub>2</sub>O<sub>2</sub> concentrations are usually considered appropriate to range between 0.3-3% (Baertschi et al., 2016). Therefore, studies in which high concentrations of H<sub>2</sub>O<sub>2</sub> are used or where the temperature is higher than room temperature are likely to produce unreliable results. What is critical is that sufficient exposure time should be considered for oxidative degradation to ensure the desired level of degradation is attained. Only in Study No. 9 (Zaman & Hassan, 2021) was an appropriate concentration of H<sub>2</sub>O<sub>2</sub> used for the experiment conducted at room temperature for 7 days with an outcome that revealed that VEL was more sensitive to oxidative stress conditions than SOF. Applying thermal stress conditions revealed that both drugs are not sensitive to thermolytic conditions, and the duration of exposure is critical to causing stress. Therefore, sufficient time should be permitted to ensure thermolytic stress can be achieved. According to the guidelines, API thermal stress studies should be performed in the solid state at high under low humidity conditions (Baertschi et al., 2016). Only five studies used API in the solid

state, and the tests were undertaken without humidity control. Photolytic stress testing revealed that both drugs were not very sensitive to the conditions.

#### **Analysis of SOF and DAC**

Two stability-indicating methods for the analysis of SOF and DAC in which stress tests were performed have been reported (Bandla & Ganapaty, 2018; Ramreddy Godela & Sowjanya, 2021).

Study No. 1, reported in (Table 4.) (Bandla & Ganapaty, 2018), used a high concentration of acid, base and H<sub>2</sub>O<sub>2</sub>. The stress testing results revealed that under acidic and basic hydrolysis in Study No. 2 (Ramreddy Godela & Sowjanya, 2021), more extensive degradation of both drugs occurred. However, SOF was more sensitive to hydrolytic conditions than DAC. In study No. 2 (Ramreddy Godela & Sowjanya, 2021), a 3% v/v H<sub>2</sub>O<sub>2</sub> solution at a temperature of 70°C was used for oxidative studies. As previously mentioned, oxidative testing with H<sub>2</sub>O<sub>2</sub> is better if performed at ambient temperatures to avoid the possible formation of hydroxyl radicals. Both drugs exhibited limited degradation under thermal and photolytic conditions. However, thermal testing in this study was performed on a solution with humidity control. According to the guidelines, it is suggested that thermal testing be performed on API in the solid state at low and high humidity conditions (Baertschi et al., 2016).

#### **Analysis of SOF, VEL and VOX**

Stability indicating analytical methods for the analysis of SOF, VEL and VOX simultaneously with stress testing was reported in 5 studies (Balaswami et al., 2018; Deepthi & Sankar, 2020; Kokkiralala & Suryakala, 2020; Lakshmi Maneka S et al., 2020; Padmini M et al., 2019).

Acid and alkali hydrolysis were performed with a high concentration of acid and alkali, and in all but one case, a temperature of 60°C was applied for 30 min. Neutral hydrolysis was also undertaken, and little degradation was observed. In all five studies (Balaswami et al., 2018; Deepthi & Sankar, 2020;



Kokkiralala & Suryakala, 2020; Lakshmi Maneka S et al., 2020; Padmini M et al., 2019), oxidative stress was undertaken with 20% v/v H<sub>2</sub>O<sub>2</sub> at a temperature of 60°C in studies No. 2 to 5 (Balaswami et al., 2018; Kokkiralala & Suryakala, 2020; Lakshmi Maneka S et al., 2020; Padmini M et al., 2019), whereas in Study No.1 (Deepthi & Sankar, 2020) the temperature used was not reported and the percentage of degradation in all three drugs was almost the same. As mentioned before, it is better to have a H<sub>2</sub>O<sub>2</sub> concentration of 3-6% and to do it at room temperature so that the DPs obtained are reliable. The thermolytic and photolytic testing conditions in these studies were similar and the results are in the same range.

#### **Analysis of SOF and LED**

The studies in which stability-indicating methods of analysis for SOF and LED are reported totals 15 (Bhavani & Maduri, 2020; El-Waey et al., 2023; El-Yazbi et al., 2020; Hassouna et al., 2017; Jahnavi & Ganapaty, 2018; Kumar & Rao, 2018; Kumari & Sankar, 2019; Mankar et al., 2019; Mastanamma et al., 2018; Narla & Pappula, 2020; Rao et al., 2017; Reddy et al., 2018; Rote et al., 2017; Suganthi et al., 2019; Veereswara Rao et al., 2018; Yeram et al., 2019).

Acid hydrolysis test conditions were considered suitable in Studies No. 13, but the alkaline stress test conditions used were unsuitable (El-Waey et al., 2023; Suganthi et al., 2019). Oxidative stress conditions in Studies No. 1,2,3,9 and 13 (Hassouna et al., 2017; Rao et al., 2017; Rote et al., 2017; Suganthi et al., 2019; Yeram et al., 2019) are better than others because an appropriate concentration of H<sub>2</sub>O<sub>2</sub> of 3-6% controlled at ambient temperature was used.

#### **CONCLUSIONS**

To analyze an API in the presence of impurities, it is necessary to design short- and long-term stability studies based on valid guidelines while developing a stability-indicating analytical method for that API before validation of that method. The conditions used for stability studies should be identified and selected according to valid guidelines so that the degradation

data generated are reliable. This review reveals that diverse approaches for the analysis of SOF are used, and the resultant data are highly variable and scattered. One of the important features of the studies reviewed is that they use short-term stability tests only and that no long-term stability testing was undertaken or reported. Since SOF has not yet been included in a monograph in any official pharmacopoeia, more detailed studies must be conducted using valid guidelines to produce important data relating to the degradation of the API, and DPs should be separated using a stability-indicating method specifically designed for routine analysis of the drug. The shortcomings identified in the studies investigated include not identifying the main DP and not reporting the kinetics or mechanism of degradation of the drug.

#### **Recommendations**

A review of published analytical studies for SOF has revealed that additional research is needed with respect to the analysis of SOF to overcome the shortcomings identified in previous studies and ensure that an accurate and reliable analytical method is designed to identify the API and its impurities. Accordingly, we have designed a study in our laboratory to perform stress and accelerated tests on the API and final product of SOF in accordance with valid guidelines. We aim to identify important DP so that a definitive stability-indicating analytical method for this API can be developed and validated. The main objectives of our study are to identify the degradation pathways, kinetics of degradation and purification of the important DP of the parent API.

#### **AUTHOR CONTRIBUTION STATEMENT**

Writing (N, HK), Writing (NN), Supervision (AM), Review and Editing (RB, W)

The contribution of authors, N, HK and NN is equal.

#### **CONFLICT OF INTEREST**

The authors declare that there is no conflict of interest.

## REFERENCES

- Abdel-Razeq, S. A., Nasr, Z. A., & S Said, N. (2019). Validated stability-indicating methods for determination of sofosbuvir by UPLC and HPTLC in pure form and tablet dosage forms. *Asian Journal of Applied Chemistry Research*, 3(4), 1-13. doi: 10.9734/ajacr/2019/v3i430097
- Agarwal, B., Jagdale, S., & Gandhi, S. (2022). Forced Degradation Study of Sofosbuvir: Identification of Degradation Products by LC-ESI-MS. *Indian Journal of Pharmaceutical Education and Research* 56(2), S181-S188. doi:10.5530/ijper.56.2s.89
- Annapurna, M. M., Teja, G. R., & Chaitanya, P. S. K. (2018). New stability indicating ultrafast liquid chromatographic method for the determination of sofosbuvir in tablets. *Asian Journal of Pharmaceutics (AJP)*, 12(1), S151-S158. doi:10.22377/ajp.v12i01.2060
- Baertschi, S. W., Alsante, K. M., & Reed, R. A. (2016). *Pharmaceutical stress testing: predicting drug degradation*: CRC Press.
- Balawami, B., Ramana, P. V., Rao, B. S., & Sanjeeva, P. (2018). A new simple stability-indicating RP-HPLC-PDA method for simultaneous estimation of triplicate mixture of sofosbuvir, velpatasvir and voxilaprevir in tablet dosage form. *Research Journal of Pharmacy and Technology*, 11(9), 4147-4156. doi:10.5958/0974-360X.2018.00762.X
- Bandla, J., & Ganapaty, S. (2017). Stability indicating RP-HPLC method development and validation for the simultaneous determination of Sofosbuvir and Velpatasvir in tablet dosage forms. *Indian Journal of Pharmaceutical and Biological Research*, 5(04), 10-16. doi:10.30750/IJPBR.5.4.3
- Bandla, J., & Ganapaty, S. (2018). Development and Validation of Stability Indicating RP-HPLC Method for the Simultaneous Estimation of Sofosbuvir and Daclatasvir Dihydrochloride in Bulk Drug and Pharmaceutical Dosage Form. *Saudi Journal of Medical and Pharmaceutical Sciences*, 4(5), 542-551. doi:10.21276/sjmps.2018.4.5.10
- Bhavani, R. P. S., & Maduri, M. S. (2020). Stability indicating method development and validation for the simultaneous estimation of ledipasvir and sofosbuvir in bulk drug by using RP-HPLC. *World Journal of Current Medical and Pharmaceutical Research*, 2(5), 307-3018. doi:10.37022/wjcmpr.vi.159
- Bhujbal, S. S., & Darkunde, S. L. (2019). Analytical method development and optimization of sofosbuvir drug-a QbD approach. *International Journal of Pharmaceutical Sciences and Research*, 10(1), 108-116. doi:10.13040/IJPSR.0975-8232.10(1).108-16
- Damle, M., & Kalaskar, P. (2020). Stability indicating HPTLC method for sofosbuvir and velpatasvir in combination. *International Journal of Pharmaceutical Science and Drug Research*, 12(2), 129-135. doi:10.25004/IJPSDR.2020.120206
- Deepthi, R., & Sankar, D. (2020). Development and Validation of a Stability-Indicating RP-HPLC Method for the Simultaneous Determination of Sofosbuvir, Velpatasvir, and Voxilaprevir in Tablet Formulation. *Global Journal of Medical Research: B Pharma, Drug Discovery, Technology & Medicine* 20(3). doi:10.34257/gjmr.vol20is3pg7
- El-Waey, A. A., Abdel-Salam, R. A., Hadad, G. M., & El-Gindy, A. (2023). Eco friendly stability indicating HPTLC method for simultaneous determination of sofosbuvir and ledipasvir in pharmaceutical tablets and HPTLC-MS characterization of their degradation products. *Microchemical Journal*, 186, 108324. doi:10.1016/j.microc.2022.108324
- El-Yazbi, A. F., Elashkar, N. E., Abdel-Hay, K. M., Talaat, W., & Ahmed, H. M. (2020). Eco-friendly HPTLC method for simultaneous analysis of sofosbuvir and ledipasvir in biological and pharmaceutical samples: Stability indicating study. *Microchemical Journal*, 154, 104584. doi:10.1016/j.microc.2019.104584

- Fakhari, A. R., Nojavan, S., Haghgoo, S., & Mohammadi, A. (2008). Development of a stability-indicating CE assay for the determination of amlodipine enantiomers in commercial tablets. *Electrophoresis*, 29(22), 4583-4592. doi:10.1002/elps.200800330
- Godela, R., & Sowjanya, G. (2020). Simultaneous estimation of velpatasvir and sofosbuvir in bulk and combined tablet dosage form by a simple validated stability indicating RP-HPLC method. *International Journal of Pharmaceutical Sciences and Research* 11(11), 5669-5678.
- Godela, R., & Sowjanya, G. (2021). Concurrent determination of daclatasvir and sofosbuvir in pure binary mixture and their combined film coated tablets by a simple stability indicating RP-HPLC method. *Research Journal of Pharmacy and Technology*, 14(11), 5913-5918. doi:10.52711/0974-360x.2021.01028
- Guideline, ICH QA1 (R2). (2003). *Stability testing of new drug substances and products*. Retrieved from <https://database.ich.org/sites/default/files/Q1A%28R2%29%20Guideline.pdf>
- Hamdache, A., Grib, L., Grib, C., Adour, L., Zatout, H., Mezrouai, A., & Saraoui, S. (2021). Forced Degradation Studies of Sofosbuvir with a Developed and Validated RP-HPLC Method as per ICH Guidelines. *Chromatographia*, 84(12), 1131-1140. doi:10.1007/s10337-021-04099-8
- Harshalatha, P., Chandrasekhar, K. B., & Mv, C. (2018). A novel stability indicating method development and validation for the simultaneous estimation of Velpatasvir & Sofosbuvir in bulk and its pharmaceutical formulations. *International Journal of Research in Pharmaceutical Sciences*, 9(2), 566-571. doi:10.26452/IJRPS.V9I2.1563
- Hassouna, M., Abdelrahman, M. M., & Mohamed, M. A. (2017). Assay and dissolution methods development and validation for simultaneous determination of sofosbuvir and ledipasvir by RP-HPLC method in tablet dosage forms. *J Forensic Sci & Criminal Inves*, 1(3), 001-011. doi:10.19080/JFSCI.2017.01.555562
- Hassouna, M., & Mohamed, M. (2018). UV-spectrophotometric and stability indicating RP-HPLC methods for the determination of the hepatitis C virus inhibitor Sofosbuvir in tablet dosage form. *Analytical Chemistry Letters*, 8(2), 217-229. doi:10.1080/22297928.2017.1410441
- Hemchand, S., Babu, R., & Annapurna, M. M. (2018). New stability indicating RP-UFLC method for the simultaneous determination of Velpatasvir and Sofosbuvir in tablets. *Research Journal of Pharmacy and Technology*, 11(12), 5637-5642. doi:10.5958/0974-360X.2018.01022.3
- Jahnavi, B., & Ganapaty, S. (2018). Development and Validation of a Stability-indicating Method for the Simultaneous Estimation of Sofosbuvir and Ledipasvir by RP-HPLC. *Indian Journal of Pharmaceutical Sciences*, 80(6), 1170-1176. doi:10.4172/pharmaceutical-sciences.1000471
- Kokkiralala, T. K., & Suryakala, D. (2020). Stability indicating RP-HPLC method development and validation for the estimation of Sofosbuvir, Velpatasvir and Voxilaprevir in bulk and pharmaceutical dosage form. *Research Journal of Pharmacy and Technology*, 13(11), 5063-5071. doi:10.5958/0974-360X.2020.00887.2
- Kumar, D. V., & Rao, J. (2018). A new validated stability indicating RP-HPLC method for simultaneous estimation of sofosbuvir and ledipasvir in tablet dosage forms. *World J Pharm Res*, 7, 763-778. doi: 10.20959/wjpr201817-13124
- Kumari, K., & Sankar, D. (2019). UPLC method for simultaneous estimation of ledipasvir and sofosbuvir in bulk and dosage forms and their stress degradation studies. *Journal of Bioanalysis and Biomedicine*, 11, 224. doi:10.4172/1948-593X.1000224
- Lakshmana Rao, A., & Pallavi, A. (2019). Method Development and Validation of Stability Indicating RP-HPLC Method for Simultaneous Estimation of Sofosbuvir and Velpatasvir in Tablet Dosage Form. *Pharmaceutical Sciences & Analytical Research Journal*, 2(1), 180014.

- Lakshmi, B., Chaitanya, P. S. K., & Chandrasekar, B. (2018). Development and validation of a stability indicating RP-UPLC method for the simultaneous quantification of sofosbuvir and velpatasvir in finished dosage form. *Indo American Journal of Pharmaceutical Research*, 8(06), 1452-1461.
- Lakshmi Maneka S, Saravanakumar RT, & Anjana, C. K. V. L. S. N. (2020). Development and Validation of Stability-indicating UPLC Method for the Simultaneous Estimation of Voxilaprevir, Sofosbuvir, and Velpatasvir in Formulations. *Asian Journal of Pharmaceutics*, 14(03), 434-443. doi:10.22377/AJP.V14I03.3759
- Lalitha, K., Reddy, J. R., & Devanna, N. (2018). Stability indicating RP-HPLC method development and validation for estimation of sofosbuvir in pharmaceutical dosage form. *The Pharma Innovation*, 7(5, Part J), 656.
- Mankar, S., Bhawar, S., & Dalavi, P. (2019). Development and Validation of Stability indicating RP-HPLC method for Simultaneous Estimation of Sofosbuvir and Ledipasvir in Bulk Tablet Dosage Form. *Journal of Drug Delivery and Therapeutics*, 9(3-s), 500-509. doi:10.22270/jddt.v9i3-s.2893
- Mastanamma, S., Chandini, S., Reehana, S., & Saidulu, P. (2018). Development and validation of stability indicating RP-HPLC method for the simultaneous estimation of Sofosbuvir and Ledipasvir in bulk and their combined dosage form. *Future Journal of Pharmaceutical Sciences*, 4(2), 116-123. doi:10.1016/J.FJPS.2017.11.003
- Mohammadi, A., Rezanour, N., Dogaheh, M. A., Bidkorbeh, F. G., Hashem, M., & Walker, R. B. (2007). A stability-indicating high-performance liquid chromatographic (HPLC) assay for the simultaneous determination of atorvastatin and amlodipine in commercial tablets. *Journal of Chromatography B*, 846(1-2), 215-221. doi:10.1016/J.JCHROMB.2006.09.007
- Montazeri, A. S., Mohammadi, A., Adib, N., & Naeemy, A. (2018). Development and Validation of a Stability-Indicating HPLC Method for the Determination of Acarbose in Pharmaceutical Dosage Forms. *Journal of Analytical Chemistry*, 73, 910-916. doi:10.1134/S1061934818090071
- Namratha, S., & Vijayalakshmi, A. (2021). A validated stability indicating UPLC method for simultaneous determination and degradation studies of Sofosbuvir and Velpatasvir in pharmaceutical dosage forms. *Research Journal of Pharmacy and Technology*, 14(3), 1658-1662. doi:10.5958/0974-360X.2021.00294.8
- Narla, D., & Pappula, N. (2020). Stability indicating UHPLC method for simultaneous estimation of sofosbuvir and ledipasvir in tablet dosage form. *International Journal of Pharmaceutical Sciences and Research*, 11, 784-790. doi:10.13040/IJPSR.0975-8232.11(2).784-90
- Nebsen, M., & Elzanfaly, E. S. (2016). Stability-indicating method and LC-MS-MS characterization of forced degradation products of sofosbuvir. *Journal of Chromatographic Science*, 54(9), 1631-1640. doi:10.1093/CHROMSCI/BMW119
- Padmini M, Venkata D, & Sankar, G. (2019). Stability-indicating RP-HPLC method for simultaneous estimation of sofosbuvir, velpatasvir, and voxilaprevir in bulk and tablet dosage forms. *Asian Journal of Pharmaceutical and Clinical Research*, 13(2), 131-139. doi:10.22159/ajpcr.2020.v13i2.36000
- Pottabathini, V., Gugulothu, V., Kaliyaperumal, M., & Battu, S. (2016). Identification, isolation and structure confirmation of forced degradation products of Sofosbuvir. *American Journal of Analytical Chemistry*, 7(11), 797-815. doi:10.4236/AJAC.2016.711071

- Pourmoslemi, S., Mirfakhraee, S., Yaripour, S., & Mohammadi, A. (2016). Development and Validation of a Stability-Indicating RP-HPLC Method for Rapid Determination of Doxycycline in Pharmaceutical Bulk and Dosage Forms. *Pharmaceutical Sciences*, 22(2), 96-104. doi:10.15171/PS.2016.16
- Priyanka, K., Vinutha, K., Sridevi, P., Ramya, B., & Bhagavan Raju, M. (2018). A Stability Indicating RP-HPLC method for simultaneous estimation of Velpatasvir and Sofosbuvir in its bulk and tablet dosage form. *American Journal of Pharmatech Research*, 8, 129-139.
- Rao, B. S., Reddy, M., & Rao, B. (2017). Simultaneous analysis of ledipasvir and sofosbuvir in bulk and tablet dosage form by stability indicating high performance liquid chromatographic method. *Global Journal for Research Analysis*, 6(4), 505-509.
- Rao, P. V., Rao, A. L., & Prasad, S. (2018). Validated Stability Indicating RP-HPLC method for estimation of antiviral class of drugs Sofosbuvir and Velpatasvir in combination and its comparison with reported methods. *Research Journal of Pharmacy and Technology*, 11(12), 5425-5430. doi:10.5958/0974-360X.2018.00990.3
- Reddy, B., Alam, M., Khanam, N., & Adhkrishnanand, P. (2018). An innovative method development and forced degradation studies for simultaneous estimation of sofosbuvir and ledipasvir by RP HPLC. *International Journal of Pharmacy and Pharmaceutical Sciences*, 11(2), 34-41. doi:10.22159/IJPPS.2019V11I2.29347
- Rote, A. P., Alhat, J., & Kulkarni, A. A. (2017). Development and validation of RP-HPLC method for the simultaneous estimation of ledipasvir and sofosbuvir in bulk and pharmaceutical dosage form. *Int J Pharm Sci Drug Res*, 9(6), 291-298. doi:10.25004/IJPSDR.2017.090602
- Saroja, J., Lakshmi, P. A., Rammohan, Y., Divya, D., & Kumar, P. S. (2018). Concurrent estimation of sofosbuvir and velpatasvir in raw and tablets using stability indicating RP-HPLC method. *Rasayan Journal of Chemistry*, 11(3), 1058-1066. doi:10.31788/RJC.2018.1132010
- Shaikh, S. N., & Manjusri, P. (2017). Development and validation of RP-HPLC method for quantitative analysis of sofosbuvir in pure and pharmaceutical formulation. *World journal of pharmacy and pharmaceutical sciences*, 6(8), 2249-2258. doi:10.20959/WJPPS20178-9909
- Singh, K., Bhatt, S., & Prasad, R. (2017). HPLC method for estimation of drug release of sofosbuvir in pharmaceutical formulations. *World journal of pharmacy and pharmaceutical sciences*, 6(8), 2249-2258.
- Souri, E., Kargar, Z., Saremi, S., Ravari, N. S., Alvandifara, F., & Amanloua, M. (2011). Development and validation of a stability-indicating HPLC method for determination of granisetron. *Journal of the Chinese Chemical Society*, 58(4), 443-449. doi:10.1002/JCCS.201190004
- Suganthi, A., Satheshkumar, S., & Ravi, T. (2019). Development of validated specific stability-indicating HPTLC method for the simultaneous determination of Ledipasvir and Sofosbuvir in fixed dose tablet formulation. *Asian J Nanosci Mater*, 2, 228-243. doi:10.26655/AJNANOMAT.2019.3.9
- Susmita, A. G., & Rajitha, G. (2018). Development and validation of stability indicating UPLC method for simultaneous estimation of sofosbuvir and velpatasvir in tablet dosage form. *International Journal of Pharmaceutical Science and Research*, 9(11), 4764-4769.
- Swain, D., Samanthula, G., Bhagat, S., Bharatam, P., Akula, V., & Sinha, B. N. (2016). Characterization of forced degradation products and in silico toxicity prediction of Sofosbuvir: A novel HCV NS5B polymerase inhibitor. *Journal of pharmaceutical and biomedical analysis*, 120, 352-363. doi:10.1016/j.jpba.2015.12.045

- Vanitha, C., Bhaskar Reddy, K., & Satyanarayana, S. V. (2018). Quality-by-design approach to selective stability indicating RP-HPLC method development and validation for estimation of sofosbuvir in bulk drug. *International Journal of Research in Pharmaceutical Sciences*, 9(2), 298-308. doi:10.26452/ijrps.v9i2.1439
- Veereswara Rao, D., Deshmukh, D., & Kumar, D. (2018). HPLC Method for The Determination of Sofosbuvir and Ledipasvir in Tablet Dosage Form. *International Journal of Research and Reviews in Pharmacy and Applied Sciences*, 8(1), 146-158.
- Vejendla, R., Subramanyam, C., & Veerabhadram, G. (2016). Estimation and validation of sofosbuvir in bulk and tablet dosage form by RP-HPLC. *International journal of pharmacy*, 6(2), 121-127.
- Wang, X.-j., & You, J.-z. (2017). Study on the thermal decomposition of sofosbuvir. *Journal of Analytical and Applied Pyrolysis*, 123, 376-384. doi:10.1016/J.JAAP.2016.11.003
- WHO. (2016). Sofosbuvir. Retrieved from [https://cdn.who.int/media/docs/default-source/essential-medicines/intellectual-property/sofosbuvir-report.pdf?sfvrsn=5a6c06ea\\_2](https://cdn.who.int/media/docs/default-source/essential-medicines/intellectual-property/sofosbuvir-report.pdf?sfvrsn=5a6c06ea_2). Retrieved 12 NOV 2023 [https://cdn.who.int/media/docs/default-source/essential-medicines/intellectual-property/sofosbuvir-report.pdf?sfvrsn=5a6c06ea\\_2](https://cdn.who.int/media/docs/default-source/essential-medicines/intellectual-property/sofosbuvir-report.pdf?sfvrsn=5a6c06ea_2)
- Yaripour, S., Rashid, S. N., Alibakhshi, H., & Mohammadi, A. (2015). Development and validation of a stability-indicating reversed phase HPLC method for the quality control of Zolpidem in bulk and tablet dosage forms. *Journal of Analytical Chemistry*, 70(6), 738-743. doi:10.1134/S1061934815060143
- Yeram, P., Hamrapurkar, P., & Mukhedkar, P. (2019). Implementation of Quality by Design approach to develop and validate stability indicating assay method for simultaneous estimation of sofosbuvir and ledipasvir in bulk drugs and tablet formulation. *International Journal of Pharmaceutical Sciences*, 10, 180-188. doi:10.13040/IJPSR.0975-8232.10(1).180-88
- Zaman, B., & Hassan, W. (2021). Development of Stability Indicating HPLC-UV Method for Determination of Process Impurities and Degradation Products in Sofosbuvir and Velpatasvir Tablets. *Pharmaceutical Chemistry Journal*, 54(12), 1295-1305. doi:10.1007/s11094-021-02359-3

# Analytical Evaluation of the Chemical Content of HTPs Compared to Conventional Cigarettes

Bensu KARAHALİL<sup>o</sup>

*Analytical Evaluation of the Chemical Content of HTPs Compared to Conventional Cigarettes*

## SUMMARY

Smoking is a major public health problem and one of the leading causes of preventable death in the world today. Despite well-known health risks, quitting remains a challenge for many smokers. This review aims to critically assess heated tobacco products (HTPs) as potentially less harmful alternatives to traditional cigarettes. This mini-review synthesizes findings from over 400 articles published in high-impact journals. Studies funded by tobacco companies or those with potential conflicts of interest were excluded to ensure unbiased results. Comprehensive analysis indicates that HTPs contain substantially fewer harmful and potentially harmful compounds (HPHCs) than conventional cigarettes. Because HTPs heat the tobacco instead of burning it, they prevent the production of harmful combustion byproducts. Nicotine levels in HTPs were found to be comparable to those in conventional cigarettes, offering similar experiences for users. HTPs are not entirely free of harmful substances, and they contain significantly fewer HPHCs due to the absence of combustion. The current body of evidence suggests that HTPs could serve as safer substitutes for smokers who have difficulty quitting. HTPs appear to be a promising option for harm reduction, mainly since they do not produce combustion byproducts, which are a significant source of carcinogens in traditional cigarettes.

**Key Words:** Electronic cigarette, heated tobacco products, nicotine, tar, tobacco harm reduction, tobacco-specific nitrosamines

*Geleneksel Sigaralara Kıyasla HTP'lerin Kimyasal İçeriğinin Analitik Değerlendirmesi*

## ÖZ

Sigara içmek önemli bir halk sağlığı sorunudur ve dünya çapında önlenebilir ölümlerin önde gelen nedenlerinden biridir. İyi bilinen sağlık risklerine rağmen, sigarayı bırakmak birçok sigara içicisi için bir zorluk olmaya devam etmektedir. Bu derleme, geleneksel sigaralara potansiyel olarak daha az zararlı alternatifler olarak ısıtılmış tütün ürünlerini (HTP'ler) eleştirel bir şekilde değerlendirmeyi amaçlamaktadır. Bu mini derleme, yüksek etkili dergilerde yayımlanan 400'den fazla makaleden elde edilen bulguları sentezlemektedir. Tütün şirketleri tarafından finanse edilen veya potansiyel çıkar çatışması olan çalışmalar, tarafsız sonuçlar elde etmek için hariç tutulmuştur. Kapsamlı analiz, HTP'lerin geleneksel sigaralara kıyasla önemli ölçüde daha az zararlı ve potansiyel olarak zararlı bileşikler (HPHC'ler) içerdiğini göstermektedir. HTP'ler tütünü yakmak yerine ısıttığından, zararlı yanma yan ürünlerinin üretimini önler. HTP'lerdeki nikotin seviyelerinin geleneksel sigaralardakilerle karşılaştırılabilir olduğu ve kullanıcılar için benzer deneyimler sunduğu bulunmuştur. HTP'ler tamamen zararlı maddelerden arınmış değildir, yanma olmadığından önemli ölçüde daha az HPHC içerirler. Mevcut kanıtlar, HTP'lerin sigarayı bırakmakta zorluk çeken tiryakiler için daha güvenli ikameler olarak hizmet edebileceğini göstermektedir. HTP'ler, özellikle geleneksel sigaralarda önemli bir karsinojen kaynağı olan yanma yan ürünleri üretmedikleri için, zarar azaltma konusunda umut verici bir seçenek olarak görünmektedir.

**Anahtar Kelimeler:** Elektronik sigara, ısıtılmış tütün ürünleri, nikotin, katran, tütün zararlarının azaltılması, tütüne özgü nitrozaminler

Received: 14.08.2024

Revised: 28.10.2024

Accepted: 13.01.2025

<sup>o</sup> ORCID: 0000-0003-1625-6337, Department of Toxicology, Faculty of Pharmacy, Gazi University, 06330, Ankara, Türkiye

## INTRODUCTION

Cigarette smoking is a serious public health problem and one of the primary preventable causes of death worldwide. Health risks (lung cancer, bladder cancer, respiratory system disorders, cardiovascular disorders, etc.) related to tobacco use have been well-established for more than 50 years. It harms nearly every organ of the body, leading to many diseases, including cancer, heart disease, stroke, asthma, and emphysema. According to the 2019 Global Burden of Disease Study, more than 1.1 billion people smoke worldwide, and 7.7 million people die every year from smoking-related diseases (GBD 2019 Tobacco Collaborators, 2009). It is expected that the number of smoking-related deaths that occur annually will continue to increase even after tobacco use starts to decrease since smoking-related diseases develop over time (WHO, 2019). Smoking, the traditional method of obtaining nicotine through the combustion of tobacco, produces emissions that contain more than 7000 chemicals. Of these chemicals, at least 250 compounds, such as hydrogen cyanide, carbon monoxide, polycyclic aromatic hydrocarbons (PAHs), and ammonia, are harmful to health (NIH, 2017). PAHs are a class of compounds composed of two or more fused benzenoid rings. They have carcinogenic and mutagenic properties. PAHs are formed due to incomplete combustion, and benzo(a)pyrene is a biomarker of them. Most PAHs are found in cigarette smoke (Vu et al., 2015). Second-hand smoke, also known as ETS, is a mixture of the smoke resulting from the burning of tobacco products during smoldering (sidestream smoke) and the part of the mainstream smoke exhaled by active smokers. Hence, not only tobacco smokers but also smokers are exposed to these chemicals and thus at risk for tobacco-related diseases. Second-hand smoke causes premature deaths among nonsmokers as well as numerous health problems such as ear infections, asthma attacks, sudden infant death syndrome, and respiratory infections, especially in infants, and

children (EPA, 2021). Due to the severe health risks of smoking, undoubtedly, the best solution to prevent the harms and health risks of smoking is to quit smoking. However, some smokers do not succeed in quitting smoking for many reasons. Due to the severe health effects of cigarettes, an alternative to cigarettes was sought for less harmful products. Over time, various products have been released to the market. These products were made to contain nicotine or to meet the ritual of smoking and were made attractive with certain flavors. Heated tobacco products (HTPs) and electronic cigarettes (e-cigarettes) were widely sold. HTPs were introduced to the market as advantageous products because they heat the tobacco at high temperatures but do not burn the tobacco, thus avoiding the formation of combustion products and providing the smoking ritual due to the tobacco it contains. Studies have been conducted to evaluate these products regarding the chemicals they contain, their emissions, and potential health risks, but with conflicting results (Bekki et al., 2017; Lu et al., 2021; Phillips et al., 2018; Titz et al., 2018).

In the present review, as mentioned above, although there are many alternatives to cigarettes, only HTPs will be mentioned because it is well-known that there are significant differences between HTPs and other alternatives (such as e-cigarettes, which are close to the smoking ritual). Nevertheless, as different possibilities are addressed in some of the studies referenced in the review, these will be briefly outlined. It should be noted, however, that the review also encompasses other subjects.

### **Heated tobacco products versus conventional cigarette**

Nicotine is the primary psychoactive substance in tobacco products that leads people to use tobacco products. Given that nicotine is a natural component of tobacco, any product that contains tobacco, of course, contains nicotine. Nicotine is a highly addictive substance, preventing even smokers who would like to quit smoking from giving up smoking.



Millions of people die every year due to smoking-related diseases. Today, however, it is not the nicotine that causes illness and death but the harmful and potentially harmful compounds (HPHCs) formed by the combustion of tobacco (FDA, 2021). Exposure to conventional tobacco smoke has no safe level. The tobacco found in a conventional cigarette transforms into ash and smoke as it burns between 400°C and above 1000°C. Three elements, i.e., tobacco, oxygen, and the necessary amount of heat to activate the reaction, should be available for combustion. Incomplete combustion, i.e., pyrolysis, of traditional cigarettes, primarily due to insufficient oxygen, also leads to the formation of HPHCs due to thermogenic degradation (Aver et al., 2017).

For smokers who cannot quit smoking for various reasons or have repeatedly tried to quit smoking but failed, novel products, such as heated tobacco products with unique mechanisms preventing the combustion of tobacco, are developed and released to the market as safer alternatives to cigarettes. Heat-not-burn tobacco (HnB) products which is a type of HTP, snus, and e-cigarettes, are other alternatives and are

also referred to as new-generation products (NGPs). HnB tobacco products heat the processed tobacco instead of combusting or burning it. HTPs are not the same as e-cigarettes since e-cigarettes heat liquids that usually contain nicotine derived from tobacco; while HTPs heat tobacco leaves, e-cigarettes do not contain tobacco. This is the first and most fundamental difference between e-cigarettes and HTPs, but when examined, it will be observed that there are significant differences between them.

HTPs are commercially available systems consisting of a charger, a holder, tobacco sticks, plugs, or capsules (Simonavicius et al., 2019; Auer et al., 2017). Among HTPs are IQOS (Phillip Morris International), PAX (PAX Labs), Glo (British American Tobacco), and Ploom (Japan Tobacco International) brand products, all of which produce aerosols that contain nicotine and other chemicals. Table 1 summarizes new generation products and leading tobacco companies. HTPs allow the users to mimic typical smoking and give the real taste of tobacco. In addition, the fact that they do not produce fire or ash is another reason smokers prefer HTPs.

**Table 1.** New generation products and main tobacco companies

Year	Company	Brand Name/Slogan	Current (C) / Discontinued (D)
1980s	Tobacco companies first developed HTP technology		
1988	ATC-RJR	Premier	D (1989) Not like taste and smell.
1996	ATC-RJR	Eclipse/ “imagine the unimaginable”	D (up to 2014)
1998	PMI	Accord/ “the time is right”	D (up to 2006) Difficult to use, not good taste; Not as satisfying as traditional cigarettes
2005	BAT	iFuse (similar to PloomTech) A hybrid product	D no longer available and was superseded by “Glo”.
2007	PMI	Heatbar (Accord is rebranded)	D Not obtaining any significant user reception; discontinued from Sweden and Australia.
2010	JTI	Ploom	D
2014	RJR (bought by BAT)	Revo (New version of “Eclipse”)	
2014	PMI	IQOS/ (New version of “Accord”) “This changes everything”	C
The second half of 2014	PMI	IQOS/ “I Quit Ordinary Smoke” The use of misleading term” according to the TCRs	C
February 2015	JTI	Ploom (later rebranded as Pax Labs)	JTI and Ploom Inc. ended their partnership
December 2016	PMI	IQOS	Applied to FDA to classify IQOS as MRTP
In February 2018	PMI	IQOS	C Around 30 countries
Early 2018	<sup>2</sup> All transnational TC	Ploom Three products available	D They remained on the market until 2019
2019	PMI	IQOS FDA partially* authorized MRTP application.	C “reduced exposure to harmful substances” and “*not reduce the risk of disease and death.”
2019	IT (Now IB)	Pulze	C
2019	BAT	Glo / 3 versions (hybrid like the iFuse) Glo Pro, glo Nano, glo Sens “a real game changer for consumers”	D
By 2019	BAT and PMI-tested devices using carbon tips as the heat source		
By July 2020	BAT	Glo Latest brand “GloHper”	C Glo website is linked to retail sites in 17 countries other than Canada.
July 2020	PMI	IQOS	partial approval applying to the marketing of IQOS
By 2021	PMI	IQOS	C 64 markets

<sup>1</sup>Brand names may vary in different countries; <sup>2</sup>Except IT included HTPs their portfolio; TC, Tobacco Company, ATC, American Tobacco Company; RJR, RJ Reynolds; TCRs, Tobacco Control researchers; PMI, Phillip Morris International; BAT, British American Tobacco; IT, Imperial Tobacco; IB, Imperial Brand; JTI, Japan Tobacco International; US, United States; FDA, Food and Drug Administration; MRTP, Modified Reduced Tobacco products;

### **Classification of Heated Tobacco Products**

The British Government categorized HTPs into three categories. In addition to these three categories, the World Health Organization (WHO) also included the new carbon-tipped devices in HTPs (WHO, 2020). These three different classes of HTPs produce vapor from tobacco or non-tobacco sources are:

1. Directly heating the processed tobacco,
2. Heating the processed tobacco in a vaporizer or
3. Passing the vapor from non-tobacco sources over processed tobacco to obtain the flavor. The HTPs that use the vapor from non-tobacco sources are called the HTP “hybrids” (Treasury, 2018).

The absence of combustion is critical in HTPs that do not produce HPHCs, including carbon monoxide. The WHO Framework Convention on Tobacco Control (FCTC) has addressed the health effects of second-hand smoke. In this regard, WHO stated in its “2018 HTPs fact sheet” that data on the health effects of second-hand exposure to HTPs are insufficient (WHO, 2018). Environmental Protection Agency (EPA) stated that second-hand smoke causes some diseases and has numerous harmful effects on nonsmoking adults and children. EPA classified second-hand smoke as a Group A carcinogen in humans (EPA, 2021). In line with EPA, the Centers for Disease Control and Prevention (CDC) reported that among nonsmoking adults, exposure to second-hand smoke contributes to death and causes diseases (stroke, lung cancer, coronary heart diseases, etc.) and in infants it causes sudden deaths (CDC, 2020). Second-hand smoke is addictive because of the nicotine alkaloid. Further independent studies are needed to clarify the health effects of second-hand exposure.

The US Family Smoking Prevention and Tobacco Control Act (FSPTCA) requires premarket authorization for all tobacco products (Section 910). It does not allow manufacturers to market tobacco products on the basis that they reduce the risk of developing tobacco-related diseases. HTPs cannot be

marketed unless authorized by the Food and Drug Administration (FDA) since FSPTCA stipulates that all tobacco products, including modified-risk tobacco products (MRTPs) such as HTPs, are regulated by FDA. For this reason, manufacturers must scientifically prove that their products reduce the risk of tobacco-related diseases before marketing them and submitting an MRTP application (Section 911) to the FDA (Lempert and Glantz, 2018). FSPTCA defines an “MRTP” as “any tobacco product sold or distributed for use to reduce harm or the risk of tobacco-related diseases associated with commercially marketed tobacco products” (FDA, 2020). Only one HTP system (IQOS and three of its tobacco-containing heat-stick products) was authorized to be marketed as MRTPs by the FDA on July 7<sup>th</sup>, 2020, since it was scientifically proven that these products heat tobacco without burning, they reduce the formation of HPHCs, and switching from regular cigarettes to these products reduces the exposure to HPHCs (FDA New Release, 2020).

It is essential to understand the health effects of HTPs that substitute cigarettes, particularly on chronic obstructive pulmonary disease (COPD) patients. However, considering that smoking is a habit with long-term exposure, there are not enough studies that compare the long-term health effects of HTPs with those of conventional cigarettes. Bekki et al. (2017) conducted the first study evaluating HTPs at the National Institute of Public Health in Japan. They measured basic HPHCs such as carbon monoxide, tar, nicotine, and tobacco-specific nitrosamines in the mainstream smoke of IQOS and its tobacco filler as well as conventional combustion cigarettes, i.e., 3R4F, a relatively high yield cigarette and 1R5F, a low yield cigarette, since nicotine and tar amounts were written on the conventional tobacco packages in Japan, but not on IQOS packages. They found that the nicotine levels in IQOS were almost the same as those in conventional cigarettes. On the other hand, the tar levels of IQOS were half or less than half of those of conventional cigarettes, and the carbon monoxide

levels of IQOS were approximately one-hundredth of conventional cigarettes. In summary, they concluded that the amounts of hazardous compounds in the mainstream smoke of IQOS were much less than those in conventional cigarettes (Bekki et al., 2017).

The previous study on the long-term health effects of HTPs was performed by Polosa et al. (2021) on two groups of patients. Group 1 consisted of 19 COPD patients who significantly reduced or stopped smoking after switching to HTPs. Group 2 consisted of 19 COPD patients with age and gender characteristics that matched the patients in Group 1 and who used HTPs for 12, 24, and 36 months. Parameters such as the number of cigarettes smoked daily, disease exacerbations, lung function test results, self-reported outcomes, and distance walked in 6 minutes were monitored in both groups for three years. Consequently, significant improvements were recorded in respiratory symptoms, and all other parameters in patients who used HTPs (Polosa et al., 2021), supporting the hypothesis asserted by tobacco companies that avoiding exposure to chemicals produced by the combustion of cigarettes by switching to HTPs will improve patients' health. It was also suggested that switching from conventional cigarettes to HTPs might be a safer alternative to conventional cigarettes (Szymanski et al., 2021). In a randomized, controlled study conducted with 180 Japanese subjects, the biomarkers of exposure (excluding nicotine and including exhaled carbon monoxide) were analyzed on day five after switching from conventional cigarettes to using glo™/THP1.0 or IQOS/THS, resulting in a reduction in smoke toxicants (Gale et al., 2018). The harm is expected to be higher when this data obtained from acute exposure is used in long-term chronic studies. Unfortunately, there have been no epidemiological studies on these products, unlike conventional cigarettes. This makes it impossible to assess the safety of not only HTPs but also other alternative products. Evaluations are currently based on acute exposures or animal experiments.

Tobacco-specific nitrosamines and carbonyl compounds regulated by WHO were also detected in the mainstream smoke of HTPs, yet in lesser amounts than conventional cigarettes. Furans derived from flavorings and pyrimidines are in lesser amounts in HTPs than conventional cigarettes. As in foods, furans in HTPs are produced by the Maillard reaction, the reaction of sugar and amino acids in tobacco leaves. Both furan and pyrimidine concentrations are lower in HTPs than in conventional cigarettes (Bekki et al., 2021). HTPs are generally used in combination with other products (including tobacco cigarettes by the youth and people who never smoke (Znyk et al., 2021). It is not possible to distinguish whether tobacco cigarettes or HTPs are responsible for any adverse health effects observed with such combined use. Independent studies have proven that harmful chemicals emitted from HTPs are less than conventional cigarettes (Znyk et al., 2021; Cancelada et al., 2019; Mallock et al., 2018 ); however, they have not been completely eliminated (Uchiyama et al., 2018). A study investigated whether IQOS, an HTP, was less harmful than conventional products and assessed its impact on indoor air quality. Consumable tobacco plugs were analyzed by gas chromatography-mass spectrometer (GC-MS) to quantify 33 volatile organic compounds in mainstream and side stream emissions of IQOS. Consequently, fewer harmful products were found in IQOS than in conventional products and that IQOS was a weak indoor air pollutant (Cancelada et al., 2019). Total particulate matter (TPM), water, aldehydes, nicotine, and other volatile organic compounds (VOCs) generated with the Health Canada Intense smoking regimen in HTP emissions were analyzed, and the nicotine levels in HTP emissions were found to be comparable to those of combusted cigarettes. In addition, it was observed that the aldehyde levels (approximately 80–95%) and VOCs (97% to 99%) were also lower in HTP emissions than in the emissions of combusted cigarettes (Mallock et al., 2018). Phillip Morris International (PMI) conducted a 90-day OECD TG 413 rat inhalation study

using carbon HTP (CHTP1.2) to determine whether, compared to combusted cigarettes, CHTP1.2 results in reduced exposure to harmful constituents and reduced respiratory tract irritation and systemic and pathological effects. CHTP is a single-use, disposable tobacco product that is similar in appearance and use to cigarettes. The CHTP device uses a fast-burning carbon heat source to heat the tobacco plug inside a specially designed rod, producing an aerosol containing nicotine and tobacco flavoring. During use, the temperature of the tobacco within the tobacco stick does not exceed a well-defined threshold, which serves to prevent combustion and, as a consequence, markedly restricts the formation and transfer of harmful smoke constituents into the aerosol. As a consequence, they found that CHTP1.2 aerosol contained approximately one-third TPM, one-twenty-fifth CO, two-fifth formaldehyde, one-eighth acetaldehyde, and one-sixth acrolein compared to those of combusted cigarettes at the same nicotine concentrations (Phillips et al., 2018).

## METHODS

### Review the PRISMA flow diagram

Simonavicius et al. (2019) conducted a systematic review of the literature published between 2009 and 2017 and indexed by databases such as Web of Science and Scopus, etc., to determine the differences between the independent and tobacco industry-funded studies on available HTPs (Figure 1 and Table 2). They found that HTP emissions under the Health Canada Intense (HCI) regimen contained 18% to 73% less nicotine,  $\geq 98\%$  less CO, and  $\geq 62\%$  fewer HPHCs and tar than cigarettes. One of the independent studies reported significantly less tar and more tobacco-specific nitrosamines in HTPs than tobacco industry-funded

studies. There were heterogeneities between the 31 reviewed studies depending on the tobacco company that funded the study. A study conducted with users and bystanders exposed to the toxicants revealed lesser amounts of harmful chemicals in HTPs than in conventional cigarettes. In this review of studies published up to November 2017, nicotine levels and HPHCs in mainstream HnB emissions compared to conventional cigarettes are reported (Simonavicius et al., 2019). In comparison, this study featured a systematic review of the literature published in the English language between January 2018 and April 2022 and indexed by PubMed, Scopus, and Elsevier databases. For this purpose, databases were searched using various synonyms and combinations of keywords such as “heat does not burn”, “heated tobacco products”, “less harmful heated tobacco products” and brand names (IQOS, Ploom, glo) and 447 publications were obtained. With the keywords given in PubMed, Scopus, Web of Science, and Elsevier databases, 447 articles were found from January 2018. The number of articles decreased to 423 after excluding articles without English text and articles outside the study’s scope. After excluding irrelevant articles in terms of title, abstract, and content, the number of articles decreased to 407. The number of articles decreased to 16, especially when studies measuring HPHC content and the most commonly used smoking regimen Health Canada Intense (HCI) (i.e., 55 ml puff volume, 2 sec. duration, 30 sec. puff interval) were included. Figure 1 summarizes the study’s inclusion and exclusion criteria (Figure 1). In addition, only independent studies were considered, and the studies carried out or sponsored by the tobacco companies, as well as the studies deemed to give rise to a conflict of interest potentially, were excluded.

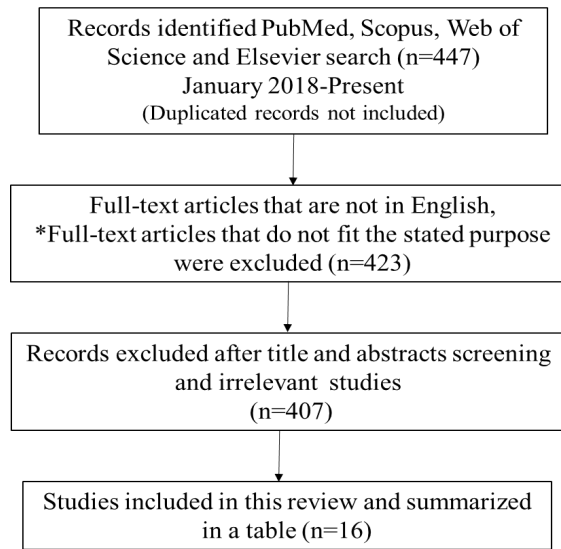


**Figure 1.** Systematic review PRISMA flow diagram according to inclusion criteria

\* Full-text articles that do not fit the stated purpose are awareness of HTPs usage, the use of HTPs and disease relation, method development for measuring HTPs etc.

**Table 2.** Studies comparing nicotine and HPHC levels in emissions of HTPs with conventional cigarettes over the last 5 years

Authors, year of publication	Heated Tobacco Products (HTPs)		Conventional Tobacco Cigarette (CTC)	Method	Results
Farsalinos et al., 2018	Formaldehyde: 5-6.4 µg/stick Acetaldehyde: 144, 1-175, 7 µg/stick ACR: 10, 4-10, 8 µg/stick PA: 11, 0-12, 8 µg/stick CA : 1, 9-2, 0 µg/stick	Formaldehyde: 0, 5-1, 0 µg/12 puffs Acetaldehyde: 0, 8-1, 5 µg/12 puffs ACR: 0, 3-0, 4 µg/12 puffs PA and CA (N.D)	Nic. Levels (1.99 ± 0.20 mg/cig) were higher than HTPs and not statistically different from e-cigarettes.	GC-NPD	CTC levels in HTPs were lower (85-95%) than CTC and higher than e-cigarettes.
Leigh et al., 2018	HTP aerosols (IQOs, Amber, Tobacco flavor) TSNA was 8-22 times lower HTP aerosols than in CTC smoke. Nic: 1.4±0.2 mg from a single HeatStick (12 puffs)	Nic: 1.3±0.2 mg per 55 puffs-	Nic 2.1±0.1 mg per cigarette (8 puffs)	GC-NPD	TSNA levels respectively, (except N-Nitrosornicotine ketone (4-(Methylnitrosamino)-1-(3-pyridyl)-butanone) (NNK) CTC>HTPs>e-cigarettes (per puff)
Caponnetto et al., 2018	IQOS Median exhaled breath CO (eCO) level (95%CI) reaching a max peak at 15 min with 4.9 (4.1;5.6) ppm	Glo Med eCO level (95%CI) reaching a max peak at 45 min with 4.5 (3.9;5.2) ppm	12 control smokers ≥10 CTC/day, 5 years CTC ≥10 ppm for at least 30 min.	A hand-held eCO meter	Baseline eCO < 5 ppm No significant changes between HTPs and Glo. Significant differences between (iQOS/GLO and CI were found.
Uchiyama et al., 2018	Total gaseous and particulate matter: 42mg/sticks Nic: 1200 µg/sticks Acetaldehyde: 360 µg/sticks Mean heating °C=210 Mainstream smoke PG: 240-850 µg/stick ACT: 140-260 µg/stick Nic content: 5.2 mg/stick, generated 1200 µg/stick	Total gaseous and particulate matter: 29mg/sticks Nic: 510 µg/sticks Acetaldehyde: 520 µg/sticks Mean heating °C= 170 PloomTECH Total gaseous and particulate matter: 18mg/sticks Nic: 230 µg/sticks Acetaldehyde: 5900 µg/sticks Mean heating °C= 23 °C Nic Content: 1.7 mg/stick; generated 510 µg/stick	Total gaseous and particulate matter: 31mg/sticks Nic: 1900 µg/sticks Acetaldehyde: 18 µg/sticks Mean heating °C=460 PG: 11-28 µg/stick ACT: 50-110µg/stick Nic content: 6.5 mg/stick; generated 230µg/stick	GC-MS, GC-TCD	Chemicals from HTP were less than those from CTCs, except water; propylene glycol, glycerol, and acetol.
Farsalinos et al., 2018	Regular Tobacco Nic content: 15.2 ± 1.1 mg/g tobacco Menthol Tobacco Nic content: 15.6 ± 1.7 mg/g tobacco Regular Tobacco Nic (aerosol): 1.40 ± 0.16 mg/12 puffs Menthol Tobacco Nic (aerosol): 1.38 ± 0.11 mg/12 puffs	(Ciga-like, eGo-style, and variable wattage) Custom-made liquid: 2% nicotine	Nic 1.99 ± 0.20 mg/cigarette		Although the Nic content in HTP was similar to in CTC, HTP yielded higher levels of Nic than aerosolized e-cigarettes but lower than CTC.

Cancelada et al., 2019	Blue, Amber, and Yellow Label Heatsticks 33 VOC quantified Acetaldehyde, DAAN, PA, BA, benzaldehyde, mACR, CA, and BUTA, IQOS emissions were higher than e-cigarettes.	TSNAs IQOS (Marlboro) (ng/cig.) Mainstream smoke NNK, NNN, NAT, NAB 0.42 ± 0.01; 0.55 ± 0.03; 0.38 ± 0.07; 0.04 ± 0.00 Sidestream smoke NNK, NNN, NAT, NAB: -;-;-;	Glo (Kent) (ng/cig.) Mainstream smoke NNK, NNN, NAT NAB 0.18 ± 0.01; ND; ND; ND Sidestream smoke NNK, NNN, NAT, NAB: -;-;-; PloomTECH (Mevius) (ng/cig.) NNK, NNN, NAT; NAB ND 0.16 ± 0.01 0.09 ± 0.01 ND Sidestream smoke NNK, NNN, NAT, NAB: -;-;-;	Isoprene, phenol, pyridine, benzene, acrylonitrile, cresols, and quinolone emissions> IQOS CC emissions from CTCs were higher than IQOS emissions, BUTA and CA, which were similar to IQOS and CTC.	Headspace GC-MS	VOC and Nic increased with temperature (IQOS heatstick-at three different headspace temperatures; 180, 200, and 220°C).
Ishizaki and Kataoka, 2019	TSNAs IQOS (Marlboro) (ng/cig.) Mainstream smoke NNK, NNN, NAT, NAB 0.42 ± 0.01; 0.55 ± 0.03; 0.38 ± 0.07; 0.04 ± 0.00 Sidestream smoke NNK, NNN, NAT, NAB: -;-;-;	TSNAs Mainstream smoke Marlboro-regular Regular: NNK, NNN, NAT, NAB (4.00 ± 0.21; 4.11 ± 0.28; 3.73 ± 0.07; 0.59 ± 0.03) Sidestream smoke Regular 2.63 ± 0.20; 1.63 ± 0.05; 0.88 ± 0.06; 0.28 ± 0.02 <b>Marlboro (Menthol), MEVIUS (Menthol, Superlight, Original); not presented</b>	TSNAs in sidestream smoke NNK > NNN > NAT > NAB  The TSNA contents were significantly lower in the mainstream smoke of HTPs than in the sidestream smoke of CTCs. CTCs are more harmful than HTPs. The TSNA content in the sidestream smoke of CTCs is relatively high and both smokers and non-smokers are exposed to it. Cancer risk is higher than not only in smokers but in non-smokers exposed to CTCs.	LC-MSMS	The complete list was not presented. Total reduction in the number and quantity of chemical components, including known HPHCs, in THS 2.2.	
Le Godec et al., 2019	Flavored Neostick (mg/stick) Total Particulate Matter: 16,24 ± 1,71 0.41 ± 0.07 Gly: 3.46 ± 0.62 Unflavored Neostick (mg/stick) Total Particulate Matter: 16,05 ± 2,01 0.40 ± 0.07 Gly: 3.44 ± 0.68	Ames Test	Flavored and unflavored neosticks-Not mutagenic (Ames test)  Flavored and unflavored neosticks-Induced mutagenicity less than 3R4F (MLA test)	Ames Test	The complete list was not presented. Total reduction in the number and quantity of chemical components, including known HPHCs, in THS 2.2.	
Bentley et al., 2019	THS 2.2. (IQOS) in mainstream aerosol 529 chemicals (majority particulate and Gas vapor) at concentrations ≥ 100ng items (excluding water, Gly, Nic) Only a few compounds in THS2.2 aerosol exceeded concentrations measured in 3R4F reference cigarette smoke.	3R4F in mainstream smoke contain 529 compounds	GCxGC-TOF MS, LC+HRAM-MS (untargeted screening)	GCxGC-TOF MS, LC+HRAM-MS (untargeted screening)	Not presented all amounts on compounds Other than some carbonyls, ammonia, NAB at least 80% lower in THS 2.2. than CTCs. Tar and nicotine were similar.	
Li et al., 2019	THS 2.2. (IQOS) Total Particulate Matter, water, tar, Hydrogene cyanide; Ammonia, NAs, phenol, and PAHs, which are carcinogenic and mutagenic. Simulated pyrolysis of THS 2.2 heating sticks	CTCs	GC × GC-MS	GC × GC-MS	Not presented all amounts on compounds Other than some carbonyls, ammonia, NAB at least 80% lower in THS 2.2. than CTCs. Tar and nicotine were similar.	



Salman et al., 2019	IQOS aerosol Total Nic, PG, Veg. Gly. ROS: 6.26±2.72 nmol H <sub>2</sub> O <sub>2</sub> /cigarette CCs: 472.4 ± 19.35 µg/cigarette			CTCs-Marlboro red CCs: 2033±35.72 µg/cigarette ROS: 46.83 ± 9.6 nmol H <sub>2</sub> O <sub>2</sub> /cigarette (Only ISO regimen data)	HPLC, GC	ROS and CC levels were 85% and 77% lower than levels emitted by CTCs. Total Nic, PG, Veg. Gly were similar.
Hirn et al., 2020	Max usage level of 400 puffs, i.e., approximately 8 HTP tobacco capsules or 40 CTCs) HTP aerosol Ammonia: 20.1±1.1 PG: 25.2±6.0 Gly: 27.6±6 Formaldehyde: 0.74±0.099 Nic: 1.97±1.7 ACT: 1.55±0.85			3R4F Ammonia: 30±1.7 PG: 0.034±0.003 Gly: 2.23±0.08 Formaldehyde: 46.8±2.5 Nic: 1.97±1.7		The HTP aerosol was compared to 3R4F using a quantitative risk assessment approach. (Total 54 analytes). >90% reduction in non-cancer and cancer risk for HTP compared to 3R4F.
Hirano et al., 2020	Nic, 25.9-257 µg/m <sup>3</sup> (Tobacco Cigarette (TC): 3 µg/m <sup>3</sup> ) Nic>TC PM <sub>2.5</sub> <standard value of 15 µg/m <sup>3</sup> /year PM <sub>2.5</sub> 492 and 413 µg/m <sup>3</sup> (SD = 667, 466) at 1.0 and 1.8 m Indoor Nic: 2.6 and 2.7 µg/m <sup>3</sup> (at 1.5 and 2.5 m from the user) PM <sub>2.5</sub> : 7.0 and 6.9 µg/m <sup>3</sup> (SD = 11.6, 4.0)	PM <sub>2.5</sub> <standard value of 15 µg/m <sup>3</sup> /year Glo is slightly higher for PM <sub>2.5</sub> PloomTECH, at 21 and 10 µg/m <sup>3</sup> (SD = 55, 6.6); Glo 330 and 99 µg/m <sup>3</sup> (SD = 564, 119) at 1.0 and 1.8 m Indoor Nic: 2.2.3 and 3.0 µg/m <sup>3</sup> (at 1.5 and 2.5 m from the user) PloomTECH PM <sub>2.5</sub> : 6.5 and 7.0 µg/m <sup>3</sup> (SD = 5.8, 2.7) Glo PM <sub>2.5</sub> : 102 and 56 mg/m <sup>3</sup> (SD = 95, 56)		PM <sub>2.5-3.5</sub> : 10,700 and >5800 µg/m <sup>3</sup> (at 1.0 and 1.8 m from the user) Indoor Nic: 130 and 160 µg/m <sup>3</sup>	LC-MSMS	Nic> Tolerable Concentration PM 2.5m <sup>3</sup> -Hazard PM 2.5m <sup>3</sup> >IQOS>Glo
Kim et al., 2020	Three major brands of HTP sticks and devices have been used to produce HTP aerosol. HTP-Heating materials <b>Sample A</b> Formaldehyde: 0.138 ± 0.016 µg/stick Acetaldehyde: 0.616 ± 0.732 µg/stick ACR: 0.121 ± 0.109 µg/stick AT: 0.181 ± 0.200 µg/stick PA: 0.102 ± 0.119 µg/stick <b>Sample B</b> Formaldehyde: 0.945 ± 0.214 µg/stick Acetaldehyde: 1.21 ± 0.650 µg/stick ACR: 0.519 ± 0.379 µg/stick AT: 0.580 ± 0.305 µg/stick PA: 0.291 ± 0.139 µg/stick <b>Sample C</b> Formaldehyde: 0.641 ± 0.092 µg/stick Acetaldehyde: 63.5 ± 18.4 µg/stick ACR: 0.220 ± 0.102 µg/stick AT: ...NA PA: 1.710 ± 0.123 µg/stick	Tobacco sticks for HTP-HTP brands <b>Sample A</b> Formaldehyde: 0.640 ± 0.528 µg/stick Acetaldehyde: 26.4 ± 42.9 µg/stick ACR: 0.473 ± 0.4029 µg/stick AT: 0.348 ± 0.480 µg/stick PA: 0.783 ± 0.7719 µg/stick <b>Sample B</b> Formaldehyde: 0.546 ± 0.364 µg/stick Acetaldehyde: 14.4 ± 24.3 µg/stick ACR: 0.143 ± 0.047 µg/stick AT: 0.317 ± 0.286 µg/stick PA: 0.682 ± 1.017139 µg/stick <b>Sample C</b> Formaldehyde: 0.539 ± 0.363 µg/stick Acetaldehyde: 24.5 ± 41.2 µg/stick ACR: 0.243 ± 0.214 µg/stick AT: 0.096 ± 0.166 µg/stick PA: 0.291 ± 0.139 µg/stick Acetaldehyde: 63.5 ± 18.4 µg/stick PA: 0.641 ± 0.854 µg/stick				Harmful compounds were come from the filter, not tobacco sticks. Heated tobacco stick filters had higher. Formaldehyde and ACR concentrations (0.945 ± 0.214 µg/stick and 0.519 ± 0.379 µg/stick) than the aerosols generated from heated tobacco consumable The amount of acetaldehyde and PA were higher in the heated filter than in the aerosol produced from heated tobacco consumable.

<p>Bitzer et al., 2020.</p>	<p>IQOS 122 ± 9.6 µg/puff 156 ± 44.6 µg/puff Glo (72 ± 10.6 µg/puff) 156 ± 44.6 µg/puff Ploom 18 ± 0 µg/puff SREC 71 ± 8.2 µg/puff Mod: ND</p>	<p>156 ± 44.6 µg/puff The hybrid (Ploom)</p>	<p>Research Cigarette-1RGF Nic 190 ± 7.9 µg/puff (except Juul) 73.9 ± 7.5 pmol GPR:2982 ± 251 pmol/mg PPR: 392 ± 61.1 pmol/mg <b>e-cigarettes</b> Juul 5,3 ± 0.5 pmol/ml SREC 40 ± 0.8 pmol/puff Mod 48 ± 1.8 pmol/puff</p>	<p>GC/ FID, EPR spectroscopy</p>	<p>No differences among HTPs (IQOS, Kent, Glo) HTPs emitted more radical than Juul. There was no particulate phase radical with IQOS, Glo, Ploom, SREC e-cigarettes emitted more radical than IQOS. 1R6F produced significantly more gas-phase radicals/ and more particulate-phase radicals than any other devices. No difference was among QOS, Glo, and SREC for Nic. The Juul and the IQOS were not different for Nic.</p>
<p>Profano et al., 2020</p>	<p>Data on indoor air-In a test room, measurements of 10, 4, 2.5, 1 µm (PM10, PM4, PM2.5, PM1) PM pollution was obtained from IQOS (n=6), Glo (n=4), Juul (n=3) in different flavors and Marlboro Gold.</p>	<p>Before and during each experiment (10–12 puff for about 5–6 min)</p>			<p>They worsen indoor air quality. Indoor PM1 was at lower conc.s than CTCs.</p>

Table abbreviations; HPHC; harmful and potentially harmful constituents; HTPs, Heated Tobacco Products; CTC; Conventional tobacco cigarettes, Med, Median; TC, Tolerable concentration; ND, Not Detected; NA, Not Available.

Test Shower Cubicle (length 0.80 m × width 0.80 m × height 2.24 m); Test Room 25m<sup>3</sup> (length 3,44 m × width 7.26 m)  
HeatSticks, regular”, “balanced regular”, “mint”, and “menthol” tobacco sticks; NeoSticks, “bright tobacco”, “fresh mix”, and “intensely fresh” tobacco sticks; Tobacco caps, “Mevius Legular”, “Cooler Green”, and “Cooler Purple” liquid capsules.

ACR, acrolein, PA, Propionaldehyde; CA, Crotonaldehyde, eg., Regular; Ment., Menthol, Nic, Nicotine; CCs, Carbonyl compounds, TSNA, tobacco-specific nitrosamines; NAB, N'-nitroso anabasine; NAT, N'-nitrosoanatabine; NNN, 4-(methylnitrosamino)-1-(3-pyridyl)-1-butanone; NNN, N'-nitrosornicotine, CO, Carbon monoxide; PG, Propylene glycol; ACT, Acetol; BUTA, Butanal; DAAN, Diacetylacetone; ACT, Aceton, BA, benzaldehyde; mACR, methacrolein; Gly, Glycerol, Veg. Gly., Vegetable glycerol; 3R4F, Reference Cigarette, AAs, Aromatic amines; VOCs, Volatile compounds; Nas, N-nitrosamine; PAH, Polycyclic aromatic hydrocarbons; PPR, Particulate phase radical; GPR, Gas Phase Radical

GC-NPD, GasChromatography equipped with Nitrogen—Phosphorous Detector; GC-MS, as chromatography—mass spectrometry; GC-ITCD, gas chromatograph/thermal conductivity detector; GCxGC-TOF MS, LC+HRAM-MS, Liquid chromatography with high-resolution accurate mass spectrometry; Two-dimensional gas chromatography with time of flight mass spectrometry; MLA, Mouse Lymphoma Assay; ISO, International Organization of Standardization; GC/FID, gas-chromatography with flame-ionization detection

## RESULTS and DISCUSSION

Carbonyl compounds in HTPs were 77-95% less than in conventional tobacco cigarettes (CTC) (Farsalinos et al., 2018; Salman et al., 2019). HPHCs (Uchiyama et al., 2018; Salman et al., 2019) and particulate matter (PM) (indoor) were also less in HTPs than in CTCs (Protano et al., 2020). Tobacco-specific nitrosamines (TSNAs) were 8–22 times less in HTP aerosols than in CTC smoke. CTCs had the highest amount of TSNAs, except 4-(methyltyramine)-1-(3-pyridyl)-1-butanone (NNK), which was followed by HTPs and then e-cigarettes (Leigh et al., 2018; Ishizaki et al., 2019). Caponnetto et al. conducted a study of exhaled breath carbon monoxide (eCO) as a combustion marker after using IQOS, Glo, and CTC. In their study, a total of 12 healthy smokers (6 Men, 6 Women) who smoked  $\geq 10$  conventional cigarettes per day for at least 5 years were recruited. During the screening, participants provided a baseline  $eCO \geq 10$  ppm (ppm) and were trained for at least 30 minutes according to the recommendations of the HTP manufacturers. Participants were asked not to smoke for at least 12 hours before each training session. By the eligibility criteria, abstinence from smoking was verified by eCO measurements of  $\leq 10$  ppm obtained with a single breath using a handheld eCO meter (Micro CO; Micro Medical Ltd., UK). Once a baseline value was obtained, eCO was recorded at 5, 10, 15, 30, and 45 minutes after the first puff of the first round. eCO concentration was significantly different ( $p < 0.0001$ ) for both HTPs (IQOS and Glo) compared to conventional smoking, but not for iQOS compared to GLO. In eCO concentrations versus time, eCO concentrations of HTPs remained below 5 ppm. The point at which the eCO concentration of conventional cigarettes did not increase, i.e. 5 ppm, represents the widely accepted eCO reference range for non-smokers (Caponnetto et al., 2018).

Significant differences were observed in nicotine levels between iQOS/GLO and CTC but not between HTPs and Glo. Nicotine levels in HTPs are similar to those of CTCs (Caponnetto et al., 2018). The

amount of nicotine in HTP aerosols was higher than in e-cigarettes but lower than in CTCs (Farsalinos et al., 2018; Salman et al., 2019; Li et al., 2019). Volatile organic compounds (VOCs) and nicotine levels increase with temperature (180°C, 200°C, and 220°C) (23). E-cigarettes reportedly emit more radicals than IQOS, whereas HTPs emit more radicals than Jull. IQOS, Kent, and Glo have similar levels of radicals (Bitzer et al., 2020). The comparison of heated tobacco sticks and heated tobacco aerosol in terms of some chemicals, such as acrolein and formaldehyde levels, revealed that the levels of these chemicals were higher in the sticks than in aerosol (Kim et al., 2020).

It is well-established that tobacco smoking causes many diseases, including cancer, and that it is the nicotine that induces tobacco use. HTPs and e-cigarettes could be less harmful smoke/aerosol alternatives that satisfy users in terms of nicotine yet minimize the health risks caused by the harmful substances found in cigarette smoke. There is also evidence that these products help smokers quit tobacco smoking. It is not the nicotine that causes harm in tobacco cigarettes, but the HPHCs formed due to incomplete combustion. It has been demonstrated that HTPs also contain HPHCs in varying proportions, similar to those found in conventional cigarettes. However, the chemical composition of these HPHCs is significantly reduced or absent due to the absence of combustion in HTPs. Since different types of harmful substances are prominent in HTPs, the possible risk assessment of these substances should be made in detail. The studies conducted in vitro and animal experiments provide limited data for the safety of HTPs. Moreover, the absence of epidemiological studies that provide the most scientifically valuable data precludes making definitive judgments about the safety of HTPs. However, HTPs, which do not contain combustion products because they do not burn, are considered to be less harmful than conventional cigarettes and may be preferable for individuals who cannot quit smoking and have severe chronic diseases (such as cardiovascular disease).

### AUTHOR CONTRIBUTION STATEMENT

Conception and design, data collection, analysis and interpretation, literature search, and preparing the text (BK).

### CONFLICT OF INTEREST

Authors declare that there is no conflict of interest.

### REFERENCES

- Auer, R., Concha-Lozano, N., Jacot-Sadowski, I., Cornuz, J., & Berthet A. (2017). Heat-not-burn tobacco cigarettes: smoke by any other name. *JAMA Intern Med.*, *177*(7), 1050-1052. doi: 10.1001/jamainternmed.2017.1419.
- Bekki, K., Inaba, Y., Uchiyama, S., & Kunugita, N. (2017). Comparison of chemicals in mainstream smoke in heat-not-burn tobacco and combustion cigarettes. *JUOEH*, *39*(3), 201-207. doi: 10.7888/juoeh.39.201.
- Bekki, K., Uchiyama, S., Inaba, Y., & Ushiyama, A. (2021). Analysis of furans and pyridines from new generation heated tobacco product in Japan. *Environ. Health Prev. Med.*, *26*(1), 89. doi: 10.1186/s12199-021-01008-1.
- Bentley, M.C., Almstetter, M., Arndt, D., Knorr, A., Martin, E., Pospisil, P., & Maeder, S. (2020). Comprehensive chemical characterization of the aerosol generated by a heated tobacco product by untargeted screening. *Anal. Bioanal. Chem.*, *412*(11), 2675-2685. doi: 10.1007/s00216-020-02502-1.
- Bitzer, Z. T., Goel, R., Trushin, N., Muscat, J., & Richie, J. P. Jr. (2020). Free radical production and characterization of heat-not-burn cigarettes in comparison to conventional and electronic cigarettes. *Chem. Res. Toxicol.*, *33*(7), 1882-1887. doi: 10.1021/acs.chemrestox.0c00088.
- Cancelada, L., Sleiman, M., Tang, X., Russell, M. L., Montesinos, V. N., Litter, M. I., Gundel, L. A., & Destailats, H. (2019). Heated Tobacco Products: Volatile Emissions and Their Predicted Impact on Indoor Air Quality. *Environ. Sci. Technol.*, *53*(13), 7866-7876. doi: 10.1021/acs.est.9b02544.
- Caponnetto, P., Maglia, M., Prosperini, G., Busà, B., & Polosa, R. (2018). Carbon monoxide levels after inhalation from new generation heated tobacco products. *Respir. Res.*, *19*(1). doi: 10.1186/s12931-018-0867-z.
- Centers for Disease Control and Prevention. 2024, Health effects, [https://www.cdc.gov/tobacco/basic\\_information/health\\_effects/index.htm](https://www.cdc.gov/tobacco/basic_information/health_effects/index.htm) Erişim tarihi: 5 Ağustos 2024.
- Environmental Protection Agency. 2024, Second-hand smoke and smoke-free homes, <https://www.epa.gov/indoor-air-quality-iaq/secondhand-smoke-and-smoke-free-homes> Erişim tarihi: 5 Ağustos 2024.
- Farsalinos, K.E., Yannovits, N., Sarri, T., Voudris, V., & Poulas, K. (2018). Nicotine delivery to the aerosol of a heat-not-burn tobacco product: comparison with a tobacco cigarette and e-cigarettes. *Nicotine Tob. Res.*, *20*(8), 1004-1009. doi: 10.1093/ntr/ntx138.
- Gale, N., McEwan, M., Eldridge, A. C., Fearon, I. M., Sherwood, N., Bowen E., McDermott, S., Holmes, E., Hedge, A., Hossack, S., Wakenshaw, L., Glew, J., Camacho, O. M., Errington, G., McAughey, J., Murphy, J., Liu, C., & Proctor, C. J. (2019). Changes in Biomarkers of Exposure on Switching from a Conventional Cigarette to Tobacco Heating Products: A Randomized, Controlled Study in Healthy Japanese Subjects. *Nicotine Tob. Res.*, *21*(9), 1220-1227. doi: 10.1093/ntr/nty104.
- GBD 2019 Tobacco Collaborators. (2021). Spatial, temporal, and demographic patterns in prevalence of smoking tobacco use and attributable disease burden in 204 countries and territories, 1990-2019: a systematic analysis from the Global Burden of Disease Study 2019. *Lancet*, *397*(10292), 2337-2360. doi: 10.1016/S0140-6736(21)01169-7.
- Ishizaki, A., & Kataoka, H. (2019). A sensitive method for the determination of tobacco-specific nitrosamines in mainstream and side stream smokes of combustion cigarettes and heated tobacco products by online in-tube solid-phase microextraction coupled with liquid

- chromatography-tandem mass spectrometry. *Anal. Chim. Acta.*, 1075, 98-105. doi: 10.1016/j.aca.2019.04.073.
- Kim, Y. H., An, Y. J., & Shin, J. W. (2020). Carbonyl compounds containing formaldehyde produced from the heated mouthpiece of tobacco sticks for heated tobacco products. *Molecules*, 25(23), 5612. doi: 10.3390/molecules25235612.
- Leigh, N. J., Palumbo, M. N., Marino, A. M., O'Connor, R. J., & Goniewicz, M. L. (2018). Tobacco-specific nitrosamines (TSNA) in heated tobacco product IQOS. *Tob. Control.*, 27(1), 37-8. doi: 10.1136/tobaccocontrol-2018-054318.
- Lempert, L. K., & Glantz, S. A. (2018). Heated tobacco product regulation under US law and the FTC. *Tob. Control.*, 27(1), 118-125. doi: 10.1136/tobaccocontrol-2018-054560.
- Li, X., Luo, Y., Jiang, X., Zhang, H., Zhu, F., Hu, S., & Pang, Y. (2019). Chemical analysis and simulated pyrolysis of tobacco heating system 2.2 compared to conventional cigarettes. *Nicotine Tob. Res.*, 21(1), 111-118. doi: 10.1093/ntr/nty005.
- Lu, F., Yu, M., Chen, C., Liu, L., Zhao, P., Shen, B., Sun, R. (2021). The Emission of VOCs and CO from Heated Tobacco Products, Electronic Cigarettes, and Conventional Cigarettes, and Their Health Risk. *Toxics*, 10(1), 8.
- Mallock, N., Böss, L., Burk, R., Danziger, M., Welsch, T., Hahn, H., Pieper, E., Henkler-Stephani, F., Hutzler, C., & Luch, A. (2018). Levels of selected analytes in the emissions of "heat not burn" tobacco products that are relevant to assess human health risks. *Arch. Toxicol.*, 92(6), 2145-2149. doi: 10.1007/s00204-018-2215-y.
- National Cancer Institute at the National Institutes of Health. 2017, What harmful chemicals does tobacco smoke contain?, <https://www.cancer.gov/about-cancer/causes-prevention/risk/tobacco/cessation-fact-sheet#what-harmful-chemicals-does-tobacco-smoke-contain> Erişim tarihi: 19 Aralık 2017.
- Phillips, B. W., Schlage, W. K., Titz, B., Kogel, U., Sciuscio, D., Martin, F., Leroy, P., Vuillaume, G., Krishnan, S., Lee, T., Velkovic, E., Elamin, A., Merg, C., Ivanov, N. V., Peitsch, M. C., Hoeng, J., & Vanscheeuwijck, P. (2018). A 90-day OECD TG 413 rat inhalation study with systems toxicology endpoints demonstrates reduced exposure effects of the aerosol from the carbon heated tobacco product version 1.2 (CHTP1.2) compared with cigarette smoke. I. Inhalation exposure, clinical pathology and histopathology. *Food Chem. Toxicol.*, 116(Pt B), 388-413. doi: 10.1016/j.fct.2018.04.015.
- Polosa, R., Morjaria, J. B., Prosperini, U., Busà, B., Pennisi, A., Gussoni, G., Rust, S., Maglia, M., Caponnetto, P. (2021). Health outcomes in COPD smokers using heated tobacco products: a 3-year follow-up. *Intern. Emerg. Med.*, 16(3), 687-696. doi: 10.1007/s11739-021-02674-3.
- Protano, C., Manigrasso, M., Cammalleri, V., Biondi Zoccai, G., Frati, G., Avino, P., & Vitali, M. (2020). Impact of electronic alternatives to tobacco cigarettes on indoor air particular matter levels. *Int. J. Environ. Res. Public Health*, 17(8), 2947. doi: 10.3390/ijerph17082947.
- Salman, R., Talih, S., El-Hage, R., Haddad, C., Karaoghlanian, N., El-Hellani, A., Saliba, N. A., & Shihadeh, A. (2019). Free-base and total nicotine, reactive oxygen species, and carbonyl emissions from IQOS, a heated tobacco product. *Nicotine Tob. Res.*, 21(9), 1285-1288. doi: 10.1093/ntr/nty235.
- Section 910. 2019, Section 910 of the Federal Food, Drug, and Cosmetic Act - Application for Review of Certain Tobacco Products. <https://www.fda.gov/tobacco-products/rules-regulations-and-guidance/section-910-federal-food-drug-and-cosmetic-act-application-review-certain-tobacco-products> Erişim tarihi: 30 Eylül 2024.

- Section 911. 2018, Section 911 of the Federal Food, Drug, and Cosmetic Act - Modified Risk Tobacco Products. <https://www.fda.gov/tobacco-products/rules-regulations-and-guidance/section-911-federal-food-drug-and-cosmetic-act-modified-risk-tobacco-products> Erişim tarihi: 30 Eylül 2024.
- Simonavicius, E., McNeill, A., Shahab, L., & Brose, L.S. (2019). Heat-not-burn tobacco products: a systematic literature review. *Tob. Control.*, 28(5), 582-594. doi: 10.1136/tobaccocontrol-2018-054419.
- Szymanski, F. M., Semczuk-Kaczmarek, K., Kuna, P. (2021) Health outcomes in COPD smokers using heated tobacco products: a 3 year follow up: comment. *Intern. Emerg. Med.*, 16(8), 2331-233. doi: 10.1007/s11739-021-02753-5.
- Titz, B., Kogel, U., Martin, F., Schlage, W. K., Xiang, Y., Nury, C., Dijon, S., Baumer, K., Peric, D., Bornand, D., Dulize, R., Phillips, B., Leroy, P., Vulliaume, G., Lebrun, S., Elamin, A., Guedj, E., Trivedi, K., Ivanov, N. V., Vanscheeuwijck, P., Peitsch, M. C., Hoeng, J. (2018). A 90-day OECD TG 413 rat inhalation study with systems toxicology endpoints demonstrates reduced exposure effects of the aerosol from the carbon heated tobacco product version 1.2 (CHTP1.2) compared with cigarette smoke. II. Systems toxicology assessment. *Food Chem. Toxicol.*, 115, 284-301.
- Treasury H. M. (2018), Tax treatment of heated tobacco products, <https://www.gov.uk/government/consultations/tax-treatment-of-heated-tobacco-products/tax-treatment-of-heated-tobacco-products> Erişim tarihi: 13 Mart 2018.
- U.S. Food & Drug Administration. 2020, FDA news release: FDA authorizes marketing of IQOS tobacco heating system with 'reduced exposure' information, <https://www.fda.gov/news-events/press-announcements/fda-authorizes-marketing-iqos-tobacco-heating-system-reduced-exposure-information> Erişim tarihi: 7 Temmuz 2020.
- U.S. Food & Drug Administration. 2024, Modified risk tobacco products, <https://www.fda.gov/tobacco-products/advertising-and-promotion/modified-risk-tobacco-products> Erişim tarihi: 7 Ağustos 2020.
- U.S. Food and Drug Administration. 2024, Nicotine is why tobacco products are addictive, <https://www.fda.gov/tobacco-products/health-effects-tobacco-use/nicotine-why-tobacco-products-are-addictive> Erişim tarihi: 5 Ağustos 2024.
- Uchiyama, S., Noguchi, M., Takagi, N., Hayashida, H., Inaba, Y., Ogura, H., & Kunugita, N. (2018). Simple determination of gaseous and particulate compounds generated from heated tobacco products. *Chem. Res. Toxicol.*, 31(7), 585-593. doi: 10.1021/acs.chemrestox.8b00024.
- Vu, A. T., Taylor, K. M., Holman, M. R., Ding, Y. S., Hearn, B., & Watson, C. H. (2015). Polycyclic Aromatic Hydrocarbons in the Mainstream Smoke of Popular U.S. Cigarettes. *Chem. Res. Toxicol.*, 28(8), 1616-26. doi: 10.1021/acs.chemrestox.5b00190.
- World Health Organization. 2019, WHO global report on trends in prevalence of tobacco smoking 2000-2025 (3rd ed.), <https://iris.who.int/bitstream/handle/10665/330221/9789240000032-eng.pdf> Erişim tarihi: 12 Nisan 2020.
- World Health Organization. (2020). Heated tobacco products: a brief. Geneva (Switzerland): WHO Regional Office for Europe. <https://iris.who.int/bitstream/handle/10665/350470/WHO-EURO-2020-4571-44334-64934-eng.pdf?sequence=3> Erişim tarihi: 21 Mayıs 2018.
- World Health Organization. 2018, Heated tobacco products (HTPS): information sheet, <https://apps.who.int/iris/bitstream/handle/10665/272875/WHO-NMH-PND-17.6-eng.pdf> Erişim tarihi: 30 Eylül 2020.
- Znyk, M., Jurewicz, J., & Kaleta, D. (2021). Exposure to heated tobacco products and adverse health effects, a systematic review. *Int. J. Environ. Res. Public Health*, 18(12), 6651. doi: 10.3390/ijerph18126651.